RELAXATION PHENOMENA OF DIELECTROPOLAR LIQUID MOLECULES UNDER LOW AND HIGH FREQUENCY ELECTRIC FIELDS

THESIS SUBMITTED FOR THE DEGREE OF DOCTOR
OF PHILOSOPHY (SCIENCE) OF THE
UNIVERSITY OF NORTH BENGAL
2002

KOUSHIK DUTTA M Sc. B Ed

STOCK TAKING - 2011

Dedicated to my parents

Sri Heramba Dutta & Smt. Depali Dutta

ACKNOWLEDGEMENT

I am highly grateful to Dr. Suprakash Acharyya M Sc. D Phil, Ex-Reader, Department of Physics, Raiganj College (University College) , Raiganj for his kind guidance, whole hearted cooperation and active supervision towards the progress of the research works presented in the thesis entitled " Relaxation phenomena of dielectropolar liquid molecules under low and high frequency electric fields". I convey my whole hearted gratitude to Dr. Tapas Kumar Chatterjee, Registrar, University of North Bengal for his constant inspiration and encouragement in the research work. I also wish to express my thanks to Prof. Subir Kumar Roy, Dept. of Spectroscopy, Indian Association for the Cultivation of Science, Kolkata for his kind permission to perform the experimental work in his laboratory.

My particular thanks, however, are due to Dr. Swapan Kumar Sit of Raiganj Polytechnic for his help in the preparation of the thesis manuscript.

I feel pleasure to thank my intimate friends Dr. Arabinda Chowdhury, Pinak Pani Nath, Susmita Karan and Dr. Aparajita Chatterjee for their constant encouragement during the tenure of my research work. I was greately helped by Dr. Rabindra Chandra Basak, Dr. Nilanjan Ghosh and Achintya Karmakar to discuss some of the topics presented here.

Thanks are due to Anirban, Arindam and Mrs. Anima Acharyya for their cooperation during the research period.

Finally I would like to use the opportunity to express my appreciation to my beloved wife Lipika, brother Raju and son Rajarshi for their unwavering love and support, without which the presented works would have remained undone.

Koushik Dutta

09.12.2002

KOUSHIK DUTTA

Department of Physics
Debinagar G. R. U. Vidyapith
PO. Debinagar, Raiganj
Dist. Uttar Dinajpur (WB)
733123. INDIA

LIST OF PUBLICATIONS

1. K Dutta, R C Basak, S K Sit and S Acharyya, *Journal of Molecular Liquids*, **88** 229-241 (2000)
2. S K Sit, K Dutta, S Acharyya, T Pal Majumder and S Roy, *Journal of Molecular Liquids*, **89** 111-126 (2000)
3. K Dutta, S K Sit and S Acharyya, *Journal of Molecular Liquids*, **92** 263-276 (2001)
4. K Dutta, S K Sit and S Acharyya, *PRAMANA: Journal of Physics*, **57** 775-793 (2001)
5. K Dutta, A Karmakar, S K Sit and S Acharyya, *Indian Journal of Pure and Applied Physics*, **40** 588-596 (2002)
6. K Dutta, A Karmakar, Mrs. L Dutta, S K Sit and S Acharyya, *Indian Journal of Pure and Applied Physics*, **40** 801-815 (2002)
7. K Dutta, S K Sit and S Acharyya, *PRAMANA: Journal of Physics*, (Communicated)
8. K Dutta, S K Sit and S Acharyya, *Journal of Physics D: Applied Physics*, (Communicated)

CONTENTS

Preface

The proposed thesis is aimed at to study the relaxation phenomena of some interesting dielectropolar liquid molecules in non-polar solvents under low and high frequency electric field at various experimental temperatures.

The relaxation phenomena in liquids and solids represent one of the most difficult unresolved problems of physics today. The presence of all relaxation phenomena in liquids under study or even for solids are related to some form of disorder. There can be no relaxation in a perfectly ordered system, because nothing can relax from perfection. Under the application of the alternating electric field in a dielectropolar liquid molecule each type of polarisations takes some time to respond the applied electric field. The lag in response to the alternation of the applied electric field is commonly known as dielectric relaxation.

The dipolar liquid molecules in non-polar solvents under low and *hf* electric fields attracted the attention of a large number of workers for its wide applications in different fields. All the information are derived from the measured relaxation parameters like real ε_{ij}', imaginary ε_{ij}'' parts of complex relative permittivity ε_{ij}^*, static relative permittivity ε_{oij} and high frequency relative permittivity $\varepsilon_{\infty ij}$ of a polar liquid molecule (j) dissolved in a non polar solvent (i) measured under any suitable experimental arrangement of the effective dispersive region of J-Band (~3 GHz), X-Band (~10 GHz) and K-Band (~24 GHz) electric fields. These data are analysed on the basis of various models like Debye, Kirkwood, Fröhlich, Onsager etc.

Out of the above models, Debye and Smyth model is very simple, straightforward and applicable to almost all rigid spherical polar liquid molecules in non-polar solvents. In such case one polar unit is assumed to be far apart from the others and remains in quasi-isolated state to eliminate polar-polar interactions almost completely.

We have therefore, become selective to chose some apparently rigid aliphatic polar molecules like chloral and ethyltrichloroacetate in non polar aromatic solvent benzene and alicyclic aliphatic solvents *n*-hexane and *n*-heptane to study their conformations under three different frequencies in GHz range. Chloral and ethyltrichloroacetate in a variety of non polar solvents under single frequency electric field show the double relaxation phenomena due to rotation of the whole molecule as well as the flexible parts attached to the parent molecules exhibiting the non-rigid nature of the molecules. The static and *hf* dipole moments for the above systems were also estimated. This investigation also includes polar liquid molecules like trifluoroethanol, trifluoroacetic acid and octanoyl chloride dissolved in benzene too.

τ_j's and μ_j's of some polysubstituted benzenes like meta-diisopropylbenzene, para-methyl benzoylchloride and ortho-chloroacetophenone in benzene at different experimental temperatures

under GHz electric field frequency were investigated to get new information about molecular environment of the polar molecules and shed more light on their structural conformations and associational behaviour. Various energy parameters like enthalpy of activation ΔH_τ, entropy of activation ΔS_τ and free energy of activation ΔF_τ were proposed from the standpoint of dielectric relaxation of the polar molecules. The molecules are complicated in nature and one of them is para compound in which peculiar behaviours are quite expected. With these facts, we are very much tempted to make a rigorous study by our well-known conductivity measurement technique.

The author also measured the relaxation parameters ε_{ij}', ε_{ij}'' ε_{oij} and $\varepsilon_{\infty ij}$ of some aprotic polar liquids like DMSO, DEF, DMF and DMA in benzene by HP 4192A impedance analyser at Dept. of Spectroscopy, IACS, Kolkata for different concentrations and at different experimental temperatures to test the theories newly developed.

Relaxation mechanism have been studied for some methyl benzenes and ketones in benzene through high frequency conductivity measurement technique to get structural and associational aspect of the molecules.

The recent trend is to study the relaxation mechanism of dielectropolar liquid molecules through *hf* dielectric orientation susceptibility χ_{ij}^* rather than permittivity ε_{ij}^* or conductivity σ_{ij}^*. The dimensionless χ_{ij}^* are directly linked with the orientation polarisation of the molecules while *hf* conductivity σ_{ij} is concerned with the transport of bound molecular charge of the polar-nonpolar liquids and ε_{ij}^* includes all the polarisations.

Relaxation phenomena in terms of dielectric orientation susceptibility measurement technique were studied for chloral and ethyltrichloroacetate in benzene, *n*-hexane and *n*-heptane and a number of disubstituted benzenes and anilines in benzene and carbon tetrachloride under *hf* electric field. The molecules are supposed to absorb electric energy much more strongly nearly 10 GHz (~X-Band) electric field to show the interesting behaviour of the molecule from relaxation phenomena.

Double relaxation phenomena seems to be the material property of some dipolar liquids in non-polar solvents. It had been extensively studied by the author for a number of alcohols in *n*-heptane under three different *hf* electric fields.

Thus the entire object of the thesis is to study the relaxation phenomena of polar liquid molecules in various non-polar solvents under high and low frequency electric field at a single or different temperatures in order to arrive at their conformational structures from the derived present formalisms on the basis of Debye and Smyth model. The correlation between the conformational structures of the compounds under investigation with the observed results enhances the scientific contents of the thesis as it adds a better understanding to the existing knowledge of dielectric relaxation phenomena so far achieved.

CHAPTER 1

GENERAL INTRODUCTION AND REVIEW OF THE PREVIOUS WORKS

1.1. Introduction:

The aim of the dielectric investigation in this thesis is to provide the reader a very simplified and significant approach to grasp the dielectric relaxation phenomena in both pure polar liquid and polar liquid molecules in non-polar solvent under low and high frequency electric fields. In order to reach the goal, the central idea of the work is concentrated to measure both the macroscopic and microscopic entities like relative permittivity ε and dipole moment μ respectively of the molecule. The electric dipole moment μ is not only significant as a reflection of the electronic structure of the molecules. But it is of prime importance in our understanding of molecular interactions. It also partly controls the transition between solid, liquid and gaseous states of a substance. The electric behaviour of dielectric molecule has wide applications in different fields. Scientists are mainly interested to predict shape, size, structure, molecular interactions and change of phase of the polar molecules. Technologists, on the other hand, find its important applications in the field of electrical engineering.

1.2. Dielectric Relaxation :

Dielectric relaxation phenomena are related to some form of disorder present in the system under study. There can be no relaxation in a perfectly ordered system, because nothing can relax from perfection. In the case of polar liquid molecules, even if for a perfectly ordered spatial array of dipoles, their orientation distribution would need to be random for the isotropic behaviour in the electric field.

If a dielectropolar substance is placed under the application of the alternating electric field, the molecule becomes polarised. There exist various types of polarisations. Each type of polarisation takes some finite time to respond the applied alternating electric field. Thus there is a considerable lag in the attainment of the equilibrium. This lag in response to the alternation of the applied electric field is commonly known as dielectric relaxation. When the external electric field is removed, all types of polarisation including the orientation polarisation decay exponentially with time. The time in which the orientation polarisation is reduced to 1/e times the initial value is called the relaxation time τ of a dielectropolar liquid molecule. In the case of static or low frequency electric field, all the polarisations are operative. When the frequency of the alternating electric field becomes high, all the polarisations are not able to attain the equilibrium before the applied electric field is reversed. The relaxation time τ is an important molecular parameter, which is usually used to determine dipole moment μ of a polar substance.

1.3. Relative Dielectric Permittivity :

Permittivity is a parameter of a dielectric medium. It arises in the calculation of force exerted on each of the electric charges placed in a medium. If two charges are placed in a homogeneous or isotropic dielectric medium, the forces on each of them is reduced by a dimensionless scalar factor ε_r called the relative dielectric permittivity which is the ratio of the capacitances of the condenser when two charged plates of opposite signs are filled up with dielectric medium and vacuum respectively. Thus ε_r is given by:

$$\varepsilon_r = \frac{C_m}{C_v}$$

where C's are the capacitance of the condenser having dielectric medium and vacuum respectively. If the relative permittivity of the material is higher the greater is the polarisability of the molecule. So the polar molecule usually has higher permittivities than the non-polar one.

1.4. Dielectric Polarisation :

Under the application of the electric field $\vec{E}$ the centres of the positive and negative charges of each molecule of dielectric material are displaced in opposite directions. This sort of relative displacement of charges is called polarisation and the dielectric is said to be polarised.

In a homogeneous or isotropic dielectric, the dielectric polarisation $\vec{P}$ per unit electric field of $\vec{E}$ is called the molecular polarisability α. The polarisability in a non-polar molecule arises from two effects. The displacement of the electrons relative to the nucleus in each atom is called the electronic polarisation and that of the atomic nuclei relative to one another is called the atomic polarisation. For a polar molecule the permanent dipole aligns along the applied electric field direction, although they have thermal motions, is called the orientation polarisation.

Therefore the total polarisability α_T of the molecule is:

$$\alpha_T = \alpha_e + \alpha_a + \alpha_o = \alpha_d + \alpha_o \qquad \ldots.(1.1)$$

where α_e, α_a and α_o are the electronic, atomic and the orientation polarisabilities respectively. α_d is called the distortion polarisability. Each of three types of polarisabilities is obviously a function of frequency of the applied electric field. As the electric field alters and reverses its sign both their distortion and average orientation polarisations must change. When the frequency is higher, this affect the orientation polarisation which takes some time of the order of 10^{-12} to 10^{-10} sec to reach the equilibrium in the cases of liquids and solids. In such frequency the distortion polarisation takes much less time than the orientation polarisation to reach equilibrium.

1.5. Clausius–Mossotti Equation and Lorentz–Lorentz Formula :

When an electric field $\vec{E}$ is applied between two plates of the condenser, the field is modified to $\vec{E}_{loc}$ by a linear liquid dielectric. The total polarisation of the molecules is given by :

$$\vec{P} = n\alpha_d \vec{E}_{loc} \qquad \ldots\ldots (1.2)$$

where 'n' is the number of molecules per unit volume of the dielectric medium and α_d is the distortion polarisability of the non-polar dielectric.

Hence, the dielectric displacement vector $\vec{D}$ is :

$$\vec{D} = \varepsilon_r \vec{E} = \vec{E} + 4\pi\vec{P} \qquad \ldots\ldots (1.3)$$

$$\varepsilon_r - 1 = \frac{4\pi n \alpha_d \vec{E}_{loc}}{\vec{E}} \qquad \ldots\ldots (1.4)$$

For a simple cubic crystal or an isotropic liquid dielectric it can be shown that

$$\vec{E}_{loc} = \vec{E} + \frac{4}{3}\pi\vec{P} \qquad \ldots\ldots (1.5)$$

From Eqs.(1.4) and (1.5) one gets,

$$\frac{\varepsilon_r - 1}{\varepsilon_r + 2} = \frac{4}{3}\pi n \alpha_d \qquad \ldots\ldots (1.6)$$

Multiplying both sides by molar volume M/ρ the above Eq.(1.6) becomes

$$\frac{\varepsilon_r - 1}{\varepsilon_r + 2}\frac{M}{\rho} = \frac{4}{3}\pi N \alpha_d \qquad \ldots\ldots (1.7)$$

where N is the Avogadro's number. The Eq.(1.7) is known as the Clausius–Mossotti equation [1.1-1.2].

The electronic polarisation occurs at frequencies corresponding to the electric transitions between different energy levels in the atom *i.e*, mostly at visible and ultra-violet frequencies. In such case the relative permittivity ε_r is replaced by the square of the refractive index n_D^2 measured at that frequency according to Maxwell's electromagnetic theory. The above relation now becomes:

$$\frac{n_D^2 - 1}{n_D^2 + 2}\frac{M}{\rho} = \frac{4}{3}\pi N \alpha_e \qquad \ldots\ldots (1.8)$$

and is called Lorentz–Lorentz formula [1.3-1.4].

1.6. Debye Equation Under Static Electric Field :

For a non-polar molecule the molecular polarisability α_d due to distortion polarisation does not depend on temperature while for a polar molecule the orientation polarisation of the molecule depends on temperature unlike distortion polarisation. The polar molecule also possesses a permanent dipole moment $\vec{\mu}_p$ which is randomly directed due to thermal agitation prevailing in the system such that net moment is zero.

Under the application of the electric field the permanent dipoles are forced to orient along the field direction and equilibrium is set up to yield the resulting orientation polarisation $\vec{P}_o$ which is inversely proportional to the absolute temperature T K. It can be shown [1.5] that:

$$\vec{P}_o = \frac{n\mu_p{}^2 \vec{E}_{loc}}{3k_B T} = n\alpha_o \vec{E}_{loc} \qquad \ldots\ldots (1.9)$$

where $\alpha_o = \mu_p^2 / 3k_B T$ is defined as the effective orientation polarisability.

Thus the total polarisability in case of polar liquid molecule, is

$$\alpha_T = \alpha_a + \alpha_e + \frac{\mu_p{}^2}{3k_B T}$$

$$\alpha_T = \alpha_d + \frac{\mu_p{}^2}{3k_B T} \qquad \ldots\ldots (1.10)$$

where α_d is the polarisability due to distortion polarisation. Hence the Clausius–Mossotti equation (1.7) becomes;

$$\frac{\varepsilon_r - 1}{\varepsilon_r + 2}\frac{M}{\rho} = \frac{4}{3}\pi N\left(\alpha_d + \frac{\mu_p{}^2}{3k_B T}\right) \qquad \ldots\ldots (1.11)$$

The Eq.(1.11) is the well known Debye equation [1.6] for a polar molecule which relates a macroscopic quantity like relative permittivity at the L.H.S of the equation to the microscopic quantity like polarisability at the R.H.S.

1.7. Onsager Equation :

The failure of Debye equation (1.11) to assume that the field due to molecules in the spherical region is equal to zero led Onsager [1.7] to develop the following model. The molecule is treated as a point dipole at the centre of a spherical cavity of molecular dimension in a continuous medium. The radius 'a' of the cavity is defined by:

$$\frac{4}{3}\pi a^3 N_1 = 1 \qquad \text{.....(1.12)}$$

where N_1= no. of dipoles per unit volume. In case of spherical molecule Onsager neglected the short range dipolar interaction among the molecules unlike long range interaction. The internal field in the spherical cavity consists of the cavity field $\vec{G}$ and the reaction field $\vec{R}$ due to external applied electric field and the polarisation by the dipole respectively. The cavity field alone orients the molecule whereas the reaction field only increases their electric moment and always remains parallel to the dipole. A relation between relative permittivity and dipole moment of nearly non-spherical polar liquid molecule is obtained by Onsager [1.7] in a continuous medium of static permittivity ε_o and refractive index n_D by:

$$\frac{(\varepsilon_o - n_D^2)(2\varepsilon_o + n_D^2)}{\varepsilon_o (n_D^2 + 2)^2} = \frac{4\pi N \rho \mu^2}{9 M k_B T} \qquad \text{.....(1.13)}$$

This theory gives a successful account of the general behaviour of pure polar liquid. The validity of Onsager's equation is limited by the assumption that molecules are point dipoles and embeded in a sphere of isotropic polarisable material. In general real molecules are non-spherical and have anisotropic polarisabilities. They have quadrupole and higher moments which may be neglected at macroscopic distances. To take such effects into account a theory would need to contain a prohitively large parameter. Later on a large number of workers [1.8-1.11] modified Debye and Onsager equations to obtain μ of a highly non-spherical polar liquid molecules.

1.8. Debye's Diffusive Model of Relaxation Phenomena :

On the basis of Einstein's theory of the Brownian motion Debye [1.6] supposed that the rotation of a polar molecule under an alternating electric field is constantly interrupted by collisions with the neighbouring molecules. The collisions among molecules may produce a resistive couple proportional to the angular frequency ω of the dielectropolar molecule. This model is applicable only to liquid molecules and helped Debye to yield the frequency dependence of the permittivity of a polar molecule.

$$\frac{\varepsilon^* - n_D^2}{\varepsilon_o - n_D^2} = \frac{1}{1 + j\omega\tau} \qquad \text{.....(1.14)}$$

where n_D is the refractive index and macroscopic relaxation time τ is related to microscopic relaxation time τ' by :

$$\tau = \frac{\varepsilon_o + 2}{n_D^2 + 2}\tau' \qquad \text{.....(1.15)}$$

1.9. Kirkwood Model of Relaxation Phenomena :

Kirkwood [1.12], however, imagined a specimen of the material containing a number of dipoles each of moment μ confined in a spherical volume. When such volume is situated in a uniform external electric field the moment of the specimen can be separated into two parts:

(i) The molecule somewhere within the specimen is fixed but the others take up all possible configurations and

(ii) The moment induced in a homogenous specimen of the fixed molecule, and the molecule itself plus local ordering of the molecules immediately round it.

The Kirkwood's equation for a dipolar liquid is given by :

$$\frac{(\varepsilon_o - 1)(2\varepsilon_o + 1)}{3\varepsilon_o} = \frac{4\pi N}{V}\left(\alpha + \frac{g\mu^2}{3k_B T}\right) \qquad \ldots\ldots (1.16)$$

where the correlation parameter g is a measure of the local ordering in the material.

1.10. Fröhlich's Model :

Fröhlich, on the other hand, assumes a spherical region of microscopic dimensions in an infinite continuous medium. The spherical region is not assumed to be an exact sphere but modified slightly. Then the equation for non polarisable dipole is deduced by Fröhlich [1.13]:

$$\frac{(\varepsilon_o - 1)(2\varepsilon_o + 1)}{3\varepsilon_o} = \frac{4\pi N}{V}\frac{\langle m.\overline{m}\rangle}{3k_B T} \qquad \ldots\ldots (1.17)$$

where $< m.\overline{m} >$ is the weighted average of electric dipole moment $\overline{m}$.

1.11. The Barrier Model of Dielectric Relaxation :

The molecules are assumed to change the orientations of a polar molecule by a series of small steps. This model is applicable to polar-nonpolar liquid mixture. A molecule in solid, may, interact with its neighbors, creating a number of " equilibrium positions". This corresponds to a minimum potential energy separated by potential barriers. This type of process was first considered by Debye [1.6].

1.12. Bauer's Theoretical Model of Dielectric Relaxation :

Bauer's [1.14] model of dielectric relaxation is closely similar to Eyring's [1.15] reaction rate theory. It explicitly refers to dipole rotation. The orientational coordinate (θ, ϕ) of a dipole in a system can be represented by a point on a unit sphere. The unit sphere can be divided into two

domains separated by a potential barrier of height H. The minimum potential energies of dipoles in two domains are 0 and U respectively.

1.13. Real and Imaginary Parts of The Relative Permittivity :

Under static electric field there is no absorption of electric energy by the dielectric material and the dielectric displacement vector $\vec{D}$ is simply related to the applied electric field $\vec{E}$ by the relation $\vec{D} = \varepsilon\vec{E}$.

When the dielectric material is placed between the plates under an alternating electric field like $\vec{E} = \vec{E}_o \cos \omega t$ there is always a dissipation of energy due to absorption of electromagnetic waves. This is called "dielectric loss" over a broad band of frequencies. Molecular forces impeding the dipole rotation dominate if the direction of the applied electric field changes sufficiently fast. The dipoles become unable to follow the changes and the orientation of permanent dipoles no longer contributes to the dielectric relaxation at such frequencies. A phase difference between $\vec{D}$ and $\vec{E}$ develops, and energy is drawn from the electrical sources by the material which is due to

(i) electrical conduction

(ii) the relaxation effect due to permanent dipoles and

(iii) the resonance effect due to rotation or vibration of atoms, ions, or electrons of the dielectric material.

Thus it is useful to describe the relationship between $\vec{E}$ and $\vec{D}$ by

$$\vec{E} = \vec{E}_o e^{j\omega t} \quad \text{and} \quad \vec{D} = \vec{D}_o e^{j(\omega t - \delta)}$$

where δ is the phase difference and $\omega = 2\pi f$, f being the frequency of the applied electric field. j = complex number $= \sqrt{-1}$.

The dielectric response of a system is described by the complex representation of the relative permittivity $\varepsilon^*(\omega)$ at frequency (ω):

$$\varepsilon^*(\omega) = \frac{\vec{D}}{\vec{E}} = \frac{\vec{D}_o}{\vec{E}_o}(\cos\delta - j\sin\delta)$$

$$\varepsilon^*(\omega) = \varepsilon'(\omega) - \varepsilon''(\omega) \qquad \ldots\ldots (1.18)$$

where $\varepsilon'(\omega)$ and $\varepsilon''(\omega)$ are the real and imaginary parts of the complex relative permittivity $\varepsilon^*(\omega)$. In the low frequency, $\varepsilon''(\omega) \to 0$, $\varepsilon'(\omega) \to \varepsilon_o$. In the high frequency *i.e* infrared region $\varepsilon'(\omega) \to \varepsilon_\infty$.

Kramers and Krönig [1.16-1.17] developed the mutual transformation relation between the two parts, dispersion and absorption of the dielectric relaxation:

$$\varepsilon'(f)-\varepsilon_\infty=\frac{2}{\pi}\int_o^\infty\frac{f'\varepsilon''(f)}{f'^2-f^2}df' \quad ; \qquad \varepsilon''(f)=-\frac{2}{\pi}\int_o^\infty\frac{\varepsilon'(f')-\varepsilon_\infty}{f'^2-f^2}df \qquad \text{.....(1.19)}$$

The frequency f must have been supplemented by a further frequency variable f' over which integration is made.

1.14. Debye Equations Under High Frequency Electric Field :

The rotation of a dipolar molecule due to an applied alternating electric field is constantly interrupted by collisions with the neighbours. These collisions may be described by a resistive couple proportional to the angular velocity of the molecule. The dipole moment μ of the molecule on which the orienting couple acts is given in terms of complex relative permittivitiy ε^* [1.6]

$$\frac{\varepsilon^*-1}{\varepsilon^*+2}\frac{M}{\rho}=\frac{4\pi N}{3}\left(\alpha_d+\frac{\mu^2}{3k_BT}\frac{1}{1+j\omega\tau'}\right) \qquad \text{.....(1.20)}$$

In the low frequency range Debye expression for the static permittivity is:

$$\frac{\varepsilon_o-1}{\varepsilon_o+2}\frac{M}{\rho}=\frac{4\pi N}{3}\left(\alpha_d+\frac{\mu^2}{3k_BT}\right) \qquad \text{.....(1.21)}$$

In the high frequency limit, *i.e* in the far infra red or visible region ($\varepsilon_\infty=n_D^2$) all types of distortion polarisation make full contribution except dipolar polarisation which is zero. In this region,:

$$\frac{\varepsilon_\infty-1}{\varepsilon_\infty+2}\frac{M}{\rho}=\frac{4\pi N}{3}\alpha_d \qquad \text{.....(1.22)}$$

On substitution of Eqs.(1.21) and (1.22) in Eq.(1.20) it can be written as

$$\frac{\varepsilon^*-1}{\varepsilon^*+2}=\frac{\varepsilon_\infty-1}{\varepsilon_\infty+2}+\left(\frac{\varepsilon_o-1}{\varepsilon_o+2}-\frac{\varepsilon_\infty-1}{\varepsilon_\infty+2}\right)\frac{1}{1+j\omega\tau'} \qquad \text{.....(1.23)}$$

The Eq.(1.23) can be rearranged to give

$$\frac{\varepsilon^*-\varepsilon_\infty}{\varepsilon_o-\varepsilon_\infty}=\frac{1}{1+j\omega\tau} \qquad \text{.....(1.24)}$$

Separating real and imaginary parts one can obtain

$$\varepsilon'=\varepsilon_\infty+\frac{\varepsilon_o-\varepsilon_\infty}{1+x^2} \qquad \text{.....(1.25)}$$

$$\varepsilon''=\frac{\varepsilon_o-\varepsilon_\infty}{1+x^2}x \qquad \text{.....(1.26)}$$

where $x = \omega\tau = \frac{\varepsilon_o + 2}{\varepsilon_\infty + 2}\omega\tau'$.

Eqs.(1.25) and (1.26) are known as Debye equations under *hf* electric field.

1.15. Murphy–Morgan Conductivity Relation :

Under the application of an alternating electric field $E=E_o e^{j\omega t}$ the conductivity of a dielectropolar liquid due to displacement current is:

$$\sigma = \frac{1}{E}\frac{dq}{dt} \qquad \ldots\ldots (1.27)$$

Again $D = 4\pi q = E + 4\pi P$ and $E = \frac{V}{d} = \frac{D}{\varepsilon}$, we have

$$\frac{dq}{dt} = \frac{1}{4\pi}\frac{dD}{dt} = \frac{\varepsilon}{4\pi d}\frac{dV}{dt} = I \text{ (say)}$$

where V is the applied alternating potential $V=V_o e^{j\omega t}$. The expression for the displacement current I is given by:

$$I = \frac{\varepsilon^*}{4\pi d}\frac{dV}{dt} \qquad \ldots\ldots (1.28)$$

Introducing $\varepsilon^*=\varepsilon'-j\varepsilon''$ and $V=V_o e^{j\omega t}$ in Eq.(1.28), the current I can be written as according to Murphy and Morgan [1.18] :

$$I = \left(\frac{\omega\varepsilon''}{4\pi} + j\frac{\omega\varepsilon'}{4\pi}\right)E_o e^{j\omega t} \qquad \ldots\ldots (1.29)$$

When eq. (1.29) is compared to Ohm's law i.e. $I=\sigma^* E_o e^{j\omega t}$, one gets σ^* where σ^* is called the *hf* complex conductivity which is:

$$\sigma^* = \sigma' + j\sigma'' \qquad \ldots\ldots (1.30)$$

Thus, σ' = the real part of *hf* complex conductivity $=\omega\varepsilon''/4\pi$ and σ'' = the imaginary part of *hf* complex conductivity $=\omega\varepsilon'/4\pi$

However, it was assumed that the conduction current due to free molecular ions and electrons in pure liquids or polar-nonpolar liquid mixtures is neglected.

The magnitude of the total *hf* conductivity σ is given by :

$$\sigma = \frac{\omega}{4\pi}\left(\varepsilon'^2 + \varepsilon''^2\right)^{\frac{1}{2}} \qquad \ldots\ldots (1.31)$$

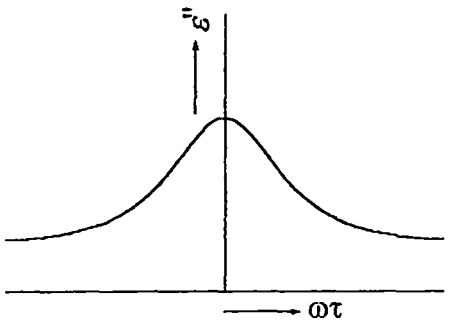

Figure 1.1: Variation of ε'' with $\omega\tau$

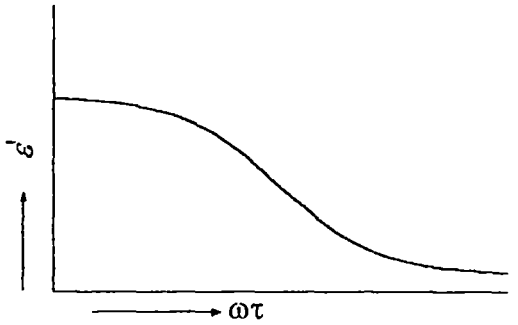

Figure 1.2: Variation of ε' with $\omega\tau$

1.16. Macroscopic and Microscopic Relaxation Time :

The gradual increase of polarisation in a dielectric medium with time to its equilibrium value under the alternating electric field is described by the decay function $f(t)$ where

$$f(t) \propto e^{-t/\tau} \qquad \ldots\ldots (1.32)$$

The relaxation time τ is independent of time but may depend on temperature. With a time dependant electric field *E(t)*, a field *E(u)* which is applied during a time interval between *u* and *u+du*; the corresponding electric displacement *D(t)* is written as:

$$D(t) = \varepsilon_\infty E(t) + \int_{-\infty}^{t} E(u) f(t-u) du \qquad \ldots\ldots (1.33)$$

On differentiating Eq.(1.33) with respect to time and multiplying both sides by τ one gets:

$$\tau \frac{dD(t)}{dt} = \varepsilon_\infty \tau \frac{dE(t)}{dt} + \tau f(o) E(t) - \int_{-\infty}^{t} E(u) f(t-u) du \qquad \ldots\ldots (1.34)$$

Adding Eqs.(1.33) and (1.34) yields:

$$\tau \frac{d}{dt}(D - \varepsilon_\infty E) + (D - \varepsilon_\infty E) = \tau f(o) E \qquad \ldots\ldots (1.35)$$

In a static electric field $D=\varepsilon_o E$

Hence from Eq.(1.35) we get

$$\tau f(o) = \varepsilon_o - \varepsilon_\infty \qquad \ldots\ldots (1.36)$$

Therefore Eq.(1.35) becomes :

$$\tau \frac{d}{dt}(D - \varepsilon_\infty E) + (D - \varepsilon_\infty E) = (\varepsilon_o - \varepsilon_\infty) E \qquad \ldots\ldots (1.37)$$

In the alternating electric field $E \propto e^{-j\omega t}$. The dielectric permittivity ε^* is complex. Hence

$$\frac{dE}{dt} = -i\omega E, \qquad D = \varepsilon^* E, \qquad \frac{dD}{dt} = -i\omega \varepsilon E \qquad \ldots\ldots (1.38)$$

Introducing this in Eq.(1.37) we get,

$$\varepsilon^* = \varepsilon_\infty + \frac{\varepsilon_o - \varepsilon_\infty}{1 + j\omega\tau} \qquad \ldots\ldots (1.39)$$

Separating the real and imaginary parts one gets

$$\frac{\varepsilon' - \varepsilon_\infty}{\varepsilon_o - \varepsilon_\infty} = \frac{1}{1 + \omega^2\tau^2} \qquad \ldots\ldots (1.40)$$

$$\frac{\varepsilon''}{\varepsilon_o - \varepsilon_\infty} = \frac{\omega\tau}{1 + \omega^2\tau^2} \qquad \ldots\ldots (1.41)$$

Although the polarisation may show a characteristic exponential decay with characteristic time τ, it does not follow that the orientation of an individual dipole decays with the same characteristic time. It is clear from (1.41) that ε'' has a maximum value for $\omega\tau = 1$ and approaches zero both for small and large values of $\omega\tau$ as shown in Fig.1.1. The variation of ε' with $\omega\tau$ is shown in Fig.1.2. The Eqs.(1.40) and (1.41) differ from Debye Eqs.(1.25) and (1.26) which contain the quantity $\tau'(\varepsilon_o+2)/(\varepsilon_\infty+2)$ instead of τ. Comparing the two equations a relation between macroscopic relaxation time τ and the microscopic relaxation time τ' is obtained by:

$$\tau = \frac{\varepsilon_o + 2}{\varepsilon_\infty + 2}\tau' \qquad \ldots\ldots (1.42)$$

On eliminating the parameter $\omega\tau$ and rearranging Eqs.(1.40) and (1.41) one gets :

$$\left(\varepsilon' - \frac{\varepsilon_o + \varepsilon_\infty}{2}\right)^2 + \varepsilon''^2 = \left(\frac{\varepsilon_o - \varepsilon_\infty}{2}\right)^2 \qquad \ldots\ldots (1.43)$$

A plot of ε'' is drawn against ε' representing the semicircle of radius $(\varepsilon_o - \varepsilon_\infty)/2$ and the center lying on the abscissa at a distance $(\varepsilon_o+\varepsilon_\infty)/2$ from the origin as illustrated in Fig.1.3. This semi-circular arc intersecting the abscissa at $\varepsilon' = \varepsilon_\infty$ and $\varepsilon' = \varepsilon_o$, is known as Debye semi-circle [1.6].

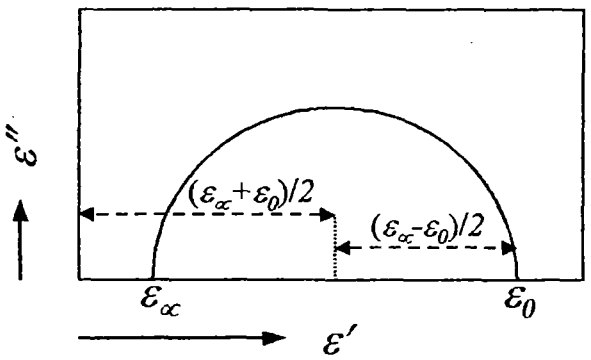

Figure 1.3: Variation of ε'' with ε' for different angular frequency ω (Debye semi-circle)

Powles [1.19] and Glarum [1.20], however, found a relation between τ and τ' by introducing a factor of approximately 3/2 given by ;

$$\tau = \frac{3\varepsilon_o}{2\varepsilon_o + \varepsilon_\infty}\tau' \qquad \ldots\ldots (1.44)$$

Another relation of macroscopic and microscopic relaxation time was given by O'Dwyer and Sack [1.21] :

$$\tau = \frac{(2\varepsilon_o^2 + 6\varepsilon_o^2\varepsilon_\infty + \varepsilon_\infty^2)}{3\varepsilon_o\varepsilon_\infty(2\varepsilon_o + \varepsilon_\infty)}\tau' \qquad \ldots\ldots (1.45)$$

1.17. Distribution of Relaxation Times :

For a dielectropolar liquid mixtures or solutions, it is found that some dipoles relax with one characteristic rate, some with another. It is impossible to study the dielectric relaxation phenomena in terms of a single Debye equation or sum of two or three Debye terms. Cole–Cole [1.22] and Davidson–Cole [1.23-1.24] relations were found to be satisfied by experimental results. But the theoretical explanation behind them has not yet been given. For most of the liquids, the experimental curve deviates from the simple normal Debye curve. In addition to Debye semi-circular behaviour, a number of distributions of relaxation times were found for different liquid dielectrics. The circular arc of Cole-Cole [1.22] plot with center lying below the abscissa as shown in Fig.1.4 exhibits symmetric distribution of relaxation time. A skewed arc, on the other hand, proposed by Cole-Davidson [1.23-1.24] is obtained to indicate an asymmetric distribution of relaxation times as shown in Fig.1.5.

Debye equation can thus be written for such a distribution of relaxation time :

$$\varepsilon^* = \varepsilon_\infty + (\varepsilon_o - \varepsilon_\infty)\int_o^\infty \frac{G(\tau)d\tau}{1 + j\omega\tau} \qquad \ldots\ldots (1.46)$$

Here, $G(\tau)d\tau$ is the distribution function for fraction of the molecules associated with relaxation times between τ and $\tau + d\tau$ such that the normalization condition for $G(\tau)$ is:

$$\int_o^\infty G(\tau)d\tau = 1 \qquad \ldots\ldots (1.47)$$

Separating the real and imaginary parts of Eq.(1.46) one gets :

$$\varepsilon' = \varepsilon_\infty + (\varepsilon_o - \varepsilon_\infty)\int_o^\infty \frac{G(\tau)d\tau}{1 + \omega^2\tau^2} \qquad \ldots\ldots (1.48)$$

and

$$\varepsilon'' = (\varepsilon_o - \varepsilon_\infty)\int_o^\infty \frac{\omega\tau G(\tau)d\tau}{1 + \omega^2\tau^2}. \qquad \ldots\ldots (1.49)$$

as Debye equations.

1.18. Cole–Cole Distribution :

The dielectric dispersion and absorption of many systems can not be described by a single relaxation time. For a large number of liquid dielectrics the experimental curve deviates from Debye curve of Fig.1.3. The broader dispersion and lower maximum loss are shown in Fig.1.4. Cole–Cole [1.22], on the other hand, found that the plot of ε'' against ε' for a dielectric material at different frequencies in a complex plane having a distribution of relaxation time is generally a semi-circular arc intersecting the abscissa axis at two points ε_∞ and ε_o. The center of semi-circle lies below the abscissa axis as found in Fig.1.4. The radius of the semi-circle makes an angle $\gamma\pi/2$ with ε' axis where γ is called the symmetric distribution parameter for $0 \leq \gamma \leq 1$. Cole and Cole modified the empirical formula of Debye by:

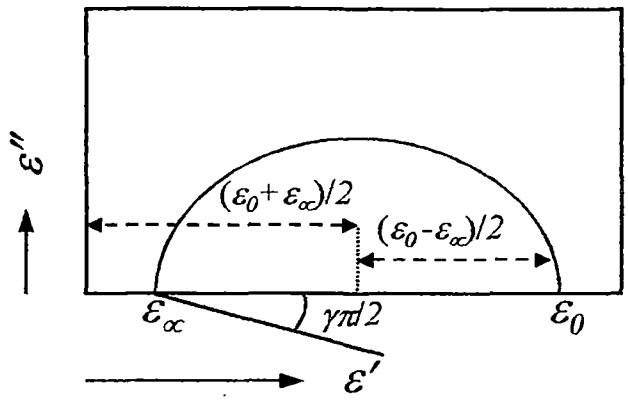

Figure 1.4: Cole-Cole Plot.

$$\varepsilon^* = \varepsilon_\infty + \frac{\varepsilon_o - \varepsilon_\infty}{1 + (j\omega\tau_s)^{1-\gamma}} \qquad \ldots\ldots (1.50)$$

where τ_s = symmetric relaxation time.

1.19. Davidson–Cole Distribution :

A skewed arc was, however, obtained by Davidson and Cole [1.23-1.24] by plotting ε'' against ε' in order to analyse asymmetrical relaxation spectra for certain dielectric materials like glycerol as sketched in Fig.1.5. The arc is obtained from a series of continuous relaxation mechanism of decreasing importance extending to the high frequency side of the main dispersion. The behaviour is represented by empirical relation:

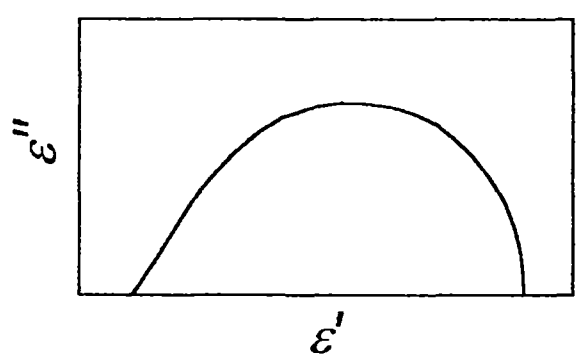

Figure 1.5: Davidson – Cole plot

$$\varepsilon^* = \varepsilon_\infty + \frac{\varepsilon_o - \varepsilon_\infty}{(1 + j\omega\tau_{cs})^{\delta}} \qquad \ldots\ldots (1.51)$$

where δ is asymmetric distribution parameter ($0< \delta \leq 1$) related to characteristic relaxation time τ_{cs} of the polar molecule. This behaviour seems to be applicable in representing the behaviour of substance at low temperature. These were well discussed by Powles in recent years [1.25]. A curve is supposed to be made up of a number of Debye semi-circular arcs with multiple relaxation times. This is displayed in Fig.1.6 to understand the asymmetric relaxation behaviour.

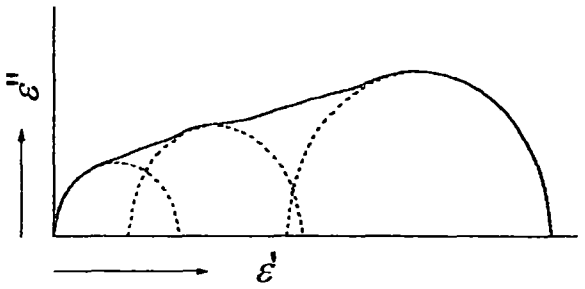

Figure 1.6: Plot of ε'' against ε' for a number of Debye semicircular arc with multiple relaxation.

1.20. Havriliak–Negami (HN) Distribution :

Dielectric relaxation behaviour of some dipolar materials is not often explained by either Cole–Cole or Davidson–Cole distribution. The most widely used distribution for the phenomenological description of dielectric experiments is the Havriliak–Negami distribution [1.26] that describes an asymmetric and broadened profile as compared to the Debye curve. The expression of the complex relative permittivity is now :

$$\varepsilon^* = \varepsilon_\infty + \frac{\varepsilon_o - \varepsilon_\infty}{[1+(j\omega\tau_{HN})^{1-\gamma}]^\delta} \qquad \ldots\ldots (1.52)$$

Eq.(1.52) reduces to Cole–Cole distribution when $\delta = 1$ and Davidson–Cole when $\gamma = 0$. Since H–N distribution is the generalization of Cole–Cole and Davidson–Cole distribution it can explain the relaxation phenomena of a wider variety of materials with different values of γ and δ parameters.

1.21. Kohlrausch–Williams–Watts (KWW) Distribution :

Under certain circumstances, the dielectric parameters are describable in the time domain by the well known stretched exponential or Kohlrausch–Williams–Watts (KWW) function [1.27-1.28] in terms of macroscopic decay function $\phi(t)$ by :

$$\phi(t) = \exp[-(t/\tau_{KWW})^\beta] \qquad \ldots\ldots (1.53)$$

where τ_{KWW} is the effective relaxation time in time domain, β is the shape parameter of the time relaxation function such that $0< \beta \leq 1$. In the frequency domain, the complex dielectric constant ε^* is written for a pure Debye process as a function of angular frequency ω and temperature T. Hence

the relationship between $\varepsilon^*(\omega,t)$ and $\phi(t,T)$ is given by one side Fourier or pure imaginary Laplace transformation of the form:

$$\frac{\varepsilon^*(\omega,T)-\varepsilon_\infty}{\varepsilon_o-\varepsilon_\infty}=\int_o^\infty\left(-\frac{d\phi}{dt}\right)\exp(-j\omega t)dt$$

$$=\pounds\left[\frac{\beta}{\tau_{KWW}}\left(\frac{t}{\tau_{KWW}}\right)^{-(1-\beta)}\exp\left\{-\left(\frac{t}{\tau_{KWW}}\right)^{\beta}\right\}\right] \qquad \ldots\ldots (1.54)$$

where $\pounds$ is the Laplace transformation of $-d\phi(t)/dt$.

Eq.(1.54) gives the single exponential Debye like distribution for β =1. KWW distribution has been widely used to describe the relaxation behaviour of glass forming liquids and complex polymeric systems.

1.22. Distribution Function of Relaxation Times :

The experimental results can satisfactorily be explained by Gaussian probability distribution function made by Wagner [1.29] and Yager [1.30] and is given by:

$$G(\tau)d\tau=\frac{b}{\sqrt{\pi}}\exp(-b^2y^2)dy \qquad \ldots\ldots (1.55)$$

Here b is the breadth of the distribution and y is defined as:

$$y=\ln(\tau/\tau_o)$$

where τ_o is the most probable relaxation time

In long chain polar molecules, like alcohols and polymers there are many possibilities of internal rotations, bending and twisting about the bond axis of the molecule each with a corresponding characteristic relaxation time. Kirkwood and Fuoss [1.31], on the other hand, defined a distribution function $G(\tau)$ in averaging to the macroscopic conditions of distribution of relaxation times for long chain polymeric dielectric molecules.

$$G(\tau)=\frac{1}{2\cosh y+2} \qquad \ldots\ldots (1.56)$$

where y =$\ln(\tau/\tau_o)$.

The experimental results were not in accord with this formula. So Fuoss and Kirkwood [1.32] further suggested that the empirical relation should represent the experimental data:

$$\varepsilon''=\varepsilon''_m\,\mathrm{sec}\,h\left[\beta\ln\frac{\omega}{\omega_m}\right] \quad \text{for } 0<\beta<1 \qquad \ldots\ldots (1.57)$$

where β is a distribution parameter and ω_m is the angular frequency corresponding to the maximum value ε_m'' of ε''. The corresponding distribution function is given by:

$$G(\tau) = \frac{\beta}{\pi} \frac{\cos(\beta\pi/2)\cosh(\beta y)}{\cos^2(\beta\pi/2) + \sinh^2(\beta y)} \qquad \ldots\ldots (1.58)$$

where $y = \log(\omega/\omega_m)$.

Another distribution function of Cole–Cole [1.22] is given by:

$$G(\tau) = \frac{\sin\gamma\pi}{2\pi}\left[\cosh\{(1-\gamma)\ln(\tau/\tau_o)\} - \cos\gamma\pi\right]^{-1} \qquad \ldots\ldots (1.59)$$

The distribution function $F(y)$ based on Havriliak–Nigami [1.26] function is :

$$F(y) = \left(\frac{1}{\pi}\right) y^{(1-\gamma)\delta} (\sin\delta\theta)\left(y^{2(1-\gamma)} + 2y^{1-\gamma}\cos\pi(1-\gamma) + 1\right) - \frac{\delta}{2} \qquad \ldots\ldots (1.60)$$

In this expression, $y = \tau/\tau_o$ and

$$\theta = \arctan\left[\frac{\sin\pi(1-\gamma)}{y^{1-\gamma} + \cos\pi(1-\gamma)}\right] \qquad \ldots\ldots (1.61)$$

Fröhlich [1.13] derived the distribution function for a molecular mechanism which leads to a distribution of relaxation time between two limiting values τ_1 and τ_2 such that $\tau_2 > \tau_1$. The distribution function is:

$$G(\tau) = (\varepsilon_o - \varepsilon_\infty)\frac{k_B T}{V_o}\frac{1}{\tau} \qquad \text{if } \tau_1 \le \tau \le \tau_2$$

$$= 0 \qquad \text{if } \tau < \tau_1 \text{ and } \tau > \tau_2 \qquad \ldots\ldots (1.62)$$

Davidson and Cole [1.23-1.24] also gave another distribution function :

$$G(\tau) = \frac{\sin\beta\pi}{\tau\pi}\left(\frac{\tau}{\tau_o - \tau}\right)^{\beta} \qquad \text{for } 0 < \tau < \tau_o$$

$$= 0 \qquad \text{for } \tau > \tau_o \qquad \ldots\ldots (1.63)$$

Similar to that of Fröhlich, Higasi *et al* [1.33] gave another distribution function $y(\tau)$ for a number of *n*-alkyl bromides at different temperatures which may be represented by :

$$y(\tau) = \frac{1}{A\tau} \qquad \text{if } \tau_1 < \tau < \tau_2$$

$$= 0 \qquad \text{if } \tau < \tau_1 \text{ and } \tau > \tau_2 \qquad \ldots\ldots (1.64)$$

where τ_1 is the relaxation time of the rotational orientation of the CH_2Br group about its bond to the rest of the molecule, while upper limit τ_2 is the relaxation time of the largest orienting unit, usually the molecule as a whole.

Matsumoto and Higasi [1.34] also suggested a more general distribution function $y(\tau)$ in order to explain the dielectric properties of some non rigid alkyl halides at lower temperature from the same principle which describes the dielectric properties of the same substance at higher temperature like:

$$y(\tau) = \frac{1}{A\tau^n} \qquad \text{if } \tau_1 < \tau < \tau_2$$

$$= 0 \qquad \text{if } \tau < \tau_1 \text{ and } \tau > \tau_2 \qquad \text{..... (1.65)}$$

and $0<n<\infty$.

1.23. Debye Equation in Solution:

In pure polar liquids, one polar molecule is surrounded by a large number of similar molecules and eventually polar-polar interaction occurs. In order to avoid the polar-polar interaction it is better to study the relaxation phenomena of dipolar liquids dissolved in non-polar solvents. In such case one polar unit is assumed to be far apart from the others and remains in the quasi-isolated state to eliminate polar-polar interactions almost completely.

Let a polar liquid (j) is dissolved in a non-polar solvent (i). Let α_i and α_j are the polarisabilities of solvent and solute of molecular weights M_i and M_j respectively. If the relative permittivitiy of the liquid mixture is ε_{ij} then Debye equation [1.6] for polar-nonpolar liquid mixture is:

$$\frac{\varepsilon_{ij}-1}{\varepsilon_{ij}+2}\frac{M_i f_i + M_j f_j}{\rho_{ij}} = \frac{4\pi N}{3}\left[\alpha_i f_i + \alpha_j f_j + \frac{\mu_s^2}{3k_B T} f_j\right]$$

$$= \frac{4\pi N \alpha_i}{3} + \frac{4\pi N}{3}\frac{\mu_s^2}{3k_B T} f_j \qquad \text{..... (1.66)}$$

Here f_i and f_j are the mole fractions of the solvent and solute defined by $f_i = n_i/(n_i+n_j)$; $f_j = n_j/(n_i+n_j)$, where n_i and n_j are the number of molecules per unit volume of the respective liquids and $\alpha_i = \alpha_j$

Eq.(1.66) is written as :

$$\frac{\varepsilon_{ij}-1}{\varepsilon_{ij}+2}V_{ij} = \frac{\varepsilon_i - 1}{\varepsilon_i + 2}V_i + \frac{4\pi N}{3}\frac{\mu_s^2}{3k_B T} f_j \qquad \text{..... (1.67)}$$

V_i and V_{ij} are the specific volumes of the solvent and solution respectively.

In case of neutral dielectrics $\varepsilon_{ij} = n_{Dij}^2$, where n_{Dij} is the refractive index. The equation can be written as:

$$\frac{n_{Dij}^{\ 2}-1}{n_{Dij}^{\ 2}+2}V_{ij} = \frac{n_{Di}^{\ 2}-1}{n_{Di}^{\ 2}+2}V_i \qquad \ldots\ldots (1.68)$$

Eqs.(1.67) and (1.68) can, however, be used to measure the dipole moment of any dipolar liquid treated as a solute in a solution.

From Eqs.(1.67) and (1.68) one gets :

$$\left(\frac{\varepsilon_{ij}-1}{\varepsilon_{ij}+2}-\frac{n_{Dij}^{\ 2}-1}{n_{Dij}^{\ 2}+2}\right)=\left(\frac{\varepsilon_i-1}{\varepsilon_i+2}-\frac{n_{Di}^{\ 2}-1}{n_{Di}^{\ 2}+2}\right)\frac{V_i}{V_{ij}}+\frac{4\pi N}{3}\frac{\mu_s^{\ 2}}{3k_BT}\frac{f_j}{V_{ij}} \qquad \ldots\ldots (1.69)$$

Introducing molar concentration c_j ie $c_j = f_j/V_{ij}$ and for extremely dilute solution $(V_i/V_{ij}) \rightarrow 1$ Eq.(1.69) is given by:

$$\left(\frac{\varepsilon_{ij}-1}{\varepsilon_{ij}+2}-\frac{n_{Dij}^{\ 2}-1}{n_{Dij}^{\ 2}+2}\right)=\left(\frac{\varepsilon_i-1}{\varepsilon_i+2}-\frac{n_{Di}^{\ 2}-1}{n_{Di}^{\ 2}+2}\right)+\frac{4\pi N}{3}\frac{\mu_s^{\ 2}}{3k_BT}c_j \qquad \ldots\ldots (1.70)$$

The Eq.(1.70) is a simple, straightforward and useful one to determine μ_s of a dipolar liquid molecule at infinite dilution. It is the well-known Debye equation [1.6] for a polar-nonpolar liquid mixture.

1.24. Extrapolation Technique and Guggenheim Equation :

In order to measure μ_s of a dipolar liquid molecule at infinite dilution a large number of workers used the extrapolation technique of different dielectric relaxation parameters. The methods suggested by Hedestrand [1.35], Cohen Henrique [1.36] and Le Fevre [1.37] had some inherent uncertainties in the calculation of $\left(\partial\rho_{ij}/\partial x_j\right)_{x_j\rightarrow 0}$ and $\left(\partial n_{Dij}/\partial x_j\right)_{x_j\rightarrow 0}$ by graphical extrapolation technique.

Higasi [1.38] measured μ_s of different polar-nonpolar liquid mixtures from the empirical formula:

$$\mu_s = \beta\left(\frac{\Delta\varepsilon}{x_j}\right)^{1/2} \qquad \ldots\ldots (1.71)$$

where $\Delta\varepsilon = \varepsilon_{ij} - \varepsilon_i$ and the constant β depends upon the solvent used. Guggenheim [1.8], on the other hand, introduced a fictitious atomic polarisability to make the solution free from atomic polarisation. The simpler method suggested is to calculate μ_s in which the need for measuring densities of liquid mixtures was not necessary. The slope of the curve drawn through the experimental parameters of Δ

where $\Delta = 3(\varepsilon_{ij} - n_{Dij}^2)/(\varepsilon_{ij} + 2)(n_{Dij}^2 + 2)$ against mole fraction c_j gave μ_s of a dielectropolar liquid molecule dissolved in a non-polar solvent. The quantity $\Delta = [(\varepsilon_{ij} - n_{Dij}^2) - (\varepsilon_i - n_{Di}^2)]$ was found from the extrapolated value of Δ / c_j at infinite dilution to calculate μ_s from the relation :

$$\mu_s^2 = \frac{9k_BT}{4\pi N} \frac{3}{(\varepsilon_i + 2)(n_{Di}^2 + 2)} \left(\frac{\Delta}{c_j} \right)_{c_j \to 0} \qquad \ldots\ldots (1.72)$$

In the meantime many workers [1.39-1.41] suggested different modified formulations to calculate μ_s by smoothing the experimental data extrapolated to infinite dilution. Smith [1.39] following Guggenheim [1.8] subsequently introduced the idea of weight fraction w_j instead of c_j where,

$$c_j = \frac{\rho_{ij}}{M_j} w_j \qquad \ldots\ldots (1.73)$$

Guggenheim [1.42], later on, accepted the view of extrapolation technique of other workers [1.39-1.41] to modify the Eq.(1.72) for μ_s :

$$\mu_s^2 = \frac{9k_BT}{4\pi N} \frac{3}{(\varepsilon_i + 2)^2} \frac{M_j}{\rho_i} \left(\frac{\Delta}{w_j} \right)_{w_j \to 0} \qquad \ldots\ldots (1.74)$$

where

$$\left(\frac{\Delta}{w_j} \right)_{w_j \to 0} = \left[\left(\frac{\varepsilon_{ij} - \varepsilon_i}{w_j} \right)_{w_j \to 0} - \left(\frac{n_{Dij}^2 - n_{Di}^2}{w_j} \right)_{w_j \to 0} \right] \qquad \ldots\ldots (1.75)$$

M_j is the molecular weight of the dipolar liquid and ρ_i is the density of the solvent.

Palit and Banerjee [1.43] made an analysis of the error involved in the Guggenheim–Smith approximate equation to find how far solution density measurement are necessary for calculation of μ_s of a polar molecule in a non-polar solvent. Botcher [1.44], however, calculated μ_s for a large number of polar-nonpolar liquid mixture using different extrapolation techniques and found different μ_s's. Later on, Krishna and Srivastava [1.45] used the following relation:

$$\mu_s = \beta \left(\frac{d\varepsilon_{ij}}{dx_j} \right)_{x_j \to 0}^{1/2} \qquad \ldots\ldots (1.76)$$

to calculate μ_s of some dielectropolar solute in liquid state.

Srivastava and Charandas [1.46] found the constant β was different for different polar liquids. A question, therefore, arises regarding the validity of Higasi's method [1.38]. Prakash [1.47], however, showed that Eq.(1.76) is a special case of Debye equation (1.70) when ε_{ij} is very

nearly equal to unity. Since $\varepsilon_{ij} \cong 1$ is not true for any polar-nonpolar liquid mixture, Higasi's [1.38] method can not be regarded as a universal one to compute μ_s at all concentrations of the polar liquid. The Eq.(1.72) was modified to calculate μ_s at $w_j \to 0$.

$$\mu_s^2 = \frac{27 M_j k_B T}{4\pi N \rho_i} \left(\frac{\delta X_{ij}}{\delta w_j} \right)_{w_j=0} \qquad \text{.....(1.77)}$$

Here,

$$\left(\frac{\delta X_{ij}}{\delta w_j} \right)_{w_j=0} = \left[\frac{1}{(\varepsilon_i + 2)^2} \left(\frac{\delta \varepsilon_{ij}}{\delta w_j} \right)_{w_j \to 0} - \frac{2 n_{Di}}{(n_{Di}^2 + 2)^2} \left(\frac{\delta n_{Dij}}{\delta w_j} \right)_{w_j \to 0} \right] \qquad \text{.....(1.78)}$$

Eq.(1.77) is the famous Guggenheim Eq.(1.74) when $\varepsilon_i = n_{Di}^2$. Thus one can conclude that Guggenheim equation is a special case of Debye formula if $\varepsilon_i = n_{Di}^2$. Therefore one should know the extrapolated values at $w_j \to 0$ from the measured relaxation parameters of different w_j's to estimate μ_s's of dipolar liquids. Le Fevre and Smyth [1.41] and Guggenheim [1.42] obtained two different values of μ_s i,e 0.91 D and 0.83 D for trimethyl amine in benzene at 25 ^{0}C using different extrapolation technique. Therefore in order to calculate μ_s accurately one should choose what type of extrapolation technique is needed to be used.

Guha *et al* [1.48] and Ghosh and Acharyya [1.49] tried to develop the dielectric theory within the frame work of Debye model [1.6] by introducing a new concept of w_j instead of c_j where $c_j = \rho_{ij} w_j / M_j$ and $w_i + w_j = 1$. But the density of solution ρ_{ij} is a function of w_j

$$\rho_{ij} = \frac{\rho_i}{1 - \gamma w_j} \qquad \text{.....(1.79)}$$

where $\gamma = (1 - \rho_i / \rho_j)$, ρ_i, and ρ_j are the densities of solvent and solute used.

Here Eq.(1.70) can now be written as

$$\frac{\varepsilon_{ij} - n_{Dij}^2}{(\varepsilon_{ij} + 2)(n_{Dij}^2 + 2)} = \frac{\varepsilon_i - n_{Di}^2}{(\varepsilon_i + 2)(n_{Di}^2 + 2)} + \frac{4\pi N \mu_s^2 \rho_i}{27 k_B T M_j} \frac{w_j}{1 - \gamma w_j}$$

$$X_{ij} = X_i + \frac{4\pi N \mu_s^2}{27 M_j k_B T} \rho_i (w_j + \gamma w_j^2 + ...) \qquad \text{.....(1.80)}$$

$$X_{ij} = a + b w_j + c w_j^2 \qquad \text{.....(1.81)}$$

where X_{ij} and X_i are the experimentally measured static or low frequency parameters and μ_s is the dipole moment of the polar liquid under static electric field.

The Eq.(1.81) is highly converging in nature in the low concentration region of the polar-nonpolar liquid mixture and μ_s can easily be calculated from the derived equation

$$\mu_s = \left(\frac{27 k_B T M_j b}{4\pi N \rho_i}\right)^{1/2} \qquad \text{.....(1.82)}$$

The theory mentioned above is applied for a large number of polar-nonpolar liquid mixtures [1.48-1.50] in order to calculate μ_s.

Suryavanshi and Mehrotra [1.51], on the other hand, suggested the least squares extrapolation technique to calculate μ of a dipolar liquid from the Eq.(1.82) of Acharyya *et al* [1.48]. The results were in excellent agreement with the reported values. One may, therefore, conclude that the least squares extrapolation [1.44] is one of the accurate techniques to study the dielectric relaxation of polar-nonpolar liquid mixture.

1.25. Eyring's Rate Theory in Dielectric Relaxation :

Eyring [1.15] treated dipole rotation in analogy with chemical rate process. He considered the chemical reaction of the type $A+B \rightarrow C$. The reaction takes place in the following way: A and B first form an 'activated complex' AB. The activated complex must acquire a certain amount of electric energy to form it which will react to form C later. When this model is applied to dipole rotation in angular coordinates, the two states '$A+B$' and 'C' are considered to have two different equilibrium of the orientations of the dipole while the activated state AB as the state in which the dipole has sufficient energy to pass from one equilibrium position to the other over a potential barrier as shown in Fig.1.7. Applying this theory to the case of dipole rotation, Eyring identified that a dipole requires sufficient energy to pass over the potential barrier from one equilibrium position to the other with relaxation time τ by :

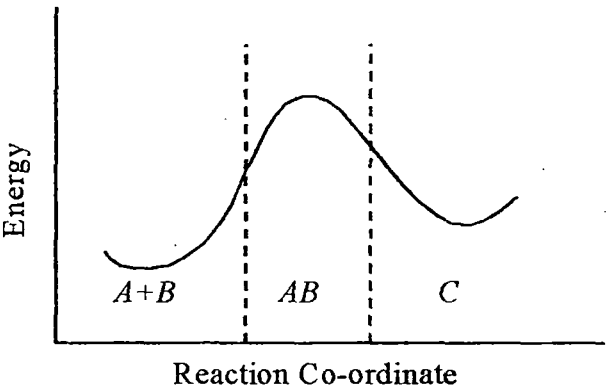

Figure 1.7: Variation of activation energy eith reaction co-ordinate

$$\tau = \frac{h}{k_B T}\exp(\Delta F_\tau / RT)$$

$$= \frac{h}{k_B T}\exp(-\Delta S_\tau / R)\exp(\Delta H_\tau / RT) \qquad \text{.....(1.83)}$$

where,

ΔF_τ= molar free energy of activation

ΔS_τ= molar entropy of activation

ΔH_τ= molar enthalpy of activation

Eyring has also obtained an expression for the viscosity flow of a dipolar liquid in terms of reaction rates as:

$$\eta = \frac{Nh}{V}\exp\left(-\Delta S_\eta / R\right)\exp\left(\Delta H_\eta / RT\right) \qquad \text{.....(1.84)}$$

where V is the molar volume of the liquid. Eyring thus arrives at the equation :

$$\tau T \propto \eta V \qquad \text{..... (1.85)}$$

only if the enthalpies of activation are the same for both the processes.

Kauzmann [1.52] critically analysed Eyring's rate theory and gave a general theory of dielectric relaxation in terms of the frequency of discontinuous molecular reorientations called '*jumps*'. Assuming the relaxation process as a chemical reaction he defined the relaxation time $\tau = 1/k_o$ such that in this time the polarisation will fall to $1/e$ th of its initial value. Here k_o is the rate constant for the activation of dipoles and is known as the dielectric relaxation rate. The reaction rate is:

$$k = K\frac{k_B T}{h}e^{\Delta S_\tau / R}e^{-\Delta E_\tau / RT} \qquad \text{..... (1.86)}$$

The main importance of the above formulations is that one can know the thermodynamics of the normal and the activated states from the observed reaction rate.

1.26. Brief Review of Relaxation Phenomena :

A large number of workers [1.1-1.4, 1.53-1.58] studied the relaxation phenomena of dipolar gases and liquids from dielectric polarisation. The observations are found in good agreement with the gas kinetic values except for substances having high dielectric constants [1.55-1.59] due to the presence of the substituent polar groups like –OH or $-NH_2$ in them. The anomalous behaviour of dispersion for liquids having –OH or $-NH_2$ groups was first observed by Drude [1.56] under relatively longer wavelength electric fields. Debye [1.6] explained this anomalous dispersion due to dielectric relaxation under *rf* electric field of the polar molecules. The radii of molecules of some ketones and glycerine were found to be smaller than the gas kinetic values as measured by Mizushima [1.60-1.61] based on Debye theory. The dipole moment μ for methyl, ethyl and amyl alcohols in benzene were measured by Stranathan [1.62] and found to be temperature independent in accordance with Debye theory. Rocard [1.63] modified Debye's theory by considering the influence

of moment of inertia of the molecules on the relaxation process. Fischer and Frank [1.64], however, measured ε'' under 4.3 metre wavelength electric field in order to estimate τ of aromatic halides. The shorter τ's were claimed for the rotation of CH_2–X group around their bond ring. But the theory could not explain the behaviour of alcohols for the strong interaction of –OH groups due to formation of hydrogen bonding. Budo [1.65] proposed the theory of dielectric relaxation considering the intra-molecular and inter-molecular rotations of the molecule. The analyses of dielectric relaxations of some non-spherical polar liquid molecules in non-polar solvent were made by Gross [1.66] to show the solvent effect under an isotropic electric field.

Onsagar [1.67] ,Plumley [1.68] and Pao [1.69] interpreted the origin of ionic conduction in dielectric liquids even in the purest hydrocarbons like hexane. Ryhel [1.70] and Eck [1.71] showed that ionic conduction occurs due to existence of ionic clusters in the liquids. Whiffen and Thompson [1.72] obtained relaxation time, dipole moment and different energy parameters of toluene, o-xylene, p-cymene chloroform etc. in non-polar solvent from –70 ^{0}C to +80 ^{0}C to predict the limitations of different rate processes in solutions. Jackson and Powles [1.73] estimated τ of polar molecules in benzene and paraffin only to show their dependence on the viscosity of solvents. The relaxation phenomena of polar liquid molecules under *rf* electric field were studied by Schallamach [1.74] in order to facilitate the rearrangement under single relaxation process. Macke and Reuter [1.75] measured relative permittivities of normal alcohols and phenols in benzene, carbon tetrachloride and cyclohexane at different temperatures to infer the molecular associations. The absorption of high frequency electric energy in dipolar aliphatic chlorides and alcohols were performed by Kremmling [1.76]. It was found difficult to sort out the effects of molecular association due to H-bond formation to change the shape of molecules. Further, the internal rotation, multiple relaxation times etc. could, however, be predicted.

Curties *et al* [1.77] observed that τ's were different in different solutions of pure polar or polar-nonpolar liquid mixtures of almost same viscosity. Methyl and ethyl alcoholic solutions of electrolytes have been studied by Lane and Saxton [1.78] who clearly established that the presence of ions reduces the permittivities of the media more markedly than that of water. Smyth *et al* [1.79] made a systematic studies on relaxation phenomena of some flexible polar molecules (alkyl halides) in liquid state in which dipole can reorient and play a significant role in the observed relaxation time. Jaffe and Lemay [1.80] concluded that dielectric liquids gave conduction current under breakdown voltage. The presence of positive ions is noticed by Green [1.81] in dielectric liquids due to dissociation of impurity molecules by external cosmic rays. Poley [1.82] estimated τ from measured ε' and ε'' for mono substituted benzene. The increase of τ occurs with molecular size. Müller [1.83], however, calculated the low molecular radii in comparison to other methods. Dielectric measurements of relaxation parameters on pure normal propyl to decayl alcohols were

carried out by Garg and Smyth [1.84] to show three different τ 's which are associated with polymeric cluster formation by the strong H-bonding between OH-groups. The intermediate τ's were attributed to the rotation of free alcohol molecules.

Simultaneous determination of τ and μ of polar-nonpolar liquid mixtures was made by Gopalakrishna [1.85]. The advantage of this method is to know only the density of the pure solvent. Different molecular associations in saturated dielectric liquids were studied by Schellman [1.86]. Srivastava and Vershri [1.87] explained the variation of ε' with concentration and temperature for binary polar mixtures of methyl and butyl alcohols with water.

Bergmann *et al* [1.88] gave a graphical method in complex plane to estimate τ_1(smaller) and τ_2(larger) that interpreted the intramolecular and molecular rotations of polar molecule respectively. Higasi *et al* [1.33] analysed the experimental data of liquid *n*-alkyl bromide in terms of distribution of τ 's between two limiting τ values.

The τ's of alkyl cyanides and alkythiols increase with the size of the molecules as observed by Krishnaji and Mansingh [1.89] from the dielectric relaxation measurement. Froster [1.90] explained the conduction in aliphatic hydrocarbons by the presence of impurities of trace polar or trapped electrons at the electrode surfaces. Experimental evidences showed electronic conduction in unsaturated hydrocarbons. Dielectric relaxation studies of ionic solutes in non-hydroxylic solutions [1.91-1.92] over a wide range of frequency established the simultaneous presence of conduction and dipole dispersion. Sinha *et al* [1.93-1.94] predicted the temperature dependence of τ and μ of polar molecule in non-polar solvent. The dependence of τ on T is, however predicted. Temperature dependence of conductivity for organic liquids were studied by Adamezewski and Jachym [1.95]. Jayprakash [1.96] estimated τ of some spherical polar molecules in non-polar solvents in excellent agreement with Gopalakrishna [1.85]. Bhattacharyya *et al* [1.97] modified Bergmann equations [1.88] in order to obtain molecular and intra-molecular τ_2 and τ_1 of phenetole, aniline and orthochloro aniline. Non-rigid molecules having two τ's and average τ could, however, be obtained by Higasi *et al* [1.98] based on single frequency measurement technique. A crude estimation of τ_1 and τ_2 can be had with a suitable equation derived from Debye model.

Lohneysen and Nageral [1.99] found the existence of natural charge carriers in liquids of two kinds of mobilities. The direct evidence of ionic conduction in polar dielectrics was found by Gaspared and Gosse [1.100] when the electrodes were membraned by teflon. The ε' and ε'' of aliphatic alcohols in non-polar solvents at different concentrations under *hf* electric field were measured by various workers [1.101-1.103]. Other group of workers [1.104-1.113] measured relative permittivities ε', ε'', ε_o and $\varepsilon_\infty = n_D^2$ of some substituted toluidines, para-compounds,

diphenylene oxide, chloral, ethyltrichloroacetate, trifluoroethanol, trifluoroacetic acid and a large number of monosubstituted and disubstituted benzenes and anilines in different non-polar solvents at various w_j's and t^0C under nearly 3 cm. wavelength electric field to estimate τ, μ and thermodynamic energy parameters. The observed results were explained in terms of molecular associations of the polar liquid molecules. Rajyam *et al* [1.114] studied the dielectric dispersion of glycerol and diethylene glycol under *rf*, *mw* and *uhf* electric fields at 80^{0}C and confirmed the Davidson-Cole type of dispersion. Mulechi *et al* [1.115] observed the self association of tertiary butyl alcohol and developed a method for simultaneous determination of three independent values of free energy of self association from experimental data.

A number of workers [1.116-1.120] estimated τ from the number density 'n' of free ions, radius 'a' of the rotating units for some straight chain alcohols, anilines, benzyl chlorides, acetone under *rf* electric field at different temperatures. τ's are observed to increase as the number of C-atom of dipolar molecules increases. The relaxation parameters from the *rf* conductivity σ has been used to study the structure of liquids.

Dhull, Sharma and Gill [1.121-1.125] measured ε' and ε'' of NMA, DMF, DMA in benzene, dioxane and carbon tetrachloride in order to obtain the different relaxation parameters. Acharyya and Chatterjee [1.126] and Acharyya *et al* [1.127] estimated τ, μ and different energy parameters ΔH_τ, ΔS_τ and ΔF_τ of some interesting polar liquid molecules in benzene and carbon tetrachloride. *Hf* conductivity σ in $\Omega^{-1}.cm^{-1}$ of a polar–nonpolar concentrated liquid mixture is liable to yield μ of dimer formation. Low concentration region σ in $\Omega^{-1}.cm^{-1}$ gives μ for monomer formation. The estimated μ_{theo} 's from the available bond angles and bond moments reveal the structural conformations. ε' and ε'' of *n*-butyl chloride, chlorobenzene and tertiary butyl alcohol in benzene were measured by Agarwal [1.128] at 32^{0}C under 9.96 GHz electric field to estimate τ. It is observed that τ is influenced by structural conformation in the following manner $\tau_{linear} > \tau_{planer} > \tau_{spherical}$. The experimental and theoretical τ 's were found in agreement in case of thiophenone, acetone, benzophenone and their mixture in *mw* electric field over a wide range of temperature as observed by Madan [1.129]. Vyas and Vashisth [1.130] explained the variation of $tan\delta$ ($=\varepsilon''/\varepsilon'$) curve against weight fraction w_j of solute in case of four aliphatic alcohols, their binary mixtures and the mixtures of alcohols with DMF and 2-fluoroaniline in benzene under 3 cm. wavelength electric field. The alcohols +DMF mixtures showed complex formations at a very low concentration. The study of alcohol+2-fluoro aniline, however, indicates dissociation effects. Gandhi and Sharma [1.131] determined τ_o, τ_1 and τ_2, distribution parameters of isobutyl-methacrylate and allyl-

methacrylate and their mixtures in benzene. The observed results reveal the existence of intra-molecular and molecular rotations.

Murthy *et al* [1.132] however, modified the work of Acharyya *et al* [1.126] and gave a new dimension in the theoretical formulation of dielectric relaxation in which simultaneous determination of τ and μ of a polar-nonpolar liquid mixture can be obtained. Makosz [1.11] calculated μ of some ellipsoidal dipolar liquids in non-polar solvents at 25^{0}C from the formula derived from Onsager's equation. Sharma and Sharma [1.133] and Sharma *et al* [1.134] measured ε_{ij}' and ε_{ij}'' of dilute solution of DMSO and DMF+DMSO mixture in benzene and carbon tetrachloride in the temperature region of 25^{0}C to 40^{0}C under 9.174 GHz electric field. τ, μ, ΔH_τ and ΔS_τ of dielectric relaxation and ΔH_η, ΔS_η and ΔF_η for viscous flow were obtained.

A series of relaxation parameters were calculated by Saha and Acharyya [1.135-1.136] from the measured relative permittivities based on newly developed methodology. Higher and lower values of μ arise due to the monomer and dimer formations. μ_{theo}'s from the available bond angles and bond moments of substituted polar groups attached to the parent molecules were estimated. The excellent agreement of μ_{theo}'s with measured *hf* μ 's shed much light on the inductive, electromeric and mesomeric moments of polar groups. The concentration variation of the measured [1.108-1.112] ε_{ij}', ε_{ij}'', ε_{oij} and $\varepsilon_{\infty ij} = n_{Dij}^2$ of a large number of disubstituted benzenes, anilines and monosubstituted anilines in benzene and carbon tetrachloride under *hf* electric field were analysed by Saha *et al* [1.137] and Sit *et al* [1.138-1.139] to estimate τ_1, τ_2 and μ_1 and μ_2 due to the rotation of the flexible polar groups attached to the parent molecules and the whole molecules themselves. The dielectric relaxation phenomena of acetophenone, DMSO and their mixtures in benzene were done by Singh and Sharma [1.140] under 9.33 GHz electric field in the temperature range of 20^{0}C to 40^{0}C. Nonlinear behaviour of τ reveals the presence of solute-solvent and solute-solute molecular associations. Jangid *et al* [1.141] made extensive study on four pure nicotinades and their quartarnary mixtures. The sufficient information about intra-molecular and inter-molecular rotations was obtained in terms of solute-solvent (monomer) and solute-solute (dimer) formations. Measurement of ε', ε'', and $tan\delta$ of polar liquids in non-polar solvents under different GHz electric fieled were made by a number of workers. The results are well explained by the rotation of –OH group about the whole molecular rotation. The molecular shapes, sizes and structures by H-bonding, and various molecular associations were interpreted by the dipole–dipole interactions.

Sengwa and Kaur [1.142] determined Kirkwood correlation factor '*g*', average τ_o, ΔF_{τ_o} of ortho-hydroxy benzaldehyde in benzene at different experimental temperatures under GHz electric field. Molecular associations hinder the intra-molecular rotations of –CHO and –OH groups in the compound to affect τ. Temperature variation of dielectric relaxation of ethylene glycol–water

mixture was carried out by Saha and Ghosh [1.143] under 1 MHz electric field. High values of τ were explained by the polymeric cluster formation of molecular association. Formation of H-bonding between two polar molecules in non-polar solvent was investigated by Dash *et al* [1.144] in some alcohols. Thakur and Sharma [1.145] measured the thermodynamic energy parameters due to dielectric relaxation and viscous flow for acetonitrile and DMF in benzene to explain the solute-solvent molecular association.

References :

[1.1] R Clausius, *Die mechanische Wärmtheorie* (Vieweg), **2** 62 (1879)

[1.2] O F Mossotti, *Mem. di Matheme di fisica in Modena*, **24 II** 49 (1850)

[1.3] H A Lorentz, *Ann. Physik*, **9** 641 (1880)

[1.4] L V Lorentz, *Ann. Physik*, **11** 70 (1880)

[1.5] P Debye, *Z. Physik*, **21** 178 (1920)

[1.6] P Debye, *Polar molecules*, Chemical Catalog Co., New York (1929)

[1.7] L Onsager, *J. Am. Chem. Soc.*, **58** 1486 (1936)

[1.8] E A Guggenheim, *Trans. Faraday Soc.*, **45** 714 (1949)

[1.9] Le Fevre, *Trans. Faraday Soc.*, **46** 1 (1950)

[1.10] A K Ghosh, K K Sarkar and S Acharyya, *Acta. Ciencia Indica*, **3** 49 (1977)

[1.11] J J Makosz, *Acta. Phys. Polon (Poland)*, **A78** 907 (1990)

[1.12] J G Kirkwood, *J. Chem. Phys.*,7 911 (1939)

[1.13] H Fröhlich, *Theory of dielectrics*, Oxford University Press, London (1949)

[1.14] E Bauer, *Cah. Phys.*, **20** 1 (1944)

[1.15] H Eyring, S Glasstone and J K Laidler, *The Theory of Rate Processes*, McGraw-Hill, New York (1941)

[1.16] A H Kramers, *Atti. Congr. Int. Fisici, Como*, **2** 545 (1927)

[1.17] R Krönig, *J. Opt. Soc. Amer.*, **12** 547 (1926)

[1.18] F J Murphy and S O Morgan, *Bell. Syst. Tech. J*, **18** 502 (1939)

[1.19] J G Powles, *J. Chem. Phys.*, **21** 633 (1953)

[1.20] S H Glarum, *J. Chem. Phys.*, **33** 1371 (1960)

[1.21] O'dwyer and R A Sack, *Aust. J. Sci. Res.*, **A5** 647 (1952)

[1.22] K S Cole and R H Cole, J. Chem. Phys, **9** 341 (1941)

[1.23] D W Davidson and R H Cole, *J. Chem. Phys.*, **18** 1417 (1951)

[1.24] D W Davidson and R H Cole, *J. Chem. Phys.*, **19** 1484 (1951)

[1.25] J G Powles, *J. Molecular Liquids*, **56** 35 (1993)

[1.26] S Havriliak and S Negami, *J. Polym. Sci. C*, **14** 99 (1966)

[1.27] F Kohlrausch, *Pogg. Ann. Phys.* **119** 352 (1863)

[1.28] G Williams and D C Watts, *Trans. Faraday Soc.*, **66** 80 (1970)

[1.29] K W Wagner, *Ann. D. Physik*, **40** 817 (1913)

[1.30] W A Yager, *Physics*, **7** 434 (1936)

[1.31] J G Kirkwood and R M Fuoss, *J. Chem. Phys.*, **9** 329 (1941)

[1.32] R M Fuoss and J G Kirkwood, *J. Amer. Chem. Soc.*, **63** 385 (1941)

[1.33] K Higasi, K Bergmann and C P Smyth, *J. Phy. Chem.*, **64** 880 (1960)

[1.34] A Matsumoto and K Higasi, *J. Chem. Phys.*, **36** 1776 (1962)

[1.35] G Z Hedestrand, *J. Phys. Chem.*, **32** 428 (1929)

[1.36] P Cohen Henrique, *Thesis Delft*, p 93 (1935)

[1.37] R J W Le Fevre and H V Vine, *J. Chem. Soc.*,1805 (1937)

[1.38] K Higasi, *Bull. Inst. Phys. Chem. Res., Tokyo* **22** 805 (1943)

[1.39] J W Smith, *Trans. Faraday Soc.*, **46** 394 (1950)

[1.40] Everard, Hill and Sutton, *Trans. Faraday Soc.*, **46** 417 (1950)

[1.41] Barclay, Le Fevre and Smyth, *Trans. Faraday Soc.*, **46** 812 (1950)

[1.42] E A Guggenheim, *Trans. Faraday Soc.*, **47** 573 (1951)

[1.43] S R Palit and B C Banerjee, *Trans. Faraday Soc.*, **47** 1299 (1951)

[1.44] C J F Bottcher, *Theory of Electric Polarization*, Elsevier Publishing Co., New York (1952)

[1.45] B Krishna and K K Srivastava, *J. Chem. Phys.*, **27** 835 (1957)

[1.46] S C Srivastava and P Charandas, *J. Chem. Phys.*, **30** 816 (1959)

[1.47] J Prakash, *Ind. J. Pure. & Appl. Phys.*, **11** 901 (1973)

[1.48] A K Guha, D K Das and S Acharyya, *Ind. J. Phys.*, **51A** 192 (1977)

[1.49] A K Ghosh and S Acharyya, *Ind. J. Phys.*, **52B** 129 (1978)

[1.50] A K Ghosh and S K Ghosh, *Ind. J. Pure & Appl. Phys.* **20** 743 (1982)

[1.51] M Suryyavanshi, S C Mehrotra, *Ind. J. Pure & Appl. Phys.* **28** 67 (1990)

[1.52] W Kauzmann, *Reviews of Modern Physics*, **14** 12 (1942)

[1.53] Ph A Guye, *Compt. Rend.*, **110** 141 (1890)

[1.54] H A Lorentz, *Arch. Nerl. Sci.*, **25** 363 (1892)

[1.55] Ch B Thwing, *Z. Phys. Chem.*, **14** 286 (1894)

[1.56] P Drude, *Z. Phys. Chem.*, **23** 267 (1897)

[1.57] J C Philipp, *Z. Phys. Chem.*, **24** 18 (1897)

[1.58] K Baedeker, *Z. Phys. Chem.*, **36** 315 (1901)

[1.59] P Walden, *Z. Phys. Chem.*, **10** 569 (1910)

[1.60] S I Mizushima, *Phys. Z.*, **28** 418 (1926)

[1.61] S I Mizushima, *Sci. Papers Inst. Phys. Chem. Research (Tokyo)*, **5** 201 (1927)

[1.62] J D Stranathan, *Phys. Rev.*, **91** 653 (1928)

[1.63] M Y Rocard, *J. Phys. Radium*, **4** 247 (1933)

[1.64] E Fischer and F C Frank, *Phys. Z.*, **40** 345 (1939)

[1.65] A Budo, *Phys. Z.*, **39** 706 (1938)

[1.66] F R Gross, *Chem. Soc. J.*, 752 (1940)

[1.67] L J Onsager, *J. Chem. Phys.*, **2** 509 (1934)

[1.68] H J Plumely, *Phys. Rev.*, **59** 200 (1941)

[1.69] C S Pao, *Phys. Rev.*, **64** 60 (1943)

[1.70] F Ryhel, *Z. Phys.*, **44** 89 (1943)

[1.71] J L Eck, *Ann. Phys.*, **4** 12 (1949)

[1.72] D H Whiffen and H W Thompson, *Discussion Faraday Soc.*, **42A** 114 (1946)

[1.73] W Jackson and J G Powles, *Trans. Faraday Soc.*, **42A** 101 (1946)

[1.74] A Schallamach, *Trans. Faraday Soc.*, **42A** 180 (1946)

[1.75] R Mecke and A Reuter, *Z. Naturforsch*, **4A** 368 (1949)

[1.76] G Kremmling, *Z. Naturforsch*, **5A** 675 (1950)

[1.77] A J Curties, P L McGree, G B Rathmann and C P Smyth, *J. Am. Chem. Soc.*, **74** 644 (1952)

[1.78] J A Lane and J A Saxton, *Proc. R. Soc.*, **214A** 531 (1952)

[1.79] F H Brannin and C P Smyth, *J. Chem. Phys.*, **20** 1121 (1952)

[1.80] G Jaffe and C Z Lemay, *J. Chem. Phys.* **21** 920 (1953)

[1.81] W B Green, *J. Appl. Phys.*, **26** 1257 (1955)

[1.82] J Ph Poley, *Appl. Scient. Res.*, **4B** 337 (1955)

[1.83] R C Müller and C P Smyth, *J. Chem. Phys.*, **24** 814 (1956)

[1.84] S K Garg and C P Smyth, *J. Chem. Phys.*, **42** 1397 (1956)

[1.85] K V Gopalakrishna, *Trans. Faraday Soc.*, **53** 767 (1957)

[1.86] J A Schellman, *J. Chem. Phys.*, **26** 1225 (1957)

[1.87] G P Srivastava and V P Vershri, *Physica*, **23** 173 (1957)

[1.88] K Bergmann, D M Roberti and C P Smyth, *J. Phys. Chem.*, **64** 665 (1960)

[1.89] Krishnaji and A Mansingh, *J. Chem. Phys.*, **41** 827 (1964)

[1.90] E O Froster, *Electro Chim. Acta.*, **9** 1319 (1964)

[1.91] M Davies and G Williams, *Trans. Faraday Soc.*, **56** 1619 (1960)

[1.92] M Davies and G Johansson, *Acta. Chim. Scand.*, **18** 1171 (1964)

[1.93] B Sinha, S B Roy and G S Kastha, *Ind. J. Phys.*, **40** 101 (1966)

[1.94] B Sinha, S B Roy and G S Kastha, *Ind. J. Phys.*, **41** 183 (1967)

[1.95] I Adamezewski and B Jachym, *Acta. Phys. Polon.*, **34** 1015 (1968)

[1.96] J Prakash, *Ind. J. Pure. & Appl. Phys.*, **8** 106 (1970)

[1.97] J Bhattacharyya, A Hassan, S B Roy and G S Kastha, *J. Phys. Soc., Japan* **28** 240 (1970)

[1.98] K Higasi, Y Koga and M Nakamura, *Bull. Chem. Soc., Japan* **44** 988 (1971)

[1.99] H V Lohneysen and H Nageral, *J. Phys. D: Appl. Phys.*, **4** 1718 (1971)

[1.100] F Gaspared and J P Gosse, *Electro. Chim. Acta.*, **15** 599 (1970)

[1.101] J Crossley, L Glasser and C P Smyth, *J. Chem. Phys.*, **55** 2197 (1971)

[1.102] H D Purohit and H S Sharma, *Ind. J. Pure & Appl. Phys.*, **9** 450 (1971)

[1.103] L Glasser, J Crossley and C P Smyth, *J. Chem. Phys.* **57** 3977 (1972)

[1.104] R L Dhar, A Mathur, J P Shukla and M C Saxena, *Ind. J. Pure & Appl. Phys.*, **11** 568 (1973)

[1.105] J P Shukla and M C Saxena, *Ind. J. Pure & Appl. Phys.*, **11** 896 (1973)

[1.106] Y Koga, H Takahasi and H Higasi, *Bull. Chem. Soc. Japan*, **46** 3359 (1973)

[1.107] H D Purohit, H S Saxena and A D Vyas, *Ind. J. Pure & Appl. Phys.*, **12** 273 (1974)

[1.108] S C Srivastava and Suresh Chandra, *Ind. J. Pure & Appl. Phys.*, **13** 101 (1975)

[1.109] S K Srivastava and S L Srivastava, *Ind. J. Pure & Appl. Phys.*, **13** 179 (1975)

[1.110] M L Arrawatia, P C Gupta and M L Sisodia, *Ind. J. Pure & Appl. Phys.*, **15** 770 (1977)

[1.111] S K S Somevanshi, S B Misra and N K Mehrotra, *Ind. J. Pure & Appl. Phys.*, **16** 57 (1978)

[1.112] P C Gupta, M L Arrawatia and M L Sisodia, *Ind. J. Pure & Appl. Phys.*, **16** 934 (1978)

[1.113] S M Khameshara and M L Sisodia, *Ind. J. Pure & Appl. Phys.*, **18** 110 (1980)

[1.114] B S Rajyam, C R K Ramasastry and C R K Murthy, *Z. Naturforsch*, **32A** 1309 (1977)

[1.115] S Mulechi, S Balanicka and J Nowak, *J. Chem. Soc. Faraday Trans.*, **2(GB)I** 42 (1980)

[1.116] S N Sen and R Ghosh, *J. Phys. Soc., Japan* **36** 743 (1974)

[1.117] A K Ghosh and S N Sen, *Ind. J. Pure & Appl. Phys.* **18** 588 (1980)

[1.118] A K Ghosh and S N Sen, *J. Phys. Soc., Japan* **48** 1219 (1980)

[1.119] R Ghosh and I Chowdhury, *Pramana : J. Phys.*, **16** 319 (1981)

[1.120] R Ghosh and I Chowdhury, *Ind. J. Pure & Appl. Phys.*, **20** 717 (1982)

[1.121] J S Dhull and D R Sharma, *J. Phys. D : Appl. Phys.*, **15** 2307 (1982)

[1.122] J S Dhull and D R Sharma, *Ind. J. Pure & Appl. Phys.*, **21** 694 (1983)

[1.123] A K Sharma and D R Sharma, *J. Phys. Soc., Japan* **53** 4771 (1984)

[1.124] A K Sharma and D R Sharma, *Ind. J. Pure & Appl. Phys.*, **23** 418 (1985)

[1.125] A K Sharma, D R Sharma and D S Gill, *J. Phys. D : Appl. Phys.*, **18** 1199 (1985)

[1.126] S Acharyya and A K Chatterjee, *Ind. J. pure & Appl. Phys.*, **23** 484 (1985)

[1.127] C R Acharyya, A K Chatterjee, P K Sanyal and S Acharyya, *Ind. J. Pure & Appl. Phys.*, **24** 234 (1986)

[1.128] C B Agarwal, *Ind. J. Pure & Appl. Phys.*, **24** 204 (1986)

[1.129] M P Madan, *J. Molecular Liquids*, **33** 203 (1987)

[1.130] A D Vyas and V M Vashisth, *J. Molecular Liquids*, **38** 11 (1988)

[1.131] J M Gandhi and G L Sharma, *J. Molecular Liquids*, **38** 23 (1988)

[1.132] M B R Murthy, R L Patil and D K Deshpande, *Ind. J. Phys.*, **63B** 494 (1989)

[1.133] A Sharma and D R Sharma, *J. Phys. Soc., Japan* **61** 1049 (1992)

[1.134] A K Sharma, D R Sharma, K C Sharma and D S Gill, *Zeitschrift fur Physika lische Chemie Neue Folge., 13d* **141S** 15 (1984)

[1.135] U Saha and S Acharyya, *Ind. J. Pure & Appl. Phys.*, **31** 181 (1993)

[1.136] U Saha and S Acharyya, *Ind. J. Pure & Appl. Phys.*, **32** 346 (1994)

[1.137] U Saha, S K Sit, R C Basak and S Acharyya, *J. Phys. D : Appl. Phys.*, **27** 596 (1994)

[1.138] S K Sit, R C Basak, U Saha and S Acharyya, *J. Phys. D : Appl. Phys.* **27** 2194 (1994)

[1.139] S K Sit, and S Acharyya, *Ind. J. Pure & Appl. Phys.*, **34** 255 (1996)

[1.140] P J Singh and K S Sharma, *Ind. J. Pure & Appl. Phys.*, **34** 1 (1996)

[1.141] R A Jangid, D Bhatnagar and J M Gandhi, *Ind. J. Pure & Appl. Phys.*, **35** 47 (1997)

[1.142] R J Sengwa and K Kaur, *Ind. J. Pure & Appl. Phys.*, **37** 469 (1999)

[1.143] U Saha and R Ghosh, *J. Phys. D : Appl. Phys.* **32** 820 (1999)

[1.144] S K Dash, J K Das and B B Swain, *Ind. J. Pure & Appl. Phys.*, **38** 791 (2000)

[1.145] N Thakur and D K Sharma, *Ind. J. Pure & Appl. Phys.*, **38** 328 (2000)

CHAPTER 2

SCOPE AND OBJECTIVE OF THE THESIS WORK

2.1. Introduction :

The aim of this chapter is to suggest simple, straightforward and significant theories on dielectric behaviour of polar liquid in suitable non-polar solvents to shed light on various molecular and intra-molecular aspects through relaxation phenomena. Several theories so far developed are based on Debye–Smyth model of polar-nonpolar liquid mixtures to get relaxation parameters like dipole moment μ, energy parameters of dielectropolar liquid molecules.

The entire formulations of the theories have been made in SI units because of its rationalised, coherent and unified nature. The more recent trend to study the dielectric relaxation mechanism of a dielectropolar liquid molecule through high frequency dielectric orientation susceptibility χ_{ij}^* rather than *hf* complex permittivity ε_{ij}^*or *hf* complex conductivity σ_{ij}^*. This chapter contains an elaborate discussion on various theories with a greater emphasis on orientational susceptibility measurement technique in comparison to the other existing theories so far derived by this research group.

Besides experimentally determining such parameters, an important aim of a worker in the field of dielectric is to analyse the experimental information from the available models. He then tried to develop a unified theory to predict the new behaviour of dielectric materials.

2.2. Relaxation Phenomena :

As stated earlier in Chapter 1, the phenomenon of dielectric relaxation in liquids and solids (DRL and DRS) is one of the greatest unresolved problems of physics today [2.1-2.4]. The dielectropolar molecular liquid dissolved in a non-polar solvent absorbs electric energy of very longer wavelengths. The absorbtion often becomes maximum at some particular wavelength. In this case, the tendency of an applied electric field is to orient the molecular dipole along the field direction. The alignment is, however, opposed by molecular inertia and thermal motion of the molecules. The viscous force of the medium, on the other hand, also imposes a lag between the alternation of the applied alternating high frequency (*hf*) electric field and the rotation of the molecules. The consequent absorbtion of electric energy leads to an anomalous dispersion. The fall of relative permittivity with decreasing wavelength and the consequent absorbtion of electric energy by the dielectropolar molecule is of particular interest so far the power loss of dielectric concerned.

The past few years have greatly advanced the available experimental information and the entire thesis work is devoted to a review of such information starting from the relative permittivity to dielectric susceptibility to interpret the relaxation phenomena (DRL) of polar-nonpolar liquid mixture. The point, which needs to be kept in mind, is that all the relaxation phenomena are usually connected with the presence of some form of disorder in the system of polar liquid in a non-polar

solvent. There can be no relaxation in a perfectly ordered system, because nothing can relax from the perfection [2.5].

Debye, however, formulated a rigorous deterministic theoretical basis for such phenomena in terms of the properties of molecular dipoles and the 'relaxation time' required for the molecular rotation. The lag in response to the alternation of the applied electric field is commonly known as dielectric relaxation and the time in which the orientation polarisation reduces to 1/e times the initial polarisation is called the relaxation time and usually denoted by τ_j. The τ_j gives a measure of the rate of restoration of random order after removal of the applied electric field. The relaxation phenomena are nowadays concerned with the various devices obtaining the relaxation time τ_j's and hence the *hf* dipole moments μ_j's along with the static or low frequency μ_s. The correlation between the conformational structures of the dipolar liquids with the observed results enhances the scientific contents of this thesis in order to add a better understanding of the existing knowledge of dielectric relaxation phenomena. However, Fröhlich, Onsager, Fuoss, Kirkwood, Eyring, Kauzmann, Bauer [2.6-2.12] and others had attempted to overcome the defects of the original theory of Debye to study the relaxation mechanism.

In addition to the novel approach to Thermally Stimulated Depolarisation Current Density (TSDCD) and Isothermal Frequency Domain AC Spectroscopy (IFDS) – a subject as old as the science of dielectrics, still the simpler Debye model mixed with Smyth and Fröhlich appears to be more reliable till now to yield more information of relaxation of dipolar molecules of Debye like behaviour found in all the materials as presented in the thesis.

2.3. Debye Equation in Solution (SI Unit) :

In SI unit, the dielectric displacement vector $\vec{D}$ for a homogeneous, isotropic dielectric medium of absolute permittivity ε in Farad.metre^{-1} can be written as:

$$\vec{D} = \varepsilon_r \varepsilon_o \vec{E} \qquad \text{.....(2.1)}$$

where ε_r is the dimensionless relative permittivity defined by $\varepsilon / \varepsilon_o$ and ε_o is the absolute permittivity of free space = 8.854×10^{-12} F.m^{-1}.

If $\vec{P}$ is the total polarisation of the medium due to external electric field $\vec{E}$, the displacement vector $\vec{D}$ is:

$$\vec{D} = \varepsilon_o \vec{E} + \vec{P} \qquad \text{.....(2.2)}$$

From Eqs.(2.1) and (2.2) one gets:

$$\vec{P} = (\varepsilon_r - 1)\varepsilon_o \vec{E} \qquad \text{.....(2.3)}$$

Again,

$$\vec{P} = n\alpha_T \vec{E}_{loc} \qquad \text{.....(2.4)}$$

where $\vec{E}_{loc}$ is local electric field within a dielectropolar liquid.

Thus the Clausius-Mossotti relation in SI unit for a non-polar liquid molecule is:

$$\frac{\varepsilon_r - 1}{\varepsilon_r + 2}\frac{M}{\rho} = \frac{N\alpha_d}{3\varepsilon_o} \qquad \text{.....(2.5)}$$

where N is the Avogadro's number, M is the molecular weight and ρ is the density of a dielectric material.

Similarly for a polar molecule Debye equation is:

$$\frac{\varepsilon_r - 1}{\varepsilon_r + 2}\frac{M}{\rho} = \frac{N}{3\varepsilon_o}\left(\alpha_d + \frac{\mu_p^2}{3k_BT}\right) \qquad \text{.....(2.6)}$$

where α_d is the polarisability due to distortion polarisation and μ_p is the permanent dipole moment of a dipolar molecule.

The same Debye equation in case of a polar-nonpolar liquid mixture is:

$$\frac{\varepsilon_{ij} - 1}{\varepsilon_{ij} + 2}\frac{M_i f_i + M_j f_j}{\rho_{ij}} = \frac{N}{3\varepsilon_o}\left(\alpha_i f_i + \alpha_j f_j\right) \qquad \text{.....(2.7)}$$

The symbols have usual meanings as in Chapter1.

The Eq.(2.7) can be written in the simplified form with the help of Eqs.(1.67), (1.68) and (1.69) respectively

$$\left(\frac{\varepsilon_{ij} - 1}{\varepsilon_{ij} + 2} - \frac{n_{Dij}^2 - 1}{n_{Dij}^2 + 2}\right) = \left(\frac{\varepsilon_i - 1}{\varepsilon_i + 2} - \frac{n_{Di}^2 - 1}{n_{Di}^2 + 2}\right) + \frac{N}{3\varepsilon_o}\frac{\mu_s^2}{3k_BT}c_j \qquad \text{.....(2.8)}$$

in SI unit in order to obtain the dipole moment μ_s of a dipolar liquid molecule.

2.4. Static Dipole Moment μ_s from Static Experimental Parameter X_{ij} :

Under static or low frequency electric field, Debye equation for polar-nonpolar liquid mixture can have the form:

$$\left(\frac{\varepsilon_{oij} - 1}{\varepsilon_{oij} + 2} - \frac{\varepsilon_{\infty ij} - 1}{\varepsilon_{\infty ij} + 2}\right) = \left(\frac{\varepsilon_{oi} - 1}{\varepsilon_{oi} + 2} - \frac{\varepsilon_{\infty i} - 1}{\varepsilon_{\infty i} + 2}\right) + \frac{N}{3\varepsilon_o}\frac{\mu_s^2}{3k_BT}\frac{\rho_{ij}}{M_j}w_j \qquad \text{.....(2.9)}$$

Here, ε_{oij}, $\varepsilon_{\infty ij}$ and ε_{oi}, $\varepsilon_{\infty i}$ are the static and infinite frequency relative permittivities of the solution and solvent respectively, w_j is the weight fraction of a polar solute and μ_s is the static dipole moment in Coulomb metre (C.m).

Let a polar solute of weight W_j and volume V_j is made to dissolve in a non-polar solvent of weight W_i and volume V_i to make a solution of density ρ_{ij}.

ρ_{ij} is given by :

$$\rho_{ij} = \frac{W_i + W_j}{V_i + V_j} = \frac{W_i + W_j}{W_i/\rho_i + W_j/\rho_j}$$

$$= \frac{\rho_i \rho_j}{w_i \rho_j + w_j \rho_i} = \frac{\rho_i}{1 - (1 - \rho_i/\rho_j) w_j} = \rho_i (1 - \gamma w_j)^{-1} \qquad \ldots\ldots (2.10)$$

where w_i ($=W_i / W_i+W_j$) and w_j ($=W_j / W_i+W_j$) are defined by the weight fractions of the solvent and solute of densities ρ_i and ρ_j respectively such that $w_i+w_j=1$. γ $=(1-\rho_i/\rho_j)$ is constant for a particular polar-nonpolar liquid mixture at a fixed temperature [2.13-2.14].

Thus Eq.(2.9) becomes :

$$\frac{\varepsilon_{oij} - \varepsilon_{\infty ij}}{(\varepsilon_{oij} + 2)(\varepsilon_{\infty ij} + 2)} = \frac{\varepsilon_{oi} - \varepsilon_{\infty i}}{(\varepsilon_{oi} + 2)(\varepsilon_{\infty i} + 2)} + \frac{N \rho_i \mu_s^2}{27 \varepsilon_o M_j k_B T} (1 - \gamma w_j)^{-1} w_j$$

$$X_{ij} = X_i + \frac{N \rho_i \mu_s^2}{27 \varepsilon_o M_j k_B T} w_j + \frac{N \rho_i \mu_s^2}{27 \varepsilon_o M_j k_B T} \gamma w_j^2 + \ldots\ldots\ldots \qquad \ldots\ldots (2.11)$$

$$X_{ij} = X_i + R w_j + R \gamma w_j^2 + \ldots\ldots\ldots \qquad \ldots\ldots (2.12)$$

The L.H.S. is defined as the static experimental parameter X_{ij} of the solution in terms of measured static and infinite frequency relative permittivities ε_{oij} and $\varepsilon_{\infty ij}$ of the solution and $R = \frac{N \rho_i \mu_s^2}{27 \varepsilon_o k_B T M_j}$. X_{ij} for most of the polar-nonpolar liquid mixtures, often behave non-linearly with w_j. This at once indicates that X_{ij} is a polynomial function of w_j like:

$$X_{ij} = a_o + a_1 w_j + a_2 w_j^2 \qquad \ldots\ldots (2.13)$$

neglecting the higher powers of w_j in Eq.(2.12) as they contain the factors arising due to orientation effect, relative density effect, dipole-dipole interactions, associations etc. It is seen that a_1 in Eq.(2.13) are free from all factors to yield a dipole moment for a quasi-isolated polar molecule. The experimental plots of X_{ij} with w_j for most of the solutions also support this statement. Equating the coefficients of the first power of w_j from Eqs.(2.13) and (2.12) one gets μ_s of a polar liquid molecule in Coulomb.metre from:

$$\mu_s = \left(\frac{27 \varepsilon_o M_j k_B T}{N \rho_i} a_1 \right)^{1/2} \qquad \ldots\ldots (2.14)$$

Here ε_o= relative permittivity in free space. k_B = Boltzmann constant, M_j = molecular weight of the solute. N = Avogadro's number and ρ_i = density of the solvent used. This theory so far derived, is tested in some interesting dipolar liquids in non-polar solvents. The findings of the study is, however, presented in Chapters 3 and 9 respectively of this thesis.

2.5. High Frequency Complex Conductivity σ_{ij}^* :

The high frequency complex conductivity σ^* of a dielectropolar material under an alternating electric field $E=E_o e^{j\omega t}$ appears in Ohm's law:

$$I = \sigma^* E_o e^{j\omega t} \qquad \ldots\ldots (2.15)$$

where I= the current density.

In SI unit the dielectric displacement D is related to charge q by:

$$D = q \qquad \ldots\ldots (2.16)$$

The *hf* complex relative permittivity ε_r^* of a system is:

$$\varepsilon_r^* = \frac{\varepsilon^*}{\varepsilon_o} \qquad \ldots\ldots (2.17)$$

where ε^* and ε_o are the absolute permittivities of the medium and free space in SI units respectively.

Again,

$$D = \varepsilon^* E = \varepsilon_o \varepsilon_r^* E \qquad \ldots\ldots (2.18)$$

Hence the current density I is given by:

$$I = \frac{dq}{dt} = \frac{dD}{dt} = \frac{d}{dt}\left(\varepsilon_o \varepsilon_r^* E_o e^{j\omega t}\right)$$

$$= \varepsilon_o \varepsilon_r^* j\omega E_o e^{j\omega t} \qquad \ldots\ldots (2.19)$$

Comparing Eqs.(2.15) and (2.19) one gets :

$$\sigma^* = j\omega\varepsilon_o\varepsilon_r^* \qquad \ldots\ldots (2.20)$$

For a polar-nonpolar liquid mixtures (*ij*) Eq.(2.20) can be written as:

$$\sigma_{ij}^* = j\omega\varepsilon_o\varepsilon_{ij}^*$$

or,

$$\sigma_{ij}' + j\sigma_{ij}'' = j\omega\varepsilon_o(\varepsilon_{ij}' - j\varepsilon_{ij}'')$$

Equating the real and imaginary parts,

$$\sigma'_{ij} = \omega\varepsilon_o\varepsilon''_{ij}$$
$$\sigma''_{ij} = \omega\varepsilon_o\varepsilon'_{ij} \qquad \text{.....(2.21)}$$

where σ_{ij}' and σ_{ij}'' are the real and imaginary parts of *hf* complex conductivity σ_{ij}^* expressed in $\Omega^{-1}\,m^{-1}$.

2.6. Relaxation Time, Dipole Moment and Conductivity of Solution under High Frequency Electric Field :

In *hf* region, the total conductivity of a polar-nonpolar liquid mixture is [2.15]:

$$\sigma_{ij} = \sqrt{\sigma_{ij}'^2 + \sigma_{ij}''^2} = \omega\varepsilon_o\sqrt{\varepsilon_{ij}'^2 + \varepsilon_{ij}''^2} \qquad \text{.....(2.22)}$$

In high frequency electric field ε_{ij}' of a solution is usually very small and is nearly equal to optical dielectric constant of the solution. But still $\varepsilon_{ij}' \gg \varepsilon_{ij}''$ where ε_{ij}'' is responsible for the absorption of electric energy by the dielectric medium to offer resistance to polarisation.

ε_{ij}' is again related to the ε_{ij}'' by [2.16]

$$\varepsilon'_{ij} = \varepsilon_{\infty ij} + \frac{1}{\omega\tau_j}\varepsilon''_{ij} \qquad \text{.....(2.23)}$$

where $\varepsilon_{\infty ij}$ is the infinite frequency relative permittivity of the solution and τ_j is the relaxation time of the polar unit in a non-polar solvent.

Multiplying both sides by $\omega\varepsilon_o$ we have,

$$\omega\varepsilon_o\varepsilon'_{ij} = \omega\varepsilon_o\varepsilon_{\infty ij} + \frac{1}{\omega\tau_j}\omega\varepsilon_o\varepsilon''_{ij}$$

$$\sigma''_{ij} = \sigma_{\infty ij} + \frac{1}{\omega\tau_j}\sigma'_{ij} \qquad \text{.....(2.24)}$$

$$\frac{d\sigma''_{ij}}{d\sigma'_{ij}} = \frac{1}{\omega\tau_j} \qquad \text{.....(2.25)}$$

The slope of the linear curve of $\sigma_{ij}''-\sigma_{ij}'$ [2.17] could provide a direct method to obtain τ_j's.

In the higher concentration, σ_{ij}'' does not vary linearly with σ_{ij}' and the polar-polar interaction seems to occur. In order to avoid this effect it is better to use the ratio of the slopes of the individual variations of σ_{ij}'' and σ_{ij}' with weight fractions w_j at $w_j \to 0$ instead of using direct slope $\left(d\sigma''_{ij}/d\sigma'_{ij}\right)_{w_j\to 0}$ of Eq.(2.25)

Hence, τ_j could, however, be measured from [2.18]

$$\left(\frac{d\sigma''_{ij}}{dw_j}\right)_{w_j\to 0} = \frac{1}{\omega\tau_j}\left(\frac{d\sigma'_{ij}}{dw_j}\right)_{w_j\to 0} \qquad \ldots\ldots (2.26)$$

Here, one polar molecule is supposed to be surrounded by a large number of non-polar solvent molecules. The polar unit thus remains in a quasi-isolated state. The polar-polar interactions are fully avoided when we use the Eq.(2.26) at $w_j \to 0$.

In *hf* region of Giga hertz range it is observed experimentally that $\sigma_{ij}'' \approx \sigma_{ij}$. Hence Eq.(2.24) can be written as [2.19]:

$$\sigma_{ij} = \sigma_{\infty ij} + \frac{1}{\omega\tau_j}\sigma'_{ij}$$

$$\left(\frac{d\sigma'_{ij}}{dw_j}\right)_{w_j\to 0} = \omega\tau_j\beta \qquad \ldots\ldots (2.27)$$

where β is the slope of the variation of σ_{ij} with w_j in the limit $w_j = 0$.

The real part of *hf* conductivity σ_{ij}' at T K of a given solution of w_j is [2.20]:

$$\sigma'_{ij} = \frac{N\rho_{ij}\mu_j^2}{27M_j k_B T}\left(\frac{\omega^2\tau_j}{1+\omega^2\tau_j^2}\right)(\varepsilon_{ij}+2)^2 w_j \qquad \ldots\ldots (2.28)$$

On differentiation with respect to w_j at $w_j \to 0$.

$$\left(\frac{d\sigma'_{ij}}{dw_j}\right)_{w_j\to 0} = \frac{N\rho_i\mu_j^2}{27M_j k_B T}\left(\frac{\omega^2\tau_j}{1+\omega^2\tau_j^2}\right)(\varepsilon_i+2)^2 \qquad \ldots\ldots (2.29)$$

Here, the density ρ_{ij} and the relative permittivity ε_{ij} of the solution become ρ_i and ε_i of the solvent only in the limit $w_j = 0$.

Comparing Eqs.(2.27) and (2.29) one gets the *hf* dipole moment μ_j of a dielectropolar molecule in a given solvent:

$$\mu_j = \left(\frac{27M_j k_B T\beta}{N\rho_i(\varepsilon_i+2)^2\omega b}\right)^{1/2} \qquad \ldots\ldots (2.30)$$

where $b = [1/(1+\omega^2\tau_j^2)]$ is the dimensionless parameter involved with the measured τ_j by both the methods mentioned above.

The formulations, so far derived in SI units, are applied in various dipolar liquids in non-polar solvents at different experimental temperatures to test the validity of the formulations arrived

at on the part of the present group. The findings are thoroughly discussed in Chapters 4, 5, 6, and 7 of this thesis.

2.7. Thermodynamic Energy Parameters from Eyring's Rate Theory :

The rotation of a dipolar unit under *hf* electric field requires activation energy sufficient to overcome the energy barrier, between two equilibrium positions. In order to infer the molecular dynamics of a polar molecule in a non-polar solvent, one can write τ from Eyring's [2.21-2.22] rate theory:

$$\tau = \frac{h}{k_B T}\exp(\Delta F_\tau / RT) \qquad \ldots\ldots (2.31)$$

The free energy of activation ΔF_τ is the difference between the free energies of the activated and non-activated states of the dipolar molecule. It is given by:

$$\Delta F_\tau = \Delta H_\tau - T\Delta S_\tau \qquad \ldots\ldots (2.32)$$

ΔH_τ and ΔS_τ are enthalpy and entropy of activation of the dielectric relaxation process respectively. Eq.(2.31) thus becomes:

$$\tau = \frac{h}{k_B T}\exp(-\Delta S_\tau / R)\exp(\Delta H_\tau / RT) \qquad \ldots\ldots (2.33)$$

$$\ln(\tau T) = \ln A + \frac{\Delta H_\tau}{RT} \qquad \ldots\ldots (2.34)$$

where $A = \frac{h}{k_B}\exp(-\Delta S_\tau / R)$.

Eq.(2.34) is satisfied by linear curve of $\ln \tau T$ against $1/T$ if ΔH_τ and ΔS_τ are independent of temperature. The thermodynamic energy parameters like ΔH_τ, ΔF_τ and ΔS_τ of relaxation process can easily be measured from the slope and the intercept of the least squares fitted curve of Eq.(2.34).

ΔH_τ gives the molecular energy involved with the relaxation process. ΔS_τ, however, indicates the stability of the activated state. The negative value of ΔS_τ often reveals that the activated states are more ordered than the normal states. On the other hand, high value of ΔS_τ indicates that the activated states are not stable due to internal resistance suffered by larger dipolar rotation.

The relaxation time τ is related to the coefficient of viscosity η of the solvent at different experimental temperatures by

$$\tau = \frac{A\eta^\gamma}{T} \qquad \ldots\ldots (2.35)$$

$$\ln(\tau T) = \ln A + \gamma \ln \eta \qquad \ldots\ldots (2.36)$$

The Eq.(2.36) is a linear plot between $\ln(\tau T)$ against $\ln\eta$ and γ can be determined from the slope of the linear curve. γ value thus obtained, signifies that the solute molecule behaves as a solid phase rotator. The ΔH_η for viscous process could, however, be obtained from γ and the relation $\Delta H_\eta = \Delta H_\tau / \gamma$. The Kalman factor $\tau T/\eta^\gamma$ at different experimental temperatures can be obtained with γ in order to compare with the Debye factor $\tau T/\eta$. The comparison often provides the applicability of Debye model of relaxation behaviour for a large number of polysubstituted benzenes in benzene presented in Chapter 4 of this thesis [2.23].

2.8. Multiple Relaxation Phenomena :

A non-rigid molecule possesses more than one τ to exhibit the distribution of τ between two limiting values of τ_1 and τ_2. The concept of existence of multiple τ for a polar molecule was first put forward by Budo [2.24] in a compact form:

$$\frac{\varepsilon^* - \varepsilon_\infty}{\varepsilon_o - \varepsilon_\infty} = \sum_j \frac{c_j}{1 + i\omega\tau_j} \qquad \ldots\ldots (2.37)$$

The complex dielectric constant ε^* is expressed as the sum of a number of non-interacting Debye type dispersions as illustrated graphically in Fig.2.1. The term c_j is the weight factor of the jth type relaxation mechanism such that $\Sigma c_j = 1$.

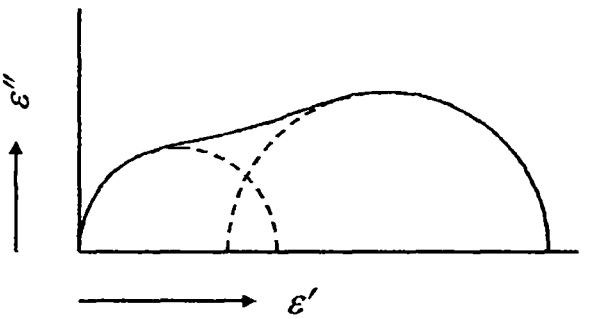

Figure 2.1: Plot of ε_{ij}'' against ε_{ij}' for two Debye semi-circle with double relaxation

Crossley *et al* [2.25] and Glasser *et al* [2.26] then proposed three relaxation phenomena in pure primary aliphatic alcohols and octanols. The lower value of τ_3 may be due to rotation of –OH group, the intermediate τ_2 due to orientation of the smaller molecular species while the longer τ_1 is associated with hydrogen bonded structure respectively. However, the relative contribution in *hf* relaxation increases for alcohols when they are diluted with non-polar solvents. The conclusion was drawn from the systematic measurement of ε_{ij}', ε_{ij}'', ε_{oij} and $\varepsilon_{\infty ij}$ at different frequencies of electric field with increasing concentration of alcohols and octanols in *n*-heptane solution.

2.9. Double Relaxation Phenomena :

Bergmann *et al* [2.27] subsequently applied the concept of two Debye type dispersions on diphenyl ether, diethyl ether, anisole and o-dimethoxy benzene respectively from ε', ε'', ε_o and ε_∞ measured under different angular frequencies ω's of the *hf* electric field in GHz range at 20°C to 80°C.

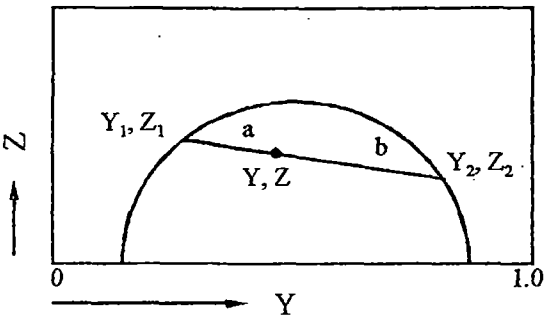

Figure 2.2: Graphical plot of Z against Y for two independent Debye type dispersions.

The Bergmann equations are:

$$\frac{\varepsilon' - \varepsilon_\infty}{\varepsilon_o - \varepsilon_\infty} = c_1 \frac{1}{1+\omega^2\tau_1^2} + c_2 \frac{1}{1+\omega^2\tau_2^2} \quad \text{..... (2.38)}$$

$$\frac{\varepsilon''}{\varepsilon_o - \varepsilon_\infty} = c_1 \frac{\omega\tau_1}{1+\omega^2\tau_1^2} + c_2 \frac{\omega\tau_2}{1+\omega^2\tau_2^2} \quad \text{..... (2.39)}$$

c_1 and c_2 are the weighted contributions due to τ_1 and τ_2 such that $c_1+c_2=1$.

The above Eqs.(2.38) and (2.39) can be put in the form:

$$Y = c_1 Y_1 + c_2 Y_2 \quad \text{..... (2.40)}$$

$$Z = c_1 Z_1 + c_2 Z_2 \quad \text{..... (2.41)}$$

where

$$Y = \frac{\varepsilon''}{\varepsilon_o - \varepsilon_\infty}; Z = \frac{\varepsilon' - \varepsilon_\infty}{\varepsilon_o - \varepsilon_\infty}$$

$$Y_1 = \frac{\omega\tau_1}{1+\omega^2\tau_1^2}; Y_2 = \frac{\omega\tau_2}{1+\omega^2\tau_2^2}$$

$$Z_1 = \frac{1}{1+\omega^2\tau_1^2}; Z_2 = \frac{1}{1+\omega^2\tau_2^2}$$

Bergmann *et al* [2.27] plotted the normalized experimental points on a complex plane as shown in Fig.2.2. A number of chords were then drawn through the experimental points to obtain a set of parameters in consistent with all the experimental points. A suitable point (Y,Z) was then selected between the points (Y_1,Z_1) and (Y_2,Z_2) of the normalized Debye semi-circle dividing the chord in the ratio $b/a=c_1/c_2$ to yield τ_1 and τ_2 [2.28]. The experimental values of ε', ε'', ε_o and ε_∞ were measured at different angular frequencies of the electric field of GHz range at a given temperature in °C.

Bhattacharyya *et al* [2.29] proposed the following equations for pure polar liquids of phenetole, aniline and o-chloro aniline molecules capable of rotations under GHz electric field as:

$$\frac{\varepsilon^* - \varepsilon_\infty}{\varepsilon_o - \varepsilon_\infty}\frac{\varepsilon_o + 2}{\varepsilon_\infty + 2} = p - iq \qquad \text{.....(2.42)}$$

where ,

$$p = c_1 \frac{1}{1+\omega^2\tau_1^2} + c_2 \frac{1}{1+\omega^2\tau_2^2}$$

$$q = c_1 \frac{\omega\tau_1}{1+\omega^2\tau_1^2} + c_2 \frac{\omega\tau_2}{1+\omega^2\tau_2^2} \qquad \text{.....(2.43)}$$

The terms τ_1, τ_2 and c_1, c_2 carry usual meanings. The above equations were simplified further in to:

$$\frac{\varepsilon_o - \varepsilon'}{\varepsilon''\omega} = (\tau_1 + \tau_2) - \frac{(\varepsilon' - \varepsilon_\infty)}{\varepsilon''}\omega\tau_1\tau_2 \qquad \text{....(2.44)}$$

provided $c_1+c_2=1$ and $\varepsilon_o \approx \varepsilon' \approx \varepsilon_\infty$ and ε'' is small for a pure polar liquid. τ_1, τ_2 and c_1, c_2 could, however, be estimated from Eq.(2.44) if ε', ε'', ε_o and ε_∞ measured at least at two different angular frequencies ω_1 and ω_2 respectively.

2.10. Double Relaxation Phenomena of a Polar-Nonpolar Liquid Mixture under Single Frequency Measurement of Relative Permittivities :

Saha *et al* [2.30] and Sit *et al* [2.31], under such context derived a very simple, straightforward and significant formulation to get τ_2 and τ_1 from the real part ε_{ij}' and imaginary part ε_{ij}'' of complex relative permittivity ε_{ij}^*, static and *hf* relative permittivities ε_{oij} and $\varepsilon_{\infty ij}$ of a polar solute (j) dissolved in a non-polar solvent (i) measured under a single GHz electric field at a given temperature. If a polar solute possesses two distinct Debye type dispersions each with a characteristic relaxation time, Bergmann equations in case of polar-nonpolar liquid mixture become:

$$\frac{\varepsilon_{ij}' - \varepsilon_{\infty ij}}{\varepsilon_{oij} - \varepsilon_{\infty ij}} = c_1 \frac{1}{1+\omega^2\tau_1^2} + c_2 \frac{1}{1+\omega^2\tau_2^2} \qquad \text{.....(2.45)}$$

$$\frac{\varepsilon_{ij}''}{\varepsilon_{oij} - \varepsilon_{\infty ij}} = c_1 \frac{\omega\tau_1}{1+\omega^2\tau_1^2} + c_2 \frac{\omega\tau_2}{1+\omega^2\tau_2^2} \qquad \text{.....(2.46)}$$

provide $c_1+c_2=1$. Here, τ_1, τ_2 and c_1, c_2 carry usual meanings [2.30-2.31].

Let us substitute $(\varepsilon_{ij}'-\varepsilon_{\infty ij})/(\varepsilon_{oij}-\varepsilon_{\infty ij})=x$, and $\varepsilon_{ij}''/(\varepsilon_{oij}-\varepsilon_{\infty ij})=y$ with $\omega\tau=\alpha$ in the Eqs.(2.45) and (2.46) one gets:

$$x = c_1 a_1 + c_2 a_2 \qquad \text{.....(2.47)}$$

$$y = c_1 b_1 + c_2 b_2 \qquad \text{.....(2.48)}$$

where $a=1/(1+\alpha^2)$ and $b=\alpha/(1+\alpha^2)$. The suffice 1 and 2 with a and b are, however, related to τ_1 and τ_2 respectively. From Eqs.(2.47) and (2.48) since $\alpha_2 \neq \alpha_1$ it is derived that

$$c_1 = \frac{(x\alpha_2 - y)(1+\alpha_1^2)}{\alpha_2 - \alpha_1} \quad \ldots\ldots (2.49)$$

$$c_2 = \frac{(y - x\alpha_1)(1+\alpha_2^2)}{\alpha_2 - \alpha_1} \quad \ldots\ldots (2.50)$$

Since $c_1+c_2=1$, one gets from Eqs.(2.49) and (2.50) the straight line equation :

$$\frac{\varepsilon_{oij} - \varepsilon'_{ij}}{\varepsilon'_{ij} - \varepsilon_{\infty ij}} = \omega(\tau_1 + \tau_2)\frac{\varepsilon''_{ij}}{\varepsilon'_{ij} - \varepsilon_{\infty ij}} - \omega^2\tau_1\tau_2 \quad \ldots\ldots (2.51)$$

between $(\varepsilon_{oij}-\varepsilon_{ij}')/(\varepsilon_{ij}'-\varepsilon_{\infty ij})$ and $\varepsilon_{ij}''/(\varepsilon_{ij}'-\varepsilon_{\infty ij})$ having slope $\omega(\tau_1+\tau_2)$ and intercept $-\omega^2\tau_1\tau_2$ respectively. Here, the angular frequency ω is $\omega=2\pi f$ and f is the frequency of the alternating electric field. The Eq.(2.51) is found to be satisfied by least squares fittings or Newton-Raphson method with ε_{ij}', ε_{ij}'', ε_{oij} and $\varepsilon_{\infty ij}$ of a polar-nonpolar liquid mixture for different w_j's under a single frequency electric field measurement at a given temperature in ^{0}C to yield the slope and intercept. They are finally used to get τ_2 and τ_1 to represent molecular and intra-molecular τ's of a polar liquid in non-polar solvent. The theory thus developed is beautifully used and discussed in Chapters 3 and 6 of this thesis.

2.11. High Frequency Dielectric Susceptibility :

The *hf* dielectric orientation susceptibility χ^* is related to P and E by:

$$P = \chi^* E \quad \ldots\ldots (2.52)$$

From the approximation of $P \propto E$ and $D \propto E$, we define the relative dielectric permittivity ε^* by

$$D = \varepsilon^* E \quad \ldots\ldots (2.53)$$

So,

$$\varepsilon^* = 1 + 4\pi\chi^* \quad \ldots\ldots (2.54)$$

Which is expressed in SI units

$$\varepsilon^* = 1 + \chi^*$$

$$\chi^* = \varepsilon^* - 1 \quad \ldots\ldots (2.55)$$

The dielectric susceptibility is given by the subtraction of either 1 or ε_∞ from the high and low frequency relative permittivities ε_r' and ε_o [2.5]. If 1 is subtracted, the susceptibility due to all operating polarisation processes results. If ε_∞ is subtracted from both ε_r' and ε_o it is only due to

orientation polarisation process [2.32]. It should be distinguished between the fast or rapidly responding component of the polarisation ε_∞ representing the processes, which respond to external fields practically instantaneously on the time domain, and the frequency dependent component referred to the dielectric susceptibility. $\chi^*(\omega)$'s refers to delayed processes. The fast component of polarisation ε_∞ is purely real since no energy loss can be involved in this rapid response. But $\chi^*(\omega)$ has a finite imaginary component. It is, therefore, a pure complex number.

The study of the dielectric relaxation becomes easier if the various processes are sufficiently well separated with respect to frequency ω of the applied electric field such that they do not overlap significantly. The dielectric behaviour of a homogeneous medium under *hf* electric field is then best represented in terms of the frequency dependent real and imaginary components of the complex dielectric orientation susceptibility $\chi^*(\omega)$:

$$\chi^*(\omega) = \chi'(\omega) - j\chi''(\omega) = \varepsilon^*(\omega) - \varepsilon_\infty \qquad \ldots\ldots (2.56)$$

where $j = \sqrt{-1}$ is a complex number.

For a polar molecule (j) dissolved in a non-polar solvent (i), the *hf* susceptibility and *hf* permittivity are related by:

$$\chi'_{ij} = \varepsilon'_{ij} - \varepsilon_{\infty ij}$$

$$\chi''_{ij} = \varepsilon''_{ij} \qquad \ldots\ldots (2.57)$$

$$\chi_{oij} = \varepsilon_{oij} - \varepsilon_{\infty ij}$$

where χ_{ij}' and χ_{ij}'' are the real and the imaginary parts of complex *hf* dielectric susceptibility χ_{ij}^* and χ_{oij} is the low frequency susceptibility, which is real. Here, $\varepsilon_{\infty ij}$ is the limit at frequencies of sufficiently high for the particular polarisation mechanism in question to show negligible loss and dispersion. The *hf* complex $\chi_{ij}^*(\omega)$ represents the dielectric response of the solution and it may be due to several independent mechanisms, which may overlap in any given frequency or time domain.

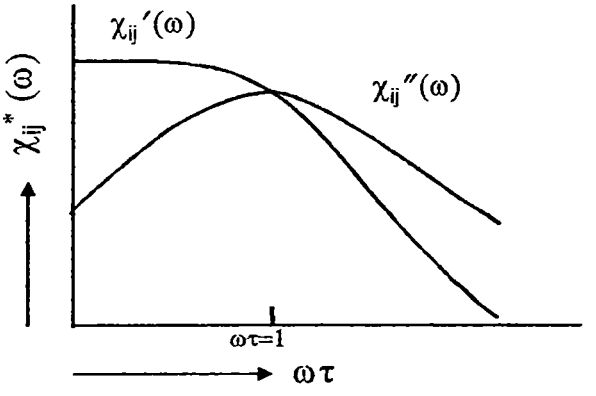

Figure 2.3: Variation of χ_{ij}' and χ_{ij}'' with $\omega\tau$

The classical Debye relation of χ_{ij}'s of a system of polar-nonpolar liquid mixture is:

$$\chi_{ij}^*(\omega) = \frac{\chi_{oij}}{1 + j\omega\tau} \qquad \ldots\ldots (2.58)$$

where τ is the temperature dependent relaxation time characterising the Debye process and $\omega\tau$ is the dimensionless parameter. Separating the real and the imaginary parts of Eq.(2.58) one gets:

$$\frac{\chi'_{ij}}{\chi_{oij}} = \frac{1}{1+\omega^2\tau^2} \qquad \ldots\ldots (2.59)$$

$$\frac{\chi''_{ij}}{\chi_{oij}} = \frac{\omega\tau}{1+\omega^2\tau^2} \qquad \ldots\ldots (2.60)$$

and their variations with respect to $\omega\tau$ are shown graphically in Fig.2.3.

2.12. Double Relaxation Phenomena of Polar-Nonpolar Liquid Mixture from *hf* Susceptibility Measurement Technique :

τ_1 and τ_2 due to rotation of the flexible parts as well as the whole molecule can be estimated from χ_{ij}'s measured under the single frequency electric field [2.33-2.34]. The equations of Bergmann *et al* [2.27] are concerned with molecular orientation polarisation processes. Thus in order to avoid the clumsiness of algebra and to exclude the fast polarisation process Bergmann equations in terms of established symbols of χ_{ij}', χ_{ij}'' and χ_{oij} can be written as:

$$\frac{\chi'_{ij}}{\chi_{oij}} = c_1\frac{1}{1+\omega^2\tau_1^2} + c_2\frac{1}{1+\omega^2\tau_2^2} \qquad \ldots\ldots (2.61)$$

$$\frac{\chi''_{ij}}{\chi_{oij}} = c_1\frac{\omega\tau_1}{1+\omega^2\tau_1^2} + c_2\frac{\omega\tau_2}{1+\omega^2\tau_2^2} \qquad \ldots\ldots (2.62)$$

Assuming that the molecule possesses two separate broad dispersions for which the relative weight factors c_1 and c_2 are such that $c_1+c_2=1$.

Let $\alpha_1=\omega\tau_1$, $\alpha_2=\omega\tau_2$, $\chi_{ij}'/\chi_{oij}= x$ and $\chi_{ij}''/\chi_{oij}= y$ Eqs.(2.61) and (2.62) take the form:

$$x = \frac{c_1}{1+\alpha_1^2} + \frac{c_2}{1+\alpha_2^2} \qquad \ldots\ldots (2.63)$$

and,

$$y = \frac{c_1\alpha_1}{1+\alpha_1^2} + \frac{c_2\alpha_2}{1+\alpha_2^2} \qquad \ldots\ldots (2.64)$$

From Eqs.(2.63) and (2.64) one gets:

$$(x\alpha_2 - y) = \frac{c_1}{1+\alpha_1^2}(\alpha_2 - \alpha_1)$$

$$c_1 = \frac{(x\alpha_2 - y)(1+\alpha_1^2)}{\alpha_2 - \alpha_1} \qquad \ldots\ldots (2.65)$$

Similarly;

$$(y - x\alpha_1) = \frac{c_2}{1+\alpha_2^2}(\alpha_2 - \alpha_1)$$

$$c_2 = \frac{(y - x\alpha_1)(1+\alpha_2^2)}{\alpha_2 - \alpha_1} \qquad \text{..... (2.66)}$$

Putting the values of x, y and α's in Eqs.(2.65) and (2.66) one gets:

$$c_1 = \frac{\left(\frac{\chi'_{ij}}{\chi_{oij}}\omega\tau_2 - \frac{\chi''_{ij}}{\chi_{oij}}\right)\left(1+\omega^2\tau_1^2\right)}{\omega(\tau_2 - \tau_1)} \qquad \text{..... (2.67)}$$

and

$$c_2 = \frac{\left(\frac{\chi''_{ij}}{\chi_{oij}} - \frac{\chi'_{ij}}{\chi_{oij}}\omega\tau_1\right)\left(1+\omega^2\tau_2^2\right)}{\omega(\tau_2 - \tau_1)} \qquad \text{..... (2.68)}$$

The experimental values of relative contributions c_1 and c_2 towards dielectric dispersions for a polar-nonpolar liquid mixture is also obtained by graphically established values of χ_{ij}'/χ_{oij} and χ_{ij}''/χ_{oij} in the limit w_j=0 from the above two Eqs.(2.67) and (2.68). The plots of χ_{ij}'/χ_{oij} and χ_{ij}''/χ_{oij} against w_j's of a given solute are obtained by least squares fitting technique with the experimental data placed upon them [2.34-2.35]. The curves are usually convex and concave nature as illustrated in Chapters 7 and 8.

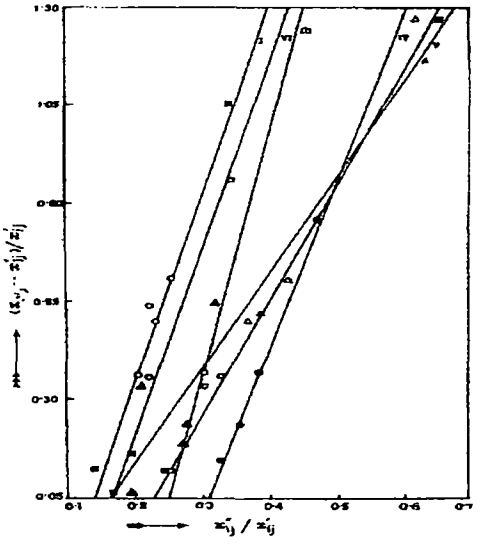

Figure 2.4: Linear plot of $(\chi_{oij}-\chi_{ij}')/\chi_{ij}'$ against χ_{ij}''/χ_{ij}' for monosubstituted anilines

The polar-nonpolar liquid mixtures under consideration are often of the complex type. A continuous distribution of τ with two discrete values of τ_1 and τ_2 could, therefore, be expected. Thus Fröhlich's equations [2.6] based on the single frequency distribution of τ between two extreme values of τ_1 and τ_2 in terms of $hf\,\chi^*_{ij}$'s can be obtained from Debye equation for a polar-nonpolar liquid mixture:

$$\frac{\chi^*_{ij}}{\chi_{oij}} = \int_o^\infty \frac{f(\tau)d\tau}{(1+j\omega\tau)} \qquad \text{..... (2.69)}$$

where $f(\tau)$ is the Fröhlich distribution function for τ such that:

$$f(\tau) = \frac{1}{A\tau}; \qquad \tau_1 < \tau < \tau_2$$
$$= 0; \qquad \tau_1 > \tau, \quad \tau_2 < \tau \qquad \text{.....(2.70)}$$

and A is the Fröhlich parameter given by $A = \ln(\tau_2 / \tau_1)$.

Separating the real and the imaginary parts of both sides of Eq.(2.69) the following equations are obtained:

$$\frac{\chi'_{ij}}{\chi_{oij}} = \frac{1}{A}\int_{\tau_1}^{\tau_2} \frac{d\tau}{\tau(1+\omega^2\tau^2)} \qquad \text{.....(2.71)}$$

$$\frac{\chi''_{ij}}{\chi_{oij}} = \frac{1}{A}\int_{\tau_1}^{\tau_2} \frac{\omega d\tau}{(1+\omega^2\tau^2)} \qquad \text{.....(2.72)}$$

Let $\ln\omega\tau = z$,

at $\tau = \tau_1$; $z = \ln\omega\tau_1$ and,

at $\tau = \tau_2$; $z = \ln\omega\tau_2$

The Eq.(2.71) is then transformed to:

$$\frac{\chi'_{ij}}{\chi_{oij}} = \frac{1}{A}\int_{\ln\omega\tau_1}^{\ln\omega\tau_2} \frac{dz}{1+e^{2z}}$$

$$= \frac{1}{A}\left[\int_{\ln\omega\tau_1}^{\ln\omega\tau_2} \frac{1+e^{2z}-e^{2z}}{1+e^{2z}} dz\right]$$

$$= \frac{1}{A}\left(\ln\frac{\omega\tau_2}{\omega\tau_1}\right) - \frac{1}{A}\int_{\ln\omega\tau_1}^{\ln\omega\tau_2} \frac{e^{2z}}{1+e^{2z}} dz$$

Again, $e^{2z}+1 = u$ so,

$$\frac{\chi'_{ij}}{\chi_{oij}} = 1 - \frac{1}{2A}\int_{1+\omega^2\tau_1^2}^{1+\omega^2\tau_2^2} \frac{du}{u}$$

$$= 1 - \frac{1}{2A}\ln\frac{1+\omega^2\tau_2^2}{1+\omega^2\tau_1^2} \qquad \text{.....(2.73)}$$

Similarly let $\omega\tau = z$ then from Eq.(2.72):

$$\frac{\chi''_{ij}}{\chi_{oij}} = \frac{1}{A}\int_{\omega\tau_1}^{\omega\tau_2} \frac{dz}{1+z^2}$$

$$= \frac{1}{A}\left[\tan^{-1}(\omega\tau_2) - \tan^{-1}(\omega\tau_1)\right] \qquad \text{.....(2.74)}$$

The above Eqs.(2.73) and (2.74) are the modified forms of Fröhlich's equations for a distribution of τ between two limiting values τ_1 and τ_2 in terms of *hf* χ_{ij}.

The theoretical values of c_1 and c_2 towards dielectric dispersion can be calculated from Eqs.(2.67); (2.68) and (2.73); (2.74) respectively with the estimated τ_1 and τ_2 in order to compare with the experimentally measured c_1 and c_2 values.

Now adding Eqs.(2.65) and (2.66) and since $c_1+c_2=1$, we have,

$$\frac{(x\alpha_2 - y)(1+\alpha_1^2)}{\alpha_2 - \alpha_1} + \frac{(y - x\alpha_1)(1+\alpha_2^2)}{\alpha_2 - \alpha_1} = 1 \qquad \text{.....(2.75)}$$

which, after simplification becomes:

$$\left(\frac{1}{x} - 1\right) = \frac{y}{x}(\alpha_2 + \alpha_1) - \alpha_1\alpha_2$$

Putting the values of x, y and α's the above equation is transformed into:

$$\frac{\chi_{oij} - \chi'_{ij}}{\chi'_{ij}} = \omega(\tau_1 + \tau_2)\frac{\chi''_{ij}}{\chi'_{ij}} - \omega^2\tau_1\tau_2 \qquad \text{.....(2.76)}$$

The Eq.(2.76) is a linear equation with the variables $(\chi_{oij}-\chi_{ij}')/\chi_{ij}'$ plotted against χ_{ij}''/χ_{ij}' for different w_j's of solute under a given angular frequency ω $(=2\pi f)$ of the electric field as illustrated in Fig.2.4 [2.35]. The intercept $-\omega^2\tau_1\tau_2$ and slope $\omega(\tau_1+\tau_2)$ of Eq.(2.76) can be used to get τ_1 and τ_2 respectively.

2.13. Dipole Moment from *hf* Dielectric Susceptibility :

Clausius-Mossotti equation in case of a polar-nonpolar liquid mixture under static or low frequency electric field is:

$$\frac{\varepsilon_{oij} - 1}{\varepsilon_{oij} + 2}\frac{M_i f_i + M_j f_j}{\rho_{ij}} = \frac{N}{3\varepsilon_o}(\alpha_i f_i + \alpha_j f_j) + \frac{N}{3\varepsilon_o}\frac{f_j\mu_j^2}{3k_BT} \qquad \text{.....(2.77)}$$

and at infinitely *hf* region (say sodium D light) the Lorentz equation is:

$$\frac{\varepsilon_{\infty ij} - 1}{\varepsilon_{\infty ij} + 2}\frac{M_i f_i + M_j f_j}{\rho_{ij}} = \frac{N}{3\varepsilon_o}(\alpha_i f_i + \alpha_j f_j) \qquad \text{.....(2.78)}$$

Subtracting Eq.(2.78) from Eq.(2.77) and after simplification one gets:

$$\frac{\varepsilon_{oij} - \varepsilon_{\infty ij}}{(\varepsilon_{oij} + 2)(\varepsilon_{\infty ij} + 2)} = \frac{N}{9\varepsilon_o}\frac{\rho_{ij}\mu_j^2}{3M_j k_B T}w_j \qquad \text{.....(2.79)}$$

where w_j is the weight fraction of the polar unit $= M_j f_j / (M_i f_i + M_j f_j)$.

Since in *hf* region it may be assumed that $\varepsilon_{oij} \approx \varepsilon_{\infty ij} \approx \varepsilon_{ij}$ where ε_{ij} is the relative permittivity of the solution and $\mu = \mu_j$ dipole moment measured under *hf* electric field, the Eq.(2.79) in terms of dielectric orientation susceptibility becomes:

$$\chi_{oij} = \frac{N\mu_j^2 \rho_{ij} F_{ij}}{3\varepsilon_o M_j k_B T} w_j \qquad \text{..... (2.80)}$$

Here F_{ij}= the local field of the solution $=(\varepsilon_{ij}+2)^2/9$.

The above Eq.(2.80) when compared with Eq.(2.60) takes the form

$$\chi''_{ij} = \frac{N\mu_j^2 \rho_{ij} F_{ij}}{3\varepsilon_o M_j k_B T} \frac{\omega\tau_j}{1+\omega^2\tau_j^2} w_j \qquad \text{..... (2.81)}$$

Differentiating Eq.(2.81) with respect to w_j in the limit $w_j \to 0$,

$$\left(\frac{d\chi''_{ij}}{dw_j}\right)_{w_j \to 0} = \frac{N\mu_j^2 \rho_i F_i}{3\varepsilon_o M_j k_B T} \frac{\omega\tau_j}{1+\omega^2\tau_j^2} \qquad \text{..... (2.82)}$$

Here, $\rho_{ij} \to \rho_i$ and $F_{ij} \to (\varepsilon_i+2)^2/9$ in the limit $w_j = 0$ where ρ_i and ε_i are density and relative permittivity of the solvent respectively.

From Eqs.(2.59) and (2.60) one gets:

$$\frac{\chi'_{ij}}{\chi''_{ij}} = \frac{1}{\omega\tau_j} \qquad \text{..... (2.83)}$$

or,

$$\left(\frac{d\chi''_{ij}}{dw_j}\right)_{w_j \to 0} = \omega\tau_j \left(\frac{d\chi'_{ij}}{dw_j}\right)_{w_j \to 0} = \omega\tau\beta \qquad \text{..... (2.84)}$$

Eqs.(2.83) and (2.84) can conveniently be used to measure τ_j's of any polar unit in a non-polar solvent.

Now, β is the slope of the variation of χ_{ij}' with w_j at $w_j \to 0$. One gets *hf* μ_j of the polar solute in a non-polar solvent from the following Eq.(2.85) by comparing Eqs.(2.82) and (2.84)

$$\mu_j = \left(\frac{27\varepsilon_o M_j k_B T \beta}{N\rho_i(\varepsilon_i+2)^2 b}\right)^{1/2} \qquad \text{..... (2.85)}$$

where $b = 1/(1+\omega^2\tau_j^2)$ is a dimensionless parameter. The methodology so far achieved in getting τ_j's and μ_j's has been used in Chapters 7, 8 and 10 of the thesis.

2.14.Substituent Polar Groups in a Dipolar Molecule under Low and *hf* Electric Field :

The measured *hf* dipole moment μ_j or static μ_s of a polar liquid molecule may be compared with the theoretical dipole moment μ_{theo} as obtained from the vector addition method of bond length and bond angles of the substituent polar groups attached to the parent molecule to get its conformational structure as displayed in different Chapters of the thesis. The bond length is the distance between the centres of two atomic nuclei when a co-valent bond links two atoms. Structural conformations of the whole molecule are studied in terms of atomic orbital, which often overlaps to form hybridised orbitals and this phenomenon is known as hybridisation. The bond due to overlap of two *s*-orbitals is called σ-bond whereas the sidewise overlap of two half filled *p*-orbitals having a nodal plane forms a π-bond. The bond angle, on the other hand, is the angle between the dipolar axis of the parent molecule and the bond axis of a flexible polar groups or atoms linked with the parent molecule. It depends on the nature of hybridisation due to size and the electro-negativity of the atoms or groups.

The slight disagreement of μ_j and μ_s with μ_{theo} is, however, observed for the presence of various effects suffered by the substituent polar groups under low and *hf* electric fields. The inductive, mesomeric and electromeric effects play the vital role to yield the conformational structure of a dipolar molecule.

The difference in electro-negativity in the atoms of a molecule produces a displacement of electrons towards the more electronegative atoms to induce a certain degree of polarity on the atom. The more or less electronegative atoms acquire a small negative δ^- or positive δ^+ charges. The inductive effect (I-effect) refers to the induced polarity in a molecule as a result of higher electro-negativity of one atom compared to another. Electron attracting groups are $-NO_2$, –F, –Cl, –Br, –I, –OH, $-C_6H_5$ etc which pull electrons away from C-atom (–I effect) while electron releasing groups are $(CH_3)_3C-$, $(CH_3)_2CH-$, CH_3CH_2-, CH_3- etc push electrons towards the C-atom (+I effect).

The mesomeric effect (M-effect) refers to the polarity produced in a molecule as a result of interaction between two π-bonds or a π-bond and lone pair of electrons. It is a permanent effect that is transmitted along the chain of C-atoms linked alternately by single and double bonds in a conjugated compound. Atoms or groups such as $-NO_2$, –C≡N, >C=O etc pull electrons away from C-atom to produce –M effect whereas –Cl, –Br, –I, $-NH_2$, $-NR_2$, –OH, $-OCH_3$ etc pushing electrons towards C-atom are said to have +M effect.

Electromeric effect, on the other hand, is a temporary effect. It involves with the complete transfer of a shared pair of π-electrons to one or other atoms joined by double or triple bonds.

Resonance, however, occurs in a polar molecule in which electrons may oscillate from one position to another. The molecule, as a result of this oscillation, may be said to have resonant

structure, each of which does not differ significantly so far the total energy is concerned. This effect involves with the delocalisation of electron cloud of a molecule by two or more structures differing only in the arrangement of electrons without shifting any atom.

All these effects were taken into account to sketch conformation structures of different dipolar liquids like dimethylsulphoxide, N,N-diethylformamide, N,N-dimethylformamide, N,N-dimethylacetamide, polysubstituted-benzenes, methyl-benzenes, ketones, chloral, ethyltrichloroacetate, trifluoroethanol, trifluoroacetic acid, octanoyl-chloride, disubstituted-benzenes and some normal and isomeric octyl alcohols etc in agreement with the measured μ_j's and μ_s's in the thesis. For all the compounds referred to above, due to their aromaticity the resonance effect combined with inductive effect known as mesomeric effect are important. The so-called mesomeric moments have significant values. These are caused by the permanent polarisation of different substituent groups acting as pusher or puller of electrons towards or away from the electrons of C-atoms attached to the parent compound. The non-polar solvent C_6H_6 unlike CCl_4, *n*-heptane and *n*-hexane is also a cyclic and planar compound having three double bonds and six *p*-electrons on C-atoms. Here π-π interaction or mesomeric effect play the role in calculating μ_{theo}. The reduction or elongation in bond moments evidently occur in almost all the polar liquids by a factor μ_s/μ_{theo} or μ_j/μ_{theo} in order to conform to the exact μ_s or μ_j.

2.15. Chi-squares Fitting Technique :

It is often found that the experimental data set may be involved with errors arising out of Gaussian, binomial, Poison etc known type of distributions. The hypothesis may be tested by comparing the experimental data of the measured dielectric relative permittivities and susceptibilities as a function of w_j's at a given experimental temperature in ^{0}C in disagreement of the assumed theoretical distribution. The parameters of this distribution will not be known from prior considerations. It will have to be estimated from the experimental data. It may be shown that if n parameters are to be determined by the method of maximum likelihood of the limiting distribution of the goodness of fit of chi-squares technique given by:

$$K_n = \sum_{i=1}^{n} \frac{(O_i - E_i)^2}{E_i} \qquad \ldots\ldots (2.86)$$

where ,

O_i = the experimentally measured value of the ith type

E_i = the theoretical value of the ith type. $i = 1, 2, 3\ldots\ldots\ldots n$

This sort of technique has been employed in Chapter 8 to show the material property of the double relaxation phenomena of systems under consideration.

2.16. Material Property of Relaxation Phenomena :

From the prolonged studies on the relaxation mechanism of dipolar liquids by Raiganj [2.34-2.35] and other groups [2.36-2.37] all over the world, it is appearing that the relaxation phenomena may be the material property of the system under consideration. If any system of polar-nonpolar liquid mixture shows double relaxation times at one frequency ω it will show the same τ_1 and τ_2 at all the ω's measurements, because τ's are expected to be independent of ω of the applied alternating electric field. The Eq.(2.73) can be written as:

$$\frac{\chi'_{ij}}{\chi_{oij}} = \frac{1}{2A}\left(2A - \ln\frac{1+\omega^2\tau_2^2}{1+\omega^2\tau_1^2}\right)$$

$$= \frac{1}{2A}\left(\ln\frac{\omega^2\tau_2^2}{\omega^2\tau_1^2} - \ln\frac{1+\omega^2\tau_2^2}{1+\omega^2\tau_1^2}\right)$$

$$= \frac{1}{2A}\left(\ln\frac{\tau_2^2(1+\omega^2\tau_1^2)}{\tau_1^2(1+\omega^2\tau_2^2)}\right) \qquad \ldots\ldots (2.87)$$

From Eqs.(2.74) and (2.87) one can write:

$$\frac{\chi''_{ij}}{\chi'_{ij}} = \frac{2\left[\tan^{-1}(\omega\tau_2) - \tan^{-1}(\omega\tau_1)\right]}{\ln\frac{\tau_2^2(1+\omega^2\tau_1^2)}{\tau_1^2(1+\omega^2\tau_2^2)}} \qquad \ldots\ldots (2.88)$$

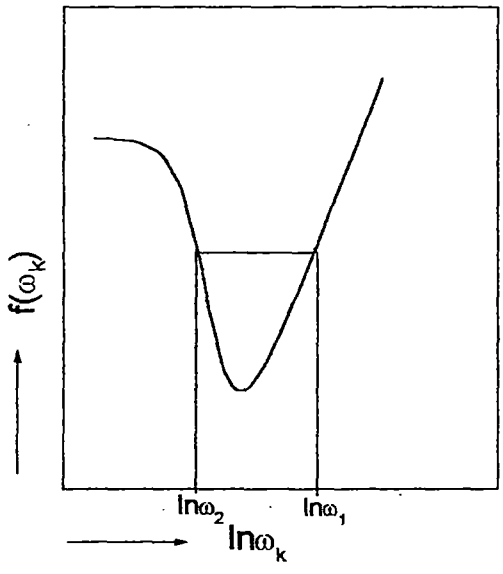

Figure 2.5: Variation of $f(\omega_k)$ with $\ln\omega_k$ for a fixed value of ω

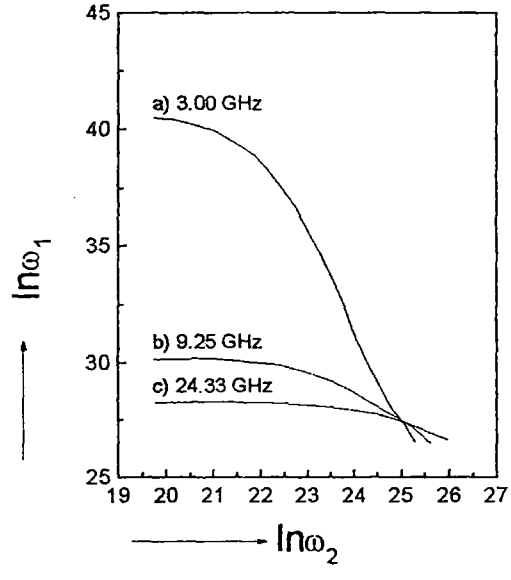

Figure 2.6: Variation of $\ln\omega_1$ against $\ln\omega_2$ of 3-methyl 3-heptanol under 3.00, 9.25 and 24.33 GHz electric field.

Assuming $\tau_1=1/\omega_1$ and $\tau_2=1/\omega_2$ such that $\omega\tau=1$ but $\omega_2<\omega_1$ Eq.(2.88), after simplification becomes [2.37]:

$$\frac{\chi''_{ij}}{\chi'_{ij}}\ln\left(\omega_1^2+\omega^2\right)+2\tan^{-1}\frac{\omega}{\omega_1}=\frac{\chi''_{ij}}{\chi'_{ij}}\ln\left(\omega_2^2+\omega^2\right)+2\tan^{-1}\frac{\omega}{\omega_2} \qquad \ldots..(2.89)$$

The Eq.(2.89) holds good for a number of $\omega_1, \omega_2, \ldots\ldots \omega_k$ i.e,

$$f(\omega_1)=f(\omega_2)=f(\omega_3)=\ldots\ldots\ldots=f(\omega_k)$$

where,

$$f(\omega_k)=\left[\frac{\chi''_{ij}}{\chi'_{ij}}\ln\left(\omega_k^2+\omega^2\right)+2\tan^{-1}\frac{\omega}{\omega_k}\right] \qquad \ldots..(2.90)$$

The term χ''_{ij}/χ'_{ij} of Eq.(2.90) is a function of w_j of a polar solute at a temperature T K and ω of the electric field. $f(\omega_k)$ is, however, made constant for a fixed τ_1 and τ_2 of a system at a given ω by introducing the least squares fitted extrapolated value of $\left(\chi''_{ij}/\chi'_{ij}\right)_{w_j\to 0}$. Eq.(2.90) then becomes:

$$f(\omega_k)=\left[\left(\frac{\chi''_{ij}}{\chi'_{ij}}\right)_{w_j\to 0}\ln\left(\omega_k^2+\omega^2\right)+2\tan^{-1}\frac{\omega}{\omega_k}\right] \qquad \ldots..(2.91)$$

A curve of $f(\omega_k)$ against $\ln\omega_k$ can be obtained by varying ω_k in order to get the arbitrary values of $\ln\omega_2$ and $\ln\omega_1$ ($\omega_2<\omega_1$) for the same $f(\omega_k)$ as sketched in Fig.2.5. Graphs of $\ln\omega_1$ vs $\ln\omega_2$ for different ω as shown in Fig.2.6 are used to obtain the points of intersection which yields the values of τ_2 and τ_1 of the polar molecular liquids. An attempt has been made in Chapter 10 of the thesis for a large number of alcohols which are supposed to behave as polymer type molecules due to their H-bonding to show the material property of the systems.

All these theoretical formulations in Chapter 2, so far derived, have been used to test their validity for a large number of dipolar liquids of different shapes, sizes and structures in all the subsequent chapters of this thesis to enhance the scientific contents of the relaxation phenomena under low and *hf* electric field.

References :

[2.1] J S Dhull and D R Sharma, *J. Phys. D: Appl. Phys.* **15** 2307 (1982)

[2.2] A K Sharma and D R Sharma, *J. Phys. Soc. Japan* **53** 4771 (1984)

[2.3] A K Sharma, D R Sharma and D S Gill, *J. Phys. D: Appl. Phys.* **18** 1199 (1985)

[2.4] A Sharma and D R Sharma, *J. Phys. Soc. Japan* **61** 1049 (1992)

[2.5] A K Jonscher, *Universal Relaxation Law*, Chelsea Dielectrics Press, London (1996)

[2.6] H Fröhlich, *Theory of Dielectrics*, Oxford University Press, London (1949)

[2.7] L Onsager, *J. Am. Chem. Soc.* **58** 1486 (1936)

[2.8] R M Fuoss and J G Kirkwood, *J. Am. Chem. Soc.* **63** 385 (1941)

[2.9] J G Kirkwood, *J. Chem. Phys.* 7 911 (1939)

[2.10] H Eyring, S Glasstone and J K Laidler, *The Theory of Rate Processes*, McGraw-Hill, New York (1941)

[2.11] W Kauzmann, *Reviews of Modern Physics*, **14** 12 (1942)

[2.12] E Bauer, *Cah. Phys.* **20** 1 (1944)

[2.13] R C Basak, S K Sit, N Nandi and S Acharyya, *Indian J. Phys.* **70B** 37 (1996)

[2.14] N Ghosh, A Karmakar, S K Sit and S Acharyya, *Indian J. Pure & Appl. Phys.* **38** 574 (2000)

[2.15] F J Murphy and S O Morgan, *Bull. Syst. Tech. J.* **18** 502 (1939)

[2.16] C P Smyth, *Dielectric Behaviour and Structure*, McGraw-Hill, New York, (1955)

[2.17] M B R Murthy, R L Patil and D K Deshpande, *Indian J. Phys.* **63B** 494 (1989)

[2.18] R C Basak, A Karmakar, S K Sit and S Acharyya, *Indian J. Pure & Appl. Phys.* **37** 224 (1999)

[2.19] K Dutta, A Karmakar, S K Sit and S Acharyya, *Indian J. Pure & Appl. Phys.* **40** 588 (2002)

[2.20] K Dutta, R C Basak, S K Sit and S Acharyya, *J. Molecular Liquids* **88** 229 (2000)

[2.21] U Saha and S Acharyya, *Indian J. Pure & Appl. Phys.* **32** 346 (1994)

[2.22] N Ghosh, R C Basak, S K Sit and S Acharyya, *J. Molecular Liquids* **85** 375 (2000)

[2.23] K Dutta, S K Sit and S Acharyya, *J. Molecular Liquids* **92** 263 (2001)

[2.24] A Budo, *Phys. Z.* **39** 706 (1938)

[2.25] J Crossley, L Glasser and C P Smyth, *J. Chem. Phys.* **55** 2197 (1971)

[2.26] L Glasser, J Crossley and C P Smyth, *J. Chem. Phys.* **57** 3977 (1972)

[2.27] K Bergmann, D M Roberti and C P Smyth, *J. Phys. Chem.* **64** 665 (1960)

[2.28] N E Hill, W E Vaughan, A H Price and M Davies, *Dielectric Properties and Molecular Behaviour*, Van Nostrand Reinhold Co.Ltd. London (1969)

[2.29] J Bhattacharyya, A Hasan, S B Roy and G S Kastha, *J. Phys. Soc. Japan* **28** 204 (1970)

[2.30] U Saha, S K Sit, R C Basak and S Acharyya, *J. Phys. D: Appl. Phys.* **27** 596 (1994)

[2.31] S K Sit, R C Basak, U Saha and S Acharyya, *J. Phys. D: Appl. Phys.* **27** 2194 (1994)

[2.32] A K Jonscher, *Inst. Phys. Conf.*, invited papers edited by CHL Goodman, Canterbury (1980)

[2.33] K Dutta, S K Sit and S Acharyya, *Pramana: J. Phys.* **57** 775 (2001)

[2.34] K Dutta, A Karmakar, L Dutta, S K Sit and S Acharyya, *Indian J. Pure & Appl. Phys.* **40** 801 (2002)

[2.35] N Ghosh, S K Sit, A K Bothra and S Acharyya, *J. Phys. D: Appl. Phys.* **34** 379 (2001)

[2.36] K Higasi, Y Koga and M Nakamura, *Bull. Chem. Soc. Japan* **44** 988 (1971)

[2.37] A Mansing and P Kumar, *J. Phys. Chem.* **69** 4197 (1965)

CHAPTER 3

DOUBLE RELAXATION TIMES, DIPOLE MOMENTS, ENERGY PARAMETERS AND MOLECULAR STRUCTURES OF SOME APROTIC POLAR MOLECULES FROM RELAXATION PHENOMENA

3.1. Introduction :

The absorption of high frequency electric energy by aprotic polar liquids in nonpolar solvents has attracted much attention [3.1-3.2]. Such liquids have wide biological applications and act as building blocks of proteins and enzymes because of their high values of dielectric constants. They showed weak molecular association of monomer or dimer formation under *X*-band (~10 GHz) electric field. Many workers [3.3-3.4] studied their structural and associational aspects in high frequency (*f*) electric field by using the concentration variation method of Gopalakrishna [3.5]. However no attempt has been made so far to observe their double relaxation phenomena in nearly 10 GHz electric field, which seems to be the most effective dispsersive region [3.6] for them.

We, therefore, measured real ε_{ij}' and imaginary ε_{ij}'' parts of complex dielectric constant ε_{ij}^* of liquids (j) like dimethylsulphoxide (DMSO) at 25^0, 30^0, 35^0 and 40^0C; N,N-diethylformamide (DEF) at 30^0C; N,N-dimethylformamide (DMF) and N,N-dimethylacetamide(DMA) at 25^0C in benzene (i) at nearly 10 GHz electric field by a Hewlett Packard Impedance Analyser 4192A together with the static and infinite frequency dielectric constants ε_{oij} (at 1 KHz) and $\varepsilon_{\infty ij}$ $(=n_{Dij}^2)$ by Abbe's refractometer within 1% accuracy [3.7-3.8]. The measured data of Table 3.1 were used to detect their possible existence of double relaxation phenomena by the recently developed single frequency measurement [3.9-3.10] method.

The relaxation times τ_2 and τ_1 due to end over end rotation for the whole molecule as well as its flexible part attached to the parent one were obtained from the slope and intercept of a derived linear equation of $(\varepsilon_{oij}-\varepsilon_{ij}')/(\varepsilon_{ij}'-\varepsilon_{\infty ij})$ with $\varepsilon_{ij}''/(\varepsilon_{ij}'-\varepsilon_{\infty ij})$ as seen graphically in Fig.3.1 for different weight fractions w_j of solutes [3.9-3.10]. The intercepts and slopes of the linear curves of Fig.3.1 together with % of errors in terms of correlation coefficients '*r*' are placed in Table 3.2. τ_1 in Table 3.2 is very close to reported τ [3.5]. The relative contributions c_1 and c_2 towards dielectric relaxation due to τ_1 and τ_2 are calculated from the values of $x=(\varepsilon_{ij}'-\varepsilon_{\infty ij})/(\varepsilon_{oij}-\varepsilon_{\infty ij})$ and $y=\varepsilon_{ij}''/(\varepsilon_{oij}-\varepsilon_{\infty ij})$ at $w_j \rightarrow 0$ from their respective plots with w_j's in Figs.3.2 and 3.3 respectively. The estimated values of c_1 and c_2 together with those from Fröhlich's equations [3.11-3.12] are presented in Table3.3 for comparison.

The dipole moments μ_2 and μ_1 of the whole and the flexible part attached to the parent molecule due to τ_2 and τ_1 in terms of slopes β of high frequency conductivities σ_{ij} against w_j's [3.13] of Fig.3.4 were estimated to present in Table 3.4. The variation of μ_2 and μ_1 of DMSO with temperature and the estimated thermodynamic energy parameters from $\ln(\tau_2 T)$ and $\ln(\tau_1 T)$ against $1/T$ respectively supports the rotation of flexible parts of molecule under GHz electric field. We have also calculated the static experimental parameter X_{ij} involved with ε_{oij} and n_{Dij}^2 at different

Table 3.1: Concentration variation of dielectric relaxation parameters like real part of dielectric constant (ε_{ij}'), dielectric loss (ε_{ij}''), static dielectric constant (ε_{oij}), optical dielectric constant ($\varepsilon_{\infty ij}$) of some aprotic polar liquids in benzene at different temperatures measured under high frequency electric field of nearly 10 Ghz.

Temperature in ^{0}C	Weight fraction w_j	ε_{ij}'	ε_{ij}''	ε_{oij} at 1 KHz	$\varepsilon_{\infty ij}=n^2_{Dij}$
		DMSO in C_6H_6 at 9.174 GHz			
	0.0022	2.311	0.0280	2.3230	2.2499
	0.0043	2.342	0.0420	2.3624	2.2530
25	0.0047	2.350	0.0460	2.3731	2.2550
	0.0069	2.381	0.0616	2.4173	2.2579
	0.0086	2.414	0.0798	2.4602	2.2620
	0.0022	2.310	0.0274	2.3210	2.2470
	0.0043	2.341	0.0400	2.3610	2.2515
30	0.0047	2.348	0.0440	2.3720	2.2500
	0.0069	2.370	0.0526	2.4045	2.2545
	0.0086	2.390	0.0648	2.4362	2.2560
	0.0022	2.290	0.0234	2.2993	2.2300
	0.0043	2.312	0.0330	2.3400	2.2320
35	0.0047	2.316	0.0360	2.3470	2.2335
	0.0069	2.350	0.0496	2.3960	2.2396
	0.0086	2.370	0.0580	2.4270	2.2440
	0.0022	2.270	0.0170	2.2849	2.2201
	0.0043	2.302	0.0282	2.3300	2.2246
40	0.0047	2.304	0.0286	2.3350	2.2256
	0.0069	2.338	0.0420	2.3838	2.2297
	0.0086	2.350	0.0500	2.4120	2.2345
		DEF in C_6H_6 at 9.695 GHz			
	0.0023	2.2780	0.0256	2.3067	2.0939
30	0.0042	2.2900	0.0288	2.3336	2.1141
	0.0079	2.3140	0.0384	2.3965	2.1543
	0.0095	2.3260	0.0448	2.4208	2.1727
		DMF in C_6H_6 at 9.987 GHz			
	0.0027	2.324	0.0256	2.3446	2.2498
25	0.0036	2.339	0.0302	2.3680	2.2518
	0.0048	2.359	0.0386	2.3968	2.2545
	0.0063	2.387	0.0484	2.4434	2.2579
		DMA in C_6H_6 at 9.987 GHz			
	0.0026	2.3250	0.0213	2.3633	2.2432
25	0.0045	2.3475	0.0278	2.3988	2.2429
	0.0056	2.3625	0.0330	2.4278	2.2427
	0.0066	2.3795	0.0381	2.4508	2.2425

w_j's of solutes [3.14] (Table 3.1). The slopes a_1's of X_{ij}–w_j curves of Fig.3.5 were then used to calculate static dipole moment μ_s. All the μ_s's together with the slopes of X_{ij}–w_j curves are placed in Table 3.5. The μ_s's of Table 3.5 when compared with μ_2 and μ_1 of Table 3.4 shows that μ_s agrees with μ_1. The conformational structures of molecules in Fig.3.6 were obtained from μ_{cal} in terms of reduced bond moments by a factor μ_s/μ_{theo} in order to take into account of the mesomeric and inductive effects of the substituent polar groups [3.14]. The theoretical dipole moment μ_{theo}'s of

polar molecules are, however, derived from the available bond moments and bond angles of polar groups of the parent molecules.

3.2. Experimental Set Up :

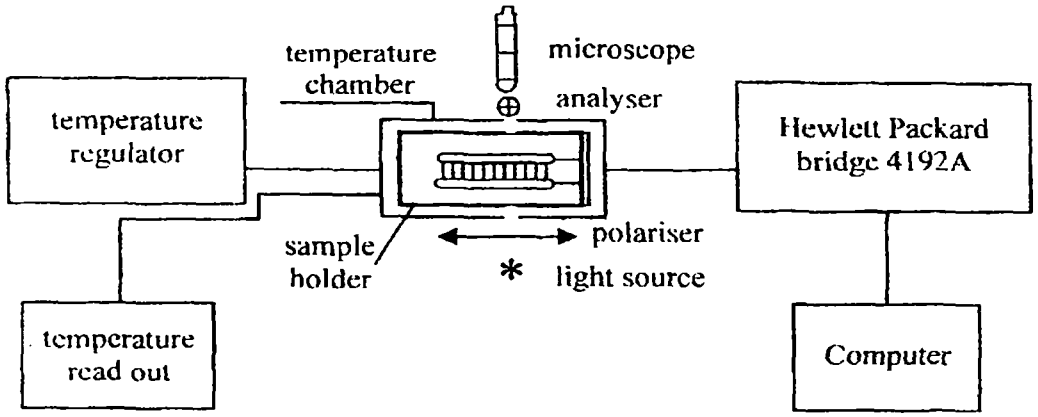

Figure A : Block diagram of the experimental setup used for dielectric measurements

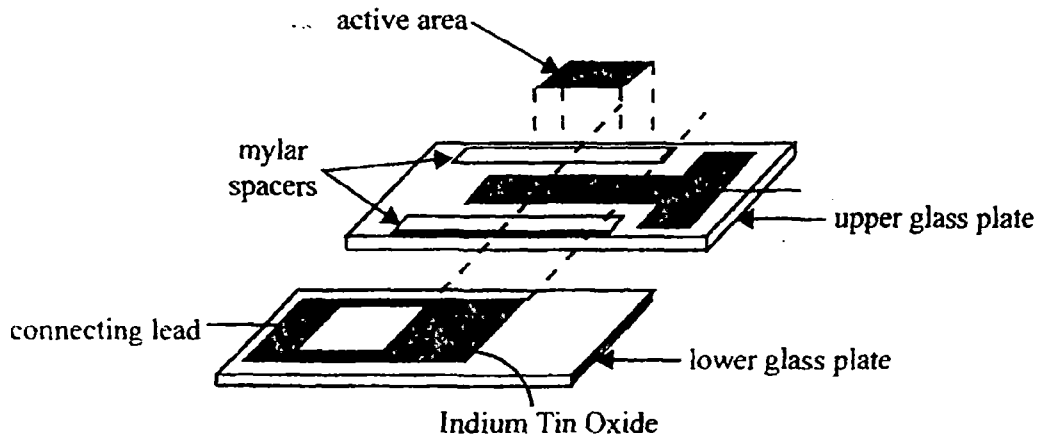

Figrure B : Inner surfaces of the lower and upper conducting glass plates.

The Block diagram for the measurement of dielectric relaxation solution (ij) data and experimental details [3.7] has been shown in the adjoining Fig.A. It consists of sample holder, temperature chamber, temperature controller and a Hewlett Packard Bridge 4192A. A cell (Fig.B) with a sample holder consists of two glass plates coated with conducting Indium Tin Oxide (ITO) in their inner surfaces. They are separated by Mylar spacer of 40 micro metre thicknesses and kept on temperature chamber Mettler Hot Stage FP 52.

The Hewlett Packard Impedance Analyser (HP 4192A) measures the complex impedance of the cell to evaluate capacitance and conductance values. Air capacitance C_0 of the cell can be written as:

$$C_o = C_L + C_S \qquad \text{.....(3.1)}$$

where C_L is the capacitance of the empty cell excluding stray capacitance C_S. When the cell is filled with the sample of known dielectric constant ε_{ij} the measured capacitance will be:

$$C = \varepsilon_{ij} C_L + C_S \qquad \text{.....(3.2)}$$

The real part of the dielectric permittivity of the sample is given by:

$$\varepsilon'_{ij} = \frac{(C - C_S)}{(C_o - C_S)} \qquad \text{.....(3.3)}$$

The dielectric loss due to absorbtion is

$$\varepsilon''_{ij} = \frac{G_{ij}}{2\pi f C_o} \qquad \text{.....(3.4)}$$

where G_{ij} and f are conductance of the solutions and frequency of the electric field.

The ITO electrode in GHz does not yield dielectric properties of the solution but rather those of the electrode materials because ITO is not sufficiently a good conductor and appropriate only upto a few MHz. The frequency range of the instrument HP 4192A was 5Hz to 13 MHz. ε_{ij}' and ε_{ij}'' for a given w_j of solute under a few MHz frequencies were carefully measured to construct the Cole-Cole semicircular arc. Both $\varepsilon_{\infty ij}$ and ε_{oij} were then accurately obtained along with ε_{ij}' and ε_{ij}'' within 5% accuracies at nearly 10 GHz to report in Table 3.1. The frequencies as quoted in Table 3.1 were found out from $(d\varepsilon_{ij}''/df)=0$ in $\varepsilon_{ij}''=a+bf+cf^2$ at which ε_{ij}' were again located. $\varepsilon_{\infty ij}$ and ε_{oij} were also verified by Abbe's refractometer and HP 4192A at 1KHz within 1% accuracy.

The solvent C_6H_6 (Spec.pure) and aprotic liquids like DMSO, DMF, DEF and DMA (E Merck, Bombay) were used after distillation. The solutions of different concentrations were made by mixing a certain weight of solute in a solvent of known weight. They were kept in dried and clean capsules for the measurement.

3.3. Theoretical Formulations :

3.3.1. Relaxation Times τ_2 and τ_1 :

The dielectric relaxation parameters under GHz electric field for two mutually independent Debye type dispersions [3.11] can be given by:

$$\frac{\varepsilon'_{ij}-\varepsilon_{\infty ij}}{\varepsilon_{oij}-\varepsilon_{\infty ij}}=c_1\frac{1}{1+\omega^2\tau_1^2}+c_2\frac{1}{1+\omega^2\tau_2^2} \qquad \ldots\ldots(3.5)$$

$$\frac{\varepsilon''_{ij}}{\varepsilon_{oij}-\varepsilon_{\infty ij}}=c_1\frac{\omega\tau_1}{1+\omega^2\tau_1^2}+c_2\frac{\omega\tau_2}{1+\omega^2\tau_2^2} \qquad \ldots\ldots(3.6)$$

Here c_1 and c_2 are the relative contributions towards dielectric relaxations due to τ_1 and τ_2 respectively.

Substituting $(\varepsilon_{ij}'-\varepsilon_{\infty ij})/(\varepsilon_{oij}-\varepsilon_{\infty ij})=x$, and $\varepsilon_{ij}''/(\varepsilon_{oij}-\varepsilon_{\infty ij})=y$, Eqs.(3.5) and (3.6) become:

$$x=c_1a_1+c_2a_2 \qquad \ldots\ldots(3.7)$$

$$y=c_1b_1+c_2b_2 \qquad \ldots\ldots(3.8)$$

where $a=1/(1+\alpha^2)$, $b=\alpha/(1+\alpha^2)$ and $\omega\tau=\alpha$. The suffices *1* and *2* with a and b are related to τ_1 and τ_2 respectively. Solving Eqs.(3.7) and (3.8) one gets:

$$c_1=\frac{(x\alpha_2-y)(1+\alpha_1^2)}{\alpha_2-\alpha_1} \qquad \ldots\ldots(3.9)$$

$$c_2=\frac{(y-x\alpha_1)(1+\alpha_2^2)}{\alpha_2-\alpha_1} \qquad \ldots\ldots(3.10)$$

provided $\alpha_2-\alpha_1\neq 0$ and $\alpha_2>\alpha_1$. Now, using $c_1+c_2=1$; one gets from Eqs.(3.9) and (3.10)

$$\frac{\varepsilon_{oij}-\varepsilon'_{ij}}{\varepsilon'_{ij}-\varepsilon_{\infty ij}}=\omega(\tau_1+\tau_2)\frac{\varepsilon''_{ij}}{\varepsilon'_{ij}-\varepsilon_{\infty ij}}-\omega^2\tau_1\tau_2 \qquad \ldots\ldots(3.11)$$

which is a straight line of $(\varepsilon_{oij}-\varepsilon_{ij}')/(\varepsilon_{ij}'-\varepsilon_{\infty ij})$ against $\varepsilon_{ij}''/(\varepsilon_{ij}'-\varepsilon_{\infty ij})$ with intercept $-\omega^2\tau_1\tau_2$ and slope $\omega(\tau_1+\tau_2)$. Here ω=angular frequency of the applied electric field of frequency f in GHz. The Eq.(3.11) is fitted with the measured ε_{ij}', ε_{ij}'', ε_{oij} and $\varepsilon_{\infty ij}$ of Table 3.1 for each aprotic polar liquid in C_6H_6 for different w_j's at a given temperature T K. The slope and intercept were used to

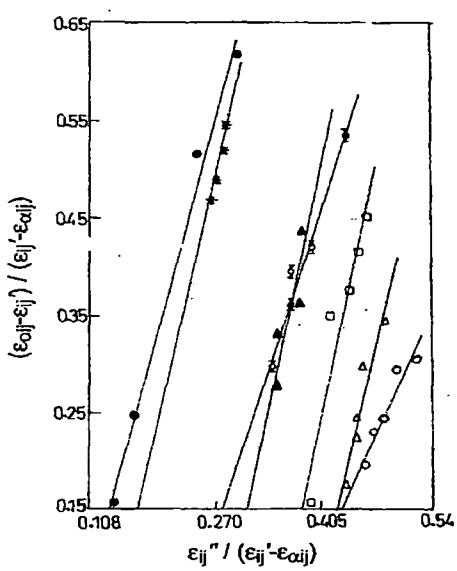

Figure 3.1: Variation of $(\varepsilon_{oij}-\varepsilon_{ij}')/(\varepsilon_{ij}'-\varepsilon_{\alpha ij})$ against $\varepsilon_{ij}''/(\varepsilon_{ij}'-\varepsilon_{\alpha ij})$ for different weight fraction w_j of some aprotic polar liquids in benzene.

DMSO (–O–,–Δ–,–□–,–Ω–) at 25°C, 30°C, 35°C, and 40°C respectively; DEF (–●–) at 30°C; DMF (–▲–) at 25°C; DMA (–✶–) at 25°C.

yield τ_1 and τ_2 as shown in Table 3.2, with the reported τ [3.5].

Table 3.2: The estimated intercepts and slopes of straight line equation of $(\varepsilon_{oij}-\varepsilon_{ij}')/(\varepsilon_{ij}'-\varepsilon_{\infty ij})$ against $\varepsilon_{ij}''/(\varepsilon_{ij}'-\varepsilon_{\infty ij})$, Correlation coefficients (r), % of error involved in regression technique, the most probable relaxation time $\tau_o=\sqrt{\tau_1\tau_2}$, and reported τ of some non-spherical aprotic polar liquids under *hf* electric field of nearly 10 GHz.

System with sl. no	Temp in ^{0}C	Intercepts and slopes of Eq.(3.11)		Correl. Coeff 'r'	% of error	Estimated values of τ_2 and τ_1 in p-secs		$\tau_o=\sqrt{\tau_1\tau_2}$	Reported τ in p sec (GK Method)
(I)DMSO in C_6H_6 M_j=78 gm	25	0.5671	1.6817	0.9605	2.34	21.08	8.10	13.07	5.37
(II)DMSO in C_6H_6 M_j=78 gm	30	1.3024	3.4358	0.9429	3.35	52.11	7.53	19.81	4.96
(III)DMSO in C_6H_6 M_j=78 gm	35	1.2899	3.8162	0.9377	3.64	59.73	6.51	19.72	4.70
(IV)DMSO in C_6H_6 M_j=78 gm	40	0.5376	2.4880	0.9862	0.83	39.04	4.15	12.73	4.33
(V)DEF in C_6H_6 M_j=101.15 gm	30	0.2592	3.0829	0.9933	0.45	49.21	1.42	8.36	2.42
(VI)DMF in C_6H_6 M_j=73 gm	25	1.0183	3.8186	0.8896	7.03	56.28	4.60	16.09	5.09
(VII)DMA in C_6H_6 M_j=87 gm	25	0.4936	3.7032	0.9011	6.34	56.81	2.21	11.20	6.53

Fröhich's theory of dielectric relaxation is based on the concept of a distribution of relaxation times with a minimum τ_1 and a maximum τ_2 values. The double relaxation method is, however, concerned with these two discrete relaxation times as the limiting values of Fröhlich's theory [3.12]. c_1 and c_2 towards dielectric relaxations are, therefore, calculated from the theoretical formulations of x and y of Fröhlich [3.12].

$$x=\frac{\varepsilon_{ij}'-\varepsilon_{\infty ij}}{\varepsilon_{oij}-\varepsilon_{\infty ij}}=1-\frac{1}{2A}\ln\left(\frac{1+e^{2A}\omega^2\tau_s^2}{1+\omega^2\tau_s^2}\right) \qquad \ldots\ldots(3.12)$$

$$y=\frac{\varepsilon_{ij}''}{\varepsilon_{oij}-\varepsilon_{\infty ij}}=\frac{1}{A}\left[\tan^{-1}(e^A\omega\tau_s)-\tan^{-1}(\omega\tau_s)\right] \qquad \ldots\ldots(3.13)$$

and are shown in Table 3.3. Here τ_S =small limiting relaxations time $=\tau_1$ and A = Fröhlich parameter $=\ln(\tau_2/\tau_1)$. 'A' is a constant which can be expressed in terms of the difference in activation energies E_2 and E_1 of a rotating unit at a given temperature because $\tau_2/\tau_1=\exp[(E_2-E_1)/k_BT]$ where k_B is the

Boltzmann constant. The values of x and y at $w_j \rightarrow 0$ from the graphical plots of Figs.3.2 and 3.3 can also be had to get c_1 and c_2. The L.H.S. of Bergmann's equatioins [3.11] are fixed for once estimated τ_1 and τ_2 from the intercept and slope of Eq.(3.11).

Table 3.3: Fröhlich parameter A, relative contributions c_1 and c_2 due to τ_1 and τ_2, theoretical values of x and y due to Fröhlich Eqs.(3.12) and (3.13) and those by graphical method at infinite dilution for some aprotic polar liquids at different and single temperature under *hf* electric field.

System with sl. no	Temp in ^{0}C	Fröhlich para meter A	Theoretical values of x and y from Eqs.(3.12) and (3.13)		Theoretical values of c_1 and c_2 from Eqs.(3.9) and (3.10)		Estimated values of x and y at $w_j \rightarrow 0$ from Figs.3.2 and 3.3		Estimated values of c_1 and c_2 from graphical technique	
			x	y	c_1	c_2	x	y	c_1	c_2
(I) DMSO in C_6H_6	25	0.9565	0.629	0.466	0.486	0.569	0.892	0.363	1.174	-0.178
(II) DMSO in C_6H_6	30	1.9345	0.449	0.434	0.423	0.934	0.900	0.338	1.094	-0.206
(III) DMSO in C_6H_6	35	2.2165	0.454	0.419	0.425	1.043	0.834	0.295	0.958	-0.075
(IV) DMSO in C_6H_6	40	2.2415	0.610	0.409	0.507	0.794	0.848	0.225	0.885	0.067
(V) DEF in C_6H_6	30	3.5454	0.677	0.328	0.588	0.924	0.988	0.055	1.006	-0.104
(VI) DMF in C_6H_6	25	2.5043	0.497	0.405	0.451	1.086	0.872	0.210	0.959	-0.173
(VII) DMA in C_6H_6	25	3.2467	0.600	0.357	0.530	1.096	0.736	0.126	0.743	0.096

3.3.2. High Frequency Dipole Moments μ_1, μ_2 of τ_1, τ_2 :

The high frequency complex conductivity σ_{ij}^* of liquid mixture is expressed by $\sigma_{ij}^* = \sigma_{ij}' + j\sigma_{ij}''$ while the total conductivity is

$$\sigma_{ij} = \frac{\omega}{4\pi}\left(\varepsilon_{ij}'^2 + \varepsilon_{ij}''^2\right)^{1/2} \qquad \ldots\ldots (3.14)$$

as a function of w_j. Although ε_{ij}'' offers resistance to polarisation, still in the *hf* region $\varepsilon_{ij}' \gg \varepsilon_{ij}''$.

The real part of *hf* conductivity is [3.13]:

$$\sigma_{ij}' = \frac{N\rho_{ij}\mu_j^2 F_{ij}}{3k_B T M_j}\left(\frac{\omega^2\tau}{1+\omega^2\tau^2}\right)w_j$$

which on differentiation with respect to w_j and at $w_j \to 0$ yields:

$$\left(\frac{d\sigma'_{ij}}{dw_j}\right)_{w_j \to 0} = \frac{N\rho_i \mu_j^2 F_i}{3k_B T M_j}\left(\frac{\omega^2\tau}{1+\omega^2\tau^2}\right) \qquad \ldots\ldots(3.15)$$

where F_{ij}=the local field of the solution=$(\varepsilon_{ij}+2)^2/9$. F_{ij} Becomes F_i and ρ_{ij} tends to ρ_i at $w_j \to 0$, where $F_i=(\varepsilon_i+2)^2/9$. ε_i and ρ_i are the dielectric constant and density of the solvent respectively. The other symbols carry usual significance [3.9-3.10].

Again, since $\sigma_{ij}=(\omega\varepsilon_{ij}'/4\pi)$ we have

$$\sigma_{ij} = \sigma_{\infty ij} + \frac{1}{\omega\tau}\sigma'_{ij}$$

or,

$$\left(\frac{d\sigma'_{ij}}{dw_j}\right)_{w_j \to 0} = \omega\tau\left(\frac{d\sigma_{ij}}{dw_j}\right)_{w_j \to 0} = \omega\tau\beta \qquad \ldots\ldots(3.16)$$

where β is the slope of σ_{ij}–w_j curve at $w_j \to 0$.

Table 3.4: The estimated coefficients α, β and γ of σ_{ij}–w_j curves (Fig.3.4), dimensionless parameters b_2 and b_1, dipole moments μ_j's in Debye of some non-spherical aprotic polar liquids in benzene under *hf* electric field of nearly 10 GHz at single and different temperatures.

System with sl. no. & mol. wt.	Temp. in ^{0}C	Coefficients α, β and γ of $\sigma_{ij} \times 10^{-10}=\alpha+\beta w_j+\gamma w_j^2$ in $\Omega^{-1}cm^{-1}$			Dimensionless parameters		Estimated dipole moments in Debye		Reported μ_j in Debye
					b_2	b_1	μ_2	μ_1	
(I) DMSO in C_6H_6 M_j=78 gm	25	1.047	5.649	157.35	0.4040	0.8212	4.67	3.28	3.79
(II) DMSO in C_6H_6 M_j=78 gm	30	1.043	8.180	-231.74	0.0999	0.8416	11.47	3.95	3.83
(III) DMSO in C_6H_6 M_j=78 gm	35	1.040	4.158	164.83	0.0779	0.8767	9.38	2.80	4.04
(IV) DMSO in C_6H_6 M_j=78 gm	40	1.023	8.897	-274.83	0.1650	0.9459	9.55	3.99	4.11
(V) DEF in C_6H_6 M_j=101.15 gm	30	1.098	2.839	32.45	0.1002	0.9926	7.47	2.38	3.88
(VI) DMF in C_6H_6 M_j=73 gm	25	1.141	6.544	245.95	0.0743	0.9232	10.88	3.09	3.62
(VII) DMA in C_6H_6 M_j=87 gm	25	1.153	1.884	533.11	0.0729	0.9811	6.43	1.75	3.37

From Eqs.(3.15) and (3.16) one gets

$$\mu_j = \left(\frac{27 k_B T M_j}{N \rho_i (\varepsilon_i + 2)^2} \frac{\beta}{\omega b} \right)^{1/2} \quad \ldots\ldots (3.17)$$

in order to obtain μ_1 or μ_2 in terms of b_1 and b_2 where b_1 and b_2 are the dimensionless parameters involved with τ_1 and τ_2 i.e,

$$b_1 = \frac{1}{1+\omega^2 \tau_1^2} \text{ and } b_2 = \frac{1}{1+\omega^2 \tau_2^2} \quad \ldots\ldots (3.18)$$

Both b_1 and b_2 as well as the coefficients α, β and γ of σ_{ij}– w_j equations in Fig.3.4 are shown in Table 3.4 together with μ_1 and μ_2 of the flexible part and the whole molecule of a polar liquid.

Table 3.5: Coefficients a_o, a_1 and a_2 in equation $X_{ij}=a_o+a_1 w_j+a_2 w_j^2$. static dipole moment μ_s in Debye and theoretical dipole moment μ_{theo} by considering inductive and mesomeric moments of substituent polar group of some aprotic polar liquids in benzene.

System with sl. no. & mol. wt.	Temp in ^{0}C	Coefficients a_o, a_1 and a_2 of $X_{ij} = a_o + a_1 w_j + a_2 w_j^2$			μ_s in Debye	μ_{theo} in Debye	μ_{cal} in Debye (corrected)	μ_s/μ_{theo}
(I) DMSO in C_6H_6 M_j= 78 gm	25	0.0022	0.7756	20.935	3.19	4.55	3.20	0.70
(II) DMSO in C_6H_6 M_j= 78 gm	30	0.0019	1.0315	-17.183	3.72	4.55	3.72	0.82
(III) DMSO in C_6H_6 M_j= 78 gm	35	0.0018	0.9346	0.000	3.58	4.55	3.58	0.79
(IV) DMSO in C_6H_6 M_j= 78 gm	40	0.0010	1.1913	-23.282	4.08	4.55	4.08	0.90
(V) DEF in C_6H_6 M_j= 101.15 gm	30	0.0116	0.2047	0.000	1.89	3.99	1.89	0.47
(VI) DMF in C_6H_6 M_j= 73 gm	25	0.0028	0.7301	61.438	2.99	3.82	2.99	0.78
(VII) DMA in C_6H_6 M_j= 87 gm	25	0.0044	0.6545	53.798	3.09	4.02	3.09	0.77

3.3.3. Static Dipole Moments :

The Debye equation for a polar nonpolar liquid mixture of w_j of a polar liquid under static or low frequency electric field at a given T K is [3.14].

$$\frac{\varepsilon_{oij} - n_{Dij}^2}{(\varepsilon_{oij}+2)(n_{Dij}^2+2)} = \frac{\varepsilon_{oi} - n_{Di}^2}{(\varepsilon_{oi}+2)(n_{Di}^2+2)} + \frac{4\pi N \mu_s^2 \rho_i}{27 k_B T M_j} w_j (1-\gamma w_j)^{-1}$$

or,

$$X_{ij} = X_i + \frac{4\pi N\mu_s^2\rho_i}{27k_BTM_j}w_j + \frac{4\pi N\mu_s^2\rho_i}{27k_BTM_j}\gamma w_j^2 + \ldots\ldots \qquad \ldots\ldots (3.19)$$

where X_{ij} and X_i are the static experimental parameters of the solution and solvent. $\gamma=(1-\rho_i/\rho_j)$, ρ_i and ρ_j are densities of pure solvent and solute respectively. The usual variation of X_{ij} with w_j is of the form:

$$X_{ij} = a_o + a_1 w_j + a_2 w_j^2 \qquad \ldots\ldots (3.20)$$

satisfying the experimental curves of Fig.3.5. The coefficients a_0, a_1 and a_2 of Eq.(3.20) with the measured data of Table 3.1 were, however, calculated and are placed in Table 3.5. Equating the first power of w_j of Eqs.(3.19) and (3.20) and neglecting terms of higher powers of w_j for their involvement with various interactions [3.14] one gets the static μ_s from:

$$\mu_s = \left(\frac{27k_BTM_j}{4\pi N\rho_i}a_1\right)^{1/2} \qquad \ldots\ldots (3.21)$$

in order to present them in Table 3.5 for comparison with μ_1 and μ_2 of Table 3.4 in terms of τ_1 and τ_2.

3.4. Results and Discussions :

The variations of experimental $(\varepsilon_{oij}-\varepsilon_{ij}')/(\varepsilon_{ij}'-\varepsilon_{\infty ij})$ with $\varepsilon_{ij}''/(\varepsilon_{ij}'-\varepsilon_{\infty ij})$ at different w_j's of solutes displayed in Fig.3.1 on fitted lines are derived to be linear as predicted by Eq.(3.11). The slopes and intercepts of Eq.(3.11) for aprotic polar liquids in C_6H_6 are presented in Table 3.2 along with the estimated τ_2 and τ_1. The linear variation is supported by the correlation coefficient 'r' and the corresponding % of errors placed in Table 3.2 in getting the straight lines of Fig.3.1. The errors within 10% indicate probably the accurate measurements of data of Table 3.1.

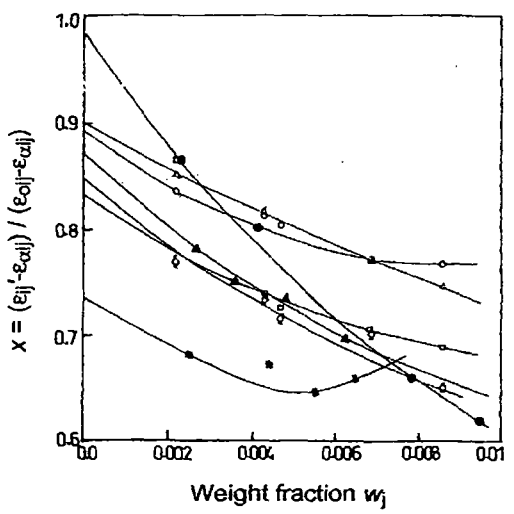

Figure 3.2: Variation of measured $x=(\varepsilon_{ij}'-\varepsilon_{\infty ij})/(\varepsilon_{oij}-\varepsilon_{\infty ij})$ with w_j of some aprotic polar liquids.

DMSO (–O–,–Δ–,–□–,–Ω–) at 25°C, 30°C, 35°C, and 40°C respectively; DEF (–●–) at 30°C; DMF (–▲–) at 25°C; DMA (–✶–) at 25°C

It is evident from Fig.3.1 that all the straight lines of DMSO in C_6H_6 shift towards the origin as the temperature increases from 25°C to 40°C. This sort of behaviour of DMSO invites a further study to see the existence of single relaxation at higher temperature. So, like electric field frequency (*f*), temperature is also a factor for such behaviour of molecules [3.10]. All the liquids show double relaxation times τ_2 and τ_1 as evident from the negative intercepts of the curves. τ_1's of the molecules [3.2-3.3] agree well with the reported τ in Table 3.2 due to Gopalakrishna's method [3.15-3.16]. It signifies that the electric field of 10 GHz frequency is the most effective dispersive region [3.6] for probable rotations of the flexible parts of these molecules [3.14]. Unlike τ_1's of DMSO; τ_2's are found to increase with temperature. The linear equation of $\ln(\tau_1 T)$ and $\ln(\tau_2 T)$ with $1/T$ were found out by [3.17]:

$$\ln(\tau_1 T) = -32.1273 + 3.6861 \times 10^3 (1/T)$$

$$\ln(\tau_2 T) = -4.8261 - 4.0995 \times 10^3 (1/T)$$

Indicating that τ_1 obeys Eyring's rate process. The energy parameters like enthalpy of activation ΔH_{τ_1}=7.32 Kcal/mole and ΔH_{τ_2} = −8.13 Kcal/mole; entropy of activation ΔS_{τ_1} are 16.79, 16.50, 16.36, 16.84 Cal/mole/K and ΔS_{τ_2} are −36.96, −38.34, −38.21, −36.98 Cal/mole/K. The corresponding free energy of activation ΔF_{τ_1} and ΔF_{τ_2} are 2.32, 2.32, 2.28, 2.05 and 2.88, 3.49, 3.64, 3.44 Kcal/mole at 25°, 30°, 35° and 40°C respectively. The data thus obtained confirm the whole molecular rotation under 10 GHz electric field as a cooperative process while the reverse is true for rotation of the flexible group.

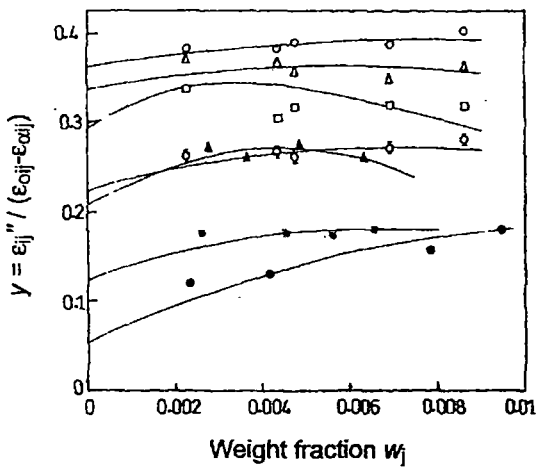

Figure 3.3: Variation of measured $y = \varepsilon_{ij}''/(\varepsilon_{oij} - \varepsilon_{\infty ij})$ with w_j of some aprotic polar liquids.

DMSO (–O–,–Δ–,–□–,–Q–) at 25°C, 30°C, 35°C, and 40°C respectively; DEF (–●–) at 30°C; DMF (–▲–) at 25°C; DMA (–✶–) at 25°C

The increase of τ_2 with the rise of temperature is due to elongation of size for monomer [3.18] formation with C_6H_6 (see Fig.3.6).

For aprotic polar molecules of greater complexity where a few experimental data are available under a single frequency electric field (Table 3.1) a continuous distribution of τ between two limiting values could be used [3.11]. The c_1 and c_2 values towards dielectric relaxations in terms of estimated τ_1 and τ_2 were, therefore, calculated from x and y of Fröhlich's Eqs.(3.12) and (3.13)

based on distribution of relaxation times. They were also obtained from $x=(\varepsilon_{ij}'-\varepsilon_{\infty ij})/(\varepsilon_{oij}-\varepsilon_{\infty ij})$ and $y=\varepsilon_{ij}''/(\varepsilon_{oij}-\varepsilon_{\infty ij})$ at $w_j\rightarrow 0$ from the graphical plots of Figs.3.2 and 3.3 as presented in Table 3.3. The explanation of the nature of variation of x and y with w_j in Figs.3.2 and 3.3 is that τ increases with w_j [3.19] the R.H.S. of Bergmann's Eqs.(3.5) and (3.6) become concave and convex cutting the ordinate axes to yield x and y respectively at $w_j\rightarrow 0$. As seen from Table 3.3; c_1 and c_2 for Fröhlich's method are positive in almost all cases. But c_2 is negative for graphical method probably due to the inertia of the flexible parts of the polar groups of the molecules [3.9].

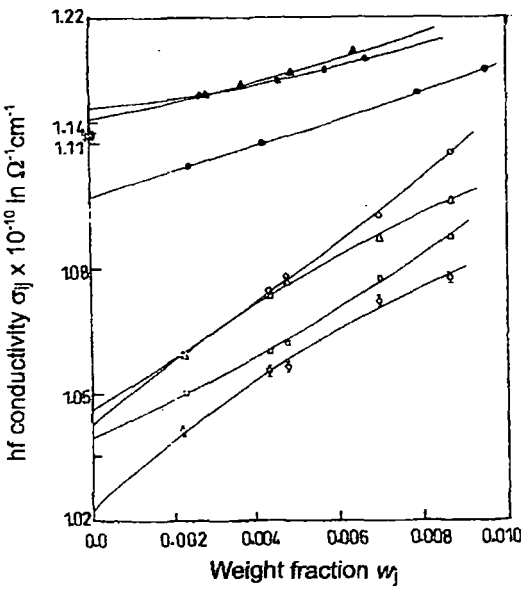

Figure 3.4: Variation of σ_{ij} with w_j of polar liquids.

DMSO (–O–,–Δ–,–□–,–Q–) at 25°C, 30°C, 35°C, and 40°C respectively; DEF (–●–) at 30°C; DMF (–▲–) at 25°C; DMA (–✶–) at 25°C

The values of μ_2 and μ_1 in terms of b's involved with τ_2's, τ_1's and slopes β's of σ_{ij}–w_j curves of Fig.3.4 were estimated from Eq.(3.17) and placed in Table 3.4. The variation of σ_{ij} with w_j are parabolic governed by α, β and γ coefficients probably due to solute-solvent associations [3.2-3.3]. The polar liquid in a given nonpolar solvent behaves as a bound charged species due to polarisation under GHz electric filed in order to have very large conductivity σ_{ij} of the order of 10^{10} $\Omega^{-1}cm^{-1}$ for different w_j's although they are insulators. They are found to decrease with the rise of temperature for DMSO for the presence of $(\rho_i F_i/T)$ in Eq.(3.15) in the limit $w_j=0$ [3.20]. It is interesting to note that μ_1 due to flexible part of the molecule agree well with the reported μ's [3.2-3.3] of Gopalakrishna's method [3.15-3.16]. This indicates that a part of the molecule is rotating under GHz electric field [3.14]. μ_2's are found to be higher in magnitudes for larger values of τ_2's according to Eq.(3.17). Both μ_2 and μ_1 vary with temperature in °C for DMSO in C_6H_6.

$$\mu_2 = -67.35 + 4.56t - 0.066t^2$$

$$\mu_1 = 8.20 - 0.32t + 0.005t^2$$

μ_2 of the parent molecule attains maximum value of 11.41 D at 34.5°C with zero dipole moments at 21.4°C and 47.7°C respectively due to monomer formation [3.2-3.3] with C_6H_6 ring (see Fig.3.6).

The degree of solubility of solutions was kept fairly constant at all temperatures and for the low concentrations of binary mixtures (Table 3.1), dimer formation [3.1-3.4] is not expected. μ_I on the other hand, decreases to a minimum value of 3.08 D at 32°C exhibiting the dimer formation of the flexible parts of their active involvement in rotation under 10 GHz electric field, unlike the whole molecule.

The static μ_s's of these liquids are also calculated from Eq.(3.21) with the measured data (Table 3.1) in terms of linear coefficients a_1's of the static experimental parameter X_{ij} against w_j curves of Fig.3.5. The coefficients a_0, a_1 and a_2 of the curves with the estimated μ_s are presented in Table 3.5. All the curves are found to be of almost same intercepts and slopes for DMSO in C_6H_6 at different temperatures signifying the fact that the static polarisability is nearly constant at all temperatures. The curves of X_{ij}–w_j in case of DMF and DMA at 25°C are, however, parabolic in nature probably due to the presence of the substituent –CH_3 group attached to the parent molecules under identical environment. But X_{ij} varies with w_j linearly in case of DEF at 30°C. All these curves in Fig.3.5 with the computed μ_s's suggest that the measured data of Table 3.1 are more than accurate.

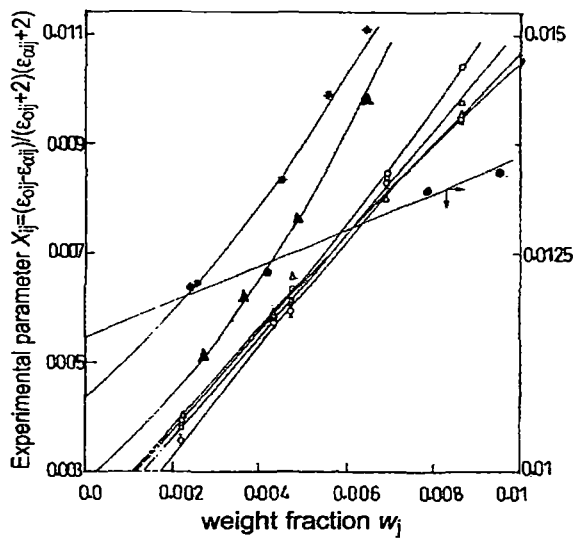

Figure 3.5: Variation of the measured X_{ij} with w_j of some aprotic polar liquids.

DMSO (–O–,–Δ–,–□–,–Ω–) at 25°C, 30°C, 35°C, and 40°C respectively; DEF (–●–) at 30°C; DMF (–▲–) at 25°C; DMA (–✶–) at 25°C

The theoretical μ_{theo}'s of polar molecules assumed to be planer ones were defined by the vector addition of the available bond moments 2.35D, 1.55D for polar groups S←CH_3, O⇐S in DMSO; 0.64D, 0.78D, 0.37D of N←CH_3, N←C_2H_5, CH_3←C in DMF, DEF and DMA. The other common bond moments are 0.3D, 0.45D, 3.10D for C←H, C←N and C⇐O respectively in them. The N atoms in DMF, DEF, DMA and S atom in DMSO molecules are thought to be slightly fractional positively charged δ^+ with benzene to make monomer formations [3.2-3.3]. The solute-solvent molecular association arises from the interaction of the π-delocalised electron cloud of the benzene ring with the fractional positive charges δ^+ on the N and S atoms of the amide groups. The bond moments of polar groups under the static and high frequency electric field are, however,

reduced by a factor μ_s/μ_{theo} in the range 0.5 and 0.9 due to inductive and mesomeric effects to yield μ_{cal} in agreement with μ_s. μ_s/μ_{theo} thus appears to exhibit the material property of the systems. The conformational structures of the polar molecules with their monomer [3.2-3.3] associations in C_6H_6 are shown in Fig.3.6. μ_{theo}'s along with μ_{cal} and μ_s/μ_{theo} are placed in Table 3.5 for comparison.

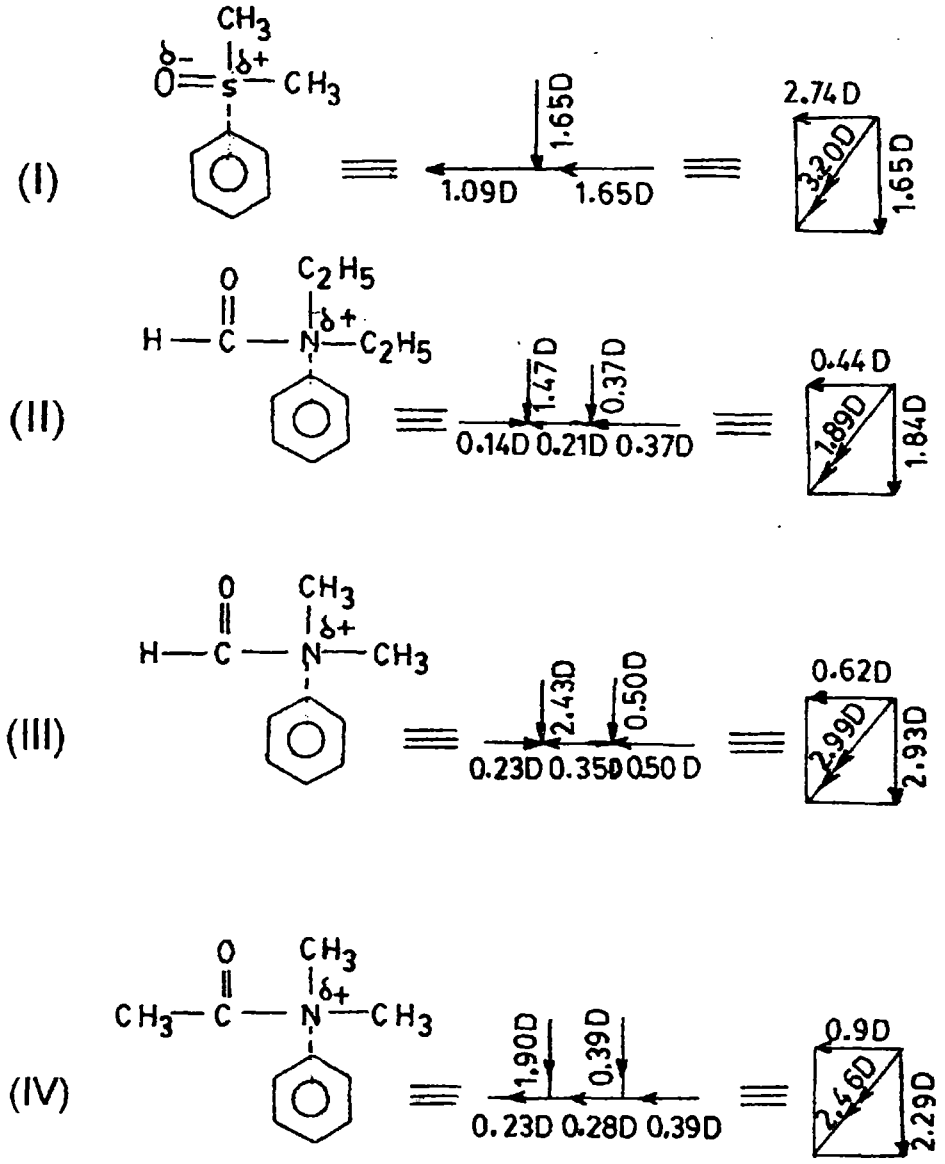

Figure 3.6: Conformational structures of aprotic polar liquids in terms of reduced bond length due to mesomeric and inductive moments of the substituent polar groups.

(I) DMSO in C_6H_6; (II) DEF in C_6H_6; (III) DMF in C_6H_6; (IV) DMA in C_6H_6

3.5. Conclusion :

The present measurements of dielectric relaxation parameters near 10 GHz electric field at different temperatures are found to exhibit double relaxation phenomena for rigid aprotic polar liquids. The procedure in obtaining τ_2 and τ_1 from the slope and intercept of a derived linear equation with ε_{oij}, $\varepsilon_{\infty ij}$, ε_{ij}' and ε_{ij}'' measured under the single frequency electric field appears to be a significant improvement over the existing ones where data at two or more frequencies are required. The % of error in terms of correlation coefficient 'r' in getting intercept and slope is made because of the linearity of the curve. The estimated τ_2 and τ_1 of the whole and the flexible part attached to the parent molecule are reliable as τ is claimed to be accurate within ±10%. It is interesting to note that unlike τ_2, τ_1 obeys Eyring's rate theory. The relative contributions c_1 and c_2 towards dielectric relaxations due to τ_1 and τ_2 are calculated by the graphical technique at $w_j \rightarrow 0$ as well as Fröhlich's method based on the concept of a distribution of τ between τ_1 and τ_2. The μ_2 and μ_1 of the whole and the flexible part attached to the parent molecule within ±5% accuracy are obtain from the slope β of σ_{ij}– w_j curves and τ_2, τ_1. The static μ_s from the linear coefficient of X_{ij}–w_j curve when compared with μ_2 and μ_1 from high frequency absorbtion reveals that μ's are little affected by the frequency (f) of the electric field. The X_{ij}–w_j curves and μ_s's may be used to test the accuracies of relaxation parameters. It is confirmed that a part of the molecule is rotating under 10 GHz electric field. Besides 'f', temperature is a factor to show mono or double relaxation behaviour for a molecule. The conformational structures of molecules from the reduced bond moments of polar groups by a factor μ_s/μ_{theo} due to mesomeric and inductive moments in them under static or low frequency electric field are in agreement with μ_s. μ_{theo} is obtained from available bond moments of polar groups. Thus the methodology, so far advanced, seems to be simple, straightforward and useful to observe interesting phenomena of *hf* absorbtion in polar-nonpolar liquid mixture.

References :

[3.1] A K Sharma and D R Sharma, *J. Phys. Soc. Japan* **53** 4771 (1984)

[3.2] J S Dhull and D R Sharma, *Indian J. Pure & Appl. Phys.* **21** 694 (1983)

[3.3] A Sharma and D R Sharma, *J. Phys. Soc. Japan* **61** 1049 (1992)

[3.4] A R Sharma, D R Sharma and M S Chauhan, *Indian J. Pure & Appl. Phys.* **31** 841 (1993)

[3.5] K V Gopalakrishna, *Trans. Faraday Soc.* **53** 767 (1957)

[3.6] S K Sit and S Acharyya, *Indian J. Pure & Appl. Phys.* **34** 255 (1996)

[3.7] T Pal Majumder, *Ph D Thesis* Jadavpur University, Calcutta (1996)

[3.8] K Higasi, K Bergmann and C P Smyth, *J. Phys. Chem.* **64** 880 (1960)

[3.9] U Saha, S K Sit, R C Basak and S Acharyya, *J. Phys. D: Appl. Phys.* **27** 596 (1994)

[3.10] S K Sit, R C Basak, U Saha and S Acharyya, *J. Phys. D: Appl. Phys.* **27** 2194 (1994)

[3.11] K Bergmann, D M Roberti and C P Smyth, *J. Phys. Chem.* **64** 665 (1960)

[3.12] H Fröhlich, *Theory of Dielectrics* (Oxford University Press) p.94 (1949)

[3.13] C P Smyth, *Dielectric Behaviour and Structure* (Mc Graw-Hill : New York) (1955)

[3.14] R C Basak, S K Sit, N Nandi and S Acharyya, *Indian J. Phys.* **70B** 37 (1996)

[3.15] J S Dhull and D R Sharma, *J. Phys. D: Appl. Phys.* **15** 2307 (1982)

[3.16] A R Saksena, *Indian J. Pure & Appl. Phys.* **16** 1079 (1978)

[3.17] H Eyring, S Glasstone and K J Laidler, *Theory of Rate Process* (Mc Graw-Hill : New York) (1941)

[3.18] U Saha and S Acharyya, *Indian J. Pure & Appl. Phys.* **32** 346 (1994)

[3.19] S N Sen and R Ghosh, *Indian J. Pure & Appl. Phys.* **10** 701 (1972)

[3.20] U Saha and S Acharyya, *Indian J. Pure & Appl. Phys.* **31** 181 (1993)

CHAPTER 4

DIELECTRIC RELAXATION PHENOMENA OF POLYSUBSTITUTED BENZENES UNDER HIGH FREQUENCY ELECTRIC FIELD

4.1. Introduction :

The dielectric relaxation phenomena of polysubstituted dielectropolar benzenes in benzene under high frequency (*hf*) electric field are of much importance to yield the structural aspect of a polar molecule. There exist several methods [4.1-4.2] to measure relaxation time τ_j and dipole moment μ_j of a polar molecule (j) from the measured real ε_{ij}' and imaginary ε_{ij}'' parts of the relative *hf* complex permittivity ε_{ij}^* of the solution (ij). However, such investigation on the relaxation phenomena of polysubstituted benzenes has not yet been made from the conductivity measurement [4.3-4.4]. Moreover, the most effective dispersive region for such polar liquids may exist at ~10 GHz (X-band) electric field [4.5]. Recently, Paul *et al* [4.6] had measured ε_{ij}', ε_{ij}'' of some polysubstituted benzenes in C_6H_6 at 30^0, 35^0, 40^0 and 45^0C under nearly 10 GHz electric field. The purpose of the study was to see the variation of τ's and μ's with temperature and concentration based on Goplakrishna's method [4.1].

Although, the molecules appear to be of outdated interest, two polar molecules have identical molecular weights in comparison to the third one, which is slightly higher. One molecule is a para-compound showing zero dipole moment at lower and higher temperatures. The substituted polar groups are attached with the parent benzene ring with different angles. We are, therefore tempted to use the measured relative permittivities [4.6] to get τ_j and μ_j of these liquids by *hf* conductivity measurement method [4.7]. The methodology is, however, involved with the transfer of dipolar charge of a polar molecule in a given solvent [4.8]. The present method of study in SI unit is superior because of its unified, coherent and rationalised nature. The dependency of τ_j's and μ_j's on t in ^{0}C is of much significance to get an idea of molecular environment and to shed more light on the structural conformations [4.9].

The measured dimensionless dielectric constants like real k_{ij}' and imaginary k_{ij}'' parts of complex dielectric constant k_{ij}^* at 30^0, 35^0, 40^0 and 45^0C are placed in Table 4.1. The real σ_{ij}' and imaginary σ_{ij}'' parts of the *hf* complex conductivity σ_{ij}^* in $\Omega^{-1}m^{-1}$ are, however, related to k_{ij}'' and k_{ij}' respectively. τ_j's are calculated from the linear slope of σ_{ij}'' against σ_{ij}' curves [4.10] for different w_j's of solute at a given temperature. The variation of σ_{ij}'' against σ_{ij}' is not strictly linear for different w_j's. (Fig.4.1). The ratio of the individual slopes of variations of σ_{ij}'' and σ_{ij}' with w_j's in Figs.4.2 and 4.3 in the limit w_j=0 may be used to get τ_j's, in which polar-polar interactions are almost eliminated. All the τ_j's are shown in Table 4.2 and are smaller than the reported τ's [4.6]. We, therefore, recalculated both τ's and μ's based on Gopalakrishna's method [4.1] which are in agreement with those of conductivity measurement. All τ's and μ's are presented in Tables 4.2 and 4.4 respectively for comparison.

Thermodynamic energy parameters: enthalpy of activation ΔH_τ, free energy of activation ΔF_τ and entropy of activation ΔS_τ for dielectric relaxations are also computed from the slope and intercept of $\ln(\tau_j T)$ against $1/T$ of Fig.4.4 with τ_j's measured by both the methods [4.11]. The values are entered in Table 4.3 in order to infer molecular dynamics of polar molecules in benzene. The enthalpy of activation ΔH_η for viscous process was, however, obtain from the linear slope γ of $\ln(\tau_j T)$ against $\ln\eta$ and ΔH_τ of Eq.(4.4). The coefficients of viscosity η of solvent C_6H_6 are $5.65\text{x}10^{-3}$, $5.30\text{x}10^{-3}$, $5.03\text{x}10^{-3}$ and $4.70\text{x}10^{-3}$ poise at 30^0, 35^0, 40^0 and 45^0C respectively.

Table 4.1: The real and imaginary parts of dimensionless dielectric constants of different aromatic polar liquids in benzene for different weight fractions w_j's at various experimental temperatures in ^{0}C.

Weight fraction	k_{ij}'	k_{ij}''	k_{ij}'	k_{ij}''	k_{ij}'	k_{ij}''	k_{ij}'	k_{ij}''
w_j	30^{0}C		35^{0}C		40^{0}C		45^{0}C	
			(I) meta-diisopropylbenzene					
0.012	2.2990	0.0424	2.3062	0.0401	2.3151	0.0393	2.3271	0.0384
0.018	2.3323	0.0570	2.3425	0.0552	2.3541	0.0545	2.3660	0.0523
0.025	2.3614	0.0721	2.3711	0.0692	2.3923	0.0660	2.4105	0.0595
0.032	2.3852	0.1083	2.4084	0.0985	2.4212	0.0854	2.4462	0.0734
0.045	2.4104	0.1251	2.4234	0.1092	2.4451	0.0982	2.4671	0.0832
			(II) para-methylbenzoylchloride					
0.011	2.1603	0.0488	2.1663	0.0440	2.1723	0.0410	2.1783	0.0381
0.018	2.1960	0.0585	2.2018	0.0553	2.2078	0.0523	2.2140	0.0492
0.028	2.2351	0.0690	2.2411	0.0662	2.2470	0.0632	2.2530	0.0603
0.039	2.2754	0.0762	2.2812	0.0731	2.2872	0.0701	2.2931	0.0672
0.050	2.3089	0.0928	2.3147	0.0899	2.3204	0.0872	2.3263	0.0842
			(III) ortho-chloroacetophenone					
0.011	2.1843	0.0351	2.1861	0.0330	2.1901	0.0310	2.1982	0.0294
0.023	2.2198	0.0462	2.2322	0.0442	2.2394	0.0450	2.2456	0.0376
0.032	2.2590	0.0573	2.2698	0.0552	2.2700	0.0491	2.2801	0.0421
0.045	2.2991	0.0692	2.3002	0.0653	2.3204	0.0551	2.3324	0.0579
0.051	2.3323	0.0810	2.3452	0.0791	2.3612	0.0770	2.3711	0.0650

Dipole moments μ_j's (shown in Table 4.4) are estimated from the linear coefficients β's of $hf\ \sigma_{ij}$ against w_j's as displayed in Fig.4.5 in the limit w_j=0. The variation of μ_j's and τ_j's with t in ^{0}C are presented in Fig.4.6. The temperature dependence of the mesomeric and inductive moments of the substituted polar groups attached to the parent molecules [4.12] are taken into account to display the theoretical dipole moments μ_{theo}'s in Fig.4.7.

Table 4.2: The slope of linear relation σ_{ij}''–σ_{ij}' curves of Fig. 4.1, correlation coefficient 'r', % of errors in regression technique, ratio of slopes of σ_{ij}''–w_j and σ_{ij}'–w_j curves at $w_j \to 0$ of Figs.4.2 and 4.3, estimated τ_j from Eq.(4.2) and reported τ in psec.

Systerm with sl. no.	t in ^{0}C	Slope of σ_{ij}''–σ_{ij}' curve of Eq.(4.2)	'r'	% of error of Eq.(4.2)	Ratio of slopes of σ_{ij}''–w_j & σ_{ij}'–w_j at $w_j \to 0$	τ_j^a	τ_j^b	Rept. τ in psec.
(I) m-diisopro-	30	1.217	0.972	1.67	1.809	13.08	8.80	10.92
pylbenzene	35	1.633	0.990	0.60	2.173	9.75	7.33	8.88
in C_6H_6	40	2.183	0.990	0.60	2.916	7.29	5.46	6.54
	45	3.227	0.988	0.72	4.207	4.93	3.79	4.30
(II) p-methyl-	30	3.491	0.988	0.72	5.858	4.56	2.72	3.85
benzoylchloride	35	3.369	0.989	0.66	4.828	4.73	3.30	4.04
in C_6H_6	40	3.342	0.988	0.72	4.931	4.77	3.23	4.05
	45	3.339	0.988	0.72	4.910	4.77	3.24	4.18
(III) o-chloro-	30	3.268	0.999	0.06	3.793	4.87	4.20	4.43
acetophenone	35	3.406	0.998	0.12	5.234	4.68	3.04	4.16
in C_6H_6	40	3.841	0.963	2.19	12.625	4.15	1.26	3.47
	45	4.614	0.987	0.78	17.625	3.45	0.90	3.09

τ_j^a = Estimated relaxation time from Eq.(4.2) with slope of σ_{ij}''–σ_{ij}'.
τ_j^b = Estimated relaxation time from Eq.(4.2) with ratio of slopes of σ_{ij}''–w_j and σ_{ij}'–w_j at $w_j \to 0$.

4.2. Theoretical Formulation :

Under electric field of giga hertz range the *hf* complex conductivity σ_{ij}^* of polar-nonpolar liquid mixture is :

$$\sigma_{ij}^* = \omega\varepsilon_o k_{ij}'' + j\omega\varepsilon_o k_{ij}' \qquad \ldots\ldots(4.1)$$

where $\omega\varepsilon_o k_{ij}'$ ($=\sigma_{ij}''$) and $\omega\varepsilon_o k_{ij}''$ ($=\sigma_{ij}'$) are the imaginary and real parts of σ_{ij}^*. $\omega(=2\pi f)$ is the angular frequency of the applied electric field of frequency f. ε_o= permittivity of free space= $8.854\text{x}10^{-12}$ F.m^{-1} and j is a complex number $=\sqrt{-1}$. The magnitude of total *hf* conductivity is :

$$\sigma_{ij} = \omega\varepsilon_o (k_{ij}''^2 + k_{ij}'^2)^{1/2}$$

σ_{ij}' and σ_{ij}'' of a given weight fraction w_j are, however, related to τ_j by :

$$\sigma_{ij}'' = \sigma_{\infty ij} + \frac{1}{\omega\tau_j}\sigma_{ij}'$$

$$\left(\frac{d\sigma_{ij}''}{d\sigma_{ij}'}\right)_{w_j \to 0} = \frac{\left(d\sigma_{ij}''/dw_j\right)_{w_j \to 0}}{\left(d\sigma_{ij}'/dw_j\right)_{w_j \to 0}} = \frac{1}{\omega\tau_j} \qquad \ldots\ldots(4.2)$$

The variation of σ_{ij}'' against σ_{ij}' for different w_j's is not always linear as shown in Fig.4.1. In such case, one may use the ratio of the individual slopes of variations of σ_{ij}'' and σ_{ij}' against w_j's as seen in Figs.4.2 and 4.3 in the limit w_j=0 to get τ_j.

Table 4.3: Thermodynamic energy parameters: enthalpy of activation ΔH_τ, entropy of activation ΔS_τ and free energy of activation ΔF_τ, value of γ from Eq.(4.4), enthalpy of activation ΔH_η due to viscous process, Debye factor and Kalman factor of the following aromatic polar liquids in benzene at different temperatures.

Systerm with sl. no.	t in ^{0}C	ΔH_τ in K J mole^{-1}	ΔS_τ in J mole^{-1} K^{-1}	ΔF_τ in K J mole^{-1}	Value of γ from Eq.(4.4)	ΔH_η from $\Delta H_\eta=\Delta H_\tau/\gamma$ in K J mole^{-1}	Debye factor $(\tau_j T/\eta)\times10^7$	Kalman Factor $\tau_j T/\eta^\gamma$
(I) m-diisopro-pylbenzene in C_6H_6	30	42.52	106.96	10.11	4.29	9.91	4.72	11.74
	35		106.07	9.85			4.26	13.08
	40		106.17	9.29			3.40	12.39
	45		106.94	8.51			2.56	11.69
(II) p-methyl-benzoylchloride in C_6H_6	30	-10.84	-59.41	7.16	-1.10	9.85	1.46	2.78×10^{-12}
	35		-60.57	7.82			1.92	3.19×10^{-12}
	40		-59.96	7.93			2.01	3.00×10^{-12}
	45		-59.58	8.11			2.19	2.83×10^{-12}
(III) o-chloro-acetophenone in C_6H_6	30	85.60	255.28	8.25	8.73	9.81	2.25	5.36×10^{10}
	35		253.25	7.60			1.77	6.89×10^{10}
	40		255.99	5.48			0.78	4.58×10^{10}
	45		254.36	4.71			0.61	6.02×10^{10}

τ_j's by both the methods of $(d\sigma_{ij}''/d\sigma_{ij}')$ and the ratio of individual slopes of Eq.(4.2) are used to get free energy of activation ΔF_τ of a polar liquid. From Eyring's rate theory [4.11] one gets:

$$\ln(\tau_j T) = \ln(Ae^{-\Delta S_\tau/R}) + \Delta H_\tau / RT \qquad \ldots\ldots (4.3)$$

Since $\Delta F_\tau = \Delta H_\tau - T\Delta S_\tau$

The intercept and slope of $\ln(\tau_j T)$ against $1/T$ as shown in Fig.4.4 are, however, related to ΔS_τ and ΔH_τ of molecules. η of C_6H_6 is related to τ_j at different temperatures by:

$$\tau_j = A\eta^\gamma / T \qquad \ldots\ldots (4.4)$$

Where γ is the slope of the linear relation of $\ln(\tau_j T)$ against $\ln\eta$. Again, σ_{ij}'' may be approximated to σ_{ij} for their identical nature of variations with w_j's as evidenced by Figs.4.2 and 4.5 respectively.

Hence Eq.(4.2) can be written as :

$$\sigma_{ij} = \sigma_{\infty ij} + \frac{1}{\omega\tau_j}\sigma_{ij}'$$

$$\left(\frac{d\sigma'_{ij}}{dw_j}\right)_{w_j\to 0} = \beta\omega\tau_j \qquad \text{.....(4.5)}$$

where β is the linear coefficient of variation of σ_{ij}–w_j curves of Fig.4.5 at $w_j\to 0$. All β's are placed in Table 4.4. The real part σ_{ij}' at T K is [4.13]:

$$\sigma'_{ij} = \frac{N\rho_{ij}\mu_j^2}{27k_BTM_j}\left(\frac{\omega^2\tau_j}{1+\omega^2\tau_j^2}\right)\left(k'_{ij}+2\right)^2 w_j$$

$$\left(\frac{d\sigma'_{ij}}{dw_j}\right)_{w_j\to 0} = \frac{N\rho_i\mu_j^2}{27k_BTM_j}\left(\frac{\omega^2\tau_j}{1+\omega^2\tau_j^2}\right)\left(k_i+2\right)^2 \qquad \text{.....(4.6)}$$

where N=Avogadro's number, ρ_i=density of solvent, k_i=dimensionless dielectric constant of solvent, M_j=molecular weight of the polar liquid (j) and k_B=Boltzmann constant. All the symbols are in SI units. From Eqs.(4.5) and (4.6) one gets μ_j of a polar molecule in Coulomb metre (C.m):

$$\mu_j = \left(\frac{27k_BTM_j}{N\rho_i(k_i+2)^2}\frac{\beta}{\omega b}\right)^{1/2} \qquad \text{.....(4.7)}$$

The dimensionless parameter b is related to τ_j by :

$$b = \frac{1}{1+\omega^2\tau_j^2} \qquad \text{.....(4.8)}$$

The measured τ_j's of the polar liquids presented in Table 4.2 are compared with the recalculated τ's based on Gopalakrishna's [4.1] method.

$$x = \frac{\varepsilon_{ij}'^2+\varepsilon'_{ij}+\varepsilon''^2_{ij}-2}{(\varepsilon'_{ij}+2)^2+\varepsilon''^2_{ij}} \qquad y = \frac{3\varepsilon''_{ij}}{(\varepsilon'_{ij}+2)^2+\varepsilon''^2_{ij}}$$

$$\tau = \frac{1}{\omega}\frac{dy}{dx} \qquad \text{.....(4.9)}$$

All the μ_j's with b's are finally found in Table 4.4 to compare with recalculated μ's from :

$$\mu = \left[\frac{9k_BTM_j}{4\pi N\rho_i}\left\{1+\left(\frac{dy}{dx}\right)^2\right\}\frac{dx}{dw_j}\right]^{1/2} \qquad \text{.....(4.10)}$$

All the computed μ_j's reported μ's along with μ_{theo}'s of Fig.4.7 are seen in Table 4.4.

4.3. Results and Discussions :

The relaxation times τ_j's of polysubstituted benzenes under 3 cm wavelength electric field, were calculated simultaneously from Eq.(4.2) with the slope of σ_{ij}'' against σ_{ij}' of *hf* conductivity σ_{ij}^* of Fig.4.1 and the ratio of slopes of the variations of σ_{ij}'' and σ_{ij}' with w_j's of Figs.4.2 and 4.3 from data of Table 4.1 at different experimental temperatures. τ_j's (Table 4.2) from slope of linear relation σ_{ij}''–σ_{ij}' curve (Fig.4.1) are slightly larger than the ratio of slopes of Eq.(4.2). The latter method is reliable as the polar-polar interactions are almost eliminated. The variation of σ_{ij}'' with σ_{ij}' is non linear (Fig.4.1) for all the liquids like σ_{ij}'' and σ_{ij}' with w_j's of Figs.4.2 & 4.3 respectively. The slopes of curves in Fig.4.1 are almost same for *p*-methylbenzoylchloride, but for o-chloroacetophenone the curves are of almost constant intercepts and slightly increasing slopes with temperature to yield almost same τ_j for their same polarity [4.14] and identical structures. Meta-diisopropylbenzene indicates the lower intercept and higher slopes as the temperature rises. τ_j's from Eq.(4.2) of σ_{ij}''–σ_{ij}' curves decrease with temperature to obey Debye relaxation mechanism like the variation of σ_{ij}'' and σ_{ij}' with w_j's for the molecules at 30^0, 35^0, 40^0 and 45^0C respectively. Nevertheless, the conductivity method yields microscopic τ_j's [4.15]. The molecule m-diisopropylbenzene has greater τ because of larger size than those of isomeric p-methylbenzoylchloride and o-chloroacetophenone. τ_j's in Table 4.2 for these molecules having the same number of C-atoms do not vary much from Eqs.(4.2) and (4.9) respectively probably for the different positions of the substituted polar groups attached to the parent molecules of Fig.4.7.

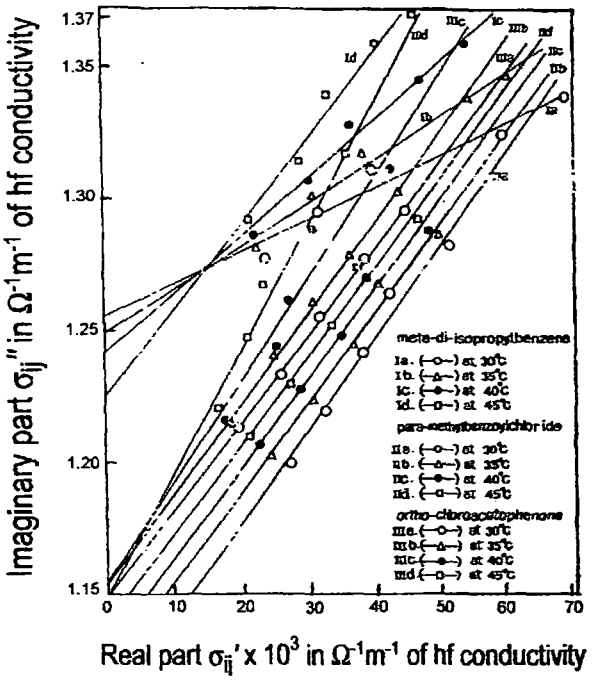

Figure 4.1: Variation of imaginary part σ_{ij}'' in $\Omega^{-1}m^{-1}$ against real part σ_{ij}' in $\Omega^{-1}m^{-1}$ of *hf* conductivity for different weight fractions w_j's of polysubstituted benzenes in benzene under 10 GHz electric field at various experimental temperatures.

For m-diisopropylbenzene both σ_{ij}'' and σ_{ij} in Figs.4.2 and 4.5 start from 1.228 $\Omega^{-1}m^{-1}$ to 1.236 $\Omega^{-1}m^{-1}$ and increase gradually to assume maximum within $0.045 \leq w_j \leq 0.051$ and then decrease as w_j increases. This sort of behaviour arises for the transfer of localised charge species of

such dipoles [4.16] which increases up to a certain w_j and then ceases gradually in the higher concentrations. Similar observation is noted in *p*-methylbenzoylchloride showing maximum at nearly w_j=0.096. All these facts indicate the phase transition of lower conductivity in the higher concentration [4.16] probably due to dimer formations. Ortho-chloroacetophenone showed a regular monotonic increase, as coefficients of quadratic term of w_j in both σ_{ij}'' and σ_{ij} are positive. The variation of σ_{ij}' with w_j's for all polar molecules in Fig.4.3 decreases with t ^{0}C to exhibit the

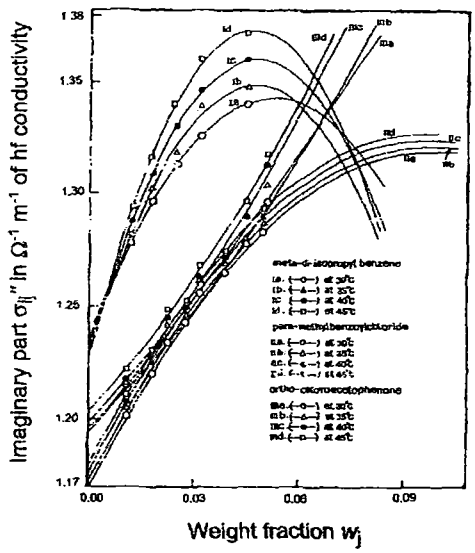

Figure 4.2: Variation of imaginary part σ_{ij}'' in $\Omega^{-1}m^{-1}$ of *hf* conductivity with weight fractions w_j's of polysubstituted benzenes in benzene under 10 GHz electric field.

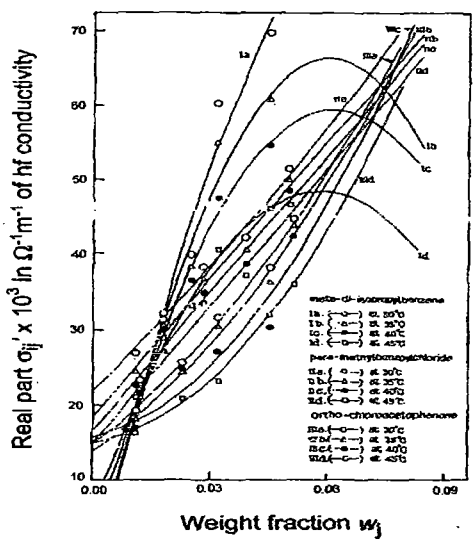

Figure 4.3: Variation of imaginary part σ_{ij}' in $\Omega^{-1}m^{-1}$ of *hf* conductivity with weight fractions w_j's of polysubstituted benzenes in benzene under 10 GHz electric field.

semiconducting nature while σ_{ij}'' and σ_{ij} of Figs.4.2 and 4.5 showed the regular increase. The percentage of errors as well as correlation coefficients r's are made for Eq.(4.2) to get τ_j's. It is interesting to note that τ_j for *m*-diisopropylbenzene and *o*-chloroacetophenone in C_6H_6 obey Debye relaxation mechanism. The energy difference between activated and normal states of the random dipole orientations increases with t ^{0}C to decrease τ_j's. τ_j's for *p*-methylbenzoylchloride initially increases and then become constant with t ^{0}C indicating the non-Debye relaxation for its asymmetry gained by two polar groups in a line. The large difference between τ_j's and reported τ's [4.6] prompted us to recalculate τ's placed in the 9th column of Table 4.2 based on Gopalakrishna's method [4.1]. The recalculated τ's and μ's are now closer to τ_j's of columns 7 and 8 of Table 4.2 and μ_j's of column 9 of Table 4.4 based on the method of conductivity measurement [4.7].

The thermodynamic energy parameters ΔH_τ, ΔS_τ and ΔF_τ (Table 4.3) were calculated from $\ln(\tau_j T)$ against $1/T$ in Fig.4.4 with the measured τ_j's by both the methods. In *p*-

methylbenzoylchloride $-\Delta S_\tau$ indicates the activated states are more stable supported by $-\Delta H_\tau$ also. ΔS_τ for *m*-diisopropylbenzene and *o*-chloroacetophenone indicates the unstability of the activated states. Unlike *p*-methylbenzoylchloride, $\gamma >$ 0.5 for *m*-diisopropylbenzene and *o*-chloroacetophenone indicates that they do not behave as solid phase rotators. Such polar liquids in C_6H_6 favour solute-solvent molecular formation. ΔH_η involved with translational and rotational energy are less than ΔH_τ due to high values of γ for all the systems. They thus need maximum energy to rotate under *hf* electric field. The γ's from the slope of $\ln(\tau_j T)$ against $\ln\eta$ are used to estimate Kalman factor $\tau_j T/\eta^\gamma$ and Debye factor $\tau_j T/\eta$ to place them in Table 4.3. Kalman factors being proportional to the volumes of the rotating units are of different orders, but constant with temperature for a given system. Debye factors, on the other hand, are of the order of 10^{-7} for all systems. This suggests the applicability of Debye-Smyth model of dielectric relaxation mechanism for all the liquids including *p*-methylbenzoylchloride although it is non-Debye in

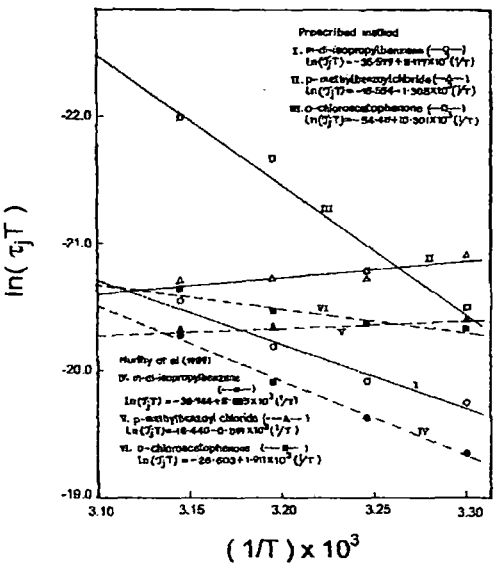

Figure 4.4: The linear plot of $\ln(\tau_j T)$ against 1/T

Table 4.4: The coefficients of *hf* conductivity σ_{ij} of aromatic polar liquid with weight fraction w_j in C_6H_6 at 30^0, 35^0, 40^0 and 45^0C in Fig.4.5, dimensionless parameters *b*'s, computed, reported and theoretical dipole moments in Coulomb metre (C.m).

Systerm with sl. no & mol. wt.	*t* in ^{0}C	Coefficients of σ_{ij}–w_j in $\Omega^{-1}m^{-1}$ of Fig.4.5 $\sigma_{ij}=\alpha+\beta w_j+\xi w_j^2$ α	β	ξ	Dimensionless parameter *b*		Computed $\mu_j\times10^{30}$ in C.m		Rept. $\mu\times10^{30}$ in C.m Eq.(4.10)	$\mu_{theo}\times10^{30}$ in C.m of Fig.4.7
(I) m-diisopro-	30	1.236	4.016	-36.919	0.597	0.766	14.34	12.66	9.07	
pylbenzene	35	1.228	5.110	-53.613	0.727	0.825	14.86	13.95	8.90	3.77
in C_6H_6	40	1.230	5.475	-56.900	0.827	0.895	14.61	14.04	8.84	
M_j=0.162 Kg	45	1.228	6.196	-65.944	0.913	0.946	14.99	14.72	8.90	
(II) p-methyl-	30	1.171	3.059	-15.421	0.924	0.972	9.87	9.63	8.17	
benzoylchloride	35	1.173	3.059	-15.464	0.919	0.959	10.03	9.82	8.27	8.80
in C_6H_6	40	1.177	3.064	-15.617	0.918	0.961	10.18	9.95	8.34	
M_j=0.156 Kg	45	1.180	3.064	-15.685	0.918	0.960	10.31	10.08	8.44	
(III) o-chloro-	30	1.197	1.477	9.038	0.915	0.935	6.90	6.82	8.07	
acetophenone	35	1.195	1.894	3.180	0.921	0.965	7.89	7.71	8.20	7.40
in C_6H_6	40	1.201	1.580	11.513	0.936	0.994	7.23	7.02	8.57	
M_j=0.156 Kg	45	1.204	1.615	11.737	0.955	0.997	7.34	7.19	8.74	

relaxation behaviour. μ_j's of the polar liquids at t ^{0}C are estimated from β's of σ_{ij}–w_j curves of Fig.4.5 and dimensionless parameters b's of Eq.(4.8) involved with the measured τ_j's from the ratio of the individual slopes of Figs.4.2 and 4.3 at $w_j \rightarrow 0$. The σ_{ij} in $\Omega^{-1}m^{-1}$ when plotted with w_j's increases with temperatures showing maximum at a certain w_j for *m*-diisopropylbenzene and *p*-methylbenzoylchloride like σ_{ij}''–w_j curves. This signifies the phase transition from higher to lower conductivity for transfer of charged species of molecules. The slopes and intercepts of σ_{ij}–w_j and σ_{ij}''–w_j curves for *p*-methylbenzoylchloride and *o*-chloroacetophenone are almost the same for their same polarity [4.14] indicating $\sigma_{ij} \approx \sigma_{ij}''$ in Eq.(4.5). The usual variations of μ_j and τ_j [4.17] with t ^{0}C

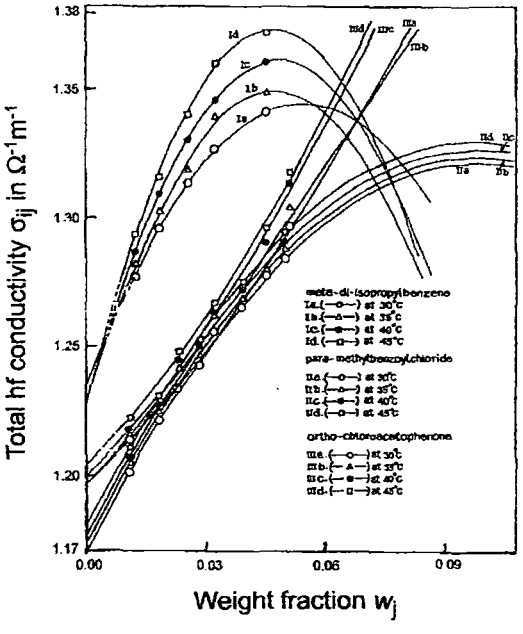

Figure 4.5: Variation of total *hf* conductivity σ_{ij} in $\Omega^{-1}m^{-1}$ with weight fractions w_j's under 10 GHz electric field at various experimental temperatures

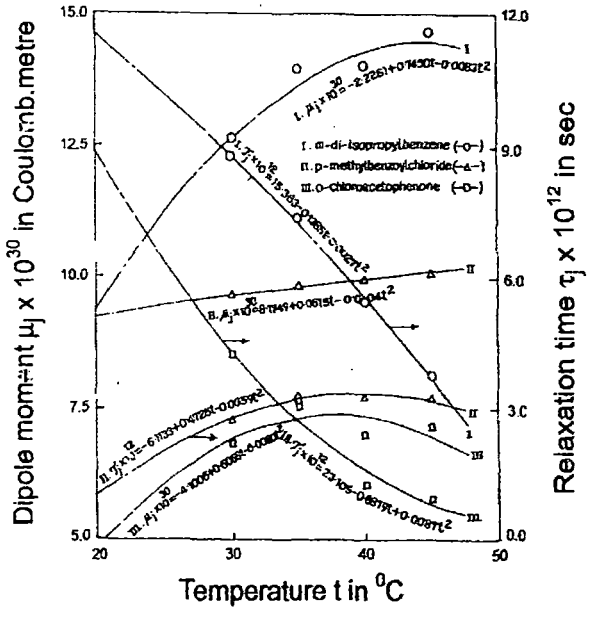

Figure 4.6: Variation of observed dipole moment μ_j and relaxation time τ_j with temperatures t in ^{0}C of different polysubstituted benzenes in benzene under 10 GHz electric field.

are shown graphically in Fig.4.6. τ_j's decrease with temperature for the curves I and III of *m*-diisopropylbenzene and *o*-chloroacetophenone. The μ_j's from Eq.(4.7) increase gradually to maximum 14.49×10^{-30} C.m at 44.88 ^{0}C, 10.54×10^{-30} C.m at 76.88^{0}C and 7.41×10^{-30} C.m at 37.93 ^{0}C respectively signifying the largest asymmetry gained by all the molecules. τ_j's are zero at 54.03 ^{0}C for the curve I and 16.22 ^{0}C, 63.88 ^{0}C for curve II. But for curve III; $\tau_j=0$ at $t=\infty$. The μ_j's are 13.80×10^{-30} C.m for the curve I and 9.07×10^{-30} C.m, 10.47×10^{-30} C.m for curve II. But undefined for curve III respectively. The variation of τ_j and μ_j with t ^{0}C are convex for curve II indicating the non-

Debye relaxation behaviour to reveal solute-solvent molecular association as observed from γ of Table 4.3.

μ_{theo} from the available bond angles and bond moments of the substituted polar groups of molecules of Fig.4.7 is placed in Table 4.4 with the reported μ from Eq.(4.10). The close agreement

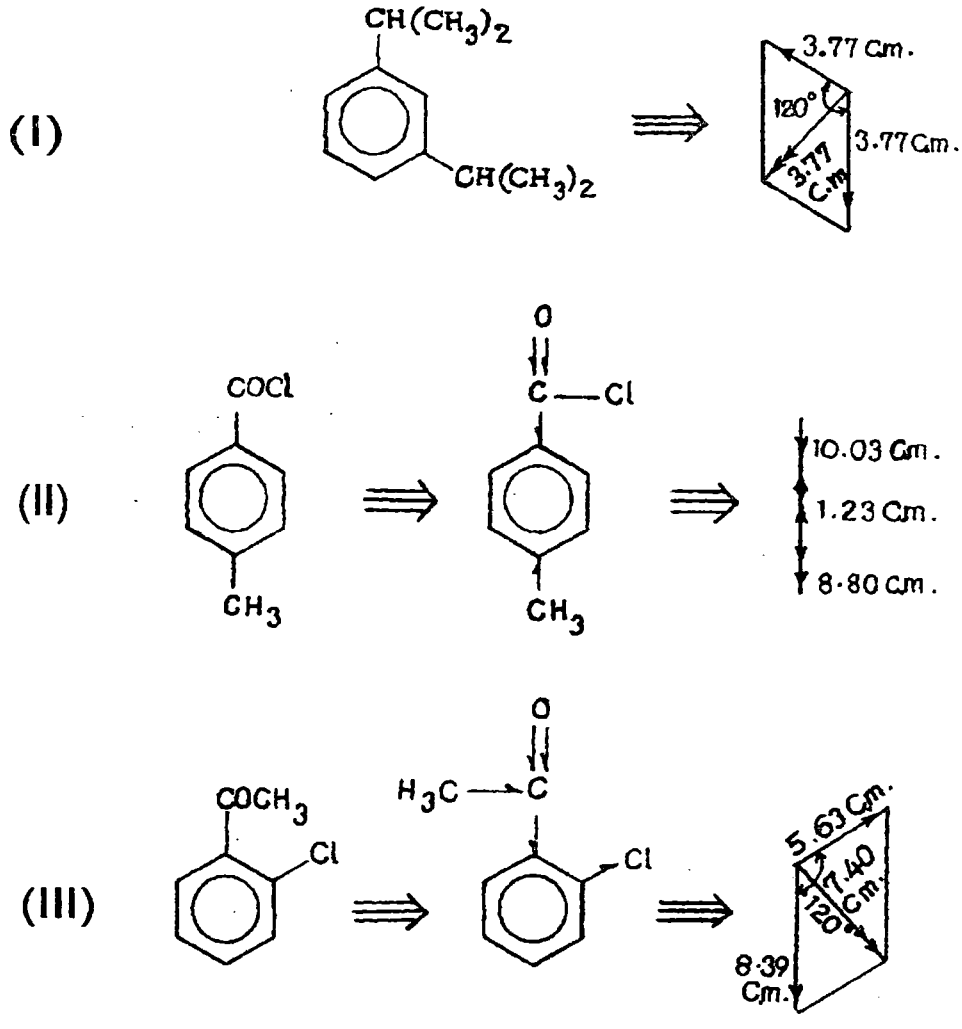

Figure 4.7: Conformational structures of (I) meta-diisopropylbenzene (II) para-methylbenzoylchloride (III) ortho-chloroacetophenone.

of μ_j's of Eq.(4.7) with Eq.(4.10) suggests the basic soundness of the present method. The wide disagreement between μ_j and μ_{theo} of Table 4.4 of the first molecule unlike the latter two suggest bond moments of the substituted polar groups are either stretched by a factor μ_j/μ_{theo} of 3.36, 3.70, 3.72, 3.90; or shortened by 0.09, 1.12, 1.13, 1.50 and 0.92, 1.04, 0.95, 0.97 respectively in order to consider inductive and mesomeric effects in them. The electromeric effect caused by >C=O in second and third molecules may be the reason to make μ_j more closer to μ_{theo} [4.18].

4.4. Conclusion :

The study of dielectric relaxation phenomena of polysubstituted benzenes in benzene under 3 cm wavelength electric field in terms of τ_j's and μ_j's in SI units at various experimental temperatures in ^{0}C by the method of *hf* conductivity measurement is more topical and significant. The use of ratio of the slopes of σ_{ij}''–w_j and σ_{ij}'–w_j curves to obtain τ_j's appears to be reliable as it avoids polar-polar interaction unlike the linear slope of σ_{ij}''–σ_{ij}' curves. The appearance of peak in σ_{ij}–w_j and σ_{ij}''–w_j curves at different t ^{0}C for systems I and II indicates the change of phase of lower conductivity as w_j increases. O-chloroacetophenone, on the other hand, showed the monotonic increase of σ_{ij} and σ_{ij}'' with w_j's at all the temperatures. The temperature dependence the of μ_j's and τ_j's although they are measured in the limit of w_j=0 supports this behaviour. τ_j is zero for *m*-diisopropylbenzene at 54.03 ^{0}C while *p*-methylbenzoylchloride at 16.22 ^{0}C and 63.88 ^{0}C respectively indicating orderness at those temperatures. *o*-chloroacetophenone showed τ_j's decreasing with temperature and becomes zero at $t=\infty$. The correspsonding μ's are $\mu_s=13.80\text{x}10^{-30}$ C.m for *m*-diisopropylbenzene and $\mu_s=9.07\text{x}10^{-30}$ C.m and $\mu_s=10.47\text{x}10^{-30}$ C.m for *p*-methylbenzoylchloride respectively as static μ_s. Both τ_j's and μ_j's in tables and figures are within 10% and 5% accuracies. The increase or decrease of μ_j's with temperature t in ^{0}C is explained by asymmetric or symmetric configurations of the molecules. The energy parameters from $\ln(\tau_j T)$ against $1/T$ with τ_j's from the ratio of individual slopes of σ_{ij}''–w_j and σ_{ij}'–w_j curves at various temperatures indicate the stability of random dipole orientations in the activated states. The deviation of μ_{theo} from the bond angles and bond moments of polar groups of molecules from measured μ_j in terms of τ_j can be explained by inductive, mesomeric and electromeric effect. The correlation between the conformational structures with the observed results enhances the scientific contents and adds a new horizon of understanding to the existing knowledge of dielectric relaxation.

References :

[4.1] K V Gopalakrishna, *Trans. Faraday Soc.* **53** 767 (1957)

[4.2] S N Sen and R Ghosh, *Indian J. Pure & Appl. Phys.* **10** 701 (1972)

[4.3] U Saha, S K Sit, R C Basak and S Acharyya, *J. Phys. D: Appl. Phys.* **27** 596 (1994)

[4.4] S K Sit, R C Basak, U Saha and S Acharyya, *J. Phys. D: Appl. Phys.* **27** 2194 (1994)

[4.5] S K Sit and S Acharyya, *Indian J. Pure & Appl. Phys.* **34** 255 (1996)

[4.6] N Paul, K P Sharma and S Chattopadhyay, *Indian J. Phys.* **71B** 711 (1997)

[4.7] R C Basak, A Karmakar, S K Sit and S Acharyya, *Indian J. Pure & Appl. Phys.* **37** 224 (1999)

[4.8] A K Jonscher, *Inst. Phys. Conf. Serial No. 58*, Invited paper presented at Physics of Dielectric Solids **8** (1980)

[4.9] N Ghosh, R C Basak, S K Sit and S Acharyya, *J. Molecular Liquids* **85** 375 (2000)

[4.10] M B R Murthy, R L Patil and D K Deshpande, *Indian J. Phys.* **63B** 491 (1989)

[4.11] H Eyring, S Glasstone and K J Laidler, *Theory of Rate Processes* (McGraw Hill: New York) (1941)

[4.12] S K Sit, N Ghosh, U Saha and S Acharyya, *Indian J. Phys.***71B** 533 (1997)

[4.13] C P Smyth, *Dielectric Behaviour and Structure* (McGraw Hill: New York) (1955)

[4.14] A K Chatterjee, U Saha, N Nandi, R C Basak and S Acharyya, *Indian J. Phys.* **66B** 291 (1992)

[4.15] S K Sit and S Acharyya, *Indian J. Phys.* **70B** 19 (1996)

[4.16] M A El shahawy, A F Mansour and H A Hashem, *Indian J. Pure & Appl. Phys.* **36** 78 (1998)

[4.17] A M Ras and P Bordewijk, *Recuel* **90** 1055 (1971)

[4.18] "*Internal Rotation in Molecules*"- Edited by W J Orville Thomas (John Wiley) (1974)

CHAPTER 5

RELAXATION PHENOMENA IN METHYL BENZENES AND KETONES FROM ULTRA HIGH FREQUENCY CONDUCTIVITY

5.1. Introduction :

Relaxation processes in dielectric polar liquid or solid material (DRL or DRS) are very encouraging to study the molecular behaviours and structures through various experimental techniques [5.1-5.2]. The methods are involved with the high frequency conductivity [5.3] or susceptibility measurements [5.4], thermally stimulated depolarisation current [5.5] (TSDC) and time or frequency domain dielectric AC spectroscopy [5.6] etc. The latter two methods consist of a tedious computer simulated calculation in comparison to others, which are very simple and straightforward within the framework of Debye and Smyth model of dielectric liquid molecule.

Vaish and Mehrotra [5.7-5.8] measured real and imaginary parts ε_{ij}' and ε_{ij}'' of complex dielectric relative permittivity ε_{ij}^* of some methyl benzenes and ketones (j) in benzene (i) under 3.13 cm wavelength electric field at 25 ^{0}C. They attempted to correlate dielectric relaxation times with those of nuclear magnetic resonance spin lattice relaxation times by using the theory of Bloembergen *et al* [5.9] in terms of measured relaxation parameters. The relaxation times τ of the molecules were calculated on the assumption that dipole-dipole (dimer) interaction occurs between the nuclear spins. The spin lattice relaxation times were obtained to compare with the Gopalakrishna, Debye and other methods. The experimental value differs significantly from those of theoretical one. This study reveals that τ plays the main role in inter and intra molecular motions and nuclear magnetic resonance (NMR) spin lattice relaxation etc.

The values of τ and dipole moment μ of these polar molecules by the conductivity technique have been calculated in the present paper. The procedures employed to get τ are those of Murthy *et al* [5.10] from the direct slope of the linear equation of imaginary $\sigma_{ij}''(=\omega\varepsilon_0\varepsilon_{ij}')$ in Ω^{-1} m^{-1} and real $\sigma_{ij}'(=\omega\varepsilon_0\varepsilon_{ij}'')$ in Ω^{-1} m^{-1} parts of the *hf* complex conductivity σ_{ij}^* (Fig.5.1) and the ratio of the individual slopes of σ_{ij}''– w_j and σ_{ij}'– w_j curves [5.11] (Figs.5.2 & 5.3) at $w_j \to 0$ respectively. The use of the ratio of individual slopes to estimate τ seems to be better as it eliminates the polar-polar interaction almost completely. Hence the purpose of the present paper is to study the success or otherwise of the proposed theory with the existing ones to infer molecular structures and associations. The graphs of σ_{ij}'' and σ_{ij}' with w_j's in Figs.5.2 & 5.3 are found to be nonlinear to indicate the presence of solute-solute associations in the mixture. τ's from linear slope are found to agree with the reported τ's from Gopalakrishna's fixed frequency method of Fig.5.4 and presented in Table 5.1 together with all the measured τ's by different procedures. Further, the polar molecules under investigation are methyl substituted aromatic and ketone substituted aliphatic compounds of highly nonspherical nature. Methyl substituted benzenes and ketones have almost similar characteristics. Some of the methyl benzenes are supposed to have apparently zero dipole moment

Table 5.1 : Slope and intercepts of Eq.(5.2), correlation coefficient r, ratio of the individual slopes of σ_{ij}''–w_j and σ_{ij}'–w_j curves at $w_j \to 0$, relaxation time τ_j from Eqs (5.3) and (5.4) and from Gopalakrishna's method of some methyl benzenes and ketones in benzene at 25°C under 9.585 GHz electric field.

System with sl.no.	Slope and intercepts of Eq.(5.3)		Corrl. coeff. r	Ratio of individual slopes of σ_{ij}''– w_j and σ_{ij}'– w_j at $w_j \to 0$	Relaxation times τ_j (x10 ^{12}) in sec.		
					τ_j^a	τ_j^b	τ_j^g
(I) toluene	1.8468	1.1385	0.9527	4.3891	8.99	3.78	8.24
(II) 1,3,5 tri methylbenzene	0.7897	1.1844	0.9755	2.8782	21.03	5.77	19.93
(III) 1,2,3,4 tetra methyl benzene	8.3666	1.1992	0.9678	6.5797	1.98	2.52	1.94
(IV) 1,2,4,5 tetra methyl benzene	1.9531	1.1854	0.9890	1.6133	8.50	10.29	8.06
(V) penta methyl benzene	1.3836	1.1770	0.9948	3.8814	12.00	4.28	11.02
(VI) *p* –fluorotoluene	4.8910	1.2071	0.9941	8.2548	3.39	2.01	3.12
(VII) butyl ethyl ketone	1.0070	1.1878	0.9481	40.3859	16.48	0.41	15.84
(VIII) methyl hexyl ketone	0.8452	1.1737	0.9993	0.6003	19.65	27.66	18.13
(IX) ethyl pentyl ketone	0.8640	1.1713	0.9686	0.6928	19.22	23.97	18.40
(X) heptyl methyl ketone	0.8203	1.1838	0.9859	1.8590	20.24	8.93	19.01

τ_j^a = Relaxation time from Eq. (5.3)
τ_j^b = Relaxation time from Eq. (5.4)
τ_j^g = Relaxation time from Gopalakrishna's method of Eq. (5.9)

from bond moment calculation. Moreover, these molecules are supposed to absorb electric energy much more strongly in the effective dispersive region of nearly 10 GHz at which peak of the absorption curve occurs. The ketones, on the other hand, are pleasant smelling liquids and widely used in petroleum industry. These liquids are used, as good solvents of synthetic rubber, wax etc. The study of the variation of τ with respect to various substituted polar groups attached to different positions of the parent molecules may throw much light on the structural conformations of the methyl benzene and ketone molecules. We had already made a detailed investigation on some polysubstituted benzenes [5.12] at various temperatures to get molecular structures by conductivity technique. Dielectric parameters are very much temperature dependent. Calculations at some other temperature may reveal a better picture. Nevertheless, from these studies it may be clear as to what theory is valid for such highly nonspherical aliphatic and aromatic compounds. A systematic comparison of τ and μ can thus be made from the measured data of 25°C.

The corresponding dipole moments μ_j's of these liquids are obtained from the linear coefficient β of *uhf* conductivity σ_{ij} curves against w_j's of Fig.5.5. All the β's and μ's are tabulated in Table 5.2 with those from Gopalakrishna and theoretical conformational calculation of Fig.5.6. The inductive, mesomeric and electromeric effects under 3 cm wavelength electric field play the vital role in determining the theoretical μ_{theo}'s of the molecules of Fig.5.6 in agreement with estimated μ_j's.

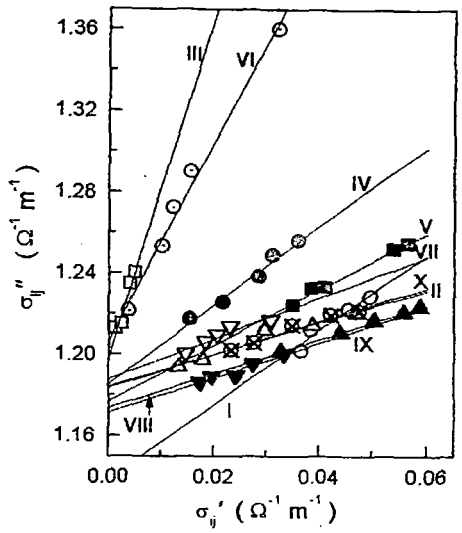

Figure.5.1 : The linear variation of imaginary part σ_{ij}'' against real part σ_{ij}' of complex *hf* conductivity σ_{ij}^* at 25°C under 9.585 GHz electric field :
(I) Toluene (-○-) (II) 1,3,5 tri methyl benzene (-Δ-) (III) 1,2,3,4 tetra methyl benzene (-□-) (IV) 1,2,4,5 tetra methyl benzene (-●-) (V) penta methyl benzene (-■-) (VI) *p*-fluoro toluene (-⊙-) (VII) Butyl ethyl ketone (-▽-) (VIII) Methyl hexyl ketone (-▲-) (IX) Ethyl pentyl ketone (-▼-) (X) heptyl methyl ketone (-⊗-)

5.2. High Frequency Conductivity Technique to Estimate τ and μ :

The ultra high frequency (*uhf*) complex conductivity [5.13] σ_{ij}^* is:

$$\sigma_{ij}^* = \sigma_{ij}' + j\sigma_{ij}'' \qquad \ldots\ldots (5.1)$$

where $\sigma_{ij}' = \omega\varepsilon_o\varepsilon_{ij}''$ and $\sigma_{ij}'' = \omega\varepsilon_o\varepsilon_{ij}'$ are the real and imaginary parts of σ_{ij}^*, ε_o= absolute permittivity of free space = 8.854×10^{-12} F.m^{-1} and $\omega(=2\pi f)$ is the angular frequency of the applied electric field of frequency, f= 9.585×10^9 Hz.

Debye equation [5.14] in the GHz region yields:

$$\sigma_{ij}'' = \sigma_{\infty ij} + \frac{1}{\omega\tau}\sigma_{ij}' \qquad \ldots\ldots (5.2)$$

$$\left(\frac{d\sigma_{ij}''}{d\sigma_{ij}'}\right) = \frac{1}{\omega\tau} \qquad \ldots\ldots (5.3)$$

Both σ_{ij}'' and σ_{ij}' are functions of w_j. Their variations are nonlinear in the higher concentration region as seen in Figs.5.2 and 5.3. In this case one can write Eq.(5.2) as:

$$\left(\frac{d\sigma_{ij}''}{dw_j}\right)_{w_j \to 0} = \frac{1}{\omega\tau}\left(\frac{d\sigma_{ij}'}{dw_j}\right)_{w_j \to 0} \qquad \ldots\ldots (5.4)$$

τ's from both the Eqs.(5.3) and (5.4) were computed and are listed in Table 5.1 for comparison with the reported τ recalculated from Gopalakrishna's method.

Table 5.2 : Coefficients of σ_{ij}–w_j curves, dimensionless parameter b [$=1/(1+\omega^2\tau^2)$], dipole moment μ_j in Coulomb.metre from τ's of Eq.(5.3), (5.4) and Gopalakrishna's method and the theoretical dipole moment μ_{theo} from the available bond angles and bond moments of some methyl benzenes and ketones in benzene at 25°C under 9.585 GHz electric field.

System with sl.no.and mol.wt.	Coefficients of $\sigma_{ij} = \alpha+\beta w_j+\xi w_j^2$			Values of b by using τ of		Dipole moment ($\times10^{-30}$) C.m			
	α	β	ξ	Eq.(5.3)	Eq.(5.4)	μ_j^a	μ_j^b	μ_j^g	μ_{theo}
(I) toluene M_j=0.092 Kg	1.1811	2.7545	–40.2180	0.7733	0.9507	7.93	7.15	7.80	1.23
(II) 1,3,5 tri methylbenzene M_j= 0.120 Kg	1.1446	3.4010	–31.2102	0.3840	0.8923	14.27	9.36	13.94	0.00
(III) 1,2,3,4 tetra methyl benzene M_j=0.134 Kg	1.1436	4.4952	–47.2133	0.9860	0.9775	10.82	10.87	10.82	0.00
(IV) 1,2,4,5 tetra methyl benzene M_j=0.134 Kg	1.1969	1.7313	–11.2125	0.7924	0.7225	7.49	7.84	7.39	0.00
(V) penta methyl benzene M_j=0.148 Kg	1.1798	1.4009	2.2168	0.6569	0.9377	7.78	6.51	7.63	1.23
(VI) p- fluoro toluene M_j=0.110 Kg	1.2039	1.9329	0.7021	0.9600	0.9856	6.52	6.43	6.53	6.23
(VII) butyl ethyl ketone M_j=0.114 Kg	1.1885	0.9115	–6.8748	0.5038	0.9994	6.29	4.46	6.19	8.09
(VIII) methyl hexyl ketone M_j=0.128 Kg	1.1790	1.8073	2.1902	0.4166	0.2649	10.32	12.94	10.05	8.14
(IX) ethyl pentyl ketone M_j=0.128 Kg	1.1820	1.7921	–27.0543	0.4274	0.3243	10.14	11.64	10.01	8.14
(X) heptyl methyl ketone M_j=0.142 Kg	1.1939	1.4569	–17.0797	0.4023	0.7757	9.93	7.15	9.60	8.20

μ_j^a = Dipole moment from Eq.(5.7) by using τ_j of Eq. (5.3)
μ_j^b = Dipole moment from Eq. (5.7) by using τ_j of Eq. (5.4)
μ_j^g = Dipole moment by Gopalakrishna's method of Eq. (5.10)
μ_{theo} = Theoretical dipole moment from the available bond angles and bond moments.

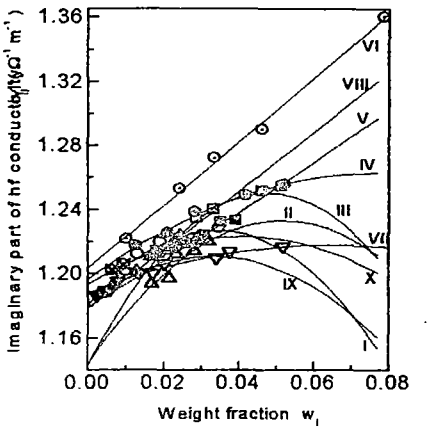

Figure.5.2: Variation of imaginary part of conductivity σ_{ij}'' against w_j at 25^{0}C under 9.585 GHz electric field :

(I) Toluene (-O-), (II) 1,3,5 tri methyl benzene (-Δ-), (III) 1,2,3,4 tetra methyl benzene (-□-), (IV) 1,2,4,5 tetra methyl benzene (-●-), (V) penta methyl benzene (-■-), (VI) *p*-fluoro toluene (-⊙-), (VII) Butyl ethyl ketone (-▽-), (VIII) Methyl hexyl ketone (-▲-), (IX) Ethyl pentyl ketone (-▼-), (X) heptyl methyl ketone (-⊗-)

Since $\varepsilon_{ij}' > \varepsilon_{ij}''$, but in *hf* region of GHz range $\varepsilon_{ij}' \cong \varepsilon_{ij}''$ where ε_{ij}'' offers resistance to polarisation and *uhf* conductivity σ_{ij} is $\sigma_{ij} = \omega\varepsilon_o(\varepsilon_{ij}'^2 + \varepsilon_{ij}''^2)^{1/2}$. We can thus write Eq.(5.2) in the following form:

$$\sigma_{ij} = \sigma_{\infty ij} + \frac{1}{\omega\tau}\sigma_{ij}'$$

$$\left(\frac{d\sigma_{ij}'}{dw_j}\right)_{w_j \to 0} = \omega\tau\beta \qquad \text{.....(5.5)}$$

β is the slope of σ_{ij}–w_j curve in the limit $w_j = 0$ as observed in Fig.5.5 and listed in Table 5.2.

The real part σ_{ij}' of *hf* complex conductivity σ_{ij}^* is given by [5.12]

$$\sigma_{ij}' = \frac{N\mu_j^2\rho_{ij}}{27M_jk_BT}\left(\frac{\omega^2\tau}{1+\omega^2\tau^2}\right)(\varepsilon_{ij}+2)^2 w_j$$

$$\left(\frac{d\sigma_{ij}'}{dw_j}\right)_{w_j \to 0} = \frac{N\mu_j^2\rho_i}{27M_jk_BT}\left(\frac{\omega^2\tau}{1+\omega^2\tau^2}\right)(\varepsilon_i+2)^2 \qquad \text{.....(5.6)}$$

where density ρ_{ij} and local field F_{ij} of the solution become ρ_i and $F_i = (\varepsilon_i + 2)^2/9$ of the solvent in the limit $w_j = 0$.

From Eqs.(5.5) and (5.6) one gets *hf* dipole moment μ_j as:

$$\mu_j = \left(\frac{27M_jk_BT\beta}{N\rho_i(\varepsilon_i+2)^2\omega b}\right)^{\frac{1}{2}} \qquad \text{.....(5.7)}$$

where,

N = Avogadro's number = 6.023×10^{23}

ρ_i = density of solvent benzene at 25°C = 874.3 Kg.m^{-3}

ε_i = relative permittivity of solvent benzene at 25°C = 2.274

M_j = molecular weight of solute in Kg.

k_B = Boltzmann constant = 1.38×10^{-23} J.mole^{-1}.K^{-1} and

b is the dimensionless parameter involved with measured τ where $b=1/(1+\omega^2\tau^2)$

Both the dipole moments μ_j's and dimensionless parameters b's are presented in Table 5.2.

5.3. Results and Discussions :

The imaginary $\sigma_{ij}''(=\omega\varepsilon_0\varepsilon_{ij}')$ Ω^{-1} m^{-1} are plotted against real $\sigma_{ij}'(=\omega\varepsilon_0\varepsilon_{ij}'')$ Ω^{-1} m^{-1} parts of *hf* complex conductivity σ_{ij}^* for different weight fractions w_j's of solute according to Eq.(5.2) to get τ of polar liquid molecules as shown in Fig.5.1. The variables are found to be almost linearly correlated as evident from the correlation coefficient 'r' of the straight line of Eq.(5.3). It appears from Fig.5.1 that the systems like (I), (II), (III) and (VII) show low values of r (Table 5.1) indicating their departure from perfect linearity of the variables. Perfect linearity is said to be achieved for $-1 \leq r \leq 1$. In such cases, the proposed method to determine τ from the ratio of the individual slopes of σ_{ij}'' and σ_{ij}' against w_j according to Eq.(5.4) seems to be a better choice and is claimed to be the best improvement over the other two because polar-polar interaction is avoided almost completely in the limit $w_j = 0$. The estimated τ's for systems (III), (IV), (VI) and (IX) from Eq.(5.4) are in agreement with those of Murthy *et al* [5.10] and reported τ. For the rest of the systems, τ's are lower from the ratio of individual slopes except methyl hexyl ketone. All the plots of $\sigma_{ij}''$and σ_{ij}'against

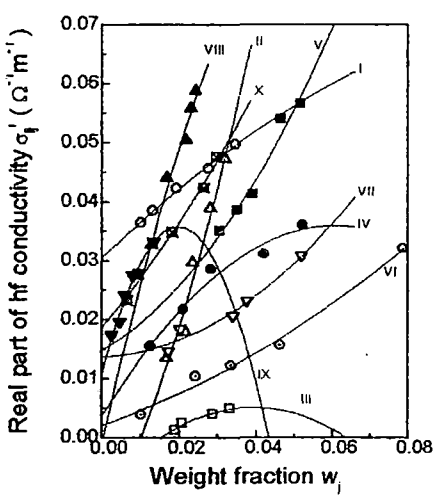

Figure 5.3 : Variation of real part of conductivity σ_{ij}' against w_j at 25°C under 9.585 GHz electric field :
(I) Toluene (-O-) (II) 1,3,5 tri methyl benzene (-Δ-) (III) 1,2,3,4 tetra methyl benzene (-□-) (IV) 1,2,4,5 tetra methyl benzene(-◉-) (V) penta methyl benzene (-■-) (VI) *p*-fluoro toluene (-⊙-) (VII) Butyl ethyl ketone (-V-) (VIII) Methyl hexyl ketone (-▲-) (IX) Ethyl pentyl ketone (-▼-) (X) heptyl methyl ketone (-⊗-)

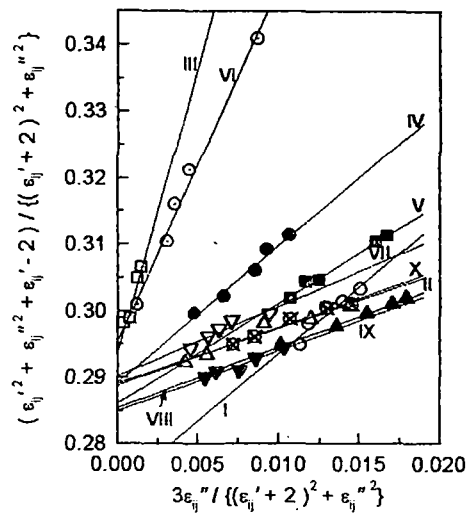

Figure 5.4: Linear plots of x against y for some methyl benzenes and ketones at 25^{0}C under 9.585 GHz electric field:

(I) Toluene (-O-), (II) 1,3,5 tri methyl benzene (-Δ-), (III) 1,2,3,4 tetra methyl benzene (-□-), (IV) 1,2,4,5 tetra methyl benzene (-●-), (V) penta methyl benzene (-■-), (VI) *p*-fluoro toluene (-⊙-), (VII) Butyl ethyl ketone (-∇-), (VIII) Methyl hexyl ketone (-▲-), (IX) Ethyl pentyl ketone (-▼-), (X) heptyl methyl ketone (-⊗-)

w_j's as sketched in Figs.5.2 and 5.3 are parabolic in nature indicating the occurrence of associational aspect of polar liquid molecules in a non-polar solvent. The systems I(-O-), II(-Δ-), III(-□-), IV(-●-), VII(-∇-), IX(-▼-) and X(-⊗-) exhibit monotonic increase of σ_{ij}'' with w_j like σ_{ij}–w_j curves of Fig.5.5 in order to attain maximum value at a certain concentration (w_j) to show the convex nature. This is perhaps due to phase transition occurring in the polar-nonpolar liquid mixture as observed elsewhere [5.12]. Similar variation σ_{ij}'' and σ_{ij} in Ω^{-1} m^{-1} with w_j as displayed graphically in Figs.5.2 and 5.5 indicates the validity of the approximation of $\sigma_{ij}'' \cong \sigma_{ij}$ of Eq.(5.5). All the curves of Figs.5.2 and 5.5 have a tendency to cut a point on the σ_{ij}–axis in the limit w_j=0 except systems (II) and (III) probably due to solvation effect [5.15] of the polar-nonpolar liquid mixture. The plots of σ_{ij}'–w_j curves of Fig.5.3 are also parabolic in nature. The variation of σ_{ij}' against w_j's for the III(-□-), IV(-●-) and IX(-▼-) systems show convex shape indicating the maximum absorption of *hf* electric energy at w_j=0.04, 0.06 and 0.02 respectively. The rest systems display gradual increase of σ_{ij}' with w_j probably due to the fact that absorbtion of electric energy increases at the higher concentration. This is authenticated by the positive coefficient of the quadratic term in the fitted equations of σ_{ij}'–w_j curves of Fig.5.3. All the τ's of the polar liquid molecules of Table 5.1 agree well with those of Murthy *et al* [5.10] from Eq.(5.3) and reported value. The reported τ's based on the standard method of Gopalakrishna were found to be much higher [5.7-5.8] which prompted us to recalculate τ's from the following expression [5.16]:

$$x = \frac{\varepsilon_{ij}'^2 + \varepsilon_{ij}' + \varepsilon_{ij}''^2 - 2}{\left(\varepsilon_{ij}' + 2\right)^2 + \varepsilon_{ij}''^2}; y = \frac{3\varepsilon_{ij}''}{\left(\varepsilon_{ij}' + 2\right)^2 + \varepsilon_{ij}''^2} \qquad \ldots\ldots (5.8)$$

The variation of x against y of Eq.(5.8) are linear as seen in Fig.5.4. One can obtain τ from:

$$\tau = \frac{1}{\omega(dx/dy)} \qquad \ldots\ldots (5.9)$$

μ_j's are recalculated by using Gopalakrishna's equation [5.16] as:

$$\mu = \left[\frac{9k_BTM_j}{4\pi N\rho_i}\left\{1+\left(\frac{dy}{dx}\right)^2\right\}\left(\frac{dx}{dw_j}\right)_{w_j\to 0}\right]^{\frac{1}{2}} \qquad \ldots\ldots (5.10)$$

τ's from the ratio of the individual slopes of Eq.(5.4), on the other hand, are found to be in better agreement for the systems: 1,2,3,4 tetramethyl benzene (III); 1,2,4,5 tetramethyl benzene (IV); *p*-fluoro toluene (VI) and ethyl pentyl ketone (IX) respectively. The other systems exhibit low values of τ from the ratio of individual slopes of σ_{ij}'' and σ_{ij}' against w_j's except methyl hexyl ketone (VIII). This behaviour can be explained on the basis of the fact that the methods of Murthy *et al* [5.10] and Gopalakrishna yield τ's of either a quasi isolated polar or a dimer (solute-solute association) molecule. The ratio of the individual slopes, on the other hand, takes into account both the processes in addition to τ of a dimer molecule. The smaller value of τ may be due to formation of monomer supported by low values of r of the systems under investigation.

Dipole moment μ_j's are computed from the slope β of *uhf* conductivity σ_{ij} against w_j curves of Fig.5.5 and dimensionless parameter b's of Eq.(5.7) to compare with the results of Eq.(5.10) of Gopalakrishna [5.16]. μ's are now found to agree well as seen in Table 5.2 with Murthy *et al* [5.10] and recalculated values of Gopalakrishna for all the systems like τ's indicating the applicability of the methods for such systems under investigation. σ_{ij}'s of polar-nonpolar liquid mixtures are, however, concerned with the bound molecular charges which may be counted by β (Table 5.2) of σ_{ij}–w_j curves of Fig.5.5. The agreement is better from Eqs.(5.4) and (5.7) with the use of the ratio of individual

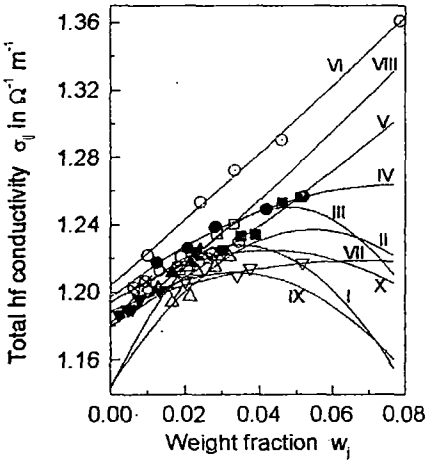

Figure 5.5 : The plot of *uhf* conductivity σ_{ij} against w_j :

(I) Toluene (-O-), (II) 1,3,5 tri methyl benzene (-Δ-), (III) 1,2,3,4 tetra methyl benzene (-□-), (IV) 1,2,4,5 tetra methyl benzene (-●-), (V) penta methyl benzene (-■-), (VI) *p*-fluoro toluene (-⊙-), (VII) Butyl ethyl ketone (-▽-), (VIII) Methyl hexyl ketone (-▲-), (IX) Ethyl pentyl ketone (-▼-), (X) heptyl methyl ketone (-⊗-)

slopes for systems (I), (III), (IV), (VI) and (IX) respectively unlike other polar liquids where μ's are slightly lower except for methyl hexyl ketone. Low values of μ's may be due to formation of monomer while high values are responsible for dimer formations. The slight difference between reported and estimated μ's may occur due to existence of steric hindrances among the substituted polar groups.

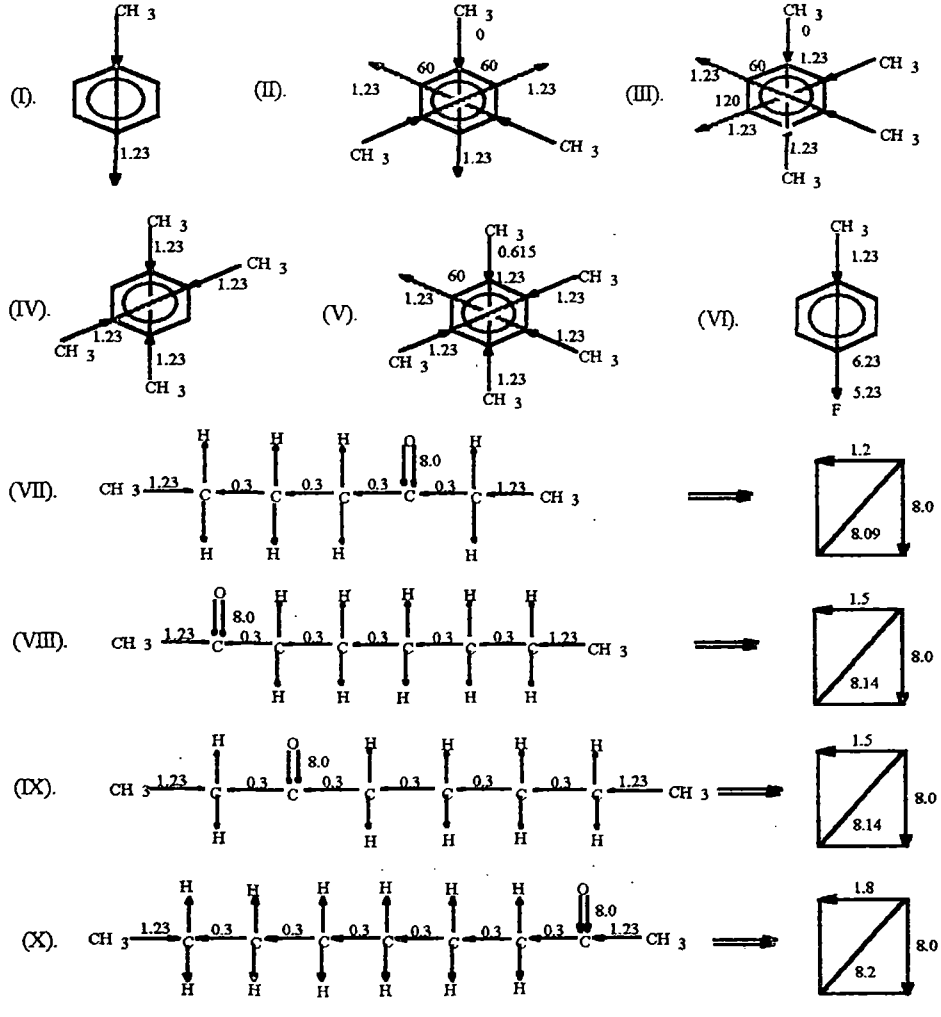

Figure 5.6: Conformational structures of polar molecules in terms of bond angles and bond moments(x 10^{-30} Coulomb. metre) of the substituent groups.

(I) Toluene, (II) 1,3,5 tri methyl benzene, (III) 1,2,3,4 tetra methyl benzene (IV), 1,2,4,5 tetra methyl benzene, (V) penta methyl benzene, (VI) p-fluoro toluene, (VII) Butyl ethyl ketone, (VIII) Methyl hexyl ketone, (IX) Ethyl pentyl ketone, (X) heptyl methyl ketone.

The theoretical dipole moments μ_{theo}'s are calculated on the basis of planar structures for the molecules from the available bond moments of $CH_3 \rightarrow C$, $C \Leftarrow O$, $C \leftarrow C$, $C \rightarrow F$ and $C \rightarrow H$ of 1.23 x 10^{-30}, 8 x 10^{-30}, 0.3 x 10^{-30}, 5.23 x 10^{-30} and 1 x 10^{-30} in Coulomb-metre (C.m) respectively.

$CH_3 \rightarrow C$ makes an angle 180^0 with the bond axis. The direction of C←C bond moment is taken in the reverse direction of bond axis [5.17]. All the substituted polar groups have the usual nature of either pushing or pulling electrons from the adjacent atoms of the parent molecules. Thus there exists a difference in electron affinity within each atom of the substituted polar groups causing inductive, mesomeric and electromeric effects in them, which play a role in the structure of the polar molecules of Fig.5.6. The solvent C_6H_6 due to its aromaticity is a cyclic planar compound having three alternate single and double bonds and six *p*-electrons on six C-atoms. The sp^2 hybridised electrons provide delocalised π-electrons to each atom of the substituted polar groups of the molecules. $CH_3^{\delta+} \rightarrow C^{\delta-}$ is a strong electron pushing (+I effect) while $>C^{\delta+} \Leftarrow O^{\delta-}$ is responsible for both the mesomeric (–M effect) and electromeric effect. Thus all the substituted polar groups may be responsible to form either solute-solvent (monomer) or solute-solute (dimer) association to yield lower and higher μ_j's respectively depending upon the solvent used. The difference $\Delta\mu$ between μ_j's and μ_{theo}'s of Fig.5.6 for the methyl substituted benzenes are 5.92, 9.36, 8.74, 7.84, 5.28 and 0.2 $\times 10^{-30}$ C.m for the six systems while the rest of the four ketones have –3.63, 4.8, 3.5 and –1.05 $\times 10^{-30}$ C.m respectively. This indicates the mesomeric and electromeric effects which are maximum for 1,3,5 trimethyl benzene and methyl hexyl ketone probably due to presence of strong electron repelling character of $CH_3 \rightarrow C$ group. The μ_{theo} of 1,3,5 tri methyl benzene, 1,2,3,4 tetra methyl benzene and 1,2,4,5 tetra methyl benzene are found to be of zero. The bond moment of $CH_3 \rightarrow C$ group acts in opposite direction in a plane to yield zero value. The molecules may have considerable μ_{theo} values if they are three dimensional structure. All these effects may be taken into account to get exact μ_j's of Table 5.2 from μ_{theo} by the factor μ_{expt}/μ_{theo} (5.81, 5.29, 1.03, 0.55, 1.59, 1.43, 0.87) except for three molecules.

5.4. Conclusion :

The structural information of some aromatic methyl benzenes and aliphatic ketones are obtained from the conductivity measurement at 25^0C under the most effective dispersive region of 9.585 GHz electric field. Modern internationally accepted symbols of dielectric relaxation terminologies and parameters in SI units seem to be more topical, significant and useful contribution to obtain τ and μ of a dipolar liquid dissolved in nonpolar solvent. τ_j's measured from the slope of the linear σ_{ij}''–σ_{ij}' curves are not in agreement for all cases with those from the ratio of the individual slopes of σ_{ij}''–w_j and σ_{ij}'–w_j in the limit $w_j = 0$. The latter method is more significant because in this case one polar molecule is surrounded by a large number of non-polar molecules and thus polar-polar interactions are supposed to be completely eliminated. This method is thus supposed to yield monomeric or often dimeric structure of polar molecules. μ_j's are measured from

the linear coefficient β of σ_{ij}–w_j curve at $w_j \rightarrow 0$. σ_{ij} or σ_{ij}'' in Ω^{-1} m^{-1} for some systems increase gradually in order to attain the maximum value for a certain concentration of solute and then decrease. This indicates the change of phase of the systems under investigation. Similar nature of variation of σ_{ij}'' with w_j indicates maximum absorption of *hf* electric energy for some systems. τ_j's and μ_j's claimed to be accurate within 10% and 5% are also compared with those from Gopalakrishna's fixed frequency method. The slight disagreement between experimental μ_j with the theoretical dipole moment μ_{theo} for some molecules reveals different associational aspects of dipolar liquid molecules in a non-polar solvent from the frequency dependence of relaxation parameters. This study also exhibits the presence of mesomeric, inductive and electromeric effects of the substituent polar groups of the molecules. The theoretical μ_{theo} for systems II, III and IV are zero although they possess a considerable μ_j. This invariably rules out the planar structure of the molecules and establish a three dimensional formation.

References :

[5.1] N Paul, K P Sharma and S Chattopadhyay, *Indian J. Phys.*, **71B** 71 (1997)

[5.2] S N Sen and R Ghosh, *J. Phys. Soc. (Japan)*, **33** 838 (1972)

[5.3] K Dutta, R C Basak, S K Sit and S Acharyya, *J. Molecular Liquids*, **88** 229 (2000)

[5.4] N Ghosh, S K Sit, A K Bothra and S Acharyya, *J. Phys. D: Appl. Phys.*, **34** 379 (2001)

[5.5] M D Migahed, M T Ahmed and A E Kotp, *J. Phys. D: Appl. Phys.*, **33** 2108 (2000)

[5.6] A Bello, E Laredo, M Grimau, A Nogales and T A Ezquerra, *J. Chem. Phys.*, **113** 863 (2000)

[5.7] S K Vaish and N K Mehrotra, *Indian J. Pure. & Appl. Phys.*, **37** 881 (1999)

[5.8] S K Vaish and N K Mehrotra, *Indian J. Pure. & Appl. Phys.*, **37** 778 (1999)

[5.9] N Bloembergen, E M Purcel and R V Pound, *Physical Review*, **73** 673 (1948)

[5.10] M B R Murthy, R L Patil and D K Deshpande, *Indian J. Phys.*, **63B** 491 (1989)

[5.11] R C Basak, S K Sit, N Nandi and S Acharyya, *Indian J. Phys.*, **70B** 37 (1996)

[5.12] K Dutta, S K Sit and S Acharyya, *J. Molecular Liquid*, **92** 263 (2001)

[5.13] F J Murphy and S O Morgan, *Bell. Syst. Tech. J.*, **18** 502 (1939)

[5.14] N E Hill, W E Vaughan, A H Price and M Davies, *Dielectric Properties and Molecular Behaviour* (Van Nostrand Reinhold Company, London) 1969

[5.15] S K Sit, R C Basak, U Saha and S Acharyya, *J. Phys. D : Appl. Phys.*, **27** 2194 (1994)

[5.16] K V Gopalakrishna, *Trans. Faraday. Soc.*, **53** 767 (1957)

[5.17] S K Sit and S Acharyya, *Indian J. Phys.*, **70B** 19 (1996)

CHAPTER 6

DIELECTRIC RELAXATION PHENOMENA AND HIGH FREQUENCY CONDUCTIVITY OF RIGID POLAR LIQUIDS IN DIFFERENT SOLVENTS

6.1. Introduction :

Dielectric relaxation studies of polar liquids in non-polar solvents are of much importance as they provide interesting information on solute-solvent and solute-solute molecular formations [6.1-6.2] under high frequency (*hf*) electric field. In order to predict associational aspects of polar liquids one must analyse the measured relaxation parameters to know the relaxation time τ and the dipole moment μ of a polar liquid by Cole-Cole [6.3], Cole-Davidson [6.4] plots or by single frequency concentration variation method [6.5].

Srivastava and Srivastava [6.6] studied the relaxation behaviour of chloral and ethyltrichloroacetate in different non-polar solvents under 4.2, 9.8 and 24.6 GHz electric field frequencies from the measured dimensionless dielectric constants like real k_{ij}', imaginary k_{ij}'', static k_{oij} and infinite frequency dielectric constant $k_{\infty ij}$ of polar solute (j) in different non-polar solvents (i) at 30^0C to predict their solute-solvent or solute-solute molecular associations. They, however, inferred that such molecules may possess two or more relaxation processes towards dielectric dispersion phenomena [6.6]. The molecule chloral is widely used in medicine and in the manufacture of D.D.T as insecticide. Ethyltrichloroacetate, on other hand, is used for artificial fragrance of fruits and flowers.

All these facts inspired us to use the measured relaxation data [6.6] for such polar liquids only to detect the double relaxation times τ_1 and τ_2 from the single frequency measurement technique [6.7-6.8]. Earlier investigations have been made on different chain like polar molecules like alcohols in a non-polar solvent [6.9-6.10] to see the double relaxation phenomena at three different electric field frequencies. However, no such study is made so far on such rigid aliphatic polar liquids in different non-polar solvents under various electric field frequencies by the double relaxation formalism derived from single frequency measurements of dielectric relaxation parameters [6.7-6.8]. It is better to study the relaxation phenomena in terms of dimensionless dielectric constants in SI units because of its rationalised coherent and unified nature.

Five systems out of twelve as presented in Table 6.1 show the double relaxation times τ_2 and τ_1 due to rotation of the whole and the flexible parts of the molecule. τ_2 and τ_1 were calculated from the slope and intercept of the linear Eq.(6.7) (see later). All the straight lines are shown graphically in Fig.6.1.

The dipole moments μ_2 and μ_1 of Table 6.2 due to τ_2 and τ_1 were computed in terms of slopes β's of total *hf* conductivity σ_{ij} against w_j curves of Fig.6.2. All the parabolic curves of conductivities σ_{ij}'s with w_j's are found to increase with frequency of the electric field.

The calculated μ's are compared with the theoretical dipole moment μ_{theo} due to available bond angles and bond moments which are sketched in Fig.6.3 showing the associational aspect of

the polar molecules with solvents to observe the mesomeric and inductive moments in them under *hf* electric field. They are finally compared with the reported μ's and μ_1 obtained from $\mu_1=\mu_2(c_1/c_2)^{½}$ assuming two relaxation processes are equally probable.

Table 6.1: The estimated relaxation time τ_2 and τ_1 from the slope and the intercept of straight line Eq.(6.5) with errors and correlation coefficients (r) together with measured τ from $\sigma_{ij}''-\sigma_{ij}'$ curve and τ_2's from single broad dispersion for apparently rigid aliphatic molecules at 30°C under different frequencies of electric fields.

System with sl. no. & mol. wt.M_j	Frequency f in GHz	Slope and intercept of Eq.(8.3)		Corrl. coeff. r	% of error in regression technique	Estimated τ_2 and τ_1 in p-sec		Measured τ in psec	Reported τ in psec	τ_2's in psec from single broad dispersion
(I) Chloral	(a) 4.2	-0.3872	-0.0732	-0.91	5.54	5.27	-	4.77	-	4.78
in benzene	(b) 9.8	3.7238	0.5497	0.99	0.09	57.98	2.50	2.36	1.78*	-
M_j=0.1475 Kg	(c) 24.6	-0.1936	-0.2161	-0.41	25.08	2.45	-	1.73	-	2.01
(II) Chloral	(a) 4.2	-2.7611	-0.4191	-0.78	12.81	5.44	-	3.74	-	40.87
in *n*-heptane	(b) 9.8	1.6593	0.1040	0.93	3.89	25.89	1.06	1.82	0.46*	-
M_j=0.1475 Kg	(c) 24.6	1.7458	0.1752	0.95	2.56	10.60	0.69	0.91	-	-
(III) Ethyltri-	(a) 4.2	0.3545	-0.0699	0.37	23.75	18.78	-	23.00	-	18.71
chloroacetate	(b) 9.8	1.5123	-0.1797	0.96	1.87	26.36	-	7.28	6.50**	32.53
in benzene M_j=0.1915 Kg	(c) 24.6	-2.7470	-3.3227	-0.24	25.86	5.88	-	3.34	-	37.19
(IV) Ethyltri-	(a) 4.2	-1.7251	-0.9325	-0.26	25.68	16.38	-	16.53	-	20.13
chloroacetate	(b) 9.8	1.5182	0.0549	0.66	15.40	24.05	0.60	6.28	5.70**	-
in *n*-hexane M_j=0.1915 Kg	(c) 24.6	2.9891	1.6141	0.98	0.83	14.76	4.58	5.76	-	-

*= Cole-Cole plot **= Gopalakrishna's method

The relative contributions c_1 and c_2 towards dielectric dispersions for the five systems were obtained from the theoretical values of $x=(k_{ij}'-k_{\infty ij})/(k_{oij}-k_{\infty ij})$ and $y=k_{ij}''/(k_{oij}-k_{\infty ij})$ of Fröhlich's theory [6.11] in terms of estimated τ_2 and τ_1 of Table 6.1. They were also computed from the values of x and y at $w_j\rightarrow 0$ of graphical technique [6.7-6.8] and placed in Table 6.3 for comparison with Fröhilch's c_1 and c_2. The variations of x and y with w_j of solute of Figs.6.4 and 6.5 are the least squares fitted parabolae with the experimental data. They are of convex and concave shapes except ethyltrichloroacetate in *n*-hexane at 9.8 and 24.6 GHz electric fields. This sort of behaviours was not observed earlier [6.7-6.8]. With these values of x and y at $w_j\rightarrow 0$ the symmetric and asymmetric distribution parameters γ and δ of the molecules at those frequencies are computed and are placed in Table 6.3 to indicate the non-rigidity of the molecules in *hf* electric field.

6.2. Theoretical Formulations :

Assuming the molecules to possess two separate board dispersions under *hf* electric field. Bergmann equations [6.12] are:

$$\frac{k'_{ij}-k_{\infty ij}}{k_{oij}-k_{\infty ij}} = c_1\frac{1}{1+\omega^2\tau_1^2}+c_2\frac{1}{1+\omega^2\tau_2^2} \qquad \ldots\ldots(6.1)$$

$$\frac{k''_{ij}}{k_{oij}-k_{\infty ij}} = c_1\frac{\omega\tau_1}{1+\omega^2\tau_1^2}+c_2\frac{\omega\tau_2}{1+\omega^2\tau_2^2} \qquad \ldots\ldots(6.2)$$

such that the sum of the relative weight factors c_1 and c_2 towards dielectric dispersion is unity i.e $c_1+c_2=1$.

Table 6.2: Estimated intercept and slope of σ_{ij}–w_j equations, dimensionless parameters b_2, b_1 [Eq.(6.13)], estimated dipole moments μ_2, μ_1 from Eq.(6.12) and μ_{theo} from bond angles and bond moment together with μ_1 from $\mu_1=\mu_2(c_1/c_2)^{1/2}$ and reported μ in Coulomb.metre (C.m).

System with sl. no. & mol. wt.M_j	f in GHz	Intercept & slope of σ_{ij}–w_j equation		Dimensionless parameter		Estimated $\mu X10^{30}$ in C.m		Reported $\mu X10^{30}$ in C.m	Estimated $\mu_1 X10^{30}$ in C.m from $\mu_1=\mu_2(c_1/c_2)^{1/2}$	μ_{theo} in C.m
		α	β	b_1	b_2	μ_2	μ_1			
(I) Chloral	4.2	5.990	4.208	-	0.981	5.02	-	5.01*	-	
in benzene	9.8	13.791	10.800	0.977	0.073	19.32	5.27	4.87**	13.26	10.02
M_j=0.1475 Kg	24.6	34.880	26.010	-	0.875	5.46	-	5.28*	-	
(II) Chloral	4.2	5.058	3.619	-	0.980	5.78	-	5.72*	-	
in *n*-heptane	9.8	11.772	6.001	0.996	0.282	9.07	4.83	6.00**	9.71	10.02
M_j=0.1475 Kg	24.6	29.631	16.513	0.989	0.271	9.69	5.08	5.10*	9.63	
(III) Ethyltri-	4.2	5.990	9.057	-	0.803	9.27	-	9.72*	-	
chloroacetate	9.8	14.100	10.334	-	0.275	11.07	-	6.50**	-	10.50
in benzene	24.6	34.188	39.357	-	0.548	9.67	-	8.05*	-	
M_j=0.1915 Kg										
(IV) Ethyltri-	4.2	4.984	5.599	-	0.843	8.97	-	8.99*	-	
chloroacetate	9.8	11.522	12.722	0.999	0.313	14.53	8.14	8.67**	17.15	10.50
in *n*-hexane	24.6	28.160	36.525	0.666	0.161	21.66	10.65	11.64*	16.37	
M_j=0.1915 Kg										

** Ref [6.5] *Computed from conductivity

Solving Eqs.(6.1) and (6.2) for c_1 and c_2 one gets:

$$c_1 = \frac{(x\alpha_2 - y)(1+\alpha_1^2)}{\alpha_2-\alpha_1} \qquad \ldots\ldots(6.3)$$

$$c_2 = \frac{(y - x\alpha_1)(1+\alpha_2^2)}{\alpha_2-\alpha_1} \qquad \ldots\ldots(6.4)$$

where $x = (k_{ij}' - k_{\infty ij})/(k_{oij} - k_{\infty ij})$ and $y = k_{ij}''/(k_{oij} - k_{\infty ij})$. The term $\alpha = \omega\tau$ and suffices 1 and 2 are, however, related to τ_1 and τ_2 respectively. Adding Eqs.(6.3) and (6.4) one gets:

$$\frac{k_{oij} - k_{ij}'}{k_{ij}' - k_{\infty ij}} = \omega(\tau_1 + \tau_2)\frac{k_{ij}''}{k_{ij}' - k_{\infty ij}} - \omega^2\tau_1\tau_2 \qquad \ldots\ldots (6.5)$$

as a linear equation having intercept $-\omega^2\tau_1\tau_2$ and slope $\omega(\tau_1+\tau_2)$ which are obtained from the measured dielectric constants at different w_j's of solutes under a single frequency electric field at a given temperature by applying linear regression technique and ω= the angular frequency $=2\pi f$, f being the frequency in GHz.

Assuming a single broad Debye like dispersion for the polar molecules the Eq.(6.5) is reduced to the from [6.8] with $\tau_1=0$.

$$\frac{k_{oij} - k_{ij}'}{k_{ij}' - k_{\infty ij}} = \omega\tau_2 \frac{k_{ij}''}{k_{ij}' - k_{\infty ij}} \qquad \ldots\ldots (6.6)$$

in order to get τ_2 for seven polar-nonpolar liquid mixtures placed in the 11th column Table 6.1.

Again, the complex *hf* conductivity σ_{ij}^* is related to k_{ij}' and k_{ij}'' by the relation:

$$\sigma_{ij}^* = \sigma_{ij}' + j\sigma_{ij}''$$

where $\sigma_{ij}' = \omega\varepsilon_o k_{ij}''$ and $\sigma_{ij}'' = \omega\varepsilon_o k_{ij}'$ are the real and imaginary parts of the complex conductivity σ_{ij}^*. The magnitude of total *hf* conductivity is given by:

$$\sigma_{ij} = \omega\varepsilon_o (k_{ij}''^2 + k_{ij}'^2)^{1/2} \qquad \ldots\ldots (6.7)$$

σ_{ij}'' is related to σ_{ij}' by the relation:

$$\sigma_{ij}'' = \sigma_{\infty ij} + \frac{1}{\omega\tau_j}\sigma_{ij}' \qquad \ldots\ldots (6.8)$$

where τ_j is the measured relaxation time of a polar unit and $\sigma_{\infty ij}$ is constant conductivity at $w_j \to 0$.

In the *hf* region, total conductivity $\sigma_{ij} \cong \sigma_{ij}''$, hence Eq.(6.8) is written as:

$$\sigma_{ij} = \sigma_{\infty ij} + \frac{1}{\omega\tau_j}\sigma_{ij}'$$

$$\left(\frac{d\sigma_{ij}}{dw_j}\right)_{w_j \to 0} = \frac{1}{\omega\tau_j}\left(\frac{d\sigma_{ij}'}{dw_j}\right)_{w_j \to 0}$$

$$\beta = \frac{1}{\omega\tau_j}\left(\frac{d\sigma_{ij}'}{dw_j}\right)_{w_j \to 0} \qquad \ldots\ldots (6.9)$$

The real part of *hf* conductivity σ_{ij}' at T K for w_j of a solute is [6.13-6.14]:

$$\sigma_{ij}' = \frac{N\rho_{ij}\mu_j^2}{27k_BTM_j}\left(\frac{\omega^2\tau_j}{1+\omega^2\tau_j^2}\right)(k_{ij}'+2)^2 w_j \qquad \ldots\ldots (6.10)$$

On differentiation with respect to w_j and at $w_j \to 0$, Eq.(6.10) becomes:

$$\left(\frac{d\sigma_{ij}'}{dw_j}\right)_{w_j\to 0} = \frac{N\rho_i\mu_j^2}{27k_BTM_j}\left(\frac{\omega^2\tau_j}{1+\omega^2\tau_j^2}\right)(k_i+2)^2 \qquad \ldots\ldots (6.11)$$

where all the symbols expressed is S I units carry usual meanings [6.14]. From Eqs.(6.9) and (6.11) one gets *hf* dipole moment μ_j from:

$$\mu_j = \left(\frac{27k_BTM_j}{N\rho_i(k_i+2)^2}\frac{\beta}{\omega b}\right)^{1/2} \qquad \ldots\ldots (6.12)$$

The dimensionless parameter b is related to τ by:

$$b = \frac{1}{1+\omega^2\tau_j^2} \qquad \ldots\ldots (6.13)$$

all the μ_j's, b's and β's as computed for chloral and ethyltrichloroacetate are presented in Table 6.2.

Table 6.3: Fröhlich parameter A [$=\ln(\tau_2/\tau_1)$], relative contributions c_1 and c_2 due to τ_1 and τ_2, theoretical values of x and y from Fröhlich Eqs.(6.14) and (6.15) and from fitting equations as shown in Figs.6.4 and 6.5 at $w_j \to 0$ and symmetric and asymmetric distribution parameters γ and δ for the five polar-nonpolar liquid mixtures at 30°C.

System with sl. no.	f in GHz	A	Theoretical values of x and y from Eqs. (6.14) & (6.15)		Theoretical values of c_1 and c_2		Estimated values of x and y at $w_j \to 0$		Estimated values of c_1 and c_2		Estimated values of γ and δ	
(I) Chloral in benzene	9.8	3.14	0.587	0.364	0.52	1.10	0.362	0.228	0.32	0.69	0.42	0.38
(II) Chloral in *n*-heptane	9.8	3.12	0.803	0.296	0.65	0.56	0.610	0.318	0.43	0.64	0.26	0.42
	24.6	2.73	0.763	0.336	0.60	0.61	0.671	0.287	0.54	0.52	0.29	0.35
(IV) Ethyltri-chloroacetate in *n*-hexane	9.8	3.69	0.843	0.255	0.69	0.49	0.446	0.284	0.26	0.59	0.34	0.42
	24.6	1.17	0.394	0.463	0.42	0.73	-0.327	0.383	-1.07	2.41	-0.62	–

The molecules under consideration are of complex type and only a few data are available under single frequency measurement. In the case of a continuous distribution of τ's between the two

extreme values [6.12] of τ_1 and τ_2, Fröhlich's theory [6.11] based on distribution of τ yields:

$$x = \frac{k'_{ij} - k_{\infty ij}}{k_{oij} - k_{\infty ij}} = 1 - \frac{1}{2A} \ln\left(\frac{1+\omega^2\tau_2^{\,2}}{1+\omega^2\tau_1^{\,2}}\right) \qquad \ldots\ldots (6.14)$$

$$y = \frac{k''_{ij}}{k_{oij} - k_{\infty ij}} = \frac{1}{A}\left[\tan^{-1}(\omega\tau_2) - \tan^{-1}(\omega\tau_1)\right] \qquad \ldots\ldots (6.15)$$

where A=Fröhlich parameter=$\ln(\tau_2/\tau_1)$. The theoretical values of x and y of Eqs.(6.14) and (6.15) were used to get c_1 and c_2. The values of c_1 and c_2 can be had from the graphical plots of x and y at $w_j \to 0$ as seen in Figs.6.4 and 6.5 respectively. c_1 and c_2 thus obtained by both the methods are shown in Table 6.3 for comparison.

The molecules under five different environments show double relaxation phenomena (Table 6.1) indicating their non-rigidity. In such cases dielectric relaxation behaviour may be represented by [6.3-6.4]:

$$\frac{k^*_{ij} - k_{\infty ij}}{k_{oij} - k_{\infty ij}} = \frac{1}{1+(j\omega\tau_s)^{1-\gamma}} \qquad \ldots\ldots (6.16)$$

$$\frac{k^*_{ij} - k_{\infty ij}}{k_{oij} - k_{\infty ij}} = \frac{1}{(1+j\omega\tau_{cs})^{\delta}} \qquad \ldots\ldots (6.17)$$

where γ and δ are symmetric and asymmetric distribution parameters which are, however, related to symmetric and characteristic relaxation times τ_s and τ_{cs} respectively.

Separating the real and the imaginary parts from Eq.(6.16) we have,

$$\gamma = \frac{2}{\pi}\tan^{-1}\left[(1-x)\frac{x}{y} - y\right] \qquad \ldots\ldots (6.18)$$

where $x = (k_{ij}' - k_{\infty ij})/(k_{oij} - k_{\infty ij})$ and $y = k_{ij}''/(k_{oij} - k_{\infty ij})$ are obtained at $w_j \to 0$ from Figs.6.4 and 6.5 respectively. Similarly, δ can be calculated as:

$$\tan(\phi\delta) = \frac{y}{x} \qquad \ldots\ldots (6.19)$$

$$\log(\cos\phi)^{1/\phi} = \frac{\log(x/\cos\phi\delta)}{\phi\delta} \qquad \ldots\ldots (6.20)$$

where $\tan\phi = \omega\tau_{cs}$. To get δ, a theoretical curve of $\log(\cos\phi)^{1/\phi}$ against ϕ is drawn as seen in Fig.6.6. Knowing $\delta\phi$ from Eq.(6.19), ϕ can be found out from curve of Fig.6.6. With the known ϕ, δ can be estimated. γ and δ are entered in the 12th and 13th columns of Table 6.3.

6.3. Results and Discussions :

Fig.6.1 showed the linear variation of $(k_{oij}-k_{ij}')/(k_{ij}'-k_{\infty ij})$ against $k_{ij}''/(k_{ij}'-k_{\infty ij})$ for different w_j's of chloral and ethyltrichloroacetate in different non-polar solvents under 4.2, 9.8 and 24.6 GHz electric field frequencies at 30°C. The linearity is expressed in terms of correlation coefficients r's as seen in Table 6.1. The percentage of errors in terms of r's in the regression technique were calculated in order to place them in Table 6.1. The estimated values of τ_2 and τ_1 from intercepts and slopes of Eq.(6.5) are shown in the 7th and 8th columns of Table 6.1. Double relaxation phenomena are, however, observed for chloral in n-heptane and ethyltrichloroacetate in n-hexane at 9.8 and 24.6 GHz electric fields. Chloral in benzene at 9.8 GHz also showed the same phenomenon. This observation reveals that the probability of showing double relaxation phenomena in aliphatic non-polar solvents at higher frequencies is maximum for such rigid aliphatic polar liquids. The electrostatic interaction of polar molecules with π-delocalised electron cloud of C_6H_6 – ring increases the rigidity to show τ_2 only for the whole molecular rotation. The interaction appears to be absent for aliphatic polar liquids in alicyclic aliphatic non-polar solvents and thus the double relaxation times τ_2 and τ_1 are seen to occur in higher frequencies for their flexibility. Chloral in C_6H_6 at 9.8 GHz is exception probably due to the fact that the effective dispersive region [6.15] lies near 10 GHz electric field for such systems. τ_2's for the rest seven systems showing single relaxation phenomena were also calculated assuming single broad Debye like dispersion [6.8] in them. They are placed in the 11th column of Table 6.1. It is interesting to note that τ_1's for the five systems agree well with the measured τ from Eq.(6.8) of conductivity measurement. This fact shows that *hf* conductivity measurement always yields the average microscopic τ whereas the double relaxation phenomena offer a better understanding of microscopic as well macroscopic molecular τ

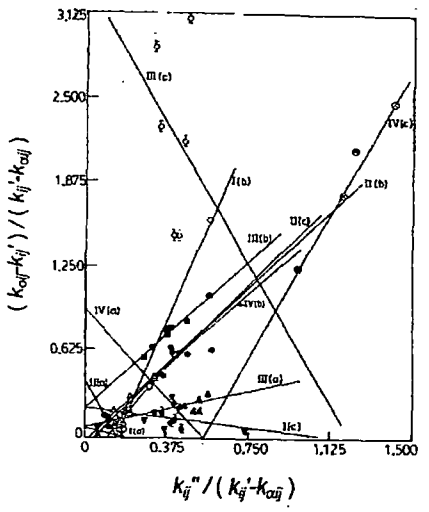

Figure 6.1: Linear variation of $(k_{oij}-k_{ij}')/(k_{ij}'-k_{\infty ij})$ against $k_{ij}''/(k_{ij}'-k_{\infty ij})$ for different w_j's at 30°C. I(a), I(b) and I(c) for chloral in benzene (⧗, ○ , ▼); II(a), II(b) and II(c) for chloral in n-heptane (◑ Δ, □); III(a), III(b) and III(c) for ethyltrichloroacetate in benzene (▲ , ■ , ⬙); IV(a), IV(b) and IV(c) for ethyltrichloroacetate in n-hexane (◆, ●, ⊕ ,) under 4.2, 9.8 and 24.6 GHz electric fields respectively

as observed elsewhere [6.9]. τ_2 of Table 6.1 is higher at 9.8 GHz and decrease gradually both at 4.2 GHz and 24.6 GHz electric fields in different solvents. This type of behaviour is probably due to larger size of the rotating unit in the effective dispersive region of nearly 10 GHz due to solute-solvent or solute-solute molecular associations which break up with the increase or decrease from nearly 10 GHz electric field frequency. All the τ and τ_1 agree well with the available reported τ placed in the 10th column of Table 6.1 establishing the fact that the rotation of a part of the molecule is possible under *hf* electric field [6.16].

The dipole moments μ_2 and μ_1 of the polar molecules were calculated in terms of dimensionless parameters b's involved with τ's of Eq.(6.13) and slope β of σ_{ij}–w_j curve of Fig.6.2 as seen in Table 6.2. The polar liquid in a given non-polar solvent behaves as a bound charged species due to polarisation under GHz electric field in order to have large *hf* conductivity σ_{ij} for different w_j although they are insulators. The parabolic variation of σ_{ij} with w_j increases with the electric field frequency as found in Fig.6.2 yielding different slopes β's which are usually used to calculate *hf* μ_j of a polar liquid from Eqs.(6.12) and (6.13) at a given temperature. μ_2's are found to increase from 4.2 GHz electric fields for chloral in *n*-heptane and ethyltrichloroacetate in *n*-hexane. This type of behaviour is probably due to rupture of solute-solute and solute-solvent molecular association in the *hf* electric field and the corresponding increase in the absorbtion for smaller molecular species [6.17]. But chloral and ethyltrichloroacetate in benzene show higher values of μ_2 at 9.8 GHz and decrease gradually from 24.6 GHz to 4.2 GHz electric fields. Such type of behaviour may be due to strong absorbtion of electric energy at 9.8 GHz and solute-solvent association of the polar solute with benzene ring. μ_2 and μ_1 are, however, compared with the μ_{theo}'s due to available bond angles and bond moments 8.0×10^{-30}, 5.0×10^{-30}, 0.3×10^{-30} and 2.4×10^{-30} Coulomb-metre for >C⇐O, C←Cl, C←C and C→OCH_3 (making an angle 57^0 with bond axis) respectively as displayed in Fig.6.3. μ_{theo}'s are

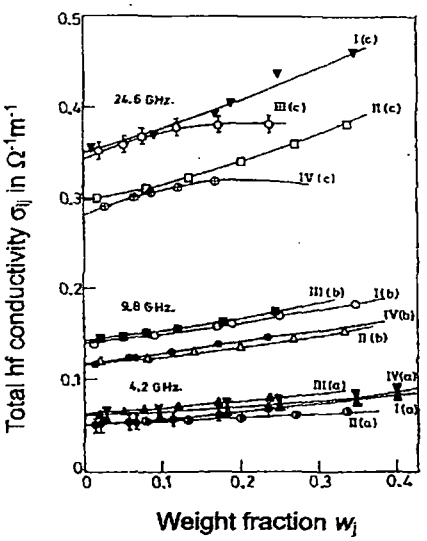

Figure 6.2: Total *hf* conductivity σ_{ij} in $\Omega^{-1}m^{-1}$ against w_j's at 30^0C. I(a), I(b) and I(c) for chloral in benzene (⧗, O , ▼); II(a), II(b) and II(c) for chloral in *n*-heptane (◑,Δ, □); III(a), III(b) and III(c) for ethyltrichloroacetate in benzene (▲ , ■ ,◊); IV(a), IV(b) and IV(c) for ethyltrichloroacetate in *n*-hexane (◆, ●,⊕ ,) under 4.2, 9.8 and 24.6 GHz electric fields respectively

placed in the 11th column of Table 6.2. The molecule chloral shows slightly larger μ_{theo} probably due to solute-solute molecular associations [Fig.6.3(ii)] in the comparatively concentrated solution as expected. The solute-solute associations may arise due to interaction of fractional positive charge δ^+ on C-atom and negative charge δ^- on O-atom of >C⇐O group between two solute molecules.

The solute-solvent association with benzene is explained on the basis of the interaction between C

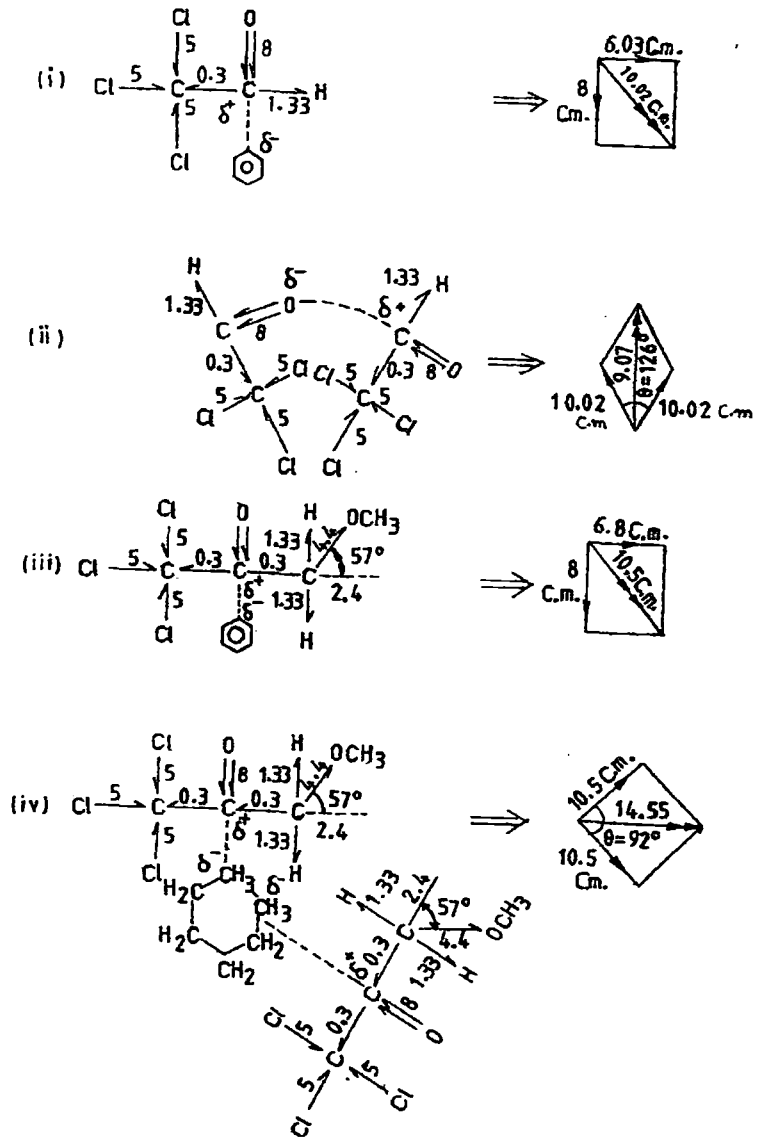

Figure 6.3: Conformational structures of chloral and ethyltrichloroacetate from bond angles and bond moments in multiple of 10^{-30} Coulomb.metre.

(i) Solute-solvent association of chloral in benzene; (ii) Solute-solute association of chloral; (iii) Solute-solvent association of ethyltrichloroacetate in benzene and (iv) Solute-solute association of ethyltrichloroacetate in *n*-hexane.

atom of >C⇐O group and π-delocalised electron cloud of C_6H_6 ring. Ethyltrichloroacetate, on the other hand, shows μ_{theo} in agreement with the estimated μ_j's in C_6H_6. This is due to solute-solvent association as sketched in Fig.6.3[(i) and (iii)] which confirms the orientation of the bond angles and bond moments of the substituents polar groups of the molecules in C_6H_6. The slight disagreement between the observed and theoretical μ's may be either due to the steric hindrances or the mesomeric, inductive and electromeric effects existing within the polar groups attached to the parent ones. Larger values of measured μ_j's invariably suggest the solute-solute interactions in alicyclic solvent *n*-hexane due to interaction between adjacent C and O atoms of >C⇐O groups of two molecules as shown in Fig.6.3 [(ii) and (iv)]. However, the reduced bond moments by μ_j/μ_{theo}'s in agreement with the estimated μ_j's reveals the mesomeric, inductive and electromeric effects within the polar groups of the molecules under consideration.

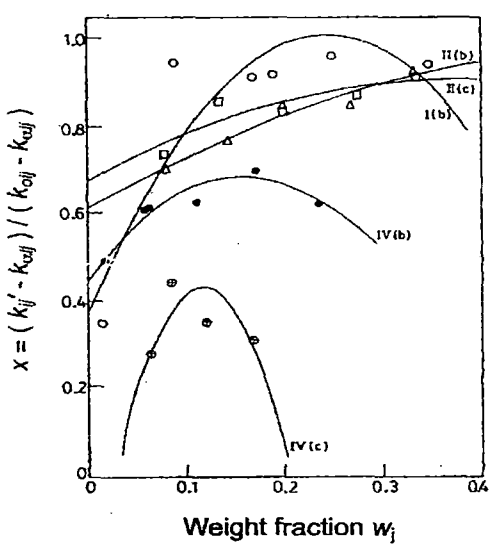

Figure 6.4: Variation of $x = (k_{ij}' - k_{\alpha ij})/(k_{oij} - k_{\alpha ij})$ with w_j's of chloral and ethyltrichloroacetate at 30°C
I(b) for chloral in benzene at 9.8 GHz (O); II(b) and II(c) for chloral in *n*-heptane at 9.8 and 24.6 GHz (Δ, □); IV(b) and IV(c) for ethyltrichloroacetate in *n*-hexane at 9.8 and 24.6 GHz (●, ⊕) electric fields.

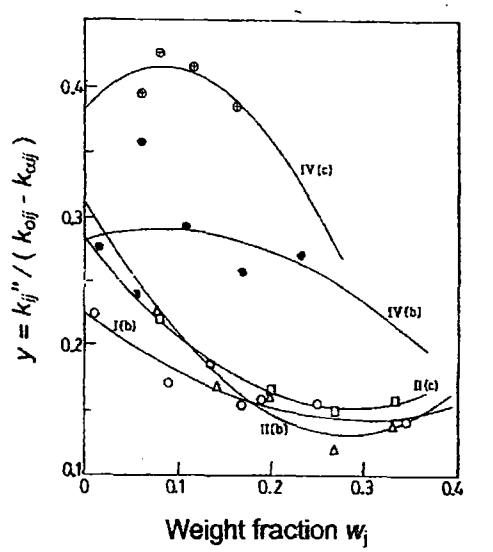

Figure 6.5: Variation of $y = k_{ij}''/(k_{oij} - k_{\alpha ij})$ with w_j's of chloral and ethyltrichloroacetate at 30°C
I(b) for chloral in benzene at 9.8 GHz (O); II(b) and II(c) for chloral in *n*-heptane at 9.8 and 24.6 GHz (Δ, □); IV(b) and IV(c) for ethyltrichloroacetate in *n*-hexane at 9.8 and 24.6 GHz (●, ⊕) electric fields

The relative contributions c_1 and c_2 toward dielectric dispersions due to τ_1 and τ_2 are, however, calculated from $x = (k_{ij}' - k_{\alpha ij})/(k_{oij} - k_{\alpha ij})$ and $y = k_{ij}''/(k_{oij} - k_{\alpha ij})$ of Eqs.(6.14) and (6.15) of Fröhlich's methods [6.11]. They are compared with those due to x and y from graphical methods

of Figs.6.4 and 6.5 at $w_j \to 0$. Both the methods yield $c_1+c_2 \cong 1$ suggesting the applicability of the methods. The nature of variation of x and y with w_j is convex and concave (except ethyltrichloroacetate in *n*-hexane at 9.8 GHz and 24.6 GHz) which is not usual as observed earlier [6.7-6.8]. Such type of behaviour explained that unlike increase of τ [6.18] it decreases with w_j probably due to solute-solute and solute-solvent molecular association. All the values of c_1 and c_2 are placed in Table 6.3 for comparison. In order to test the rigidity of the molecules the symmetric and asymmetric distribution parameter γ and δ were estimated from Eqs.(6.18) and (6.19) for fixed values of x and y at $w_j \to 0$ of Figs.6.4 and 6.5. The values of $\log(\cos\phi)^{1/\phi}$ against ϕ in degree as shown in Fig.6.6 is essential to get δ. Knowing ϕ from the curve of Fig.6.6, δ's were obtained. Both γ and δ are placed in Table 6.3. The values of γ establish the fact that the molecules obey the symmetric relaxation phenomena as δ's are very low [6.19].

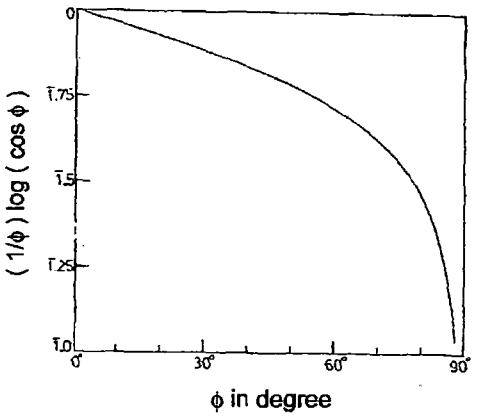

Figure 6.6: Plot of $(1/\phi)\log(\cos\phi)$ against ϕ in degree

6.4. Conclusions :

The study of dielectric relaxation mechanism by dimensionless dielectric constants gives a new insight into polar-polar and polar-nonpolar molecular interactions. The single frequency measurement of dielectric relaxation parameters provides a unique method to get macroscopic and microscopic relaxation times τ_2 and τ_1 and hence dipole moments μ_2 and μ_1 of the whole and the flexible part of the molecule. The estimation of τ_j or τ_1 and τ_2 from a linear equation is very simple and straightforward to get μ_j or μ_1 and μ_2 in terms of slope of σ_{ij}–w_j curve. The errors in measurement of τ_j and μ_j can be computed by correlation coefficients and are claimed to be accurate within 10% and 5% respectively. The molecules under different states of environment show interesting phenomena of double or single relaxation mechanism. When the solute-solvent molecular interaction is almost absent in the polar solute in alicyclic aliphatic solvent; flexible part along with the whole molecule rotates under *hf* electric field giving rise what is known as double relaxation. The solute-solvent association, on the other hand, favours the existence of single relaxation phenomena by the whole molecular rotations as π-delocalised electron clouds of solvent interact

with the flexible parts to cease their rotations. The probability of showing double relaxation is, thus greater in aliphatic solvents. Various types of molecular associations like solute-solute and solute-solvent interactions are inferred from departure of the graphical plots of $x = (k_{ij}' - k_{\infty ij})/(k_{oij} - k_{\infty ij})$ and $y = k_{ij}''/(k_{oij} - k_{\infty ij})$ with w_j of Bergmann's equations. Nonrigid characteristics of the molecules are confirmed by estimation of symmetric γ and asymmetric distribution parameter δ. The molecular associations are also supported by the conformational structures of the molecules in which the presence of mesomeric, inductive and electromeric moments due to >C⇐O group are found to play their vital role. The correlation between the conformational structures of such polar liquids with the observed results enhances the scientific content of the paper in order to add a better understanding of the existing knowledge of dielectric relaxation phenomena.

References :

[6.1] A K Sharma, D R Sharma and D S Gill, *J. Phys. D: Appl. Phys.* **18** 1199 (1985)

[6.2] A Sharma and D R Sharma, *J. Phys. Soc. Japan* **61** 1049 (1992)

[6.3] K S Cole and R H Cole, *J. Chem. Phys.* **9** 341 (1941)

[6.4] D W Davidson and R H Cole, *J. Chem. Phys.* **19** 1484 (1951)

[6.5] K V Gopalakrishna, *Trans. Faraday Soc.* **53** 767 (1957)

[6.6] S K Srivastava and S L Srivastava, *Indian J. Pure & Appl. Phys.* **13** 179 (1975)

[6.7] U Saha, S K Sit, R C Basak and S Acharyya, *J. Phys. D: Appl. Phys.* **27** 596 (1994)

[6.8] S K Sit, R C Basak, U Saha and S Acharyya, *J. Phys. D: Appl. Phys.* **27** 2194 (1994)

[6.9] S K Sit and S Acharyya, *Indian J. Phys.* **70B** 19 (1996)

[6.10] S K Sit, N Ghosh and S Acharyya, *Indian J. Pure & Appl. Phys.* **35** 329 (1997)

[6.11] H Frohlich, *Theory of Dielectrics* (Oxford University Press) p.94 (1949)

[6.12] K Bergmann, D M Roberti and C P Smyth, *J. Phys. Chem.* **64** 665 (1960)

[6.13] C P Smyth, *Dielectric Behaviour and Structure* (New York: McGraw Hill) (1955)

[6.14] R C Basak, A K Karmakar, S K Sit and S Acharyya, *Indian J. Pure & Appl. Phys.* **37** 224 (1999)

[6.15] S K Sit and S Acharyya, *Indian J. Pure & Appl. Phys.* **34** 255 (1996)

[6.16] R C Basak, S K Sit, N Nandi and S Acharyya, *Indian J. Phys.* **70B** 37 (1996)

[6.17] L Glasser, J Crossley and C P Smyth, *J. Chem. Phys.* **57** 3977 (1972)

[6.18] S N Sen and R Ghosh, *Indian J. Pure & Appl. Phys.* **10** 701 (1972)

[6.19] S Chandra and J Prakash, *J. Phys. Soc. Japan* **35** 876 (1975)

CHAPTER 7

DOUBLE RELAXATION PHENOMENA OF DISUBSTITUTED BENZENES AND ANILINES IN NONPOLAR APROTIC SOLVENTS UNDER HIGH FREQUENCY ELECTRIC FIELD

7.1. Introduction :

The dielectric relaxation phenomena of non-spherical and rigid polar liquid molecule in different nonpolar solvents at a given temperature, under a high frequency (*hf*) electric field attracted the attention of a large number of workers [7.1-7.2]. The dipole moment μ from the relaxation time τ of the polar liquid molecule is of much importance [7.3-7.4] to determine the shape, size, structure and molecular association of a polar molecule. The real ε_{ij}' and imaginary ε_{ij}'' parts of complex relative permittivity ε_{ij}^*, static and infinite frequency relative permittivities ε_{oij} and $\varepsilon_{\infty ij}$ of a polar liquid molecule (j) in a non-polar solvent (i) at a fixed experimental temperature under a single frequency electric field of GHz range are used to obtain the double relaxation times τ_2 and τ_1 due to rotation of the whole molecule as well as the flexible part attached to the parent molecule [7.5].

Khameshara and Sisodia [7.6], Gupta *et al* [7.7] and Arrawatia *et al* [7.8] measured the relative permittivities of some disubstituted benzenes and anilines in aprotic non-polar solvents C_6H_6 and CCl_4 under 9.945 GHz electric field at 35^{0}C to predict the conformation of the molecules in terms of the relaxation time τ based on the single frequency concentration variation method of Gopalakrishna [7.9] and the dipole moment μ by Higasi's method [7.10]. The compounds are very interesting for the different functional groups like $-NH_2$, $-CH_3$, $-NO_2$, $-Cl$ etc. attached to the parent molecules. The samples were of purest quality and supplied by M/s Fluka and M/s E Merck respectively. The solvents C_6H_6 and CCl_4 of M/s BDH were used after double distillation and suitably dried over NaCl and $CaCl_2$. ε_{oij} at 35^{0}C was measured by heterodyne beat method at 300 KHz. $\varepsilon_{\infty ij}=n_{Dij}^2$, where the refractive index n_{Dij} was measured by an Abbe's refractometer. The weight fraction w_j of the respective solute which is defined by the weight of the solute per unit weight of the solution was taken up to four decimal place as the accuracy in the measurement was 0.0012 %. ε_{ij}' and ε_{ij}'' within 1% and 5% accuracies were carried out by using the voltage standing wave ratio in slotted line and short circuiting plunger based on the method of Heston *et al* [7.11]. The possible existence of τ_1 and τ_2 of the compounds was, however, detected from the relative permittivity measurements [7.12] under 9.945 GHz electric field at 35^{0}C.

Nowadays, the usual practice [7.13] is to study the dielectric relaxation phenomena in terms of dielectric orientation susceptibilities χ_{ij}'s. χ_{ij}'s are linked with the orientation polarisation of a polar molecule. So it is better to work with χ_{ij}'s rather than ε_{ij}'s or conductivity σ_{ij}'s as the latters are involved with all the polarisation processes and the transport of bound molecular charges respectively [7.14]. The real $\chi_{ij}'(=\varepsilon_{ij}'-\varepsilon_{\infty ij})$ and imaginary $\chi_{ij}''(=\varepsilon_{ij}'')$ parts of the complex dielectric orientation susceptibility $\chi_{ij}^*(=\varepsilon_{ij}^*-\varepsilon_{\infty ij})$ and the low frequency susceptibility $\chi_{oij}(=\varepsilon_{oij}-\varepsilon_{\infty ij})$ which is real of the disubstituted benzenes and anilines in C_6H_6 and CCl_4 of Table 7.1 are used to obtain their

Table 7.1: The real χ_{ij}' and imaginary χ_{ij}'', parts of the complex dielectric orientation susceptibility χ_{ij}^* and static dielectric susceptibility χ_{oij} which is real for various weight fraction w_j of different disubstituted benzenes and anilines in C_6H_6 and CCl_4 at 35 °C under 9.945 GHz electric field.

Weight fraction w_j	χ_{ij}'	χ_{ij}''	χ_{oij}	Weight fraction w_j	χ_{ij}'	χ_{ij}''	χ_{oij}
(I) o-chloronitrobenzene in C_6H_6				(II) 4-chloro 3-nitro benzotrifluoride inCCl_4			
0.0109	0.117	0.066	0.167	0.0050	0.122	0.019	0.155
0.0173	0.169	0.100	0.254	0.0101	0.145	0.037	0.185
0.0217	0.197	0.126	0.305	0.0147	0.150	0.054	0.233
0.0280	0.253	0.165	0.376	0.0193	0.167	0.068	0.266
0.0330	0.284	0.192	0.461	0.0231	0.179	0.075	0.302
(III) 4-chloro 3-nitro toluene in C_6H_6				(IV) 4-chloro 3-nitro toluene in CCl_4			
0.0072	0.075	0.046	0.132	0.0041	0.145	0.039	0.208
0.0144	0.098	0.088	0.241	0.0087	0.173	0.071	0.315
0.0224	0.150	0.133	0.310	0.0128	0.190	0.101	0.419
0.0323	0.200	0.179	0.464	0.0162	0.218	0.138	0.482
0.0453	0.271	0.252	0.630	0.0203	0.241	0.165	0.586
(V) o-nitrobenzotrifluoride in C_6H_6				(VI) m-nitrobenzotrifluoride in C_6H_6			
0.0085	0.094	0.058	0.154	0.0096	0.082	0.032	0.094
0.0167	0.166	0.108	0.257	0.0173	0.103	0.060	0.157
0.0244	0.226	0.159	0.384	0.0245	0.129	0.082	0.202
0.0335	0.297	0.205	0.495	0.0326	0.157	0.106	0.265
0.0402	0.353	0.255	0.604	0.0380	0.187	0.128	0.323
(VII) 2-chloro 6-methyl aniline in C_6H_6				(VIII) 3-chloro 2-methyl aniline in C_6H_6			
0.0184	0.072	0.017	0.075	0.0083	0.059	0.018	0.065
0.0305	0.096	0.026	0.097	0.0207	0.099	0.043	0.128
0.0417	0.117	0.040	0.138	0.0270	0.128	0.055	0.166
0.0573	0.163	0.058	0.191	0.0363	0.165	0.073	0.221
0.0636	0.183	0.065	0.214	0.0421	0.193	0.086	0.255
(IX) 3-chloro 4-methyl aniline in C_6H_6				(X) 4-chloro 2-methyl aniline in C_6H_6			
0.0214	0.088	0.032	0.099	0.0196	0.124	0.063	0.151
0.0374	0.123	0.060	0.167	0.0300	0.157	0.090	0.219
0.0403	0.133	0.066	0.185	0.0417	0.199	0.121	0.304
0.0548	0.166	0.091	0.244	0.0481	0.216	0.138	0.354
(XI) 5-chloro 2-methyl aniline in C_6H_6							
0.0194	0.094	0.050	0.123				
0.0249	0.110	0.064	0.153				
0.0307	0.129	0.081	0.191				
0.0480	0.182	0.129	0.292				
0.0569	0.206	0.150	0.362				

conformational structures in terms of molecular and intra-molecular dipole moments μ_2 and μ_1 involved with the estimated τ_2 and τ_1. The disubstituted benzenes and anilines are thought to absorb electric energy much more strongly in nearly 10 GHz electric field to yield considerable values of τ_1 and τ_2. The eleven polar-nonpolar liquid mixtures under investigation are found to show the double relaxation phenomena. The most of the polar molecules are isomers of aniline and benzene. Some of the polar solutes are dissolved in C_6H_6 while a few in CCl_4 to observe the solvent effect too. Moreover, a few of the polar molecules are para-compounds in which a peculiar feature of relaxation phenomena is expected [7.15]. A strong conclusion of double relaxation phenomena of polar molecule in a non-polar solvent based on the single frequency measurement of relaxation parameters can be made only if the accurate value of χ_{oij} (±1%) involved with ε_{oij} and $\varepsilon_{\infty ij}$ is available. The use of n_{Dij}^2 for $\varepsilon_{\infty ij}$ often introduces [7.6-7.8] an additional error in the calculation since $\varepsilon_{\infty ij}$ is approximately equal to 1 to 1.5 times of n_{Dij}^2.

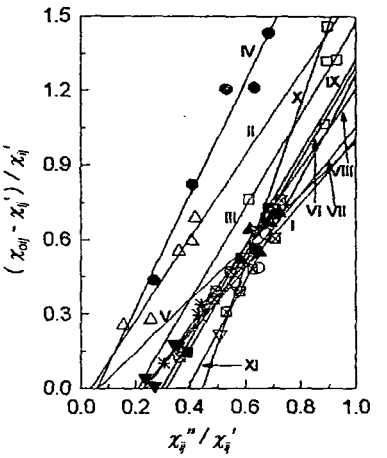

Figure 7.1: Linear variation of $(\chi_{oij} - \chi_{ij}')/\chi_{ij}'$ with χ_{ij}''/χ_{ij}' for different w_j's at 35°C under 9.945 GHz electric field.
I. o-chloronitrobenzene in C_6H_6 (–○–); II. 4-chloro 3-nitrobenzotrifluoride in CCl_4 (–△–); III. 4-chloro 3-nitrotoluene in C_6H_6 (–□–); IV. 4-chloro 3-nitrotoluene in CCl_4 (–●–); V. o-nitrobenzotrifluoride in C_6H_6 (–▲–); VI. m-nitrobenzotrifluoride in C_6H_6 (–■–); VII. 2-chloro 6-methyl aniline in C_6H_6 (–▼–); VIII. 3-chloro 2-methyl aniline in C_6H_6 (–✶ –); IX. 3-chloro 4-methyl aniline in C_6H_6 (–⊗–); X. 4-chloro 2-methyl aniline in C_6H_6 (–▽–) and XI. 5-chloro 2-methyl aniline in C_6H_6 (–⊠ –)

Bergmann *et al* [7.16] however devised a graphical method to obtain τ_1 and τ_2 for a pure polar liquid. The respective weighted contributions c_1 and c_2 towards dielectric relaxations were estimated in terms of τ_1 and τ_2. Bhattacharyya *et al* [7.17] subsequently attempted to simplify the procedure of Bergmann *et al* [7.16] to get the same for a pure polar molecule with ε', ε'', ε_o and ε_∞ measured at two different frequencies in GHz range. The graphical analysis advanced by Higasi *et al* [7.18] on polar-nonpolar liquid mixture was also a crude one.

Thus the object of the present paper is to detect τ_1 and τ_2 and hence to measure μ_1 and μ_2 using χ_{ij}'s based on the single frequency measurement technique [7.12, 7.19]. The aspect of molecular orientation polarisation is, however, achieved by introducing χ_{ij}'s because $\varepsilon_{\infty ij}$ which includes fast polarisation, frequently appears as a subtracted term in Bergmann equations. Thus to

Table 7.2: The relaxation times τ_2 and τ_1 from the slope and intercept of straight line Eq.(7.3), correlation coefficients r's and % of error in regression technique, measured τ_j from the slope of χ_{ij}'' vs χ_{ij}' of Eq.(7.15) and the ratio of the individual slopes of χ_{ij}'' vs w_j and χ_{ij}' vs w_j at $w_j \to 0$ of Eq.(7.16), reported τ, symmetric and characteristic relaxation times τ_s and τ_{cs} for different disubstituted benzenes and anilines at 35^{0}C under 9.945 GHz electric field.

System with sl.no..	Slope & intercept of Eq.(7.3)		'r'	% of error	Estimated τ_2 and τ_1 in psec		Measured τ_j in psec fromEqs (7.15) &(7.16)		Rept. τ in psec	τ_s in psec	τ_{cs} in psec
(I) o-chloro nitro benzene in C_6H_6	1.310	0.301	0.82	9.88	16.21	4.76	12.08	10.13	13.5	7.87	17.08
(II) 4-chloro 3-nitrobe-nzotrifluoride in CCl_4	1.666	0.059	0.95	2.94	26.08	0.58	16.43	22.66	21.1	0.00	--
(III) 4-chloro 3-nitro toluene in C_6H_6	1.865	0.389	0.88	6.80	26.02	3.83	16.13	19.89	20.9	10.76	39.65
(IV) 4-chloro 3-nitro toluene in CCl_4	2.283	0.134	0.98	1.19	35.57	0.96	21.47	22.61	35.0	1.47	38.84
(V) o- nitrobenzo trifluoride in C_6H_6	1.063	0.067	0.70	15.38	15.93	1.08	12.09	11.08	13.7	10.89	28.83
(VI) m-nitrobenzotri fluoride in C_6H_6	1.898	0.597	0.99	0.60	24.01	6.37	14.33	36.57	19.7	6.20	--
(VII) 2-chloro 6-methyl aniline in C_6H_6	1.371	0.313	0.93	4.08	17.31	4.63	7.05	14.55	7.8	4.08	--
(VIII) 3-chloro 2-me thyl aniline in C_6H_6	1.596	0.386	0.99	0.60	20.79	4.76	7.98	11.49	9.9	4.57	--
(IX) 3-chloro 4- methyl aniline in C_6H_6	1.891	0.561	0.99	0.67	24.37	5.90	12.07	13.65	13.6	7.28	--
(X) 4-chloro 2-methyl aniline in C_6H_6	3.217	1.428	0.99	0.67	42.97	8.51	12.80	11.04	18.5	7.59	--
(XI) 5-chloro 2-methyl aniline in C_6H_6	2.075	0.811	0.97	1.78	24.85	8.36	14.34	14.35	16.6	5.60	4.52

avoid the clumsiness of algebra and to exclude the fast polarisation process Bergmann equations [7.16] are simplified by the established symbols of χ_{ij}',χ_{ij}'' and χ_{oij} of Table 7.1 in SI units:

$$\frac{\chi_{ij}'}{\chi_{oij}} = \frac{c_1}{1+\omega^2\tau_1^{\,2}} + \frac{c_2}{1+\omega^2\tau_2^{\,2}} \qquad \ldots\ldots(7.1)$$

$$\frac{\chi_{ij}''}{\chi_{oij}} = c_1\frac{\omega\tau_1}{1+\omega^2\tau_1^{\,2}} + c_2\frac{\omega\tau_2}{1+\omega^2\tau_2^{\,2}} \qquad \ldots\ldots(7.2)$$

assuming two broad Debye type dispersions for which the sum of c_1 and c_2 is unity. The Eqs.(7.1) and (7.2) are now solved to get:

$$\frac{\chi_{oij}-\chi'_{ij}}{\chi'_{ij}} = \omega(\tau_1+\tau_2)\frac{\chi''_{ij}}{\chi'_{ij}} - \omega^2\tau_1\tau_2 \qquad \ldots\ldots(7.3)$$

The variables $(\chi_{oij}-\chi_{ij}')/\chi_{ij}'$ and χ_{ij}''/χ_{ij}' are plotted against each other for different w_j's of the polar liquid under a single angular frequency $\omega\,(=2\pi f)$ of the electric field to get a straight line with intercept $-\omega^2\tau_1\tau_2$ and slope $\omega(\tau_1+\tau_2)$, as shown in Fig.7.1. The intercept and slope of Eq.(7.3) are obtained by linear regression analysis made with the measured χ_{ij}'s of solutes in CCl_4 and C_6H_6 to get τ_2 and τ_1 as found in the 6 and 7 columns of Table 7.2.The variables of Eq.(7.3) are extracted from Table 7.1 where all the data are collected together system wise up to three decimals in close agreement with the expected [7.12] τ_2 and τ_1 of Table 7.2. Both τ_2 and τ_1 were found to deviate significantly when the data of Table 7.1 were taken up to two decimal places with the claimed accuracy of measurement. The correlation coefficients r's and the % of errors were worked out to place them in Table 7.2 only to see how far the variables of Eq.(7.3) are collinear to each other.

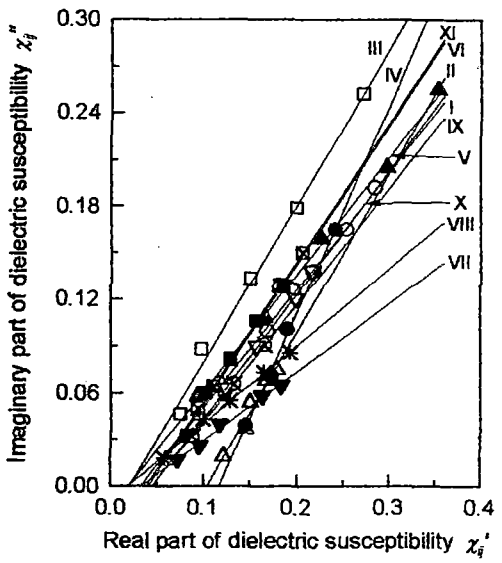

Figure 7.2: Linear variation of χ_{ij}'' with χ_{ij}' for different w_j's.

I. o-chloronitrobenzene in C_6H_6 (–○–); II. 4-chloro 3-nitrobenzotrifluoride in CCl_4 (–△–); III. 4-chloro 3-nitrotoluene in C_6H_6 (–□–); IV. 4-chloro 3-nitrotoluene in CCl_4 (–●–); V. o-nitrobenzotrifluoride in C_6H_6 (–▲–); VI. m-nitrobenzotrifluoride in C_6H_6 (–■–); VII. 2-chloro 6-methyl aniline in C_6H_6 (–▼–); VIII. 3-chloro 2-methyl aniline in C_6H_6 (–✱ –); IX. 3-chloro 4-methyl aniline in C_6H_6 (–⊗–); X. 4-chloro 2-methyl aniline in C_6H_6 (–▽–) and XI. 5-chloro 2-methyl aniline in C_6H_6 (–⊠ –)

The relaxation times τ's due to Debye model are measured from the slope of χ_{ij}'' vs χ_{ij}' curves of Fig.7.2 and the ratio of the individual slopes of χ_{ij}'' vs w_j and χ_{ij}' vs w_j curves at $w_j\to 0$ of Figs.7.3 and 7.4 respectively. τ's from both the methods are entered in the 8 and 9 columns of Table 7.2 only to see how far they agree with τ_1 and τ_2 due to double relaxation method of Eq.(7.3).

The theoretical c_1 and c_2 towards dielectric dispersions for τ_1 and τ_2 of different disubstituted benzenes and anilines in C_6H_6 and CCl_4 were calculated from Fröhlich's [7.20] theoretical formulations of χ_{ij}'/χ_{oij} and χ_{ij}''/χ_{oij}. The experimental c_1 and c_2, on the other hand, were found out from $(\chi_{ij}'/\chi_{oij})_{wj\to 0}$ and $(\chi_{ij}''/\chi_{oij})_{wj\to 0}$ by graphical variations of χ_{ij}'/χ_{oij} and χ_{ij}''/χ_{oij} with w_j's of Figs.7.5 and 7.6 in order to place them in Table 7.3 for comparison. The plots of χ_{ij}'/χ_{oij} and χ_{ij}''/χ_{oij} against w_j of the polar liquids in Figs.7.5 and 7.6 are the least squares fitted curves with the experimental points placed upon them. With the values of the intercepts presented in Table 7.3 from Figs.7.5 and 7.6 and the graphical plot of $(1/\phi)\log(\cos\phi)$ against ϕ in degrees given elsewhere [7.4], the symmetric and asymmetric distribution parameters γ and δ related to symmetric and characteristic relaxation times τ_s and τ_{cs} of the molecules were determined. They are seen in Table 7.3. The object of such determinations of γ, δ, τ_s and τ_{cs} is to conclude the molecular nonrigidity and distribution of relaxation behaviour as well.

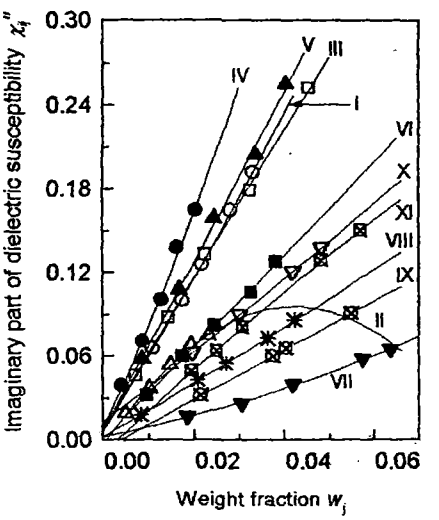

Figure 7.3: Variation of χ_{ij}'' against w_j of solutes

I. o-chloronitrobenzene in C_6H_6 (–O–) II. 4-chloro 3-nitrobenzotrifluoride in CCl_4 (–△–); III. 4-chloro 3-nitrotoluene in C_6H_6 (–□–); IV. 4-chloro 3-nitrotoluene in CCl_4 (–●–); V. o-nitrobenzotrifluoride in C_6H_6 (–▲–); VI. m-nitrobenzotrifluoride in C_6H_6 (–■–); VII. 2-chloro 6-methyl aniline in C_6H_6 (–▼–); VIII. 3-chloro 2-methyl aniline in C_6H_6 (–✶ –); IX. 3-chloro 4-methyl aniline in C_6H_6 (–⊗–); X. 4-chloro 2-methyl aniline in C_6H_6 (–▽–) and XI. 5-chloro 2-methyl aniline in C_6H_6 (–⊠ –)

The dipole moments μ_2 and μ_1 were then measured in terms of dimensionless parameters b's involved with measured τ's of Table 7.2 and coefficients β_1's and β_2's presented in Table 7.4 of the variations of *hf* χ_{ij}' and total *hf* conductivity σ_{ij} with w_j's of Figs.7.4 and 7.7 respectively. The measured μ's are found in Table 7.4 in order to compare with theoretical dipole moment μ_{theo}'s derived from available bond angles and bond moments of the substituent polar groups attached to the parent molecules as sketched in Fig.7.8. The structural aspect of some interesting polar molecules in Fig.7.8 exhibits the prominent mesomeric, inductive and electromeric effects of the substituted polar groups. All these effects are taken into account by the ratio μ_{expt}/μ_{theo} in agreement with the measured μ's [7.6-7.8] of Table 7.4.

Table 7.3: Fröhlich's parameter A, theoretical and experimental values of χ_{ij}'/χ_{oij} & χ_{ij}''/χ_{oij} of Fröhlich equations (7.6) and (7.7) and from fitting Eqs. of Figs.7.5 and 7.6 at $w_j \to 0$ respectively, theoretical and experimental relative contributions c_1 and c_2 towards dielectric dispersion due to τ_1 and τ_2, symmetric and asymmetric distribution parameters γ and δ for polar-nonpolar liquid mixtures of disubstituted benzenes and anilines at 35°C under 9.945 GHz electric field.

System with sl.no	A	Theoretical values of χ_{ij}'/χ_{oij} & χ_{ij}''/χ_{oij} from Eqs (7.6) & (7.7)		Theoretical values of c_1 and c_2		Expt. values of χ_{ij}'/χ_{oij} & χ_{ij}''/χ_{oij} at $w_j \to 0$ of Figs. (7.5) & (7.6)		Expt. values of c_1 & c_2		Estimated values of γ and δ	
(I) o-chloronitro benzene in C_6H_6	1.225	0.746	0.410	0.526	0.533	0.733	0.349	0.599	0.371	0.13	0.0095
(II) 4-chloro 3-nitrobenzotrifluoride in CCl_4	3.806	0.830	0.259	0.687	0.525	0.890	0.027	0.894	-0.012	0.82	—
(III) 4-chloro 3nitro toluene in C_6H_6	1.916	0.677	0.409	0.527	0.649	0.600	0.309	0.508	0.435	0.28	0.0070
(IV) 4-chloro 3-nitro toluene in CCl_4	3.612	0.754	0.301	0.638	0.703	0.863	0.144	0.823	0.253	0.38	0.0024
(V) o-nitrobenzotrifluoride in C_6H_6	2.691	0.873	0.266	0.653	0.444	0.616	0.347	0.288	0.655	0.21	0.0084
(VI) m-nitrobenzotrifluoride in C_6H_6	1.327	0.611	0.455	0.485	0.625	1.134	0.261	1.514	-0.561	-0.45	—
(VII) 2-chloro 6-methyl aniline in C_6H_6	1.319	0.737	0.412	0.527	0.544	1.078	0.141	1.402	-0.468	-0.40	—
(VIII) 3-chloro 2-methyl aniline in C_6H_6	1.474	0.693	0.424	0.518	0.585	1.023	0.232	1.192	-0.194	-0.20	—
(IX) 3-chloro 4- methyl aniline in C_6H_6	1.418	0.622	0.449	0.490	0.632	1.244	0.254	1.614	-0.588	-0.62	—
(X) 4-chloro 2-methyl aniline in C_6H_6	1.619	0.427	0.448	0.416	0.842	1.062	0.419	1.449	-0.556	-0.33	—
(XI) 5-chloro 2-methyl aniline in C_6H_6	1.089	0.547	0.475	0.462	0.627	0.907	0.312	1.354	-0.536	-0.03	0.0210

7.2. Formulations of c_1 and c_2 for τ_1 and τ_2 :

The Eqs.(7.1) and (7.2) are now solved to get c_1 and c_2 where

$$c_1 = \frac{(\chi_{ij}'\alpha_2 - \chi_{ij}'')(1+\alpha_1^2)}{\chi_{oij}(\alpha_2 - \alpha_1)} \quad \ldots\ldots (7.4)$$

$$c_2 = \frac{(\chi_{ij}'' - \chi_{ij}'\alpha_1)(1+\alpha_2^2)}{\chi_{oij}(\alpha_2 - \alpha_1)} \quad \ldots\ldots (7.5)$$

where $\alpha_1=\omega\tau_1$ and $\alpha_2=\omega\tau_2$ provided $\alpha_2>\alpha_1$. The molecules under consideration are of complex type and only a few data are available under single frequency measurement in the low concentration region. A continuous distribution of τ with two discrete values of τ_1 and τ_2 could, therefore, be expected. Thus from Fröhlich's equations [7.20] based on distribution of τ between the two extreme values of τ_1 and τ_2 one gets:

$$\frac{\chi'_{ij}}{\chi_{oij}} = 1 - \frac{1}{2A}\ln\left(\frac{1+\omega^2\tau_2^{\,2}}{1+\omega^2\tau_1^{\,2}}\right) \qquad \ldots\ldots(7.6)$$

$$\frac{\chi''_{ij}}{\chi_{oij}} = \frac{1}{A}\left[\tan^{-1}(\omega\tau_2) - \tan^{-1}(\omega\tau_1)\right] \qquad \ldots\ldots(7.7)$$

where the Fröhlich parameter A is given by $A=\ln(\tau_2/\tau_1)$. The theoretical values of χ_{ij}'/χ_{oij} and χ_{ij}''/χ_{oij} of Eqs.(7.6) and (7.7) were used to get theoretical c_1 and c_2 from Eqs.(7.4) and (7.5) in order to compare them with the experimental values of c_1 and c_2 from the graphical plots of χ_{ij}'/χ_{oij} and χ_{ij}''/χ_{oij} at $w_j\rightarrow 0$ as seen in Figs.7.5 and 7.6 respectively. Both the theoretical and experimental c_1 and c_2 are presented in Table 7.3 for comparison.

7.3. Distribution Parameters γ and δ Related to Symmetric and Characteristic Relaxation Times τ_s and τ_{cs} :

The molecules are expected to show either symmetrical circular arc or a skewed arc in addition to other models [7.21] when the values of χ_{ij}''/χ_{oij} are plotted against χ_{ij}'/χ_{oij} at $w_j\rightarrow 0$ for various frequencies of the electric field to yield:

$$\frac{\chi^*_{ij}}{\chi_{oij}} = \frac{1}{1+(j\omega\tau_s)^{1-\gamma}} \qquad \ldots\ldots(7.8)$$

$$\frac{\chi^*_{ij}}{\chi_{oij}} = \frac{1}{(1+j\omega\tau_{cs})^{\delta}} \qquad \ldots\ldots(7.9)$$

Here, γ and δ are the symmetric and asymmetric distribution parameters related to symmetric and characteristic relaxation times τ_s and τ_{cs} respectively. Separating the real and imaginary parts of Eq.(7.8) one gets:

$$\gamma = \frac{2}{\pi}\tan^{-1}\left[\left(1-\frac{\chi'_{ij}}{\chi_{oij}}\right)\frac{\chi'_{ij}/\chi_{oij}}{\chi''_{ij}/\chi_{oij}} - \frac{\chi''_{ij}}{\chi_{oij}}\right] \qquad \ldots\ldots(7.10)$$

$$\tau_s = \frac{1}{\omega}\left[1\Big/\left(\frac{\chi'_{ij}/\chi_{oij}}{\chi''_{ij}/\chi_{oij}}\cos\frac{\gamma\pi}{2} - \sin\frac{\gamma\pi}{2}\right)\right]^{\frac{1}{1-\gamma}} \qquad \text{.....(7.11)}$$

where χ_{ij}'/χ_{oij} and χ_{ij}''/χ_{oij} are obtained from intercepts of each variable with w_j's of Figs.7.5 and 7.6 in the limit w_j=0. Again δ and τ_{cs} can be had from Eq.(7.9) as:

$$\tan(\phi\delta) = \frac{\left(\chi''_{ij}/\chi_{oij}\right)_{wj\to 0}}{\left(\chi'_{ij}/\chi_{oij}\right)_{wj\to 0}} \qquad \text{.....(7.12)}$$

$$\tau_{cs} = \frac{1}{\omega}\tan\phi \qquad \text{.....(7.13)}$$

Since ϕ can not be evaluated directly, a theoretical curve of $(1/\phi)\log(\cos\phi)$ with ϕ in degrees was drawn as shown elsewhere [7.4] from which

$$\frac{1}{\phi}\log(\cos\phi) = \frac{\log\left[\left(\chi'_{ij}/\chi_{oij}\right)/\cos(\phi\delta)\right]}{\phi\delta} \qquad \text{.....(7.14)}$$

was found out. The known values of $(1/\phi)\log(\cos\phi)$ was then used to obtain ϕ. With known ϕ and δ, τ_{cs} were obtained from Eqs.(7.12) and (7.13) for each molecule. The estimated γ and δ are presented in columns 11 and 12 of Table 7.3. τ_s and τ_{cs} are entered in columns 11 and 12 of Table 7.2 to conclude symmetric relaxation behaviour for disubstituted anilines and asymmetric relaxation behaviour for disubstituted benzenes respectively.

7.4. Theoretical Formulation for Dipole Moments μ_2 and μ_1 :

The Debye equation [7.22] for a polar-nonpolar liquid mixture under *hf* electric field in terms of χ_{ij}'s is written as:

$$\frac{d\chi''_{ij}}{d\chi'_{ij}} = \omega\tau \qquad \text{.....(7.15)}$$

$$\frac{\left(d\chi''_{ij}/dw_j\right)_{wj\to 0}}{\left(d\chi'_{ij}/dw_j\right)_{wj\to 0}} = \omega\tau \qquad \text{.....(7.16)}$$

τ's of the polar liquids could, however, be estimated from Eqs.(7.15) and (7.16) as seen in 8 and 9 columns of Table 7.2. Again the imaginary part χ_{ij}'' of the complex *hf* susceptibility χ_{ij}^* as a function of w_j of a solute can be written as [7.23-7.24]:

$$\chi''_{ij} = \frac{N\rho_{ij}\mu_j^{\,2}}{27\varepsilon_o k_B T M_j}\frac{\omega\tau}{1+\omega^2\tau^2}\left(\varepsilon_{ij}+2\right)^2 w_j$$

Table 7.4: Slope β_1 of χ_{ij}' vs w_j and β_2 of σ_{ij} vs w_j curves, measured dipole moments μ_j from susceptibility measurement technique and *hf* conductivity method from Eqs.(7.19) and (7.26) respectively, reported dipole moment, theoretical dipole moment μ_{theo} from available bond angles and bond moments expressed in Coulomb.metre (C.m) and the values of μ_{expt}/μ_{theo} for different disubstituted benzenes and anilines at 35 ^{0}C under 9.945 GHz electric field.

System with sl.no. & mol.wt.	Slope of χ_{ij}'-w_j & σ_{ij}- w_j curves		Dipole moments μ_j (x 10^{-30}) in Coulomb.metre								μ_{expt}/μ_{theo}
			From Eq (7.19)		From Eq (7.26)		μ_j^a	μ_j^b	μ_j^r	μ_{theo}	
	β_1	β_2	μ_2	μ_1	μ_2	μ_1					
(I) o-chloronitro benzene in C_6H_6 M_j=0.1575 Kg	8.326	4.706	16.93	12.41	17.11	12.54	14.90	14.07	14.50	17.60	0.96
(II) 4-chloro3-nitrobenzotrifluoride in CCl_4 M_j=0.2255 Kg	3.358	1.875	13.02	6.81	13.08	6.84	9.76	11.80	10.57	12.60	1.03
(III) 4-chloro 3-nitro toluene in C_6H_6 M_j=0.1715 Kg	4.490	2.570	17.39	9.37	17.69	9.53	12.94	14.54	14.97	18.60	0.93
(IV) 4-chloro 3-nitro toluene in CCl_4 M_j=0.1715 Kg	4.854	3.001	17.40	7.15	18.39	7.56	11.95	12.36	15.60	18.50	0.94
(V) o-nitrobenzotrifluoride in C_6H_6 M_j=0.1910 Kg	8.598	4.662	18.78	13.34	18.59	13.20	16.68	16.18	16.54	20.60	0.91
(VI) m-nitrobenzotrifluoride in C_6H_6 M_j=0.1910 Kg	1.426	0.702	9.77	5.83	9.22	5.50	7.27	13.52	12.24	12.47	0.78
(VII) 2-chloro 6-methyl aniline in C_6H_6 M_j=0.1415 Kg	0.728	0.560	4.91	3.47	5.79	4.09	3.64	4.50	7.73	6.16	0.56
(VIII) 3-chloro 2-methylaniline in C_6H_6 M_j=0.1415 Kg	2.674	1.693	10.47	6.66	11.20	7.13	7.14	7.86	10.07	8.27	0.81
(IX) 3-chloro4-methyl aniline in C_6H_6 M_j=0.1415 Kg	2.128	1.269	10.38	6.07	10.78	6.30	7.14	7.49	8.70	7.33	0.83
(X) 4-chloro2-methyl aniline in C_6H_6 M_j=0.1415 Kg	3.650	2.063	21.38	8.45	21.61	8.54	9.56	9.07	10.94	10.20	0.83
(XI) 5-chloro2-methyl aniline in C_6H_6 M_j=0.1415 Kg	3.481	2.196	13.46	8.22	14.37	8.78	9.79	9.79	0.34	9.44	0.87

μ_j^a = dipole moment by using τ from the direct slope of Eq (7.15)

μ_j^b = dipole moment by using τ from the ratio of individual slopes of Eq (7.16)

μ_j^r = reported dipole moment

μ_{theo} = theoretical dipole moment from the available bond angles and bond moments.

which on differentiation with respect to w_j and at $w_j \to 0$ yields:

$$\left(\frac{d\chi''_{ij}}{dw_j}\right)_{w_j \to 0} = \frac{N\rho_i \mu_j^{\,2}}{27\varepsilon_o k_B T M_j} \frac{\omega\tau}{(1+\omega^2\tau^2)} (\varepsilon_i + 2)^2 \qquad \ldots\ldots (7.17)$$

where the density of the solution ρ_{ij} becomes ρ_i=density of solvent, $(\varepsilon_{ij}+2)^2$ becomes $(\varepsilon_i+2)^2$ at $w_j \to 0$, k_B=Boltzmann constant, N=Avogadro's number, ε_i=relative permittivity of solvent and ε_o=permittivity of free space = 8.854 x 10^{-12} Farad. metre^{-1}. All are expressed in SI units.

Comparing Eqs.(7.16) and (7.17) one gets:

$$\left(\frac{d\chi'_{ij}}{dw_j}\right)_{w_j \to 0} = \frac{N\rho_i \mu_j^{\,2}}{27\varepsilon_o k_B T M_j} \frac{1}{(1+\omega^2\tau^2)} (\varepsilon_i + 2)^2 = \beta_1 \qquad \ldots\ldots (7.18)$$

where β_1 is the slope of χ_{ij}' vs w_j curves of Fig.7.4 at $w_j \to 0$. Here no approximation in determination of μ_j is made like the conductivity measurement technique [7.4] given below.

After simplification, the *hf* dipole moment μ_j is given by:

$$\mu_j = \left(\frac{27\varepsilon_o k_B T M_j \beta_1}{N\rho_i (\varepsilon_i + 2)^2 b}\right)^{\frac{1}{2}} \qquad \ldots\ldots (7.19)$$

here dimensionless parameter b is given by :

$$b = 1/(1+\omega^2\tau^2) \qquad \ldots\ldots (7.20)$$

7.5. Dipole Moments μ_2 and μ_1 from *hf* Conductivity :

The complex *hf* conductivity σ_{ij}^* of polar-nonpolar liquid mixture in a GHz electric field is given by [7.25]:

$$\sigma_{ij}^* = \sigma'_{ij} + j\sigma''_{ij} \qquad \ldots\ldots (7.21)$$

where $\sigma_{ij}'(=\omega\varepsilon_o\varepsilon_{ij}'')$ and $\sigma_{ij}''(=\omega\varepsilon_o\varepsilon_{ij}')$ are the real and imaginary parts of the complex conductivity σ_{ij}^* in $\Omega^{-1}.m^{-1}$. The magnitude of the total *hf* conductivity is:

$$\sigma_{ij} = \omega\varepsilon_o \left(\varepsilon_{ij}''^{\,2} + \varepsilon_{ij}'^{\,2}\right)^{1/2} \qquad \ldots\ldots (7.22)$$

Although $\varepsilon_{ij}' >> \varepsilon_{ij}''$, but in the high frequency region, $\varepsilon_{ij}' \cong \varepsilon_{ij}''$. ε_{ij}'' is responsible for absorbtion of electric energy and offers resistance to polarisation. Hence σ_{ij}'' is related to σ_{ij}' by the relation [7.25]:

$$\sigma''_{ij} = \sigma_{\infty ij} + \frac{1}{\omega\tau}\sigma'_{ij}$$

$$\sigma_{ij} = \sigma_{\infty ij} + \frac{1}{\omega\tau}\sigma'_{ij} \qquad \text{.....(7.23)}$$

Here the approximation $\sigma_{ij}'' \cong \sigma_{ij}$ is made. Differentiation of Eq.(7.23) with respect to w_j at $w_j \to 0$ yields:

$$\left(\frac{d\sigma'_{ij}}{dw_j}\right)_{w_j \to 0} = \omega\tau\left(\frac{d\sigma_{ij}}{dw_j}\right)_{w_j \to 0} = \omega\tau\beta_2 \qquad \text{.....(7.24)}$$

where β_2 is the slope of σ_{ij} vs w_j curves of Fig.7.7 at infinite dilution $w_j \to 0$ and placed in Table 7.4. The real part of *hf* conductivity σ_{ij}' at T K [7.23] is given by:

$$\sigma'_{ij} = \frac{N\rho_{ij}\mu_j^{\,2}}{27k_BTM_j}\frac{\omega^2\tau}{1+\omega^2\tau^2}(\varepsilon_{ij}+2)^2 w_j$$

$$\left(\frac{d\sigma'_{ij}}{dw_j}\right)_{w_j \to 0} = \frac{N\rho_i\mu_j^{\,2}}{27k_BTM_j}\frac{\omega^2\tau}{1+\omega^2\tau^2}(\varepsilon_i+2)^2 \qquad \text{.....(7.25)}$$

Comparing Eqs.(7.24) and (7.25) one gets the dipole moment μ_j from:

$$\mu_j = \left(\frac{27k_BTM_j\beta_2}{N\rho_i(\varepsilon_i+2)^2\omega b}\right)^{\frac{1}{2}} \qquad \text{.....(7.26)}$$

All the measured dipole moments μ_j's from the susceptibility measurement technique of Eq.(7.19) and *hf* conductivity method of Eq.(7.26) are entered in the 4,5 and 6,7 columns of Table 7.4 respectively.

7.6. Results and Discussions :

The double relaxation times τ_1 and τ_2 for the polar liquid molecules in different solvents are found out from the slope and intercept of Eq.(7.3) as shown in Fig.7.1 in terms of the orientation susceptibility parameters χ_{ij}'s of Table 7.1. The χ_{ij}'s are, however, derived from the relative permittivities ε_{ij}'s [7.6-7.8] for different weight fractions w_j's of the polar liquids. The variables of Eq.(7.3) i.e $(\chi_{oij}-\chi_{ij}')/\chi_{ij}'$ and χ_{ij}''/χ_{ij}' are plotted against each other for different w_j's of solutes under 9.945 GHz electric field at 35°C to get linear equation by regression analysis. From Fig.7.1 it revealed that the fitting is good for some cases, but poor in other cases. It appears that the linear fit for II (–△–), III (–□–) and IV (–●–) in Figs.7.1 and 7.2 often passes through two among five data, others being off from the fit. Nevertheless, the regression analysis was made on the basis of Eq. (7.3). However, the accuracy of Fig.7.1 is tested by the correlation coefficients r's, which were

found to be close to unity indicating the variables are almost collinear. The % of errors in terms of r's in getting the intercepts and slopes were worked out to find the accuracies of τ_1 and τ_2 respectively. In order to locate the double relaxation phenomena of the polar liquid molecules in non-polar aprotic solvents under investigation, accurate measurement of χ_{oij} involved with ε_{oij} and $\varepsilon_{\infty ij}$ is necessary. The refractive index n_{Dij} measured by Abbe's refractrometer often yields $\varepsilon_{\infty i}=n_{Dij}^2$, although Cole Cole [7.26] and Cole Davidson [7.27] plots usually give $\varepsilon_{\infty ij} \cong 1.0$ to 1.5 times of n_{Dij}^2. This often introduces an additional error in the calculations. Nevertheless, the accuracies of χ_{ij}'', χ_{ij}' and χ_{oij} are of 5% and 1% respectively derived from measured [7.6-7.8] relative permittivities ε_{ij}'', ε_{ij}', ε_{oij} and $\varepsilon_{\infty ij}$. The estimated τ_2 and τ_1 are placed in Table 7.2 in order to compare them with those of Murthy *et al* [7.28] of Eq.(7.15) and by the ratio of the individual slopes of the variations of χ_{ij}'' and χ_{ij}' with w_j's in the limit $w_j=0$ of Eq.(7.16). The latter method seems to be better to calculate τ since it eliminates polar-polar interaction almost completely. The linear plot of χ_{ij}'' against χ_{ij}' of Fig.7.2 for different w_j's of solute has intercepts although it was expected from Eq.(7.15) that they should pass through the origin. Nevertheless, τ's are found to be in close agreement with those calculated from the ratio of the individual slopes of the variations of χ_{ij}'' and χ_{ij}' with w_j at $w_j \to 0$ of Eq.(7.16) as shown in Figs.7.3 and 7.4. The experimental points as shown in Figs.7.3 and 7.4 with the fit are tabulated to back up the results of Eq.(7.16) due to Debye model. χ_{ij}'' increases monotonically with w_j's and has a tendency to meet the origin for all the curves. This type of behaviour indicates that χ_{ij}'' tends to pass through the origin at $w_j \to 0$ under 9.945 GHz electric field.

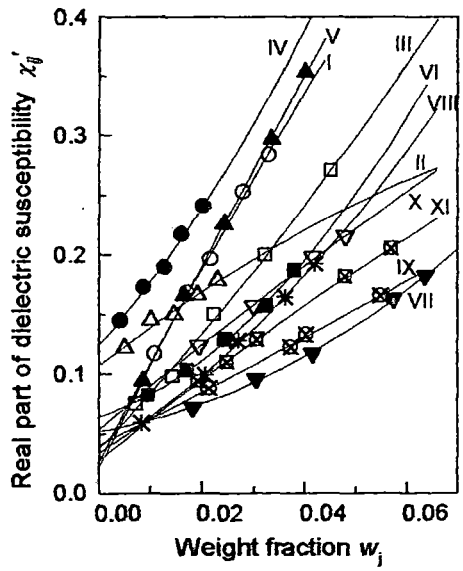

Figure 7.4 : Variation of χ_{ij}' against w_j of solutes

I. o-chloronitrobenzene in C_6H_6 (–○–); II. 4-chloro 3-nitrobenzotri-fluoride in CCl_4 (–△–); III. 4-chloro 3-nitrotoluene in C_6H_6 (–□–); IV. 4-chloro 3-nitrotoluene in CCl_4 (–●–); V. o-nitrobenzotriflu-oride in C_6H_6 (–▲–); VI. m-nitrobenzotrifluoride in C_6H_6 (–■–); VII. 2-chloro 6-methyl aniline in C_6H_6 (–▼–); VIII. 3-chloro 2-me-thyl aniline in C_6H_6 (–* –) IX. 3-chloro 4-methyl aniline in C_6H_6 (–⊗–) X. 4-chloro 2-methyl aniline in C_6H_6 (–▽–) and XI. 5-chloro 2-methyl aniline in C_6H_6 (–⊠ –)

It is evident from Table 7.2 that all the disubstituted benzenes exhibit the whole molecular rotation while the disubstituted anilines show the rotation of the flexible parts under 10 GHz electric field when τ_1's and τ_2's are compared with the reported data. This indicates the flexible parts are more rigid in the disubstituted benzenes rather than the disubstituted anilines. The assumptions of symmetric and asymmetric relaxation behaviours from Eqs.(7.8) and (7.9) for such non rigid polar molecules yield τ_s and τ_{cs} from Eqs.(7.11) and (7.13) to place them in the last two columns of Table 7.2. It reveals that the symmetric and asymmetric relaxation processes are more probable since τ_s and τ_{cs} are almost in agreement with the reported τ's in a solution. The characteristic relaxation times τ_{cs} are sometimes very high through asymmetric distribution parameter δ and often could not be determined for most of the molecules. The disubstituted benzenes showed τ_2's in agreement with the reported τ's and τ_{cs} except *o*-nitrobenzotrifluoride in C_6H_6 which agrees with τ_s only. But 4-chloro 3-nitrobenzotrifluoride in CCl_4 and *m*-nitrobenzotrifluoride in C_6H_6 yield τ_2 in close agreement with reported τ's although they showed $\tau_s \cong \tau_1$. Only 2-chloro 6-methyl aniline and 3-chloro 2-methyl aniline in C_6H_6 showed τ_1's in excellent agreement with the calculated τ_s's. For the rest disubstituted anilines τ_1's agree well with the calculated τ_s's, but the agreement is not better with the measured τ's from Eqs.(7.15) and (7.16). It thus reveals that a part of the disubstituted anilines is rotating, obeying symmetric relaxation behaviour while most of the disubstituted benzenes showed asymmetric relaxation process for their whole molecular rotations.

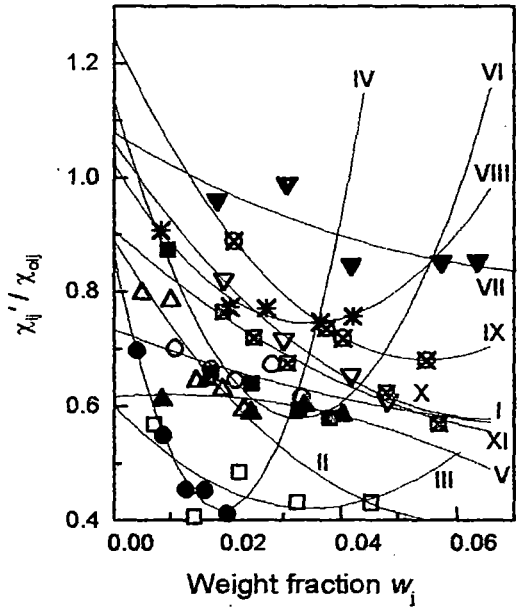

Figure 7.5 : Plot of χ_{ij}'/χ_{oij} with w_j of solutes

I. o-chloronitrobenzene in C_6H_6 (–○–); II. 4-chloro 3-nitrobenzotrifluoride in CCl_4 (–△–); III. 4-chloro 3-nitrotoluene in C_6H_6 (–□–); IV. 4-chloro 3-nitrotoluene in CCl_4 (–●–); V. o-nitrobenzotrifluoride in C_6H_6 (–▲–); VI. m-nitrobenzotrifluoride in C_6H_6 (–■–); VII. 2-chloro 6-methyl aniline in C_6H_6 (–▼–); VIII. 3-chloro 2-methyl aniline in C_6H_6 (–✶ –); IX. 3-chloro 4-methyl aniline in C_6H_6 (–⊗–); X. 4-chloro 2-methyl aniline in C_6H_6 (–▽–) and XI. 5-chloro 2-methyl aniline in C_6H_6 (–⊠ –)

The relative weighted contributions c_1 and c_2 towards dielectric dispersions due to τ_1 and τ_2 are estimated and placed in Table 7.3 by using Fröhlich's Eqs.(7.6) and (7.7). They are compared with the experimental c_1 and c_2 from the fitted curves of χ_{ij}''/χ_{oij} and χ_{ij}'''/χ_{oij} against w_j in the limit $w_j \to 0$ of Figs.7.5 and 7.6. The nonlinear fit with only five points for III (–□–) and IV (–●–) of Fig.7.5 appeared to be non-convincing and misguiding. But three accurate experimental points are enough for such fit. However, the fit is done with a PC and software. All the curves of Figs.7.5 and 7.6 vary usually [7.12] except the convex curve V for *o*-nitrobenzotrifluoride in C_6H_6. The variations of χ_{ij}''/χ_{oij} with w_j are, however, concave and convex in nature for all systems as observed elsewhere [7.12]. The left hand sides of Eqs.(7.1) and (7.2) vary with w_j's in concave and convex manner according to Figs.7.5 and 7.6 are now fixed for τ_1 and τ_2 once estimated from intercept and slope of Eq.(7.3) to yield experimental c_1 and c_2 values from Eqs.(7.4) and (7.5) at $w_j \to 0$. This study is supposed to yield the accurate values of c_1 and c_2 unlike the earlier one [7.12] based on the graphical extrapolated values of $(\varepsilon_{ij}' - \varepsilon_{\infty ij})/(\varepsilon_{oij} - \varepsilon_{\infty ij})$ and $\varepsilon_{ij}''/(\varepsilon_{oij} - \varepsilon_{\infty ij})$ at $w_j \to 0$ drawn on the basis of scientific judgment. Although, the nature of variations remains unaltered, it is evident from Table 7.3 that c_2's are often negative for 4-chloro 3-nitrobenzotrifluoride in CCl_4, *m*-nitrobenzotrifluoride in C_6H_6 and for all the disubstituted anilines unlike other systems. This perhaps signifies that the rotation of the flexible parts of the polar molecules are not in accord with the whole molecular rotation due to inherent inertia of the substituted parts of the molecules under *hf* electric field. The theoretical values of c_1+c_2 are found to be greater than the sum of the experimental ones as listed in Table 7.3. The experimental values show that $c_1+c_2 \cong 1$ for almost all the non-spherical polar liquid molecules. But

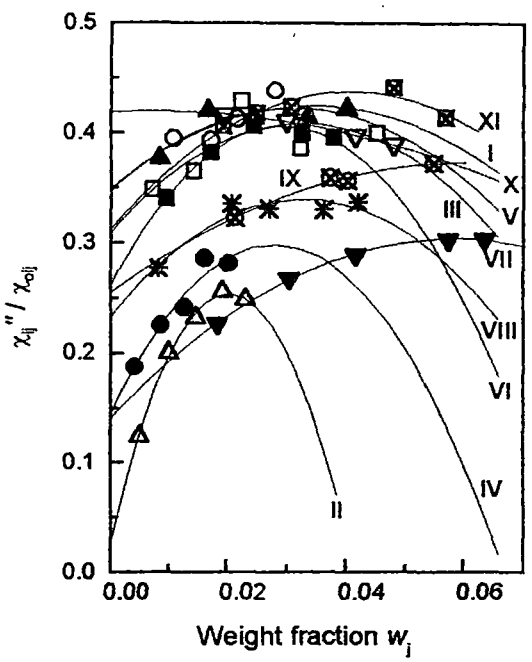

Figure 7.6 : Plot of χ_{ij}''/χ_{oij} with w_j of solutes

I. o-chloronitrobenzene in C_6H_6 (–O–); II. 4-chloro 3-nitrobenzotrifluoride in CCl_4 (–△–) III. 4-chloro 3-nitrotoluene in C_6H_6 (–□–); IV. 4-chloro 3-nitrotoluene in CCl_4 (–●–); V. o-nitrobenzotrifluoride in C_6H_6 (–▲–); VI. m-nitrobenzotrifluoride in C_6H_6 (–■–); VII. 2-chloro 6-methyl aniline in C_6H_6 (–▼–); VIII. 3-chloro 2-methyl aniline in C_6H_6 (–✱ –); IX. 3-chloro 4-methyl aniline in C_6H_6 (–⊗–); X. 4-chloro 2-methyl aniline in C_6H_6 (–▽–) and XI. 5-chloro 2-methyl aniline in C_6H_6 (–⊠ –)

(II) 4-chloro 3-nitrobenzotrifluoride in CCl_4 (–△–), (X) 4-chloro 2-methyl aniline (–▽–) and (XI) 5-chloro 2-methyl aniline (–⊠–) in C_6H_6 show considerably lower values of c_1+c_2. This may indicate the reliability of Eq.(7.3) so far derived for such molecules, although they show high correlation coefficients r's and the corresponding very low % of errors to get the intercept and slope of Eq.(7.3). The largest theoretical c_1+c_2 value for (IV) 4-chloro 3-nitro toluene in CCl_4 (–●–) is 1.34, showing a deviation of nearly 34% unlike the other systems. The possible existence of more than two broad Debye type dispersions may be taken into account for such molecules of varying complexities as reported in Tables and Figures.

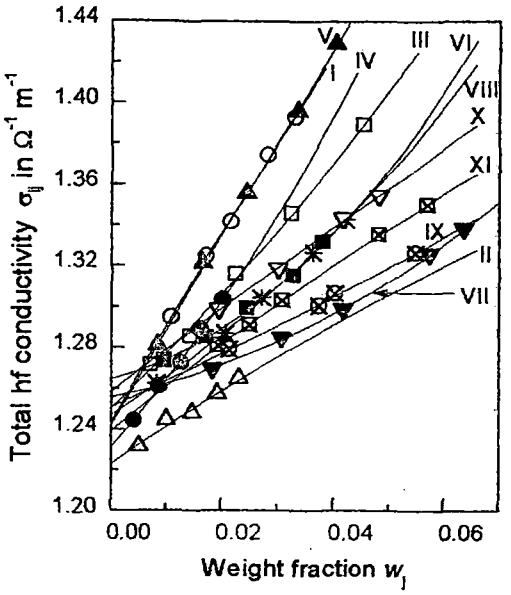

Figure 7.7 : Variation of σ_{ij} against w_j of solutes

I. o-chloronitrobenzene in C_6H_6 (–○–); II. 4-chloro 3-nitrobenzotrifluoride in CCl_4 (–△–); III. 4-chloro 3-nitrotoluene in C_6H_6 (–□–); IV. 4-chloro 3-nitrotoluene in CCl_4 (–●–); V. o-nitrobenzotrifluoride in C_6H_6 (–▲–); VI. m-nitrobenzotrifluoride in C_6H_6 (–■–); VII. 2-chloro 6-methyl aniline in C_6H_6 (–▼–); VIII. 3-chloro 2-methyl aniline in C_6H_6 (–✶ –); IX. 3-chloro 4-methyl aniline in C_6H_6 (–⊗–); X. 4-chloro 2-methyl aniline in C_6H_6 (–▽–) and XI. 5-chloro 2-methyl aniline in C_6H_6 (–⊠ –)

Dipole moments μ_2 and μ_1 due to rotation of the whole molecule as well as the flexible parts were, however, measured from Eq.(7.19) using dimensionless parameters b's involved with τ's by both the methods and slope β_1's of χ_{ij}' vs w_j curves of Fig.7.4. The measured values of μ_2 and μ_1 are presented in Table 7.4.The variations of all the χ_{ij}'s of polar-nonpolar liquid mixtures are found to be parabolic with w_j's of polar compounds as evident from Fig.7.4. They are found to cut the ordinate axis at w_j=0 within $0.0238 \leq \chi_{ij}' \leq 0.0645$ except 4-chloro 3-nitrobenzotrifluoride in CCl_4 (–△–), 4-chloro 3-nitrotoluene in CCl_4 (–●–). This behaviour probably reflects the solvent effects on the polar compounds under investigation. The interaction of solute on solvent CCl_4 may occur due to slightly positive charge δ^+ on C atom of CCl_4 and negative charge δ^- on Cl atom of the substituted group in the benzene ring as seen in Fig.7.8. All the systems are of similar nature having monotonic increase of χ_{ij}' with w_j . The dipole moments μ_2 and μ_1 are also derived from the conductivity measurement technique of Eq.(7.26) using the slope β_2's of σ_{ij} vs w_j curves of Fig.7.7 and are placed in Table 7.4 for comparison. The total hf conductivity σ_{ij} of all the polar-nonpolar liquid mixtures increase monotonically with w_j and cut the ordinate axis within the range

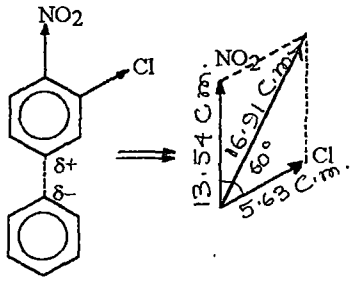

I. o-chloronitrobenzene in C $_6$H$_6$

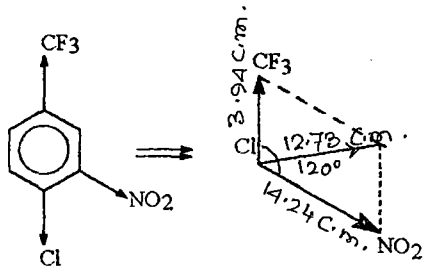

II. 4-chloro 3-nitrobenzotrifluoride in CCl $_4$

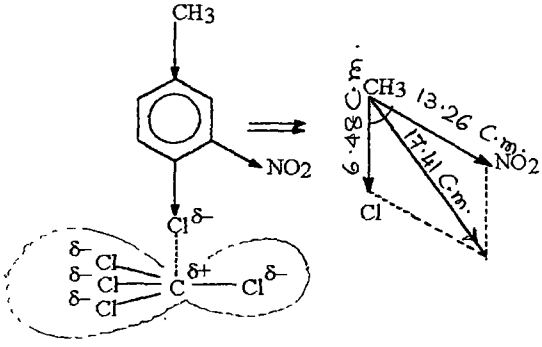

IV. 4-chloro 3-nitro toluene in CCl $_4$

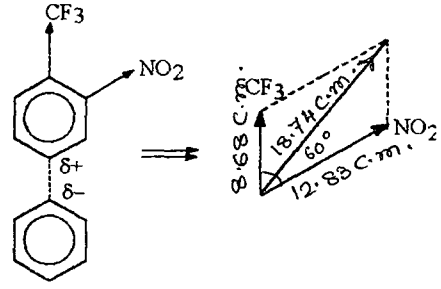

V. o-nitrobenzotrifluoride in C $_6$H$_6$

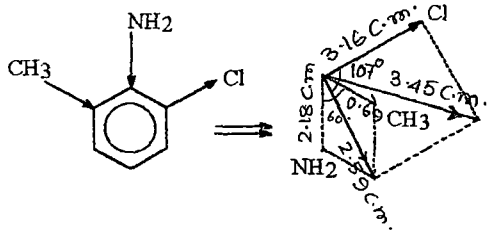

VII. 2-chloro 6-methyl aniline in C $_6$H$_6$

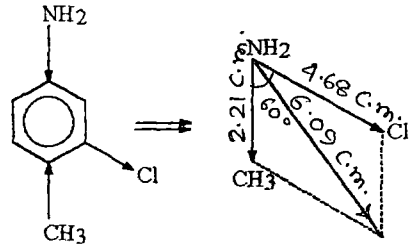

IX. 3-chloro 4-methyl aniline in C $_6$H$_6$

Figure 7.8: Conformational structures of solutes from bond angles and bond moments in multiple 10^{-30} Coulomb. metre (C.m)

$1.2233 \leq \sigma_{ij} \leq 1.2646$ at w_j=0 as seen in Fig.7.7.The slight disagreement of μ_1 and μ_2 derived from both the methods is due to the fact that the *hf* conductivity includes the fast polarisation probably for the bound molecular charge associated with the molecule. All μ_2's for disubstituted benzenes and μ_1's for disubstituted anilines are found to agree with the reported μ's placed in Table 7.4. This indicates that the flexible parts of the disubstituted benzenes are more rigid in comparison to disubstituted anilines.

The *hf* dipole moment μ_j's are calculated by using τ from both the methods of direct slope of Eq.(7.15) and the ratio of the individual slopes of Eq.(7.16) in order to place them in Table 7.4. μ_j's by using τ from the ratio of the individual slopes are in close agreement with the reported values suggesting the fact that the latter method to get τ is more realistic. In such case one polar molecule is surrounded by a large number of non-polar solvent molecules and remains in a quasi-isolated state.

A special attention is, therefore, paid to obtain the conformational structures of some of the complex molecules as shown schematically in Fig.7.8. The inductive, electromeric and resonance effects combined with mesomeric effect of the substituted polar groups play the key role to yield the theoretical dipole moment μ_{theo}'s depending on the electron affinity of C–atom of the benzene ring. The molecules have C→CF_3, C←NH_2 ($\angle 142^0$), C→NO_2 , C→Cl C←CH_3 polar groups of bond moments 9.53 x 10^{-30}, 4.93 x 10^{-30}, 14.10 x 10^{-30}, 5.63 x 10^{-30}, 1.23 x 10^{-30} Coulomb.metre (C.m) respectively [7.12,7.19] aligned in different angles in a plane to yield μ_{theo}. Out of these, only –NO_2 and –NH_2 groups are in the habit to show resonance effect (–R or +R) in the molecules either by pulling or pushing electrons towards C–atom of the benzene ring. This resonance effect is more stronger than inductive effects (+I or –I) to exhibit the peculiar behaviours as seen in the χ_{ij}''/χ_{oij} vs w_j and χ_{ij}''/χ_{oij} vs w_j curves for the disubstituted benzenes II, IV, V, VI including all the disubstituted anilines. The structure of these polar molecules is of special interest as sketched in Fig.7.8 in view of rearrangement of charge density in them. All the disubstituted anilines include –Cl, –NH_2 and –CH_3 polar groups of which –Cl and –CH_3 have very weak inductive effects (+I or –I). They are easily influenced by the GHz electric field to show the rotation of their flexible parts. Further, the observed difference in μ values for a polar molecule in two aprotic non-polar solvents may arise due to weak polarity of CCl_4 as shown in Fig.7.8. The difference between μ_{theo}'s and experimental μ_j's establishes the non consideration of inductive and mesomeric effects. All these effects may be taken into account by the factor μ_{expt}/μ_{theo} to yield the exact μ_1 and μ_2 values of the molecules. All the polar molecules have sp^2 hybridized carbon atoms of benzene ring and the substituted parts are associated with sp^3 orbital. The interaction of orbitals may lead to gain knowledge on accumulation of charge on the substituted groups in addition to various effects present in them. The conformational structures of other molecules except six of Fig.7.8 were already shown elsewhere [7.12,7.19].

7.7. Conclusions :

The study of relaxation phenomena of disubstituted benzenes and anilines in C_6H_6 and CCl_4 by the modern established symbols of dielectric orientation susceptibilities χ_{ij}'s measured under a

single frequency electric field is very encouraging. It seems to be more topical, significant and useful contribution to predict the conformational structures and various molecular associations of the molecules at any given temperature. The intercept and slope of the derived linear Eq.(7.3) by the regression analysis on the measured data of χ_{ij}'s of different w_j's are used to get τ_2 and τ_1. The methodology so far developed in SI units is superior because of the unified, coherent and rationalised nature of the established symbols of dielectric terminologies and parameters which are directly linked with orientation polarisation of the molecules. The significant Eqs.(7.15) and (7.16) to obtain τ_j's and hence μ_j's from Eq.(7.19) help the future workers to shed more light on the relaxation phenomena of the complicated non-spherical polar liquids and liquid crystals. The prescribed method to obtain τ_j's from Eq.(7.16) with the use of the ratio of the individual slopes of χ_{ij}'' vs w_j and χ_{ij}' vs w_j curves at $w_j \rightarrow 0$ is a significant improvement over the existing ones as it eliminates polar-polar interaction almost completely in τ_j's and μ_j's respectively. τ_j's and μ_j's are usually claimed to be accurate within 10% and 5% respectively. But the correlation coefficient r and % of errors of Eq.(7.3) demand τ's and μ's are more than accurate. The non-spherical disubstituted benzene and aniline molecules absorb electric energy much more strongly nearly 10 GHz electric field at which the ε'' for absorbtion against frequency ω showed the peak. This invited the attention to get the double relaxation times τ_2 and τ_1 from Eq.(7.3). The corresponding sum of the experimental and theoretical values of weighted contributions c_1 and c_2 towards dielectric dispersions due to estimated τ_2 and τ_1 differ significantly to indicate more than two Debye type relaxations in such molecules because of their complexity. The τ's for disubstituted benzenes as seen in Table 7.2 show the whole molecular rotation while the flexible parts of the disubstituted anilines rotate under 10 GHz electric field. Disubstituted anilines exhibit the symmetric relaxation behaviour while the asymmetric relaxation behaviour occurs in disubstituted benzenes in C_6H_6 except 4-chloro 3-nitrobenzotrifluoride in CCl_4 and *m*-nitro benzotrifluoride in C_6H_6 respectively. μ_2 and μ_1 due to τ_2 and τ_1 are expected to be smaller when they are measured from the susceptibility measurement technique rather than the *hf* conductivity method where the approximation of $\sigma_{ij} \cong \sigma_{ij}''$ is usually made. The difference of μ_2 for the first six systems and of μ_1 for the rest five systems of Table 7.4 between conductivity and susceptibility measurement may arise either by elongation or reduction of the bond moments of the substituted polar groups by the factor μ_{expt}/μ_{theo} in agreement with the measured μ's to take into account of the inductive, mesomeric and electromeric effects of the polar groups in the molecules. Thus the correlation between the conformational structures with the observed results enhances the scientific content to add a new horizon of understanding to the existing knowledge of dielectric relaxation phenomena.

References :

[7.1] J S Dhull and D R Sharma, *J. Phys. D: Appl. Phys.* **15** 2307 (1982)

[7.2] A K Sharma and D R Sharma, *J. Phys. Soc. Japan* **53** 4771 (1984)

[7.3] A C Kumbharkhane, S M Puranic, C G Akode and S C Mehrotra, *Indian. J. Phys.* **74A** 471 (2000)

[7.4] K Dutta, R C Basak, S K Sit and S Acharyya, *J. Molecular Liquids* **88** 229 (2000)

[7.5] S K Sit, K Dutta, S Acharyya, T Palmajumder and S Roy, *J. Molecular Liquids* **89** 111 (2001)

[7.6] S M Khameshara and M L Sisodia, *Indian J. Pure Appl. Phys.* **18** 110 (1980)

[7.7] P C Gupta, M L Arrawatia and M L Sisodia, *Indian J. Pure Appl. Phys.***16** 451 (1978)

[7.8] M L Arrawatia, P C Gupta and M L Sisodia, *Indian J. Pure Appl. Phys.* **15** 770 (1977)

[7.9] K V Gopalakrishna, *Trans.Faraday Soc.* **53** 767 (1957)

[7.10] K Higasi, *Bull.Chem.Soc.Japan* **39** 2157 (1966)

[7.11] W M Heston, A D Franklin, E J Henneley and C P Smyth, *J. Am. Chem. Soc.* **72** 3443 (1950)

[7.12] U Saha, S K Sit, R C Basak and S Acharyya, *J. Phys. D: Appl. Phys.* **27** 596 (1994).

[7.13] A K Jonscher, *Physics of Dielectric Solids*, invited papers edited by CHL Goodman (1980).

[7.14] A K Jonscher, *Universal Relaxation Law*, Chelsea Dielectric Press, London (1996)

[7.15] N Ghosh, R C Basak, S K Sit and S Acharyya, *J. Molecular Liquids* **85** 375 (2000)

[7.16] K Bergmann, D M Roberti and C P Smyth, *J. Phys. Chem.* **64** 665 (1960)

[7.17] J Bhattacharyya, A Hasan, S B Roy and G S Kastha, *J. Phys. Soc. Japan* **28** 204 (1970)

[7.18] K Higasi, Y Koga and M Nakamura, *Bull. Chem. Soc. Japan* **44** 988 (1971)

[7.19] S K Sit, R C Basak, U Saha and S Acharyya, *J. Phys. D: Appl. Phys.* **27** 2194 (1994)

[7.20] H Fröhlich, *Theory of Dielectrics*, Oxford University Press (1949)

[7.21] J G Powles, *J. Molecular Liquids* **56** 35 (1993)

[7.22] N E Hill, W E Vaughan, A H Price and M Davies, *Dielectric Properties and Molecular Behaviour* (London: Van Nostrand Reinhold Company) (1969).

[7.23] C P Smyth, *Dielectric Behaviour and Structure* (McGrew Hill) (1955)

[7.24] K Dutta, S K Sit and S Acharyya, *Pramana: J. of Physics* **57** 775 (2001)

[7.25] F J Murphy and S O Morgan, *Bell. Syst. Tech. J.* **18** 502 (1939)

[7.26] K S Cole and R H Cole, *J. Chem. Phys.* **9** 341 (1941)

[7.27] R H Cole and D W Davidson, *J. Chem. Phys.* **19** 1484 (1951)

[7.28] M B R Murthy, R L Patil and D K Deshpande, *Indian J. Phys.* **63B** 491 (1989)

CHAPTER 8

DIELECTRIC RELAXATION PHENOMENA OF RIGID POLAR LIQUID MOLECULES UNDER GIGA HERTZ ELECTRIC FIELD

8.1. Introduction :

Dielectric relaxation studies of polar liquids in non-polar solvents are of much importance as they provide interesting information of solute–solvent or solute–solute molecular association [8.1-8.2] under high frequency (*hf*) electric field. The associational aspects of polar liquids can, however be inferred from the measured relaxation time τ by Cole-Cole [8.3], Cole-Davidson [8.4] plot or by single frequency concentration variation method [8.5] and dipole moment μ from the measured *hf* conductivity σ_{ij} and estimated τ [8.6].

Srivastava and Srivastava [8.7] measured the real ε_{ij}' and imaginary ε_{ij}'' parts of complex relative permittivity ε_{ij}^* of chloral and ethyltrichloroacetate in benzene, *n*-heptane and *n*-hexane in 4.2, 9.8 and 24.6 GHz electric field by Smyth's method [8.8] at 30^{0}C.The polar solutes (j) chloral (CCl_3CHO) and ethyltrichloroacetate ($CCl_3COOCH_2CH_3$) were of puram grade of M/s BDH, England, *n*-hexane and *n*-heptane from M/s E Merck Darmstadt, Germany. Both solutes and solvents were doubly distilled before making solutions of varying concentrations called the weight fractions w_j of solutes that are defined as the weight of the solute per unit weight of the solution up to four decimal places as shown in Table 8.1 in each solvent. The static relative permittivity ε_{oij} at 100 KHz and refractive index n_{Dij} of the solutions were measured. The purpose of this study was to observe the solute-solvent or solute-solute molecular interactions. They, however, inferred that these molecules might possess two or more relaxation processes towards dielectric dispersions.

Nowadays, the usual practice is to study the dielectric relaxation processes in terms of *hf* dielectric orientation susceptibility χ_{ij}^* rather than ε_{ij}^* or *hf* conductivity σ_{ij}^* [8.9-8.10]. ε_{ij}^* includes within it all the polarisation processes while σ_{ij}^* is more linked to transport of bound molecular charges. It is, therefore, better to work with susceptibilities χ_{ij}'s as they are concerned with orientation polarisation. The dielectric susceptibilities real $\chi_{ij}'(=\varepsilon_{ij}'-\varepsilon_{\infty ij})$ and imaginary $\chi_{ij}''(=\varepsilon_{ij}'')$ parts of complex dielectric susceptibility $\chi_{ij}^*(=\varepsilon_{ij}^*-\varepsilon_{\infty ij})$ and the low frequency dielectric susceptibility $\chi_{oij}(=\varepsilon_{oij}-\varepsilon_{\infty ij})$ which is real were derived from measured relative permittivities [8.7]. The experimental results thus collected together are placed in Table 8.1. One could not make a strong conclusion of double relaxation phenomena of polar molecule in a nonpolar solvent based on the single frequency measurement of relaxation parameters provided the accurate value of χ_{oij} involved with ε_{oij} and $\varepsilon_{\infty ij}$ is not available. The use of n_{Dij}^2 for $\varepsilon_{\infty ij}$ [8.7] often introduces the additional error in the calculation. Nevertheless, the data of Table 8.1 are accurate up to 5% for χ_{ij}'' and 2% for χ_{ij}' and χ_{oij} respectively.

The non-spherical as well as nonrigid polar liquid molecules often possess two or more τ in GHz electric field for the rotation of different flexible polar groups attached to the parent molecule

Table 8.1: Concentration variation of the real χ_{ij}' and imaginary χ_{ij}'' parts of dimensionless complex dielectric orientation susceptibility χ_{ij}^* and the static dielectric orientation susceptibility χ_{oij} which is real derived from the measured relative permittivities ε_{ij}', ε_{ij}'', ε_{oij} and $\varepsilon_{\alpha\infty ij}$ of chloral and ethyltrichloroacetate in different non-polar solvents at 30 ^{0}C

Frequency in GHz	Weight fraction w_j	$\chi_{ij}'=\varepsilon_{ij}'-\varepsilon_{\alpha\infty ij}$	$\chi_{ij}''=\varepsilon_{ij}''$	$\chi_{oij}=\varepsilon_{oij}-\varepsilon_{\alpha\infty ij}$	Weight fraction w_j	$\chi_{ij}'=\varepsilon_{ij}'-\varepsilon_{\alpha\infty ij}$	$\chi_{ij}''=\varepsilon_{ij}''$	$\chi_{oij}=\varepsilon_{oij}-\varepsilon_{\alpha\infty}$
	I Chloral in benzene				II Chloral in *n*-heptane			
(a) 4.2	0.0255	0.0750	0.005	0.0790	0.1349	0.1853	0.022	0.2052
	0.0977	0.2107	0.031	0.2117	0.2008	0.2996	0.029	0.3238
	0.1813	0.3984	0.080	0.4004	0.2706	0.4128	0.045	0.4531
	0.2511	0.5653	0.088	0.5703	0.3366	0.5356	0.060	0.5787
(b) 9.8	0.0899	0.1803	0.041	0.2024	0.0807	0.0891	0.029	0.1271
	0.1711	0.3377	0.057	0.3719	0.1416	0.1646	0.036	0.2146
	0.1903	0.3695	0.072	0.4153	0.2003	0.2599	0.050	0.3099
	0.2510	0.5149	0.083	0.5608	0.2683	0.3828	0.055	0.4528
	0.3476	0.7333	0.099	0.8183	0.3324	0.5262	0.080	0.5722
(c) 24.6	0.0152	0.0632	0.047	0.0664	0.0795	0.0795	0.024	0.1079
	0.0899	0.1603	0.066	0.2024	0.1349	0.1753	0.038	0.2052
	0.1711	0.3177	0.104	0.3719	0.2008	0.2696	0.054	0.3238
	0.1903	0.3895	0.146	0.4153	0.2706	0.3928	0.068	0.4531
	0.3476	0.7333	0.208	0.8183	0.3366	0.5256	0.091	0.5787
	III Ethyltrichloroacetate in benzene				IV Ethyltrichloroacetate in *n*-hexane			
(a) 4.2	0.0211	0.1031	0.043	0.1292	0.0595	0.1430	0.052	0.1700
	0.0521	0.2061	0.095	0.2513	0.0649	0.1525	0.066	0.1839
	0.0755	0.2885	0.154	0.3457	0.1137	0.2673	0.108	0.3154
	0.1202	0.4432	0.224	0.5312	0.1722	0.3908	0.185	0.4887
	0.1734	0.5891	0.310	0.7610				
	0.2388	0.7969	0.454	1.0569				
(b) 9.8	0.0207	0.0835	0.023	0.1315	0.0210	0.0369	0.021	0.0755
	0.0498	0.1456	0.046	0.2406	0.0595	0.1030	0.041	0.1700
	0.0802	0.2083	0.079	0.3643	0.0649	0.1125	0.066	0.1839
	0.1193	0.2934	0.115	0.5264	0.1137	0.1973	0.093	0.3154
	0.1764	0.4199	0.194	0.7759	0.1722	0.3408	0.126	0.4887
	0.2444	0.6074	0.226	1.0824	0.2360	0.4333	0.190	0.6970
(c) 24.6	0.0211	0.0331	0.010	0.1292	0.0639	0.0522	0.073	0.1842
	0.0521	0.0761	0.025	0.2513	0.0845	0.1008	0.098	0.2298
	0.0755	0.1385	0.059	0.3457	0.1193	0.1167	0.137	0.3297
	0.1202	0.2132	0.086	0.5312	0.1683	0.1512	0.185	0.4782
	0.1734	0.2391	0.105	0.7610				

and the whole molecule itself [8.11]. Bergmann *et al* [8.12], however, devised a graphical method to obtain τ_1 and τ_2 for a pure polar liquid. The respective weighted contributions c_1 and c_2 towards dielectric relaxations were also estimated in terms of τ_1 and τ_2. A graphical method [8.13] was, soon employed from Fröhlich's distribution function [8.14] to get τ_2 and τ_1 of a pure polar solute. The

methods indicate that a single frequency measurement is not sufficient to have correct τ_1 and τ_2. Bhattacharya *et al* [8.15] subsequently attempted to get τ_1, τ_2 and c_1, c_2 for a polar molecule with ε', ε'' ε_o and ε_∞ measured at two different frequencies in GHz region. The graphical analysis made by Higasi *et al* [8.16] on polar-nonpolar liquid mixture was, also a crude approximation.

Saha *et al* [8.6] and Sit *et al* [8.17] recently put forward an analytical method based on single frequency measurement of relative permittivities ε_{ij}', ε_{ij}'' ε_{oij} and $\varepsilon_{\infty ij}$ of polar-nonpolar liquid mixtures of different w_j's at a given temperature to get τ_1, τ_2 and c_1, c_2 respectively. Earlier investigation had been made on different chain-like polar molecules like alcohols in nonpolar solvents [8.18-8.19] to see the double relaxation phenomena at three different electric field frequencies in terms of relative permittivities. However, no such study is made on the aforesaid rigid aliphatic polar liquid molecules in different solvents under various electric field frequencies from measured χ_{ij}'s of Table 8.1. Chloral is widely used in medicine as drug to induce sleep and relieve pain and in the manufacture of D.D.T. as insecticides. Ethyltrichloroacetate, on the other hand, is used for artificial fragrance of fruits and flowers.

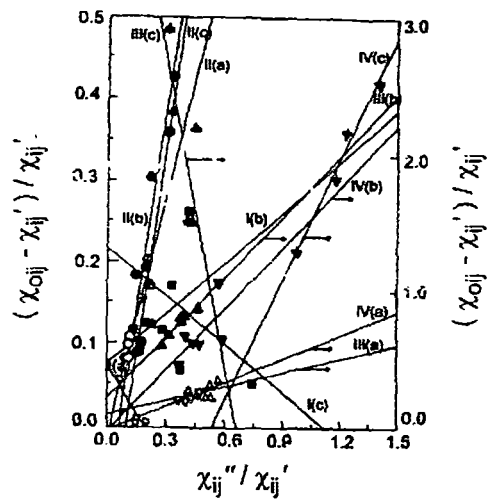

Figure 8.1: Linear variation of $(\chi_{oij}-\chi_{ij}')/\chi_{ij}'$ against χ_{ij}''/χ_{ij}' for different w_j's at 30^{0}C.
I(a), I(b) and I(c) for chloral in benzene (–□–, –■–, –⊞–); II(a), II(b) and II(c) for chloral in *n*-heptane (–○–, –●–, –⊕–); III(a), III(b) and III(c) for ethyltrichloroacetate in benzene (–Δ–, –▲–, –▲–)and IV(a), IV(b) and IV(c) for ethyltrichloroacetate in *n*-hexane (–▽–, –▼–, –▼–) at 4.2, 9.8 and 24.6 GHz electric fields respectively

Thus the object of the present paper is to detect the existence of double relaxation times τ_1, and τ_2 due to rotation of the flexible part and the whole molecules themselves using χ_{ij}'s based on the single frequency measurement technique [8.6-8.17]. The aspect of molecular orientation polarisation is, however, accomplished by introducing χ_{ij}'s because $\varepsilon_{\infty ij}$ .which includes fast polarisation frequently appears as a subtracted term in Bergmann's equations. Thus in order to avoid the clumsiness of algebra and exclude the fast polarisation Bergmann equations [8.12] in terms of established symbols of χ_{ij}', χ_{ij}'' and χ_{oij} can be written as:

$$\frac{\chi'_{ij}}{\chi_{oij}} = c_1 \frac{1}{1+\omega^2\tau_1^2} + c_2 \frac{1}{1+\omega^2\tau_2^2} \qquad \ldots\ldots (8.1)$$

$$\frac{\chi''_{ij}}{\chi_{oij}} = c_1 \frac{\omega\tau_1}{1+\omega^2\tau_1^2} + c_2 \frac{\omega\tau_2}{1+\omega^2\tau_2^2} \qquad \ldots\ldots (8.2)$$

assuming two separate broad dispersions for which the sum of c_1 and c_2 is unity. Eqs.(8.1) and (8.2) are solved to get

$$\frac{\chi_{oij} - \chi'_{ij}}{\chi'_{ij}} = \omega(\tau_1 + \tau_2)\frac{\chi''_{ij}}{\chi'_{ij}} - \omega^2\tau_1\tau_2 \qquad \ldots\ldots (8.3)$$

When the variables $(\chi_{oij}-\chi_{ij}')/\chi_{ij}'$ are plotted against χ_{ij}''/χ_{ij}' for different w_j's of solute under a given angular frequency ω $(=2\pi f)$ of the electric field, a straight line results with the intercept $-\omega^2\tau_1\tau_2$ and slope $\omega(\tau_1+\tau_2)$, as displayed in Fig.8.1. The intercept and slope of Eq.(8.3) are obtained by linear regression analysis made on the measured susceptibilities for different w_j's of chloral in *n*-heptane and ethyltrichloroacetate in *n*-hexane of Table 8.1 to get τ_1 and τ_2 as found in columns 7 and 8 of Table 8.2 extracted from the data of Table 8.1 based on minimum chi-squares value.

Table 8.2: The estimated relaxation time τ_2 and τ_1 from the slope and the intercept of straight line Eq.(8.3) with correlation coefficients (r) and minimum chi-squares values together with measured τ from the slope of $\chi_{ij}''-\chi_{ij}'$ of Eq.(8.16) and τ_2's from single broad dispersion from Eq.(8.4) for rigid aliphatic polar molecules at 30°C under different frequencies of electric fields.

System with sl. no. & mol. wt.M_j	Frequency f in GHz	Slope and intercept of Eq.(8.3)		Corrl. coeff. r	Minimum chi-squares value of Eq.(8.3)	Estimated τ_2 and τ_1 in p-sec		τ^a	τ^b	τ^c
(I) Chloral	(a) 4.2	-0.3872	-0.0732	-0.91	-0.010	5.27	-	7.53	-	4.77
in benzene	(b) 9.8	0.2101	-0.0733	0.49	0.006	6.42	-	1.88	1.78*	10.12
M_j=0.1475 Kg	(c) 24.6	-0.1936	-0.2161	-0.41	0.180	2.45	-	1.72	-	2.01
(II) Chloral	(a) 4.2	0.9995	0.0175	0.69	0.003	37.16	0.67	4.09	-	-
in *n*-heptane	(b) 9.8	1.6592	0.1040	0.93	0.053	25.89	1.06	1.78	0.46*	-
M_j=0.1475 Kg	(c) 24.6	1.7431	0.1748	0.96	0.020	10.60	0.69	0.90	-	-
(III) Ethyltrichloro-	(a) 4.2	0.3546	-0.0698	0.37	0.047	18.78	-	23.00	-	18.71
acetate in benzene	(b) 9.8	1.5115	-0.1800	0.97	0.005	26.36	-	7.28	6.50**	32.53
M_j=0.1915 Kg	(c) 24.6	-7.4034	-4.8872	-0.76	0.337	3.95	-	3.18	-	35.35
(IV) Ethyltrichloro-	(a) 4.2	0.5843	0.0382	0.86	0.004	19.30	2.86	18.66	-	-
acetate in *n*-hexane	(b) 9.8	1.5181	0.0548	0.66	0.153	24.05	0.60	6.28	5.70**	-
M_j=0.1915 Kg	(c) 24.6	2.9886	1.6134	0.99	0.010	14.76	4.58	7.09	-	-

τ^a = Measured τ in p-sec from Eq.(8.16)

τ^b = Reported τ in p-sec

τ^c = τ_2 in p-sec from single broad dispersion of Eq.(8.4)

Assuming a single Debye-like broad dispersion for a polar molecule in a given solvent, Eq.(9.3) is reduced to [9.17] with τ_1=0,

$$\frac{\chi_{oij} - \chi'_{ij}}{\chi'_{ij}} = \omega\tau_2 \frac{\chi''_{ij}}{\chi'_{ij}} \qquad \ldots\ldots (8.4)$$

in order to get τ_2 for the two polar liquids in benzene as seen in the 11th column of Table 8.2. Both the correlation coefficients r's and the minimum chi-squares values are entered in the 5th and 6th columns of Table 8.2.

The theoretical c_1 and c_2 towards dielectric dispersions for chloral and ethyltrichloroacetate in n-heptane and n-hexane were calculated from Fröhlich's [8.14] theoretical equations of χ_{ij}'/χ_{oij} and χ_{ij}''/χ_{oij} with the estimated τ_2 and τ_1 of Table 8.2. The experimental c_1 and c_2, on the other hand, were computed form the values χ_{ij}'/χ_{oij} and χ_{ij}''/χ_{oij} at $w_j \to 0$ by graphical method of Figs.8.2 and 8.3 in order to place them in Table 8.3 for comparison. The plot of χ_{ij}'/χ_{oij} and χ_{ij}''/χ_{oij} against w_j of the respective solutes in Figs.8.2 and 8.3 are the least squares fitted parabolae with the experimental data placed upon them. They are of convex and concave shapes except ethyltrichloroacetate in n-hexane at 9.8 and 24.6 GHz electric fields.

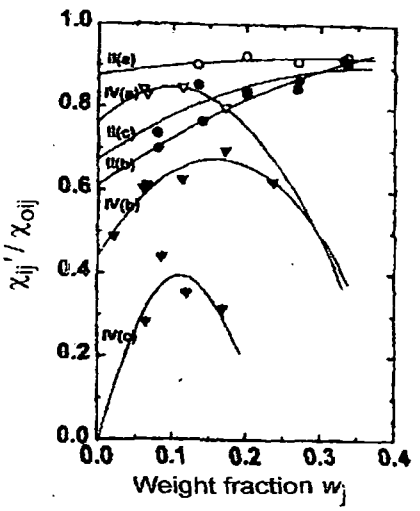

Figure 8.2: Variation of χ_{ij}''/χ_{oij} against w_j's of chloral and ethyltrichloroacetate at 30^{0}C.
II(a), II(b) and II(c) for chloral in n-heptane (–○–, –●–, –⊕–); and IV(a), IV(b) and IV(c) for ethyltrichloroacetate in n-hexane (–▽–, –▼–, –⧨–) at 4.2, 9.8 and 24.6 GHz electric fields respectively

With the values of χ_{ij}'/χ_{oij} and χ_{ij}''/χ_{oij} in the limit of w_j=0 of Figs.8.2 and 8.3, and the graphical plot of $(1/\phi)\log(\cos\phi)$ against ϕ in degrees of Fig.8.4, the symmetric and asymmetric distribution parameters γ and δ related to symmetric and characteristic relaxation times τ_s and τ_{cs} of the molecules were determined and are placed in Table 8.3 to conclude the molecular non-rigidity and symmetric distribution as well.

The dipole moments μ_2 and μ_1 of Table 8.4 from τ_2 and τ_1 of Table 8.2 were then measured in terms of the linear coefficients β's of the variations of χ_{ij}'s with w_j's of Fig.8.5. All the familiar parabolic curves χ_{ij}'s with w_j's are found to increase with frequency (f) of the electric field. The

measured μ's are compared with theoretical dipole moment μ_{theo}'s derived from available bond angles and bond moments of the substituent polar groups attached to the parent ones as sketched in Fig.8.6. The associational aspect of the polar molecules with solvents in Fig.8.6 exhibits the mesomeric, inductive and electromeric effects. All these effects are taken into account by the ratio of μ_{expt}/μ_{theo} in agreement with the experimental results as seen in Table 8.4. They are finally compared with the reported μ's and μ_1's obtained from $\mu_1=\mu_2(c_1/c_2)^{1/2}$ assuming both the relaxation processes are equally probable.

Table 8.3: Fröhlich parameter A [$=\ln(\tau_2/\tau_1)$], relative contributions c_1 and c_2 towards dielectric dispersion due to τ_1 and τ_2, theoretical and experimental values of χ_{ij}'/χ_{oij} and χ_{ij}''/χ_{oij} of Fröhlich's Eqs.(8.7) and (8.8) and from fitting equations of Figs.8.2 and 8.3 at $w_j\rightarrow 0$ respectively and symmetric and asymmetric distribution parameters γ and δ related to symmetric and characteristic relaxation times τ_s and τ_{cs} for polar-nonpolar liquid mixtures at 30°C.

System with sl. no.	f in GHz	A	Theoretical values of χ_{ij}'/χ_{oij} and χ_{ij}''/χ_{oij} from Eq.(8.7) and (8.8)		Theoretical values of c_1 and c_2		Experimental values of χ_{ij}'/χ_{oij} and χ_{ij}''/χ_{oij} at $w_j\rightarrow 0$		Experimental values of c_1 and c_2		Estimated values of γ and δ		τ_s and τ_{cs} in p-sec	
(II)	4.2	4.0137	0.9161	0.1886	0.7373	0.3512	0.880	0.161	0.7287	0.2927	0.29	0.18	4.60	59.71
Chloral in	9.8	3.1956	0.8028	0.2958	0.6463	0.5639	0.615	0.320	0.4334	0.6492	0.25	0.42	10.52	35.51
n-heptane	24.6	2.7319	0.7634	0.3355	0.6043	0.6111	0.675	0.289	0.5395	0.5211	0.28	0.36	3.13	13.49
(IV)														
Ethyltrichl	4.2	1.9093	0.9411	0.2071	0.6310	0.3950	0.765	0.325	0.1494	0.7762	0.14	0.50	16.18	39.29
oroacetate	9.8	3.6910	0.8429	0.2547	0.6891	0.4943	0.445	0.286	0.2583	0.5968	0.33	0.43	20.48	65.69
in	24.6	1.1702	0.3937	0.4629	0.4152	0.7264	-0.015	0.298	-0.3167	1.2155	-0.21	-	18.73	-
n-hexane														

8.2. Theoretical Formulations of c_1 and c_2 for τ_1 and τ_2 :

Eqs.(8.1) and (8.2) are solved for c_1 and c_2 to get

$$c_1=\frac{(\chi_{ij}'\alpha_2-\chi_{ij}'')(1+\alpha_1^2)}{\chi_{oij}(\alpha_2-\alpha_1)} \qquad \ldots\ldots(8.5)$$

$$c_2=\frac{(\chi_{ij}''-\chi_{ij}'\alpha_1)(1+\alpha_2^2)}{\chi_{oij}(\alpha_2-\alpha_1)} \qquad \ldots\ldots(8.6)$$

where $\alpha_1=\omega\tau_1$ and $\alpha_2=\omega\tau_2$, provided $\alpha_2>\alpha_1$. The molecules under consideration are of complex type and only a few data are available under single frequency measurement in the low concentration region. A continuous distribution of τ with two discrete values of τ_1 and τ_2 could, therefore, be

expected [8.12]. Thus from Fröhlich's theory[8.14] based on distribution of τ between the two extreme values of τ_1 and τ_2 one gets

$$\frac{\chi'_{ij}}{\chi_{oij}} = 1 - \frac{1}{2A}\ln\left(\frac{1+\omega^2\tau_2^{\,2}}{1+\omega^2\tau_1^{\,2}}\right) \qquad \ldots\ldots (8.7)$$

$$\frac{\chi''_{ij}}{\chi_{oij}} = \frac{1}{A}\left[\tan^{-1}(\omega\tau_2) - \tan^{-1}(\omega\tau_1)\right] \qquad \ldots\ldots (8.8)$$

where A=Fröhlich parameter=$\ln(\tau_2/\tau_1)$. The theoretical values of χ_{ij}'/χ_{oij} and χ_{ij}''/χ_{oij} of Eqs.(8.7) and (8.8) were used to get theoretical c_1 and c_2 from Eqs.(8.1) and (8.2) in order to compare them with c_1 and c_2 from the graphical plots of χ_{ij}'/χ_{oij} and χ_{ij}''/χ_{oij} at $w_f \to 0$ as seen in Figs.8.2 and 8.3. Both the theoretical and experimental c_1 and c_2 are placed in Table 8.3.

8.3. Distribution Parameters γ and δ Related to τ_s and τ_{cs} :

All the chemical systems are almost identical for the three frequencies employed. Nevertheless, the existence of double relaxations for chloral in *n*-heptane and ethyltrichloroacetate in *n*-hexane reflects the material property of the chemical systems (Table 8.2) indicating the molecular non-rigidity. In such case, the molecule may either show symmetrical circular arc or a skewed arc [8.20] when the values of χ_{ij}''/χ_{oij} is plotted against χ_{ij}'/χ_{oij} at $w_f \to 0$ for various frequencies of the electric field to yield:

$$\frac{\chi^*_{ij}}{\chi_{oij}} = \frac{1}{1+(j\omega\tau_s)^{1-\gamma}} \qquad \ldots\ldots (8.9)$$

$$\frac{\chi^*_{ij}}{\chi_{oij}} = \frac{1}{(1+j\omega\tau_{cs})^{\delta}} \qquad \ldots\ldots (8.10)$$

Here, γ and δ are the symmetric and asymmetric distribution parameters which are, related to symmetric and characteristic relaxation times τ_s and τ_{cs} respectively. Separating the real and imaginary parts from Eq.(8.9) one has

$$\gamma = \frac{2}{\pi}\tan^{-1}\left[\left(1 - \frac{\chi'_{ij}}{\chi_{oij}}\right)\frac{\chi'_{ij}/\chi_{oij}}{\chi''_{ij}/\chi_{oij}} - \frac{\chi''_{ij}}{\chi_{oij}}\right] \qquad \ldots\ldots (8.11)$$

$$\tau_s = \frac{1}{\omega}\left[1\Big/\left(\frac{\chi'_{ij}/\chi_{oij}}{\chi''_{ij}/\chi_{oij}}\cos\frac{\gamma\pi}{2} - \sin\frac{\gamma\pi}{2}\right)\right]^{\frac{1}{1-\gamma}} \qquad \ldots\ldots (8.12)$$

where χ_{ij}'/χ_{oij} and χ_{ij}''/χ_{oij} are obtained from Figs.8.2 and 8.3 at $w_j \to 0$. Again δ and τ_{cs} can be had from Eq.(8.10)as:

$$\tan(\phi\delta) = \frac{\chi''}{\chi'} \qquad \ldots\ldots (8.13)$$

and

$$\tau_{cs} = \frac{1}{\omega}\tan\phi \qquad \ldots\ldots (8.14)$$

Since ϕ cannot be evaluated directly, a theoretical curve of $(1/\phi)\log(\cos\phi)$ with ϕ in degrees was drawn in Fig.8.4 from which

$$\frac{1}{\phi}\log(\cos\phi) = \frac{\log\left[\left(\chi_{ij}'/\chi_{oij}\right)/\cos(\phi\delta)\right]}{\phi\delta} \qquad \ldots\ldots (8.15)$$

can be found out. The known value of $(1/\phi)\log(\cos\phi)$ was then use to obtain ϕ. With known ϕ and δ, τ_{cs} were found out from Eqs.(8.13) and (8.14). The estimated γ and δ are entered in columns 12 and 13 with τ_s and τ_{cs} in columns 14 and 15 of Table 8.3 to conclude the symmetric relaxation behaviour for such liquids.

8.4. Theoretical Formulation for Dipole Moments μ_2 and μ_1 :

The Debye equation [8.14] for a polar-nonpolar liquid mixture under *hf* electric field in terms of χ_{ij}'s is written as:

$$\frac{d\chi_{ij}''}{d\chi_{ij}'} = \omega\tau$$

or,

$$\left(\frac{d\chi_{ij}''}{dw_j}\right)_{w_j\to 0} = \omega\tau\left(\frac{d\chi_{ij}'}{dw_j}\right)_{w_j\to 0} \qquad \ldots\ldots (8.16)$$

τ's of the polar liquid could, however, be estimated from Eq.(8.16) in order to place in column 9 of Table 8.2. Again, the imaginary part of dielectric orientation susceptibility χ_{ij}'' as a function of w_j of a solute can be written as [8.21-8.22]

$$\chi_{ij}'' = \frac{N\rho_{ij}\mu_j^{\,2}}{27\varepsilon_o k_B T M_j}\frac{\omega\tau}{1+\omega^2\tau^2}(\varepsilon_{ij}+2)^2 w_j$$

Differentiation of the above equation with respect to w_j and at $w_j \to 0$ yields:

$$\left(\frac{d\chi''_{ij}}{dw_j}\right)_{w_j\to 0} = \frac{N\rho_i\mu_j^{\,2}}{27\varepsilon_o k_B T M_j}\left(\frac{\omega\tau}{1+\omega^2\tau^2}\right)(\varepsilon_i+2)^2 \qquad \ldots\ldots (8.17)$$

where the density of the solution ρ_{ij} becomes ρ_i= density of solvent, $(\varepsilon_{ij}+2)^2\to(\varepsilon_i+2)^2$ at $w_j\to 0$, k_B=Boltzmann constant, N=Avogadro's number, ε_i=relative permittivity of solvent and ε_o=permittivity of free space=$8.854\text{x}10^{-12}$ F.m $^{-1}$. All are expressed in SI units.

Comparing Eqs.(8.16) and (8.17) one gets

$$\omega\tau\left(\frac{d\chi'_{ij}}{dw_j}\right)_{w_j\to 0} = \frac{N\rho_i\mu_j^{\,2}}{27\varepsilon_o k_B T M_j}\left(\frac{\omega\tau}{1+\omega^2\tau^2}\right)(\varepsilon_i+2)^2 = \omega\tau\beta \qquad \ldots\ldots (8.18)$$

where β is the slope of χ_{ij}'–w_j curves of Fig.8.5 at $w_j\to 0$. Here, no approximation in determination of μ_j is made like the conductivity measurement technique done elsewhere [8.23].

After simplification, the *hf* dipole moment μ_j is given by:

$$\mu_j = \left(\frac{27\varepsilon_o k_B T M_j \beta}{N\rho_i(\varepsilon_i+2)^2 b}\right)^{\frac{1}{2}} \qquad \ldots\ldots (8.19)$$

where

$$b = 1/(1+\omega^2\tau^2) \qquad \ldots\ldots (8.20)$$

is the dimensionless parameter involved with measured τ's of Table 8.2. All the μ's, b's and β's as computed for chloral and ethyltrichloroacetate in different solvents at 30^{0}C are placed in Table 8.4 to compare with μ_{theo}'s from the available bond angles and bond moments in Coulomb-metre (C.m).

8.5. Results and Discussions :

The double or single relaxation phenomena for chloral and ethyltrichloroacetate in benzene, *n*-heptane and *n*-hexane under 24.6, 9.8 and 4.2 GHz electric field frequencies were studied from the slopes and intercepts of linear plots in Fig.8.1 for the variables $(\chi_{oij}-\chi_{ij}')/\chi_{ij}'$ against χ_{ij}''/χ_{ij}' of theoretical formulation of Eq.(8.3) for different w_j's of solutes at 30^{0}C. The dielectric orientation susceptibilities χ_{ij}', χ_{ij}'' and χ_{oij} are collected together in Table 8.1 from the measured relative permittivities of ε_{ij}', ε_{ij}'' ε_{oij} and $\varepsilon_{\infty ij}$ [8.7]. The linear regression analysis made on Eq.(8.3) with the data of Table 8.1 was, however, done by the use of a PC and software. The correlation coefficients r's are placed in Table 8.2 in getting the intercepts and slopes of Eq.(8.3) to see how far the data of Table 8.1 are collinear. The errors involved in the linear regression analysis of Eq(8.3) are expressed by chi-squares values which were initially very large in some cases. One therefore, should have become selective to choose a few date for some systems for which chi-squares values were adjusted

Table 8.4: Estimated coefficients of χ_{ij}'–w_j equations, dimensionless parameters b_2, b_1 [Eq.(8.20)], estimated dipole moments μ_2 and μ_1 from Eq.(8.19) and μ_{theo} from bond angle and bond moment together with μ_1 from $\mu_1=\mu_2(c_1/c_2)^{½}$ and reported μ in Coulomb.metre (C.m).

System with sl. no. & mol. wt.M_j	f in GHz	Coefficients of χ_{ij}'–w_j equation $\chi_{ij}'=\alpha+\beta w_j+\xi w_j^2$			Dimensionless parameter		Estimated $\mu X10^{30}$ in C.m		Reported $\mu X10^{30}$ in C.m	Estimated $\mu_1 X10^{30}$ in C.m from $\mu_1=\mu_2(c_1/c_2)^{½}$	μ_{theo}
		α	β	ξ	b_1	b_2					
(I) Chloral	4.2	0.0291	1.7212	1.6641	-	0.9810	-	5.21	5.17*	-	
in benzene	9.8	0.0218	1.6402	1.1834	-	0.8648	-	5.42	4.87**	-	10.02
M_j=0.1475 Kg	24.6	0.0333	1.4368	1.6834	-	0.8746	-	5.04	4.73*	-	
(II) Chloral	4.2	-0.0250	1.5050	0.4654	0.9997	0.5098	5.99	8.39	6.13*	12.16	
in *n*-heptane	9.8	0.0150	0.7168	2.4649	0.9958	0.2824	4.14	7.78	6.00**	8.33	10.02
M_j=0.1475 Kg	24.6	-0.0223	1.2478	1.1078	0.9888	0.2714	5.48	10.47	5.63*	10.41	
(III) Ethyltrichl-	4.2	0.0295	3.5204	-1.3400	-	0.8028	-	9.39	9.70*	-	
oroacetate	9.8	0.0490	1.7935	1.9676	-	0.2751	-	11.45	6.50**	-	10.50
in benzene	24.6	-0.0309	2.7329	-6.6401	-	0.7285	-	8.68	8.13*	-	
M_j=0.1915 Kg											
(IV) Ethyltrichl-	4.2	2.6215	2.6215	-1.7604	0.9943	0.7940	9.16	10.28	10.30*	12.98	
oroacetate	9.8	1.9711	1.9711	-0.2513	0.9986	0.3132	7.95	14.19	8.67**	16.74	10.50
in *n*-hexane	24.6	2.4108	2.4108	-6.6385	0.6662	0.1612	10.76	21.87	13.27*	16.53	
M_j=0.1915 Kg											

to be minimum for the effective utilization of the experimental data [8.7]. The large chi-squares values initially obtained for Eq.(8.3) further indicate the probable uncertainty in the measurements. The minimum chi-squares values so adjusted on the data are presented in column 6 of Table 8.2. The data for chloral in benzene (–□–, –⊞–) at 4.2 and 24.6 GHz and ethyltrichloroacetate in *n*-hexane (–▼–) at 9.8 GHz do not appear to lie on the straight line. The display of data set for ethyltrichloroacetate in benzene (–Δ–, –▲–) at 4.2 and 24.6 GHz and in *n*-hexane (–▽–) at 4.2 GHz is over a narrow range, which often renders the linear regression of doubtful validity. Perfect linearity between variables of Eq.(8.3) is said to be achieved if r=–1 or +1 although, the correlation coefficient r's for the systems (–⊞–, –□–, –▼–) are –0.41, –0.91 and 0.66 respectively. The high value of r =–0.91 for chloral in benzene (–□–) at 4.2 GHz indicates that the variables of Eq.(8.3) are almost linearly correlated with each other while comparatively lower values of r's of –0.41 and 0.66 for chloral in benzene at 24.6 GHz (–⊞–) and ethyltrichloroacetate in *n*-hexane at 9.8 GHz (–▼–) may occur for the experimental difficulty of the accurate measurements of the relative permittivities in the 24.6 GHz electric field. The desired variables $(\chi_{oij}-\chi_{ij}')/\chi_{ij}'$ and χ_{ij}''/χ_{ij}' of Eq.(8.3) for ethyltrichloroacetate in benzene (–Δ–) and *n*-hexane (–▽–) at 4.2 GHz and ethyltrichloroacetate in benzene at 24.6 GHz (–▲–) are incidentally of narrow range although the relative permittivities

were measured [8.7] for a wide range of concentration as seen in Table 8.1. Nevertheless, the straight lines of the data set for the systems under consideration as displayed in Fig.8.1 are made on the basis of minimum chi-squares values mathematically adjusted between two variables. The high values of r's as shown in Table 8.2 signify the applicability of linear regression analysis on the data set mentioned above.

Four data set out of six, showed mono while other two double relaxations which are important. Nevertheless, the measurement technique employed and sampling of the polar-nonpolar liquid mixtures for various concentrations called w_j's were so prepared [8.7-8.8] that χ_{ij}', χ_{oij} and χ_{ij}'' of Table 8.1 for different w_j's are of 2% and 5% accuracies. This type of anomaly showed in benzene and *n*-hexane the associational aspects [8.24] of polar molecules. The estimated values of τ_2 and τ_1 from the intercepts and slopes of Table 8.2 are placed in the 7th and 8th columns of Table 8.2. Double relaxation phenomena are, however, observed for chloral in *n*-heptane and ethyltrichloroacetate in *n*-hexane at 4.2 GHz (*J*-band) 9.8 GHz (*X*-band) and 24.6 GHz (*Q*-band) *hf* electric field. This fact indicates that the phenomena of double or single relaxation are the material property of the chemical system in addition to the dependency on solvent used. It further reveals that the existence of double relaxation phenomena in aliphatic solvents at all the frequencies is greater than in the aromatic solvent. Both chloral and ethyltrichloroacetate in benzene showed the single relaxation by showing τ_2 only. The existence of fractional +ve charge δ^+ on C-atom and δ^- on O-atom of >C⇐ O group in both the polar liquids produces electromeric effect to form π-complexes with the delocalised π-electron cloud δ^- of benzene ring. This prefers the solute-solvent molecular association and yields single τ_2 in benzene. The τ_2's were calculated from Eq.(8.4) assuming single broad Debye-like dispersion [8.17]. They are placed in column 11 of Table 8.2. It is interesting to note that τ_1's for two molecules agree well with the measured τ from Eq.(8.16) involved with measured susceptibility.

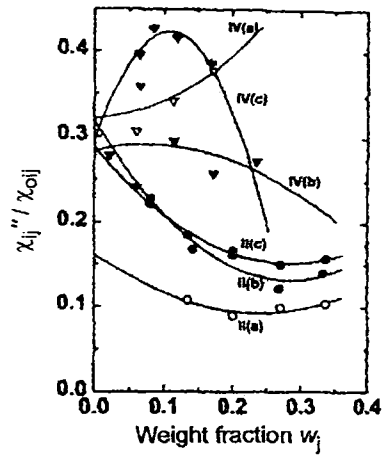

Figure 8 3: Variation of χ_{ij}''/χ_{oij} against w_j's of chloral and ethyltrichloroacetate at 30^{0}C.
II(a), II(b) and II(c) for chloral in *n*-heptane (–O–, –●–, –⊕–); and IV(a), IV(b) and IV(c) for ethyltrichloroacetate in *n*-hexane (–∇–, –▼–, –⧨–) at 4.2, 9.8 and 24.6 GHz electric fields respectively

Thus the *hf* susceptibility measurement always yields the microscopic as well as macroscopic τ as observed for double relaxation phenomena through conductivity measurements [8.18].

Almost all τ_2's of Table 8.2 are higher at 9.8 GHz, but of low values both at 4.2 and 24.6 GHz electric field in different solvents. Such behaviour occurs probably due to strong absorbtion of electric energy in the effective dispersive region of 9.8 GHz. The solute-solvent or solute-solute molecular association break up at higher and lower frequencies from nearly 10 GHz electric field. Almost all the τ_1 agree with the reported τ seen in the 10th column Table 8.2 exhibiting the probability of rotation of a part of the molecule under *hf* electric field [8.9]

The theoretical values of the relative contributions and c_1 and c_2 towards dielectric dispersions due to τ_1 and τ_2 are, however, calculated from Eqs.(8.5) and (8.6) with the theoretical values of χ_{ij}'/χ_{oij} and χ_{ij}''/χ_{oij} of Fröhlich's [8.14] Eqs.(8.7) and (8.8). They are compared with the experimental c_1 and c_2 derived from Eqs.(8.5) and (8.6) with the graphically estimated χ_{ij}'/χ_{oij} and χ_{ij}''/χ_{oij} of Figs.8.2 and 8.3 at $w_j \rightarrow 0$. Both the methods yield $c_1+c_2 \cong 1$ suggesting the applicability of the methods. The variations of χ_{ij}'/χ_{oij} and χ_{ij}''/χ_{oij} with w_j are convex and concave unlike the observation made earlier [8.6, 8.17], except ethyltrichloroacetate in *n*-hexane at 9.8 and 24.6 GHz both of which show the convex variation. Such type of behaviour is explained by the fact that unlike increase of τ [8.25] it decreases with w_j probably due to solute-solute or solute-solvent molecular associations. All the experimental values of c_1 and c_2 are placed in Table 8.3 for comparison with the theoretical c_1 and c_2.

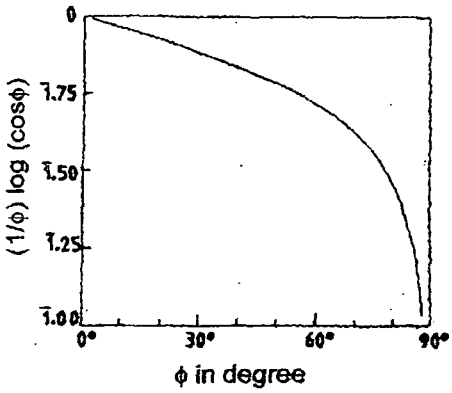

Figure 8.4: Plot of $(1/\phi)\log(\cos\phi)$ against ϕ in degree.

In order to test the non-rigid relaxation behaviour of the molecules the symmetric and asymmetric distribution parameters γ and δ were estimated from Eqs.(8.11) and (8.13) for fixed values of χ_{ij}'/χ_{oij} and χ_{ij}''/χ_{oij} at $w_j \rightarrow 0$ from Figs.8.2 and 8.3. γ and δ are, however, related to symmetric and asymmetric relaxation times τ_s and τ_{cs} of Eqs.(8.12) and (8.14). The values of $(1/\phi)\log(\cos\phi)$ against ϕ in degrees as shown in Fig.8.4 is essential to get δ. Knowing ϕ from the curve of Fig.8.4; δ's were found out. Both γ, δ and τ_s, τ_{cs} are placed in Table 8.3. The values of γ establish the non-rigid and symmetrical distribution of dielectric parameters of the molecules in *n*-hexane and *n*-heptane at all the frequencies unlike δ, as they are found to be very low [8.26].

The dipole moments μ_2 and μ_1 of polar molecules as presented in Table 8.4 were estimated from Eq.(8.19) in terms of dimensionless parameters b's of Eq.(8.20) and slope β of the familiar χ_{ij}'–w_j curves of Fig.8.5 as seen Table 8.4. The variation of χ_{ij}' with w_j are almost similar as seen Fig.8.5 and Table 8.4 like conductivity measurement presented elsewhere [8.23]. Estimated dipole moments are found in agreement with the reported μ's to signify the applicability of the present method. μ_2's are found to increase from 24.6 GHz to 4.2 GHz electric field showing the maximum values at 9.8 GHz for both chloral and ethyltrichloroacetate in benzene. This type of behaviour may be due to strong absorbtion of electric energy at 9.8 GHz and solute-solvent association of polar solute with benzene ring. But μ_2's for chloral in n-heptane and ethyltrichloroacetate in n-hexane increase gradually from 4.2 GHz. This sort of variation is probably due to rupture of solute-solute and solute-solvent molecular associations in the *hf* electric field and the corresponding increase in the absorbtion for smaller molecular species [8.27].

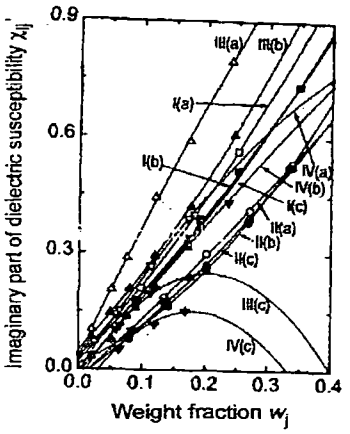

Figure 8.5: Variation of real part of dielectric susceptibility χ_{ij}' witht w_j of solutes at 30^{0}C.
I(a), I(b) and I(c) for chloral in benzene (–□–, –■–, –⊞–); II(a), II(b) and II(c) for chloral in n-heptane (–○–, –●–, –⊕–); III(a), III(b) and III(c) for ethyltrichloroacetate in benzene (–Δ–, –▲–, –⯅–)and IV(a), IV(b) and IV(c) for ethyltrichloroacetate in n-hexane (–▽–, –▼–, –⯆–) at 4.2, 9.8 and 24.6 GHz electric fields respectively

The μ_2 and μ_1 for chloral in n-heptane and ethyltrichloroacetate in n-hexane at 4.2, 9.8 and 24.6 GHz as well as μ_2 of those liquids in benzene (Table 8.4) are, however, compared with μ_{theo}'s due to available bond angles and bond moments 8.0, 5.0, 0.3 and 2.4 multiple of 10^{-30} Coulomb metre (C.m) for the substituent polar groups of C⇐O, C⇐Cl, C←C and C→OCH_3 (making an angle 57^0 with bond axis) respectively with the parent molecules of Fig.8.6. μ_{theo}'s are entered in column 12 of Table 8.4. Chloral shows slightly larger μ_{theo} for solute-solute molecular associations [Fig.8.6 (ii)] in the comparatively concentrated solution as expected [8.28]. The solute-solute molecular association arises due to interaction of fractional positive change δ^+ on C-atom and negative change δ^- on O-atom of >C⇐O group of two solute molecules. Only >C⇐O exhibits electromeric effect. The solvent C_6H_6 on the other hand, is a cyclic compound with three double bonds and six p-electrons on six C-atoms. Hence π–π interaction or resonance effect combined with

inductive effect known as mesomeric effect is expected to play an important role in the measured *hf* μ_j. Special attention is, therefore, paid to study the solute-solvent molecular association with C_6H_6. This is explained by the interaction between C-atom of carbonyl group and π-delocalised electron

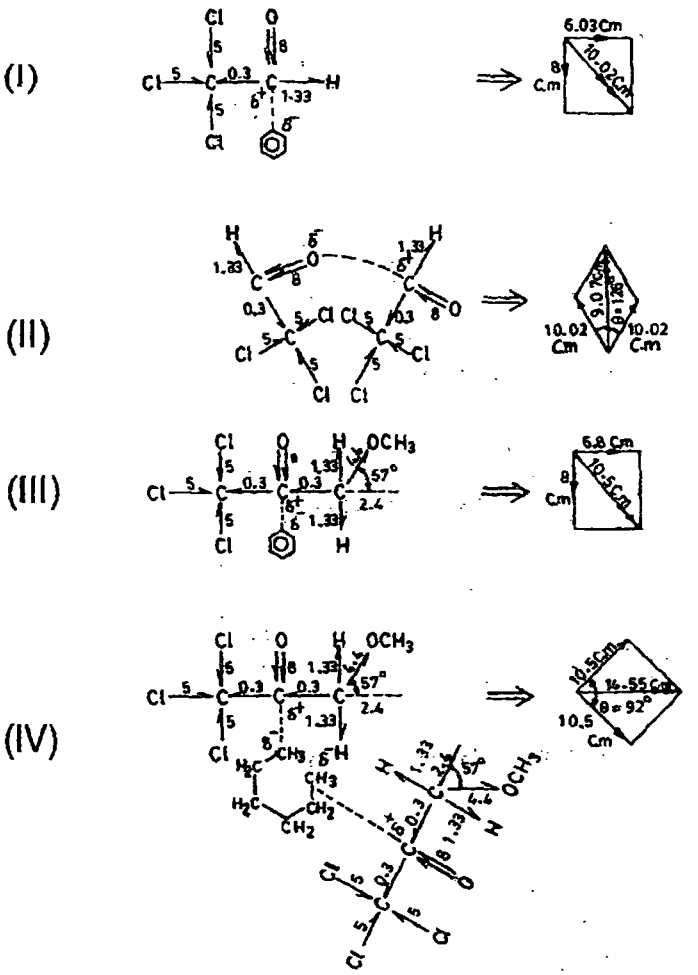

Figure 8.6: Conformational structures of chloral and ethyltrichloroacetate from bond angles and bond moments (expressed in multiple of 10^{-30} Coulomb.metre).

(I) Solute-solvent molecular association of chloral in benzene, (II) Solute-solute molecular association of chloral in *n*-heptane, (III) Solute-solvent molecular association of ethyltrichloroacetate in benzene and (IV) Solute-solute molecular association of ethyltrichloroacetate in *n*-hexane

cloud of benzene ring. Ethyltrichloroacetate, on the other hand, shows μ_{theo} in agreement with the estimated μ's in C_6H_6. This is due to solute-solvent molecular association as sketched in Fig.8.6(i) and (iii). Larger values of measured μ's are explained by the solute-solute molecular interactions in

solvent *n*-hexane due to interaction between adjacent C and O atoms of >C⇐O groups of two molecules as shown in Fig.8.6(iv). However, the reduced bond moments by μ_{expt}/μ_{theo} corroborate μ_{theo}'s in agreement with the experimental μ's to measure mesomeric, inductive and electromeric effects of the substituent polar groups of the molecules.

8.6. Conclusion :

Theoretical considerations for the effective utilization of the established symbols of dielectric terminologies and parameters in terms of dielectric susceptibilities from dielectric relative permittivities appear to be more topical, significant and useful contribution in the study of dielectric relaxation mechanism as they are directly concerned with orientation polarisation of the polar molecules. The significant formulations so far derived in terms of χ_{ij}', χ_{ij}'' and χ_{oij} measured under the single frequency measurements of relative permittivities help one to grasp a new physical insight into the molecular interactions. The single frequency measurement of relaxation parameters provide a unique method to get macroscopic and microscopic relaxation times and hence dipole moments of the whole and the flexible part of a molecule. The estimation of τ_1 and τ_2 from the linear Eq.(8.3) is simple and straightforward to get μ from Eq.(8.19) in terms of slope of familiar χ_{ij}'–w_j curve. The correlation coefficient and chi-squares values signify the minimum error introduced into the desired parameters. The molecules under identical state of environment show interesting phenomena of double or even single relaxation depending upon the solvent used. Aliphatic polar molecules have the greater probability of showing double relaxation in non-polar aliphatic solvents. Various types of molecular associations like solute-solute and solute–solvent association are thus inferred from the usual departure of the graphical plots of χ_{ij}'/χ_{oij} and χ_{ij}''/χ_{oij} with w_j following Bergmann's equations. Non-rigid characteristics of the molecules are ascertained by the symmetric distribution parameter in solvents. The molecular associations are supported by the conformational structures of the molecules in which the mesomeric, inductive and electromeric effects play and important role. The correlation between the conformational structures of the compounds with the observed results enhances the scientific contents and adds a new horizon to understanding the existing knowledge of dielectric relaxation.

References:

[8.1] A K Sharma, D R Sharma and D S Gill, *J. Phys. D: Appl. Phys.* **18** 1199 (1985)

[8.2] A Sharma and D R Sharma, *J. Phys. Soc. Jpn.* **61** 1049 (1992)

[8.3] K S Cole and R H Cole, *J. Chem. Phys.* **9** 341 (1941)

[8.4] D W Davidson and R H Cole, *J. Chem. Phys.* **19** 1484 (1951)

[8.5] K V Gopalakrishna, *Trans. Faraday Soc.* **53** 767 (1957)

[8.6] U Saha, S K Sit, R C Basak and S Acharyya, *J. Phys. D: Appl. Phys.* **27** 596 (1994)

[8.7] S K Srivastava and S L Srivastava, *Indian J. Pure & Appl. Phys.* **13** 179 (1975)

[8.8] A D Franklin, W M Heston, E J Hennelly and C P Smyth, *J. Am. Chem. Soc.* **72** 3447 (1950)

[8.9] K Dutta, R C Basak, S K Sit and S Acharyya, *J Molecular Liquids* **88** 229 (2000)

[8.10] A K Johnscher, *Physics of Dielectric solids, invited papers edited by CHL Goodman* (1980) p.7

[8.11] A Budo, *Phys. Z.* **39** 706 (1938)

[8.12] K Bergmann, D M Roberti and C P Smyth, *J. Phys. Chem.* **64** 665 (1960)

[8.13] A Mansing and P Kumar, *J. Phys. Chem.* **69** 4197 (1965)

[8.14] H Frohlich, *Theory of Dielectrics (Oxford University Press, Oxford)* 1949 p.94

[8.15] J Bhattacharyya, A Hasan, S B Roy and G S Kastha, *J. Phys. Soc. Jpn.* **28** 204 (1970)

[8.16] K Higasi, Y Koga and M Nakamura, *Bull. Chem. Soc. Jpn.* **44** 988 (1971)

[8.17] S K Sit, R C Basak, U Saha and S Acharyya, *J. Phys. D: Appl. Phys.* **27** 2194 (1994)

[8.18] S K Sit and S Acharyya, *Indian J. Phys. B* **70** 19 (1996)

[8.19] S K Sit, N Ghosh and S Acharyya, *Indian J. Pure & Appl. Phys.* **35** 329 (1997)

[8.20] J G Powles, *J. Molecular Liquids* **56** 35 (1993)

[8.21] C P Smyth, *Dielectric Behaviour and Structure (Mc Graw Hill)* 1955 p.140

[8.22] N Ghosh, S K Sit, A K Bothra and S Acharyya, *J. Phys. D: Appl. Phys.* **34** 379 (2001)

[8.23] K Dutta, S K Sit and S Acharyya, *J. Molecular Liquids* **92** 263 (2001)

[8.24] H D Purohit, H S Sharma and A D vyas, *Indian J. Pure & Appl. Phys.* **12** 273 (1974)

[8.25] S N Sen and R Ghosh, *Indian J. Pure & Appl. Phys.* **10** 701 (1972)

[8.26] S Chandra and J Prakash, *J. Phys. Soc. Jpn.* **35** 876 (1975)

[8.27] L Glasser, J Crossley and C P Smyth, *J. Chem. Phys.* **57** 3977 (1972)

[8.28] R J Sengwa and K Kaur, *Indian J. Pure & Appl. Phys.* **37** 469 (1999)

CHAPTER 9

RELAXATION PHENOMENA OF POLAR NON-POLAR LIQUID MIXTURES UNDER LOW AND HIGH FREQUENCY ELECTRIC FIELD

9.1. Introduction :

The dielectric relaxation phenomena of dipolar liquid molecules in non-polar solvents under high frequency electric field is of special importance to study the structure as well as different inter and intra molecular interactions besides solute-solvent and solute-solute molecular associations [9.1-9.2]. Nowadays, it is being thought to be an essential tool to investigate the inductive, mesomeric and electromeric moments of the substituent polar groups present in the polar molecule through the time and frequency domain AC spectroscopy [9.3] or dielectric orientation susceptibility [9.4] or conductivity measurement technique [9.5]. The *hf* conductivity σ_{ij} is concerned with only bound molecular charges while the *hf* susceptibility χ_{ij} contains only orientation polarisation of the dipolar molecule. The dipole moment μ_j and the relaxation time τ_j are, however, easily measured from the conductivity measurements.

Purohit *et al* [9.6-9.7] and Srivastava & Srivastava [9.8] had measured the real ε_{ij}', imaginary ε_{ij}'' parts of the complex relative permittivities ε_{ij}^*, static or low frequency and infinite frequency relative permittivities ε_{oij} and $\varepsilon_{\infty ij}$ of some aliphatic molecules (j) chloral [CCl_3CHO], ethyltrichloroacetate [$CCl_3COOCH_2CH_3$], trifluoroethanol [CF_3CH_2OH], trifluoroacetic acid [CF_3COOH] and octanoyl chloride [$CH_3(CH_2)_6COCl$] in non-polar solvents (i) under 9.8 GHz electric field at 30°C ,25°C and 35°C respectively. The inductive, mesomeric and electromeric moments of the substituent polar groups attached to the parent molecules play the vital role in the formation of solute-solute (dimer) and solute-solvent (monomer) molecular associations. Chloral is widely used in medicine as a drug to induce sleep and relieve pain and in the manufacture of DDT as insecticides. Ethyltrichloroacetate, on the other hand, is used as artificial fragrance of fruits and flowers. Trifluoroethanol and Trifluoroacetic acid in C_6H_6 have a tendency to form either monomer or dimer formations through hydrogen bonding except octanoyl chloride. The liquids were of puram grade of M/s BDH, England but octanoyl chloride was of puram grade of M/s Fluka, AG.

We, therefore, thought to restudy all these polar molecules from *hf* complex conductivity σ_{ij}^* in terms of the internationally accepted symbols of dielectric terminologies and parameters in SI units to predict their τ and μ. The molecules have often a tendency to exhibit double relaxation times τ_1 and τ_2 due to rotation of their flexible polar groups attached to parent molecules and the whole molecules themselves [9.9] under a single frequency electric field of GHz range at a given temperature. The polar molecules showed double relaxation phenomena in a particular solvent when the measured data are adjusted to chi-squares minimization [9.10]. The most effective dispersive region of almost all the polar molecules lies in the neighbourhood of 10 GHz electric field [9.11]. Moreover, the comparison of *hf* μ_j obtained from *hf* conductivity σ_{ij} measurement with the static μ_s from the measured static parameter X_{ij} seems to be interesting to see how far μ_j involved with τ_j

Table 9.1: Static relative permittivity ε_{oij}, infinite frequency relative permittivity. $\varepsilon_{\infty ij}$, real part ε_{ij}' and imaginary part ε_{ij}'' of complex relative permittivity ε_{ij}^* of chloral, ethyltrichloro acetate, at 30°C,trifluoroethanol, trifluoroacetic acid at 25°C and octanoyl chloride at 35°C in different non polar solvents under 9.8 GHz electric field.

System with sl. no .& mol.wt	Weight fraction w_j	ε_{oij}	$\varepsilon_{\infty ij}$	Weight fraction w_j	ε_{ij}'	ε_{ij}''
(I) Chloral in benzene M_j=0.1475 Kg	0.0255	2.314	2.2350	0.0152	2.26	0.015
	0.0977	2.441	2.2293	0.0899	2.42	0.035
	0.1813	2.622	2.2216	0.1711	2.56	0.057
	0.2511	2.785	2.2147	0.1903	2.60	0.066
	0.3493	3.011	2.2067	0.2510	2.75	0.087
	0.4019	3.189	2.2020	0.3476	2.97	0.116
(II) Chloral in *n*-heptane M_j=0.1475 Kg	0.0224	1.925	1.9154	0.0224	1.93	0.017
	0.0807	2.048	1.9209	0.0807	2.01	0.029
	0.1416	2.140	1.9254	0.1416	2.09	0.036
	0.2003	2.240	1.9301	0.2003	2.19	0.050
	0.2683	2.390	1.9372	0.2683	2.32	0.055
	0.3324	2.516	1.9438	0.3324	2.47	0.080
(III)Ethyltrichloro-acetate in benzene M_j=0.1915 Kg	0.0207	2.368	2.2365	0.0207	2.32	0.023
	0.0498	2.475	2.2344	0.0498	2.38	0.046
	0.0802	2.596	2.2317	0.0802	2.44	0.079
	0.1193	2.753	2.2266	0.1193	2.52	0.115
	0.1764	2.996	2.2201	0.1764	2.64	0.194
	0.2444	3.295	2.2126	0.2444	2.82	0.226
(IV)Ethyltrichloro-acetate in *n*-hexane M_j=0.1915 Kg	0.0266	1.980	1.8837	0.0210	1.92	0.021
	0.0639	2.072	1.8878	0.0595	1.99	0.041
	0.0845	2.119	1.8892	0.0649	2.00	0.066
	0.1193	2.223	1.8933	0.1137	2.09	0.093
	0.1683	2.377	1.8988	0.1722	2.24	0.126
				0.2360	2.34	0.190
(V) Trifluoro-ethanol in benzene M_j=0.1000 Kg	0.0030	2.284	2.1994	0.0113	2.332	0.007
	0.0060	2.301	2.2132	0.0215	2.396	0.041
	0.0226	2.405	2.3061	0.0313	2.458	0.073
	0.0311	2.456	2.3537	0.0416	2.515	0.118
	0.0411	2.525	2.4109	0.0523	2.638	0.189
(VI) Trifluoroacetic acid in benzene M_j=0.1140 Kg	0.0066	2.327	2.2370			
	0.0130	2.368	2.2731	0.0130	2.315	0.035
	0.0271	2.411	2.3082	0.0271	2.350	0.056
	0.0391	2.449	2.3452	0.0391	2.377	0.069
	0.0515	2.484	2.3671	0.0515	2.398	0.084
	0.0630	2.519	2.3940	0.0630	2.420	0.100
(VII) Octanoyl chloride in benzene M_j=0.1625 Kg	0.0183	2.369	2.2218	0.0181	2.306	0.033
	0.0349	2.444	2.2176	0.0358	2.350	0.076
	0.0497	2.526	2.2142	0.0516	2.393	0.111
	0.0648	2.582	2.2110	0.0702	2.439	0.147
	0.0808	2.661	2.2080	0.0802	2.486	0.184

agree with μ_s and μ_{theo}. A systematic comparison of τ_j's with the reported τ's and the estimated τ_1 and τ_2 of the molecules by double relaxation method [9.9] enables one to conclude either a part or a whole molecule is rotating under GHz electric field. μ_{theo}'s were, however, obtained from available bond angles and bond moments of the substituent polar groups attached to the parent molecule [9.9-9.10]. Earlier investigations on different polar molecules [9.5] showed that a part of the molecule is rotating under *hf* electric field of nearly 3 cm wavelength. The purpose of the present paper is thus to observe how the apparently rigid aliphatic polar molecules behave under static or low frequency and 9.8 GHz electric fields.

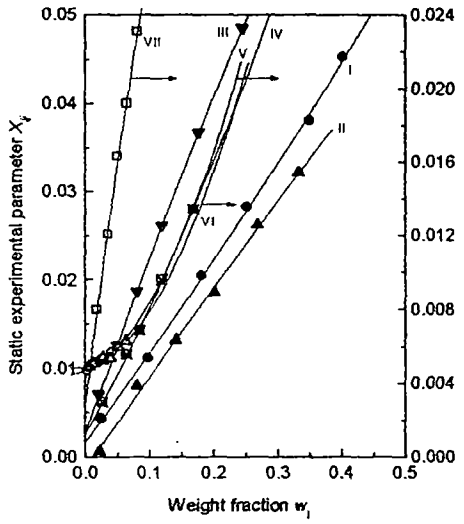

Figure 9.1: Variation of measured experimental parameter X_{ij} with weight fraction w_j of solutes,

I Chloral in benzene (–●–); II Chloral in *n*-heptane (–▲–); III Ethyltrichloroacetate in benzene (–▼–); IV Ethyltrichloroace-tate in *n*-hexane (–⊗–); V Trifluoroethanol in benzene (–O–); VI Trifluoroacetic acid in benzene (–Δ–) and VII Octanoyl chloride in benzene (–□–).

The static or low frequency μ_s's were measured from the linear coefficient of the variation of X_{ij}'s with w_j's of a polar solute. The variables X_{ij} is, however, related with ε_{oij} and $\varepsilon_{\infty ij}$ of the polar liquids. μ_s's are estimated from the measured data of Table 9.1 and placed in Table 9.3 in order to compare with the *hf* μ_j's involved with τ_j's measured from Eqs.(9.9) and (9.10) as derived later on. The concentration variation of X_{ij}'s are displayed in Fig.9.1 by Newton-Raphson's method with the experimental points placed upon them.

The percentage of errors in getting X_{ij}–w_j curves was computed from correlation coefficients '*r*' for all the systems. The errors introduced in a_1's are very low because *r*'s are very close to unity establishing the fact X_{ij}'s are correlated almost exactly with w_j's of Table 9.1. The μ_s's of Table 9.3 are found to be almost equal with *hf* μ_j's except systems V (–O–) and VI (–Δ–). μ_j's are estimated from the linear coefficient β's of the curves of *hf* conductivity σ_{ij}'s against w_j's of polar liquids at infinite dilution and the estimated τ_j's. τ_j's are, however, obtained from the linear slope of σ_{ij}''–σ_{ij}' curves of Fig.9.2 and the ratio of individual slopes of σ_{ij}'' and σ_{ij}' with w_j curves

at $w_j \rightarrow 0$ shown in Figs.9.3 and 9.4. τ_j's are placed in Table 9.2 and were used to calculate μ_j's of Table 9.3. μ_j's from both the methods are found to agree excellently for all the systems except ethyltrichloroacetate and octanoyl chloride in benzene.

Table 9.2: Slope of σ_{ij}''–σ_{ij}' curves, correlation coefficients r, percentage of error in regression technique, relaxation time τ_j using Eq.(9.9), ratio of slopes of σ_{ij}''–w_j and σ_{ij}'–w_j curves at $w_j \rightarrow 0$, percentage of error in σ_{ij}''–w_j and σ_{ij}'–w_j curves, corresponding τ_j using Eq.(9.10) and reported τ for chloral, ethyltrichloroacetate at 30°C, trifluoroethanol, trifluoroacetic acid at 25°C and octanoyl chloride at 35°C in different non-polar solvents under 9.8 GHz electric field.

System with sl.no	Slope of σ_{ij}''–σ_{ij} curve	Corrl .coef r	% of error	τ_j x10^{12} sec from Eq (9.9)	Ratio of slopes of σ_{ij}''–w_j& σ_{ij}'–w_j curves at $w_j \rightarrow 0$	% of error in regression technique σ_{ij}''–w_j curve	% of error in regression technique σ_{ij}'–w_j curve	τ_jx 10^{12} sec from Eq.(9.10)	Rept τx 10^{12} sec
(I)Chloral in benzene	6.8735	0.9987	0.07	2.36	6.5416	0.08	0.11	2.48	1.78*
(II) Chloral in *n*-heptane	8.9472	0.9881	0.65	1.82	8.8940	0.02	1.53	1.83	0.46*
(III) Ethyltrichloro acetate in benzene	2.2289	0.9820	0.98	7.29	1.3768	0.03	0.79	11.80	6.5**
(IV) Ethyltrichloro acetate in *n*-hexane	2.5845	0.9826	0.95	6.28	3.1959	0.27	0.95	5.08	5.7**
(V)Trifluoroethanol in benzene	1.6508	0.9982	0.11	9.84	3.2082	0.50	0.16	5.06	13.85+
(VI)Trifluoroacetic acid in benzene	1.6337	0.9973	0.16	9.94	2.1001	0.05	0.14	7.73	9.23+
(VII) Octanoyl chlo ride in benzene	1.2019	0.9989	0.07	3.51	0.8443	0.31	0.38	19.24	18.60++

*= Cole–Cole plot,.
**= Gopalakrishna's method,
+= Calculated by Gopalakrishna's method,
++= Higasi's method.

μ_j's thus obtained are compared with the theoretical dipole moment μ_{theo}'s derived from the available bond angles and bond moments of the substituent polar groups of the molecules [9.9-9.10] and presented in Table 9.3. In Fig.9.6 conformations of five dipolar molecules are displayed by taking into account of the reduced bond length by a factor μ_s / μ_{theo} due to inductive, mesomeric and electromeric effects of the substituent polar groups attached to the parent molecules.

9.2. Theoretical Formulation of X_{ij} to Estimate Static μ_s :

The low frequency or static dipole moment μ_s of a polar solute (j) in a non-polar solvent (i) at any temperature T K is given by [9.12]:

$$\frac{\varepsilon_{oij}-1}{\varepsilon_{oij}+2}-\frac{\varepsilon_{\infty ij}-1}{\varepsilon_{\infty ij}+2}=\frac{\varepsilon_{oi}-1}{\varepsilon_{oi}+2}-\frac{\varepsilon_{\infty i}-1}{\varepsilon_{\infty i}+2}+\frac{N\mu_s^2 c_j}{9\varepsilon_o k_B T} \qquad .....(9.1)$$

where ε_{oij} and $\varepsilon_{\infty ij}$ are the dimensionless low and infinite frequency relative permittivities of solution (ij) of Table 9.1. The molar concentration c_j can be expressed by weight fraction w_j of the polar solute:

$$c_j=\frac{\rho_{ij} w_j}{M_j}$$

k_B is the Boltzmann constant, N is the Avogadro's number and ε_o= permittivity of the free space= $8.854\text{x}10^{-12}$ Farad.metre^{-1}.

The weight W_i and volume V_i of a non-polar solvent is mixed with a polar solute of weight W_j and volume V_j to give the solution density ρ_{ij}, where,

$$\rho_{ij}=\frac{W_i+W_j}{V_i+V_j}=\frac{W_i+W_j}{\frac{W_i}{\rho_i}+\frac{W_j}{\rho_j}}=\frac{\rho_i\rho_j}{\frac{W_i\rho_j}{W_i+W_j}+\frac{W_j\rho_i}{W_i+W_j}}$$

$$=\frac{\rho_i\rho_j}{\rho_j w_i+\rho_i w_j}=\rho_i(1-\gamma w_j)^{-1} \qquad .....(9.2)$$

The weight fraction w_i and w_j of solvent and solute are:

$$w_i=\frac{W_i}{W_i+W_j} \text{ and } w_j=\frac{W_j}{W_i+W_j}$$

such that $w_i+w_j=1$ and $\gamma=(1-\rho_i/\rho_j)$ where ρ_i and ρ_j are densities of pure solvent and pure solute respectively in SI units.

Now Eq.(9.1) may be written as :

$$\frac{\varepsilon_{oij}-\varepsilon_{\infty ij}}{(\varepsilon_{oij}+2)(\varepsilon_{\infty ij}+2)}=\frac{\varepsilon_{oi}-\varepsilon_{\infty i}}{(\varepsilon_{oi}+2)(\varepsilon_{\infty i}+2)}+\frac{N\rho_i\mu_s^2}{27\varepsilon_o M_j k_B T}w_j(1-\gamma w_j)^{-1}$$

or,

$$X_{ij}=X_i+\frac{N\rho_i\mu_s^2}{27\varepsilon_o M_j k_B T}w_j+\frac{N\rho_i\mu_s^2}{27\varepsilon_o M_j k_B T}\gamma w_j^2+..... \qquad .....(9.3)$$

The above equation can be expressed as a best fitted polynomial equation of w_j like

$$X_{ij} = a_o + a_1 w_j + a_2 w_j^2 + \ldots\ldots \qquad \ldots\ldots(9.4)$$

Now equating the coefficients of first power of w_j of Eqs.(9.3) and (9.4) one gets ;

$$\mu_s = \left(\frac{27 \varepsilon_o M_j k_B T a_1}{N \rho_i} \right)^{1/2} \qquad \ldots\ldots(9.5)$$

where a_1 is the slope of X_{ij}–w_j curve of Fig.9.1. But μ_s from the coefficients of higher powers of w_j of Eqs.(9.3) and (9.4) are not reliable as they are involved with various effects of solvent, relative density, solute-solute association, internal field, macroscopic viscosity etc. μ_s from Eq.(9.5) along with a_1 are placed in Table 9.3 to compare with *hf* μ_j's as well as μ_1 and μ_2 from double relaxation method and μ_{theo} from the available bond angles and bond moments.

Table 9.3: Values of coefficients of $X_{ij} = a_0 + a_1 w_j + a_2 w_j^2$ and $\sigma_{ij} = \alpha + \beta w_j + \xi w_j^2$ curves, static and *hf* dipole moment μ_s, and μ_j , theoretical dipole moment μ_{theo}, reported dipole moment μ and estimated μ_1 and μ_2 of the flexible part and the whole molecule by double relaxation method for chloral, ethyltrichloroacetate at 30°C, trifluoroethanol, trifluoroacetic acid at 25°C and octanoyl chloride at 35°C in different non-polar solvents under 9.8 GHz electric field.

System with sl.no. & mol.wt	Coeff. of X_{ij}–w_j curve a_0, a_1, a_2	Coeff. of σ_{ij}–w_j curve α, β, ξ	μ_s X 10^{30} in C.m	μ_j^a X 10^{30} in C.m	μ_j^b X 10^{30} in C.m	μ_{theo} x10^{30} in C.m	Rept μ X 10^{30} in C.m	$\frac{\mu_s}{\mu_{theo}}$	Corrc μ_{theo} x10^{30} in C.m	μ_1 X 10^{30} in C.m	μ_2 X 10^{30} in C.m
(I) Chloral in benzene	0.0017	1.2206									
	0.0992	0.9559	5.28	5.27	5.27	10.02	4.87	0.53	5.31	5.27	19.32
M_j = 0.1475 Kg	0.0207	0.5611									
(II) Chloral in	-0.0013	1.0419									
n-heptane	0.1053	0.5311	6.17	4.85	4.85	10.02	6.00	0.62	6.21	4.83	9.07
M_j = 0.1475 Kg	-0.0144	1.1538									
(III) Ethyltrichloro-	0.0028	1.2468									
acetate in benzene	0.2049	0.9425	8.65	6.46	7.29	10.50	6.50	0.82	8.61	–	11.07
M_j = 0.1915 Kg	-0.0719	1.0703									
(IV) Ethyltrichloro	0.0027	1.0198									
acetate in *n*-hexane	0.1299	1.1260	7.96	8.71	8.52	10.50	8.67	0.76	7.97	8.13	14.53
M_j = 0.1915 Kg	0.1231	-0.0323									
(V) Trifluoroeth-	0.0047	1.2535									
anol in benzene	0.0144	1.3716	1.64	5.93	5.31	2.78	9.98	0.59	1.64	–	–
M_j = 0.1000 Kg	0.2276	41.238									
(VI) Trifluoroace-	0.0049	1.2430									
tic acid in benzene	0.0077	1.5621	1.28	6.77	6.40	8.47	5.58	0.15	1.27	–	8.77
M_j = 0.1140 Kg	0.2279	-5.3871									
(VII) Octanoyl	0.0028	1.2396									
chloride in benzene	0.2870	0.8981	9.54	6.99	8.33	11.62	9.14	0.82	9.55	–	7.02
M_j = 0.1625 Kg	-0.4601	6.9372									

μ_j^a = *hf* dipole moment by using τ_j of Eq.(9.9) μ_j^b = *hf* dipole moment by using τ_j of Eq.(9.10)

9.3. Formulation of *hf* Conductivity σ_{ij} to Estimate τ_j and *hf* μ_j:

The complex relative dielectric permittivity ε_{ij}^* under *hf* electric field is:

$$\varepsilon_{ij}^* = \varepsilon_{ij}' - j\varepsilon_{ij}''$$

where ε_{ij}' and ε_{ij}'' are the real and imaginary parts of ε_{ij}^*. The *hf* complex conductivity σ_{ij}^* of a polar-nonpolar liquid mixture for a given weight fraction w_j is [9.12]

$$\sigma_{ij}^* = \sigma_{ij}' + j\sigma_{ij}''$$

or,

$$\sigma_{ij}^* = \omega\varepsilon_o\varepsilon_{ij}'' + j\omega\varepsilon_o\varepsilon_{ij}' \qquad \text{.....(9.6)}$$

where $\omega\varepsilon_o\varepsilon_{ij}'' = \sigma_{ij}'$ and $\omega\varepsilon_o\varepsilon_{ij}' = \sigma_{ij}''$ are the real and imaginary parts of complex conductivity, ε_o= permittivity of free space = 8.854×10^{-12} F.m^{-1} and j is a complex number = $\sqrt{-1}$.

The total *hf* conductivity σ_{ij} is given by:

$$\sigma_{ij} = \omega\varepsilon_o(\varepsilon_{ij}''^2 + \varepsilon_{ij}'^2)^{1/2} \qquad \text{.....(9.7)}$$

Again, σ_{ij}'' is related to σ_{ij}' by

$$\sigma_{ij}'' = \sigma_{\infty ij} + \frac{1}{\omega\tau_j}\sigma_{ij}' \qquad \text{.....(9.8)}$$

$\sigma_{\infty ij}$ is the constant conductivity at infinite dilution of w_j=0 and τ_j is the relaxation time of a dipolar liquid. Eq.(9.8) on differentiation w.r.to σ_{ij}' yields

$$\frac{d\sigma_{ij}''}{d\sigma_{ij}'} = \frac{1}{\omega\tau_j} \qquad \text{.....(9.9)}$$

which provides a convenient method to obtain τ_j of a polar molecule. It is, however, better to use the ratio of the individual slopes of variation of σ_{ij}'' and σ_{ij}' with w_j in order to avoid the polar-polar interaction at $w_j \to 0$ in a given solvent to get τ_j from:

$$\frac{\left(d\sigma_{ij}''/dw_j\right)_{w_j\to 0}}{\left(d\sigma_{ij}'/dw_j\right)_{w_j\to 0}} = \frac{1}{\omega\tau_j} \qquad \text{.....(9.10)}$$

where $\omega = 2\pi f$ and f is the frequency of the applied *hf* electric field.

In *hf* region of GHz range, it is generally observed $\sigma_{ij}'' \approx \sigma_{ij}$ as evident from Figs.9.3 and 9.5 hence Eq.(9.8) becomes

$$\sigma_{ij} = \sigma_{\infty ij} + \frac{1}{\omega\tau_j}\sigma_{ij}'$$

$$\beta = \frac{1}{\omega\tau_j}\left(\frac{d\sigma'_{ij}}{dw_j}\right)_{w_j\to 0} \qquad \text{.....(9.11)}$$

Here $\beta = \left(d\sigma_{ij}/dw_j\right)_{w_j\to 0}$ is the slope of σ_{ij}–w_j curves of Fig.9.5 at $w_j\to 0$.

The real part σ_{ij}' of a polar-nonpolar liquid mixture of w_j at T K is [9.12] given by:

$$\sigma'_{ij} = \frac{N\rho_{ij}\mu_j^2}{27M_j k_B T}\left(\frac{\omega^2\tau}{1+\omega^2\tau^2}\right)\left(\varepsilon_{oij}+2\right)\left(\varepsilon_{\infty ij}+2\right)w_j$$

$$\left(\frac{d\sigma'_{ij}}{dw_j}\right)_{w_j\to 0} = \frac{N\rho_i\mu_j^2}{3M_j k_B T}\left(\frac{\varepsilon_i+2}{3}\right)^2\left(\frac{\omega^2\tau}{1+\omega^2\tau^2}\right) \qquad \text{.....(9.12)}$$

Now, comparing Eqs.(9.11) and (9.12) one gets the $hf\ \mu_j$ from :

$$\mu_j = \left[\frac{27M_j k_B T\beta}{N\rho_i(\varepsilon_i+2)^2\omega b}\right]^{1/2} \qquad \text{.....(9.13)}$$

wherer,

$$b = 1/(1+\omega^2\tau_j^2) \qquad \text{.....(9.14)}$$

is a dimensionless parameter involved with τ_j's obtained from Eqs.(9.9) and (9.10). The other symbols used in Eq.(9.13) are N= Avogadro's number, ρ_i = density of the solvent, ε_i = relative permittivity of the solvent, M_j= molecular weight of the solute and k_B= Boltzmann constant. All are expressed in SI units. All the computed $hf\ \mu_j$'s in terms of β's and b's are presented in Table 9.3. They are compared with μ_1 and μ_2 of the flexible part and the whole molecule by the double relaxation method [9.9] as entered in Table 9.3. The computed τ_j's are, however, placed in Table 9.2 to compare with those by other methods and freshly calculated Gopalakrishna's method for the last three systems.

9.4. Results and Discussion :

The dipole moments μ_s's of the polar molecule under static or low frequency electric field are estimated from the slope a_1 of the X_{ij}–w_j curves of Fig.9.1. X_{ij} is related to static and infinite frequency relative permittivities ε_{oij} and $\varepsilon_{\infty ij}$ of Eq.(9.1) at different w_j 's of polar solutes presented in Table 9.1. All the curves of X_{ij} against w_j were, however, drawn by best-fitted regression analysis made on available experimental data extracted from Table 9.1 in order to plot Fig.9.1. Each system consists of a polar solute in different non-polar solvents usually shows almost same slopes as seen in Fig.9.1. This signifies the almost same polarity of the molecules under investigation [9.13].

Polarisations are found to be slightly larger for ethyltrichloroacetate in benzene, *n*-hexane and octanoyl chloride in benzene in comparison to other molecules. The increase in polarisation is due to the increase in dipole moment which means that dimerisation takes place in such a manner that in the dimeric molecule, the dipoles are inclined at an angle less than 90^0 so that the dipole moment is more than that of the monomer. The correlation coefficients r's in getting the coefficients of X_{ij}–w_j curves of Fig.9.1 were very close to unity *i.e*, 0.9993, 0.9978, 0.9999, 0.9998, 0.9693, 0.9574 and 0.9980 for seven systems of tables and figures respectively and hence percentage of errors in terms of r's were very small.

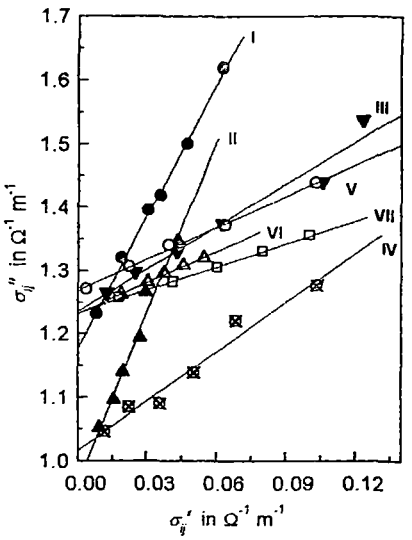

Figure 9.2: Linear plot of σ_{ij}'' against σ_{ij}' for different weight fraction w_j,
I. Chloral in benzene (–●–); II. Chloral in *n*-heptane (–▲–); III. Ethyltrichloroacetate in benzene (–▼–); IV. Ethyltrichloroacetate in *n*-hexane (–⊗–); V. Trifluoroethanol in benzene (–○–); VI. Trifluoroacetic acid in benzene (–Δ–) and VII. Octanoyl chloride in benzene (–□–).

The relaxation time τ_j of the molecules are estimated by using the linear slope of σ_{ij}''–σ_{ij}' curve of Murthy *et al* [9.14] and the ratio of individual slopes of σ_{ij}''–w_j and σ_{ij}'–w_j at $w_j \rightarrow 0$. It is evident from Table 9.2 that τ_j's agree well in both the methods except ethyltrichloroacetate (III), trifluoroethanol (V) and octanoyl chloride (VII) all in benzene. This behaviour is explained on the basis of solute-solute (dimer) molecular association in the higher concentration region which turn into solute-solvent (monomer) association due to rupture of dimer. In such case it is better to use the ratio of individual slopes of σ_{ij}'' and σ_{ij}' in $\Omega^{-1}m^{-1}$ against w_j at infinite dilution as seen in Figs.9.3 and 9.4 where polar-polar interaction is almost avoided completely to compute τ_j. The curves of σ_{ij}''–σ_{ij}' in Fig.9.2 are not perfectly linear with the experimental data according to Eq.(9.9) for the systems III (–▼–), IV (–⊗–) and V (–○–). In such cases polar-polar interaction in the higher concentration region or solute-solvent association in the lower concentration region may be the cause for such non-linear behaviour. The almost parallel nature of the curves I and II ; III and IV in Fig.9.3 of σ_{ij}''–w_j curves indicates the same polarity of the molecules of chloral and ethyltrichloroacetate in different solvents. The higher magnitude of σ_{ij}'' in $\Omega^{-1}m^{-1}$ in benzene for each solute of Fig.9.3 may reveal the solute-solute (dimer) interaction of the polar molecules. Curve VI (trifluoroacetic acid in benzene) of Fig.9.3 are found to increase

gradually to show maximum at w_j =0.1401. This type of behaviour may be due to transition of phase [9.15] occurred after a certain concentration of the solute. Like systems II and IV in *n*-heptane and *n*-hexane, the other curves of Fig.9.3 for solvent benzene meet at a point on the ordinate axis 1.2206 $\leq \sigma_{ij}'' \leq$ 1.2526 at w_j=0 exhibiting the probable solvation effect of polar solute in same non-polar solvent. It is evident from Fig.9.3 that all the curves are almost same as total *hf* conductivity σ_{ij} in $\Omega^{-1}m^{-1}$ plotted against w_j in Fig.9.5. This indicates the validity of the approximation $\sigma_{ij}'' \approx \sigma_{ij}$ in Eq.(9.11). All the curves of σ_{ij}' in Fig.9.4 increase gradually with w_j and become closer to yield $\sigma_{ij}' \approx 0$ at w_j=0. Such nature of curves are explained on the basis of the fact that absorbtion of *hf* electric energy increases with concentration. The magnitude of absorbtion is maximum for trifluoroethanol in benzene (V) and minimum for chloral in *n*-heptane (II) although concentration of polar solute of the latter system is higher than the former.

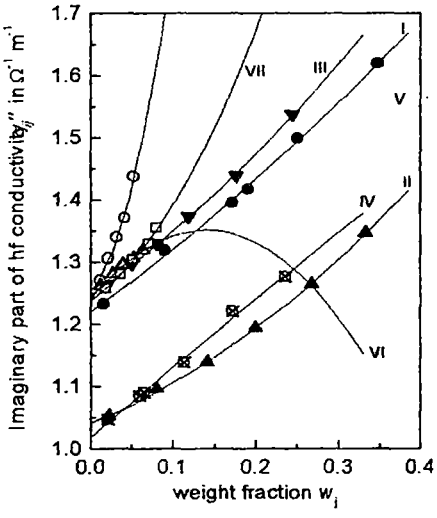

Figure 9.3: Variation of imaginary part of *hf* complex conductivity σ_{ij}'' with weight fraction w_j

I. Chloral in benzene (–●–); II. Chloral in *n*-heptane (–▲–); III. Ethyltrichloroacetate in benzene (–▼–); IV. Ethyltrichloroacetate in *n*-hexane (–⊗–); V. Trifluoroethanol in benzene (–O–); VI. Trifluoroacetic acid in benzene (–Δ–) and VII. Octanoyl chloride in benzene (–□–).

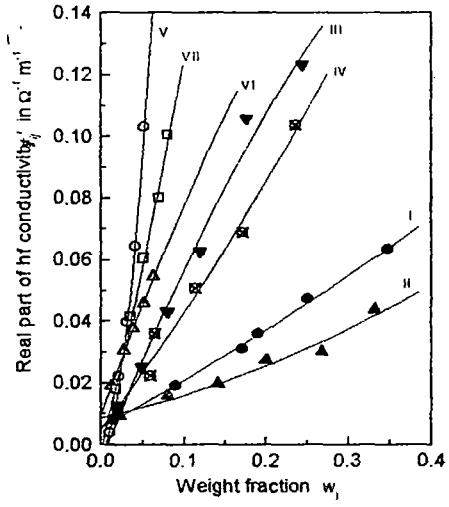

Figure 9.4: Variation of real part of *hf* complex conductivity σ_{ij}' with weight fraction w_j.

I. Chloral in benzene (–●–); II. Chloral in *n*-heptane (–▲–); III. Ethyltrichloroacetate in benzene (–▼–); IV. Ethyltrichloroacetate in *n*-hexane (–⊗–); V. Trifluoroethanol in benzene (–O–); VI. Trifluoroacetic acid in benzene (–Δ–) and VII. Octanoyl chloride in benzene (–□–).

The high frequency dipole moments μ_j of the polar liquids are estimated in terms of slope β of σ_{ij}–w_j curve of Fig.9.5 and dimensionless parameter *b*'s in order to show them in Table 9.3. They are compared with μ_s, μ_1, μ_2 and reported μ's respectively. All the curves of total *hf* conductivity σ_{ij} in $\Omega^{-1}m^{-1}$ against w_j of Fig.9.5 are parabolic as evident from the coefficients α, β and ξ of Table 9.3. This indicates that conductivity of the mixture with the absorbtion of *hf* electric energy increases with w_j's of solute except system VI. These curve when extrapolated beyond the experimental data

exhibits maximum σ_{ij} at $w_j = 0.1401$ and then decreases gradually thereafter like σ_{ij}''–w_j curves of Fig.9.3 probably due to transition of phase [9.15] occurred at that concentration. This type of behaviour invariably demands experimental measurement beyond this concentration of polar liquid already taken up.

The *hf* μ_j's are found to agree well with the static μ_s for chloral, ethyltrichloroacetate and octanoyl chloride in benzene, *n*-heptane and *n*-hexane (system I, II, III, IV, and VII). It reveals the fact that dimerisation takes place both in static and high frequency electric field probably the available data of relative permittivities are in higher concentration regions. μ_j's of trifluoroethanol and trifluoroacetic acid are higher than μ_s indicating the strong solute-solvent association due to hydrogen bonding. μ_j's when compared with μ_1 and μ_2 by double relaxation method indicate that chloral in benzene, *n*-heptane and ethyltrichloroacetate in *n*-hexane show double relaxation phenomena in X-band electric field. This is due to rotations of the whole molecules as well as the flexible parts attached to the parent molecules. The other systems show the mono relaxation behaviour due to their solvation effect with benzene.

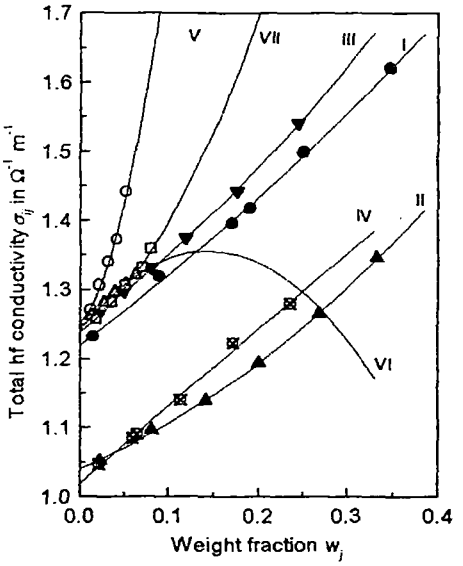

Figure 9.5: Variation of total *hf* conductivity σ_{ij} with weight fraction w_j

I Chloral in benzene (–●–); II. Chloral in *n*-heptane (–▲–); III. Ethyltrichloroacetate in benzene (–▼–); IV. Ethyltrichloroacetate in *n*-hexane (–⊗–); V. Trifluoroethanol in benzene (–○–); VI. Trifluoroacetic acid in benzene (–Δ–) and VII. Octanoyl chloride in benzene (–□–).

Assuming the planar structure of the molecules the theoretical dipole moments μ_{theo}'s for the polar molecules were estimated from the available bond angles and bond moments of C←Cl, C←C, C→F, C⇐O, C→OH and C→OCH_3 of 5.00, 0.30, 4.67, 8.00, 4.67 and 4.40 times of 10^{-30} Coulomb.metre (C.m) making angles 62^0 and 57^0 with the bond axis by C→OH and C→OCH_3 groups only and were shown elsewhere [9.9-9.10]. μ_{theo}'s thus obtained are placed in Table 9.3. A little disagreement among the estimated μ_s and μ_j with μ_{theo} occurs due to inductive, mesomeric and electromeric effects of the substituent polar groups attached to the parent molecules under static or *hf* electric field. The so called mesomeric moments have significant values. This is caused by the permament polarisation of different substituent groups acting as pusher or puller of electron towards

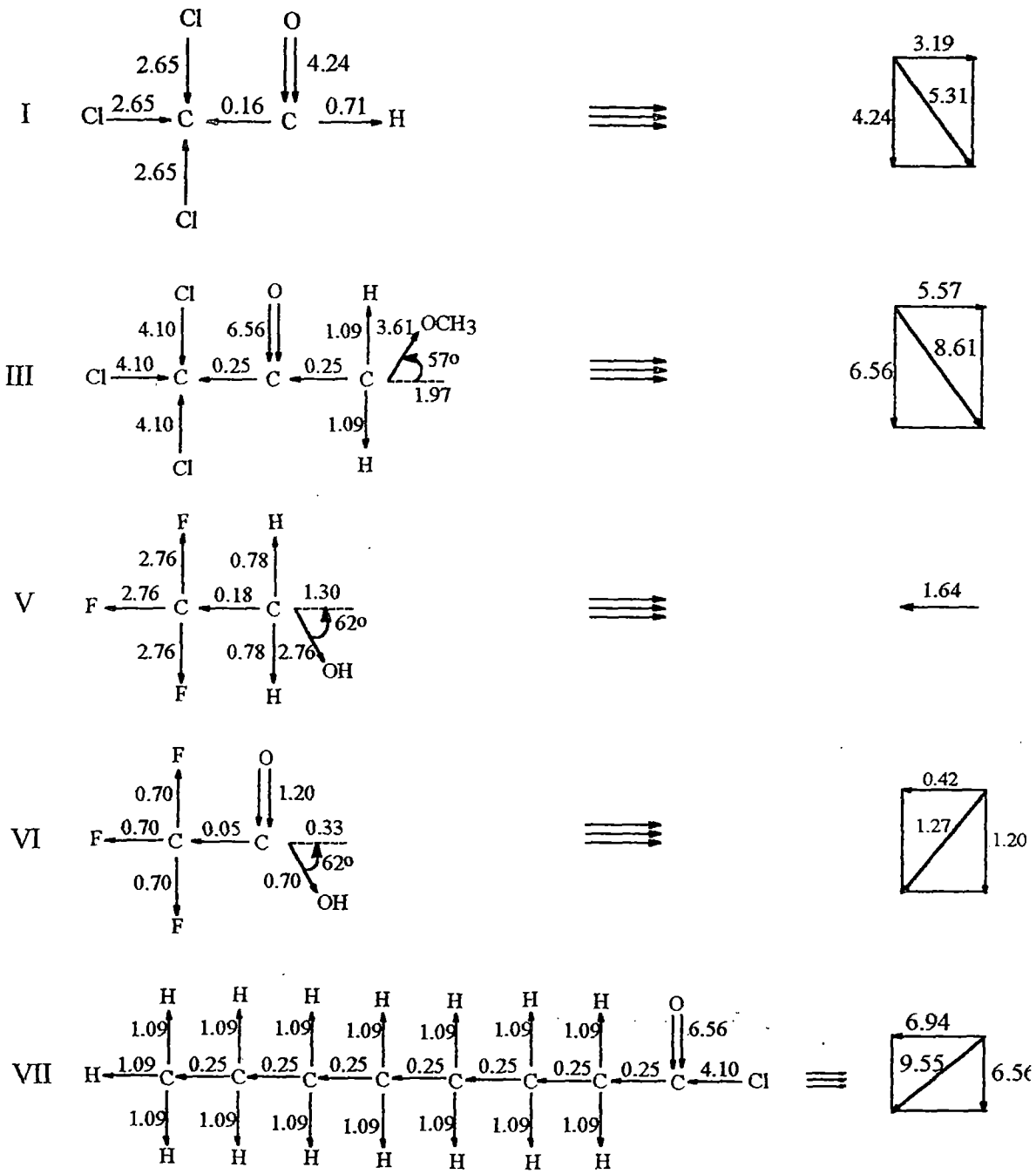

Figure 9.6: Conformational structures of the molecules by taking into account the reduced bond moments in multiple of 10^{-30} Coulomb metre.

I. Chloral, III. Ethyltrichloroacetate, V. Trifluoroethanol, VI. Trifluoroacetic acid, VII. Octanoyl chloride

or away from C-atoms of the compounds. The larger values of μ_{theo}'s from the available bond angles and bond moments in comparison to μ_s indicate that the bond length of the substituent polar groups of the dipolar molecules are reduced by a factor μ_s/μ_{theo}. The reduction in bond moments

evidently occurs in all polar liquids by a factor μ_s/μ_{theo} lying in the range 0.5 to 0.8 except trifluoroacetic acid (0.15) to conform to the exact μ_s. The structural conformations of five compounds with reduced bond lengths, in agreement with μ_j or μ_s are sketched in Fig.9.6.

9.5. Conclusion :

A convenient and useful method is thus suggested to calculate the relaxation time τ_j and hence *hf* dipole moment μ_j under the most effective dispersive region of 10 GHz electric field along with the static μ_s in SI units of some non-spherical rigid aliphatic polar molecules in non-polar solvents. The existing method by using the slope of *hf* σ_{ij}''–σ_{ij}' curves of Murthy *et al* (1998) to obtain τ_j when compared with those from the ratio of the slopes of the individual variations of σ_{ij}''–w_j and σ_{ij}'– w_j at $w_j \to 0$ reveals the fact that both the methods yield almost the same τ_j's both in higher and lower concentration of dipolar molecules. The latter method to get τ_j is a significant improvement over the former one as it eliminates the polar-polar interaction almost completely in a given solvent. The slope β's of *hf* σ_{ij}–w_j curves could, however, be used to calculate *hf* μ_j's in terms of τ_j's by the latter method. The comparison of μ_j and μ_s with μ_1 and μ_2 of the flexible part and the whole molecules by double relaxation method and μ_{theo} from available bond angles and bond moments of the substituent polar groups seems to be interesting phenomenon to offer deep insight into the dielectric relaxation mechanism. The μ_j's and μ_s are almost equal in some cases revealing the fact that μ_s are little affected by frequency of the electric field in higher concentration region while lower μ_s's than μ_j's in the lower concentration region support monomer and dimer formation in the static and *hf* electric field respectively. Moreover, the X_{ij}–w_j curves can be used to taste the accuracies of the measurement of all the relative permittivities. The X_{ij}'s are involves with the low and infinitely *hf* ε_{oij} and $\varepsilon_{\infty ij}$ permittivities of a given polar-nonpolar liquid mixtures. The computation of τ_j, μ_j and μ_s from σ_{ij} and X_{ij} measurement of a polar unit in a given solvent appears to be more simple, straightforward and unique to locate their correlation coefficient r's and percentage of errors involved. In this method it is claimed that τ_j, μ_j and μ_s are claimed to be accurate within 10% and 5% respectively. Both μ_j and μ_s are found to agree with μ_1 only to show that a part of the molecule is rotating under GHz electric field. μ_s/μ_{theo}'s are almost constant for all the molecule under study revealing the material property of the systems. The reduction in bond moments of the substituent polar groups by the factor μ_s/μ_{theo} exhibits the presence of mesomeric, inductive and electromeric moments in them under static or low and *hf* electric fields.

References :

[9.1] A Sharma and D R Sharma , *J. Phys. Soc. (Jpn)*, **61** 1049 (1992).

[9.2] A K Sharma, D R Sharma, K C Sharma and D S Gill, *Zeitschrift fur Physikalische Chemie Neue Folge Bd* **141S** 15 (1984).

[9.3] F Alvarez, A Alegria and J Colmenero, *J. Chem. Phys.* **103(2)** 798 (1995)

[9.4] A K Jonscher, *Inst. Phys. Conf. (Canterbury)*, Invited papers edited by CHL Goodman, (1980)

[9.5] R C Basak, S K Sit, N Nandi and S Acharyya, *Indian J. Phys.* **70B** 37 (1996)

[9.6] H D Purohit and H S Sharma, *Indian J. Pure & Appl. Phys.* **11** 664 (1973)

[9.7] H D Purohit, H S Sharma and A D Vyas, *Indian J. Pure & Appl. Phys.* **12** 273 (1974)

[9.8] S K Srivastava and S L Srivastava, *Indian J. Pure & Appl. Phys.* **13** 179 (1975)

[9.9] K Dutta, R C Basak, S K Sit and S Acharyya, *J. Molecular Liquids* **88** 241 (2000)

[9.10] K Dutta, S K Sit and S Acharyya, *Pramana: J. Physics* **57** 775 (2001)

[9.11] S K Sit and S Acharyya, *Indian J. Pure & Appl. Phys.* **34** 255 (1996)

[9.12] R C Basak, A Karmakar, S K Sit and S Acharyya, *Indian J. Pure & Appl. Phys.* **37** 224 (1999)

[9.13] A K Chatterjee,U Saha, N Nandi, R C Basak and S Acharyya, *Indian J. Phys.* **66B** 291 (1992)

[9.14] M B R Murthy, R L Patil and D K Deshpande, *Indian J. Phys.* **63B** 491 (1989)

[9.15] K Dutta, S K Sit and S Acharyya, *J. Molecular Liquids*, **92** 263 (2001)

CHAPTER 10

MATERIAL PROPERTY OF DIPOLAR LIQUID IN NONPOLAR SOLVENT THROUGH RELAXATION PHENOMENA UNDER HIGH FREQUENCY ELECTRIC FIELD – A NOVEL IDEA

10.1. Introduction :

Relaxation phenomena is an important tool to measure relaxation time τ_j, dipole moment μ_j, shape, size as well as molecular interactions of a dipolar liquid molecule in a non-polar solvent under high frequency (*hf*) electric field [10.1-10.2]. There are various established techniques [10.3-10.4] like thermally stimulated depolarisation current (TSDC) and isothermal frequency domain AC spectroscopy by which one can estimate μ_j and τ_j of a polar liquid molecule. Nevertheless, one can use Debye and Smyth model to determine τ_j and μ_j of a dipolar liquid molecule because of its simplicity and straightforwardness. Crossley *et al* [10.5] and Glasser *et al* [10.6] proposed that the normal and isomeric octyl alcohols were expected to show triple relaxation times under *hf* electric field of GHz range when they are diluted with non-polar solvent *n*-heptane. Alcohols show double relaxation times [10.7-10.8] τ_2 and τ_1 due to end over end rotation as well as rotation of the flexible part of the molecule at all frequencies of 3.00, 9.25 and 24.33 GHz electric field.

We, therefore, thought to study these alcohols again because of its diverse nature in different environments. The alcohols are hydrogen bonded polymer type molecules. Some of the octyl alcohols are isomers. They usually showed α, β and γ relaxation in *hf* electric field. It was observed [10.9] that μ_j's of alcohols vary slightly when measurements are done in terms of either relative permittivities ε_{ij}'s or conductivity σ_{ij}'s in SI units. The other parameter τ_j, however, remains same in both cases. Nowadays, it is the practice to study the relaxation phenomena in terms of orientation susceptibilities χ_{ij}'s [10.10-10.11] rather than ε_{ij}'s or σ_{ij}'s. ε_{ij} includes all types of polarisations whereas σ_{ij} is concerned with the bound molecular charges. χ_{ij}'s, on the other hand, are related to orientation polarisations of the molecule. The purpose of the present paper is to study the existence of double relaxation times of alcohols between two limiting τ's in terms of *hf* χ_{ij}'s. The chemical systems under consideration are identical and they are in same environment. If any system shows double relaxation times at one frequency it will show the same double relaxation times τ_1 and τ_2 at all the frequencies because the double relaxation phenomenon is the material property of the system. Saha *et al* and Sit *et al* [10.12-10.13] proposed a very simple and easy technique to measure the double relaxation times of a polar-nonpolar liquid mixture at a given experimental temperature under a single frequency of the electric field. The estimated τ's are different in different frequencies of the electric field. Moreover, τ_1 and τ_2 from the single frequency measurement technique is not so reliable [10.14-10.15].

In this context, we propose a graphical technique to estimate τ_1 and τ_2 of some alcohols (j) in a non-polar solvent (i) in terms of real χ_{ij}' and imaginary χ_{ij}'' parts of *hf* complex dielectric orientation susceptibilities χ_{ij}^* under 3.00, 9.25 and 24.33 GHz electric field and low frequency

Table 10.1: Concentration variation of the real part χ_{ij}' and imaginary part χ_{ij}'' of dimensionless complex dielectric orientation susceptibility χ_{ij}^* and the static dielectric orientation susceptibility χ_{oij} which is real of some normal and isomeric octyl alcohols in *n*-heptane under 3.00, 9.25 and 24.33 GHz electric fields.

Frequency f in GHz	Weight fraction w_j	χ_{ij}'	χ_{ij}''	χ_{oij}	Weight fraction w_j	χ_{ij}'	χ_{ij}''	χ_{oij}
		I. 1-Butanol				II. 1-Hexanol		
3.00	0.0451	0.049	0.0114	0.055	0.0459	0.033	0.0065	0.044
	0.0697	0.072	0.0188	0.093	0.0703	0.051	0.0117	0.063
	0.1163	0.123	0.0460	0.197	0.1028	0.070	0.0214	0.094
	0.1652	0.180	0.0782	0.381	0.1688	0.123	0.0446	0.207
	0.2072	0.224	0.1119	0.601	0.2335	0.184	0.0755	0.358
					0.2901	0.232	0.1097	0.562
9.25	0.0451	0.040	0.0121	0.055	0.0459	0.026	0.0083	0.044
	0.0697	0.057	0.0220	0.093	0.0703	0.038	0.0121	0.063
	0.1163	0.088	0.0416	0.197	0.1028	0.045	0.0226	0.094
	0.1652	0.121	0.0637	0.381	0.1688	0.085	0.0454	0.207
	0.2072	0.152	0.0956	0.601	0.2335	0.126	0.0688	0.358
					0.2901	0.161	0.1000	0.562
24.33	0.0451	0.036	0.0147	0.055	0.0459	0.024	0.0131	0.044
	0.0697	0.053	0.0236	0.093	0.0703	0.032	0.0190	0.063
	0.1163	0.082	0.0425	0.197	0.1028	0.031	0.0296	0.094
	0.1652	0.105	0.0644	0.381	0.1688	0.048	0.0425	0.207
	0.2072	0.124	0.0818	0.601	0.2335	0.086	0.0569	0.358
					0.2901	0.116	0.0748	0.562
		III. 1-Heptanol				IV. 1-Decanol		
3.00	0.0735	0.053	0.0111	0.056	0.0572	0.032	0.0051	0.036
	0.1175	0.086	0.0216	0.109	0.1351	0.067	0.0194	0.086
	0.1909	0.128	0.0456	0.236	0.2140	0.098	0.0371	0.157
	0.2465	0.173	0.0651	0.313	0.2640	0.121	0.0496	0.212
	0.2970	0.217	0.0864	0.456	0.3353	0.156	0.0690	0.316
9.25	0.0735	0.040	0.0129	0.056	0.0572	0.028	0.0090	0.036
	0.1175	0.060	0.0232	0.109	0.1351	0.047	0.0228	0.086
	0.1909	0.090	0.0438	0.236	0.2140	0.065	0.0386	0.157
	0.2465	0.112	0.0609	0.313	0.2640	0.069	0.0484	0.212
	0.2970	0.149	0.0774	0.456	0.3353	0.093	0.0656	0.316
24.33	0.0735	0.030	0.0182	0.056	0.0572	0.025	0.0120	0.036
	0.1175	0.050	0.0265	0.109	0.1351	0.039	0.0273	0.086
	0.1909	0.087	0.0482	0.236	0.2140	0.046	0.0400	0.157
	0.2465	0.095	0.0567	0.313	0.2640	0.056	0.0513	0.212
	0.2970	0.118	0.0694	0.456	0.3353	0.067	0.0637	0.316
		V. 2-methyl 3-heptanol				VI. 3-methyl 3-heptanol		
3.00	0.0437	0.040	0.0040	0.041	0.0450	0.040	0.0043	0.040
	0.1299	0.086	0.0137	0.093	0.1334	0.099	0.0131	0.103
	0.2522	0.143	0.0309	0.165	0.2538	0.162	0.0272	0.176
	0.4081	0.215	0.0583	0.276	0.4085	0.242	0.0489	0.277
9.25	0.0437	0.037	0.0088	0.041	0.0450	0.034	0.0103	0.040
	0.1299	0.078	0.0244	0.093	0.1334	0.079	0.0263	0.103
	0.2522	0.108	0.0412	0.165	0.2538	0.126	0.0458	0.176
	0.4081	0.164	0.0710	0.276	0.4085	0.192	0.0766	0.277
24.33	0.0437	0.030	0.0156	0.041	0.0450	0.031	0.0187	0.040
	0.1299	0.056	0.0362	0.093	0.1334	0.061	0.0394	0.103
	0.2522	0.088	0.0565	0.165	0.2538	0.099	0.0674	0.176
	0.4081	0.115	0.0809	0.276	0.4085	0.131	0.0928	0.277

Frequency f in GHz	Weight fraction w_j	χ_{ij}'	χ_{ij}''	χ_{oij}	Weight fraction w_j	χ_{ij}'	χ_{ij}''	χ_{oij}
	VII. 4-methyl 3-heptanol				VIII. 5-methyl 3-heptanol			
3.00	0.0466	0.039	0.0046	0.040	0.1228	0.084	0.0143	0.092
	0.1326	0.090	0.0147	0.096	0.2489	0.134	0.0337	0.164
	0.2590	0.156	0.0338	0.174	0.3898	0.202	0.0554	0.275
	0.4124	0.224	0.0572	0.287				
9.25	0.0466	0.034	0.0091	0.040	0.1228	0.068	0.0225	0.092
	0.1326	0.076	0.0262	0.096	0.2489	0.095	0.0441	0.164
	0.2590	0.112	0.0472	0.174	0.3898	0.143	0.0706	0.275
	0.4124	0.168	0.0766	0.287				
24.33	0.0466	0.028	0.0146	0.040	0.1228	0.051	0.0297	0.092
	0.1326	0.055	0.0376	0.096	0.2489	0.071	0.0511	0.164
	0.2590	0.093	0.0616	0.174	0.3898	0.107	0.0675	0.275
	0.4124	0.115	0.0849	0.287				
	IX. 2-octanol				X. 4-octanol			
3.00	0.1236	0.078	0.0156	0.065	0.1201	0.081	0.0129	0.092
	0.2479	0.137	0.0419	0.199	0.2445	0.120	0.0302	0.151
	0.3844	0.207	0.0791	0.374	0.3838	0.181	0.0549	0.251
9.25	0.1236	0.061	0.0227	0.065	0.1201	0.063	0.0198	0.092
	0.2479	0.093	0.0467	0.199	0.2445	0.087	0.0397	0.151
	0.3844	0.133	0.0786	0.374	0.3838	0.128	0.0616	0.251
24.33	0.1236	0.047	0.0285	0.065	0.1201	0.052	0.0266	0.092
	0.2479	0.072	0.0513	0.199	0.2445	0.070	0.0449	0.151
	0.3844	0.105	0.0680	0.374	0.3838	0.109	0.0659	0.251

susceptibility χ_{oij} which is real. The data set for alcohols and octanols are presented in Table 10.1. Several values of $\ln\omega_1$ and $\ln\omega_2$ ($\omega_1>\omega_2$) are chosen for same $f(\omega_k)$ plotted against $\ln\omega_k$ in Fig.10.1 at constant ω. τ_1 and τ_2 are estimated from the intersection points of $\ln\omega_1$ vs $\ln\omega_2$ curve of Fig.10.2. They are placed in Table 10.2. τ_1 and τ_2 are also estimated from the linear plot of $(\chi_{oij}-\chi_{ij}')/\chi_{ij}'$ against χ_{ij}''/χ_{ij} at different w_j's as shown in Fig.10.3 and are presented in Table 10.2. μ_1 and μ_2 are calculated in terms of slope β of χ_{ij}'-w_j curve (Fig.10.4). All the μ's along with theoretical μ_{theo}'s from Fig.10.5 are placed in Table 10.3 for comparison.

10.2. Theoretical Formulations for τ_1 and τ_2 :

Debye equation for a polar-nonpolar liquid mixture in terms of the complex *hf* χ_{ij}^* for a distribution of τ is :

$$\frac{\chi_{ij}^*}{\chi_{oij}} = \int_0^\infty \frac{f(\tau)d\tau}{(1+j\omega\tau)} \qquad \ldots\ldots (10.1)$$

where $f(\tau)$ is the Fröhlich distribution function for the relaxation time such that:

$$f(\tau) = \frac{1}{A\tau} \qquad \tau_1 < \tau < \tau_2$$
$$= 0 \qquad \tau_1 > \tau; \tau_2 < \tau \qquad \text{.....(10.2)}$$

and A= Fröhlich parameter = $\ln\frac{\tau_2}{\tau_1}$

Table 10.2: Intercepts of χ_{ij}''/χ_{ij}' against w_j curve at $w_j \to 0$, values of $\ln\omega_2$ and $\ln\omega_1$ from Fig.10.2 and their average τ_2 and τ_1, τ_2 and τ_1 from single frequency measurement of Eq.(10.8) under 3.00, 9.25 and 24.33 GHz electric fields of some normal and isomeric octyl alcohols in *n*-heptane at 25°C.

System with sl. no		Frequency f in GHz	Intercept of χ_{ij}''/χ_{ij}'–w_j at $w_j \to 0$		Values of $\ln\omega_2$ and $\ln\omega_1$ from the Fig.10.2		Average τ_2 and τ_1 in psec		τ_2 and τ_1 from single frequency measurement		Average τ_2 and τ_1 in psec	
I. 1-Butanol	a)	3.00	0.1262	ab)	23.5015	30.8189	48.41	0.08	211.41	9.10	122.63	4.96
	b)	9.25	0.2120	bc)	24.2051	29.8712			101.87	3.73		
	c)	24.33	0.3231	ca)	23.6737	30.1101			54.60	2.04		
II. 1-Hexanol	a)	3.00	0.1246	ab)	23.2412	31.8059	57.03	0.04	204.26	9.17	110.44	5.01
	b)	9.25	0.1933	bc)	24.1343	30.4314			85.24	3.76		
	c)	24.33	0.2928	ca)	23.5801	30.6780			41.81	2.10		
III. 1-Heptanol	a)	3.00	0.0711	ab)	23.8767	33.6138	18.80	0.91	208.81	9.20	113.91	4.98
	b)	9.25	0.1306	bc)	26.4479	27.0234			83.03	3.30		
	c)	24.33	0.4503	ca)	25.2871	27.7518			49.89	2.43		
IV. 1-Decanol	a)	3.00	0.0438	ab)	25.5281	27.9946	13.12	0.29	135.66	6.89	83.68	5.27
	b)	9.25	0.1620	bc)	24.5801	30.5149			83.14	5.61		
	c)	24.33	0.2631	ca)	25.3244	29.7019			32.25	3.30		
V. 2-methyl 3-heptanol	a)	3.00	0.0700	ab)	24.9650	28.6944	11.19	0.90	73.31	5.41	50.96	4.3
	b)	9.25	0.1974	bc)	25.6712	27.3056			49.61	4.10		
	c)	24.33	0.4952	ca)	25.1384	27.6667			29.96	3.39		
VI. 3-methyl 3-heptanol	a)	3.00	0.0921				13.75	1.24	73.55	6.17	43.80	4.41
	b)	9.25	0.2882		25.0098	27.4128			43.34	4.37		
	c)	24.33	0.5807						14.52	2.68		
VII. 4-methyl 3-heptanol	a)	3.00	0.0892				5.81	2.01	84.34	6.71	51.61	4.74
	b)	9.25	0.2174		25.8707	26.9313			45.08	4.21		
	c)	24.33	0.4932						25.40	3.31		
VIII. 5-methyl 3-heptanol	a)	3.00	0.0358				3.39	1.36	101.22	6.58	57.13	4.15
	b)	9.25	0.1040		26.4103	27.3200			52.36	4.21		
	c)	24.33	0.3276						17.83	1.66		
IX. 2-octanol	a)	3.00	0.0604				16.51	0.20	160.41	7.83	94.46	4.94
	b)	9.25	0.1964		24.8271	29.2251			92.00	5.11		
	c)	24.33	0.3447						30.97	1.89		
X. 4-octanol	a)	3.00	0.0286				3.17	0.67	85.13	4.72	49.55	3.11
	b)	9.25	0.0699		26.4780	28.0264			42.74	2.64		
	c)	24.33	0.2409						20.77	1.97		

Separating the real and imaginary parts of both sides of Eq.(10.1), the following equations are obtained.

$$\frac{\chi'_{ij}}{\chi_{oij}} = \frac{1}{A}\int_{\tau_1}^{\tau_2} \frac{d\tau}{\tau(1+\omega^2\tau^2)} \qquad \text{..... (10.3)}$$

$$\frac{\chi''_{ij}}{\chi_{oij}} = \frac{1}{A}\int_{\tau_1}^{\tau_2} \frac{\omega d\tau}{(1+\omega^2\tau^2)} \qquad \text{..... (10.4)}$$

where $\chi_{ij}'=(\varepsilon_{ij}'-\varepsilon_{\infty ij})$, $\chi_{ij}''=\varepsilon_{ij}''$ and $\chi_{oij}=(\varepsilon_{oij}-\varepsilon_{\infty ij})$, are the real, imaginary and low frequency dielectric susceptibilities χ_{ij}'s expressed in terms of relative permittivities ε_{ij}'s.

Dividing Eq.(10.4) by (10.3) and evaluating the integral one gets:

$$\frac{\chi''_{ij}}{\chi'_{ij}} = \frac{2[\tan^{-1}(\omega\tau_2)-\tan^{-1}(\omega\tau_1)]}{\ln\frac{\tau_2^2}{\tau_1^2}\frac{(1+\omega^2\tau_1^2)}{(1+\omega^2\tau_2^2)}} \qquad \text{..... (10.5)}$$

Assuming smaller relaxation time $\tau_1 = 1/\omega_1$, larger relaxation time $\tau_2 = 1/\omega_2$ and on rearrangement of Eq.(10.5) becomes [10.16]:

$$\frac{\chi''_{ij}}{\chi'_{ij}}\ln(\omega_1^2+\omega^2) + 2\tan^{-1}\frac{\omega}{\omega_1} = \frac{\chi''_{ij}}{\chi'_{ij}}\ln(\omega_2^2+\omega^2) + 2\tan^{-1}\frac{\omega}{\omega_2}$$

or, $f(\omega_1) = f(\omega_2) = f(\omega_k)$

where,

$$f(\omega_k) = \left[\left(\frac{\chi''_{ij}}{\chi'_{ij}}\right)\ln(\omega_k^2+\omega^2) + 2\tan^{-1}\frac{\omega}{\omega_k}\right] \qquad \text{..... (10.6)}$$

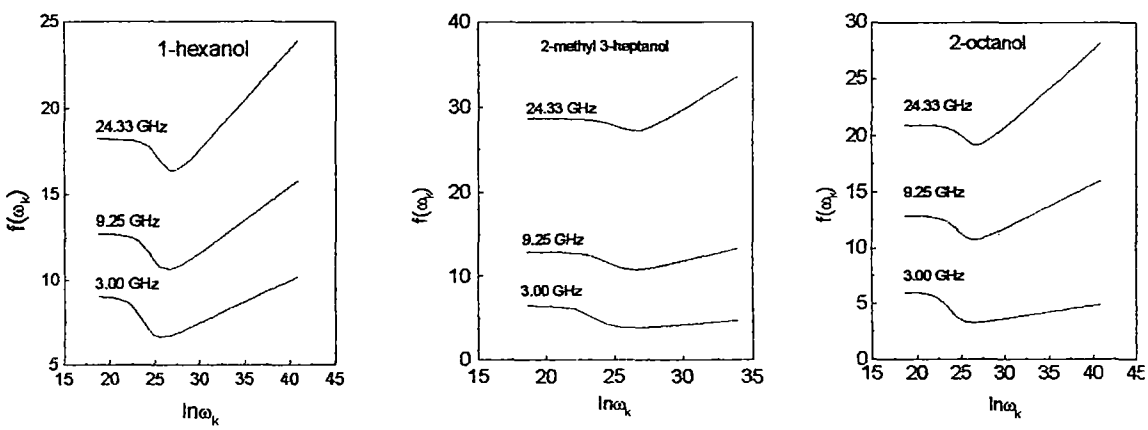

Figure 10.1: Variation of $f(\omega_k)$ with $\ln\omega_k$ for 1-hexanol, 2-methyl 3-heptanol and 2-octanol in *n*-heptane under 3.00, 9.25 and 24.33 GHz electric field at 25°C.

The term χ_{ij}''/χ_{ij}' of Eq.(10.6) is a function of weight fraction w_j of polar solute at a temperature T and angular frequency ω of the electric field. The factor $f(\omega_k)$ is, however, made constant for a fixed τ_1 and τ_2 at a given angular frequency ω by introducing the following term in the Eq.(10.6).

$$f(\omega_k) = \left(\frac{\chi_{ij}''}{\chi_{ij}'}\right)_{w_j \to 0} \ln(\omega_k^2 + \omega^2) + 2\tan^{-1}\frac{\omega}{\omega_k} \qquad \ldots\ldots (10.7)$$

Table 10.3: Slope β of χ_{ij}'–w_j curve at $w_j \to 0$, dipole moment from Eq.(10.13), dipole moment from single frequency measurement and theoretical dipole moment μ_{theo} from the available bond angles and bond moments in Coulomb.metre (C.m).

System with sl. no & mol. wt	Frequency f in GHz	Slope β of χ_{ij}'–w_j at $w_j \to 0$	$\mu \times 10^{30}$ (C.m) from average τ_2 and τ_1 of Fig.10.2		$\mu \times 10^{30}$ (C.m) from single frequency measurement		Theoretical dipole moment $\mu_{theo} \times 10^{30}$ in C.m
			μ_2	μ_1	μ_2	μ_1	
I. 1-Butanol M_j= 0.074 Kg	a) 3.00	1.028	4.67	3.45	17.44	4.30	
	b) 9.25	0.627	8.04	2.69	22.07	3.77	4.95
	c) 24.33	0.796	22.69	3.04	29.17	3.63	
II. 1-Hexanol M_j= 0.102 Kg	a) 3.00	0.608	4.57	3.11	16.87	4.30	
	b) 9.25	0.330	7.95	2.29	18.77	3.80	4.35
	c) 24.33	-0.089	–	–	21.20	3.43	
III. 1-Heptanol M_j= 0.116 Kg	a) 3.00	0.447	3.02	2.85	17.40	4.33	
	b) 9.25	0.213	2.91	1.97	18.40	3.80	4.05
	c) 24.33	0.588	9.94	3.30	27.01	3.73	
IV. 1-Decanol M_j= 0.158 Kg	a) 3.00	0.383	3.17	3.08	11.94	4.40	
	b) 9.25	0.192	2.74	2.18	18.40	3.93	3.15
	c) 24.33	0.133	4.06	1.81	17.24	3.83	
V. 2-methyl 3-heptanol M_j= 0.130 Kg	a) 3.00	0.530	3.36	3.28	6.93	4.10	
	b) 9.25	0.376	3.30	2.77	11.30	3.80	5.85
	c) 24.33	0.359	5.35	2.73	16.00	3.83	
VI. 3-methyl 3-heptanol M_j= 0.130 Kg	a) 3.00	0.663	3.79	3.67	7.27	4.30	
	b) 9.25	0.477	3.99	3.12	10.70	4.07	5.85
	c) 24.33	0.414	6.75	2.95	8.60	30.83	
VII. 4-methyl 3-heptanol M_j= 0.130 Kg	a) 3.00	0.643	3.64	3.62	7.83	4.20	
	b) 9.25	0.413	3.06	2.92	10.64	3.90	5.85
	c) 24.33	0.424	3.93	3.07	13.90	3.90	
VIII. 5-methyl 3-heptanol M_j= 0.130 Kg	a) 3.00	0.277	2.38	2.37	8.47	3.97	
	b) 9.25	0.038	0.90	0.88	11.17	3.60	5.85
	c) 24.33	0.024	0.79	0.71	9.50	3.37	
IX. 2-octanol M_j= 0.130 Kg	a) 3.00	0.420	3.06	2.92	12.94	4.10	
	b) 9.25	0.207	2.84	2.05	18.90	3.63	3.58
	c) 24.33	0.143	4.63	1.71	16.00	3.43	
X. 4-octanol M_j= 0.130 Kg	a) 3.00	0.142	1.70	1.70	7.10	3.77	
	b) 9.25	0.053	1.06	1.04	9.07	3.43	3.58
	c) 24.33	-0.041	–	–	10.97	3.43	

where $(\chi_{ij}''/\chi_{ij}')_{wj\to 0}$ is the intercept of χ_{ij}''/χ_{ij}' against w_j curve at $w_j\to 0$. The graphs are drawn by adopting least squares fitting technique of the experimental data at different w_j's of solute of Table10.1. The values of $(\chi_{ij}''/\chi_{ij}')_{wj\to 0}$ are placed in Table 10.2. Curves of $f(\omega_k)$ against $\ln\omega_k$ [10.16] for 1-hexanol, 2-methyl 3-heptanol and 2-octanol are drawn in Fig.10.1 by varying ω_k independently for a constant angular frequency ω to get two values of $\ln\omega_2$ and $\ln\omega_1$ ($\omega_2<\omega_1$) for same $f(\omega_k)$. Finally graphs of $\ln\omega_1$ vs $\ln\omega_2$ are plotted in Fig.10.2 for three different values of $\omega(=2\pi f)$, f being the frequency of the electric field of 3.00, 9.25 and 24.33 GHz respectively. The points of intersection of the curves yield the values of τ_2 and τ_1 of the polar molecules. They are placed in Table 10.2 along with those from double relaxation method by single frequency measurement technique [10.7-10.8].

τ's are also estimated from the following equation [10.11]:

$$\frac{\chi_{oij}-\chi_{ij}'}{\chi_{ij}'}=\omega(\tau_2+\tau_1)\frac{\chi_{ij}''}{\chi_{ij}'}-\omega^2\tau_1\tau_2 \qquad \text{..... (10.8)}$$

The term $(\chi_{oij}-\chi_{ij}')/\chi_{ij}'$ vs χ_{ij}''/χ_{ij}' on both sides of Eq.(10.8) are functions of w_j's of polar solute at a constant angular frequency ω and fixed τ_1 and τ_2. Graphs of $(\chi_{oij}-\chi_{ij}')/\chi_{ij}'$ with χ_{ij}''/χ_{ij}' are drawn against different w_j's at 3.00, 9.25 and 24.33 GHz electric fields to get fixed intercepts and slopes from which τ_1's and τ_2's were obtained. They are placed in Table 10.2. Three sets of τ_1 and τ_2 are obtained for alcohols at 3.00, 9.25 and 24.33 GHz electric fields respectively. The average τ_1 and τ_2 are placed in Table10.2 for comparison with the graphical method.

10.3. Estimation of μ_1 and μ_2 from τ_1 and τ_2 :

The Debye equation[10.17] for a polar-nonpolar liquid mixture under *hf* electric field in terms of χ_{ij}'s is written as:

$$\frac{d\chi_{ij}''}{d\chi_{ij}'}=\omega\tau \qquad \text{..... (10.9)}$$

$$\frac{\left(d\chi_{ij}''/dw_j\right)_{w_j\to 0}}{\left(d\chi_{ij}'/dw_j\right)_{w_j\to 0}}=\omega\tau \qquad \text{..... (10.10)}$$

Again, the imaginary part χ_{ij}'' of the complex *hf* susceptibility χ_{ij}^* as a function of w_j of a solute can be written as[10.17]

$$\chi_{ij}''=\frac{N\rho_{ij}\mu_j^{\,2}}{27\varepsilon_o k_B T M_j}\frac{\omega\tau}{1+\omega^2\tau^2}\left(\varepsilon_{ij}+2\right)^2 w_j$$

which on differentiation with respect to w_j and at $w_j \to 0$ yields:

$$\left(\frac{d\chi_{ij}''}{dw_j}\right)_{w_j \to 0} = \frac{N\rho_i \mu_j^2}{27\varepsilon_o k_B T M_j} \frac{\omega\tau}{1+\omega^2\tau^2}(\varepsilon_i+2)^2 \qquad \ldots\ldots (10.11)$$

where the density of the solution ρ_{ij} becomes ρ_i = density of solvent, $(\varepsilon_{ij}+2)^2$ becomes $(\varepsilon_i+2)^2$ at $w_j \to 0$, k_B=Boltzmann constant, N= Avogadro's number, ε_i= relative permittivity of solvent and ε_o= permittivity of free space = 8.854 x 10^{-12} Farad. metre^{-1}. All are expressed in SI units.

Comparing Eqs.(10.10) and (10.11) one gets:

$$\left(\frac{d\chi_{ij}'}{dw_j}\right)_{w_j \to 0} = \frac{N\rho_i \mu_j^2}{27\varepsilon_o k_B T M_j} \frac{1}{1+\omega^2\tau^2}(\varepsilon_i+2)^2 = \beta \qquad \ldots\ldots (10.12)$$

where β is the slope of χ_{ij}'-w_j curves of Fig.10.4 at $w_j \to 0$. Here no approximation in determination of μ_j is made like the conductivity measurement technique[10.9]. After simplification, the *hf* dipole moment μ_j is given by:

$$\mu_j = \left(\frac{27\varepsilon_o k_B T M_j \beta}{N\rho_i(\varepsilon_i+2)^2 b}\right)^{\frac{1}{2}} \qquad \ldots\ldots (10.13)$$

The dimensionless parameter b in terms of τ of Eq.(10.13) is given by:

$$b = 1/(1+\omega^2\tau^2) \qquad \ldots\ldots (10.14)$$

where τ is estimated from the graphical plots of $\ln\omega_1$ vs $\ln\omega_2$ of Fig.10.2. All the τ's are placed in Table 10.2.

10.4. Results and Discussions :

The data of χ_{ij}', χ_{ij}'' and χ_{oij} at different w_j's of dipolar alcohols in *n*-heptane at 25^{0}C under 3.00, 9.25 and 24.33 GHz electric fields are extracted from the measured permittivities ε_{ij}'s of Crossley *et al* [10.5] and Glasser *et al* [10.6] as presented in Table 10.1. The terms χ_{ij}''/χ_{ij}' for each alcohol are plotted against different w_j's for 3.00, 9.25 and 24.33 GHz electric fields. Eventually, the least squares fitted curves are found to be parabolic in nature. The values of intercepts of (χ_{ij}''/χ_{ij}')–w_j curves at $w_j \to 0$ are placed in column 3 of Table10.2. For several arbitrary values of angular frequency ω_k, three graphs of $f(\omega_k)$ against $\ln\omega_k$ of Eq.(10.6) for each alcohol are drawn for 3.00, 9.25 and 24.33 GHz electric fields. The variations of $f(\omega_k)$ against $\ln\omega_k$ are shown for three peculiar dipolar alcohols like 1-hexanol, 2-methyl 3-heptanol and 2-octanol at 3.00, 9.25 and 24.33 GHz electric fields. They are sketched in Fig.10.1. The graphs are drawn by using a PC which show the

gradual decrease of $f(\omega_k)$ with the increase of $\ln\omega_k$ to exhibit minimum at a certain frequency ω_k and then increase afterwards [10.16]. A large number of arbitrary values of $\ln\omega_2$ and $\ln\omega_1$ ($\ln\omega_2 < \ln\omega_1$) are selected for a fixed $f(\omega_k)$ in order to draw the graphs of $\ln\omega_1$ vs $\ln\omega_2$ at 3.00, 9.25 and 24.33 GHz electric fields. All the graphs as shown in Fig.10.2 are similar in nature. They show larger values initially and decrease gradually in order to cut at a point for all most all the dipolar liquids to yield significant values of τ_2 and τ_1 respectively. Unlike other systems, 1-butanol, 1-hexanol, 1-heptanol, 1-decanol and 2-methyl 3-heptanol, the curves meet at three points to exhibit three values of τ_2 and τ_1. This type of behaviour may be due to some uncertainty in measurements

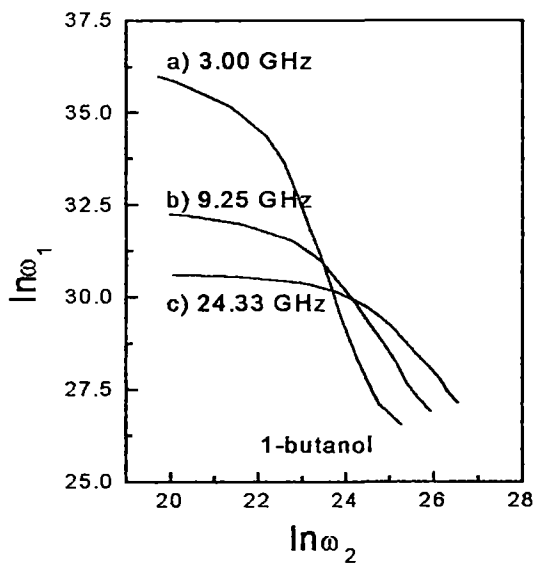

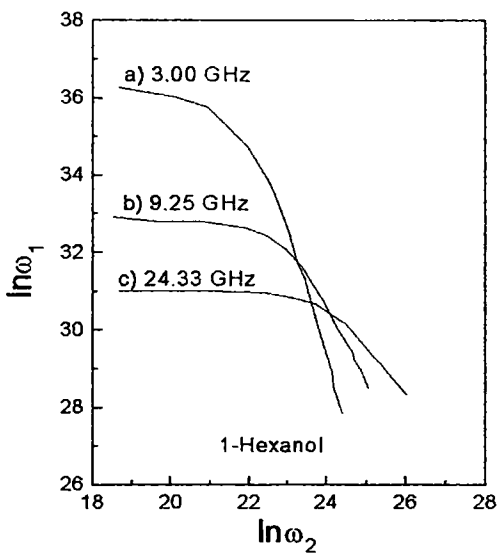

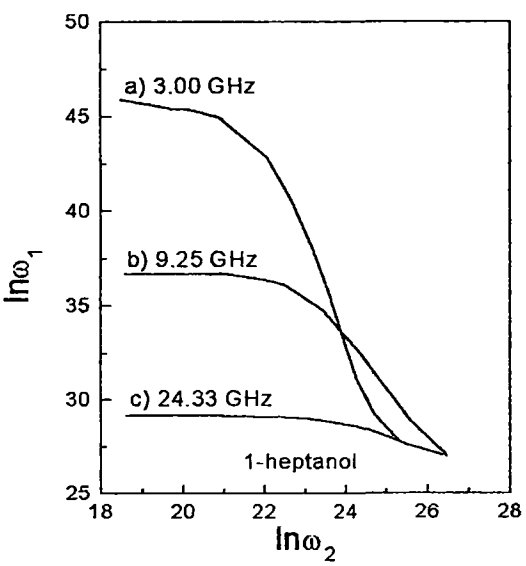

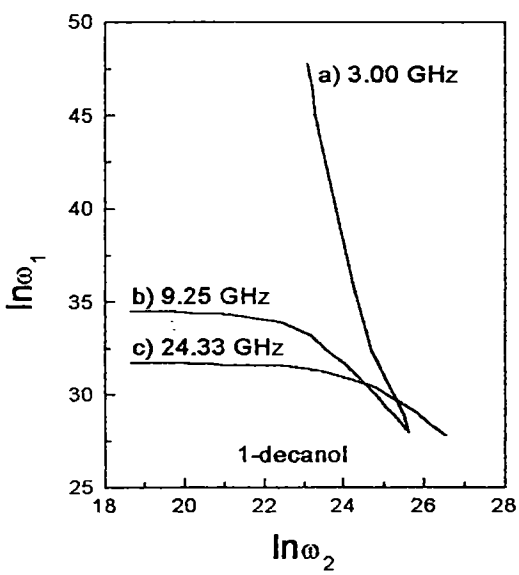

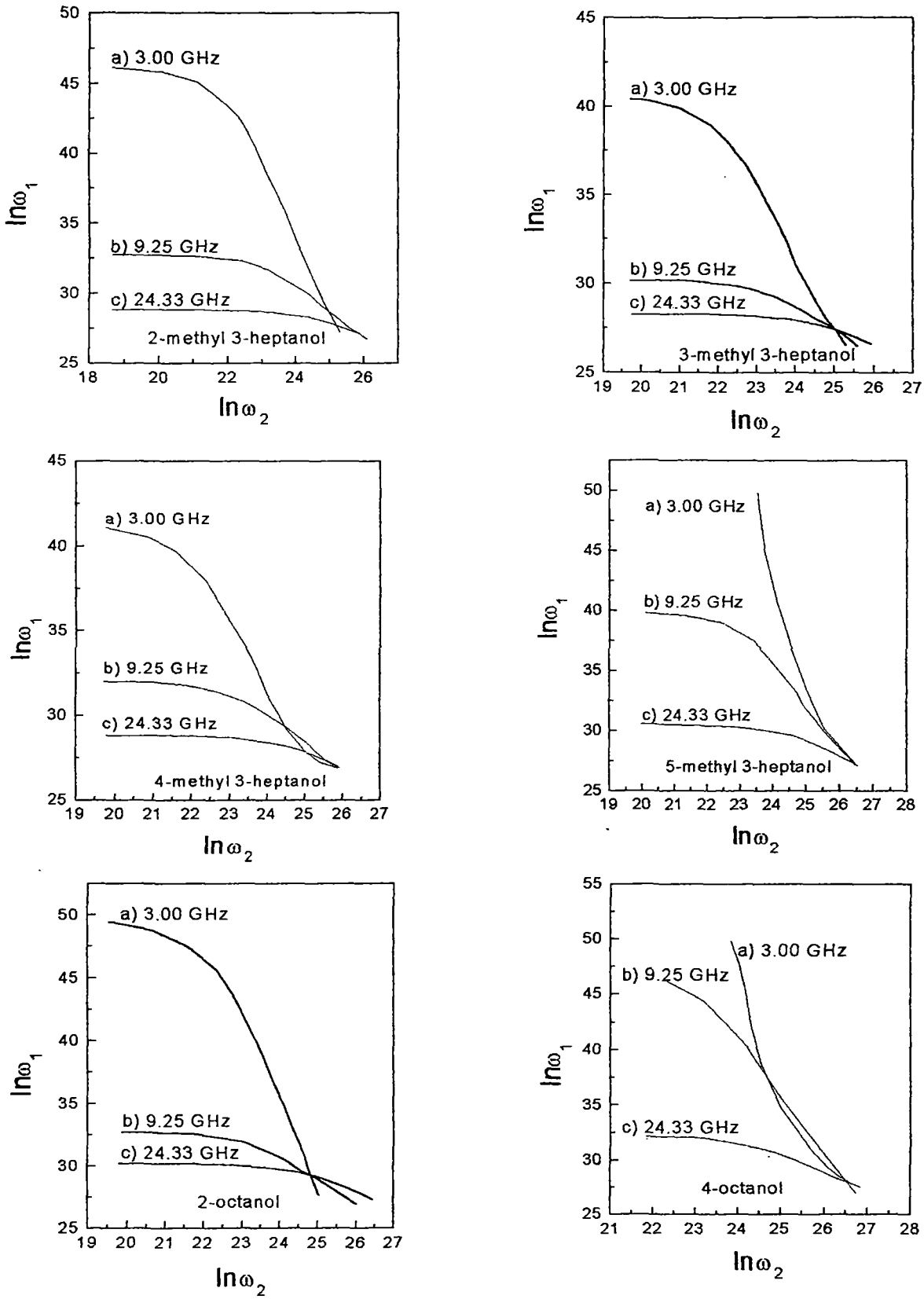

Figure 10.2: Plot of $\ln\omega_1$ against $\ln\omega_2$ for some normal alcohols and isomeric octyl alcohols in *n*-heptane under 3.00, 9.25 and 24.33 GHz electric fields at 25°C.

of experimental data (Table 10.1) of polar-nonpolar liquid mixtures at different *hf* electric fields. The average of the three τ's along with single τ_2 and τ_1 for the rest five systems are placed in Table 10.2.

τ_2 and τ_1 are also calculated from the slopes and intercepts of straight line Eq.(10.8) from single frequency measurement technique [10.11]. The plots of $(\chi_{oij}-\chi_{ij}')/\chi_{ij}'$ against χ_{ij}''/χ_{ij}' at different w_j's of alcohols for 24.33 GHz electric field are shown in Fig.10.3 only to see the soundness of the theory. The alcohols usually show peak at 24.33 GHz electric field when dielectric loss ($\chi_{ij}''=\varepsilon_{ij}''$) is plotted against angular frequency ω ($=2\pi f$), f being the frequency of the electric field at a fixed weight fraction w_j's of solute [10.9]. The estimated τ_2 and τ_1 are placed in ninth and tenth column of Table 10.2. They are found to be dependent on frequency of the applied electric field. The alcohols under investigation are in the same environment and are expected to show fixed τ_2 and τ_1 at all the three frequencies in order to exhibit the material property of the systems. The τ_2 and τ_1 thus obtained from the straight line Eq.(10.8) are made average and placed in the 11th column of Table 10.2. They are compared with those of graphical technique adopted here. The values from single relaxation technique are greater than the graphical method. τ_2 from graphical method agree well with τ_1 of Eq.(10.8) for almost all the octyl alcohols except 2-methyl 3-heptanol and 2-octanol.This type of behaviour may reveal the applicability of both the methods for the systems under study. Moreover, the graphical technique based on Debye-Fröhlich model provides better understanding to reflect the material property of the systems.

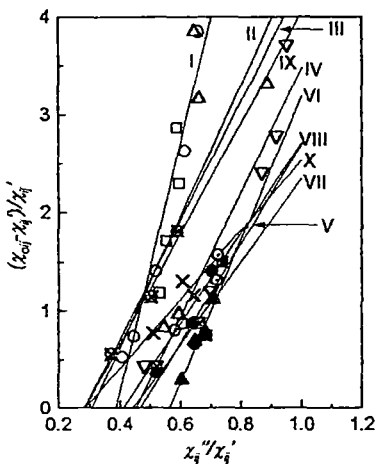

Figure 10.3: Plot of $(\chi_{oij}-\chi_{ij}')/\chi_{ij}'$ against χ_{ij}''/χ_{ij}' for different w_j's under 24.33 GHz electric field at 25^{0}C.

I. 1-butanol (○), II. 1-hexanol (△), III. 1-heptanol (□), IV. 1-decanol (▽), V. 2-methyl 3-heptanol (●), VI. 3 methyl 3-heptanol (▲), VII. 4-methyl 3-heptanol (⊠), VIII. 5-methyl 3-heptanol (⊙), IX. 2-octanol (⊗) and X. 4-octanol (✳) in *n*-heptane.

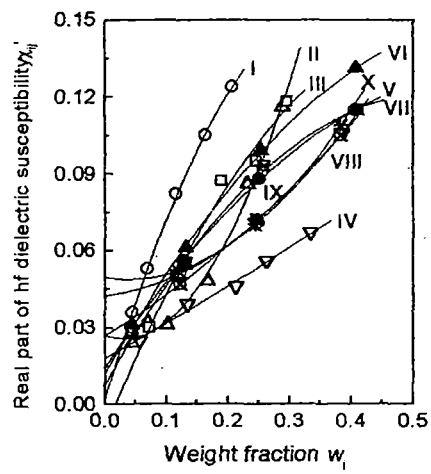

Figure 10.4: Variation of real part of complex dielectric orientation susceptibility χ_{ij}' with w_j's under 24.33 GHz electric field at 25^{0}C.

I. 1-butanol (○), II. 1-hexanol (△), III. 1-heptanol (□), IV. 1-decanol (▽), V. 2-methyl 3-heptanol (●), VI. 3 methyl 3-heptanol (▲), VII. 4-methyl 3-heptanol (⊠), VIII. 5-methyl 3-heptanol (⊙), IX. 2-octanol (⊗) and X. 4-octanol (✳) in *n*-heptane.

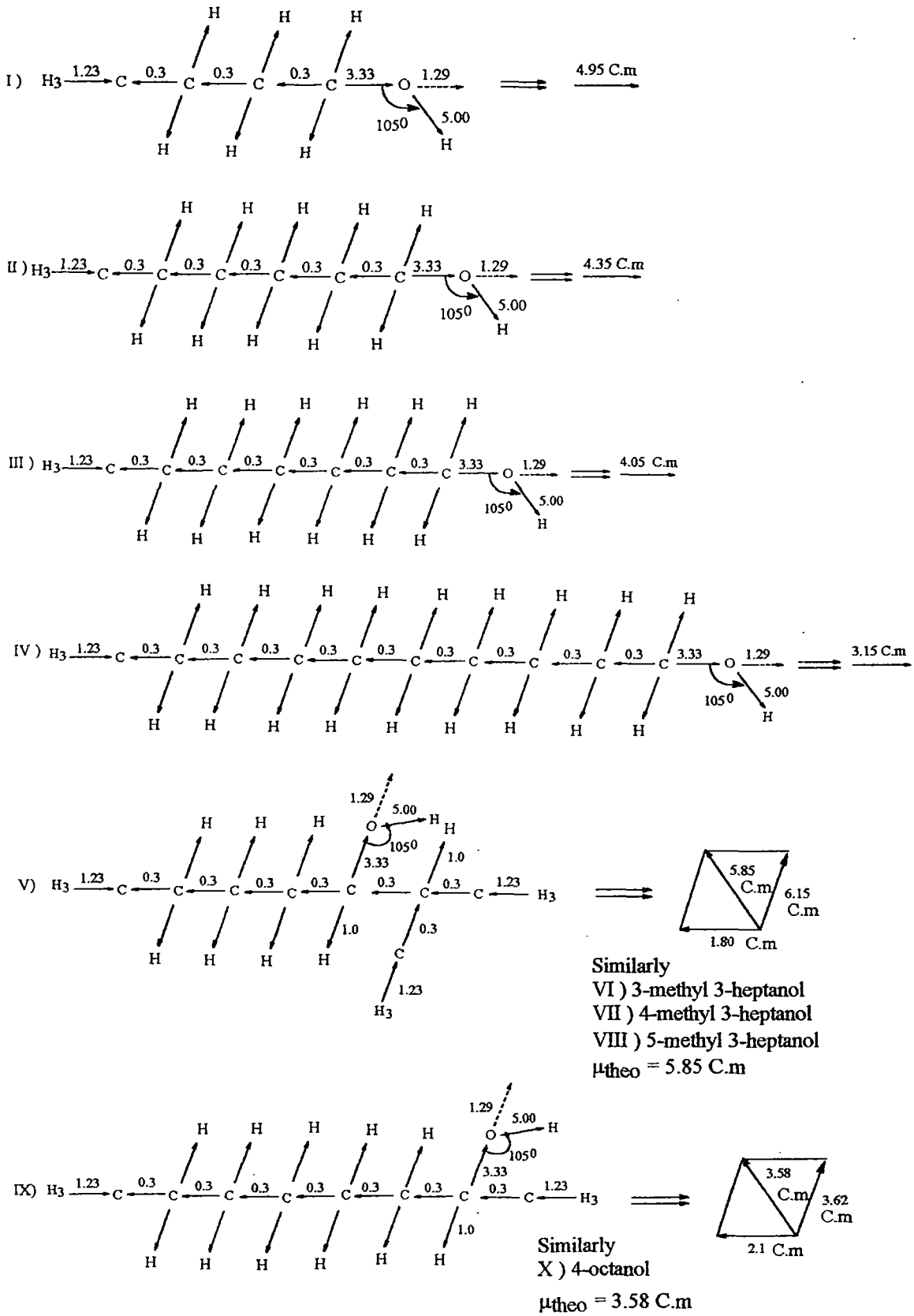

Figure 10.5: Conformational structures of polar molecules in terms of bond angles and bond moments ($x10^{-30}$ Coulomb. metre) of the substituents groups: I.) 1-Butanol, II.) 1-Hexanol, III.) 1-Heptanol, IV.) 1-Decanol, V.) 2-methyl 3-heptanol and IX.) 2-octanol.

The alcohols show effective dispersive region nearly 24.33 GHz electric field as observed elsewhere [10.9]. The dipole moments μ_2 and μ_1 of the whole and flexible parts of the dipolar alcohols in terms of τ_2 and τ_1 of Eq.(10.13) and slope β of χ_{ij}'-w_j curves are calculated at 3.00, 9.25 and 24.33 GHz electric fields. They are shown in Table 10.3. Plot of χ_{ij}' against w_j for all the alcohols at 24.33 GHz electric field are made in Fig.10.4. The variations are parabolic in nature. The graphs are almost same for the systems 5-methyl 3-heptanol (VIII), 2-octanol (IX) and 4-octanol (X) respectively. This may be due to almost same polarity of the molecules [10.18]. The convex or concave nature of all the curves may perhaps reveal the solute-solute molecular association in the higher concentration region due to hydrogen bonding. Besides 24.33 GHz electric field dipole moments are almost constant for all the systems at 3.00 and 9.25 GHz electric fields. Difference in μ_2 and μ_1 are, however, observed in case of 1-butanol (I), 1-hexanol (II) and 1-heptanol (III). This may indicate that the accurate measurement of $\varepsilon_{\infty ij}$ is needed [10.7] to get a sharp cutting of plot of $\ln\omega_1$ against $\ln\omega_2$ instead of little spread in Fig.10.2 for such molecules. μ_2 and μ_1 are in agreement with the single frequency measurement technique. Little disagreement among μ's may be due to steric hindrances and various effects like inductive, mesomeric and electromeric effects present in the substituent polar groups. The theoretical dipole moment μ_{theo}'s are sketched in Fig.10.5 considering planar structure of the alcohols. The available bond moments of $H_3\rightarrow C$, $C\leftarrow C$, $C\rightarrow O\rightarrow$ and $O\rightarrow H$ (making an angle 105^0) substituted polar groups are 1.23 C.m, 0.3 C.m, 3.33 C.m and 5.00 C.m respectively. In these polar molecules inductive and mesomeric effects among substituted groups play vital role to yield conformational structure. They can be taken into account by taking the ratio of μ_1/μ_{theo} which may be multiplied to the bond moment value to get μ_{theo}'s in exact agreement with calculated μ_1's.

References:

[10.1] A K Sharma, D R Sharma and D S Gill, *J. Phys. D: Appl. Phys.* **18** 1199 (1985)

[10.2] A Sharma and D R Sharma, *J. Phys. Soc. Japan* **61** 1049 (1992)

[10.3] M D Migahed, M T Ahmed and A E Kotp, *J. Phys. D: Appl. Phys.* **33** 2108 (2000)

[10.4] A Bello, E Laredo, M Grimau, A Nogales and T A Ezquerra, *J. Chem. Phys.* **113** 863 (2000)

[10.5] J Crossley, L Glasser and C P Smyth, *J. Chem. Phys.* **55** 2197 (1971)

[10.6] L Glasser, J Crossley and C P Smyth, *J. Chem. Phys.* **37** 3978 (1973)

[10.7] S K Sit and S Acharyya, *Indian J. Phys.* **70B** 19 (1996)

[10.8] S K Sit, N Ghosh and S Acharyya, *Indian J. Pure & Appl. Phys.* **35** 329 (1997)

[10.9] N Ghosh, A Karmakar, S K Sit and S Acharyya, *Ind. J. Pure & Appl. Phys.* **38** 574 (2000)

[10.10] A K Jonscher, *Inst. Phys. Conf. (Canterbury)*, invited papers edited by CHL Goodman (1980)

[10.11] K Dutta, S K Sit and S Acharyya, *Pramana: J. Phys.* **57** 775 (2001)

[10.12] U Saha, S K Sit, R C Basak and S Acharyya, *J. Phys. D: Appl. Phys.* **27** 596 (1994)

[10.13] S K Sit, R C Basak, U Saha and S Acharyya, *J. Phys. D: Appl. Phys.* **27** 2194 (1994)

[10.14] K Higasi, K Bergmann and C P Smyth, *J. Phys. Chem.* **64** 880 (1960)

[10.15] K Higasi, Y Koga and M Nakamura, *Bull. Chem. Soc. Japan* **44** 988 (1971)

[10.16] A Mansingh and P Kumar, *J. Phys. Chem.* **69** 4197 (1965)

[10.17] K Dutta, A Karmakar, L Dutta, S K Sit and S Acharyya, *Indian J. Pure & Appl. Phys.* **40** 801 (2002)

[10.18] A K Chatterjee, U Saha, N Nandi, R C Basak and S Acharyya, *Inian J. Phys.* **66B** 291 (1992)

SUMMARY AND CONCLUSION

The subject matter of the thesis work titled "*Relaxation phenomena of dielectropolar liquid molecules under low and high frequency electric fields*" has been divided into a large number of chapters. All the chapters are highly informative to shed more light on the relaxation phenomena of dipolar liquid molecules in non-polar solvents under low and high frequency (*hf*) electric fields.

A brief account of early works on dielectric relaxation of liquids (DRL) by different groups of workers has been presented in Chapter 1. The fundamental theories to explain the relaxation phenomena of polar molecules both in pure state and in suitable non-polar solvents have been well discussed in this chapter in C.G.S. units. An extensive review of polarisation is included at the end of this chapter in order to get a chronological development of the subject.

The theoretical formulations recently derived and used by the present author to estimate *hf* relaxation time τ_j, static or low frequency dipole moments μ_s, *hf* dipole moment μ_j, double relaxation times and dipole moments τ_1, τ_2 and μ_1, μ_2 under *hf* electric fields of GHz range are presented in Chapter 2. The aim of this chapter is to provide a comprehensive theoretical formulation in SI units in order to study the relaxation phenomena of polar-nonpolar liquid mixtures in terms of the measured relative permittivities under low and *hf* electric fields. The concept of relaxation mechanism of polar molecules in non-polar solvents is, however, gained through μ_s, μ_j, μ_1 and μ_2 based on Smyth's model. The different thermodynamic energy parameters of enthalpy of activation ΔH_τ, entropy of activation ΔS_τ and free energy of activation ΔF_τ can, however, be obtained from the temperature variation of measured τ_j's of polar molecules in non-polar solvents to throw much light on the concept of rigid phase rotators of the molecules in a given solvent. The Chapter 2 approaches with different objects in view: It provides an archetypal example of the application of dielectric relaxation, to help and elucidate the shape, size and structure of dielectropolar molecules in liquid states.

The theoretical formulations, so far derived in Chapter 2, were tested by an experimental measurement as shown in Chapter 3 to support the applicability of the method based on Debye-Smyth model. The block diagram of the experimental set up of HP 4192A Impedance Analyser has been sketched along with a brief description of measurements of ε_{ij}', ε_{ij}'' ε_{oij} and $\varepsilon_{\infty ij}$ at various concentrations and temperatures of aprotic polar liquids like dimethylsulphoxide (DMSO), N,N-diethylformamide (DEF), N,N-dimethylformamide (DMF) and N,N-dimethylacetamide (DMA) all in C_6H_6. From the linear curve of $(\varepsilon_{oij}-\varepsilon_{ij}')/(\varepsilon_{ij}'-\varepsilon_{\infty ij})$ against $\varepsilon_{ij}''/(\varepsilon_{ij}'-\varepsilon_{\infty ij})$ it was observed that all the systems show double relaxation times τ_2 and τ_1 due to end over end rotation of the whole molecules as well as the flexible parts attached to the parent molecules. The τ_1, in agreement with reported τ, signifies that a part of the molecules is rotating under 10 GHz electric field. The support of this fact came from the measured thermodynamic energy parameters ΔH_τ, ΔS_τ and ΔF_τ from

$\ln(\tau_j T)$ against $1/T$ for DMSO. The theoretical values c_1 and c_2 of weighted contributions towards dielectric relaxations for the measured τ_1 and τ_2 were ascertained from Fröhlich theoretical equations. They are compared with the experimental c_1 and c_2 as obtained by the graphical technique. The corresponding dipole moments μ_2 and μ_1 were obtained from τ_2 and τ_1 in order to compare with the static μ_s's, reported μ and theoretical dipole moments μ_{theo}'s from the available bond angles and bond moments of the substituent polar groups attached to the parent molecules in Debye units. The molecular conformations are, however, sketched by μ_{cal} from μ_s/μ_{theo} which takes into account of the existence of mesomeric and inductive effects of different polar groups of such molecules.

Chapter 4 presents a beautiful study of the relaxation phenomena of some polysubstituted benzenes in C_6H_6 through *hf* conductivity σ_{ij}'s measurements. τ_j's measured from the ratio of the slopes of the individual variations of imaginary part σ_{ij}'' and real part σ_{ij}' of complex *hf* conductivity σ_{ij}^* with w_j's in the limit $w_j=0$ at a given temperature is more reliable in comparison to the direct slope of the variation of $\sigma_{ij}''-\sigma_{ij}'$ at different w_j's. τ_j's were found in close agreement with the reported values. ΔH_τ, ΔS_τ and ΔF_τ were computed by applying Eyring's rate theory with the measured τ in order to get solvent environment. The estimated values of γ and ΔH_η show the solid phase rotators of the molecule in a solvent. ΔH_η is involved with the translation and the rotational energies. The comparison of the Kalman factor $\tau_j T/\eta^\gamma$ and Debye factor $\tau_j T/\eta$ suggests the applicability of Debye model of dielectric relaxation for such dipolar liquid molecules. The excellent agreement of the measured μ_j's in terms of measured τ_j's and slope β's of $\sigma_{ij}-w_j$ curves with the reported μ's establishes the basic soundness of the conductivity measurement technique used. The slight disagreement between μ_j's and μ_{theo}'s reveals the existence of mesomeric, inductive and electromeric effects within the polar groups attached to the parent benzene ring. The temperature dependence of τ_j's and μ_j's is much more significant to conceive the solvent environment of the polar molecules and the molecular dynamics of the systems. It sheds more light on their structural conformations.

The Chapter 5 reports the measured τ_j and μ_j of some methyl benzenes and ketones in C_6H_6 at 25^0C under 9.585 GHz electric field from the measured ε_{ij}' and ε_{ij}'' at various w_j's. The methodology to get τ_j from the ratio of the individual slopes of σ_{ij}'' and σ_{ij}' against w_j seems to be a significant improvement over the existing one of the linear slope of $\sigma_{ij}''-\sigma_{ij}'$ curve. The variation of $\sigma_{ij}-w_j$ like $\sigma_{ij}''-w_j$ curve is often convex in nature indicating the probable occurrence of phase change of the liquid state after a certain concentration. The estimated μ_j by using τ_j from both the methods are compared with those of Gopalakrishna and theoretical ones to establish the applicability of the method.

The double relaxation phenomena in apparently rigid aliphatic polar liquids like chloral and ethyltrichloroacetate in non-polar solvents benzene, *n*-heptane and *n*-hexane under 4.2, 9.8 and 24.6 GHz electric field at 30°C have been extensively studied in Chapter 6. Five systems of polar-nonpolar liquid mixtures show τ_1, τ_2 and μ_1, μ_2 due to rotation of their flexible parts and the whole molecules. The probability of showing double relaxation phenomena is greater in aliphatic solvents at 9.8 and 24.6 GHz electric fields indicating their non rigidity. This is also supported by the symmetric and asymmetric distribution parameters γ and δ estimated from the values of x [$=(\varepsilon_{ij}'-\varepsilon_{\infty ij})/(\varepsilon_{oij}-\varepsilon_{\infty ij})$] and y [$=\varepsilon_{ij}''/(\varepsilon_{oij}-\varepsilon_{\infty ij})$] at $w_j \rightarrow 0$. The unusual variations of x and y with w_j's predict their probable solute-solute and solute-solvent molecular associations under *hf* electric field. μ_{theo}'s in terms of the available bond angles and bond moments conform the estimated μ_j's only to establish the existence of mesomeric, inductive and electromeric effects in them.

In Chapter 7, the relaxation phenomena of some disubstituted benzenes and anilines in C_6H_6 and CCl_4 through *hf* susceptibility χ_{ij} measurement technique have been presented. The main advantage of this method is that it is directly linked with the orientation polarisation and excluded the fast polarisation process. τ_2 and τ_1 were obtained from the intercept and slope of a linear equation of $(\chi_{oij}-\chi_{ij}')/\chi_{ij}'$ against χ_{ij}''/χ_{ij}' for different w_j's. τ_j's were calculated from the ratio of the individual slopes of χ_{ij}'' and χ_{ij}' with w_j's at $w_j \rightarrow 0$ assuming single Debye like dispersion and compared with those of Murthy *et al* and Gopalakrishna. The relative contributions c_1 and c_2 towards dielectric relaxations for τ_1 and τ_2 can, however, be obtained from the Fröhlich theoretical formulations of χ_{ij}'/χ_{oij} and χ_{ij}''/χ_{oij} and compared with those from the experimentally measured values of $(\chi_{ij}'/\chi_{oij})_{wj \rightarrow 0}$ and $(\chi_{ij}''/\chi_{oij})_{wj \rightarrow 0}$ graphically. The symmetric and characteristic relaxation times τ_s and τ_{cs} were determined in order to establish the different relaxation behaviours for such polar molecules. μ_2 and μ_1 for the rotations of the whole molecules as well as the flexible parts were ascertained from τ_2 and τ_1 and the linear coefficient β of $\chi_{ij}'-w_j$ curve. μ_j's were finally compared with the reported μ and μ_{theo} to conclude that for disubstituted anilines a part of the molecule is rotating while the whole molecular rotation occurs for disubstituted benzenes.

Chloral and ethyltrichloroacetate showed double relaxation phenomena in aliphatic solvents through chi-squares minimization of the measured data. High frequency susceptibility χ_{ij} measurement under 4.2, 9.8 and 24.6 GHz electric fields at 30°C has been applied. The findings were displayed in Chapter 8. The measured τ_2, τ_1 and μ_2, μ_1 were found to be little deviated from *hf* σ_{ij} measurement technique. The *hf* χ_{ij} measurement, although is very simple, it does not include any approximation in the calculation of μ_j. Nevertheless, the variation of χ_{ij}'/χ_{oij} and χ_{ij}''/χ_{oij} with w_j's remain almost unaltered with respect to σ_{ij} measurement technique. The measured μ_j's when compared with μ_{theo}'s established the associational aspects of the polar

molecules with solvents and solutes. The mesomeric and inductive moments of the molecules could, however, be studied. The existence of fractional +ve charge δ^+ on C-atom and –ve charge δ^- on O-atom of C⇐O group in both the polar liquids showed the electromeric effect to form π–complex with the π–delocalised electron clouds of benzene ring.

In Chapter 9, the static or low frequency μ_s of some aliphatic polar liquids in different non-polar solvents were studied in terms of static experimental parameter X_{ij}. X_{ij}'s are related with ε_{oij} and $\varepsilon_{\infty ij}$ of polar-nonpolar liquid mixtures at different w_j's. A comparison is, however, made with the *hf* μ_j from *hf* σ_{ij} measurement technique and μ_{theo}. A little disagreement is caused by the permanent polarisation of different substituent polar groups acting as pusher or puller of electrons towards or away from C-atom of the compounds. The reduction in bond moments evidently occur in all the polar liquids by a factor μ_s/μ_{theo} to conform to the exact μ_s or μ_j.

With all these discussions made above, a [illegible] conclusion regarding the relaxation phenomena can, however, be reached by other and our groups. The findings are presented in Chapter 10. In course of our prolonged studies on relaxation phenomena of polar-nonpolar liquid mixtures it reveals that the existence of double relaxation phenomena reflects the material property of the chemical system under investigation and is not dependent on the measurement frequency. Although relative permittivities ε_{ij}' and $\varepsilon_{\infty ij}$, dielectric loss ε_{ij}'' vary with frequency, the fundamental dielectric parameters such as dielectric decrement and relaxation time which describe the relaxation properties of the system, do not. The theoretical consideration in the chapters 6 and 8 appears to be sound in getting τ_1 and τ_2. But chloral in C_6H_6 in Chapter 6 exhibited double relaxation behaviour at 9.8 GHz. This should be reflected at all the frequencies. The analysis is expected to produce the same τ_1 and τ_2 at all the three frequencies. We then applied the chi-squares minimisation on the data set in Chapter 8 to predict τ_1 and τ_2 of chloral and ethyltrichloroacetate in aliphatic solvents. Under such context we, therefore, decided to restudy a number of normal and isomeric octyl alcohols in *n*-heptane at 25^{0}C under 3.00, 9.25 and 24.33 GHz electric fields through *hf* susceptibility χ_{ij}'s measurements. Three graphs of $f(\omega_k)$ against $\ln\omega_k$ were drawn at those frequencies for a number of arbitrary angular frequencies ω_k's. $\ln\omega_2$ and $\ln\omega_1$ for a fixed value of $f(\omega_k)$ of $f(\omega_k)$–$\ln\omega_k$ curve, however yield the same τ_2 and τ_1 for a system from the intersection points of $\ln\omega_1$ against $\ln\omega_2$ curve for three different frequencies. τ_2 and τ_1 were then compared with the average τ's of our single frequency measurement technique stated elsewhere. The estimated μ_2 and μ_1 in terms of the linear coefficients β's of χ_{ij}'–w_j curves and the measured τ_2 and τ_1 by different methods showed that μ's were slightly different in different frequencies because rotation of the whole molecule as well as the flexible parts are probably affected by the frequency of the applied alternating electric field. The measured μ_j's were then compared with μ_{theo}'s of almost all the alcohols.

The dielectric theories are presented in SI units in some chapters. SI units used are of unified, coherent and rationalised nature. The curves with the available experimental points in all the figures of different chapters show the validity of the theoretical formulations so far derived. The correlation coefficient r's, % of errors and chi-squares minimisation testing computed on the various data at a given experimental temperature go to support the reliability of the derived formulations. Theories of dielectric relaxations have been formulated in terms of relative permittivities ε_{ij}'s. Measurement of τ_j's and μ_j's were carried out in terms of *hf* conductivity σ_{ij} which is concerned with bound molecular charges of polar molecules.

Nowadays, the study of dielectric relaxation phenomena is preferred in terms of dielectric orientation susceptibility χ_{ij}'s in SI units as seen in Chapters 7, 8 and 10 of this thesis. χ_{ij}'s are supposed to be involved only with orientation polarisation of molecules. It is to be noted that the dielectric susceptibilities χ's are given by the subtraction of either 1 or ε_∞ from relative permittivity ε_r. If 1 is subtracted, the susceptibility due to all operating polarisation processes results, while if ε_∞ is subtracted from the low frequency value of ε_r, the susceptibility due only to orientation polarisation processes is given. But Thermally Stimulated Depolarisation Current Density (TSDCD) and Isothermal Frequency Domain AC Spectroscopy (IFDS) can recently be used to study the dielectric relaxation phenomena. These may give a firm answer to the problem of polar-nonpolar liquid mixtures with which the present author is concerned. But the latter two methods consist of a tedious computer simulated calculation unlike σ_{ij} or χ_{ij} measurement quoted above. Thus the methods appear to be much simpler, straightforward and easy to arrive at the expected conclusion. Moreover, the polar-nonpolar liquid mixtures can be studied by taking into account of the concept of other models like Onsager, Kirkwood, Fröhlich etc. But those models are not so simpler like Debye-Smyth. Further work can be carried out to predict the relaxation phenomena by assuming moment of inertia of the polar molecules under *uhf* electric field. Numerical calculation on relaxation parameters may be carried out on the basis of Newton-Raphson method to arrive at the results.

The thesis thus provides the future workers in liquid dielectrics to open a new and vast scope to work further on the interesting dielectropolar liquids in non-polar solvents under *hf* electric field. It can thus be concluded that the relaxation phenomena of highly non-spherical polar liquid molecules in non-polar solvents could be explained by the Debye-Smyth model which was supposed to be applicable to the nearly spherical molecules of simpler configuration. The correlation between the conformational structures obtained from the available bond angles and bond lengths with the observed results enhances the scientific contents and adds a new horizon of understanding to the existing knowledge of dielectric relaxation phenomena.

Reprints

ELSEVIER

Journal of Molecular Liquids 88 (2000) 229–241

journal of MOLECULAR LIQUIDS

www.elsevier.nl/locate/molliq

Dielectric relaxation phenomena and high frequency conductivity of rigid polar liquids in different solvents.

K Dutta, R C Basak, S K Sit and S Acharyya,

Dept. of Physics, Raiganj College (University College)
P.O. Raiganj, Dist. Uttar Dinajpur (W.B.) PIN–733134, INDIA

Received 14 March 2000; accepted 03 July 2000

ABSTRACT

The double relaxation phenomena in apparently rigid aliphatic polar liquids (j) like chloral and ethyltrichloroacetate in nonpolar solvents (i) benzene, n-hexane and n-heptane under 4.2, 9.8 and 24.6 GHz electric fields at 30°C have been studied. Only five systems of polar-nonpolar liquid mixtures show the double relaxation times τ_1 and τ_2 due to rotation of their flexible parts and the whole molecules. The probability of showing the double relaxation phenomena is greater in aliphatic solvents at 9.8 and 24.6 GHz electric fields indicating their nonrigidity. This is also supported by the symmetric and asymmetric distribution parameters γ and δ estimated from values of x and y at $w_j \rightarrow 0$ involved with dimensionless dielectric constants k'_{ij}, k''_{ij}, k_{oij} and $k_{\infty ij}$ of solutions. The variation of x and y with weight fractions w_j's of solutes are found to be unusual predicting their probable solute-solvent and solute-solute molecular association under high frequency (hf) electric fields. The dipole moments μ_1 and μ_2 of the flexible parts and the whole molecules from the slopes β's of hf conductivities σ_{ij}'s with w_j's and the estimated τ_1 and τ_2 reveal their solute-solute associations in the aliphatic solvents. The theoretical dipole moments μ_{theo}'s in terms of available bond angles and bond moments conform the estimated μ_j's only to establish the existence of mesomeric, inductive and electromeric effects in them.

1. INTRODUCTION

Dielectric relaxation studies of polar liquids in nonpolar solvents are of much importance as they provide interesting information on solute-solvent and solute-solute molecular formations [1-2] under high frequency (hf) electric field. In order to predict associational aspects of polar liquids one must analyze the measured relaxation parameters to know the relaxation time τ and the dipole moment μ of a polar liquid by Cole-Cole [3], Cole-Davidson [4] plots or by single frequency concentration variation method [5].

Srivastava and Srivastava [6] studied the relaxation behaviour of chloral and ethyltrichloroacetate in different nonpolar solvents under 4.2, 9.8 and 24.6 GHz electric field frequencies from the measured relaxation permittivities like real ε'_{ij} imaginary ε''_{ij}, static ε_{oij} and infinite frequency permittivity $\varepsilon_{\infty ij}$ of polar solute (j) in different nonpolar solvents (i) at 30°C to predict their solute-solvent or solute-solute molecular associations. They, however, inferred that such molecules may possess two or more relaxation processes towards dielectric dispersion phenomena [6]. The molecule chloral is widely used in medicine and in the manufacture of

0167-7322/00/$ - see front matter
PII S0167-7322(00) 00142-2

D.D.T. as insecticide. Ethyltrichloroacetate, on the other hand, is used for artificial fragrance of fruits and flowers.

All these facts inspired us to use the measured relaxation data [6] for such polar liquids only to detect the double relaxation times τ_1 and τ_2 from the single frequency measurement technique [7-8]. Earlier investigations have been made on different chain like polar molecules like alcohols in a nonpolar solvent [9-10] to see the double relaxation phenomena at three different electric field frequencies. However, no such study is made so far on such rigid aliphatic polar liquids in different nonpolar solvents under various electric field frequencies by the double relaxation formalism derived from single frequency measurements of dielectric relaxation parameters [7-8]. Moreover, their measured permittivities [6] have dimensions of Farad metre^{-1} (F.m^{-1}) in SI units. It is, therefore, better to replace them in terms of dimensionless dielectric constants in SI units because of its rationalised coherent and unified nature.

Five systems out of twelve as presented in Table 1 show the double relaxation times τ_2 and τ_1 due to rotation of the whole and the flexible part of the molecule. τ_2 and τ_1 were calculated from the slope and intercept of the linear equation (7) (see later). All the straight lines are shown graphically in Figure 1.

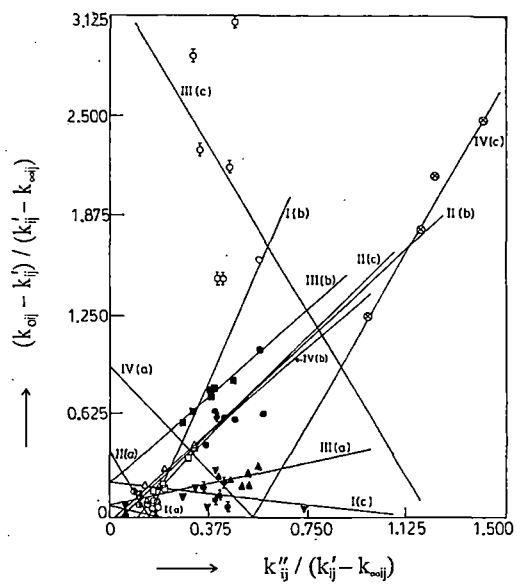

Figure 1 : Linear variation of $(k_{oij} - k'_{ij}) / (k'_{ij} - k_{\infty ij})$ against $k''_{ij} / (k'_{ij} - k_{\infty ij})$ for different w_j's of chloral and ethyltrichloroacetate under three different hf electric fields at 30°C. I(a), I(b) and I(c) for chloral in benzene (⧗, ○, ▼) ; II(a), II(b) and II(c) for chloral in n-heptane (◑, △, □); III(a), III(b) and III(c) for ethyltrichloroacetate in benzene (▲, ■, ◊) and IV(a), IV(b) and IV(c) for ethyltrichloroacetate in n-hexane (◈, ●, ⊕) at 4.2, 9.8 and 24.6 GHz electric fields respectively.

The dipole moments μ_2 and μ_1 of Table 2 due to τ_2 and τ_1 were computed in terms of slopes β's of total hf conductivity σ_{ij} against w_j curves of Figure 2. All the parabolic curves of conductivities σ_{ij}'s with w_j's are found to increase with frequency of the electric field.

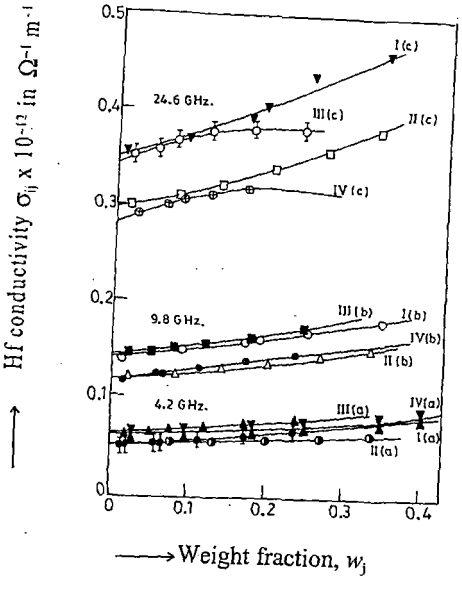

Figure 2 ; Hf conductivity σ_{ij} x 10^{-12} in Ω^{-1} m^{-1} against w_j of solutes at 30°C. I(a), I(b) and I(c) for chloral in benzene (⧗, ○, ▼) ; II(a), II(b) and II(c) for chloral in n-heptane (◑, △, □); III(a), III(b) and III(c) for ethyltrichloroacetate in benzene (▲, ■, ◊) and IV(a), IV(b) and IV(c) for ethyltrichloroacetate in n-hexane (◆, ●, ⊕) at 4.2, 9.8 and 24.6 GHz electric fields respectively.

The calculated μ's are compared with the theoretical dipole moment μ_{theo} due to available bond angles and bond moments which are sketched in Figure 3 showing the associational aspect of the polar molecules with solvents to observe the mesomeric and inductive moments in them under hf electric field. They are finally compared with the reported μ's and μ_1 obtained from $\mu_1=\mu_2(c_1/c_2)^{1/2}$ assuming two relaxation processes are equally probable.

The relative contributions c_1 and c_2 towards dielectric dispersions for the five systems were obtained from the theoretical values of $x = (k'_{ij} - k_{\infty ij}) / (k_{oij} - k_{\infty ij})$ and $y = k''_{ij} / (k_{oij} - k_{\infty ij})$ of Fröhlich's theory [11] in terms of estimated τ_2 and τ_1 of Table 1. They were also computed from the values of x and y at $w_j \rightarrow 0$ of graphical technique [7-8] and placed in Table 3 for comparison with Fröhlich's c_1 and c_2. The variations of x and y with w_j of solute of Figures 4 and 5 are the least squares fitted parabolae with the experimental data. They are of convex and concave shapes except ethyltrichloroacetate in n-hexane at 9.8 and 24.6 GHz electric fields. This sort of behaviours was not observed earlier [7-8]. With these values of x and y at $w_j \rightarrow 0$ the symmetric and asymmetric distribution parameters γ and δ of the molecules at those frequencies are computed and are placed in Table 3 to indicate the nonrigidity of the molecules in hf electric field.

2. THEORETICAL FORMULATIONS

Assuming the molecules to possess two separate broad dispersions under hf electric field, Bergmann equations [12] are :

$$\frac{\varepsilon'_{ij}-\varepsilon_{\infty ij}}{\varepsilon_{oij}-\varepsilon_{\infty ij}} = \frac{c_1}{1+\omega^2\tau_1^2} + \frac{c_2}{1+\omega^2\tau_2^2} \quad (1)$$

$$\frac{\varepsilon''_{ij}}{\varepsilon_{oij}-\varepsilon_{\infty ij}} = c_1\frac{\omega\tau_1}{1+\omega^2\tau_1^2} + c_2\frac{\omega\tau_2}{1+\omega^2\tau_2^2} \quad (2)$$

such that the sum of the relative weight factors c_1 and c_2 towards dielectric dispersion is unity i.e. $c_1 + c_2 = 1$.

When the dielectric relaxation permittivities in equations (1) and (2) are expressed *in terms of* internationally accepted symbols like real k'_{ij} ($= \varepsilon'_{ij}/\varepsilon_o$), imaginary k''_{ij} ($= \varepsilon''_{ij}/\varepsilon_o$) parts of complex dimensionless dielectric constant k^*_{ij}, static k_{oij} ($= \varepsilon_{oij}/\varepsilon_o$) and infinite frequency dielectric constant $k_{\infty ij}$ ($= \varepsilon_{\infty ij}/\varepsilon_o$) where ε_o = permittivity of free space = 8.854×10^{-12} F.m^{-1}, the Bergmann equations (1) and (2) are given by :

$$\frac{k'_{ij}-k_{\infty ij}}{k_{oij}-k_{\infty ij}} = \frac{c_1}{1+\omega^2\tau_1^2} + \frac{c_2}{1+\omega^2\tau_2^2} \quad (3)$$

$$\frac{k''_{ij}}{k_{oij}-k_{\infty ij}} = c_1\frac{\omega\tau_1}{1+\omega^2\tau_1^2} + c_2\frac{\omega\tau_2}{1+\omega^2\tau_2^2} \quad (4)$$

Solving equations (3) and (4) for c_1 and c_2 one gets,

$$c_1 = \frac{(x\alpha_2 - y)(1+\alpha_1^2)}{\alpha_2-\alpha_1} \quad (5)$$

$$c_2 = \frac{(y - x\alpha_1)(1+\alpha_2^2)}{\alpha_2-\alpha_1} \quad (6)$$

where $x = (k'_{ij}-k_{\infty ij}) / (k_{oij}-k_{\infty ij})$ and $y = k''_{ij} / (k_{oij}-k_{\infty ij})$. The term $\alpha = \omega\tau$ and suffices 1 and 2 are, however, related to τ_1 and τ_2 respectively.

Adding equations (5) and (6) one gets,

$$\frac{k_{oij}-k'_{ij}}{k'_{ij}-k_{\infty ij}} = \omega(\tau_1+\tau_2)\frac{k''_{ij}}{k'_{ij}-k_{\infty ij}} - \omega^2\tau_1\tau_2 \quad (7)$$

as a linear equation having intercept $-\omega^2\tau_1\tau_2$ and slope $\omega(\tau_1+\tau_2)$ which are obtained from the measured dielectric constants at different w_j's of solutes under a single frequency electric field at a given temperature by applying linear regression technique and ω = the angular frequency $= 2\pi f$, f being the frequency in GHz.

Assuming a single broad Debye like dispersion for the polar molecules the equation (7) is reduced to the form [8] with $\tau_1 = 0$;

$$\frac{k_{oij} - k'_{ij}}{k'_{ij} - k_{\infty ij}} = \omega\tau_2 \frac{k''_{ij}}{k'_{ij} - k_{\infty ij}} \qquad (8)$$

in order to get τ_2 for seven polar-nonpolar liquid mixtures placed in the 11th column of Table 1.

Table – 1 : The estimated relaxation times τ_2 and τ_1 from the slopes and intercepts of the straightline equ (7) with errors and correlation coefficients (r) together with measured τ from $\sigma''_{ij} - \sigma'_{ij}$ curve and τ_2's from single broad dispersion for apparently rigid aliphatic molecules at 30^0C under different frequencies of electric fields.

System with sl. no. & mol.wt. in Kg.	Frequency in GHz (f)	Intercept & slope of equ (7)		Correlation coefficient (r)	% of error in regression technique	Estimated values of τ_2 and τ_1 in psec		Measured τ in psec.	Reported τ in psec	τ_2's in psec from single broad dispersion of equ (8)
		m	c							
(I) chloral in benzene	(a) 4.2	-0.3872	-0.0732	-0.91	5.54	5.27	--	4.77	--	4.78
	(b) 9.8	3.7238	0.5497	0.99	0.09	57.98	2.50	2.36	1.78*	--
M_j = 0.1475Kg	(c) 24.6	-0.1936	-0.2161	-0.41	25.08	2.45	--	1.73	--	2.01
(II) chloral in n-heptane	(a) 4.2	-2.7611	-0.4191	-0.78	12.81	5.44	--	3.74	--	40.87
	(b) 9.8	1.6593	0.1040	0.93	3.89	25.89	1.06	1.82	0.46*	--
M_j = 0.1475Kg	(c) 24.6	1.7458	0.1752	0.95	2.56	10.60	0.69	0.91	--	--
(III) ethyltri chloroacetate	(a) 4.2	0.3545	-0.0699	0.37	23.75	18.78	--	23.00	--	18.71
	(b) 9.8	1.5123	-0.1797	0.96	1.87	26.36	--	7.28	6.5**	32.53
in benzene M_j = 0.1915Kg	(c) 24.6	-2.7470	-3.3227	-0.24	25.86	5.88	--	3.34	--	37.19
(IV) ethyltri chloroacetate	(a) 4.2	-1.7251	-0.9325	-0.26	25.68	16.38	--	16.53	--	20.13
	(b) 9.8	1.5182	0.0549	0.66	15.40	24.05	0.60	6.28	5.7**	--
in n-hexane M_j = 0.1915Kg	(c) 24.6	2.9891	1.6141	0.98	0.83	14.76	4.58	5.76	--	--

* Cole-Cole plot ** Gopalakrishna's method

Again, the complex hf conductivity σ_{ij}^{*} is related to k_{ij}' and k_{ij}'' by the relation :

$$\sigma_{ij}^{*} = \sigma_{ij}' + j\sigma_{ij}''$$

where $\sigma_{ij}' = \omega \varepsilon_o k_{ij}''$ and $\sigma_{ij}'' = \omega \varepsilon_o k_{ij}'$ are the real and imaginary parts of the complex conductivity, σ_{ij}^{*}.

The magnitude of total hf conductivity is given by :

$$\sigma_{ij} = \omega \varepsilon_o (k_{ij}''^2 + k_{ij}'^2)^{1/2} \qquad (9)$$

σ_{ij}'' is related to σ_{ij}' by the relation :

$$\sigma_{ij}'' = \sigma_{\infty ij} + (1/\omega\tau)\ \sigma_{ij}' \qquad (10)$$

where τ is the measured relaxation time of a polar unit and $\sigma_{\infty ij}$ is the constant conductivity at $w_j \to 0$.

In the hf region, total conductivity $\sigma_{ij} \cong \sigma_{ij}''$, hence equation (10) is written as :

$$\sigma_{ij} = \sigma_{\infty ij} + (1/\omega\tau)\ \sigma_{ij}'$$

$$\text{or } (d\sigma_{ij} / dw_j)_{w_j \to 0} = (1/\omega\tau) (d\sigma_{ij}' / dw_j)_{w_j \to 0}$$

$$\text{or } \beta = (1/\omega\tau) (d\sigma_{ij}' / dw_j)_{w_j \to 0} \qquad (11)$$

The real part of hf conductivity σ_{ij}' at T K for w_j of a solute is [13-14] :

$$\sigma_{ij}' = \frac{N\rho_{ij}\mu_j^2}{27\varepsilon_o k_B T M_j} \left(\frac{\omega^2\tau}{1+\omega^2\tau^2}\right) (\varepsilon_o k_{oij} + 2) (\varepsilon_o k_{\infty ij} + 2) w_j \qquad (12)$$

On differentiation with respect to w_j and at $w_j \to 0$, equation (12) becomes :

$$\left(\frac{d\sigma_{ij}'}{dw_j} \right)_{w_j \to 0} = \frac{N\rho_i\mu_j^2}{3\varepsilon_o k_B T M_j} \left(\frac{\varepsilon_i + 2}{3} \right)^2 \left(\frac{\omega^2\tau}{1+\omega^2\tau^2} \right) \qquad (13)$$

where all the symbols expressed in S I units carry usual meanings [14].
From equations (11) and (13) one gets hf dipole moment μ_j from :

$$\mu_j = \left(\frac{27\varepsilon_o k_B T M_j}{N\rho_i (\varepsilon_i + 2)^2} \frac{\beta}{\omega b} \right)^{1/2} \qquad (14)$$

The dimensionless parameter b is related to τ by :

$$b = 1/(1+\omega^2\tau^2) \qquad (15)$$

All the μ_j's, b's and β's as computed for chloral and ethyltrichloroacetate are presented in Table 2.

Table-2 : Estimated intercept and slope of σ_{ij} - w_j equations, dimensionless parameters b_2, b_1 [equ. (15)], estimated dipole moments μ_2, μ_1 [equ (14)], μ_{theo} from bond angles and bond moments together with μ_1 from $\mu_1 = \mu_2 (c_1 / c_2)^{1/2}$ and reported μ in Coulomb-metre (C.m).

System with sl. no. & mol.wt. in Kg.	Frequency in GHz (f)	Intercept & slope of σ_{ij} against w_j equations		Dimensionless parameter		Estimated dipole moments in C.m.		Reported $\mu \times 10^{30}$, in C.m	Estimated $\mu_1 \times 10^{30}$ in C.m from $\mu_1 = \mu_2 (c_1 / c_2)^{1/2}$	$\mu_{theo} \times 10^{30}$ in C.m
		$\alpha \times 10^{-10}$	$\beta \times 10^{-10}$	b_1	b_2	$\mu_2 \times 10^{30}$	$\mu_1 \times 10^{30}$			
(I) chloral in benzene M_j = 0.1475Kg	(a) 4.2	5.990	4.208	--	0.981	5.02	--	5.01*	--	
	(b) 9.8	13.791	10.800	0.977	0.073	19.32	5.27	4.87**	13.26	10.02
	(c) 24.6	34.880	26.010	--	0.875	5.46	--	5.28*	--	
(II) chloral in n-heptane M_j = 0.1475Kg	(a) 4.2	5.058	3.619	--	0.980	5.78	--	5.72*	--	
	(b) 9.8	11.772	6.001	0.996	0.282	9.07	4.83	6.00**	9.71	10.02
	(c) 24.6	29.631	16.513	0.989	0.271	9.69	5.08	5.10*	9.63	
(III) ethyltri chloroacetate in benzene M_j = 0.1915Kg	(a) 4.2	5.990	9.057	--	0.803	9.27	--	9.72*	--	
	(b) 9.8	14.100	10.334	--	0.275	11.07	--	6.50**	--	10.5
	(c) 24.6	34.188	39.357	--	0.548	9.67	--	8.05*	--	
(IV) ethyltri chloroacetate in n-hexane M_j = 0.1915Kg	(a) 4.2	4.984	5.599	--	0.843	8.97	--	8.99*	--	
	(b) 9.8	11.522	12.722	0.999	0.313	14.53	8.14	8.67**	17.15	10.5
	(c) 24.6	28.160	36.525	0.666	0.161	21.66	10.65	11.64*	16.37	

** Ref [5] * Computed from the conductivity.

The molecules under consideration are of complex type and only a few data are available under single frequency measurement. In the case of a continuous distribution of τ's between the two extreme values [12] of τ_1 and τ_2, Fröhlich's theory [11] based on distribution of τ yields :

$$x = \frac{k_{ij}' - k_{\infty ij}}{k_{oij} - k_{\infty ij}} = 1 - \frac{1}{2A} \ln \left(\frac{1+\omega^2\tau_2^2}{1+\omega^2\tau_1^2} \right) \quad (16)$$

$$y = \frac{k_{ij}''}{k_{oij} - k_{\infty ij}} = \frac{1}{A} [\tan^{-1}(\omega\tau_2) - \tan^{-1}(\omega\tau_1)] \quad (17)$$

where A = Fröhlich parameter = ln (τ_2 / τ_1). The theoretical values of x and y of equations (16) and (17) were used to get c_1 and c_2. The values of c_1 and c_2 can be had from the graphical plots of x and y at $w_j \rightarrow 0$ as seen in Figures 4 and 5 respectively. c_1 and c_2 thus obtained by both the methods are shown in Table 3 for comparison.

Table – 3. Fröhlich parameter A, relative contributions c_1 and c_2 due to τ_1 and τ_2, theoretical values of x and y from Fröhlich's equations (16) and (17) and from fitting equations as shown in Figures 4 and 5 at $w_j \rightarrow 0$ and symmetric and asymmetric distribution parameters γ and δ for the five polar – nonpolar liquid mixutres at 30^0C.

System with sl. no.	Frequency in GHz (f)	Fröhlich parameter A= $\ln(\tau_2/\tau_1)$	Theoretical values of x and y from equs.(16) & (17)		Theoretical values of c_1 and c_2		Estimated values of x and y at $w_j \rightarrow 0$		Estimated values of c_1 and c_2		Estimated values of γ and δ	
			x	y	c_1	c_2	x	y	c_1	c_2	γ	δ
(I) chloral in benzene	(b) 9.8	3.14	0.587	0.364	0.52	1.10	0.362	0.228	0.32	0.69	0.42	0.38
(II) chloral in n-heptane	(b) 9.8	3.12	0.803	0.296	0.65	0.56	0.610	0.318	0.43	0.64	0.26	0.42
	(c) 24.6	2.73	0.763	0.336	0.60	0.61	0.671	0.287	0.54	0.52	0.29	0.35
(IV) ethyltrichloroacetate in n-hexane	(b) 9.8	3.69	0.843	0.255	0.69	0.49	0.44	0.284	0.26	0.59	0.34	0.42
	(c) 24.6	1.17	0.394	0.463	0.42	0.73	-0.32	0.383	-1.07	2.41	-0.62	--

The molecules under five different environments show double relaxation phenomena (Table 1) indicating their nonrigidity. In such cases dielectric relaxation behaviour may be represented by [3 - 4] :

$$\frac{k_{ij}^{*} - k_{\infty ij}}{k_{oij} - k_{\infty ij}} = \frac{1}{1+(j\omega\tau_s)^{1-\gamma}} \qquad (18)$$

$$\frac{k_{ij}^{*} - k_{\infty ij}}{k_{oij} - k_{\infty ij}} = \frac{1}{(1+j\omega\tau_{cs})^{\delta}} \qquad (19)$$

where γ and δ are symmetric and asymmetric distribution parameters which are, however, related to symmetric and characteristic relaxation times τ_s and τ_{cs} respectively.

Separating the real and the imaginary parts from equation (18) we have,

$$\gamma = \frac{2}{\pi} \tan^{-1} \left[(1-x)\frac{x}{y} - y \right] \qquad (20)$$

where $x = (k_{ij}' - k_{\infty ij}) / (k_{oij} - k_{\infty ij})$ and $y = k_{ij}'' / (k_{oij} - k_{\infty ij})$ are obtained at $w_j \rightarrow 0$ from Figures 4 and 5 respectively.

Similarly, δ can be calculated as :

$$\tan(\delta\phi) = y / x \tag{21}$$

$$\log(\cos\phi)^{1/\phi} = \frac{\log(x / \cos\phi\delta)}{\phi\delta} \tag{22}$$

where $\tan\phi = \omega\tau_{CS}$. To get δ, a theoretical curve of $\log(\cos\phi)^{1/\phi}$ against ϕ is drawn as seen in Figure 6. Knowing $\delta\phi$ from equation (21), ϕ can be found out from curve of Figure 6. With the known ϕ, δ can be estimated. γ and δ are entered in the 12th and 13th columns of Table 3.

3. RESULTS AND DISCUSSIONS

Figure 1 showed the linear variation of $(k_{oij} - k'_{ij}) / (k'_{ij} - k_{\infty ij})$ against $k''_{ij} / (k'_{ij} - k_{\infty ij})$ for different w_j's of chloral and ethyltrichloroacetate in different nonpolar solvents under 4.2, 9.8, and 24.6 GHz electric field frequencies at 30°C. The linearity is expressed in terms of correlation coefficients *r*'s as seen in Table 1. The percentage of errors in terms of *r*'s in the regression technique were calculated in order to place them in Table 1. The estimated values of τ_2 and τ_1 from intercepts and slopes of equation (7) are shown in the 7th and 8th columns of Table 1. Double relaxation phenomena are, however, observed for chloral in n-heptane and ethyltrichloroacetate in n-hexane at 9.8 and 24.6 GHz electric field. Chloral in benzene at 9.8 GHz also showed the same phenomenon. This observation reveals that the probability of showing double relaxation phenomena in aliphatic nonpolar solvents at higher frequencies is maximum for such rigid aliphatic polar liquids.The electrostatic interaction of polar molecules with π – delocalised electron cloud of C_6H_6 – ring increases the rigidity to show τ_2 only for the whole molecular rotation. The interaction appears to be absent for aliphatic polar liquids in alicyclic aliphatic nonpolar solvents and thus the double relaxation times τ_2 and τ_1 are seen to occur in higher frequencies for their flexibility. Chloral in C_6H_6 at 9.8 GHz is exception probably due to the fact that the effective dispersive region [15] lies near 10 GHz electric field for such system. τ_2's for the rest seven systems showing single relaxation phenomena were also calculated assuming single broad Debye like dispersion [8] in them. They are placed in the 11th column of Table 1. It is interesting to note that τ_1's for the five systems agree well with the measured τ from equation (10) of conductivity measurement. This fact shows that hf conductivity measurement always yields the average microscopic τ whereas the double relaxation phenomena offer a better understanding of microscopic as well as macroscopic molecular τ as observed elsewhere [9]. τ_2 of Table 1 is higher at 9.8 GHz and decrease gradually both at 4.2 GHz and 24.6 GHz electric fields in different solvents. This type of behaviour is probably due to larger size of the rotating unit in the effective dispersive region of nearly 10 GHz due to solute-solvent or solute-solute molecular associations which breakup with the increase or decrease from nearly 10 GHz electric field frequency. All the τ and τ_1 agree well with the available reported τ placed in the 10th column of Table 1 establishing the fact that the rotation of a part of the molecule is possible under hf electric field [16].

The dipole moments μ_2 and μ_1 of the polar molecules were calculated in terms of dimensionless parameters b's involved with τ's of equation (15) and slope β of $\sigma_{ij} - w_j$ curve of Figure 2 as seen in Table 2. The polar liquid in a given nonpolar solvent behaves as a bound charged species due to polarisation under GHz electric field in order to have very large hf conductivity

σ_{ij} x 10^{12} Ω^{-1} m^{-1} for different w_j's; although they are insulators. The parabolic variation of σ_{ij} x 10^{-12} Ω^{-1} m^{-1} with w_j's increases with the electric field frequency as found in Figure 2 yielding different slopes β's which are usually used to calculate hf μ_j of a ploar liquid from equation (14) and (15) at a given temparature. μ_2's are found to increase from 4.2 GHz electric fields for chloral in n-heptane and ethyltrichloro-acetate in n-hexane. This type of behaviour is probably due to rupture of solute-solute and solute-solvent molecular association in the hf electric field and the corresponding increase in the absorption for smaller molecular species [17]. But

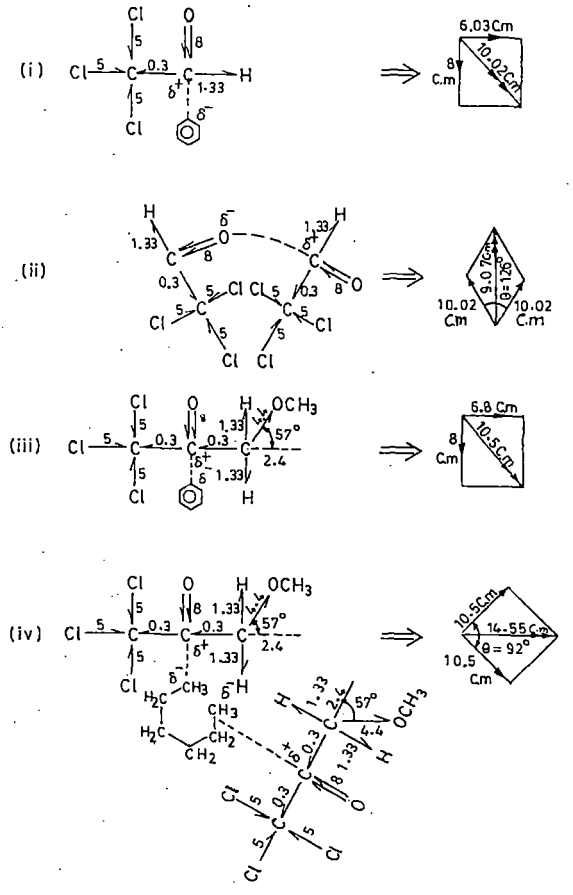

Figure 3 : Conformational structures of chloral and ethyltrichloroacetate from bond angles and bond moments in multiple of 10^{-30} Coulomb-metre. (i) Solute-solvent association of chloral in benzene; (ii) Solute-solute association of chloral; (iii) Solute-solvent association of ethyltrichloroacetate in benzene and (iv) Solute-solute association of ethyltrichloroacetate in n-hexane.

chloral and ethyltrichloroacetate in benzene show higher values of μ_2 at 9.8 GHz and decrease gradually from 24.6 GHz to 4.2 GHz electric fields. Such type of behaviour may be due to strong absorption of electric energy at 9.8 GHz and solute-solvent association of the polar solute with benzene ring. μ_2 and μ_1 are, however, compared with the μ_{theo}'s due to available bond angles and bond moments 8.0 x 10^{-30}, 5.0 x 10^{-30} 0.3 x 10^{-30} and 2.4 x 10^{-30} Coulomb-metre for > C ≤ O, C←Cl, C←C and C→OCH_3 (making an angle 57° with bond axis) respectively as displayed in Figure 3. μ_{theo}'s are placed in the 11th column of Table 2. The molecule chloral shows slightly larger μ_{theo} probably due to solute-solute molecular associations [Figure 3(ii)] in the comparatively concen-trated solution as expected. The solute-solute association may arise due to interaction of fractional positive charge δ^+ on C atom and negative charge δ^- on O atom of > C ≤ O group between two solute molecules. The solute-solvent association with benzene is explained on the basis of the interaction between C atom of > C ≤ O group and π – delocalised electron cloud of C_6H_6 ring. Ethyltrichloroacetate, on the other hand, shows μ_{theo} in agreement with the estimated

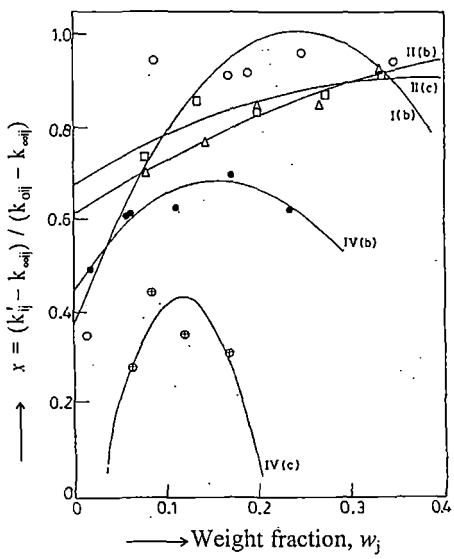

Figure 4 : Variation of $x = (k'_{ij} - k_{\infty ij})/(k_{oij} - k_{\infty ij})$ against different w_j's of chloral and ethyltrichloroacetate at 30°C under various frequencies of GHz range. I(b) for chloral in benzene at 9.8 GHz (O); II(b) and II(c) for chloral in n-heptane at 9.8 and 24.6 GHz (△, □); IV(b) and IV(c) for ethyltrichloroacetate in n-hexane at 9.8 and 24.6 GHz. (●, ⊕)

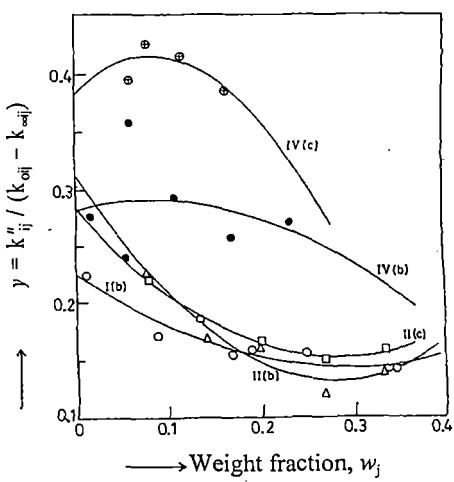

Figure 5 : Variation of $y = k''_{ij} / (k_{oij} - k_{\infty ij})$ against different w_j's of chloral and ethyltrichloroacetate at 30°C under various frequencies of GHz range. I(b) for chloral in benzene at 9.8 GHz (O); II(b) and II(c) for chloral in n-heptane at 9.8 and 24.6 GHz (△, □); IV(b) and IV(c) for ethyltrichloroacetate in n-hexane at 9.8 and 24.6 GHz. (●, ⊕)

μ_j's in C_6H_6. This is due to solute-solvent association as sketched in Figure 3[(i) and (iii)] which confirms the orientation of the bond angles and bond moments of the substituents polar groups of the molecules in C_6H_6. The slight disagreement between the observed and the theoretical μ's may be either due to the steric hindrances or the mesomeric, inductive and electromeric effects existing within the polar groups attached to the parent ones. Larger values of measured μ_j's invariably suggest the solute-solute interactions in alicyclic solvent n-hexane due to interaction between adjacent C and O atoms of $> C \leftarrow O$ groups of two molecules as shown in Figure 3 [(ii) and (iv)]. However, the reduced bond moments by μ_j / μ_{theo}'s in agreement with the estimated μ_j's reveals the mesomeric, inductive and electromeric effects within the polar groups of the molecules under consideration.

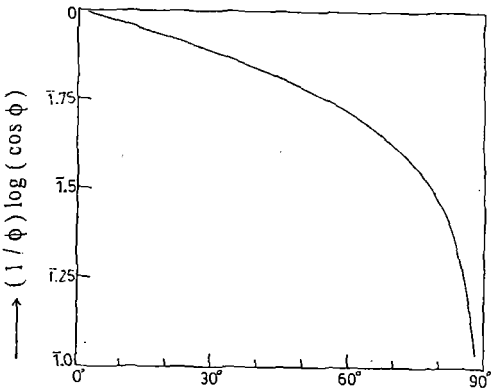

Figure 6 : Plot of (1 / ϕ) log (cos ϕ) against ϕ in degree.

The relative contributions c_1 and c_2 toward dielectric dispersions due to τ_1 and τ_2 are : however, calculated from $x = (k'_{ij} - k_{\infty ij}) / (k_{oij} - k_{\infty ij})$ and $y = k''_{ij} / (k_{oij} - k_{\infty ij})$ of equations (16) and (17) of Fröhlich's methods [11]. They are compared with those due to x and y from graphical methods of Figures 4 and 5 at $w_j \rightarrow 0$. Both the methods yield $c_1 + c_2 \cong 1$ suggesting the applicability of the methods. The nature of variation of x and y with w_j is convex and concave (except ethyltricchloroacetate in n-hexane at 9.8 and 24.6 GHz) which is not usual as observed earlier [7 - 8]. Such type of behaviour explained that unlike increase of τ [18] it decreases with w_j probably due to solute-solute and solute-solvent molecular association. All the values of c_1 and c_2 are placed in Table 3 for comparison. In order to test the rigidity of the molecules the symmetric and asymmetric distribution parameters γ and δ were estimated from equations (20) and (21) for fixed values of x and y at $w_j \rightarrow 0$ of Figures 4 and 5. The values of $(1/\phi)$ log $(\cos\phi)$ against ϕ in degree as shown in Figure 6, is essential to get δ knowing ϕ from the curve of Figure 6 : δ's were obtained. Both γ and δ are placed in Table 3. The values of γ establish the fact that the molecules obey the symmetric relaxation phenomena as δ's are very low [19].

4. CONCLUSION

The study of dielectric relaxation mechanism by dimensionless dielectric constants gives a new insight into polar-polar and polar-nonpolar molecular interactions. The single frequency measurement of dielectric relaxation parameters provides a unique method to get macroscopic and microscopic relaxation times τ_2 and τ_1 and hence dipole moments μ_2 and μ_1 of the whole and the flexible part of the molecule. The estimation of τ_j or τ_1 and τ_2 from a linear equation is very simple and straightforward to get μ_j or μ_1 and μ_2 in terms of slope of $\sigma_{ij} - w_j$ curve. The errors in

measurement of τ_j and μ_j can be computed by correlation coefficients and are claimed to be accurate within 10% and 5% respectively. The molecules under different states of environment show interesting phenomena of double or single relaxation mechanism. When the solute-solvent molecular interaction is almost absent in the polar solute in alicyclic aliphatic solvent; flexible part alongwith the whole molecule rotates under hf electric field giving rise what is known as double relaxation. The solute-solvent association, on the other hand, favours the existence of single relaxation phenomena by the whole molecular rotations as π–delocalised electron clouds of solvent interact with the flexible parts to cease their rotations. The probability of showing double relaxation is, thus greater in aliphatic solvents. Various types of molecular associations like solute-solute and solute-solvent interactions are inferred from departure of the graphical plots of $x = (k'_{ij} - k_{\infty ij})/(k_{oij} - k_{\infty ij})$ and $y = k''_{ij} / (k_{oij} - k_{\infty ij})$ with w_j of Bergmann's equations. Nonrigid characteristics of the molecules are confirmed by estimation of symmetric γ and asymmetric distribution parameter δ. The molecular associations are also supported by the conformational structures of the molecules in which the presence of mesomeric, inductive and electromeric moments due to > C ≤ O group are found to play their vital role. The correlation between the conformational structures of such polar liquids with the observed results enhances the scientific content of the paper in order to add a better understanding of the existing knowledge of dielectric relaxation phenomena.

5. ACKNOWLEDGEMENT

The authors are thankful to Mr. A. Chowdhury for computational works.

REFERENCES

1. A.K. Sharma, D.R. Sharma and D.S. Gill, J. Phys. D : Appl. Phys **18** (1985) 1199.
2. A. Sharma and D.R. Sharma, J. Phys. Soc. Japan **61** (1992) 1049.
3. K.S. Cole and R.H. Cole, J. Chem. Phys. **9** (1941) 341.
4. D.W. Davidson and R.H. Cole, J. Chem. Phys. **19** (1951) 1484.
5. K.V. Gopalakrishna, Trans. Faraday Soc. **53** (1957) 767.
6. S.K. Srivastava and S.L. Srivastava, Indian J. Pure Appl. Phys. **13** (1975) 179.
7. U. Saha, S.K. Sit, R.C. Basak and S. Acharyya, J. Phys. D : Appl. Phys. **27** (1994) 596.
8. S.K. Sit, R.C. Basak, U. Saha and S. Acharyya, J. Phys. D : Appl. Phys. **27** (1994) 2194.
9. S.K. Sit and S. Acharrya, Indian J. Phys. **70B** (1996) 19.
10. S.K. Sit, N. Ghosh and S. Acharyya, Indian J. Pure Appl. Phys. **35** (1997) 329.
11. H. Fröhlich, Theory of Dielectrics (Oxford : Oxford University Press) (1949) P 94.
12. K. Bergmann, D.M. Roberti and C.P. Smyth, J. Phys. Chem. **64** (1960) 665.
13. C.P. Smyth, Dielectric Behaviour and Structure (New York : McGrawHill) (1955).
14. R.C. Basak, A.K. Karmakar, S.K. Sit and S. Acharyya, Indian J. Pure Appl. Phys. **37** (1999) 224.
15. S.K. Sit and S. Acharyya, Indian J. Pure Appl. Phys. **34** (1996) 255.
16. R.C. Basak, S.K. Sit, N. Nandi and S. Acharyya, Indian J. Phys **70B** (1996) 37.
17. L. Glasser, J. Crossley and C.P. Smyth, J Chem. Phys. **57** (1972) 3977.
18. S.N. Sen and R. Ghosh, Indian J. Pure Appl. Phys. **10** (1972) 701.
19. S. Chandra and J. Prakash, J. Phys. Soc. Japan **35** (1975) 876.

ELSEVIER

Journal of Molecular Liquids 89 (2000) 111–126

journal of MOLECULAR LIQUIDS

www.elsevier.nl/locate/molliq

Double relaxation times, dipole moments, energy parameters and molecular structures of some aprotic polar molecules from relaxation phenomena.

S K Sit[a], K Dutta[a], S Acharyya[a], T Pal Majumder[b] and S Roy[b]

[a] Department of Physics, Raiganj College (University College)
P.O. Raiganj, Dist. Uttar Dinajpur (W.B.) 733134, India

[b] Department of Spectroscopy, Indian Association for the Cultivation of Science, Calcutta-32, (W.B.), India

Received 20 January 2000; accepted 20 October 2000

ABSTRACT

The real ε'_{ij} and imaginary ε''_{ij} parts of complex dielectric constant ε^*_{ij} of some aprotic polar molecules (j) like dimethylsulphoxide (DMSO) : N, N-diethylformamide (DEF) : N, N-dimethylformamide (DMF) and N,N-dimethylacetamide (DMA) in benzene (i) for different weight fractions w_j's of solutes are located at different temperatures under nearly 10 GHz electric field together with the static and infinite frequency dielectric constants ε_{oij} and $\varepsilon_{\infty ij}$. All the molecules show the double relaxation times τ_1 and τ_2 for rotations of their flexible parts and the whole molecules by the single frequency measurement technique. The τ_1 in agreement with reported τ signifies that a part of the molecule is rotating under 10 GHz electric field. It is also supported by energy parameters ΔH_τ, ΔS_τ and ΔF_τ measured from ln (τ T) against 1/T curves for DMSO. The relative contributions c_1 and c_2 towards dielectric relaxations for τ_1 and τ_2 are ascertained from Fröhlich's equations and graphical technique. The corresponding dipole moments μ_2 and μ_1 of the whole and the flexible part of the molecule are obtained from τ_2 and τ_1 and the slope β of high frequency conductivity σ_{ij} against w_j in order to compare with the measured static μ_s and reported μ's. μ_1's are found to agree with μ_j and static μ_s. The molecular conformational structures are obtained by μ_{cal} from μ_s/μ_{theo} by considering mesomeric and inductive effects of the substituent polar groups. μ_{theo}'s are obtained from available bond moments and bond angles. The comparison of all the μ's shows little dependence on electric field frequency.

1. INTRODUCTION

The absorbtion of high frequency electric energy by aprotic polar liquids in nonpolar solvents has attracted much attention [1-2]. Such liquids have wide biological applications and act as building blocks of proteins and enzymes because of their high values of dielectric constants. They showed weak molecular association of monomer or dimer formation under the X-band (~10GHz) electric field. Many workers [3-4] studied their structural and associational aspects in high frequency (f) electric field by using the concentration variation method of Gopalakrishna [5]. However no attempt has been made so far to observe their double relaxation phenomena in nearly 10 GHz electric field which seems to be the most effective dispersive region [6] for them.

0167-7322/00/$ - see front matter
PII S0167-7322(00) 00164-1

Table 1. : Concentration variation of dielectric relaxation parameters like real part of dielectric constant (ε'_{ij}), dielectric loss (ε''_{ij}), static dielectric constant (ε_{oij}), optical dielectric constant ($\varepsilon_{\infty ij}$) of some aprotic polar liquids in benzene at different temperatures measured under high frequency electric field of nearly 10 GHz.

Temperature in ^{0} C	Weight fraction w_i	ε'_{ij}	ε''_{ij}	ε_{oij} at 1KHz	$\varepsilon_{\infty ij} = n^2_{Dij}$
	DMSO in C_6H_6 at 9.174 GHz				
	0.0022	2.311	0.0280	2.3230	2.2499
	0.0043	2.342	0.0420	2.3624	2.2530
25	0.0047	2.350	0.0460	2.3731	2.2550
	0.0069	2.381	0.0616	2.4173	2.2579
	0.0086	2.414	0.0798	2.4602	2.2620
	0.0022	2.310	0.0274	2.3210	2.2470
	0.0043	2.341	0.0400	2.3610	2.2515
30	0.0047	2.348	0.0440	2.3720	2.2500
	0.0069	2.370	0.0526	2.4045	2.2545
	0.0086	2.390	0.0648	2.4362	2.2560
	0.0022	2.290	0.0234	2.2993	2.2300
	0.0043	2.312	0.0330	2.3400	2.2320
35	0.0047	2.316	0.0360	2.3470	2.2335
	0.0069	2.350	0.0496	2.3960	2.2396
	0.0086	2.370	0.0580	2.4270	2.2440
	0.0022	2.270	0.0170	2.2849	2.2201
	0.0043	2.302	0.0282	2.3300	2.2246
40	0.0047	2.304	0.0286	2.3350	2.2256
	0.0069	2.338	0.0420	2.3838	2.2297
	0.0086	2.350	0.0500	2.4120	2.2345
	DEF in C_6H_6 at 9.695 GHz				
	0.0023	2.2780	0.0256	2.3067	2.0939
30	0.0042	2.2900	0.0288	2.3336	2.1141
	0.0079	2.3140	0.0384	2.3965	2.1543
	0.0095	2.3260	0.0448	2.4208	2.1727
	DMF in C_6H_6 at 9.987 GHz				
	0.0027	2.324	0.0256	2.3446	2.2498
25	0.0036	2.339	0.0302	2.3680	2.2518
	0.0048	2.359	0.0386	2.3968	2.2545
	0.0063	2.387	0.0484	2.4434	2.2579
	DMA in C_6H_6 at 9.987 GHz				
	0.0026	2.3250	0.0213	2.3633	2.2432
25	0.0045	2.3475	0.0278	2.3988	2.2429
	0.0056	2.3625	0.0330	2.4278	2.2427
	0.0066	2.3795	0.0381	2.4508	2.2425

We, therefore, measured real ε'_{ij} and imaginary ε''_{ij} parts of complex dielectric constant ε^*_{ij} of liquids (j) like dimethylsulphoxide (DMSO) at 25°, 30°, 35° and 40°C; N, N-diethylformamide (DEF) at 30°C; N, N-dimethylformamide (DMF) and N, N-dimethylacetamide (DMA) at 25°C in benzene (i) at nearly 10 GHz electric field by a Hewlett Packard Impedance Analyser 4192A together with the static and infinite frequency dielectric constants ε_{oij} (at 1 KHz) and $\varepsilon_{\infty ij}$ ($=n^2_{Dij}$)by Abbe's refractometer within 1% accuracy [7-8]. The measured data of Table 1 were used to detect their possible existence of double relaxation phenomena by the recently developed single frequency measurement [9–10] method.

The relaxation times τ_2 and τ_1 due to end over end rotation for the whole molecule as well as its flexible part attached to the parent one were obtained from the slope and intercept of a derived linear equation of $(\varepsilon_{oij}-\varepsilon'_{ij}) / (\varepsilon'_{ij}-\varepsilon_{\infty ij})$ with $\varepsilon''_{ij} / (\varepsilon'_{ij}-\varepsilon_{\infty ij})$ as seen graphically in Figure 1 for different weight fractions w_j of solutes [9-10]. The intercepts and slopes of the linear curves of Figure 1 together with % of errors in terms of correlation coefficients 'r' are placed in Table 2. τ_1 in Table 2 is very close to reported τ [5]. The relative contributions c_1 and c_2 towards dielectric relaxation due to τ_1 and τ_2 are calculated from the values of $x = (\varepsilon'_{ij}-\varepsilon_{\infty ij}) / (\varepsilon_{oij}-\varepsilon_{\infty ij})$ and $y = \varepsilon''_{ij} / (\varepsilon_{oij}-\varepsilon_{\infty ij})$ at $w_j \rightarrow 0$ from their respective plots with w_j's in Figures 2 and 3 respectively.

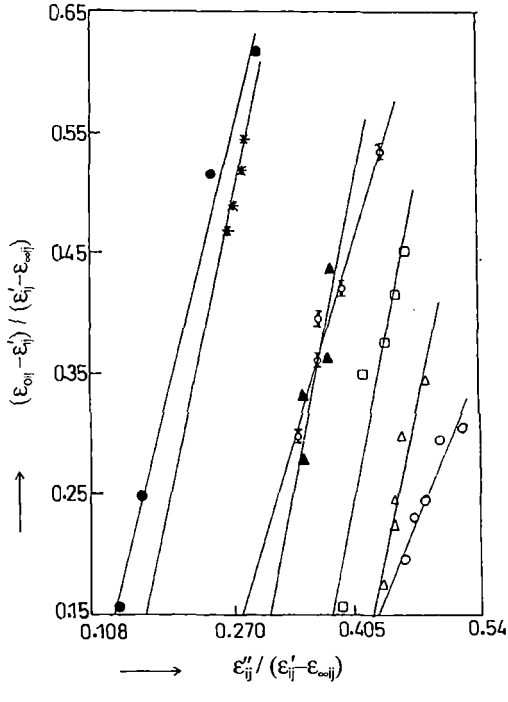

Figure 1. Variation of $(\varepsilon_{oij}-\varepsilon'_{ij}) / (\varepsilon'_{ij}-\varepsilon_{\infty ij})$ against $\varepsilon''_{ij} / (\varepsilon'_{ij}-\varepsilon_{\infty ij})$ for different weight fraction w_j of some aprotic polar liquids in benzene :
DMSO (– O –, – △ –, – □ –, – ◊ –) at 25°C, 30°C, 35°C and 40°C respectively; DEF (– ● –) at 30°C; DMF (– ▲ –) at 25°C; DMA (– ✱ –) at 25°C

The estimated values of c_1 and c_2 together with those from Fröhlich's equations [11-12] are presented in Table 3 for comparison.

Table 2. : The estimated intercepts and slopes of straight line equation of $(\varepsilon_{oij}-\varepsilon'_{ij}) / (\varepsilon'_{ij}-\varepsilon_{\infty ij})$ against $\varepsilon''_{ij} / (\varepsilon'_{ij}-\varepsilon_{\infty ij})$, correlation coefficients (r), % of error involved in regression technique, the most probable relaxation time $\tau_0 = \sqrt{\tau_1\tau_2}$ and reported τ of some nonspherical aprotic polar liquids under hf electric field of nearly 10 GHz.

System with Sl. no. & mol.wt.	Tem-pera-ture in ^{0}C	Intercept & slope of equ (11) m	c	Correlat ion coefficie nt (r)	% of error in regre-ssion tech-nique	Estimated values of τ_2 and τ_1 in psec		Most probable relaxation time $\tau_0=\sqrt{\tau_1\tau_2}$ in psec	Reported τ in psec. (G.K. Method)
(I) DMSO in C_6H_6 M_j = 78gm.	25	0.5671	1.6817	0.9605	2.34	21.08	8.10	13.07	5.37
(II) DMSO in C_6H_6 M_j = 78gm.	30	1.3024	3.4358	0.9429	3.35	52.11	7.53	19.81	4.96
(III) DMSO in C_6H_6 M_j = 78gm.	35	1.2899	3.8162	0.9377	3.64	59.73	6.51	19.72	4.70
(IV) DMSO in C_6H_6 M_j = 78gm.	40	0.5376	2.4880	0.9862	0.83	39.04	4.15	12.73	4.33
(V) DEF in C_6H_6 M_j = 101.15gm.	30	0.2592	3.0829	0.9933	0.45	49.21	1.42	8.36	2.42
(VI) DMF in C_6H_6 M_j = 73gm.	25	1.0183	3.8186	0.8896	7.03	56.28	4.60	16.09	5.09
(VII) DMA in C_6H_6 M_j = 87gm.	25	0.4936	3.7032	0.9011	6.34	56.81	2.21	11.20	6.53

The dipole moments μ_2 and μ_1 of the whole and the flexible part attached to the parent molecule due to τ_2 and τ_1 in terms of slopes β's of high frequency conductivities σ_{ij} against w_j's [13] of Figure 4 were estimated to present in Table 4. The variation of μ_2 and μ_1 of DMSO with temperature and the estimated thermodynamic energy parameters from $\ln(\tau_2 T)$ and $\ln(\tau_1 T)$ against 1/T respectively supports the rotation of flexible parts of molecule under GHz electric field. We have also calculated the static experimental parameter X_{ij} involved with ε_{oij} and n^2_{Dij} at different w_j's of solutes [14] (Table 1). The slopes a_i's of X_{ij}–w_j curves of Figure 5 were then used to calculate static dipole moment μ_s. All the μ_s's together with the slopes of X_{ij}–w_j curves are placed in Table 5. The μ_s of Table 5 when compared with μ_2 and μ_1 of Table 4 shows that μ_s agrees with μ_1. The conformational structures of molecules in Figure 6 were obtained from μ_{cal} in terms of reduced bond moments by a factor μ_s / μ_{theo} in order to take into account of the mesomeric and inductive effects of the substituent polar groups [14]. The theoretical dipole moment μ_{theo}'s of polar molecules are, however, derived from the available bond moments and bond angles of polar groups of the parent molecules.

2. EXPERIMENTAL SET UP

The Block diagram for the measurement of dielectric relaxation solution (ij) data and experimental details [7] has been shown in the adjoining Figure A. It consists of sample holder, temperature chamber, temperature controller and a Hewlett Packard Bridge 4192 A. A cell (Figure B) with a sample holder consists of two glass plates coated with conducting Indium Tin Oxide (ITO) in their inner surfaces. They are separated by mylar spacer of 40 μm thickness and kept on temperature chamber Mettler Hot Stage FP 52.

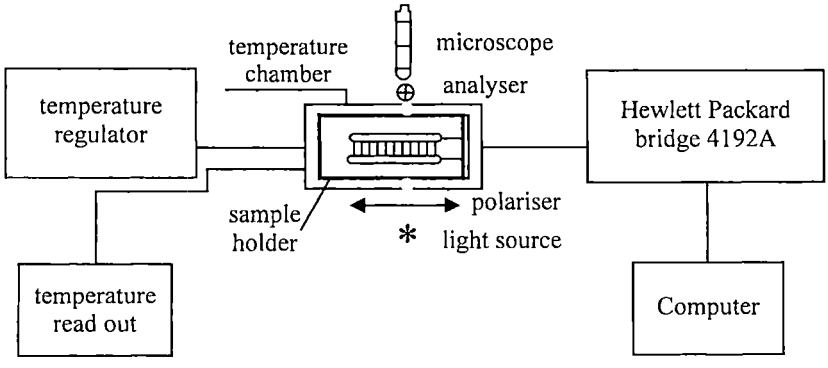

Figure A : Block diagram of the experimental setup used for dielectric measurements

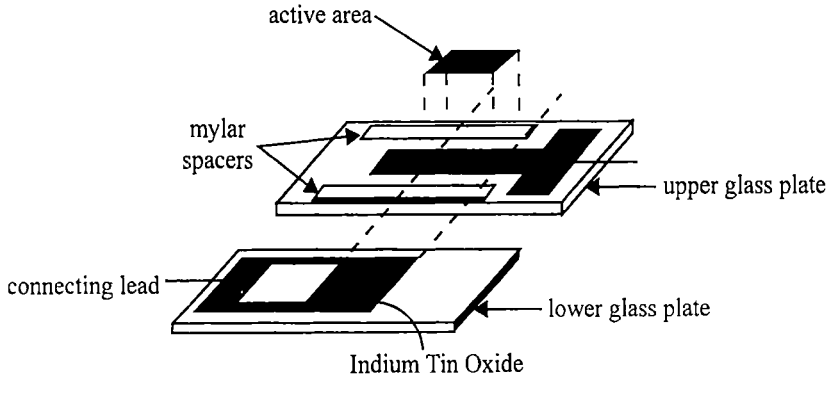

Figrure B : Inner surfaces of the lower and upper conducting glass plates.

The Hewlett Packard Impedance Analyser (HP 4192A) measures the complex impedance of the cell to evaluate capacitance and conductance values. Air capacitance C_0 of the cell can be written as

$$C_0 = C_L + C_S \tag{1}$$

where C_L is the capacitance of the empty cell excluding stray capacitance C_S. When the cell is filled with the sample of known dielectric constant ε_{ij}, the measured capacitance will be :

$$C = \varepsilon_{ij} C_L + C_S \tag{2}$$

The real part of the dielectric permittivity of the sample is given by :

$$\varepsilon'_{ij} = (C - C_S)/(C_0 - C_S) \tag{3}$$

The dielectric loss due to absorbtion is

$$\varepsilon''_{ij} = G_{ij} / 2\pi f C_0 \tag{4}$$

where G_{ij} and f are conductance of the solutions and frequency of the electric field.

The ITO electrode in GHz does not yield dielectric properties of the solution but rather those of the electrode materials because ITO is not sufficiently a good conductor and appropriate only upto a few MHz. The frequency range of the instrument HP 4192A was 5Hz to 13 MHz. ε'_{ij} and ε''_{ij} for a given w_j of solute under a few MHz frequencies were carefully measured to construct the Cole-Cole semicircular arc. Both $\varepsilon_{\infty ij}$ and ε_{oij} were then accurately obtained along with ε'_{ij} and ε''_{ij} within 5% accuracies at nearly 10 GHz to report in Table 1. The frequencies as quoted in Table 1 were found out from $(d\varepsilon''_{ij}/df)=0$ in $\varepsilon''_{ij} = a + bf + cf^2$ at which ε'_{ij} were again located. $\varepsilon_{\infty ij}$ and ε_{oij} were also verified by Abbe's refractometer and HP 4192A at 1KHz within 1% accuracy.

The solvent C_6H_6 (Spec.pure) and aprotic liquids like DMSO, DMF, DEF and DMA (E Merck, Bombay) were used after distillation. The solutions of different concentrations were made by mixing a certain weight of solute in a solvent of known weight. They were kept in dried and clean capsules for the measurement.

3. THEORETICAL FORMULATIONS

3.1. Relaxation times τ_2 and τ_1 :

The dielectric relaxation parameters under GHz electric field for two mutually independent Debye type dispersions [11] can be given by :

$$\frac{\varepsilon'_{ij} - \varepsilon_{\infty ij}}{\varepsilon_{oij} - \varepsilon_{\infty ij}} = \frac{c_1}{1+\omega^2\tau_1^2} + \frac{c_2}{1+\omega^2\tau_2^2} \tag{5}$$

$$\frac{\varepsilon''_{ij}}{\varepsilon_{oij} - \varepsilon_{\infty ij}} = c_1 \frac{\omega\tau_1}{1+\omega^2\tau_1^2} + c_2 \frac{\omega\tau_2}{1+\omega^2\tau_2^2} \tag{6}$$

Here c_1 and c_2 are the relative contributions towards dielectric relaxations due to τ_1 and τ_2 respectively.

Substituting $(\varepsilon_{ij}'-\varepsilon_{\infty ij}) / (\varepsilon_{oij}-\varepsilon_{\infty ij}) = x$ and $\varepsilon_{ij}'' / (\varepsilon_{oij}-\varepsilon_{\infty ij}) = y$ equations (5) and (6) become :

$$x = c_1 a_1 + c_2 a_2 \tag{7}$$

$$y = c_1 b_1 + c_2 b_2 \tag{8}$$

where $a = 1 / (1+\alpha^2)$, $b = \alpha / (1+\alpha^2)$ and $\omega\tau = \alpha$
The suffices 1 and 2 with a and b are related to τ_1 and τ_2 respectively.
Solving equations (7) and (8) one gets :

$$c_1 = \frac{(x\alpha_2 - y)(1+\alpha_1^2)}{\alpha_2 - \alpha_1} \tag{9}$$

$$c_2 = \frac{(y - x\alpha_1)(1+\alpha_2^2)}{\alpha_2 - \alpha_1} \tag{10}$$

provided $\alpha_2 - \alpha_1 \neq 0$ and $\alpha_2 > \alpha_1$
Now, using $c_1 + c_2 = 1$; one gets from equations (9) and (10)

$$\frac{\varepsilon_{oij} - \varepsilon_{ij}'}{\varepsilon_{ij}' - \varepsilon_{\infty ij}} = \omega(\tau_1 + \tau_2) \frac{\varepsilon_{ij}''}{\varepsilon_{ij}' - \varepsilon_{\infty ij}} - \omega^2 \tau_1 \tau_2 \tag{11}$$

which is a straight line of $(\varepsilon_{oij} - \varepsilon_{ij}') / (\varepsilon_{ij}' - \varepsilon_{\infty ij})$ against $\varepsilon_{ij}'' / (\varepsilon_{ij}' - \varepsilon_{\infty ij})$ with intercept $-\omega^2\tau_1\tau_2$ and slope $\omega(\tau_1 + \tau_2)$. Here ω = angular frequency of the applied electric field of frequency f in GHz. The equation (11) is fitted with the measured ε_{ij}', ε_{ij}'', ε_{oij} and $\varepsilon_{\infty ij}$ of Table 1 for each aprotic polar liquid in C_6H_6 for different w_j's at a given temperature T K. The slope and intercept were used to yield τ_1 and τ_2, as shown in Table 2, with the reported τ [5].

Fröhlich's theory of dielectric relaxation is based on the concept of a distribution of relaxation times with a minimum τ_1 and a maximum τ_2 values. The double relaxation method is, however, concerned with these two discrete relaxation times as the limiting values of Fröhlich's theory [12]. c_1 and c_2 towards dielectric relaxations are, therefore, calculated from the theoretical formulations of x and y of Fröhlich [12].

$$x = \frac{\varepsilon_{ij}' - \varepsilon_{\infty ij}}{\varepsilon_{oij} - \varepsilon_{\infty ij}} = 1 - \frac{1}{2A} \ln\left(\frac{1+e^{2A}\omega^2\tau_S^2}{1+\omega^2\tau_S^2}\right) \tag{12}$$

$$y = \frac{\varepsilon_{ij}''}{\varepsilon_{oij} - \varepsilon_{\infty ij}} = \frac{1}{A}\left[\tan^{-1}(e^A\omega\tau_S) - \tan^{-1}(\omega\tau_S)\right] \tag{13}$$

and are shown in Table 3. Here τ_S = small limiting relaxation time = τ_1 and A=Fröhlich parameter = $\ln(\tau_2 / \tau_1)$. 'A' is a constant which can be expressed in terms of the difference in activation energies E_2 and E_1 of a rotating unit at a given temperature because $\tau_2 / \tau_1 = \exp(E_2 - E_1) / k_BT$ where k_B is the Boltzmann constant. The values of x and y at $w_j \rightarrow 0$ from the graphical plots of Figures 2 and 3 can also be had to get c_1 and c_2. The L.H.S. of Bergmann's equations [11] are fixed for once estimated τ_1 and τ_2 from the intercept and slope of equation (11).

Table 3. : Fröhlich parameter A, relative contributions c_1 and c_2 due to τ_1 and τ_2, theoretical values of x and y due to Fröhlich equations (12) and (13) and those by graphical method at infinite dilution for some aprotic polar liquids at different and single temperature under hf electric field

System with sl. no.	Tem pera ture in ^{0}C	Fröhlich parameter A= $\ln(\tau_2/\tau_1)$	Theoretical values of x and y from equations (12) & (13)		Theoretical values of c_1 and c_2 from equations (9) & (10)		Estimated values of x and y at $w_j \rightarrow 0$ from figures 2 & 3		Estimated values of c_1 and c_2 from graphical technique	
			x	y	c_1	c_2	x	y	c_1	c_2
(I) DMSO in C_6H_6	25	0.9565	0.629	0.466	0.486	0.569	0.892	0.363	1.174	-0.178
(II) DMSO in C_6H_6	30	1.9345	0.449	0.434	0.423	0.934	0.900	0.338	1.094	-0.206
(III) DMSO in C_6H_6	35	2.2165	0.454	0.419	0.425	1.043	0.834	0.295	0.958	-0.075
(IV) DMSO in C_6H_6	40	2.2415	0.610	0.409	0.507	0.794	0.848	0.225	0.885	0.067
(V) DEF in C_6H_6	30	3.5454	0.677	0.328	0.588	0.924	0.988	0.055	1.006	-0.104
(VI) DMF in C_6H_6	25	2.5043	0.497	0.405	0.451	1.086	0.872	0.210	0.959	-0.173
(VII) DMA in C_6H_6	25	3.2467	0.600	0.357	0.530	1.096	0.736	0.126	0.743	0.096

Table 4. : The estimated coefficients α, β and γ of $\sigma_{ij} - w_j$ curves (Figure 4), dimensionless parameters b_2 and b_1, dipole moments μ_j's in Debye of some nonspherical aprotic polar liquids in benzene under hf electric field of nearly 10 GHz at single and different temperatures.

System with sl. no. & mol.wt.	Tem perat ure in ^{0}C	Co-efficients α, β and γ of $\sigma_{ij}\times10^{-10} = \alpha + \beta w_j + \gamma w_j^2$ in $\Omega^{-1}cm^{-1}$			Dimensionless parameters		Estimated dipole moments in Debye		Reported dipole moment μ_j in Debye
					b_2	b_1	μ_2	μ_1	
(I) DMSO in C_6H_6 M_j = 78gm.	25	1.047	5.649	157.35	0.4040	0.8212	4.67	3.28	3.79
(II) DMSO in C_6H_6 M_j = 78gm.	30	1.043	8.180	-231.74	0.0999	0.8416	11.47	3.95	3.83
(III) DMSO in C_6H_6 M_j = 78gm.	35	1.040	4.158	164.83	0.0779	0.8767	9.38	2.80	4.04
(IV) DMSO in C_6H_6 M_j = 78gm.	40	1.023	8.897	-274.83	0.1650	0.9459	9.55	3.99	4.11
(V) DEF in C_6H_6 M_j = 101.15gm.	30	1.098	2.839	32.45	0.1002	0.9926	7.47	2.38	3.88
(VI) DMF in C_6H_6 M_j = 73gm.	25	1.141	6.544	245.95	0.0743	0.9232	10.88	3.09	3.62
(VII) DMA in C_6H_6 M_j = 87gm.	25	1.153	1.884	533.11	0.0729	0.9811	6.43	1.75	3.37

3.2. High frequency dipole moments μ_1, μ_2 of τ_1, τ_2 :

The high frequency complex conductivity σ^*_{ij} of liquid mixture is expressed by $\sigma^*_{ij} = \sigma'_{ij} + j\sigma''_{ij}$ while the total conductivity is

$$\sigma_{ij} = (\omega / 4\pi)\ (\varepsilon'^{2}_{ij} + \varepsilon''^{2}_{ij})^{1/2} \tag{14}$$

as a function of w_j. Although ε''_{ij} offers resistance to polarisation, still in the hf region $\varepsilon'_{ij} >> \varepsilon''_{ij}$. The real part of hf conductivity is [13] :

$$\sigma'_{ij} = \frac{N\rho_{ij}\mu_j^2 F_{ij}}{3k_B TM_j} \left(\frac{\omega^2\tau}{1+\omega^2\tau^2}\right) w_j$$

which on differentiation with respect to w_j and at $w_j \to 0$ yields :

$$\left(\frac{d\sigma'_{ij}}{dw_j}\right)_{w_j \to 0} = \frac{N\rho_i\mu_j^2 F_i}{3k_B TM_j} \left(\frac{\omega^2\tau}{1+\omega^2\tau^2}\right) \tag{15}$$

where F_{ij} = the local field of the solution = $(\varepsilon_{ij}+2)^2 / 9$. F_{ij} becomes F_i and ρ_{ij} tends to ρ_i at $w_j \to 0$, where $F_i = (\varepsilon_i+2)^2 / 9$. ε_i and ρ_i are the dielectric constant and density of the solvent respectively. The other symbols carry usual significance [9,10].
Again, since $\sigma_{ij} = (\omega\varepsilon'_{ij} / 4\pi)$ we have

$$\sigma_{ij} = \sigma_{\infty ij} + (1/\omega\tau)\ \sigma'_{ij}$$

$$\text{or, } (d\sigma'_{ij} / dw_j)_{w_j \to 0} = \omega\tau\ (d\sigma_{ij} / dw_j)_{w_j \to 0} = \omega\tau\beta \tag{16}$$

where β is the slope of σ_{ij}– w_j curve at $w_j \to 0$.
From equations (15) and (16) one gets

$$\mu_j = \left(\frac{27k_B TM_j}{N\rho_i (\varepsilon_i+2)^2} \frac{\beta}{\omega b}\right)^{1/2} \tag{17}$$

in order to obtain μ_1 or μ_2 in terms of b_1 and b_2 where b_1 and b_2 are the dimensionless parameters involved with τ_1 and τ_2 i.e.

$$b_1 = 1 / (1 + \omega^2\tau_1^2) \quad \text{and} \quad b_2 = 1 / (1+\omega^2\tau_2^2) \tag{18}$$

Both b_1 and b_2 as well as the coefficients α,β and γ of σ_{ij}– w_j equations of curves in Figure 4 are shown in Table 4 together with μ_1 and μ_2 of the flexible part and the whole molecule of a polar liquid.

3.3. Static dipole moments :

The Debye equation for a polar nonpolar liquid mixture of w_j of a polar liquid under static or low frequency electric field at a given T K is [14]

$$\frac{\varepsilon_{oij} - n^2_{Dij}}{(\varepsilon_{oij}+2)(n^2_{Dij}+2)} = \frac{\varepsilon_{oi} - n^2_{Di}}{(\varepsilon_{oi}+2)(n^2_{Di}+2)} + \frac{4\pi N\mu_S^2\rho_i}{27k_B TM_j} w_j (1-\gamma w_j)^{-1}$$

$$\text{or, } X_{ij} = X_i + \frac{4\pi N\mu_S^2\rho_i}{27k_B TM_j} w_j + \frac{4\pi N\mu_S^2\rho_i}{27k_B TM_j} \gamma w_j^2 + \ldots \tag{19}$$

where X_{ij} and X_i are the static experimental parameters of the solution and solvent.
$\gamma = (1 - \rho_i / \rho_j)$, ρ_i and ρ_j are densities of pure solvent and solute respectively.
The usual variation of X_{ij} with w_j is of the form :

$$X_{ij} = a_0 + a_1 w_j + a_2 w_j^2 \quad (20)$$

satisfying the experimental curves of Figure 5. The coefficients a_0, a_1 and a_2 of equation (20) with the measured data of Table 1 were, however, calculated and are placed in Table 5. Equating the first power of w_j of equations (19) and (20) and neglecting terms of higher powers of w_j for their involvement with various interactions [14] one gets the static μ_s from :

$$\mu_s = \left(\frac{27 k_B T M_j}{4\pi N \rho_i} \, a_1 \right)^{1/2} \quad (21)$$

in order to present them in Table 5 for comparison with μ_1 and μ_2 of Table 4 in terms of τ_1 and τ_2.

Table 5. : Coefficients a_0, a_1 and a_2 in equation $X_{ij} = a_0 + a_1 w_j + a_2 w_j^2$, static dipole moment μ_s in Debye, and theoretical dipole moment μ_{theo} by considering inductive and mesomeric moments of substituents polar group of some aprotic polar liquids in benzene.

System with sl. no. & mol.wt.	Temperature in ^{0}C	Co-efficients a_0, a_1, a_2 of $X_{ij}=a_0+a_1w_j+a_2w_j^2$			μ_s in Debye	μ_{theo} in Debye	μ_{cal} in Debye (corrected)	μ_s/μ_{theo}
(I) DMSO in C_6H_6 M_j = 78gm.	25	0.0022	0.7756	20.935	3.19	4.55	3.20	0.70
(II) DMSO in C_6H_6 M_j = 78gm.	30	0.0019	1.0315	-17.183	3.72	4.55	3.72	0.82
(III) DMSO in C_6H_6 M_j = 78gm.	35	0.0018	0.9346	0.000	3.58	4.55	3.58	0.79
(IV) DMSO in C_6H_6 M_j = 78gm.	40	0.0010	1.1913	-23.282	4.08	4.55	4.08	0.90
(V) DEF in C_6H_6 M_j = 101.15gm.	30	0.0116	0.2047	0.000	1.89	3.99	1.89	0.47
(VI) DMF in C_6H_6 M_j = 73gm.	25	0.0028	0.7301	61.438	2.99	3.82	2.99	0.78
(VII) DMA in C_6H_6 M_j = 87gm.	25	0.0044	0.6545	53.798	3.09	4.02	3.09	0.77

4. RESULTS AND DISCUSSIONS

The variation of experimental $(\varepsilon_{oij}-\varepsilon'_{ij}) / (\varepsilon'_{ij}-\varepsilon_{\infty ij})$ with $\varepsilon''_{ij} / (\varepsilon'_{ij}-\varepsilon_{\infty ij})$ at different w_j's of solutes displayed in Figure 1 on fitted lines are derived to be linear as predicted by equation (11). The slopes and intercepts of equation (11) for aprotic polar liquids in C_6H_6 are presented in Table 2 alongwith the estimated τ_2 and τ_1. The linear variation is supported by the correlation coefficient 'r' and the corresponding % of errors placed in Table 2 in getting the straight lines of Figure 1. The errors within 10% indicate probably the accurate measurements of data of Table 1. It is evident from Figure 1 that all the straight lines of DMSO in C_6H_6 shift towards the origin as the temperature increases from 25°C to 40°C. This sort of behaviour of DMSO invites a further

study to see the existence of single relaxation at higher temperature. So, like electric field frequency (*f*), temperature is also a factor for such behaviour of molecules [10]. All the liquids show double relaxation times τ_2 and τ_1 as evident from the negative intercepts of the curves. τ_1's of the molecules [2-3] agree well with the reported τ in Table 2 due to Gopalakrishna's method [15-16]. It signifies that the electric field of 10 GHz frequency is the most effective dispersive region [6] for probable rotations of the flexible parts of these molecules [14]. Unlike τ_1's of DMSO; τ_2's are found to increase with temperature. The linear equation of $\ln(\tau_1 T)$ and $\ln(\tau_2 T)$ with 1 / T were found out by [17]

$$\ln(\tau_1 T) = -32.1273 + 3.6861 \times 10^3 \, (1 / T)$$
$$\ln(\tau_2 T) = -4.8261 - 4.0995 \times 10^3 \, (1 / T)$$

indicating that τ_1 obeys Eyring's rate process. The energy parameters like enthalpy of activation $\Delta H_{\tau_1} = 7.32$ Kcal/mole and $\Delta H_{\tau_2} = -8.13$ Kcal/mole; entropy of activation ΔS_{τ_1} are 16.79, 16.50, 16.36, 16.84Cal/mole/K and ΔS_{τ_2} are -36.96, -38.34, -38.21, -36.98 Cal/mole/K. The corresponding free energy of activation ΔF_{τ_1} and ΔF_{τ_2} are 2.32, 2.32, 2.28, 2.05 and 2.88, 3.49, 3.64, 3.44 Kcal/mole at 25°, 30°, 35° and 40°C respectively. The data thus obtained confirm the whole molecular rotation under 10 GHz electric field as a co-operative process while the reverse is true for rotation of the flexible group. The increase of τ_2 with the rise of temperature is due to elongation of size for monomer [18] formation with C_6H_6 (see Figure 6).

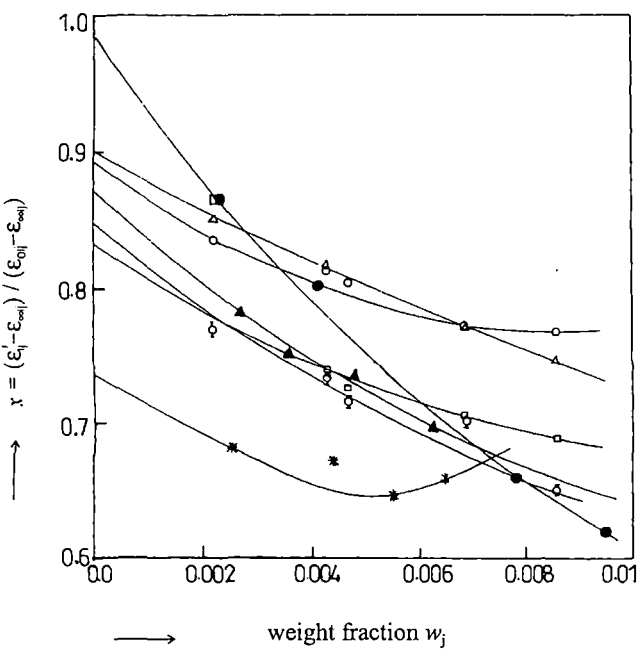

Figure 2. Variation of measured $x = (\varepsilon'_{ij} - \varepsilon_{\infty ij}) / (\varepsilon_{0ij} - \varepsilon_{\infty ij})$ with weight fraction w_j of some aprotic polar liquids :
DMSO (– O –, – △ –, – □ –, – ◇ –) at 25°C, 30°C, 35°C and 40°C respectively; DEF (– ● –) at 30°C; DMF (– ▲ –) at 25°C; DMA (– ✱ –) at 25°C

For aprotic polar molecules of greater complexity where a few experimental data are available under a single frequency electric field (Table 1) a continuous distribution of τ between two limiting values could be used [11]. The c_1 and c_2 values towards dielectric relaxations in terms of estimated τ_1 and τ_2 were, therefore, calculated from *x* and *y* of Fröhlich's equations (12) and (13) based on distribution of relaxation times. They were also obtained from

$x = (\varepsilon'_{ij}-\varepsilon_{\infty ij}) / (\varepsilon_{0ij}-\varepsilon_{\infty ij})$ and $y = \varepsilon''_{ij} / (\varepsilon_{0ij}-\varepsilon_{\infty ij})$ at $w_j \rightarrow 0$ from the graphical plots of Figures 2 and 3 as presented in Table 3. The explanation of the nature of variation of x and y with w_j in Figures 2 and 3 is that as τ increases with w_j [19] the R.H.S. of Bergmann's equations (5) and (6) become concave and convex cutting the ordinate axes to yield x and y respectively at $w_j \rightarrow 0$. As seen from Table 3; c_1 and c_2 for Fröhlich's method are positive in almost all cases. But c_2 is negative for graphical method probably due to the inertia of the flexible parts of the polar groups of the molecules [9].

The values of μ_2 and μ_1 in terms of b's involved with τ_2's and τ_1's and slopes β's of σ_{ij}–w_j curves of Figure 4 were estimated from equation (17) and placed in Table 4. The variation of σ_{ij} with w_j are parabolic governed by α, β and γ coefficients probably due to solute-solvent associations [2-3]. The polar liquid in a given nonpolar solvent behaves as a bound charged species due to polarisation under GHz electric field in order to have very large conductivity σ_{ij} of the order of $10^{10}\,\Omega^{-1}\,cm^{-1}$ for different w_j's although they are insulators. They are found to decrease with the rise of temperature for DMSO for the presence of $(\rho_i F_i/T)$ in equation (15) in the limit $w_j = 0$ [20]. It is interesting to note that μ_1 due to flexible part of the molecule agree well with the reported μ's [2-3] of Gopalakrishna's method [15-16]. This indicates that a part of the molecule is rotating under GHz electric field [14]. μ_2's are found to be higher in magnitudes for larger values of τ_2's according to equation (17). Both μ_2 and μ_1 vary with temperature t in °C for DMSO in C_6H_6 :

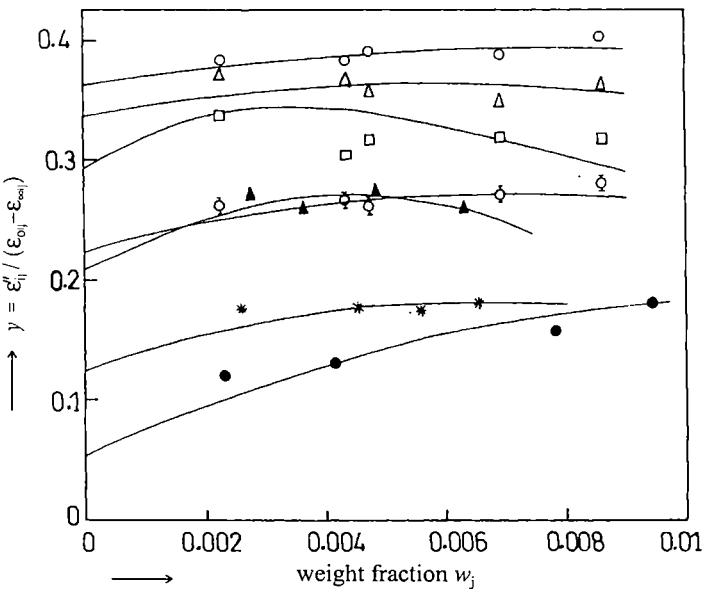

Figure 3. Variation of measured $y = \varepsilon''_{ij} / (\varepsilon_{0ij}-\varepsilon_{\infty ij})$ with weight fraction w_j of some aprotic polar liquids : DMSO (– O –, – △ –, – □ –, – ◊ –) at 25°C, 30°C, 35°C and 40°C respectively; DEF (– ● –) at 30°C; DMF (– ▲ –) at 25°C; DMA(– ✱ –) at 25°C

$$\mu_2 = -67.35 + 4.56\,t - 0.066\,t^2$$
$$\mu_1 = 8.20 - 0.32\,t + 0.005\,t^2$$

μ_2 of the parent molecule attains maximum value of 11.41 D at 34.5°C with zero dipole moments at 21.4°C and 47.7°C respectively due to monomer formation [2-3] with C_6H_6 ring (see Figure6).

The degree of solubility of solutions were kept fairly constant at all temperatures and for the low concentrations of binary mixtures (Table 1), dimer formation [1-4] is not expected. μ_i, on the other hand, decreases to a minimum value of 3.08 D at 32°C exhibiting the dimer formation of

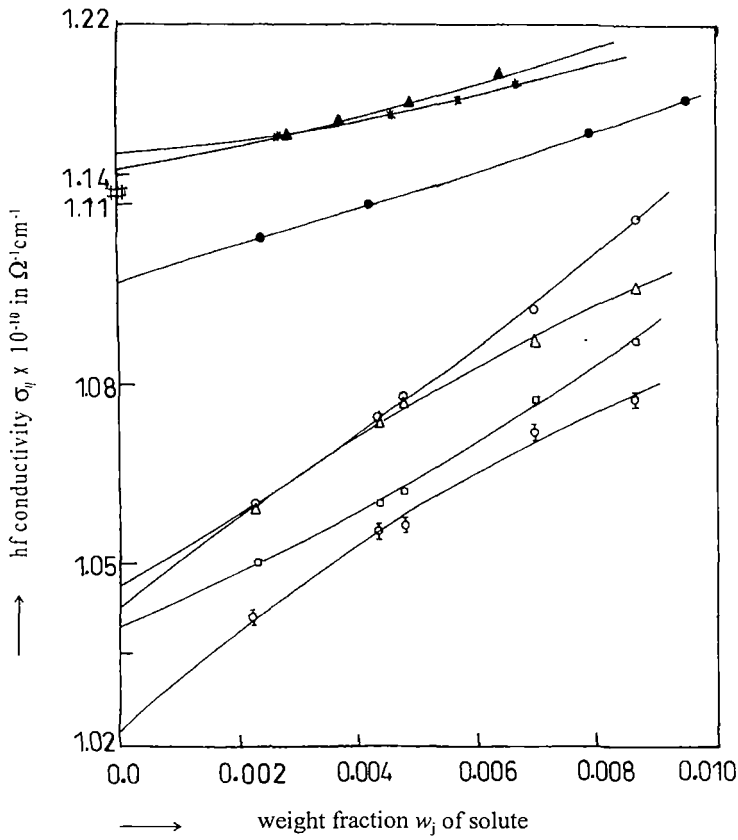

Figure 4. Vriation of hf conductivity σ_{ij} as a function of weight fraction w_j of polar liquids : DMSO (– O –, – △ –, – □ –, – ◇ –) at 25°C, 30°C, 35°C and 40°C respectively; DEF (– ● –) at 30°C; DMF (– ▲ –) at 25°C; DMA (– ✱ –) at 25°C

the flexible parts for their active involvement in rotation under 10 GHz electric field, unlike the whole molecule.

The static μ_s's of these liquids are also calculated from equation (21) with the measured data (Table 1) in terms of linear coefficients a_i's of the static experimental parameter X_{ij} against w_j curves of Figure 5. The coefficients a_0, a_1 and a_2 of the curves with the estimated μ_s are presented in Table 5. All the curves are found to be of almost same intercepts and slopes for DMSO in C_6H_6 at different temperatures signifying the fact that the static polarisability is nearly constant at all temperatures. The curves of $X_{ij} - w_j$ in case of DMF and DMA at 25°C are,

however, parabolic in nature probably due to the presence of the substituent – CH_3 group attached to the parent molecules under indentical environment. But X_{ij} varies with w_j linearly in case of DEF at 30°C. All these curves in Figure 5 with the computed μ_s's suggest that the measured data of Table 1 are more than accurate.

The theoretical μ_{theo}'s of polar molecules assumed to be planar ones were defined by the vector addition of the available bond moments 2.35D, 1.55D for polar groups S←CH_3, O⇐S in DMSO; 0.64 D, 0.78 D, 0.37 D of N←CH_3, N←C_2H_5, CH_3←C in DMF, DEF and DMA. The

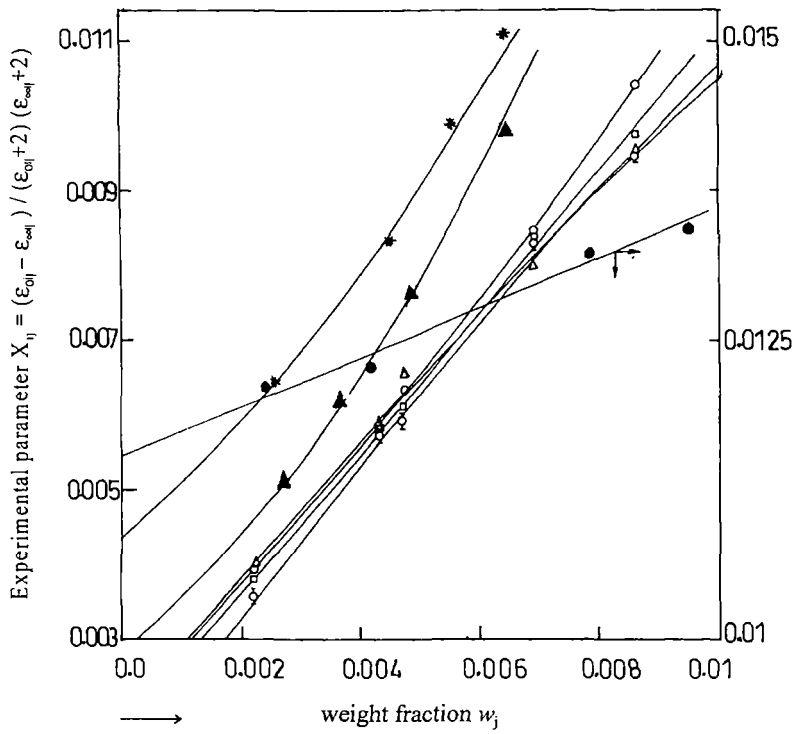

Figure 5. Variation of the measured values of the experimental parameter X_{ij} with weight fraction w_j of some aprotic polar liquids in benzene :
DMSO (– O –, – △ –, – □ –, – ◇ –) at 25°C, 30°C, 35°C and 40°C respectively; DEF (– ● –) at 30°C; DMF (– ▲ –) at 25°C; DMA (– ✱ –) at 25°C

other common bond moments are 0.3 D, 0.45 D, 3.10 D for C←H, C←N and C⇐0 respectively in them. The N atoms in DMF, DEF, DMA and S atom in DMSO molecules are thought to be the site of fractional positive charge of δ^+ with benzene to make monomer formations [2-3]. The solute-solvent molecular association arises from the interaction of the π–delocalised electron cloud of the benzene ring with the fractional positive charges δ^+ on the N and S atoms of the amide groups. The bond moments of polar groups under the static and high frequency electric

field are, however, reduced by a factor μ_s/μ_{theo} in the range 0.5 and 0.9 due to inductive and mesomeric effects to yield μ_{cal} in agreement with μ_s. μ_s/μ_{theo} thus appears to exhibit the material property of the syetems. The conformational structures of the polar molecules with their monomer [2-3] associations in C_6H_6 are shown in Figure 6. μ_{theo}'s alongwith μ_{cal} and μ_s/μ_{theo} are placed in Table 5 for comparison.

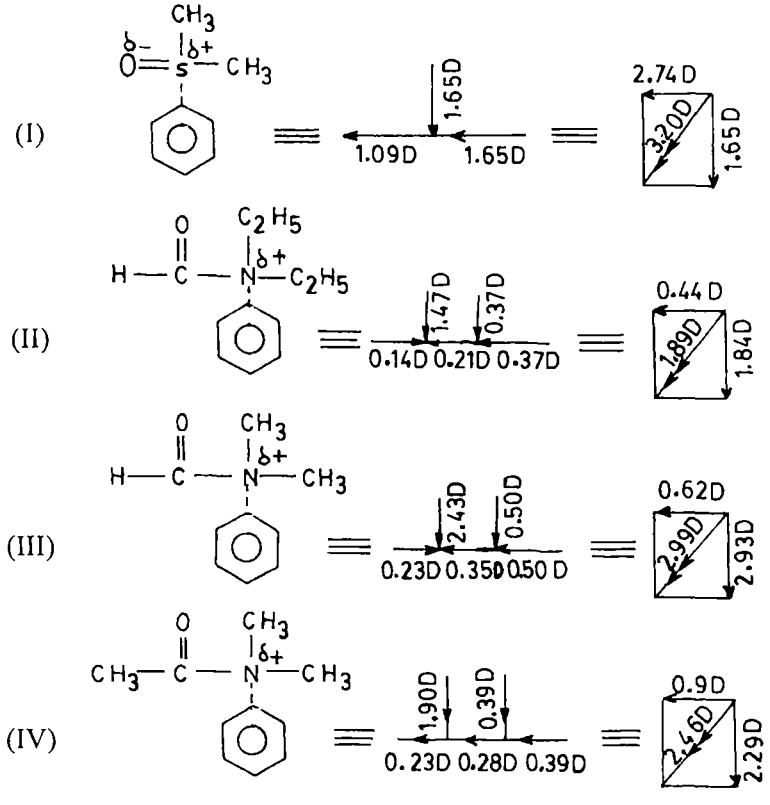

Figure 6. Conformational structures of aprotic polar liquids in terms of reduced bond lenght due to mesomeric and inductive moments of the substituent polar groups :
(I) DMSO in C_6H_6 ; (II) DEF in C_6H_6 ; (III) DMF in C_6H_6; (IV) DMA in.C_6H_6

5. CONCLUSION

The present measurements of dielectric relaxation parameters near 10 GHz electric field at different temperatures are found to exhibit double relaxation phenomena for rigid aprotic polar liquids. The procedure in obtaining τ_2 and τ_1 from the slope and intercept of a derived linear equation with ε_{oij}, $\varepsilon_{\infty ij}$, ε'_{ij} and ε''_{ij} measured under the single frequency electric field appears to be

a significant improvement over the existing ones where data at two or more frequencies are required. The % of error in terms of correlation coefficient 'r' in getting intercept and slope is made because of the linearity of the curve. The estimated τ_2 and τ_1 of the whole and the flexible part attached to the parent molecule are reliable as τ is claimed to be accurate within $\pm 10\%$. It is interesting to note that unlike τ_2, τ_1 obeys Eyring's rate theory. The relative contributions c_1 and c_2 towards dielectric relaxations due to τ_1 and τ_2 are calculated by the graphical technique at $w_j \rightarrow 0$ as well as Fröhlich's method based on the concept of a distribution of τ between τ_1 and τ_2. The μ_2 and μ_1 of the whole and the flexible part attached to the parent molecule within $\pm 5\%$ accuracy are obtained from the slope β of σ_{ij}–w_j curves and τ_2, τ_1. The static μ_s from the linear coefficient of X_{ij}–w_j curve when compared with μ_2 and μ_1 from high frequency absorbtion reveals that μ's are little affected by the frequency (f) of the electric field. The X_{ij}–w_j curves and μ_s's may be used to test the accuracies of relaxation parameters. It is confirmed that a part of the molecule is rotating under 10 GHz electric field. Besides 'f', temperature is a factor to show mono or double relaxation behaviour for a molecule. The conformational structures of molecules from the reduced bond moments of polar groups by a factor μ_s/μ_{theo} due to mesomeric and inductive moments in them under static or low frequency electric field are in agreement with μ_s. μ_{theo} is obtained from available bond moments of polar groups. Thus the methodology, so far advanced, seems to be simple, straightforward and useful to observe interesting phenomena of hf absorbtion in polar-nonpolar liquid mixture.

REFERENCES

[1] A K Sharma and D R Sharma, J. Phys. Soc. Japan **53** (1984) 4771
[2] J S Dhull and D R Sharma, Indian J. Pure Appl. Phys. **21** (1983) 694
[3] A Sharma and D R Sharma, J. Phys. Soc. Japan **61** (1992) 1049
[4] A R Sharma, D R Sharma and M S Chauhan, Indian J. Pure Appl. Phys. **31** (1993) 841
[5] K V Gopalakrishna, Trans. Faraday Soc. **53** (1957) 767
[6] S K Sit and S Acharyya, Indian J. Pure Appl. Phys. **34** (1996) 255
[7] T Pal Majumder, Ph.D.thesis (1996) Jadavpur University, Calcutta
[8] K Higasi, K Bergmann and C P Smyth, J. Phys. Chem. **64** (1960) 880
[9] U Saha, S K Sit, R C Basak and S Acharyya, J. Phys. D: Appl. Phys. **27** (1994) 596
[10] S K Sit, R C Basak, U Saha and S Acharyya, J. Phys. D : Appl. Phys. **27** (1994) 2194
[11] K Bergmann, D M Roberti and C P Smyth, J.Phys. Chem. **64** (1960) 665
[12] H Fröhlich, Theory of Dielectrics (Oxford University Press) (1949) P 94
[13] C P Smyth, Dielectric Behaviour and Structure (New York : Mc Graw-Hill) 1955
[14] R C Basak, S K Sit, N Nandi and S Acharyya, Indian J.Phys. **70B** (1996) 37
[15] J S Dhull and D R Sharma, J.Phys. D : Appl. Phys. **15** (1982) 2307
[16] A R Saksena, Indian J. Pure Appl. Phys. **16** (1978) 1079
[17] H Eyring, S Glasstone and K J Laidler,4 Theory of Rate Process (Mc Graw - Hill : New York) 1941
[18] U Saha and S Acharyya, Indian J. Pure Appl. Phys. **32** (1994) 346
[19] S N Sen and R Ghosh, Indian J. Pure Appl. Phys. **10** (1972) 701
[20] U Saha and S Acharyya, Indian J. Pure Appl. Phys **31** (1993) 181

ELSEVIER

Journal of Molecular Liquids 92 (2001) 263–276

journal of MOLECULAR LIQUIDS

www.elsevier.nl/locate/molliq

Dielectric relaxation phenomena of polysubstituted benzenes under high frequency electric field.

K Dutta, S K Sit and S Acharyya

Department of Physics, Raiganj College (University College)
P.O. Raiganj, Uttar Dinajpur, 733134 (W.B.), INDIA.

ABSTRACT

The relaxation times τ_j's and the dipole moments μ_j's in SI units of polysubstituted benzenes like meta-diisopropylbenzene, para-methylbenzoylchloride and ortho-chloroacetophenone in benzene are estimated at 30°, 35°, 40° and 45 °C from the real k_{ij}' imaginary k_{ij}'' parts of the dimensionless complex hf dielectric constants k_{ij}^* measured under 3 cm wavelength electric field. τ_j's measured from the ratio of the slopes of the variations of imaginary σ_{ij}'' and real σ_{ij}' parts of complex hf conductivity σ_{ij}^* with the weight fractions w_j's in the limit $w_j = 0$ at a given temperature are reliable in comparison to the linear coefficients of variation of σ_{ij}'' against σ_{ij}' of different w_j's (Murthy et al 1989). In the former case the polar-polar interactions are fully eliminated. The thermodynamic energy parameters with the estimated τ_j's reveal the cooperative process for p-methylbenzoylchloride unlike other two molecules besides the solute-solute and solute-solvent molecular associations. The variation of μ_j's with temperature t in °C when compared to theoretical dipole moments μ_{theo}'s from available bond angles and bond moments establishes the temperature dependence of the inductive, mesomeric and electromeric effects of the substituted polar groups of molecules.

1. INTRODUCTION

The dielectric relaxation phenomena of a polysubstituted dielectropolar benzenes in benzene under high frequency (hf) electric field are of much importance to yield the structural aspect of a polar molecule. There exist several methods [1,2] to measure relaxation time τ_j and dipole moment μ_j of a polar molecule (j) from the measured real ε_{ij}' and imaginary ε_{ij}'' parts of the relative hf complex permittivity ε_{ij}^* of the solution (ij). However, such investigation on the relaxation phenomena of polysubstituted benzenes has not yet been made from the conductivity measurement [3, 4]. Moreover, the most effective dispersive region for such polar liquids may exist at ~10GHz (X-band) electric field [5]. Recently, Paul et al [6] had measured ε_{ij}', ε_{ij}'' of some polysubstituted benzenes in C_6H_6 at 30°, 35°, 40° and 45°C under nearly 10 GHz electric field. The purpose of the study was to see the variation of τ's and μ's with temperature and concentration based on Gopalakrishna's method [1].

Although, the molecules appear to be of outdated interest, two polar molecules have identical molecular weights in comparison to the third one which is slightly higher. One molecule is a para-compound showing zero dipole moment at lower and higher temperatures. The substituted

0167-7322/01/$ - see front matter
PII S0167-7322(01) 00197-0

polar groups are attached with the parent benzene ring with different angles. We are, therefore, tempted to use the measured relative permittivity [6] to get τ_j and μ_j of these liquids by hf conductivity measurement method [7]. The methodology is, however, involved with the transfer of dipolar charge of a polar molecule in a given solvent [8]. The present method of study in SI unit is superior because of its unified, coherent and rationalised nature. The dependency of τ_j's and μ_j's on t in ^{0}C is of much significance to get an idea of molecular environment and to shed more light on the structural conformations [9].

Table-1. The real and imaginary parts of dimensionless dielectric constants of different aromatic polar liquids in benzene for different weight fractions w_j's at various experimental temperatures in ^{0}C

Weight fraction w_j	k'_{ij}	k_{ij}''	k'_{ij}	k_{ij}''	k'_{ij}	k_{ij}''	k'_{ij}	k_{ij}''
	30 ^{0}C		35 ^{0}C		40 ^{0}C		45 ^{0}C	
				(I) meta-di-isopropylbenzene				
0.012	2.2990	0.0424	2.3062	0.0401	2.3151	0.0393	2.3271	0.0384
0.018	2.3323	0.0570	2.3425	0.0552	2.3541	0.0545	2.3660	0.0523
0.025	2.3614	0.0721	2.3711	0.0692	2.3923	0.0660	2.4105	0.0595
0.032	2.3852	0.1083	2.4084	0.0985	2.4212	0.0854	2.4462	0.0734
0.045	2.4104	0.1251	2.4234	0.1092	2.4451	0.0982	2.4671	0.0832
				(II) para-methylbenzoylchloride				
0.011	2.1603	0.0488	2.1663	0.0440	2.1723	0.0410	2.1783	0.0381
0.018	2.1960	0.0585	2.2018	0.0553	2.2078	0.0523	2.2140	0.0492
0.028	2.2351	0.0690	2.2411	0.0662	2.2470	0.0632	2.2530	0.0603
0.039	2.2754	0.0762	2.2812	0.0731	2.2872	0.0701	2.2931	0.0672
0.050	2.3089	0.0928	2.3147	0.0899	2.3204	0.0872	2.3263	0.0842
				(III) ortho-chloroacetophenone				
0.011	2.1843	0.0351	2.1861	0.0330	2.1901	0.0310	2.1982	0.0294
0.023	2.2198	0.0462	2.2322	0.0442	2.2394	0.0450	2.2456	0.0376
0.032	2.2590	0.0573	2.2698	0.0552	2.2700	0.0491	2.2801	0.0421
0.045	2.2991	0.0692	2.3002	0.0653	2.3204	0.0551	2.3324	0.0579
0.051	2.3323	0.0810	2.3452	0.0791	2.3612	0.0770	2.3711	0.0650

The measured dimensionless dielectric constants like real k'_{ij} and imaginary k_{ij}'' parts of complex dielectric constant k_{ij}^* at 30^0, 35^0, 40^0 and 45^{0}C are placed in Table 1. The real σ'_{ij} and imaginary σ_{ij}'' parts of the hf complex conductivity σ_{ij}^* in $\Omega^{-1}m^{-1}$ are, however, related to k_{ij}'' and k'_{ij} respectively. τ_j's are calculated from the linear slope of σ_{ij}'' against σ'_{ij} curves [10] for different w_j's of solute at a given temperature. The variation of σ_{ij}'' against σ'_{ij} is not strictly linear for different w_j's. (Figure 1). The ratio of the individual slopes of variations of σ_{ij}'' and σ'_{ij} with w_j's in Figures 2 & 3 in the limit $w_j = 0$ may be used to get τ_j's, in which polar-polar interactions are almost eliminated. All

the τ_j's are shown in table 2 and are smaller than the reported τ's [6]. We, therefore, recalculated both τ's and μ's based on Gopalakrishna's method [1] which are in agreement with those of conductivity measurement. All τ's and μ's are now presented in Tables 2 and 4 respectively for comparison.

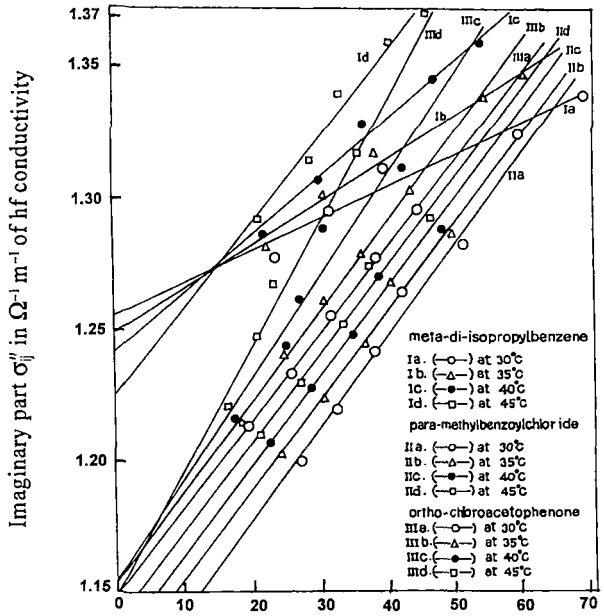

Figure 1 : Variation of imaginary part σ''_{ij} in Ω^{-1} m^{-1} against real part σ'_{ij} in Ω^{-1} m^{-1} of hf conductivity for different weight fractions w_j's of polysubstituted benzenes in benzene under 10 GHz electric field at various experimental temperatures.

Thermodynamic energy parameters : enthalpy of activation ΔH_τ, free energy of activation ΔF_τ and entropy of activation ΔS_τ for dielectric relaxations are also computed from the slope and intercept of ln (τ_jT) against 1/T of Figure 4 with τ_j's measured by both the methods [11]. The values are entered in Table 3 in order to infer molecular dynamics of polar molecules in benzene. The enthalpy of activation ΔH_η for viscous process was, however, obtained from the linear slope γ of ln (τ_jT) against lnη and ΔH_τ of eq (4). The coefficient of viscosity η of solvent C_6H_6 are 5.65 x 10^{-3}, 5.30 x 10^{-3}, 5.03 x 10^{-3} and 4.70 x 10^{-3} poise at 30°, 35°, 40° and 45°C respectively.

Dipole moments μ_j's (shown in Table 4) are estimated from the linear coefficients β's of hf σ_{ij} against w_j's as displayed in Figure 5 in the limit $w_j = 0$. The variation of μ_j's and τ_j's with t in °C are presented in Figure 6. The temperature dependence of the mesomeric and inductive moments of the substituted polar groups attached to the parent molecules [12] are taken into account to display the theoretical dipole moments μ_{theo}'s in Figure 7.

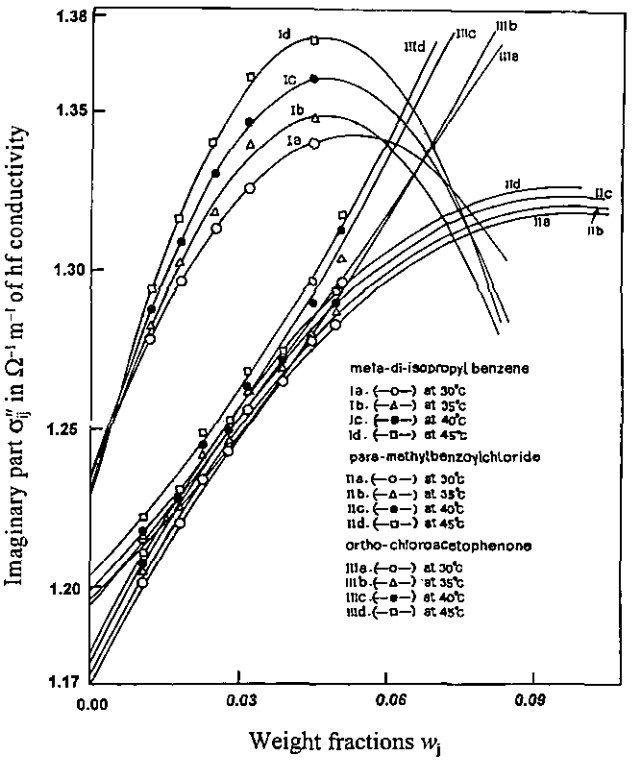

Figure 2 : Variation of imaginary part σ''_{ij} in Ω^{-1} m^{-1} of hf conductivity with weight fractions w_j's of polysubstituted benzenes in benzene under 10 GHz electric field at various experimental temperatures.

2. THEORETICAL FORMULATION

Under electric field of giga hertz range the hf complex conductivity σ^*_{ij} of polar-nonpolar liquid mixture is :

$$\sigma^*_{ij} = \omega \varepsilon_o k''_{ij} + j\omega \varepsilon_o k'_{ij} \qquad (1)$$

where $\omega \varepsilon_o k'_{ij}$ ($= \sigma''_{ij}$) and $\omega \varepsilon_o k''_{ij}$ ($= \sigma'_{ij}$) are the imaginary and real parts of σ^*_{ij}. ω ($= 2\pi f$) is the angular frequency of the applied electric field of frequency f. ε_o = permittivity of free space = 8.854×10^{-12} F.m^{-1} and j is a complex number $= \sqrt{-1}$. The magnitude of total hf conductivity is:

$$\sigma_{ij} = \omega \varepsilon_o (k''^2_{ij} + k'^2_{ij})^{1/2}$$

σ'_{ij} and σ''_{ij} of a given weight fraction w_j are, however, related to τ_j by :

$$\sigma''_{ij} = \sigma_{\infty ij} + (1/\omega\tau_j)\ \sigma'_{ij}$$

Table-2. The slope of linear relation $\sigma_{ij}'' - \sigma_{ij}'$ curves of Figure 1, correlation coefficient r, % of errors in regression technique, ratio of slopes of $\sigma_{ij}'' - w_j$ and $\sigma_{ij}' - w_j$ curves at $w_j \rightarrow 0$ of figures 2 and 3, estimated τ_j from eq (2) and reported τ in psec.

System with Sl. no.	t in ^0C	Slope of $\sigma_{ij}'' - \sigma_{ij}'$ curve of eq. (2)	Corrl. coeff. (r)	% of error in regression technique of eq. (2)	Ratio of slopes of $\sigma_{ij}'' - w_j$ & $\sigma_{ij}' - w_j$ at $w_j \rightarrow 0$ of eq. (2)	Estimated τ_j in psec		Reported τ in psec.
						from eq. (2) with slope of $\sigma_{ij}'' - \sigma_{ij}'$	from eq. (2) with ratio of slopes of $\sigma_{ij}'' - w_j$ and $\sigma_{ij}' - w_j$	
(I) m-diiso	30	1.217	0.972	1.67	1.809	13.08	8.80	10.92
propylbenz	35	1.633	0.990	0.60	2.173	9.75	7.33	8.88
ene in C_6H_6	40	2.183	0.990	0.60	2.916	7.29	5.46	6.54
	45	3.227	0.988	0.72	4.207	4.93	3.79	4.30
(II) p-meth	30	3.491	0.988	0.72	5.858	4.56	2.72	3.85
ylbenzoylc	35	3.369	0.989	0.66	4.828	4.73	3.30	4.04
hloride in	40	3.342	0.988	0.72	4.931	4.77	3.23	4.05
C_6H_6	45	3.339	0.988	0.72	4.910	4.77	3.24	4.18
(III) o-chlo	30	3.268	0.999	0.06	3.793	4.87	4.20	4.43
roacetophe	35	3.406	0.998	0.12	5.234	4.68	3.04	4.16
none in	40	3.841	0.963	2.19	12.625	4.15	1.26	3.47
C_6H_6	45	4.614	0.987	0.78	17.625	3.45	0.90	3.09

The intercept and slope of $\ln(\tau_j T)$ against 1/T as shown in Figure 4 are, however, related to ΔS_τ and ΔH_τ of molecules. η of C_6H_6 is related to τ_j at different temperatures by :

$$\tau_j = A\eta^\gamma / T \qquad (4)$$

where γ is the slope of the linear relation of $\ln(\tau_j T)$ against $\ln\eta$. Again, σ_{ij}'' may be approximated to σ_{ij}' for their identical nature of variations with w_j's as evidenced by Figures 2 and 5 respectively. Hence eq (2) can be written as :

$$\sigma_{ij} = \sigma_{\infty ij} + (1/\omega\tau)\ \sigma_{ij}'$$

$$\text{or } (d\sigma_{ij}'/dw_j)_{w_j \rightarrow 0} = \beta\omega\tau_j \qquad (5)$$

where β is the linear coefficient of variation of $\sigma_{ij} - w_j$ curves of Figure 5 at $w_j \rightarrow 0$. All β's are placed in Table 4. The real part σ_{ij}' at T K is [13] :

$$\sigma_{ij}' = \frac{N\rho_{ij}\mu_j^2}{27k_B TM_j} \left(\frac{\omega^2\tau_j}{1+\omega^2\tau_j^2} \right) (k_{ij}' + 2)^2\ w_j$$

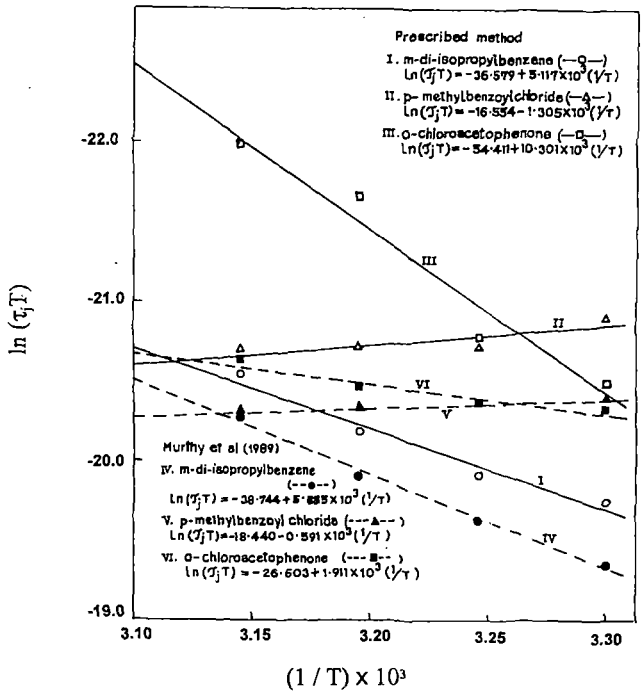

Figure 4 : The linear plot of ln ($\tau_j T$) against 1 / T of different polysubstituted benzenes in benzene under 10 GHz electric field.

$$\text{or} \left(\frac{d\sigma_{ij}'}{dw_j} \right)_{w_j \to 0} = \frac{N\rho_i \mu_j^2}{27 k_B T M_j} \left(\frac{\omega^2 \tau_j}{1 + \omega^2 \tau_j^2} \right) (k_i + 2)^2 \qquad (6)$$

where N = Avogadro's number, ρ_i = density of solvent, k_i = dimensionless dielectric constant of solvent. M_j = molecular weight of the polar liquid (j) and k_B = Boltzmann constant. All the symbols are in S I units. From eqs (5) and (6) one gets μ_j of a polar molecule in Coulomb metre (C.m) :

$$\mu_j = \left(\frac{27 k_B T M_j}{N\rho_i (k_i+2)^2} \frac{\beta}{\omega b} \right)^{1/2} . \qquad (7)$$

The dimensionless parameter b is related to τ_j by :

$$b = 1 / (1 + \omega^2 \tau_j^2) \qquad (8)$$

The measured τ_j's of the polar liquids presented in Table 2 are compared with the recalculated τ's based on Gopalakrishna's [1] method :

$$x = \frac{\varepsilon_{ij}'^2 + \varepsilon_{ij}' + \varepsilon_{ij}''^2 - 2}{(\varepsilon_{ij}' + 2)^2 + \varepsilon_{ij}''^2} \qquad y = \frac{3\varepsilon_{ij}''}{(\varepsilon_{ij}' + 2)^2 + \varepsilon_{ij}''^2}$$

$$\tau = (1 / \omega) (dy / dx) \quad (9)$$

All the μ_j's with b's are finally found in Table 4 to compare with recalculated μ's from :

$$\mu = \left[\frac{9k_B T M_j}{4\pi N \rho_i} \left\{ 1 + \left(\frac{dy}{dx} \right) 2 \right\} \frac{dx}{dw_j} \right]^{1/2} \quad (10)$$

All the computed μ_j's, reported μ's along with μ_{theo}'s of Figure 7 are seen in Table 4.

Table-3 : The thermodynamic energy parameters:enthalpy of activation ΔH_τ, entropy of activation ΔS_τ and free energy of activation ΔF_τ , value of γ from eq. (4), enthalpy of activation ΔH_η, Debye factor and Kalman factor of the following aromatic polar liquids in benzene at different temperatures.

System with Sl. no.	t in ^0C	ΔH_τ in K J mole^{-1}	ΔS_τ in J mole^{-1} K^{-1}	ΔF_τ in K J mole^{-1}	Value of γ from eq (4)	ΔH_η from $\Delta H_\eta = \Delta H_\tau/\gamma$ in K J mole^{-1}	Debye factor $(\tau_j T / \eta) \times 10^7$	Kalman factor $\tau_j T / \eta^\gamma$
(I) m-diis	30		106.96	10.11			4.72	11.74
opropylbe	35	42.52	106.07	9.85	4.29	9.91	4.26	13.08
nzene in	40		106.17	9.29			3.40	12.39
C_6H_6	45		106.94	8.51			2.56	11.69
(II) p-me	30		-59.41	7.16			1.46	2.78×10^{-12}
thylbenzoy	35	-10.84	-60.57	7.82	-1.10	9.85	1.92	3.19×10^{-12}
lchloride	40		-59.96	7.93			2.01	3.00×10^{-12}
in C_6H_6	45		-59.58	8.11			2.19	2.83×10^{-12}
(III) o-chl	30		255.28	8.25			2.25	5.36×10^{10}
oroacetoph	35	85.60	253.25	7.60	8.73	9.81	1.77	6.89×10^{10}
enone in	40		255.99	5.48			0.78	4.58×10^{10}
C_6H_6	45		254.36	4.71			0.61	6.02×10^{10}

3. RESULTS AND DISCUSSION

The relaxation times τ_j's of polysubstituted benzenes under 3 cm wavelength electric field, were calculated simultaneously from eq. (2) with the slope of σ_{ij}'' against σ_{ij}' of hf conductivity σ_{ij}^* of Figure 1 and the ratio of slopes of the variations of σ_{ij}'' and σ_{ij}' with w_j's of Figures 2 and 3 from data of Table 1 at different experimental temperatures. τ_j's (Table 2) from slope of linear relation $\sigma_{ij}'' - \sigma_{ij}'$ curve (Figure 1) are slightly larger than the ratio of slopes of eq. (2). The latter method is reliable as the polar-polar interactions are almost eliminated. The variation of σ_{ij}'' with σ_{ij}' is non linear (Figure 1) for all the liquids like σ_{ij}'' and σ_{ij}' with w_j's of Figures 2 & 3 respectively. The slopes of curves in Figure 1 are almost same for p-methylbenzoylchloride, but for o-chloroacetophenone the curves are of almost constant intercepts and slightly increasing slopes with temperature to yield almost same τ_j for their same polarity [14] and identical structures.

Meta-diisopropylbenzene indicates the lower intercept and higher slopes as the temperature rises. τ_j's from eq. (2) of $\sigma_{ij}'' - \sigma_{ij}'$ curves decrease with temperature to obey Debye relaxation mechanism like the variation of σ_{ij}'' and σ_{ij}' with w_j's for the molecules at 30°, 35°, 40° and 45°C respectively. Nevertheless, the conductivity method yields microscopic τ_j's [15]. The molecule m-diisopropylbenzene has greater τ because of larger size than those of isomeric p-methylbenzoylchloride and o-chloroacetophenone. τ_j's in Table 2 for these molecules having the same number of C-atoms do not vary much from eqs (2) & (9) respectively probably for the different positions of the substituted polar groups attached to the parent molecules of Figure 7.

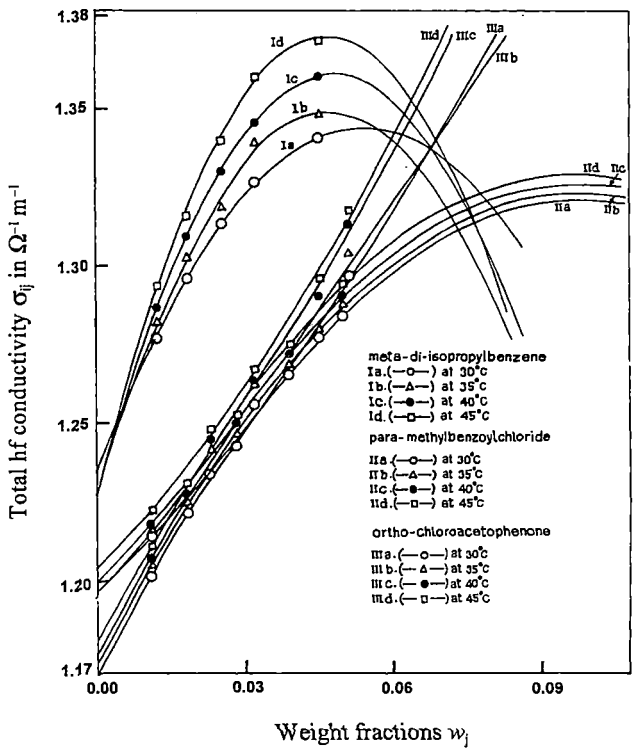

Figure 5 : Variation of total hf conductivity σ_{ij} in Ω^{-1} m^{-1} with weight fractions w_j's of polysubstituted benzenes in benzene under 10 GHz electric field at various experimental temperatures.

For m-diisopropylbenzene both σ_{ij}'' and σ_{ij} in Figures 2 and 5 start from 1.228 Ω^{-1} m^{-1} to 1.236 Ω^{-1} m^{-1}and increase gradually to assume maximum within $0.045 \leq w_j \leq 0.051$ and then decrease as w_j increases. This sort of behaviour arises for the transfer of localised charge species of such dipoles [16] which increases upto a certain w_j and then ceases gradually in the higher concentrations. Similar observation is noted in p-methylbenzoylchloride showing maximum at

nearly $w_j = 0.096$. All these facts indicate the phase transition of lower conductivity in the higher concentration [16] probably due to dimer formations. Ortho-chloroacetophenone showed a regular monotonic increase as coefficients of quadratic term of w_j in both σ_{ij}'' and σ_{ij} are positive. The variation of σ_{ij}' with w_j's for all polar molecules in Figure 3 decreases with t °C to exhibit the semiconducting nature while σ_{ij}'' and σ_{ij} of Figures 2 and 5 showed the regular increase. The percentage of errors as well as correlation coefficients r's are made for eq (2) to get τ_j's. It is interesting to note that τ_j for m-diisopropylbenzene and o-chloroacetophenone in C_6H_6 obey Debye relaxation mechanism. The energy difference between activated and normal states of the random dipole orientations increases with t °C to decrease τ_j's. τ_j's for p-methylbenzoylchloride initially increases and then become constant with t °C indicating the non-Debye relaxation for its asymmetry gained by two polar groups in a line. The large difference between τ_j's and reported τ's [6] prompted us to recalculate τ's placed in the 9th column of Table 2 based on Gopalakrishna's method [1]. The recalculated τ's and μ's are now closer to τ_j's of columns 7 and 8 of Table 2 and μ_j's of column 9 of Table 4 based on the method of conductivity measurement [7].

Table-4. The coefficients of hf conductivity σ_{ij} of aromatic polar liquid with weight fraction w_j in C_6H_6 at 30°, 35°, 40° and 45 °C in Figure 5, dimensionless parameters b's, computed, reported and theoretical dipole moments in Coulomb metre (C.m).

System with sl. no. & mol. wt.	t in °C	Coefficients of $\sigma_{ij} - w_j$ eq. in $\Omega^{-1}m^{-1}$ of Fig. 5 $\sigma_{ij} = \alpha + \beta w_j + \gamma w_j^2$			Dimensionless parameter b		Computed $\mu_j \times 10^{30}$ in Coulomb metre (C.m)		Reported $\mu \times 10^{30}$ in C.m eq. (10)	Theoretical $\mu \times 10^{30}$ in C.m of Fig.7
		α	β	γ	from eq.(2) of Fig.1	from eq.(2) of Figs 2 & 3				
(I) m-diisopropylbenzene M_j = 0.162 Kg.	30	1.236	4.016	-36.919	0.597	0.766	14.34	12.66	9.07	3.77
	35	1.228	5.110	-53.613	0.727	0.825	14.86	13.95	8.90	
	40	1.230	5.475	-56.900	0.827	0.895	14.61	14.04	8.84	
	45	1.228	6.196	-65.944	0.913	0.946	14.99	14.72	8.90	
(II) p-methylbenzoylchloride M_j = 0.156 Kg.	30	1.171	3.059	-15.421	0.924	0.972	9.87	9.63	8.17	8.80
	35	1.173	3.059	-15.464	0.919	0.959	10.03	9.82	8.27	
	40	1.177	3.064	-15.617	0.918	0.961	10.18	9.95	8.34	
	45	1.180	3.064	-15.685	0.918	0.960	10.31	10.08	8.44	
(III) o-chloroacetophenone M_j = 0.156 Kg.	30	1.197	1.477	9.038	0.915	0.935	6.90	6.82	8.07	7.40
	35	1.195	1.894	3.180	0.921	0.965	7.89	7.71	8.20	
	40	1.201	1.580	11.513	0.936	0.994	7.23	7.02	8.57	
	45	1.204	1.615	11.737	0.955	0.997	7.34	7.19	8.74	

The thermodynamic energy parameters ΔH_τ , ΔS_τ and ΔF_τ (Table 3) were calculated from $\ln(\tau_j T)$ against 1 / T in Figure 4 with the measured τ_j's by both the methods. In p-methylbenzoylchloride – ΔS_τ indicates the activated states are more stable supported by – ΔH_τ also. ΔS_τ for m-diisopropylbenzene and o-chloroacetophenone indicates the unstability of the activated states. Unlike p-methylbenzoylchloride, $\gamma > 0.5$ for m-diisopropylbenzene and o-chloroacetophenone indicates that they do not behave as solid phase rotators. Such polar liquids in C_6H_6 favour solute-solvent molecular formation. ΔH_η involved with translational and rotational energy are less than ΔH_τ due to high values of γ for all the systems. They thus need maximum energy to rotate under hf electric field. The γ's from the slope of $\ln(\tau_j T)$ against $\ln\eta$ are used to estimate Kalman factor $\tau_j T / \eta^\gamma$ and Debye factor $\tau_j T / \eta$ to place them in Table 3. Kalman factors being proportional to the volumes of the rotating units are of different orders, but constant with temperature for a given system. Debye factors, on the other hand, are of the order of 10^{-7} for all systems. This suggests, the applicability of Debye – Smyth model of dielectric relaxation mechanism for all the liquids including p-methylbenzoylchloride although it is non-Debye in relaxation behaviour.

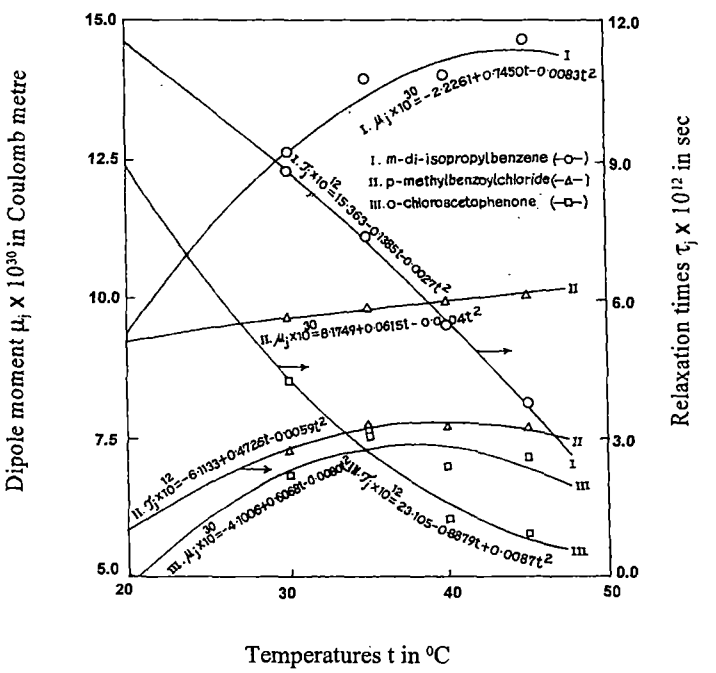

Figure 6 : Variation of observed dipole moment μ_j in Coulomb metre and relaxation times τ_j in p-sec with temperatures t in °C of different polysubstituted benzenes in benzene under 10 GHz electric field.

μ_j's of the polar liquids at t °C are estimated from β's of $\sigma_{ij} - w_j$ curves of Figure 5 and dimensionless parameters b's of eq (8) involved with the measured τ_j's from the ratio of the individual slopes of Figures 2 and 3 at $w_j \to 0$. The σ_{ij} in $\Omega^{-1} m^{-1}$ when plotted with w_j's increases with temperatures showing maximum at a certain w_j for m-diisopropylbenzene and p-methylbenzoylchloride like $\sigma''_{ij} - w_j$ curves. This signifies the phase transition from higher to lower conductivity for transfer of charged species of molecules. The slopes and intercepts of $\sigma_{ij} - w_j$ and $\sigma''_{ij} - w_j$ curves for p-methylbenzoylchloride and o-chloroacetophenone are almost the same for their same polarity [14] indicating $\sigma_{ij} \simeq \sigma''_{ij}$ in eq. (5). The usual variations of μ_j and τ_j [17] with t °C are shown graphically in Figure 6. τ_j's decrease with temperature for the curves I and III of m-diisopropylbenzene and o-chloroacetophenone. The μ_j's from eq (7) increase gradually to maximum 14.49×10^{-30} C.m at 44.88 °C, 10.54×10^{-30} C.m at 76.88 °C and 7.41×10^{-30} C.m. at 37.93 °C respectively signifying the largest asymmetry gained by all the molecules. τ_j's are zero at 54.03 °C for the curve I and 16.22 °C, 63.88 °C for curve II. But for curve III; $\tau_j = 0$ at $t = \infty$. The μ_j's are 13.80×10^{-30} C.m, for the curve I and 9.07×10^{-30} C.m, 10.47×10^{-30} C.m for curve II, but undefined for curve III respectively. The variation of τ_j and μ_j with t °C are convex for curve II indicating the non-Debye relaxation behaviour to reveal solute-solvent molecular association as observed from γ of Table 3.

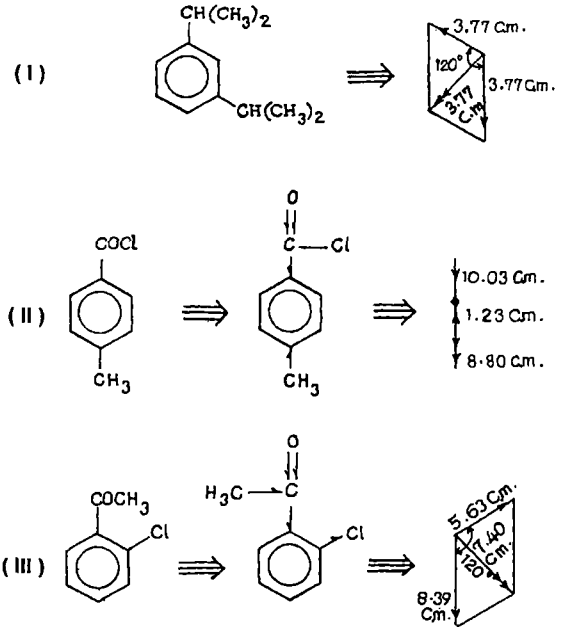

Figure 7 : Conformational structures of different polysubstituted benzenes.
(I) meta-diisopropylbenzene
(II) para-methylbenzoylchloride
(III) ortho-chloroacetophenone

μ_{theo} from the available bond angles and bond moments of the substituted polar groups of molecules of Figure 7 is placed in Table 4 with the reported μ from eq. (10). The close agreement of μ_j's of eq (7) with eq (10) suggests the basic soundness of the present method. The wide disagreement between μ_j and μ_{theo} of Table 4 of the first molecule unlike the latter two suggest bond moments of the substituted polar groups are either stretched by a factor μ_j / μ_{theo} of 3.36, 3.70, 3.72, 3.90; or shortened by 0.09, 1.12, 1.13, 1.50 and 0.92, 1.04, 0.95, 0.97 respectively in order to consider inductive and mesomeric effects in them. The electromeric effect caused by >C=0 in second and third molecules may be the reason to make μ_j more closer to μ_{theo} [18].

4. CONCLUSION

The study of dielectric relaxation phenomena of polysubstituted benzene in benzene under 3cm wavelength electric field in terms of τ_j's and μ_j's in SI units at various experimental temperatures in °C by the method of hf conductivity measurement is more topical and significant. The use of ratio of the slopes of $\sigma_{ij}'' - w_j$ and $\sigma_{ij}' - w_j$ curves to obtain τ_j's appears to be reliable as *it avoids polar – polar interaction unlike the linear slope of $\sigma_{ij}'' - \sigma_{ij}'$ curves. The appearance of* peak in $\sigma_{ij} - w_j$ and $\sigma_{ij}'' - w_j$ curves at different t °C for systems I and II indicates the change of phase of lower conductivity as w_j increases. O-chloroacetophenone, on the other hand, showed the monotonic increase of σ_{ij} and σ_{ij}'' with w_j's at all the temperatures. The temperature dependence of μ_j's and τ_j's although they are measured in the limit of $w_j = 0$ supports this behaviour. τ_j is zero for m-diisopropylbenzene at 54.03 °C while p-methylbenzoylchloride at 16.22 °C and 63.88 °C respectively indicating orderness at those temperatures. O-chloroacetophenone, showed τ_j's decreasing with temperature and becomes zero at $t = \infty$. The corresponding μ_j's are $\mu_s = 13.80 \times 10^{-30}$ C.m for m-diisopropylbenzene and $\mu_s = 9.07 \times 10^{-30}$ C.m and $\mu_s = 10.47 \times 10^{-30}$ C.m for p-methylbenzoylchloride respectively as static μ_s. Both τ_j's and μ_j's in tables and figures are within 10% and 5% accuracies. The increase or decrease of μ_j's with temperature t in °C is explained by asymmetric or symmetric configurations of the molecules. The energy parameters from ln (τ_jT) against 1/T with τ_j's from the ratio of individual slopes of $\sigma_{ij}'' - w_j$ and $\sigma_{ij}' - w_j$ curves at various temperatures indicate the stability of random dipole orientations in the activated states. The deviation of μ_{theo} from the bond angles and bond moments of polar groups of molecules from measured μ_j in terms of τ_j can be explained by inductive, mesomeric and electromeric effects. The correlation between the conformational structures with the observed results enhances the scientific contents and adds a new horizon of understanding to the existing knowledge of dielectric relaxation.

REFERENCE

[1] K V Gopalakrishna, Trans. Faraday Soc. **53** (1957) 767
[2] S N Sen and R Ghosh, Indian J. Pure & Appl. Phys. **10** (1972) 701
[3] U Saha, S K Sit, R C Basak and S Acharyya, J. Phys. D : Appl. Phys **27** (1994) 596
[4] S K Sit, R C Basak, U Saha and S Acharyya, J. Phys D : Appl. Phys **27** (1994) 2194
[5] S K Sit and S Acharyya, Indian J. Pure & Appl. Phys **34** (1996) 255
[6] N Paul, K P Sharma and S Chattopadhyay, Indian J. Phys **71B** (1997) 711
[7] R C Basak, A Karmakar, S K Sit and S Acharyya, Indian J. Pure & Appl. Phys. **37** (1999) 224

[8] A K Jonscher, Inst. Phys. Conf. Serial No. 58, Invited paper presented at Phys. of Dielectric *Solids. 8-11 (1980)*
[9] N Ghosh, R C Basak, S K Sit and S Acharyya, J. Molecular Liquids **85** (2000) 375
[10] M B R Murthy, R L Patil and D K Deshpande, Indian J. Phys **63B** (1989) 491
[11] H Eyring, S Glasstone and K J Laidler, Theory of Rate Processes (New York : Mc Graw Hill, 1941)
[12] S K Sit, N Ghosh, U Saha and S Acharyya, Indian J. Phys **71B** (1997) 533
[13] C P Smyth, Dielectric Behaviour and Structure (Mc Graw-Hill : New York) 1955
[14] A K Chatterjee, U Saha, N Nandi, R C Basak and S Acharyya, Indian J. Phys **66B** (1992) 291
[15] S K Sit and S Acharyya, Indian J. Phys **70B** (1996) 19
[16] M A El shahawy, A F Mansour and H A Hashem, Indian J. Pure & Appl. Phys **36** (1998) 78
[17] A M Ras and P Bordewijk, Recuel **90** (1971) 1055
[18] "Internal rotation in molecules" - Edited by W J Orville Thomas (John Wiley) (1974)

PRAMANA
— journal of
physics

Vol. 57, No. 4
October 2001
pp. 775–793

Dielectric relaxation phenomena of rigid polar liquid molecules under giga hertz electric field

K DUTTA, S K SIT and S ACHARYYA
Department of Physics, Raiganj College (University College), P.O. Raiganj,
Dist. Uttar Dinajpur 733 134, India

MS received 22 May 2000; revised 19 March 2001

Abstract. The dielectric relaxation phenomena of rigid polar liquid molecules chloral and ethyltrichloroacetate (j) in benzene, n-hexane and n-heptane (i) under 4.2, 9.8 and 24.6 GHz electric fields at 30°C are studied to show the possible existence of double relaxation times τ_2 and τ_1 for rotations of the whole and the flexible parts of molecules. The probability of showing double relaxation is more in aliphatic solvents indicating their nonrigidity. The symmetric and asymmetric distribution parameters γ and δ are obtained from χ'_{ij}/χ_{0ij} and χ''_{ij}/χ_{0ij} at $w_j \to 0$ where χ'_{ij} and χ''_{ij} are real and imaginary parts of the complex orientational susceptibility χ^*_{ij} and χ_{0ij} is the low frequency susceptibility which is real. χ_{ij}'s are involved with the measured dielectric relative permittivities ε'_{ij}, ε''_{ij}, ε_{0ij} and $\varepsilon_{\infty ij}$ of solutions. The theoretical weighted contributions c_1 and c_2 towards dielectric dispersions by Fröhlich's method are compared with the experimental ones obtained from the graphical variation of χ'_{ij}/χ_{0ij} and χ''_{ij}/χ_{0ij} with weight fractions w_j's at $w_j \to 0$. The measured dipole moments μ_2 and μ_1 of the whole and the flexible part of a polar molecule in terms of the linear coefficients β's of χ'_{ij}'s with w_j's and the estimated τ_2 and τ_1 reveal their associations with aliphatic solvents. The theoretical dipole moments μ_{theo}'s from the available bond angles and bond moments of the substituent polar groups of the molecules with the estimated μ's suggest the mesomeric, inductive and electromeric effects in them under GHz electric field.

Keywords. Relaxation time; hf conductivity; dipole moment.

PACS No. 77.22.Gm

1. Introduction

Dielectric relaxation studies of polar liquids in nonpolar solvents are of much importance as they provide interesting information of solute–solvent or solute–solute molecular association [1,2] under high frequency (hf) electric field. The associational aspects of polar liquids can, however, be inferred from the measured relaxation time τ by Cole–Cole [3], Cole–Davidson [4] plot or by single frequency concentration variation method [5] and dipole moment μ from the measured hf conductivity σ_{ij} and estimated τ [6].

Srivastava and Srivastava [7] measured the real ε'_{ij} and imaginary ε''_{ij} parts of complex relative permittivity ε^*_{ij} of chloral and ethyltrichloroacetate in benzene, n-heptane and n-hexane in 4.2, 9.8 and 24.6 GHz electric field by Smyth's method [8] at 30°C. The polar

solutes (j) chloral (CCl_3CHO) and ethyltrichloroacetate ($CCl_3COOCH_2CH_3$) were of puram grade of M/s. BDH, England, *n*-hexane and *n*-heptane from M/s. E Merck Darmstadt, Germany. Both solutes and solvents were doubly distilled before making solutions of varying concentrations called the weight fractions w_j's of solutes which are defined as the weight of the solute per unit weight of the solution up to four decimal places as shown in table 1 in each solvent. The static relative permittivity ε_{0ij} at 100 KHz and refractive index n_{Dij} of the solutions were measured. The purpose of this study was to observe the solute–solvent or solute–solute molecular interactions. They, however, inferred that these molecules may possess two or more relaxation processes towards dielectric dispersions.

Now a days, the usual practice is to study the dielectric relaxation processes in terms of hf dielectric orientational susceptibility χ_{ij}^* rather than ε_{ij}^* or hf conductivity σ_{ij}^* [9,10]. ε_{ij}^* includes within it all the polarization processes while σ_{ij}^* is more linked to transport of bound molecular charges. It is, therefore, better to work with susceptibilities χ_{ij}'s as they are concerned with orientational polarization. The dielectric susceptibilities real $\chi_{ij}'(=\varepsilon_{ij}' - \varepsilon_{\infty ij})$ and imaginary $\chi_{ij}''(=\varepsilon_{ij}'')$ parts of complex dielectric susceptibility $\chi_{ij}^*(=\varepsilon_{ij}^* - \varepsilon_{\infty ij})$ and the low frequency dielectric susceptibility $\chi_{0ij}(=\varepsilon_{0ij} - \varepsilon_{\infty ij})$ which is real were derived from measured relative permittivities [7]. The experimental results thus collected together are placed in table 1. One could not make a strong conclusion of double relaxation phenomena of polar molecule in a nonpolar solvent based on the single frequency measurement of relaxation parameters provided the accurate value of χ_{0ij} involved with ε_{0ij} and $\varepsilon_{\infty ij}$ is not available. The use of n_{Dij}^2 for $\varepsilon_{\infty ij}$ [7] often introduces the additional error in the calculation. Nevertheless, the data of table 1 are accurate up to 5% for χ_{ij}'' and 2% for χ_{ij}' and χ_{0ij} respectively.

The nonspherical as well as nonrigid polar liquid molecules often possess two or more τ's in GHz electric field for the rotation of different flexible polar groups attached to the parent molecule and the whole molecule itself [11]. Bergmann *et al* [12], however, devised a graphical method to obtain τ_1 and τ_2 for a pure polar liquid. The respective weighted contributions c_1 and c_2 towards dielectric relaxations were also estimated in terms of τ_1 and τ_2. A graphical method [13] was, soon employed from Fröhlich's distribution function [14] to get τ_2 and τ_1 of a pure polar solute. The methods indicate that a single frequency measurement is not sufficient to have correct τ_1 and τ_2. Bhattacharyya *et al* [15] subsequently attempted to get τ_1, τ_2 and c_1, c_2 for a polar molecule with $\varepsilon', \varepsilon'', \varepsilon_0$ and ε_∞ measured at two different frequencies in GHz region. The graphical analysis made by Higasi *et al* [16] on polar–nonpolar liquid mixture was, also a crude approximation.

Saha *et al* [6] and Sit *et al* [17] recently put forward an analytical method based on single frequency measurement of relative permittivities ε_{ij}', ε_{ij}'', ε_{0ij} and $\varepsilon_{\infty ij}$ of polar–nonpolar liquid mixtures of different w_j's at a given temperature to get τ_1, τ_2 and c_1, c_2 respectively. Earlier investigation had been made on different chain-like polar molecules like alcohols in nonpolar solvents [18,19] to see the double relaxation phenomena at three different electric field frequencies in terms of relative permittivities. However, no such study is made on the aforesaid rigid aliphatic polar liquid molecules in different solvents under various electric field frequencies from measured χ_{ij}'s of table 1. Chloral is widely used in medicine as drug to induce sleep and relieve pain and in the manufacture of D.D.T. as insecticides. Ethyltrichloroacetate, on the other hand, is used for artificial fragrance of fruits and flowers.

Thus the object of the present paper is to detect the existence of double relaxation times τ_1 and τ_2 due to rotation of the flexible part and the whole molecules themselves using

Table 1. Concentration variation of the real χ'_{ij} and imaginary χ''_{ij} parts of dimensionless complex dielectric orientational susceptibility χ^*_{ij} and the static dielectric orientational susceptibility χ_{0ij} which is real derived from the measured relative permittivities $\varepsilon'_{ij}, \varepsilon''_{ij}, \varepsilon_{0ij}$ and $\varepsilon_{\infty ij}$ of chloral and ethyltrichloroacetate in different non-polar solvents at 30°C.

Frequency f in GHz	Weight fraction, w_j	$\chi'_{ij} = \varepsilon'_{ij} - \varepsilon_{\infty ij}$	$\chi''_{ij} = \varepsilon''_{ij}$	$\chi_{0ij} = \varepsilon_{0ij} - \varepsilon_{\infty ij}$
		I chloral in benzene		
(a) 4.2	0.0255	0.0750	0.005	0.0790
	0.0977	0.2107	0.031	0.2117
	0.1813	0.3984	0.080	0.4004
	0.2511	0.5653	0.088	0.5703
(b) 9.8	0.0899	0.1803	0.041	0.2024
	0.1711	0.3377	0.057	0.3719
	0.1903	0.3695	0.072	0.4153
	0.2510	0.5149	0.083	0.5608
	0.3476	0.7333	0.099	0.8183
(c) 24.6	0.0152	0.0632	0.047	0.0664
	0.0899	0.1603	0.066	0.2024
	0.1711	0.3177	0.104	0.3719
	0.1903	0.3895	0.146	0.4153
	0.3476	0.7333	0.208	0.8183
		II chloral in *n*-heptane		
(a) 4.2	0.1349	0.1853	0.022	0.2052
	0.2008	0.2996	0.029	0.3238
	0.2706	0.4128	0.045	0.4531
	0.3366	0.5356	0.060	0.5787
(b) 9.8	0.0807	0.0891	0.029	0.1271
	0.1416	0.1646	0.036	0.2146
	0.2003	0.2599	0.050	0.3099
	0.2683	0.3828	0.055	0.4528
	0.3324	0.5262	0.080	0.5722
(c) 24.6	0.0795	0.0795	0.024	0.1079
	0.1349	0.1753	0.038	0.2052
	0.2008	0.2696	0.054	0.3238
	0.2706	0.3928	0.068	0.4531
	0.3366	0.5256	0.091	0.5787
		III ethyltrichloroacetate in benzene		
(a) 4.2	0.0211	0.1031	0.043	0.1292
	0.0521	0.2061	0.095	0.2513
	0.0755	0.2885	0.154	0.3457
	0.1202	0.4432	0.224	0.5312
	0.1734	0.5891	0.310	0.7610
	0.2388	0.7969	0.454	1.0569

(b) 9.8	0.0207	0.0835	0.023	0.1315
	0.0498	0.1456	0.046	0.2406
	0.0802	0.2083	0.079	0.3643
	0.1193	0.2934	0.115	0.5264
	0.1764	0.4199	0.194	0.7759
	0.2444	0.6074	0.226	1.0824
(c) 24.6	0.0211	0.0331	0.010	0.1292
	0.0521	0.0761	0.025	0.2513
	0.0755	0.1385	0.059	0.3457
	0.1202	0.2132	0.086	0.5312
	0.1734	0.2391	0.105	0.7610
	IV ethyltrichloroacetate in *n*-hexane			
(a) 4.2	0.0595	0.1430	0.052	0.1700
	0.0649	0.1525	0.066	0.1839
	0.1137	0.2673	0.108	0.3154
	0.1722	0.3908	0.185	0.4887
(b) 9.8	0.0210	0.0369	0.021	0.0755
	0.0595	0.1030	0.041	0.1700
	0.0649	0.1125	0.066	0.1839
	0.1137	0.1973	0.093	0.3154
	0.1722	0.3408	0.126	0.4887
	0.2360	0.4333	0.190	0.6970
(c) 24.6	0.0639	0.0522	0.073	0.1842
	0.0845	0.1008	0.098	0.2298
	0.1193	0.1167	0.137	0.3297
	0.1683	0.1512	0.185	0.4782

χ_{ij}'s based on the single frequency measurement technique [6,17]. The aspect of molecular orientational polarization is, however, accomplished by introducing χ_{ij}'s because $\varepsilon_{\infty ij}$ which includes fast polarization, frequently appears as a subtracted term in Bergmann's equations. Thus in order to avoid the clumsiness of algebra and exclude the fast polarization Bergmann's equations [12] in terms of established symbols of χ'_{ij}, χ''_{ij} and χ_{0ij} can be written as

$$\frac{\chi'_{ij}}{\chi_{0ij}} = \frac{c_1}{1+\omega^2\tau_1^2} + \frac{c_2}{1+\omega^2\tau_2^2}, \tag{1}$$

$$\frac{\chi''_{ij}}{\chi_{0ij}} = c_1\frac{\omega\tau_1}{1+\omega^2\tau_1^2} + c_2\frac{\omega\tau_2}{1+\omega^2\tau_2^2}, \tag{2}$$

assuming two separate broad dispersions for which the sum of c_1 and c_2 is unity. Equations (1) and (2) are solved to get

$$\frac{\chi_{0ij}-\chi'_{ij}}{\chi'_{ij}} = \omega(\tau_1+\tau_2)\frac{\chi''_{ij}}{\chi'_{ij}} - \omega^2\tau_1\tau_2. \tag{3}$$

When the variables $(\chi_{0ij}-\chi'_{ij})/\chi'_{ij}$ are plotted against χ''_{ij}/χ'_{ij} for different w_j's of solute

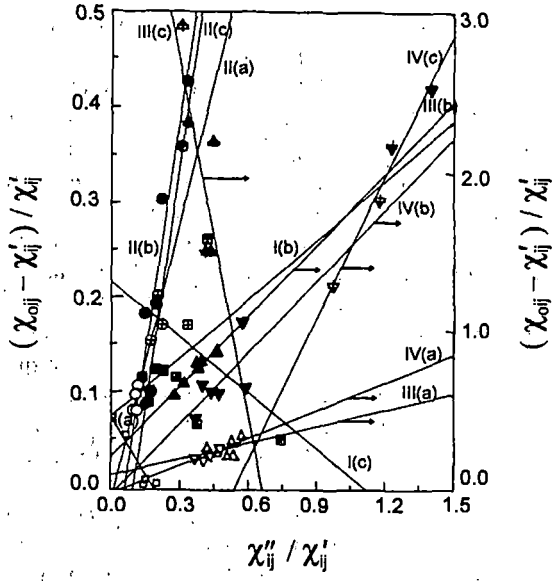

Figure 1. Linear variation of $(\chi_{0ij}-\chi'_{ij})/\chi'_{ij}$ against χ''_{ij}/χ'_{ij} for different w_j's of chloral and ethyltrichloroacetate under three different hf electric fields at 30°C. Curves I(a), I(b) and I(c) for chloral in benzene (−□−, −■−, −⊞−); curves II(a), II(b) and II(c) for chloral in *n*-heptane (−○−, −●−, −⊕−); curves III(a), III(b) and III(c) for ethyltrichloroacetate in benzene (−Δ−, −▲−, −⧋−); curve IV(a), IV(b) and IV(c) for ethyltrichloroacetate in *n*-hexane (−∇−, −▼−, −▽−) at 4.2, 9.8 and 24.6 GHz electric fields respectively.

under a given angular frequency $\omega(=2\pi f)$ of the electric field, a straight line results with the intercept $-\omega^2\tau_1\tau_2$ and slope $\omega(\tau_1+\tau_2)$, as displayed in figure 1. The intercept and slope of eq. (3) are obtained by linear regression analysis made on the measured susceptibilities for different w_j's of chloral in *n*-heptane and ethyltrichloroacetate in *n*-hexane of table 1 to get τ_1 and τ_2 as found in columns 7 and 8 of table 2 extracted from the data of table 1 based on minimum chi-square value.

Assuming a single Debye-like broad dispersion for a polar molecule in a given solvent, eq. (3) is reduced to [17] with $\tau_1 = 0$,

$$\frac{\chi_{0ij}-\chi'_{ij}}{\chi'_{ij}} = \omega\tau_2\frac{\chi''_{ij}}{\chi'_{ij}}, \tag{4}$$

in order to get τ_2 for the two polar liquids in benzene as seen in the 11th column of table 2. Both the correlation coefficients r's and the minimum chi-square values are entered in the 5th and 6th columns of table 2.

The theoretical c_1 and c_2 towards dielectric dispersions for chloral and ethyltrichloroacetate in *n*-heptane and *n*-hexane were calculated from Fröhlich's [14] theoretical equations of χ'_{ij}/χ_{0ij} and χ''_{ij}/χ_{0ij} with the estimated τ_2 and τ_1 of table 2. The experimental c_1 and c_2, on the other hand, were computed from the values of χ'_{ij}/χ_{0ij} and χ''_{ij}/χ_{0ij} at $w_j \to 0$

by graphical method of figures 2 and 3 in order to place them in table 3 for comparison. The plot of χ'_{ij}/χ_{0ij} and χ''_{ij}/χ_{0ij} against w_j of the respective solutes in figures 2 and 3 are the least square fitted parabolae with the experimental data placed upon them. They are of convex and concave shapes except ethyltrichloroacetate in n-hexane at 9.8 and 24.6 GHz electric fields. With the values of χ'_{ij}/χ_{0ij} and χ''_{ij}/χ_{0ij} in the limit of $w_j = 0$ of figures 2 and 3, and the graphical plot of $(1/\phi)\log(\cos\phi)$ against ϕ in degrees of figure 4, the symmetric and asymmetric distribution parameters γ and δ related to symmetric and characteristic relaxation times τ_s and τ_{cs} of the molecules were determined and are placed in table 3 to conclude the molecular nonrigidity and symmetric distribution as well.

The dipole moments μ_2 and μ_1 of table 4 from τ_2 and τ_1 of table 2 were then measured in terms of the linear coefficients β's of the variations of χ'_{ij} with w_j's of figure 5. All the familiar parabolic curves of χ'_{ij}'s with w_j's are found to increase with frequency (f) of the electric field. The measured μ's are compared with theoretical dipole moment μ_{theo}'s derived from available bond angles and bond moments of the substituent polar groups attached to the parent ones as sketched in figure 6. The associational aspect of the polar molecules with solvents in figure 6 exhibits the mesomeric, inductive and electromeric effects. All these effects are taken into account by the ratio of $\mu_{\text{expt}}/\mu_{\text{theo}}$ in agreement with the experimental results as seen in table 4. They are finally compared with the reported μ's and μ_1's obtained from $\mu_1 = \mu_2(c_1/c_2)^{1/2}$ assuming both the relaxation processes are equally probable.

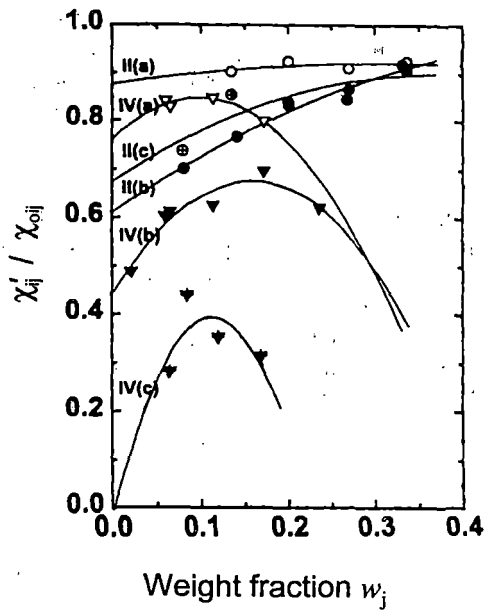

Figure 2. Variation of χ'_{ij}/χ_{0ij} against different w_j's of chloral and ethyltrichloroacetate at 30°C under various frequencies of GHz range. Curves II(a), II(b) and II(c) for chloral in n-heptane (−○−, −●−, −⊕−); curve IV(a), IV(b) and IV(c) for ethyltrichloroacetate in n-hexane (−▽−, −▼−, −▽̸−) at 4.2, 9.8 and 24.6 GHz electric fields respectively.

Table 2. The estimated relaxation times τ_2 and τ_1 from the slope and the intercept of straight line equation (3) with correlation coefficients (r) and minimum chi square values together with measured τ from the slope of $\chi''_{ij} - \chi'_{ij}$ of eq. (16) and τ_2's from single broad dispersion from eq. (4) for rigid aliphatic polar molecules at 30°C under different frequencies of electric fields.

System with sl. no. and mol. wt. M_j	Frequency in GHz(f)	Slope and intercept of eq. (3)		Correlation coefficient (r)	Minimum chi square value of eq. (3)	Estimted τ_2 and τ_1 in psec (eq. (3))		Measured τ in psec from eq. (16)	Reported τ in psec	τ_2 in psec from single broad dispersion of eq. (4)
		$\omega(\tau_1+\tau_2)$	$-\omega^2\tau_1\tau_2$							
(I) Chloral in benzene $M_j = 0.1475$ Kg	(a) 4.2	−0.3872	−0.0732	−0.91	−0.010	5.27	-	7.53	-	4.77
	(b) 9.8	0.2101	−0.0733	0.49	0.006	6.42	-	1.88	1.78*	10.12
	(c) 24.6	−0.1936	−0.2161	−0.41	0.180	2.45	-	1.72	-	2.01
(II) Chloral in n-heptane $M_j = 0.1475$ Kg	(a) 4.2	0.9995	0.0175	0.69	0.003	37.16	0.67	4.09	-	-
	(b) 9.8	1.6592	0.1040	0.93	0.053	25.89	1.06	1.78	0.46*	-
	(c) 24.6	1.7431	0.1748	0.96	0.020	10.60	0.69	0.90	-	-
(III) Ethyltrichloroacetate in benzene $M_j = 0.1915$ Kg	(a) 4.2	0.3546	−0.0698	0.37	0.047	18.78	-	23.00	-	18.71
	(b) 9.8	1.5115	−0.1800	0.97	0.005	26.36	-	7.28	6.50**	32.53
	(c) 24.6	−7.4034	−4.8872	−0.76	0.337	3.95	-	3.18	-	35.35
(IV) Ethyltrichloroacetate in n-hexane $M_j = 0.1915$ Kg	(a) 4.2	0.5843	0.0382	0.86	0.004	19.30	2.86	18.66	-	-
	(b) 9.8	1.5181	0.0548	0.66	0.153	24.05	0.60	6.28	5.70**	-
	(c) 24.6	2.9886	1.6134	0.99	0.010	14.76	4.58	7.09		-

*Cole–Cole plot; **Gopalakrishna's method.

Table 3. Fröhlich's parameter A, relative contributions c_1 and c_2 towards dielectric dispersion due to τ_1 and τ_2, theoretical and experimental values of χ'_{ij}/χ_{0ij} and χ''_{ij}/χ_{0ij} of Fröhlich's equations (7) and (8) and from fitting equations of figures 2 and 3 at $w_j \to 0$ respectively and symmetric and asymmetric distribution parameter γ and δ related to symmetric and characteristic relaxation times τ_s and τ_{cs} for polar-nonpolar liquid mixtures at 30°C.

System with sl. no.	Frequency in GHz	Fröhlich's parameter $A = \ln(\tau_2/\tau_1)$	Theoretical values of χ'_{ij}/χ_{0ij} and χ''_{ij}/χ_{0ij} from eqs (7) and (8)		Theoretical values of c_1 and c_2		Experimental values of χ'_{ij}/χ_{0ij} and χ''_{ij}/χ_{0ij} at $w_j \to 0$		Experimental values of c_1 and c_2		Estimated values of γ and δ		τ_s and τ_{cs} in psec	
(II) Chloral in *n*-heptane	4.2	4.0137	0.9161	0.1886	0.7373	0.3512	0.880	0.161	0.7287	0.2927	0.29	0.18	4.60	59.71
	9.8	3.1956	0.8028	0.2958	0.6463	0.5639	0.615	0.320	0.4334	0.6492	0.25	0.42	10.52	35.51
	24.6	2.7319	0.7634	0.3355	0.6043	0.6111	0.675	0.289	0.5395	0.5211	0.28	0.36	3.13	13.49
(IV) Ethyl-trichloro-acetate in *n*-hexane	4.2	1.9093	0.9411	0.2071	0.6310	0.3950	0.765	0.325	0.1494	0.7762	0.14	0.50	16.18	39.29
	9.8	3.6910	0.8429	0.2547	0.6891	0.4943	0.445	0.286	0.2583	0.5968	0.33	0.43	20.48	65.69
	24.6	1.1702	0.3937	0.4629	0.4152	0.7264	−0.015	0.298	−0.3167	1.2155	−0.21	-	18.73	-

Table 4. Estimated coefficients of $\chi'_{ij} - w_j$ equations, dimensionless parameters b_2, b_1 (eq. (20)), estimated dipole moments μ_2 and μ_1 from eq. (19) and μ_{theo} from bond angle and bond moment together with μ_1 from $\mu_1 = \mu_2(c_1/c_2)1/2$ and reported μ in Coulomb-metre (C.m.).

System with sl. no. and mol. wt. M_j	Frequency in GHz (f)	Coefficients of $\chi'_{ij} - w_j$ equation $\chi'_{ij} = \alpha + \beta w_j + \gamma w_j^2$			Dimensionless parameter		Estimated $\mu \times 10^{30}$ in C.m.		Reported $\mu \times 10^{30}$ in C.m.	Estimated $\mu_1 \times 10^{30}$ in C.m. from $\mu_1 = \mu_2(c_1/c_2)^{1/2}$	Conformational $\mu_{\text{theo}} \times 10^{30}$ in C.m.
		α	β	γ	b_1	b_2	μ_1	μ_2			
(I) Chloral in	4.2	0.0291	1.7212	1.6641	-	0.9810	-	5.21	5.17*	-	
benzene	9.8	0.0218	1.6402	1.1834	-	0.8648	-	5.42	4.87**	-	10.02
$M_j = 0.1475$ Kg	24.6	0.0333	1.4368	1.6836	-	0.8746	-	5.04	4.73*	-	
(II) Chloral in	4.2	−0.0250	1.5050	0.4654	0.9997	0.5098	5.99	8.39	6.13*	12.16	10.02
n-heptane	9.8	0.0150	0.7168	2.4649	0.9958	0.2824	4.14	7.78	6.00**	8.33	
$M_j = 0.1475$ Kg	24.6	−0.0223	1.2478	1.1078	0.9888	0.2714	5.48	10.47	5.63*	10.41	
(III) Ethyl-	4.2	0.0295	3.5204	−1.3400	-	0.8028	-	9.39	9.70*	-	
trichloroacetate	9.8	0.0490	1.7935	1.9676	-	0.2751	-	11.45	6.50**	-	
in benzene	24.6	−0.0309	2.7329	−6.6401	-	0.7285	-	8.68	8.13*	-	10.50
$M_j = 0.1915$ Kg											
(IV) Ethyl-	4.2	−0.0084	2.6215	−1.7604	0.9943	0.7940	9.16	10.28	10.30*	12.98	
trichloroacetate	9.8	−0.0108	1.9711	−0.2513	0.9986	0.3132	7.95	14.19	8.67**	16.74	
in n-hexane	24.6	−0.0683	2.4108	−6.6385	0.6662	0.1612	10.76	21.87	13.27*	16.53	10.50
$M_j = 0.1915$ Kg											

*Computed from the susceptibility measurement of eq. (16); **Ref. [7].

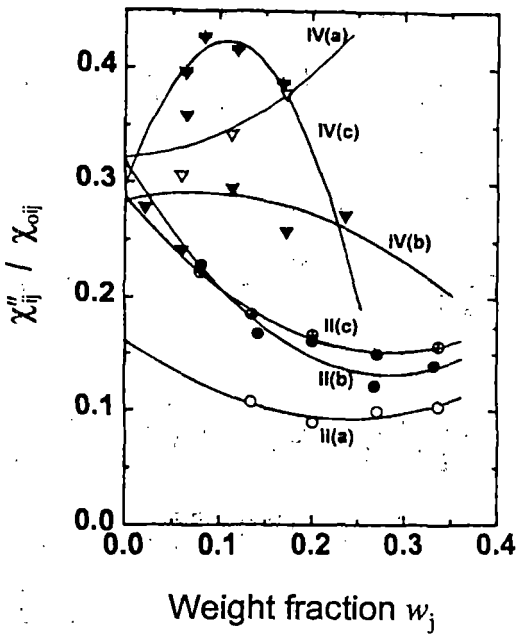

Figure 3. Variation of χ''_{ij}/χ_{0ij} against different w_j's of chloral and ethyltrichloro acetate at 30°C under various frequencies of GHz range. Curves II(a), II(b) and II(c) for chloral in *n*-heptane ($-\circ-, -\bullet-, -\oplus-$); curve IV(a), IV(b) and IV(c) for ethyltrichloroacetate in *n*-hexane ($-\nabla-, -\blacktriangledown-, -\boxtimes-$) at 4.2, 9.8 and 24.6 GHz electric fields respectively.

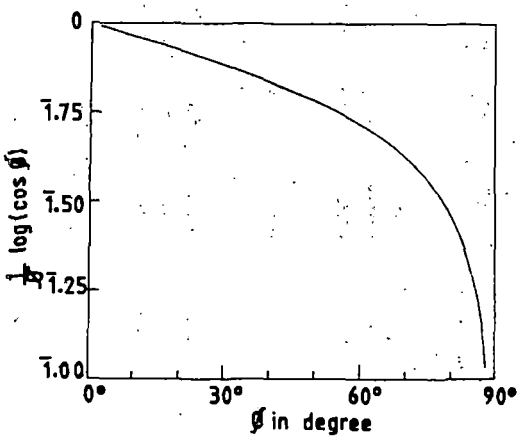

Figure 4. Plot of $(1/\phi)\log(\cos\phi)$ against ϕ in degree.

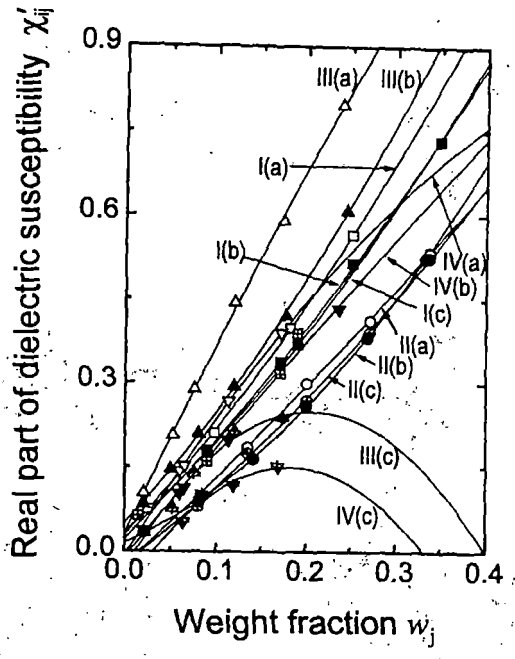

Figure 5. Plot of real part of dielectric susceptibility χ'_{ij} against w_j's of solutes for 4.2, 9.8 and 24.6 GHz electric fields at 30°C. Curves I(a), I(b) and I(c) for chloral in benzene (–□–, –■–, –⊞–); curves II(a), II(b) and II(c) for chloral in *n*-heptane (–○–, –●–, –⊕–); curves III(a), III(b) and III(c) for ethyltrichloroacetate in benzene (–Δ–, –▲–, –⧋–). Curve IV(a), IV(b) and IV(c) for ethyltrichloroacetate in *n*-hexane (–▽–, –▼–, –⧩–) at 4.2, 9.8 and 24.6 GHz electric fields respectively.

2. Theoretical formulations of c_1 and c_2 for τ_1 and τ_2

Equations (1) and (2) are solved for c_1 and c_2 to get

$$c_1 = \frac{(\chi'_{ij}\alpha_2 - \chi''_{ij})(1+\alpha_1^2)}{\chi_{0ij}(\alpha_2 - \alpha_1)}, \tag{5}$$

$$c_2 = \frac{(\chi''_{ij} - \chi'_{ij}\alpha_1)(1+\alpha_2^2)}{\chi_{0ij}(\alpha_2 - \alpha_1)}, \tag{6}$$

where $\alpha_1 = \omega\tau_1$ and $\alpha_2 = \omega\tau_2$, provided $\alpha_2 > \alpha_1$. The molecules under consideration are of complex type and only a few data are available under single frequency measurement in the low concentration region. A continuous distribution of τ with two discrete values of τ_1 and τ_2 could, therefore, be expected [12]. Thus from Fröhlich's theory [14] based on distribution of τ between the two extreme values of τ_1 and τ_2 one gets

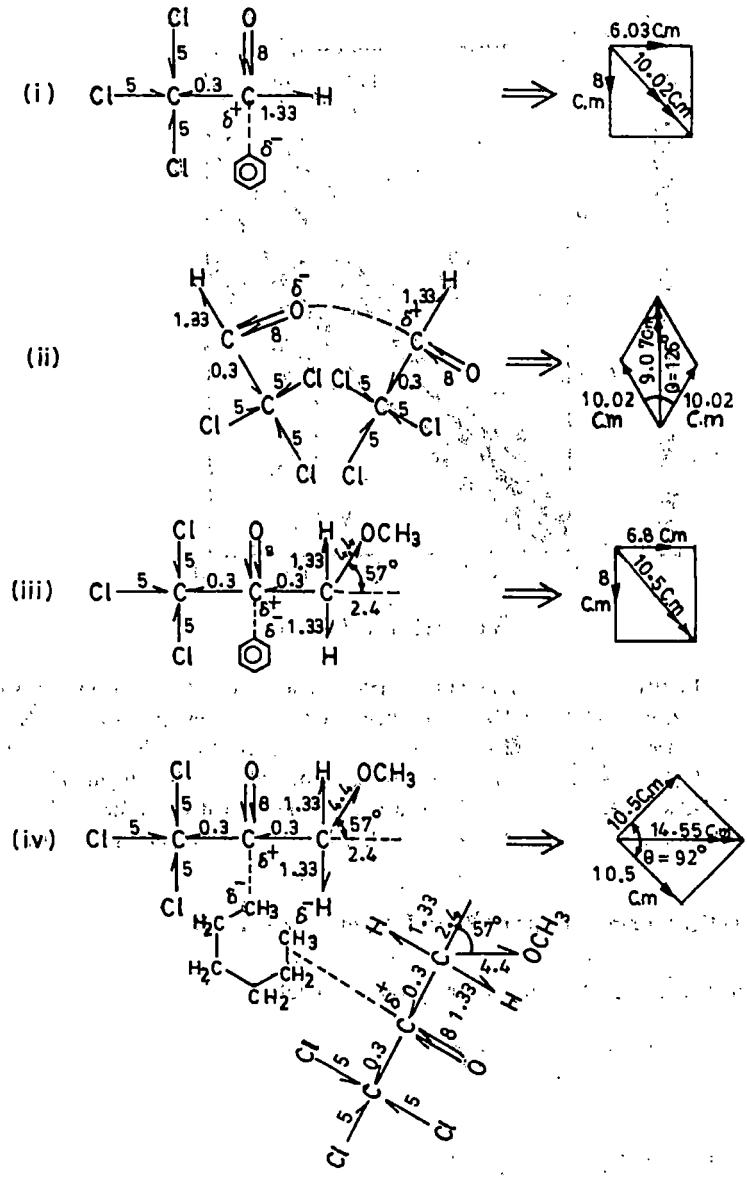

Figure 6. Conformational structures of chloral and ethyltrichloroacetate from bond angles and bond moments (expressed in multiple of 10^{-30} Coulomb metre). (i) Solute–solvent molecular association of chloral in benzene. (ii) Solute–solute molecular association of chloral in *n*-heptane. (iii) Solute–solvent molecular association of ethyltrichloroacetate in benzene. (iv) Solute–solute molecular association of ethyltrichloroacetate in *n*-hexane.

$$\frac{\chi'_{ij}}{\chi_{0ij}} = 1 - \frac{1}{2A}\ln\left(\frac{1+\omega^2\tau_2^2}{1+\omega^2\tau_1^2}\right), \tag{7}$$

$$\frac{\chi''_{ij}}{\chi_{0ij}} = \frac{1}{A}[\tan^{-1}(\omega\tau_2) - \tan^{-1}(\omega\tau_1)], \tag{8}$$

where A = Fröhlich parameter = $\ln(\tau_2/\tau_1)$. The theoretical values of χ'_{ij}/χ_{0ij} and χ''_{ij}/χ_{0ij} of eqs (7) and (8) were used to get theoretical c_1 and c_2 from eqs (1) and (2) in order to compare them with c_1 and c_2 from the graphical plots of χ'_{ij}/χ_{0ij} and χ''_{ij}/χ_{0ij} at $w_j \to 0$ as seen in figures 2 and 3. Both the theoretical and experimental c_1 and c_2 are placed in table 3.

3. Distribution parameters γ and δ related to τ_s and τ_{cs}

All the chemical systems are almost identical for the three frequencies employed. Nevertheless, the existence of double relaxations for chloral in *n*-heptane and ethyltrichloroacetate in *n*-hexane reflects the material property of the chemical systems (table 2) indicating the molecular nonrigidity. In such case, the molecule may either show symmetrical circular arc or a skewed arc [20] when the values of χ''_{ij}/χ_{0ij} is plotted aginst χ'_{ij}/χ_{0ij} at $w_j \to 0$ for various frequencies of the electric field to yield

$$\frac{\chi^*_{ij}}{\chi_{0ij}} = \frac{1}{1+(j\omega\tau_s)^{1-\gamma}}, \tag{9}$$

$$\frac{\chi^*_{ij}}{\chi_{0ij}} = \frac{1}{(1+j\omega\tau_{cs})^{\delta}}. \tag{10}$$

Here, γ and δ are the symmetric and asymmetric distribution parameters which are, related to symmetric and characteristic relaxation times τ_s and τ_{cs} respectively. Separating the real and imaginary parts from eq. (9) one has

$$\gamma = \frac{2}{\pi}\tan^{-1}\left[\left(1-\frac{\chi'_{ij}}{\chi_{0ij}}\right)\frac{\chi'_{ij}}{\chi''_{ij}} - \frac{\chi''_{ij}}{\chi_{0ij}}\right], \tag{11}$$

$$\tau_s = \frac{1}{\omega}\left[1\Big/\left\{\left(\frac{\chi'_{ij}}{\chi''_{ij}}\right)\cos\left(\frac{\gamma\pi}{2}\right) - \sin\left(\frac{\gamma\pi}{2}\right)\right\}\right]^{1/(1-\gamma)}, \tag{12}$$

where χ'_{ij}/χ_{0ij} and χ''_{ij}/χ_{0ij} are obtained from figures 2 and 3 at $w_j \to 0$. Again δ and τ_{cs} can be had from eq. (10) as

$$\tan(\phi\delta) = \frac{\chi''_{ij}}{\chi'_{ij}} \tag{13}$$

and

$$\tau_{cs} = \frac{1}{\omega}\tan\phi. \tag{14}$$

Since ϕ cannot be evaluated directly, a theoretical curve of $(1/\phi)\log(\cos\phi)$ with ϕ in degrees was drawn in figure 4 from which

$$\frac{1}{\phi}\log(\cos\phi) = \frac{\log[(\chi'_{ij}/\chi_{0ij})/\cos(\phi\delta)]}{\phi\delta} \tag{15}$$

can be found out. The known value of $(1/\phi)\log(\cos\phi)$ was then used to obtain ϕ. With known ϕ and δ, τ_{cs} were found out from eqs (13) and (14). The estimated γ and δ are entered in 12 and 13 with τ_s and τ_{cs} in columns 14 and 15 of table 3 to conclude the symmetric relaxation behaviour for such liquids.

4. Theoretical formulation for dipole moments μ_2 and μ_1

The Debye equation [14] for a polar–nonpolar liquid mixture under hf electric field in terms of χ_{ij}'s is written as

$$\mathrm{d}\chi''_{ij}/\mathrm{d}\chi'_{ij} = \omega\tau \quad \text{or} \quad \left(\frac{\mathrm{d}\chi''_{ij}}{\mathrm{d}w_j}\right)_{w_j\to 0} = \omega\tau\left(\frac{\mathrm{d}\chi'_{ij}}{\mathrm{d}w_j}\right)_{w_j\to 0}. \tag{16}$$

τ's of the polar liquids could, however, be estimated from eq. (16) in order to place in column 9 of table 2. Again, the imaginary part of dielectric orientational susceptibility χ''_{ij} as a function of w_j of a solute can be written as [21,22]

$$\chi''_{ij} = \frac{N\rho_{ij}\mu_j^2}{27\varepsilon_0 k_B T M_j}\left(\frac{\omega\tau}{1+\omega^2\tau^2}\right)(\varepsilon_{ij}+2)^2 w_j.$$

Differentiation of the above equation with respect to w_j and at $w_j \to 0$ yields

$$\left(\frac{\mathrm{d}\chi''_{ij}}{\mathrm{d}w_j}\right)_{w_j\to 0} = \frac{N\rho_i\mu_j^2}{27\varepsilon_0 k_B T M_j}\left(\frac{\omega\tau}{1+\omega^2\tau^2}\right)(\varepsilon_i+2)^2, \tag{17}$$

where the density of the solution ρ_{ij} becomes ρ_i = density of solvent, $(\varepsilon_{ij}+2)^2 \to (\varepsilon_i+2)^2$ at $w_j \to 0$, k_B = Boltzmann constant, N = Avogadro's number, ε_i = relative permittivity of solvent and ε_0 = permittivity of free space = 8.854×10^{-12} F.m^{-1}. All are expressed in SI units.

Comparing eqs (16) and (17) one gets

$$\omega\tau\left(\frac{\mathrm{d}\chi'_{ij}}{\mathrm{d}w_j}\right)_{w_j\to 0} = \frac{N\rho_i\mu_j^2}{27\varepsilon_0 k_B T M_j}\left(\frac{\omega\tau}{1+\omega^2\tau^2}\right)(\varepsilon_i+2)^2 = \omega\tau\beta, \tag{18}$$

where, β is the slope of $\chi'_{ij} - w_j$ curves of figure 5 at $w_j \to 0$. Here, no approximation in determination of μ_j is made like the conductivity measurement technique done elsewhere [23].

After simplification, the hf dipole moment μ_j is given by

$$\mu_j = \left(\frac{27\varepsilon_0 k_B T M_j}{N\rho_i(\varepsilon_i+2)^2}\,\frac{\beta}{b}\right)^{1/2}, \tag{19}$$

where

$$b = 1/(1+\omega^2\tau^2) \tag{20}$$

is the dimensionless parameter involved with measured τ's of table 2. All the μ's, b's and β's as computed for chloral and ethyltrichloroacetate in different solvents at 30°C are placed in table 4 to compare with μ_{theo}'s from the available bond angles and bond moments in Coulomb-metre (C.m).

5. Results and discussions

The double or single relaxation phenomena for chloral and ethyltrichloroacetate in benzene, *n*-heptane and *n*-hexane under 24.6, 9.8 and 4.2 GHz electric field frequencies were studied from the slopes and intercepts of linear plots in figure 1 for the variables $(\chi_{0ij}-\chi'_{ij})/\chi'_{ij}$ against χ''_{ij}/χ'_{ij} of theoretical formulation of eq. (3) for different w_j's of solutes at 30°C. The dielectric orientational susceptibilities χ'_{ij}, χ''_{ij} and χ_{0ij} are collected together in table 1 from the measured relative permittivities of $\varepsilon'_{ij}, \varepsilon''_{ij}, \varepsilon_{0ij}$ and $\varepsilon_{\infty ij}$ [7]. The linear regression analysis made on eq. (3) with the data of table 1 was, however, done by the use of a PC and software. The correlation coefficients r's are placed in table 2 in getting the intercepts and slopes of (3) to see how far the data of table 1 are collinear. The errors involved in the linear regression analysis of (3) are expressed by chi-square values which were initially very large in some cases. One therefore, should have become selective to choose a few data for some systems for which chi-square values were adjusted to be minimum for the effective utilization of the experimental data [7]. The large chi-square values initially obtained for (3) further indicate the probable uncertainty in the measurements. The minimum chi-square values so adjusted on the data are presented in column 6 of table 2. The data for chloral in benzene ($-\square-, -\boxplus-$); at 4.2 and 24.6 GHz and ethyltrichloroacetate in *n*-hexane ($-\blacktriangledown-$); at 9.8 GHz do not appear to lie on the straight line. The display of data set for ethyltrichloroacetate in benzene ($-\Delta-, -\blacktriangle-$); at 4.2 and 24.6 GHz and in *n*-hexane ($-\nabla-$); at 4.2 GHz is over a narrow range which often renders the linear regression of doubtful validity. Perfect linearity between variables of eq. (3) is said to be achieved if $r = -1$ or $+1$ although, the correlation coefficients r's for the systems ($-\boxplus-, -\square-, -\blacktriangledown-$) are -0.41, -0.91 and 0.66 respectively. The high value of $r = -0.91$ for chloral in benzene ($-\square-$) at 4.2 GHz indicates that the variables of eq. (3) are almost linearly correlated with each other while comparatively lower values of r's of -0.41 and 0.66 for chloral in benzene at 24.6 GHz ($-\boxplus-$) and ethyltrichloroacetate in *n*-hexane at 9.8 GHz ($-\blacktriangledown-$) may occur for the experimental difficulty of the accurate measurements of the relative permittivities in the 24.6 GHz electric field. The desired variables $(\chi_{0ij}-\chi'_{ij})/\chi'_{ij}$ and χ''_{ij}/χ'_{ij} of eq. (3) for ethyltrichloroacetate in benzene ($-\Delta-$) and *n*-hexane ($-\nabla-$) at 4.2 GHz and ethyltrichloroacetate in benzene at 24.6 GHz ($-\blacktriangle-$) are incidentally of narrow range although the relative permittivities were measured [7] for a wide range of concentrations as seen in table 1. Nevertheless, the straight lines of the data set for the systems under consideration as displayed in figure 1 are made on the basis

of minimum chi square values mathematically adjusted between two variables. The high values of r's as shown in table 2 signify the applicability of linear regression analysis on the data set mentioned above.

Four data set out of six, showed mono while other two double relaxations which are important. Nevertheless, the measurement technique employed and sampling of the polar–nonpolar liquid mixtures for various concentrations called w_j's were so prepared [7,8] that χ'_{ij}, χ_{0ij} and χ''_{ij} of table 1 for different w_j's are of 2% and 5% accuracies. This type of anomaly showed in benzene and n-hexane the associational aspects [24] of polar molecules. The estimated values of τ_2 and τ_1 from the intercepts and slopes of table 2 are placed in the 7th and 8th columns of table 2. Double relaxation phenomena are, however, observed for chloral in n-heptane and ethyltrichloroacetate in n-hexane at 4.2 GHz (J-band), 9.8 GHz (X-band) and 24.6 GHz (Q-band) hf electric field. This fact indicates that the phenomena of double or single relaxation are the material property of the chemical system in addition to the dependency on solvent used. It further reveals that the existence of double relaxation phenomena in aliphatic solvents at all the frequencies is greater than in the aromatic solvent. Both chloral and ethyltrichloroacetate in benzene showed the single relaxation by showing τ_2 only. The existence of fractional +ve charge δ^+ on C atom and δ^- on O atom of $> C \Longleftarrow O$ group in both the polar liquids produces electromeric effect to form π-complexes with the delocalized π electron cloud δ^- of benzene ring. This prefers the solute–solvent molecular association and yields single τ_2 in benzene. The τ_2's were calculated from eq. (4) assuming single broad Debye-like dispersion [17]. They are placed in column 11 of table 2. It is interesting to note that τ_1's for two molecules agree well with the measured τ from eq. (16) involved with measured susceptibility. Thus the hf susceptibility measurement always yields the microscopic as well as macroscopic τ as observed for double relaxation phenomena through conductivity measurements [18].

Almost all τ_2's of table 2 are higher at 9.8 GHz, but of low values both at 4.2 and 24.6 GHz electric field in different solvents. Such behaviour occurs probably due to strong absorbtion of electric energy in the effective dispersive region of 9.8 GHz. The solute–solvent of solute–solute molecular associations break up at higher and lower frequencies from nearly 10 GHz electric field. Almost all the τ_1 agree with the reported τ seen in the 10th column of table 2 exhibiting the probability of rotation of a part of the molecule under hf electric field [9].

The theoretical values of the relative contributions c_1 and c_2 towards dielectric dispersions due to τ_1 and τ_2 are, however, calculated from eqs (5) and (6) with the theoretical values of χ'_{ij}/χ_{0ij} and χ''_{ij}/χ_{0ij} of Fröhlich's [14] eqs (7) and (8). They are compared with the experimental c_1 and c_2 derived from eqs (5) and (6) with the graphically estimated χ'_{ij}/χ_{0ij} and χ''_{ij}/χ_{0ij} of figures 2 and 3 at $w_j \to 0$. Both the methods yield $c_1 + c_2 \cong 1$ suggesting the applicability of the methods. The variations of χ'_{ij}/χ_{0ij} and χ''_{ij}/χ_{0ij} with w_j are convex and concave unlike the observation made earlier [6,17], except ethyltrichloroacetate in n-hexane at 9.8 and 24.6 GHz both of which show the convex variation. Such type of behaviour is explained by the fact that unlike increase of τ [25] it decreases with w_j probably due to solute–solute or solute–solvent molecular associations. All the experimental values of c_1 and c_2 are placed in table 3 for comparison with the theoretical c_1 and c_2.

In order to test the non-rigid relaxation behaviour of the molecules the symmetric and asymmetric distribution parameters γ and δ were estimated from eqs (11) and (13) for fixed values of χ'_{ij}/χ_{0ij} and χ''_{ij}/χ_{0ij} at $w_j \to 0$ from figures 2 and 3. γ and δ are, however

related to symmetric and asymmetric relaxation times τ_s and τ_{cs} of eqs (12) and (14). The values of $(1/\phi)\log(\cos\phi)$ against ϕ in degrees as shown in figure 4 is essential to get δ. Knowing ϕ from the curve of figure 4; δ's were found out. Both γ, δ and τ_s, τ_{cs} are placed in table 3. The values of γ establish the nonrigid and symmetrical distribution of dielectric parameters of the molecules in *n*-hexane and *n*-heptane at all the frequencies unlike δ, as they are found to be very low [26].

The dipole moments μ_2 and μ_1 of polar molecules as presented in table 4 were estimated from eq. (19) in terms of dimensionless parameters b's of eq. (20) and slope β of the familiar $\chi'_{ij} - w_j$ curves of figure 5 as seen in table 4. The variation of χ'_{ij} with w_j are almost similar as seen in figure 5 and table 4 like conductivity measurement presented elsewhere [23]. Estimated dipole moments are found in agreement with the reported μ's to signify the applicability of the present method. μ_2's are found to increase from 24.6 GHz to 4.2 GHz electric field showing the maximum values at 9.8 GHz for both chloral and ethyltrichloroacetate in benzene. This type of behaviour may be due to strong absorbtion of electric energy at 9.8 GHz and solute–solvent association of polar solute with benzene ring. But μ_2's for chloral in *n*-heptane and ethyltrichloroacetate in *n*-hexane increase gradually from 4.2 GHz. This sort of variation is probably due to rupture of solute– solute and solute–solvent molecular associations in the hf electric field and the corresponding increase in the absorbtion for smaller molecular species [27].

The μ_2 and μ_1 for chloral in *n*-heptane and ethyltrichloroacetate in *n*-hexane at 4.2, 9.8 and 24.6 GHz as well as μ_2 of those liquids in benzene (table 4) are, however, compared with μ_{theo}'s due to available bond angles and bond moments 8.0, 5.0, 0.3 and 2.4 multiple of 10^{-30} Coulomb metre (C.m) for the substituent polar groups of C⇐=O, C⇐=Cl, C←—C and C→OCH_3 (making an angle 57° with bond axis) respectively with the parent molecules of figure 6. μ_{theo}'s are entered in column 12 of table 4. Chloral shows slightly larger μ_{theo} for solute–solute molecular associations (figure 6(ii)) in the comparatively concentrated solution as expected [28]. The solute–solute molecular association arises due to interaction of fractional positive charge δ^+ on C atom and negative charge δ^- on O atom of >C⇐=O group of two solute molecules. Only >C⇐=O exhibits electromeric effect. The solvent C_6H_6 on the other hand, is a cyclic compound with three double bonds and six *p*-electrons on six C atoms. Hence π–π interaction or resonance effect combined with inductive effect known as mesomeric effect is expected to play an important role in the measured hf μ_j. Special attention is, therefore, paid to study the solute–solvent molecular association with C_6H_6. This is explained by the interaction between C atom of carbonyl group and π-delocalized electron cloud of benzene ring. Ethyltrichloroacetate, on the other hand, shows μ_{theo} in agreement with the estimated μ's in C_6H_6. This is due to solute–solvent molecular association as sketched in figure 6(i) and (iii). Larger values of measured μ's are explained by the solute–solute molecular interactions in solvent *n*-hexane due to interaction between adjacent C and O atoms of >C⇐=O groups of two molecules as shown in figure 6(iv). However, the reduced bond moments by μ_{expt}/μ_{theo} corroborate μ_{theo}'s in agreement with the experimental μ's to measure mesomeric, inductive and electromeric effects of the substituent polar groups of the molecules.

6. Conclusion

Theoretical considerations for the effective utilization of the established symbols of dielectric terminologies and parameters in terms of dielectric susceptibilities from dielectric relative permittivities appear to be more topical, significant and useful contribution in the

study of dielectric relaxation mechanism as they are directly concerned with orientational polarization of the polar molecules. The significant formulations so far derived in terms of χ'_{ij}, χ''_{ij} and χ_{0ij} measured under the single frequency measurements of relative permittivities help one to grasp a new physical insight into the molecular interactions. The single frequency measurement of relaxation parameters provide a unique method to get macroscopic and microscopic relaxation times and hence dipole moments of the whole and the flexible part of a molecule. The estimation of τ_1 and τ_2 from the linear equation (3) is simple and straightforward to get μ from eq. (19) in terms of slope of familiar $\chi'_{ij} - w_j$ curve. The correlation coefficient and chi-square values signify the minimum error introduced into the desired parameters. The molecules under identical state of environment show interesting phenomena of double or even single relaxation depending upon the solvent used. Aliphatic polar molecules have the greater probability of showing double relaxation in nonpolar aliphatic solvents. Various types of molecular associations like solute–solute and solute–solvent associations are thus inferred from the usual departure of the graphical plots of χ'_{ij}/χ_{0ij} and χ''_{ij}/χ_{0ij} with w_j following Bergmann's equations. Nonrigid characteristics of the molecules are ascertained by the symmetric distribution parameter in solvents. The molecular associations are supported by the conformational structures of the molecules in which the mesomeric, inductive and electromeric effects play an important role. The correlation between the conformational structures of the compounds with the observed results enhances the scientific contents and adds a new horizon to understanding the existing knowledge of dielectric relaxation.

References

[1] A K Sharma, D R Sharma and D S Gill, *J. Phys.* **D18**, 1199 (1985)
[2] A Sharma and D R Sharma, *J. Phys. Soc. Jpn.* **61**, 1049 (1992)
[3] K S Cole and R H Cole, *J. Chem. Phys.* **9**, 341 (1941)
[4] D W Davidson and R H Cole, *J. Chem. Phys.* **19**, 1484 (1951)
[5] K V Gopalakrishna, *Trans. Faraday Soc.* **53**, 767 (1957)
[6] U Saha, S K Sit, R C Basak and S Acharyya, *J. Phys.* **D27**, 596 (1994)
[7] S K Srivastava and S L Srivastava, *Indian J. Pure Appl. Phys.* **13**, 179 (1975)
[8] A D Franklin, W M Heston, E J Hennelly and C P Smyth, *J. Am. Chem. Soc.* **72**, 3447 (1950)
[9] K Dutta, R C Basak, S K Sit and S Acharyya, *J. Molecular Liquids* **88**, 229 (2000)
[10] A K Jonscher, *Physics of dielectric solids*, invited papers edited by C H L Goodman (1980) p. 7
[11] A Budo, *Phys. Z.* **39**, 706 (1938)
[12] K Bergmann, D M Roberti and C P Smyth, *J. Phys. Chem.* **64**, 665 (1960)
[13] A Mansing and P Kumar, *J. Phys. Chem.* **69**, 4197 (1965)
[14] H Fröhlich, *Theory of dielectrics* (Oxford University Press, Oxford, 1949) p. 94
[15] J Bhattacharyya, A Hasan, S B Roy and G S Kastha, *J. Phys. Soc. Jpn.* **28**, 204 (1970)
[16] K Higasi, Y Koga and M Nakamura, *Bull. Chem. Soc. Jpn.* **44**, 988 (1971)
[17] S K Sit, R C Basak, U Saha and S Acharyya, *J. Phys.* **D27**, 2194 (1994)
[18] S K Sit and S Acharyya, *Indian J. Phys.* **B70**, 19 (1996)
[19] S K Sit, N Ghosh and S Acharyya, *Indian J. Pure Appl. Phys.* **35**, 329 (1997)
[20] J G Powles, *J. Molecular Liquids* **56**, 35 (1993)
[21] C P Smyth, *Dielectric behaviour and structure* (Mc Graw Hill, 1955) p. 140
[22] N Ghosh, S K Sit, A K Bothra and S Acharyya, *J. Phys.* **34**, 379 (2001)
[23] K Dutta, S K Sit and S Acharyya, *J. Molecular Liquids* **92**, 263 (2001)
[24] H D Purohit, H S Sharma and A D Vyas, *Indian J. Pure Appl. Phys.* **12**, 273 (1974)

[25] S N Sen and R Ghosh, *Indian J. Pure Appl. Phys.* **10**, 701 (1972)
[26] S Chandra and J Prakash, *J. Phys. Soc. Jpn.* **35**, 876 (1975)
[27] L Glasser, J Crossley and C P Smyth, *J. Chem. Phys.* **57**, 3977 (1972)
[28] R J Sengwa and K Kaur, *Indian J. Pure Appl. Phys.* **37**, 469 (1999)

Indian Journal of Pure & Applied Physics
Vol. 40, August 2002, pp.588-596

Relaxation phenomena in methyl benzenes and ketones from ultra high frequency conductivity

K Dutta, A Karmakar, S K Sit & S Acharyya

Department of Physics, Raiganj College (University College), PO Raiganj, Dist Uttar Dinajpur (WB) 733 134

e-mail: koushikduttajsm@rediffmail.com

Received 30 August 2001; revised 14 February 2002; accepted 30 May 2002

The relaxation time τ and dipole moment μ of some methyl benzenes and ketones (j) in a non-polar solvent benzene (i) at 25 °C under 9.585 GHz electric field have been obtained from the measured real and imaginary parts ε_{ij}' and ε_{ij}'' of hf complex relative permittivity ε_{ij}^* at various weight fractions w_j's of a polar liquid. The methodology to get τ from the ratio of the individual slopes of real $\sigma_{ij}'(=\omega\varepsilon_0\varepsilon_{ij}'')$ and imaginary $\sigma_{ij}''(=\omega\varepsilon_0\varepsilon_{ij}')$ parts of complex hf conductivity σ_{ij}^* curve against w_j's, seems to be a significant improvement over the existing one like the linear slope of $\sigma_{ij}''-\sigma_{ij}'$ curve. The variation of $\sigma_{ij} - w_j$ curve like $\sigma_{ij}''- w_j$ curve is often convex indicating the probable occurrence of phase change in the polar-nonpolar liquid mixture after a certain concentration. The convex nature of $\sigma_{ij}'- w_j$ curves for some systems indicate the maximum absorption of hf electric energy unlike other systems. The estimated μ's from slope β of hf conductivity $\sigma_{ij} - w_j$ curve and τ from both the methods are compared with the work of Gopalakrishna to establish the applicability of the methods. Theoretical dipole moments μ_{theo}'s from available bond angles and bond moments are calculated by considering inductive, mesomeric and electromeric effects of the substituent polar groups of the molecules.

1 Introduction

Relaxation processes in dielectric polar liquid or solid material (DRL or DRS) are very encouraging to study the molecular behaviour and structures through various experimental techniques[1,2]. The methods are involved with the high frequency conductivity[3] or susceptibility measurements[4], thermally stimulated de-polarisation current[5] (TSDC) and time or frequency domain dielectric ac spectroscopy[6] etc. The latter two methods consist of a tedious computer simulated calculation in comparison to others, which are very simple and straightforward within the framework of Debye & Smyth model of dielectric liquid molecule.

Vaish & Mehrotra[7,8] measured real and imaginary parts (ε_{ij}' and ε_{ij}'') of complex dielectric relative permittivity ε_{ij}^* of some methyl benzenes and ketones (j) in benzene (i) under 3.13 cm wavelength electric field at 25 °C. They attempted to correlate dielectric relaxation times with those of nuclear magnetic resonance spin lattice relaxation times by using the theory of Bloembergen *et al.*[9] in terms of measured relaxation parameters. The relaxation times τ of the molecules were calculated on the assumption that dipole-dipole (dimer) interaction occurs between the nuclear spins. The spin lattice relaxation times were obtained to compare with the Gopalakrishna, Debye and other methods. The experimental values differ significantly from those of theoretical one. This study reveals that, τ plays the main role in inter and intra molecular motions and nuclear magnetic resonance (NMR) spin lattice relaxation etc.

The values of τ and dipole moment μ of these polar molecules by the conductivity technique have been calculated in the present paper. The procedures employed to get τ are those of Murthy *et al.*[10] from the direct slope of the linear equation of imaginary $\sigma_{ij}''(=\omega\varepsilon_0\varepsilon_{ij}')$ and real $\sigma_{ij}'(=\omega\varepsilon_0\varepsilon_{ij}'')$ in Ω^{-1} m^{-1} parts of the hf complex conductivity σ_{ij}^* (Fig. 1) and the ratio of the individual slopes of $\sigma_{ij}''- w_j$ and $\sigma_{ij}'- w_j$ curves[11] (Figs 2 and 3) at $w_j\rightarrow 0$ respectively. The use of the ratio of individual slopes to estimate τ seems to be better as it eliminates the polar-polar interaction almost completely. Hence, the purpose of the present paper is to study the success or otherwise of the proposed theory with the existing ones to infer molecular structures and associations. The graphs of σ_{ij}'' and σ_{ij}' with w_j's in Figs 2 and 3 are found to be non-linear to indicate the presence of solute-solute associations in the mixture. The τ's

from linear slope are found to agree with the reported τ's from Gopalakrishna's fixed frequency method (Fig. 4) and are presented in Table 1 together with all the measured τ's by different procedures. Further, the polar molecules under

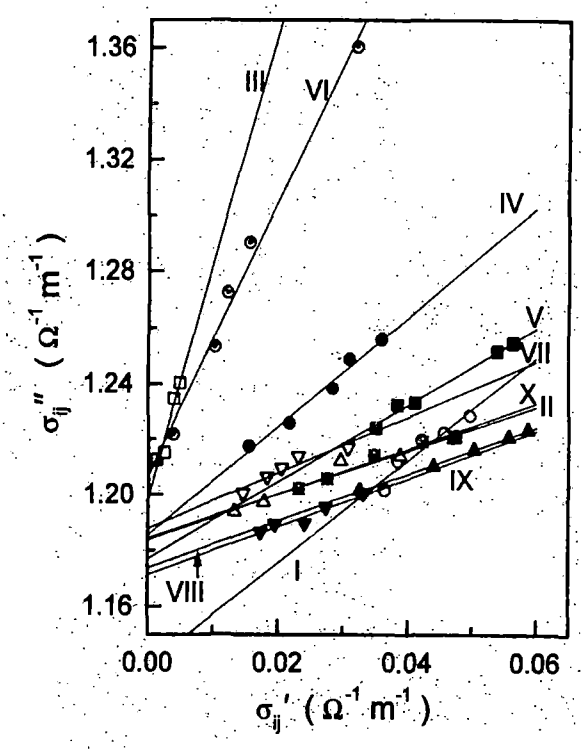

Fig. 1 — The linear variation of imaginary part σ_{ij}'' against real part σ_{ij}' of complex hf conductivity σ_{ij}^* at 25 °C under 9.585 GHz electric field : (I) toluene (-○-); (II) 1,3,5 tri methyl benzene (-Δ-); (III) 1,2,3,4 tetra methyl benzene (-□-); (IV) 1,2,4,5 tetra methyl benzene (-●-); (V) penta methyl benzene (-■-); (VI) p-fluoro toluene (-⊙-);(VII) butyl ethyl ketone(-∇-); (VIII) methyl hexyl ketone (-▲-); (IX) ethyl pentyl ketone (-▼-); (X) heptyl methyl ketone (-⊗-)

investigation are methyl substituted aromatic and ketone substituted aliphatic compounds of highly non-spherical nature. Methyl substituted benzenes and ketones have almost similar characteristics. Some of the methyl benzenes are supposed to have apparently zero dipole moment from bond moment calculation. Moreover, these molecules are supposed to absorb electric energy much more strongly in the effective dispersive region of nearly 10 GHz at which peak of the absorption curve occurs. The ketones, on the other hand, are pleasant smelling liquids and widely used in petroleum industry. These liquids are used as good solvents of synthetic rubber, wax etc. The study of the variation of τ with respect to various substituted polar groups attached to different positions of the parent molecules may throw much light on the structural conformations of the methyl benzene and ketone molecules. The authors had already made a detailed investigation on some poly-substituted benzenes[12] at various temperatures to get molecular structures by conductivity technique. Dielectric parameters are very much temperature- dependent. Calculations at some other temperature may reveal a better picture. Nevertheless, from these studies it may be clear as to what theory is valid for such highly non-spherical aliphatic and aromatic compounds. A systematic comparison of τ and μ can thus be made from the measured data at 25 °C.

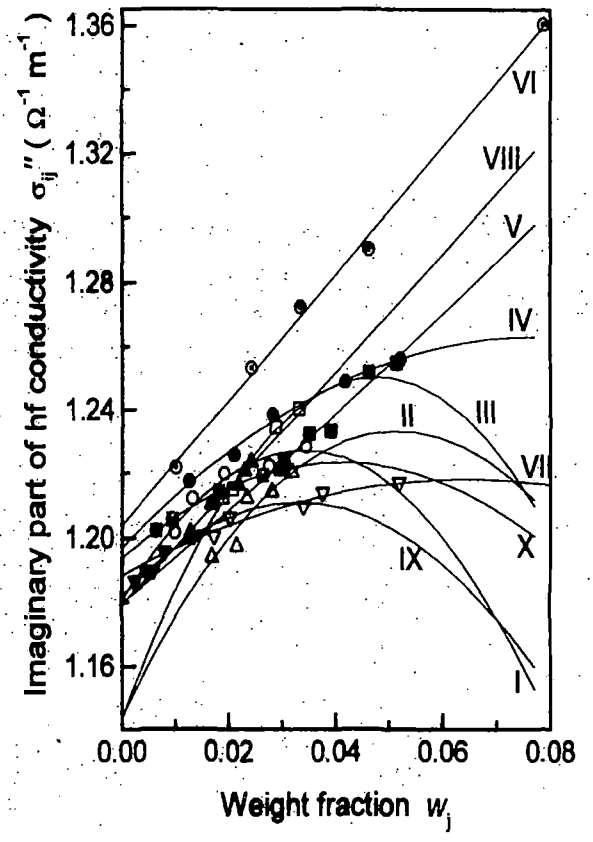

Fig. 2 — Variation of imaginary part of conductivity σ_{ij}'' against w_j at 25 °C under 9.585 GHz electric field : (I) toluene (-○-); (II) 1,3,5 tri methyl benzene (-Δ-); (III) 1,2,3,4 tetra methyl benzene (-□-); (IV) 1,2,4,5 tetra methyl benzene (-●-); (V) penta methyl benzene (-■-); (VI) p-fluoro toluene (-⊙-); (VII)butyl ethyl ketone(-∇-); (VIII) methyl hexyl ketone (-▲-); (IX) ethyl pentyl ketone (-▼-); (X) heptyl methyl ketone (-⊗-)

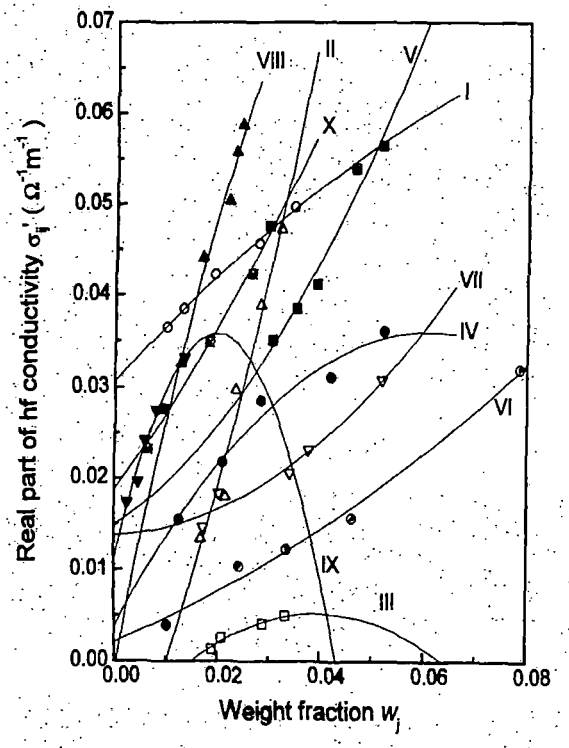

Fig. 3 — Variation of real part of conductivity σ_{ij}' against w_j at 25 °C under 9.585 GHz electric field : (I) toluene (-○-); (II) 1,3,5 tri methyl benzene (-Δ-); (III) 1,2,3,4 tetra methyl benzene (-□-); (IV) 1,2,4,5 tetra methyl benzene (-●-); (V) penta methyl benzene (-■-); (VI) p-fluoro toluene (-⊙-); (VII) butyl ethyl ketone (-∇-); (VIII) methyl hexyl ketone (-▲-); (IX) ethyl pentyl ketone (-▼-); (X) heptyl methyl ketone (-⊗-)

The corresponding dipole moments μ_j's of these liquids are obtained from the linear coefficient β of uhf conductivity σ_{ij} curves against w_j's (Fig. 5). All the β's and μ's are tabulated in Table 2 with those from Gopalakrishna and theoretical conformational calculation of Fig. 6. The inductive, mesomeric and electromeric effects under 3 cm wavelength electric field play the vital role in determining the theoretical μ_{theo}'s of the molecules of Fig. 6 in agreement with estimated μ_j's.

2 HF Conductivity Technique to Estimate τ and μ

The ultra high frequency (uhf) complex conductivity[13] σ_{ij}^* is :

$$\sigma_{ij}^* = \sigma_{ij}' + j\sigma_{ij}'' \qquad \ldots(1)$$

where $\sigma_{ij}' = \omega\varepsilon_o\varepsilon_{ij}''$ and $\sigma_{ij}'' = \omega\varepsilon_o\varepsilon_{ij}'$ are the real and imaginary parts of σ_{ij}^*, ε_o is absolute permittivity of free space = 8.854×10^{-12} F.m^{-1} and $\omega(=2\pi f)$ is the angular frequency of the applied electric field of frequency, $f = 9.585 \times 10^9$ Hz.

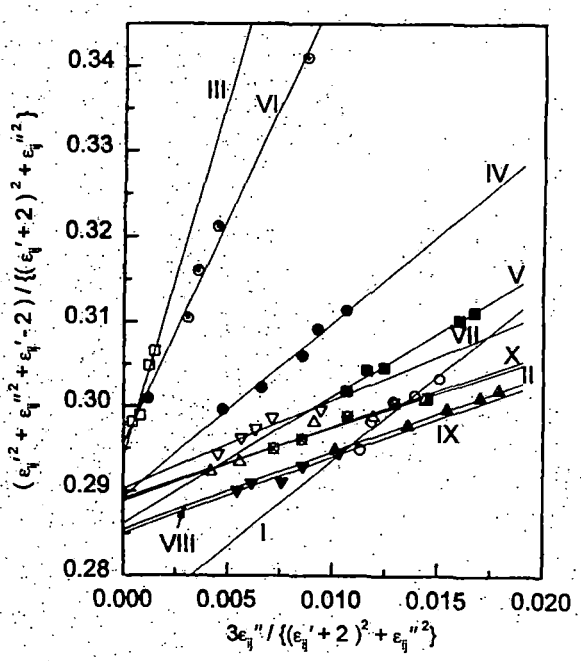

Fig. 4 — Linear plots of x against y for some methyl benzenes and ketones at 25 °C under 9.585 GHz electric field: (I) toluene (-○-); (II) 1,3,5 tri methyl benzene (-Δ-); (III) 1,2,3,4 tetra methyl benzene (-□-); (IV) 1,2,4,5 tetra methyl benzene (-●-); (V) penta methyl benzene (-■-); (VI) p-fluoro toluene (-⊙-); (VII) butyl ethyl ketone (-∇-); (VIII) methyl hexyl ketone(-▲-); (IX) ethyl pentyl ketone (-▼-); (X) heptyl methyl ketone (-⊗-)

Debye equation[14] in the GHz region yields:

$$\sigma_{ij}'' = \sigma_{\infty ij} + \frac{1}{\omega\tau}\sigma_{ij}' \qquad \ldots(2)$$

$$\left(\frac{d\sigma_{ij}''}{d\sigma_{ij}'}\right) = \frac{1}{\omega\tau} \qquad \ldots(3)$$

Both σ_{ij}'' and σ_{ij}' are functions of w_j. Their variations are non-linear in the higher concentration region as seen in Figs 2 and 3. In this case, one can write Eq. (2) as:

$$\left(\frac{d\sigma_{ij}''}{dw_j}\right)_{w_j \to 0} = \frac{1}{\omega\tau}\left(\frac{d\sigma_{ij}'}{dw_j}\right)_{w_j \to 0} \qquad \ldots(4)$$

the τ's from both the Eqs (3) and (4) were computed and are listed in Table 1 for comparison with the reported τ recalculated from Gopalakrishna's method.

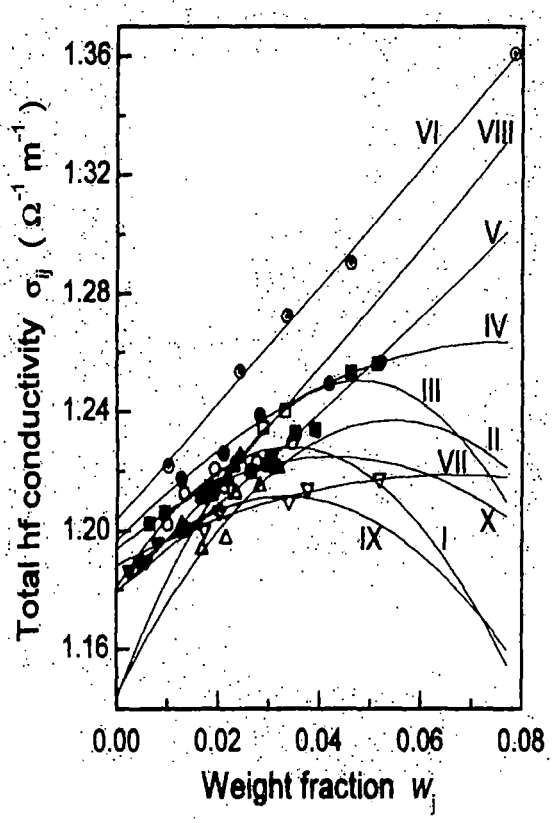

Fig. 5 — The plot of uhf conductivity σ_{ij} against w_j :(I) toluene (-○-); (II) 1,3,5 tri methyl benzene (-Δ-); (III) 1,2,3,4 tetra methyl benzene (-□-); (IV) 1,2,4,5 tetra methyl benzene (-●-); (V) penta methyl benzene (-■-); (VI) p-fluoro toluene (-⊙-); (VII) butyl ethyl ketone (-▽-); (VIII) methyl hexyl ketone(-▲-); (IX) ethyl pentyl ketone (-▼-); (X) heptyl methyl ketone (-⊗-)

Since $\varepsilon_{ij}' > \varepsilon_{ij}''$, but in hf region of GHz range $\varepsilon_{ij}' \equiv \varepsilon_{ij}''$ where ε_{ij}'' offers resistance to polarisation and uhf conductivity $\sigma_{ij} = \omega\varepsilon_0 (\varepsilon_{ij}'^2 + \varepsilon_{ij}''^2)^{1/2}$. Eq. (2) can thus be written in the following form:

$$\sigma_{ij} = \sigma_{\infty ij} + \frac{1}{\omega\tau}\sigma_{ij}'$$

$$\left(\frac{d\sigma_{ij}'}{dw_j}\right)_{w_j \to 0} = \omega\tau\beta \qquad \ldots(5)$$

β is the slope of σ_{ij}– w_j curve in the limit $w_j = 0$ as observed in Fig. 5 and listed in Table 2.

The real part σ_{ij}' of hf complex conductivity σ_{ij}^* is given by[12]:

$$\sigma_{ij}' = \frac{N\mu_j^2\rho_{ij}}{27M_j k_B T}\left(\frac{\omega^2\tau}{1+\omega^2\tau^2}\right)(\varepsilon_{ij}+2)^2 w_j$$

$$\left(\frac{d\sigma_{ij}'}{dw_j}\right)_{w_j \to 0} = \frac{N\mu_j^2\rho_i}{27M_j k_B T}\left(\frac{\omega^2\tau}{1+\omega^2\tau^2}\right)(\varepsilon_i+2)^2 \qquad \ldots(6)$$

where density ρ_{ij} and local field F_{ij} of the solution become ρ_i and $F_i = (\varepsilon_i + 2)^2/9$ of the solvent in the limit w_j=0.

From Eqs (5) and (6) one gets hf dipole moment μ_j as:

$$\mu_j = \left(\frac{27M_j k_B T\beta}{N\rho_i(\varepsilon_i+2)^2\omega b}\right)^{\frac{1}{2}} \qquad \ldots(7)$$

where

N = Avogadro's number = 6.023×10^{23}

ρ_i = density of solvent benzene at 25 °C = 874.3 Kg.m^{-3}

ε_i = relative permittivity of solvent benzene at 25 °C = 2.274

M_j = molecular weight of solute in Kg

k_B = Boltzmann constant = 1.38×10^{-23} J.mole^{-1}.K^{-1} and b is the dimensionless parameter involved with measured τ where $b = 1/(1+\omega^2\tau^2)$

Both the dipole moments μ_j's and dimensionless parameters b's are presented in Table 2.

3 Results and Discussion

The imaginary $\sigma_{ij}''(=\omega\varepsilon_0\varepsilon_{ij}')$ Ω^{-1} m^{-1} are plotted against real $\sigma_{ij}'(=\omega\varepsilon_0\varepsilon_{ij}'')$ Ω^{-1} m^{-1} parts of hf complex conductivity σ_{ij}^* for different weight fractions w_j's of solute according to Eq. (2) to get τ of polar liquid molecules as shown in Fig. 1. The variables are found to be almost linearly correlated as evident from the correlation coefficient r of the straight line of Eq. (3). It appears from Fig. 1 that, the systems like (I), (II), (III) and (VII) show low values of r (Table 1) indicating their departure from perfect linearity of the variables. Perfect linearity is said to

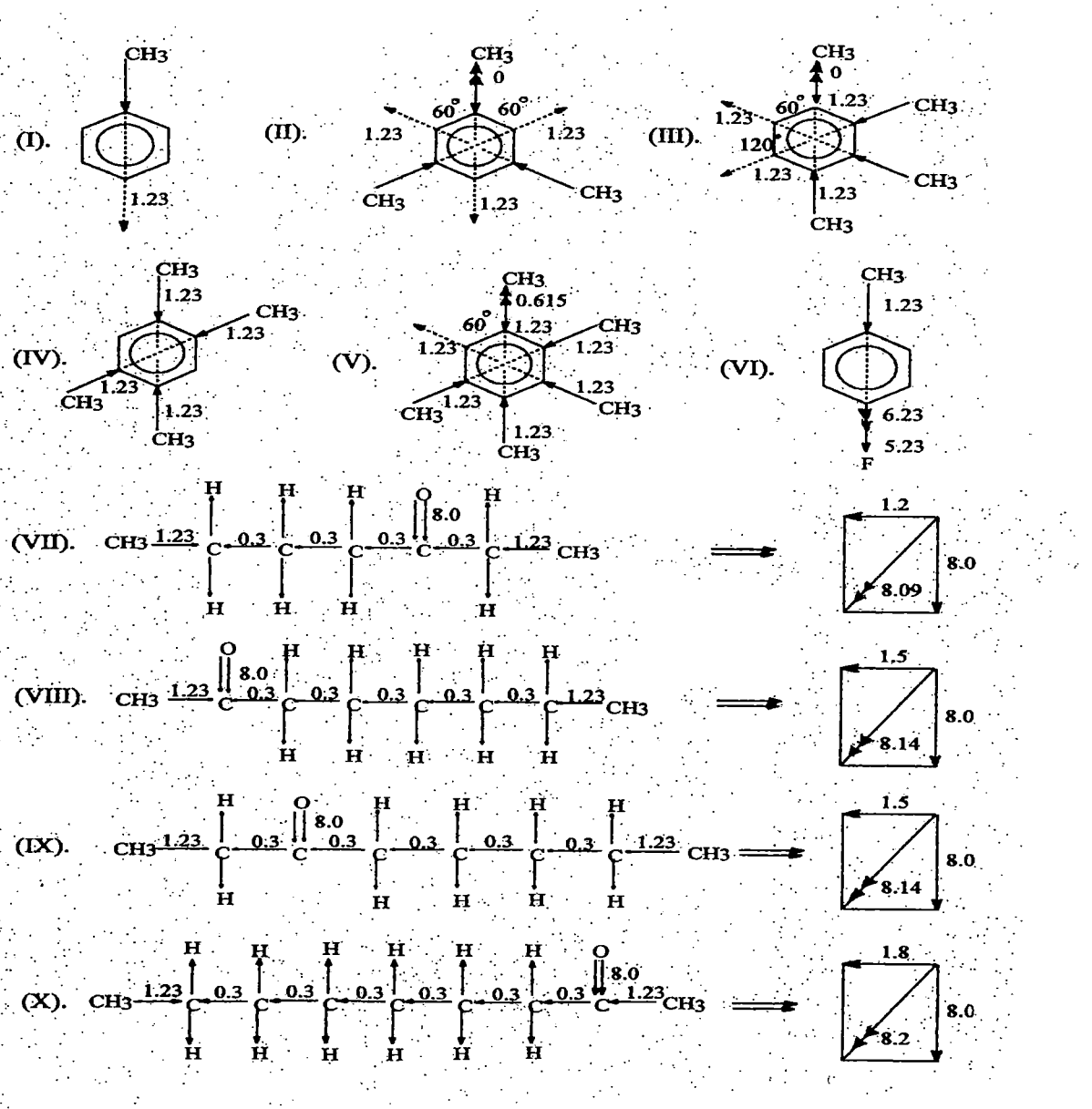

Fig. 6 — Conformational structures of polar molecules in terms of bond angles and bond moments ($\times 10^{-30}$ Coulomb. metre) of the substituent groups: (I) toluene; (II) 1,3,5 tri methyl benzene; (III) 1,2,3,4 tetra methyl benzene (IV) 1,2,4,5 tetra methyl benzene; (V)penta methyl benzene ; (VI) p-fluoro toluene; (VII) butyl ethyl ketone; (VIII) methyl hexyl ketone ; (IX) ethyl pentyl ketone; (X)heptyl methyl ketone

be achieved for $-1 \leq r \leq 1$. In such cases, the proposed method to determine τ from the ratio of the individual slopes of σ_{ij}'' and σ_{ij}' against w_j according to Eq. (4) seems to be a better choice and is claimed to be the best improvement over the other two because polar-polar interaction is avoided almost completely in the limit $w_j = 0$. The estimated τ's for systems (III), (IV), (VI) and (IX) from Eq. (4) are in agreement with those of Murthy *et al.*[10]

and reported τ. For the rest of the systems, τ's are lower from the ratio of individual slopes, except methyl hexyl ketone. All the plots of σ_{ij}'' and σ_{ij}' against w_j's as sketched in Figs 2 and 3 are parabolic in nature indicating the occurrence of associational aspect of polar liquid molecules in a non-polar solvent. The systems I(-○-), II(-Δ-), III(-□-), IV(-●-), VII(-∇-), IX(-▼-) and X(-⊗-) exhibit monotonic increase of σ_{ij}'' with w_j like σ_{ij}– w_j curves

of Fig. 5 in order to attain maximum value at a certain concentration (w_j) to show the convex nature. This is perhaps due to phase transition occurring in the polar-non-polar liquid mixture as observed elsewhere[12]. Similar variation σ_{ij}'' and σ_{ij} in Ω^{-1} m^{-1} with w_j as displayed graphically in Figs 2 and 5 indicates the validity of the approximation of $\sigma_{ij}'' \cong \sigma_{ij}$ of Eq. (5). All the curves of Figs 2 and 5 have a tendency to cut a point on the σ_{ij} -axis in the limit $w_j = 0$ except systems (II) and (III) probably due to solvation effect[15] of the polar-non-polar liquid mixture. The plots of $\sigma_{ij}' - w_j$ curves of Fig. 3 are also parabolic in nature. The variation of σ_{ij}' against w_j's for the III(-□-), IV(-●-) and IX(-▼-) systems show convex shape indicating the maximum absorption of hf electric energy at $w_j = 0.04$, 0.06 and 0.02, respectively. The rest of the systems display gradual increase of σ_{ij}' with w_j probably due to the fact that absorption of electric energy increases at the higher concentration. This is authenticated by the positive coefficient of the quadratic term in the fitted equations of $\sigma_{ij}'-w_j$ curves of Fig. 3. All the τ's of the polar liquid molecules of Table 1 agree well with those of Murthy *et al.*[10] from Eq. (3) and reported value. The reported τ's based on the standard method of Gopalakrishna were found to be much higher[7,8] which prompted us to recalculate τ's from the following expression[16]:

$$x = \frac{\varepsilon_{ij}'^2 + \varepsilon_{ij}' + \varepsilon_{ij}''^2 - 2}{(\varepsilon_{ij}' + 2)^2 + \varepsilon_{ij}''^2}; y = \frac{3\varepsilon_{ij}''}{(\varepsilon_{ij}' + 2)^2 + \varepsilon_{ij}''^2} \quad \ldots(8)$$

The variation of x against y of Eq. (8) are linear as seen in Fig. 4. One can obtain τ from:

$$\tau = 1 \Big/ \omega\left(\frac{dx}{dy}\right) \quad \ldots(9)$$

μ_j's are recalculated by using Gopalakrishna's equation[16] as:

$$\mu = \left[\frac{9k_B T M_j}{4\pi N \rho_i}\left\{1 + \left(\frac{dy}{dx}\right)^2\right\}\left(\frac{dx}{dw_j}\right)_{w_j \to 0}\right]^{\frac{1}{2}} \quad \ldots(10)$$

τ's from the ratio of the individual slopes of Eq. (4), on the other hand, are found to be in better agreement for the systems: 1,2,3,4 tetramethyl benzene (III); 1,2,4,5 tetramethyl benzene (IV); p-fluoro toluene (VI) and ethyl pentyl ketone (IX) respectively. The other systems exhibit low values of τ from the ratio of individual slopes of σ_{ij}'' and σ_{ij}' against w_j's except methyl hexyl ketone (VIII). This behaviour can be explained on the basis of the fact that the methods of Murthy *et al.*[10] and Gopalakrishna yield τ's of either a quasi isolated polar or a dimer (solute-solute association) molecule. The ratio of the individual slopes, on the other hand, takes into account both the processes in addition to τ of a dimer molecule. The smaller value of τ may be due to formation of monomer supported by low values of r of the systems under investigation.

Dipole moments μ_j's are computed from the slope β of uhf conductivity σ_{ij} against w_j curves of Fig. 5 and dimensionless parameters b's of Eq. (7) to compare with the results of Eq. (10) of Gopalakrishna[16]. The μ's are now found to agree well as seen in Table 2 with Murthy *et al.*[10] and recalculated values of Gopalakrishna for all the systems like τ's indicating the applicability of the methods for such systems under investigation. The σ_{ij}'s of polar-non-polar liquid mixtures are, however, concerned with the bound molecular charges which may be counted by β (Table 2) of $\sigma_{ij} - w_j$ curves of Fig. 5. The agreement is better from Eqs (4) and (7) with the use of the ratio of individual slopes for systems (I), (III), (IV), (VI) and (IX) respectively unlike other polar liquids where μ's are slightly lower except for methyl hexyl ketone. Low values of μ's may be due to formation of monomer while high values are responsible for dimer formations. The slight difference between reported and estimated μ's may occur due to existence of steric hindrances among the substituted polar groups.

The theoretical dipole moments μ_{theo}'s are calculated on the basis of planar structures for the molecules from the available bond moments of $CH_3 \rightarrow C$, $C \Leftarrow O$, $C \leftarrow C$, $C \rightarrow F$ and $C \rightarrow H$ of 1.23×10^{-30}, 8×10^{-30}, 0.3×10^{-30}, 5.23×10^{-30} and 1×10^{-30} in Coulomb-metre (C.m) respectively. $CH_3 \rightarrow C$ makes an angle 180° with the bond axis. The direction of $C \leftarrow C$ bond moment is taken in the reverse direction of bond axis[17]. All the substituted polar groups have the usual nature of either pushing or pulling electrons from the adjacent atoms of the parent molecules. Thus, there exists a difference in electron affinity within each atom of the substituted

Table 1 — Slope and intercepts of Eq. (2), correlation coefficient r, ratio of the individual slopes of $\sigma_{ij}''-w_j$ and $\sigma_{ij}'-w_j$ curves at $w_j \to 0$, relaxation time τ from Eqs (3) and (4) and from Gopalakrishna's method of some methyl benzenes and ketones in benzene at 25 °C under 9.585 GHz electric field

System	Slope and intercepts of Eq. (3)		Correlation. Coefficient r	Ratio of individual slopes of $\sigma_{ij}''-w_j$ and $\sigma_{ij}'-w_j$ at $w_j \to 0$	Relaxation times τ_j ($\times 10^{-12}$) in s		
					τ_j^a	τ_j^b	τ_j^g
(I) toluene	1.8468	1.1385	0.9527	4.3891	8.99	3.78	8.24
(II) 1,3,5 tri methylbenzene	0.7897	1.1844	0.9755	2.8782	21.03	5.77	19.93
(III) 1,2,3,4 tetra methyl benzene	8.3666	1.1992	0.9678	6.5797	1.98	2.52	1.94
(IV) 1,2,4,5 tetra methyl benzene	1.9531	1.1854	0.9890	1.6133	8.50	10.29	8.06
(V) penta methyl benzene	1.3836	1.1770	0.9948	3.8814	12.00	4.28	11.02
(VI) p–fluorotoluene	4.8910	1.2071	0.9941	8.2548	3.39	2.01	3.12
(VII) butyl eyhyl ketone	1.0070	1.1878	0.9481	40.3859	16.48	0.41	15.84
(VIII) methyl hexyl ketone	0.8452	1.1737	0.9993	0.6003	19.65	27.66	18.13
(IX) ethyl pentyl ketone	0.8640	1.1713	0.9686	0.6928	19.22	23.97	18.40
(X) heptyl methyl ketone	0.8203	1.1838	0.9859	1.8590	20.24	8.93	19.01

τ_j^a = Relaxation time from Eq. (3)
τ_j^b = Relaxation time from Eq. (4)
τ_j^g = Relaxation time from Gopalakrishna's method of Eq. (9)

Table 2 — Coefficients of $\sigma_{ij}-w_j$ curves, dimensionless parameter b [$=1/(1+\omega^2\tau^2)$], dipole moment μ_j in Coulomb.metre from τ's of Eqs (3), (4) and Gopalakrishna's method and the theoretical dipole moment μ_{theo} from the available bond angles and bond moments of some methyl benzenes and ketones in benzene at 25 °C under 9.585 GHz electric field

System with mol.wt.	Coefficients of $\sigma_{ij} = \alpha+\beta w_j+\gamma w_j^2$			Values of b by using τ		Dipole moment ($\times 10^{-30}$) C.m			
	α	β	γ	of Eq. (3)	of Eq. (4)	μ_j^a	μ_j^b	μ_j^g	μ_{theo}
(I) toluene M_j=0.092 Kg	1.1811	2.7545	–40.2180	0.7733	0.9507	7.93	7.15	7.80	1.23
(II) 1,3,5 tri methylbenzene M_j= 0.120 Kg	1.1446	3.4010	–31.2102	0.3840	0.8923	14.27	9.36	13.94	0.00
(III) 1,2,3,4 tetra methyl benzene M_j=0.134 Kg	1.1436	4.4952	–47.2133	0.9860	0.9775	10.82	10.87	10.82	0.00
(IV) 1,2,4,5 tetra methyl benzene M_j=0.134 Kg	1.1969	1.7313	–11.2125	0.7924	0.7225	7.49	7.84	7.39	0.00
(V) penta methyl benzene M_j=0.148 Kg	1.1798	1.4009	2.2168	0.6569	0.9377	7.78	6.51	7.63	1.23
(VI) p- fluoro toluene M_j=0.110 Kg	1.2039	1.9329	0.7021	0.9600	0.9856	6.52	6.43	6.53	6.23
(VII) butyl ethyl ketone M_j=0.114 Kg	1.1885	0.9115	–6.8748	0.5038	0.9994	6.29	4.46	6.19	8.09
(VIII) methyl hexyl ketone M_j=0.128 Kg	1.1790	1.8073	2.1902	0.4166	0.2649	10.32	12.94	10.05	8.14
(IX) ethyl pentyl ketone M_j=0.128 Kg	1.1820	1.7921	–27.0543	0.4274	0.3243	10.14	11.64	10.01	8.14
(X) heptyl methyl ketone M_j=0.142 Kg	1.1939	1.4569	–17.0797	0.4023	0.7757	9.93	7.15	9.60	8.2

μ_j^a = dipole moment from Eq.(7) by using τ_j of Eq. (3)
μ_j^b = dipole moment from Eq. (7) by using τ_j of Eq. (4)
μ_j^g = dipole moment by Gopalakrishna's method of Eq. (10)
μ_{theo} = theoretical dipole moment from the available bond angles and bond moments

polar groups causing inductive, mesomeric and electromeric effects in them, which play a role in the structure of the polar molecules of Fig. 6. The solvent C_6H_6 due to its aromaticity is a cyclic planar compound having three alternate single and double bonds and six *p*-eleINDIAN J PURE & APPL PHYS, VOL 40, AUGUST 2002ctrons on six C-atoms. The sp^2 hybridised electrons provide de-localised π-electrons to each atom of the substituted polar groups of the molecules. $CH_3^{\delta+}\rightarrow C^{\delta-}$ is a strong electron pushing (+I effect) while $>C^{\delta+}\Leftarrow O^{\delta-}$ is responsible for both the mesomeric (–M effect) and electromeric effect. Thus all the substituted polar groups may be responsible to form either solute-solvent (monomer) or solute-solute (dimmer) association to yield lower and higher μ_j's respectively depending upon the solvent used. The difference $\Delta\mu$ between μ_j's and μ_{theo}'s of Fig. 6 for the methyl substituted benzenes are 5.92, 9.36, 8.74, 7.84, 5.28 and 0.2×10^{-30} C.m for the six systems while the rest of the four ketones have –3.63, 4.8, 3.5 and -1.05×10^{-30} C.m respectively. This indicates the mesomeric and electromeric effects which are maximum for 1,3,5 trimethyl benzene and methyl hexyl ketone probably due to presence of strong electron repelling character of $CH_3\rightarrow C$ group. The μ_{theo} of 1,3,5 tri methyl benzene, 1,2,3,4 tetra methyl benzene and 1,2,4,5 tetra methyl benzene are found to be zero. The bond moment of $CH_3\rightarrow C$ group acts in opposite direction in a plane to yield zero value. The molecules may have considerable μ_{theo} values if they are three dimensional structures. All these effects may be taken into account to get exact μ_j's of Table 2 from μ_{theo} by the factor μ_{expt}/μ_{theo} (5.81, 5.29, 1.03, 0.55, 1.59, 1.43, 0.87) except for three molecules.

4 Conclusion

The structural information of some aromatic methyl benzenes and aliphatic ketones is obtained from the conductivity measurement at 25 °C under the most effective dispersive region of 9.585 GHz electric field. Modern internationally accepted symbols of dielectric relaxation terminologies and parameters in S I units seem to be more topical, significant and useful contribution to obtain τ and μ of a dipolar liquid dissolved in non-polar solvent. The τ_j's measured from the slope of the linear $\sigma_{ij}''-\sigma_{ij}'$ curves are not in agreement with those from the ratio of the individual slopes of $\sigma_{ij}''-w_j$ and $\sigma_{ij}'-w_j$ in the limit $w_j=0$ for all cases. The latter method is more significant because in this case one polar molecule is surrounded by a large number of non-polar molecules and thus polar-polar interactions are supposed to be completely eliminated. This method is thus supposed to yield monomeric or often dimeric structure of polar molecules. The μ_j's are measured from the linear coefficient β of $\sigma_{ij}-w_j$ curve at $w_j\rightarrow 0$. The σ_{ij} or σ_{ij}'' in Ω^{-1} m^{-1} for some systems increases gradually in order to attain the maximum value for a certain concentration of solute and then decreases. This indicates the change of phase of the systems under investigation. Similar nature of variation of σ_{ij}'' with w_j indicates maximum absorption of hf electric energy for some systems. The τ_j's and μ_j's claimed to be accurate within 10 and 5 % are also compared with those from Gopalakrishna's fixed frequency method. The slight disagreement between experimental μ_j with the theoretical dipole moment μ_{theo} for some molecules reveals different associational aspects of dipolar liquid molecules in a non-polar solvent from the frequency dependence of relaxation parameters. This study also exhibits the presence of mesomeric, inductive and electromeric effects of the substituent polar groups of the molecules. The theoretical μ_{theo} for systems II, III and IV are zero although they possess a considerable μ_j. This invariably rules out the planar structure of the molecules and establish a three dimensional formation.

References

1 Paul N, Sharma K P & Chattopadhyay S, *Indian J Phys*, 71B (1997) 71.

2 Sen S N & Ghosh R, *J Phys Soc Jpn*, 33 (1972) 838.

3 Dutta K, Basak R C, Sit S K & Acharyya S, *J Molec Liq*, 88 (2000) 229.

4 Ghosh N, Sit S K, Bothra A K & Acharyya S, *J Phys D: Appl Phys*, 34 (2001) 379.

5 Migahed M D, Ahmed M T & Kotp A E, *J Phys D: Appl Phys*, 33 (2000) 2108.

6 Bello A, Laredo E, Grimau M, Nogales A & Ezquerra T A, *J Chem Phys*, 113 (2000) 863.

7 Vaish S K & Mehrotra N K, *Indian J Pure & Appl Phys*, 37 (1999) 881.

8 Vaish S K & Mehrotra N K, *Indian J Pure & Appl Phys*, 37 (1999) 778.

9 Bloembergen N, Purcel E M & Pound R V, *Phys Rev*, 73 (1948) 673.

10 Murthy M B R, Patil R L & Deshpande D K, *Indian J Phys*, 63B (1989) 491.

11 Basak R C, Sit S K, Nandi N & Acharyya S, *Indian J Phys*, 70B (1996) 37.

12 Dutta K, Sit S K & Acharyya S, *J Molec Liq*, 92 (2001) 263.

13 Murphy F J & Morgan S O, *Bell Syst Tech J*, 18 (1939) 502.

14 Hill N E, Vaughan W E, Price A H & Davies M, *Dielectric properties and molecular behaviour* (Van Nostrand Reinhold Co, London), 1969.

15 Sit S K, Basak R C, Saha U & Acharyya S, *J Phys D: Appl Phys*, 27 (1994) 2194.

16 Gopalakrishna K V, *Trans Faraday Soc*, 53 (1957) 767.

17 Sit S K & Acharyya S, *Indian J Phys*, 70B (1996) 19.

Indian Journal of Pure & Applied Physics
Vol. 40, November 2002, pp. 801-815

Double relaxation phenomena of di-substituted benzenes and anilines in non-polar aprotic solvents under high frequency electric field

K Dutta , A Karmakar, (Mrs) L Dutta, S K Sit & S Acharyya

Department of Physics, Raiganj College (University College), PO Raiganj Dist, Uttar Dinajpur 733 134

[e-mail: koushikduttajsm@rediffmail.com]

Received 1 October 2001; revised 12 February 2002; accepted 15 April 2002

The derived linear equation $(\chi_{o ij} - \chi_{ij}')/\chi_{ij}' = \omega(\tau_1+\tau_2)\ \chi_{ij}''/\chi_{ij}' - \omega^2\tau_1\tau_2$ for different weight fractions w_j of di-substituted benzenes and anilines (j) in aprotic and non-polar solvents (i) C_6H_6 and CCl_4 under 9.945 GHz electric field are obtained from the available measured dielectric relative permittivities at 35 °C. The double relaxation times τ_1 and τ_2 of the flexible part and the whole molecule are estimated from the slope and intercept of the above equation. χ_{ij}' and χ_{ij}'' are the real and imaginary parts of the high frequency complex orientational dielectric susceptibility χ_{ij}^* and $\chi_{o ij}$ is the low frequency dielectric susceptibility, which is real. They are, however, related with the measured relative permittivities. Values of τ_i are calculated from the ratio of the individual slopes of the variations of χ_{ij}'' and χ_{ij}' with w_j at $w_j \to 0$, assuming single Debye-like dispersion and compared with Murthy *et al.* [*Indian J Phys*, 63B (1989) 491] and Gopalakrishna [*Trans Faraday Soc*, 53 (1957) 767]. The weighted contributions c_1 and c_2 towards dielectric relaxations for τ_1 and τ_2 can, however, be obtained from Fröhlich's theoretical formulations of $\chi_{ij}'/\chi_{o ij}$ and $\chi_{ij}''/\chi_{o ij}$ and compared with those from the experimentally measured values of $(\chi_{ij}'/\chi_{o ij})_{wj \to 0}$ and $(\chi_{ij}''/\chi_{o ij})_{wj \to 0}$. The latter measured values are employed to get symmetric distribution parameter γ to yield symmetric relaxation time τ_s. The curve of $(1/\phi)\log(\cos\phi)$ against ϕ in degrees together with the values of $(\chi_{ij}'/\chi_{o ij})_{wj \to 0}$ and $(\chi_{ij}''/\chi_{o ij})_{wj \to 0}$ experimentally obtained, gives the asymmetric distribution parameter δ to get the characteristic relaxation time τ_{cs}. All these findings ultimately establish the different types of relaxation behaviour for such complex molecules. The dipole moments μ_1 and μ_2 for the flexible part and the whole molecule are ascertained from τ_1 and τ_2 and the linear coefficients β_1 of χ_{ij}' versus w_j and β_2 of σ_{ij} versus w_j curves respectively, where σ_{ij} is the hf conductivity. The values of μ are finally compared with the reported μ's and μ_{theo}'s derived from available bond angles and bond moments of the substituted polar groups of di-substituted anilines to conclude that a part of the molecule is rotating while the whole molecular rotation occurs for di-substituted benzenes. The slight disagreement between measured values of μ and μ_{theo} can, however, be interpreted by the inductive, mesomeric and electromeric effects of the polar groups of the parent molecules.

1 Introduction

The dielectric relaxation phenomena of nonspherical and rigid polar liquid molecule in different non-polar solvents at a given temperature, under a high frequency (hf) electric field attracted the attention of a large number of workers[1,2]. The dipole moment μ from the relaxation time τ of the polar liquid molecule is of much importance[3,4] to determine the shape, size, structure and molecular association of a polar molecule. The real ε_{ij}' and imaginary ε_{ij}'' parts of complex relative permittivity ε_{ij}^*, static and infinite frequency relative permittivities $\varepsilon_{o ij}$ and $\varepsilon_{\infty ij}$ of a polar liquid molecule (j) in a non-polar solvent (i) at a fixed experimental temperature under a single frequency electric field of GHz range are used to obtain the double relaxation times τ_2 and τ_1 due to rotation of the whole molecule as well as the flexible part attached to the parent molecule[5].

Khameshara & Sisodia[6], Gupta *et al.*[7] and Arrawatia *et al.*[8] measured the relative permittivities of some di-substituted benzenes and anilines in aprotic non-polar solvents C_6H_6 and CCl_4 under 9.945 GHz electric field at 35 °C to predict the conformation of the molecules in terms of the relaxation time τ, based on the single frequency concentration variation method of Gopalakrishna[9] and the dipole moment, μ by Higasi's method[10]. The compounds are very interesting for the different functional groups like $-NH_2$, $-CH_3$, $-NO_2$, $-Cl$, etc. attached to the parent molecules. The samples were of purest quality and supplied by M/s Fluka and M/s E Merck, respectively. The solvents C_6H_6 and CCl_4 of M/s BDH were used after double distillation and

suitably dried over NaCl and $CaCl_2$. ε_{oij} at 35 °C was measured by heterodyne beat method at 300 kHz $\varepsilon_{\infty ij}=n_{Dij}^2$, where the refractive index n_{Dij} was measured by Abbe's refractometer. The weight fraction w_j of the respective solute, which is defined by the weight of the solute per unit weight of the solution was taken up to four decimal places, as the accuracy in the measurement was 0.0012 %. ε_{ij}' and ε_{ij}'' within 1 % and 5 % accuracies were carried out by using the voltage standing wave ratio in slotted line and short-circuiting plunger, based on the method of Heston *et al.*[11]. The possible existence of τ_1 and τ_2 of the compounds was, however, detected from the relative permittivity measurements[12], under 9.945 GHz electric field at 35 °C.

Now-a-days, the usual practice[13] is to study the dielectric relaxation phenomena in terms of dielectric orientational susceptibilities χ_{ij}. χ_{ij}'s are linked with the orientational polarization of a polar molecule. So it is better to work with χ_{ij}'s rather than ε_{ij}'s or conductivity σ_{ij}'s as the latter are involved with all the polarization processes and the transport of bound molecular charges, respectively[14]. The real $\chi_{ij}'(=\varepsilon_{ij}'-\varepsilon_{\infty ij})$ and imaginary $\chi_{ij}''(=\varepsilon_{ij}'')$ parts of the complex dielectric orientational susceptibility $\chi_{ij}^*(=\varepsilon_{ij}^*-\varepsilon_{\infty ij})$ and the low frequency susceptibility $\chi_{oij}(=\varepsilon_{oij}-\varepsilon_{\infty ij})$ which is real of the di-substituted benzenes and anilines in C_6H_6 and CCl_4 of Table 1 are used to obtain their conformational structures in terms of molecular and intra-molecular dipole moments μ_2 and μ_1 involved with the estimated τ_2 and τ_1. Di-substituted benzenes and anilines are thought to absorb electric energy much more strongly, in nearly 10 GHz electric field yielding considerable values of τ_1 and τ_2. The 11 polar-non-polar liquid mixtures under investigation are found to show the double relaxation phenomena. Most of the polar molecules are isomers of aniline and benzene. Some of the polar solutes are dissolved in C_6H_6, while a few in CCl_4 to observe the solvent effect too. Moreover, a few of the polar molecules are para-compounds, in which a peculiar feature of relaxation phenomena is expected[15]. A strong conclusion of double relaxation phenomena of polar molecule in a non-polar solvent, based on the single frequency measurement of relaxation parameters can be made only if, the accurate value of χ_{oij} (±1 %) involved with ε_{oij} and $\varepsilon_{\infty ij}$ is available. The use of n_{Dij}^2 for $\varepsilon_{\infty ij}$ often introduces[6-8] an additional error in the calculation, since $\varepsilon_{\infty ij}$ is approximately equal to 1-1.5 times of n_{Dij}^2.

Bergmann *et al.*[16], however, devised a graphical method to obtain τ_1 and τ_2 for a pure polar liquid. The respective weighted contributions c_1 and c_2 towards dielectric relaxations were estimated in terms of τ_1 and τ_2. Bhattacharyya *et al.*[17] subsequently attempted to simplify the procedure of Bergmann *et al.*[16] to get the same for a pure polar molecule with ε', ε'', ε_o and ε_∞ measured at two different frequencies in GHz range. The graphical analysis advanced by Higasi *et al.*[18] on polar-non-polar liquid mixture was also a crude one.

Thus, the object of the present paper is to detect τ_1 and τ_2 and hence, to measure μ_1 and μ_2 using values of χ_{ij} based on the single frequency measurement technique[12,19]. The aspect of molecular orientational polarization is, however, achieved by introducing χ_{ij} because $\varepsilon_{\infty ij}$ which includes fast polarization, frequently appears as a subtracted term in Bergmann equations. Thus, to avoid the clumsiness of algebra and to exclude the fast polarization process, Bergmann equations[16] are simplified by the established symbols of χ_{ij}', χ_{ij}'' and χ_{oij} of Table 1 in SI units:

$$\frac{\chi_{ij}'}{\chi_{oij}}=\frac{c_1}{1+\omega^2\tau_1^2}+\frac{c_2}{1+\omega^2\tau_2^2} \qquad ...(1)$$

and

$$\frac{\chi_{ij}''}{\chi_{oij}}=c_1\frac{\omega\tau_1}{1+\omega^2\tau_1^2}+c_2\frac{\omega\tau_2}{1+\omega^2\tau_2^2} \qquad ...(2)$$

assuming two broad Debye-type dispersions for which the sum of c_1 and c_2 is unity.

Eqs (1) and (2) are now solved to get:

$$\frac{\chi_{oij}-\chi_{ij}'}{\chi_{ij}'}=\omega(\tau_1+\tau_2)\frac{\chi_{ij}''}{\chi_{ij}'}-\omega^2\tau_1\tau_2 \qquad ...(3)$$

The variables $(\chi_{oij}-\chi_{ij}')/\chi_{ij}'$ and χ_{ij}''/χ_{ij}' are plotted against each other for different values of w_j of the polar liquid under a single angular frequency ω $(=2\pi f)$ of the electric field to get a straight line with intercept $-\omega^2\tau_1\tau_2$ and slope $\omega(\tau_1+\tau_2)$, as shown in Fig.1. The intercept and slope of Eq. (3) are obtained by linear regression analysis made with the measured values of χ_{ij} of solutes in CCl_4 and C_6H_6 to get τ_2 and τ_1 as found in the 6th and 7th columns of

Table 1 — The real χ_{ij}' and imaginary χ_{ij}'', parts of the complex dielectric orientational susceptibility χ_{ij}^* and static dielectric susceptibility $\chi_{\omega ij}$ which is real for various weight fraction w_j of different di-substituted benzenes and anilines at 35 °C under 9.945 GHz electric field

Weight fraction w_j	χ_{ij}'	χ_{ij}''	$\chi_{\omega ij}$	Weight fraction w_j	χ_{ij}'	χ_{ij}''	$\chi_{\omega ij}$
	(I) o-chloronitrobenzene in C_6H_6				(II) 4-chloro 3-nitro benzotrifluoride in CCl_4		
0.0109	0.117	0.066	0.167	0.0050	0.122	0.019	0.155
0.0173	0.169	0.100	0.254	0.0101	0.145	0.037	0.185
0.0217	0.197	0.126	0.305	0.0147	0.150	0.054	0.233
0.0280	0.253	0.165	0.376	0.0193	0.167	0.068	0.266
0.0330	0.284	0.192	0.461	0.0231	0.179	0.075	0.302
	(III) 4-chloro 3-nitro toluene in C_6H_6				(IV) 4-chloro 3-nitro toluene in CCl_4		
0.0072	0.075	0.046	0.132	0.0041	0.145	0.039	0.208
0.0144	0.098	0.088	0.241	0.0087	0.173	0.071	0.315
0.0224	0.150	0.133	0.310	0.0128	0.190	0.101	0.419
0.0323	0.200	0.179	0.464	0.0162	0.218	0.138	0.482
0.0453	0.271	0.252	0.630	0.0203	0.241	0.165	0.586
	(V) o-nitrobenzotrifluoride in C_6H_6				(VI) m-nitrobenzotrifluoride in C_6H_6		
0.0085	0.094	0.058	0.154	0.0096	0.082	0.032	0.094
0.0167	0.166	0.108	0.257	0.0173	0.103	0.060	0.157
0.0244	0.226	0.159	0.384	0.0245	0.129	0.082	0.202
0.0335	0.297	0.205	0.495	0.0326	0.157	0.106	0.265
0.0402	0.353	0.255	0.604	0.0380	0.187	0.128	0.323
	(VII) 2-chloro 6-methyl aniline in C_6H_6				(VIII) 3-chloro 2-methyl aniline in C_6H_6		
0.0184	0.072	0.017	0.075	0.0083	0.059	0.018	0.065
0.0305	0.096	0.026	0.097	0.0207	0.099	0.043	0.128
0.0417	0.117	0.040	0.138	0.0270	0.128	0.055	0.166
0.0573	0.163	0.058	0.191	0.0363	0.165	0.073	0.221
0.0636	0.183	0.065	0.214	0.0421	0.193	0.086	0.255
	(IX) 3-chloro 4-methyl aniline in C_6H_6				(X) 4-chloro 2-methyl aniline in C_6H_6		
0.0214	0.088	0.032	0.099	0.0196	0.124	0.063	0.151
0.0374	0.123	0.060	0.167	0.0300	0.157	0.090	0.219
0.0403	0.133	0.066	0.185	0.0417	0.199	0.121	0.304
0.0548	0.166	0.091	0.244	0.0481	0.216	0.138	0.354
	(XI) 5-chloro 2-methyl aniline in C_6H_6						
0.0194	0.094	0.050	0.123				
0.0249	0.110	0.064	0.153				
0.0307	0.129	0.081	0.191				
0.0480	0.182	0.129	0.292				
0.0569	0.206	0.150	0.362				

Table 2. The variables of Eq. (3) are extracted from Table 1, where all the data are collected together, system-wise, up to three decimal places in close agreement with the expected[12] τ_2 and τ_1 of Table 2. Both τ_2 and τ_1 were found to deviate significantly, when the data of Table 1 were taken up to two decimal places with the claimed accuracy of measurement. The values of correlation coefficient (r) and the % error were worked out to place them in Table 2, only to see how far the variables of Eq. (3) are collinear to each other.

The relaxation times τ's due to Debye model are measured from the slope of χ_{ij}'' versus χ_{ij}' curves of Fig. 2 and the ratio of the individual slopes of χ_{ij}'' versus w_j and χ_{ij}' versus w_j curves at $w_j \to 0$ of Figs 3

and 4, respectively. Values of τ from both the methods are entered in the 8th and 9th columns of Table 2 only to see how far they agree with τ_1 and τ_2 due to double relaxation method of Eq. (3).

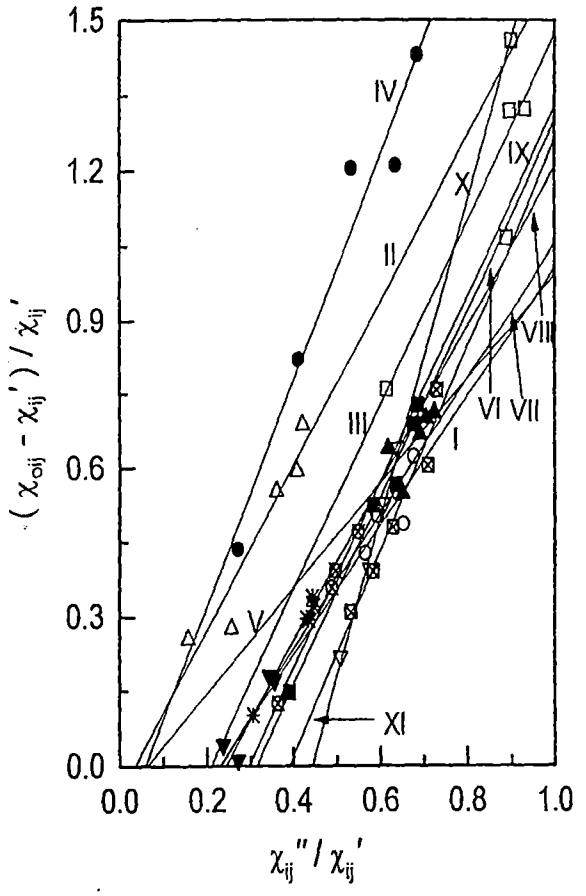

Fig. 1 — Linear variation of $(\chi_{\omega ij} - \chi_{ij}')/\chi_{ij}'$ with χ_{ij}''/χ_{ij}' for different values of w_j for: I. o-chloronitrobenzene in C_6H_6 (–○–); II. 4-chloro 3-nitrobenzotrifluoride in CCl_4 (–△–); III. 4-chloro 3-nitrotoluene in C_6H_6 (–□–); IV. 4-chloro 3-nitrotoluene in CCl_4 (–●–); V. o-nitrobenzotrifluoride in C_6H_6 (–▲–); VI. m-nitrobenzotrifluoride in C_6H_6 (–■–); VII. 2-chloro 6-methyl aniline in C_6H_6 (–▼–); VIII. 3-chloro 2-methyl aniline in C_6H_6 (–∗ –); IX. 3-chloro 4-methyl aniline in C_6H_6 (–⊗–); X. 4-chloro 2-methyl aniline in C_6H_6 (–∇–) and XI. 5-chloro 2-methyl aniline in C_6H_6 (–⊠ –) at 35 °C under 9.945 GHz electric field

The theoretical values of c_1 and c_2 towards dielectric dispersions for τ_1 and τ_2 of different di-substituted benzenes and anilines in C_6H_6 and CCl_4 were calculated from Fröhlich's[20] theoretical formulations of $\chi_{ij}'/\chi_{\omega ij}$ and $\chi_{ij}''/\chi_{\omega ij}$. The experimental values of c_1 and c_2, on the other hand, were found out from $(\chi_{ij}'/\chi_{\omega ij})_{wj\to 0}$ and $(\chi_{ij}''/\chi_{\omega ij})_{wj\to 0}$ by graphical variations of $\chi_{ij}'/\chi_{\omega ij}$ and $\chi_{ij}''/\chi_{\omega ij}$ with values of w_j of Figs 5 and 6, in order to place them in Table 3 for comparison. The plots of $\chi_{ij}'/\chi_{\omega ij}$ and $\chi_{ij}''/\chi_{\omega ij}$ against w_j of the polar liquids in Figs 5 and 6 are the least square fitted curves with the experimental points placed upon them. With the values of the intercepts presented in Table 3 from Figs 5 and 6 and the graphical plot of $(1/\phi)$ log(cos ϕ) against ϕ in degrees given elsewhere[4], the symmetric and asymmetric distribution parameters γ and δ related to symmetric and characteristic relaxation times τ_s and τ_{cs} of the molecules were determined. They are seen in Table 3. The object of such determinations of γ, δ, τ_s and τ_{cs} is to conclude the molecular non-rigidity and distribution of relaxation behaviour as well.

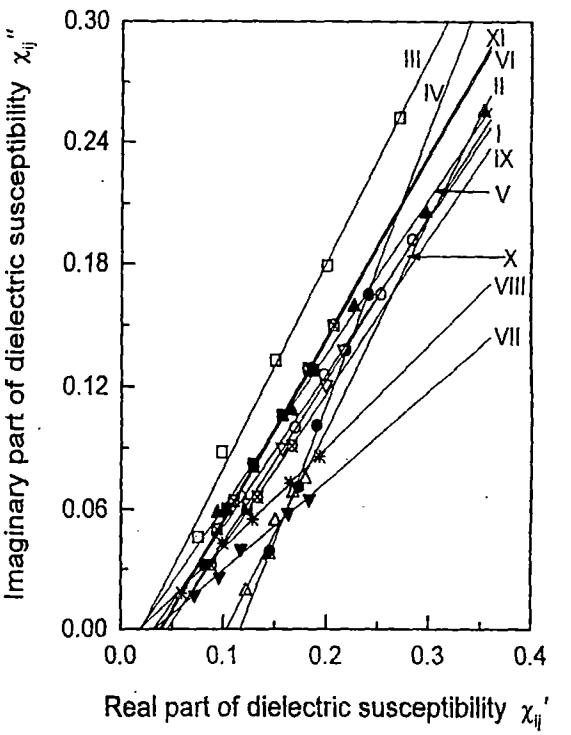

Fig. 2 — Linear variation of χ_{ij}'' with χ_{ij}' for different values of w_j for: I. o-chloronitrobenzene in $_6H_6$ (–○–); II. 4-chloro 3-nitrobenzotrifluoride in CCl_4 (–△–); III. 4-chloro 3-nitrotoluene in C_6H_6 (–□–); IV. 4-chloro 3-nitrotoluene in CCl_4 (–●–); V. o-nitrobenzotrifluoride in C_6H_6 (–▲–); VI. m-nitrobenzotrifluoride in C_6H_6 (–■–); VII. 2-chloro 6-methyl aniline in C_6H_6 (–▼–); VIII. 3-chloro 2-methyl aniline in C_6H_6 (–∗ –); IX. 3-chloro 4-methyl aniline in C_6H_6 (–⊗–); X. 4-chloro 2-methyl aniline in C_6H_6 (–∇–) and XI. 5-chloro 2-methyl aniline in C_6H_6 (–⊠ –) at 35 °C under 9.945 GHz electric field

Table 2 — The relaxation times τ_2 and τ_1 from the slope and intercept of straight line Eq. (3), correlation coefficients r's and % of error in regression technique, measured τ_j from the slope of χ_{ij}'' versus χ_{ij}' of Eq. (15) and the ratio of the individual slopes of χ_{ij}'' versus w_j and χ_{ij}' versus w_j at $w_j \to 0$ of Eq. (16), reported τ, symmetric and characteristic relaxation times τ_s and τ_{cs} for different disubstituted benzenes and anilines at 35 °C under 9.945 GHz electric field

System with S.No.	Eq. (3) Slope/Intercept		Corrl. Coeff (r)	% of Error	Estimated τ_2 and τ_1 in ps		Measured τ_j in ps from Eq. (15)	Eq.(16)	Rept. τ in ps	τ_s in ps	τ_{cs} in ps
(I) o-chloro nitro-benzene in C_6H_6	1.310	0.301	0.82	9.88	16.21	4.76	12.08	10.13	13.5	7.87	17.08
(II) 4-chloro 3-nitroben-zotrifluoride in CCl_4	1.666	0.059	0.95	2.94	26.08	0.58	16.43	22.66	21.1	0.00	--
(III) 4-chloro 3-nitro-toluene in C_6H_6	1.865	0.389	0.88	6.80	26.02	3.83	16.13	19.89	20.9	10.76	39.65
(IV) 4-chloro 3-nitro-toluene in CCl_4	2.283	0.134	0.98	1.19	35.57	0.96	21.47	22.61	35.0	1.47	38.84
(V) o- nitrobenzo-trifluoride in C_6H_6	1.063	0.067	0.70	15.38	15.93	1.08	12.09	11.08	13.7	10.89	28.83
(VI) m-nitrobenzotri-fluoride in C_6H_6	1.898	0.597	0.99	0.60	24.01	6.37	14.33	36.57	19.7	6.20	--
(VII) 2-chloro 6-methyl aniline in C_6H_6	1.371	0.313	0.93	4.08	17.31	4.63	7.05	14.55	7.8	4.08	--
(VIII) 3-chloro 2-methyl aniline in C_6H_6	1.596	0.386	0.99	0.60	20.79	4.76	7.98	11.49	9.9	4.57	--
(IX) 3-chloro 4- methyl aniline in C_6H_6	1.891	0.561	0.99	0.67	24.37	5.90	12.07	13.65	13.6	7.28	--
(X) 4-chloro 2-methyl aniline in C_6H_6	3.217	1.428	0.99	0.67	42.97	8.51	12.80	11.04	18.5	7.59	--
(XI) 5-chloro 2-methyl aniline in C_6H_6	2.075	0.811	0.97	1.78	24.85	8.36	14.34	14.35	16.6	5.60	4.52

The dipole moments μ_2 and μ_1 were then measured in terms of dimensionless parameters (b) involved with measured values of τ of Table 2 and coefficients β_1 and β_2 presented in Table 4 of the variations of hf χ_{ij}' and total hf conductivity σ_{ij} with values of w_j of Figs 4 and 7, respectively. The measured values of μ are presented in Table 4 in order to compare with theoretical dipole moment μ_{theo} derived from available bond angles and bond moments of the substituent polar groups attached to the parent molecules as sketched in Fig. 8. The structural aspect of some interesting polar molecules presented in Fig. 8 exhibits the prominent mesomeric, inductive and electromeric effects of the substituted polar groups. All these effects are taken into account by the ratio μ_{expt}/μ_{theo}, in agreement with the measured values[6-8] of μ presented in Table 4.

2 Formulations of c_1 and c_2 for τ_1 and τ_2

Eqs (1) and (2) are now solved to get c_1 and c_2, where:

$$c_1 = \frac{(\chi_{ij}'\alpha_2 - \chi_{ij}'')(1+\alpha_1^2)}{\chi_{oij}(\alpha_2 - \alpha_1)} \quad \ldots(4)$$

$$c_2 = \frac{(\chi_{ij}'' - \chi_{ij}'\alpha_1)(1+\alpha_2^2)}{\chi_{oij}(\alpha_2 - \alpha_1)} \quad \ldots(5)$$

where $\alpha_1 = \omega\tau_1$ and $\alpha_2 = \omega\tau_2$ provided $\alpha_2 > \alpha_1$. The molecules under consideration are of complex type and only little data are available under single frequency measurement in the low concentration region. A continuous distribution of τ with two discrete values of τ_1 and τ_2 could, therefore, be expected. Thus, from Fröhlich's equations[20] based

on distribution of τ between the two extreme values of τ_1 and τ_2, one gets:

$$\frac{\chi'_{ij}}{\chi_{oij}} = 1 - \frac{1}{2A}\ln\left(\frac{1+\omega^2\tau_2^{\,2}}{1+\omega^2\tau_1^{\,2}}\right) \qquad ...(6)$$

$$\frac{\chi''_{ij}}{\chi_{oij}} = \frac{1}{A}\left[\tan^{-1}(\omega\tau_2) - \tan^{-1}(\omega\tau_1)\right] \qquad ...(7)$$

where the Fröhlich parameter A is given by $A = \ln(\tau_2/\tau_1)$. The theoretical values of χ_{ij}'/χ_{oij} and χ_{ij}''/χ_{oij} of Eqs (6) and (7) were used to get theoretical c_1 and c_2 from Eqs (4) and (5) in order to compare them with the experimental values of c_1 and c_2 from the graphical plots of χ_{ij}'/χ_{oij} and χ_{ij}''/χ_{oij} at $w_j \to 0$, as seen in Figs 5 and 6, respectively. Both the theoretical and experimental values of c_1 and c_2 are presented in Table 3 for comparison.

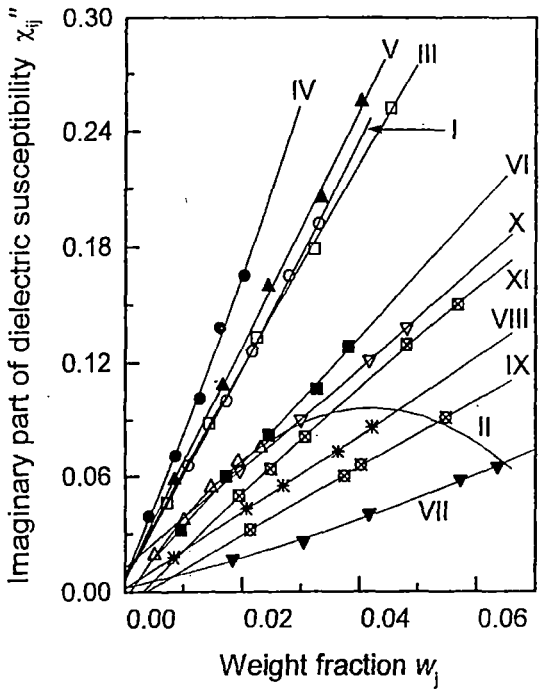

Fig. 3 — Variation of χ_{ij}'' against w_j of solutes at 35 °C under 9.945 GHz electric field for: I. o-chloronitrobenzene in C_6H_6 (–O–); II. 4-chloro 3-nitrobenzotrifluoride in CCl_4 (–△–); III. 4-chloro 3-nitrotoluene in C_6H_6 (–□–); IV. 4-chloro 3-nitrotoluene in CCl_4 (–●–); V. o-nitrobenzotrifluoride in C_6H_6 (–▲–); VI. m-nitrobenzotrifluoride in C_6H_6 (–■–); VII. 2-chloro 6-methyl aniline in C_6H_6 (–▼–); VIII. 3-chloro 2-methyl aniline in C_6H_6 (–* –); IX. 3-chloro 4-methyl aniline in C_6H_6 (–⊗–); X. 4-chloro 2-methyl aniline in C_6H_6 (–▽–) and XI. 5-chloro 2-methyl aniline in C_6H_6 (–⊠ –) at 35 °C under 9.945 GHz electric field

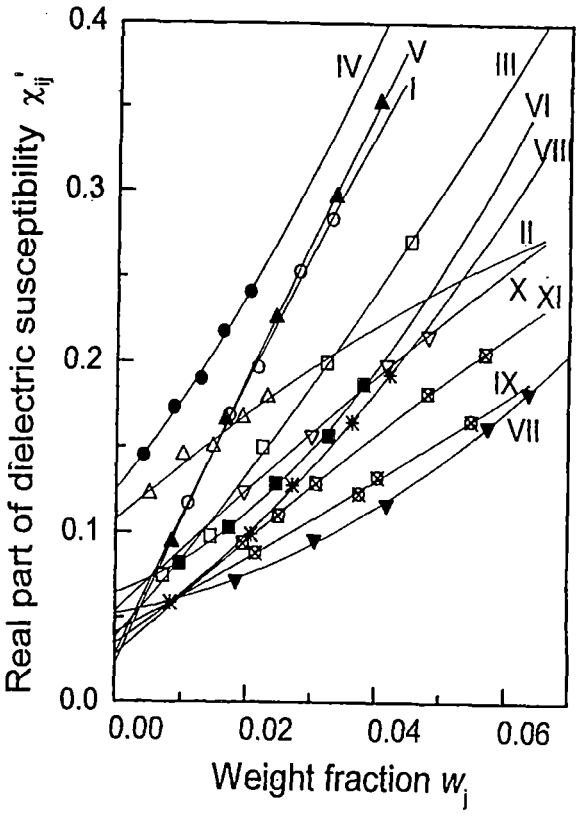

Fig. 4 — Variation of χ_{ij}' against w_j of solutes at 35 °C under 9.945 GHz electric field for: I. o-chloronitrobenzene in C_6H_6 (–O–); II. 4-chloro 3-nitrobenzotrifluoride in CCl_4 (–△–); III. 4-chloro 3-nitrotoluene in C_6H_6 (–□–); IV. 4-chloro 3-nitrotoluene in CCl_4 (–●–); V. o-nitrobenzotrifluoride in C_6H_6 (–▲–); VI. m-nitrobenzotrifluoride in C_6H_6 (–■–); VII. 2-chloro 6-methyl aniline in C_6H_6 (–▼–); VIII. 3-chloro 2-methyl aniline in C_6H_6 (–* –); IX. 3-chloro 4-methyl aniline in C_6H_6 (–⊗–); X. 4-chloro 2-methyl aniline in C_6H_6 (–▽–) and XI. 5-chloro 2-methyl aniline in C_6H_6 (–⊠ –) at 35 °C under 9.945 GHz electric field

3 Distribution Parameters Related to Symmetric and Characteristic Relaxation

The molecules are expected to show either symmetrical circular arc or a skewed arc in addition to other models[21] when the values of χ_{ij}''/χ_{oij} are plotted against χ_{ij}'/χ_{oij} at $w_j \to 0$ for various frequencies of the electric field to yield

$$\frac{\chi^*_{ij}}{\chi_{oij}} = \frac{1}{1+(j\omega\tau_s)^{1-\gamma}} \qquad ...(8)$$

$$\frac{\chi^*_{ij}}{\chi_{oij}} = \frac{1}{(1+j\omega\tau_{cs})^{\delta}} \qquad ...(9)$$

Table 3 — Fröhlich's parameter A, theoretical and experimental values of $\chi_{ij}'/\chi_{\omega ij}$ and $\chi_{ij}''/\chi_{\omega ij}$ of Fröhlich equations (6) and (7) and from fitting equations of Figs 5 and 6 at $w_j \to 0$, respectively, theoretical and experimental relative contributions c_1 and c_2 towards dielectric dispersion due to τ_1 and τ_2 symmetric and asymmetric distribution parameters γ and δ for polar-non-polar liquid mixtures of di-substituted benzenes and anilines at 35 °C under 9.945 GHz electric field

System with Sl.No.	A= Ln (τ_2/τ_1)	Theoretical values of $\chi_{ij}'/\chi_{\omega ij}$ & $\chi_{ij}''/\chi_{\omega ij}$ from Eqs (6) & (7)		Theoretical values of c_1 and c_2		Exptl. values of $\chi'_{ij}/\chi_{\omega ij}$ & $\chi''_{ij}/\chi_{\omega ij}$ at $w_j \to 0$ of Figs 5 & 6		Exptl. values of c_1 & c_2		Estimated values of γ and δ	
(I)o-chloronitro-benzene in C_6H_6	1.225	0.746	0.410	0.526	0.533	0.733	0.349	0.599	0.371	0.13	0.010
(II) 4-chloro 3-nitro-benzotrifluoride in CCl_4	3.806	0.830	0.259	0.687	0.525	0.890	0.027	0.894	-0.012	0.82	---
(III) 4-chloro 3nitro-toluene in C_6H_6	1.916	0.677	0.409	0.527	0.649	0.600	0.309	0.508	0.435	0.28	0.007
(IV) 4-chloro 3-nitro-toluene in CCl_4	3.612	0.754	0.301	0.638	0.703	0.863	0.144	0.823	0.253	0.38	0.002
(V) o-nitrobenzo-trifluoride in C_6H_6	2.691	0.873	0.266	0.653	0.444	0.616	0.347	0.288	0.655	0.21	0.008
(VI) m- nitrobenzo-trifluoride in C_6H_6	1.327	0.611	0.455	0.485	0.625	1.134	0.261	1.514	-0.561	-0.45	---
(VII) 2-chloro 6-methyl aniline in C_6H_6	1.319	0.737	0.412	0.527	0.544	1.078	0.141	1.402	-0.468	-0.40	---
(VIII) 3-chloro 2-methyl aniline in C_6H_6	1.474	0.693	0.424	0.518	0.585	1.023	0.232	1.192	-0.194	-0.20	---
(IX) 3-chloro 4- methyl aniline in C_6H_6	1.418	0.622	0.449	0.490	0.632	1.244	0.254	1.614	-0.588	-0.62	---
(X) 4-chloro 2-methyl aniline in C_6H_6	1.619	0.427	0.448	0.416	0.842	1.062	0.419	1.449	-0.556	-0.33	---
(XI) 5-chloro 2-methyl aniline in C_6H_6	1.089	0.547	0.475	0.462	0.627	0.907	0.312	1.354	-0.536	-0.03	0.021

Here, γ and δ are the symmetric and asymmetric distribution parameters related to symmetric and characteristic relaxation times τ_s and τ_{cs}, respectively. Separating the real and imaginary parts of Eq. (8) one gets:

$$\gamma = \frac{2}{\pi}\tan^{-1}\left[\left(1-\frac{\chi'_{ij}}{\chi_{\omega ij}}\right)\frac{\chi'_{ij}/\chi_{\omega ij}}{\chi''_{ij}/\chi_{\omega ij}} - \frac{\chi''_{ij}}{\chi_{\omega ij}}\right] \qquad ...(10)$$

and

$$\tau_s = \frac{1}{\omega}\left[1\Big/\left(\frac{\chi'_{ij}/\chi_{\omega ij}}{\chi''_{ij}/\chi_{\omega ij}}\cos\frac{\gamma\pi}{2} - \sin\frac{\gamma\pi}{2}\right)\right]^{\frac{1}{1-\gamma}} \qquad ...(11)$$

where $\chi_{ij}'/\chi_{\omega ij}$ and $\chi_{ij}''/\chi_{\omega ij}$ are obtained from intercepts of each variable with values of w_j of Figs 5 and 6 in the limit w_j=0. Again δ and τ_{cs} can be had from Eq. (9) as:

$$\tan(\phi\delta) = \frac{(\chi''_{ij}/\chi_{\omega ij})_{wj\to 0}}{(\chi'_{ij}/\chi_{\omega ij})_{wj\to 0}} \qquad ...(12)$$

$$\tau_{cs} = \frac{1}{\omega}\tan\phi \qquad ...(13)$$

Since, ϕ cannot be evaluated directly, a theoretical curve of $(1/\phi)\log(\cos\phi)$ with ϕ in degrees was drawn as shown elsewhere[4], from which:

$$\frac{1}{\phi}\log(\cos\phi) = \frac{\log\left[(\chi'_{ij}/\chi_{\omega ij})/\cos(\phi\delta)\right]}{\phi\delta} \qquad ...(14)$$

was found out. The known values of $(1/\phi)\log(\cos\phi)$ was then used to obtain ϕ. With known ϕ and δ, τ_{cs} were obtained from Eqs (12) and (13) for each molecule. The estimated γ and δ are presented in columns 11 and 12 of Table 3. Values of τ_s and τ_{cs} are entered in columns 11 and 12 of Table 2 to conclude symmetric relaxation behaviour for di-substituted anilines and asymmetric relaxation behaviour for di-substituted benzenes, respectively.

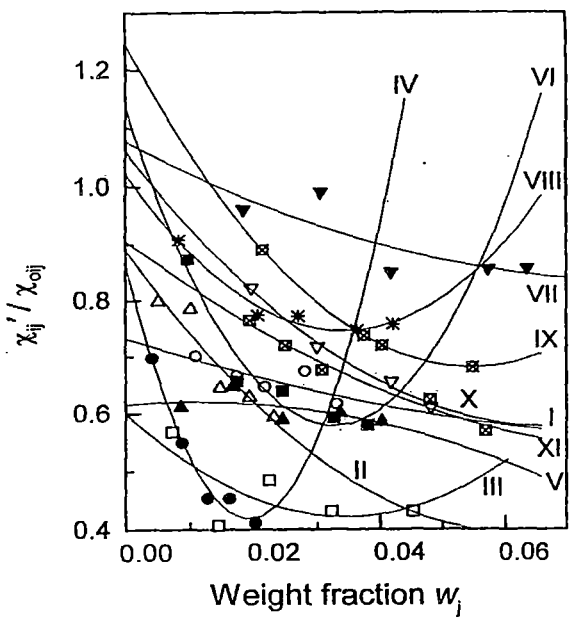

Fig. 5 — Plot of χ_{ij}'/χ_{oij} with w_j of solutes at 35 °C under 9.945 GHz electric field for: I. o-chloronitrobenzene in C_6H_6 (–○–); II. 4-chloro 3-nitrobenzotrifluoride in CCl_4 (–△–); III. 4-chloro 3-nitrotoluene in C_6H_6 (–□–); IV. 4-chloro 3-nitrotoluene in CCl_4 (–●–); V. o-nitrobenzotrifluoride in C_6H_6 (–▲–); VI. m-nitrobenzotrifluoride in C_6H_6 (–■–); VII. 2-chloro 6-methyl aniline in C_6H_6 (–▼–); VIII. 3-chloro 2-methyl aniline in C_6H_6 (–∗ –); IX. 3-chloro 4-methyl aniline in C_6H_6 (–⊗–); X. 4-chloro 2-methyl aniline in C_6H_6 (–∇–) and XI. 5-chloro 2-methyl aniline in C_6H_6 (–⊠ –) at 35 °C under 9.945 GHz electric field

4 Theoretical Formulation for Dipole Moments μ_2 and μ_1

The Debye equation[22] for a polar-nonpolar liquid mixture under hf electric field in terms of χ_{ij}'s is written as:

$$\frac{d\chi_{ij}''}{d\chi_{ij}'} = \omega\tau \qquad \ldots(15)$$

$$\frac{\left(d\chi_{ij}''/dw_j\right)_{wj\to 0}}{\left(d\chi_{ij}'/dw_j\right)_{wj\to 0}} = \omega\tau \qquad \ldots(16)$$

τ's of the polar liquids could, however, be estimated from Eqs (15) and (16) as seen in 8th and 9th columns of Table 2. Again, the imaginary part χ_{ij}'' of the complex hf susceptibility χ_{ij}^* as a function of w_j of a solute can be written as[23-24]:

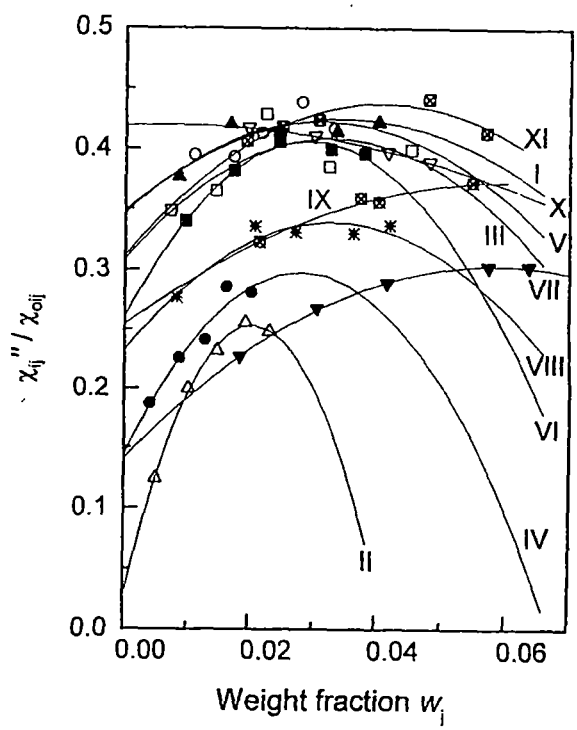

Fig. 6 — Plot of χ_{ij}''/χ_{oij} with w_j of solutes at 35 °C under 9.945 GHz electric field for: I. o-chloronitrobenzene in C_6H_6 (–○–); II. 4-chloro 3-nitrobenzotrifluoride in CCl_4 (–△–); III. 4-chloro 3-nitrotoluene in C_6H_6 (–□–); IV. 4-chloro 3-nitrotoluene in CCl_4 (–●–); V. o-nitrobenzotrifluoride in C_6H_6 (–▲–); VI. m-nitrobenzotrifluoride in C_6H_6 (–■–); VII. 2-chloro 6-methyl aniline in C_6H_6 (–▼–); VIII. 3-chloro 2-methyl aniline in C_6H_6 (–∗ –); IX. 3-chloro 4-methyl aniline in C_6H_6 (–⊗–); X. 4-chloro 2-methyl aniline in C_6H_6 (–∇–) and XI. 5-chloro 2-methyl aniline in C_6H_6 (–⊠ –) at 35 °C under 9.945 GHz electric field

$$\chi_{ij}'' = \frac{N\rho_{ij}\mu_j^2}{27\varepsilon_o k_B T M_j}\frac{\omega\tau}{1+\omega^2\tau^2}(\varepsilon_{ij}+2)^2 w_j$$

which on differentiation with respect to w_j and at $w_j\to 0$ yields:

$$\left(\frac{d\chi_{ij}''}{dw_j}\right)_{w_j\to 0} = \frac{N\rho_i\mu_j^2}{27\varepsilon_o k_B T M_j}\frac{\omega\tau}{(1+\omega^2\tau^2)}(\varepsilon_i+2)^2 \qquad \ldots(17)$$

Table 4 — Slope β_1 of χ_{ij}' versus w_j and β_2 of σ_{ij} versus w_j curves, measured dipole moments μ_j from susceptibility measurement technique and hf conductivity method from Eqs (19) and (26), respectively, reported dipole moment, theoretical dipole moment μ_{theo} from available bond angles and bond moments expressed in Coulomb-metre (C-m) and the values of μ_{expt}/μ_{theo} for different disubstituted benzenes and anilines at 35 °C under 9.945 GHz electric field

System with Sl. No. & Mol.wt.	Slope of χ_{ij}'-w_j & σ_{ij}-w_j curves		Dipole moments μ_j ($\times 10^{-30}$) in cm								μ_{expt}/μ_{theo}
			From Eq. (19)		From Eq. (26)		μ_j^a	μ_j^b	μ_j^r	μ_{theo}	
	β_1	β_2	μ_2	μ_1	μ_2	μ_1					
(I)o-chloronitro benzene in C_6H_6 M_j=0.1575 kg	8.326	4.706	16.93	12.41	17.11	12.54	14.90	14.07	14.50	17.60	0.96
(II)4-chloro3-nitrobenzotrifluoride in CCl_4 M_j=0.2255 kg	3.358	1.875	13.02	6.81	13.08	6.84	9.76	11.80	10.57	12.60	1.03
(III)4-chloro 3-nitrotoluene in C_6H_6 M_j=0.1715 kg	4.490	2.570	17.39	9.37	17.69	9.53	12.94	14.54	14.97	18.60	0.93
(IV)4-chloro 3-nitrotoluene in CCl_4 M_j=0.1715 kg	4.854	3.001	17.40	7.15	18.39	7.56	11.95	12.36	15.60	18.50	0.94
(V)o-nitrobenzotrifluoride in C_6H_6 M_j=0.1910 kg	8.598	4.662	18.78	13.34	18.59	13.20	16.68	16.18	16.54	20.60	0.91
(VI)m-nitrobenzotrifluoride in C_6H_6 M_j=0.1910 kg	1.426	0.702	9.77	5.83	9.22	5.50	7.27	13.52	12.24	12.47	0.78
(VII)2-chloro 6-methylaniline in C_6H_6 M_j=0.1415 kg	0.728	0.560	4.91	3.47	5.79	4.09	3.64	4.50	7.73	6.16	0.56
(VIII)3-chloro 2-methylaniline in C_6H_6 M_j=0.1415 kg	2.674	1.693	10.47	6.66	11.20	7.13	7.14	7.86	10.07	8.27	0.81
(IX)3-chloro4-methyl aniline in C_6H_6 M_j=0.1415 kg	2.128	1.269	10.38	6.07	10.78	6.30	7.14	7.49	8.70	7.33	0.83
(X)4-chloro2-methyl aniline in C_6H_6 M_j=0.1415 kg	3.650	2.063	21.38	8.45	21.61	8.54	9.56	9.07	10.94	10.20	0.83
(XI)5-chloro2-methyl aniline in C_6H_6 M_j=0.1415 kg	3.481	2.196	13.46	8.22	14.37	8.78	9.79	9.79	10.34	9.44	0.87

μ_j^a = dipole moment by using τ from the direct slope of Eq. (15) ; μ_j^r = reported dipole moment
μ_j^b = dipole moment by using τ from the ratio of individual slopes of Eq. (16)
μ_{theo} = theoretical dipole moment from the available bond angles and bond moments

where the density of the solution ρ_{ij} becomes ρ_i = density of solvent, $(\varepsilon_{ij}+2)^2$ becomes $(\varepsilon_i+2)^2$ at $w_j \to 0$, k_B=Boltzmann constant, N= Avogadro's number, ε_i= relative permittivity of solvent and ε_o= permittivity of free space = 8.854×10^{-12} F.m^{-1}. All are expressed in SI units.

Comparing Eqs (16) and (17) one gets:

$$\left(\frac{d\chi'_{ij}}{dw_j}\right)_{w_j\to 0} = \frac{N\rho_i\mu_j^2}{27\varepsilon_o k_B TM_j}\frac{1}{(1+\omega^2\tau^2)}(\varepsilon_i+2)^2 = \beta_1 \qquad ...(18)$$

where β_1 is the slope of χ_{ij}' versus w_j curves of Fig.4 at $w_j\to 0$. Here, no approximation in determination of μ_j is made, like the conductivity measurement technique[4] given below. After simplification, the hf dipole moment μ_j is given by:

$$\mu_j = \left(\frac{27\varepsilon_o k_B TM_j\beta_1}{N\rho_i(\varepsilon_i+2)^2 b}\right)^{\frac{1}{2}} \qquad ...(19)$$

where dimensionless parameter b is given by:

$$b = 1/(1+\omega^2\tau^2) \qquad ...(20)$$

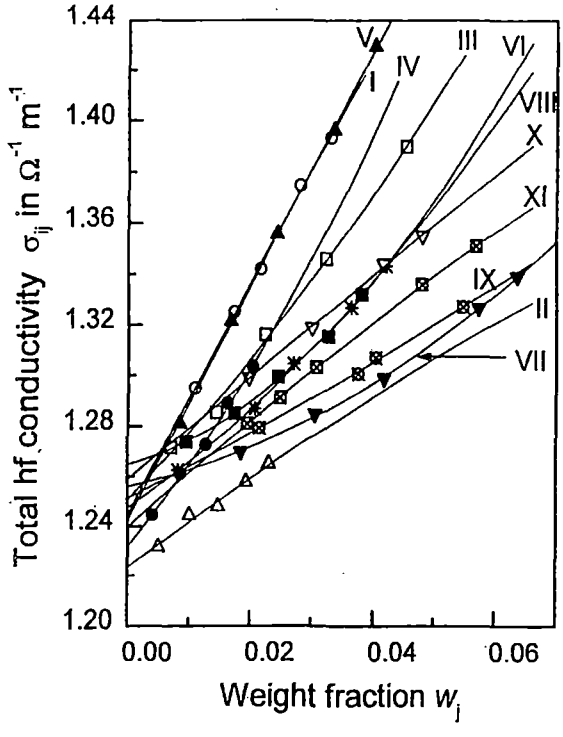

Fig. 7 — Variation of σ_{ij} against w_j of solutes at 35 °C under 9.945 GHz electric field for: I. o-chloronitrobenzene in C_6H_6 (–○–); II. 4-chloro 3-nitrobenzotrifluoride in CCl_4 (–△–); III. 4-chloro 3-nitrotoluene in C_6H_6 (–□–); IV. 4-chloro 3-nitrotoluene in CCl_4 (–●–); V. o-nitrobenzotrifluoride in C_6H_6 (–▲–); VI. m-nitrobenzotrifluoride in C_6H_6 (–■–); VII. 2-chloro 6-methyl aniline in C_6H_6 (–▼–); VIII. 3-chloro 2-methyl aniline in C_6H_6 (–∗ –); IX. 3-chloro 4-methyl aniline in C_6H_6 (–⊗–); X. 4-chloro 2-methyl aniline in C_6H_6 (–∇–) and XI. 5-chloro 2-methyl aniline in C_6H_6 (–⊠ –) at 35 °C under 9.945 GHz electric field

5 Dipole Moments μ_2 and μ_1 from hf Conductivity

The complex hf conductivity σ_{ij}^* of polar-non-polar liquid mixture in a GHz electric field is given by[25]:

$$\sigma_{ij}^* = \sigma'_{ij} + j\sigma''_{ij} \qquad ...(21)$$

where $\sigma_{ij}'(=\omega\varepsilon_o\varepsilon_{ij}'')$ and $\sigma_{ij}''(=\omega\varepsilon_o\varepsilon_{ij}')$ are the real and imaginary parts of the complex conductivity σ_{ij}^* in Ω^{-1} m^{-1}. The magnitude of the total hf conductivity is:

$$\sigma_{ij} = \omega\varepsilon_o\left(\varepsilon_{ij}''^2 + \varepsilon_{ij}'^2\right)^{1/2} \qquad ...(22)$$

Although $\varepsilon_{ij}'>>\varepsilon_{ij}''$, but in the high frequency region, $\varepsilon_{ij}'\cong\varepsilon_{ij}''$. ε_{ij}'' is responsible for absorption of electric energy and offers resistance to polarization. Hence, σ_{ij}'' is related to σ_{ij}' by the relation[26]:

$$\sigma''_{ij} = \sigma_{\infty ij} + \frac{1}{\omega\tau}\sigma'_{ij}$$

$$\sigma_{ij} = \sigma_{\infty ij} + \frac{1}{\omega\tau}\sigma'_{ij} \qquad ...(23)$$

Here, the approximation $\sigma_{ij}''\cong\sigma_{ij}$ is made. Differentiation of Eq. (23) with respect to w_j at $w_j\to 0$ yields:

$$\left(\frac{d\sigma'_{ij}}{dw_j}\right)_{w_j\to 0} = \omega\tau\left(\frac{d\sigma_{ij}}{dw_j}\right)_{w_j\to 0} = \omega\tau\beta_2 \qquad ...(24)$$

where β_2 is the slope of σ_{ij} versus w_j curves of Fig. 7 at infinite dilution $w_j\to 0$ and placed in Table 4. The real part of hf conductivity σ_{ij}' at T K (Ref. 23) is given by:

$$\sigma'_{ij} = \frac{N\rho_{ij}\mu_j^2}{27k_B TM_j}\frac{\omega^2\tau}{1+\omega^2\tau^2}(\varepsilon_{ij}+2)^2 w_j$$

$$\left(\frac{d\sigma'_{ij}}{dw_j}\right)_{w_j\to 0} = \frac{N\rho_i\mu_j^2}{27k_B TM_j}\frac{\omega^2\tau}{1+\omega^2\tau^2}(\varepsilon_i+2)^2 \qquad ...(25)$$

Comparing Eqs (24) and (25) one gets the dipole moment μ_j from:

$$\mu_j = \left(\frac{27k_B TM_j\beta_2}{N\rho_i(\varepsilon_i+2)^2\omega b}\right)^{\frac{1}{2}} \qquad ...(26)$$

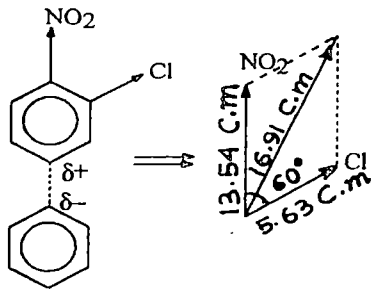

I. o-chloronitrobenzene in C_6H_6

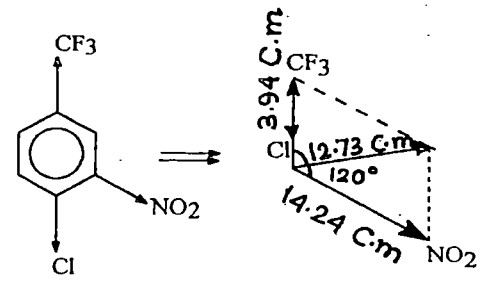

II. 4-chloro 3-nitrobenzotrifluoride in CCl_4

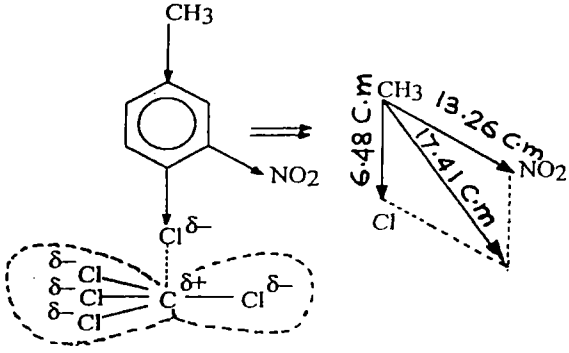

IV. 4-chloro 3-nitro toluene in CCl_4

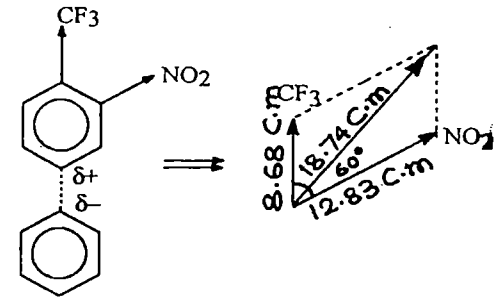

V. o-nitrobenzotrifluoride in C_6H_6

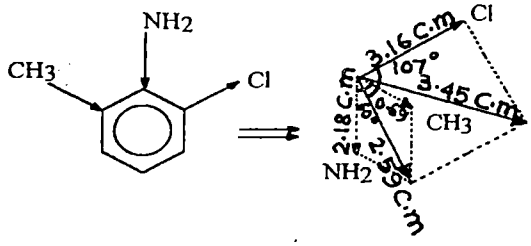

VII. 2-chloro 6-methyl aniline in C_6H_6

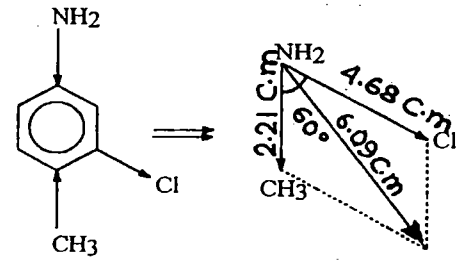

IX. 3-chloro 4-methyl aniline in C_6H_6

Fig. 8 — Conformational structures of solutes from bond angles and bond moments in multiple 10^{30} C-m

All the measured dipole moments μ_i from the susceptibility measurement technique of Eq. (19) and hf conductivity method of Eq. (26) are entered in the 4th to 7th columns of Table 4, respectively.

Results and Discussion

The double relaxation times τ_1 and τ_2 for the polar liquid molecules in different solvents are found out from the slope and intercept of Eq. (3), as

shown in Fig. 1, in terms of the orientational susceptibility parameters χ_{ij} of Table 1. The χ_{ij} values are, however, derived from the relative permittivities[6-8] ε_{ij} for different weight fractions w_j of the polar liquids. The variables of Eq. (3) i.e $(\chi_{oij} - \chi_{ij}')/\chi_{ij}'$ and χ_{ij}''/χ_{ij}' are plotted against each other for different values of w_j of solutes under 9.945 GHz electric field at 35 °C to get linear equation by regression analysis. From Fig. 1, it is revealed that, the fitting is good for some cases, but poor in other cases. It appears that the linear fit for II (–△–), III (–□–) and IV (–●–) in Figs 1 and 2 often passes through two among five data points, others being off from the fit. Nevertheless, the regression analysis was made on the basis of Eq. (3). However, the accuracy of Fig. 1 is tested by the correlation coefficients (r), which were found to be close to unity, indicating that the variables are almost collinear.

The % errors in terms of r-values in getting the intercepts and slopes were worked out to find the accuracies of τ_1 and τ_2, respectively. In order to locate the double relaxation phenomena of the polar liquid molecules in non-polar aprotic solvents under investigation, accurate measurement of χ_{oij} involved with ε_{oij} and $\varepsilon_{\infty ij}$ is necessary. The refractive index n_{Dij} measured by Abbe's refractometer often yields $\varepsilon_{\infty ij} = n_{Dij}^2$, although Cole Cole[27] and Cole Davidson[28] plots usually give $\varepsilon_{\infty ij} \cong 1.0$-$1.5$ times of n_{Dij}^2. This often introduces an additional error in the calculations. Nevertheless, the accuracies of χ_{ij}'', χ_{ij}' and χ_{oij} are of 5 % and 1 %, respectively derived from measured[6-8] relative permittivities ε_{ij}'', ε_{ij}', ε_{oij} and $\varepsilon_{\infty ij}$. The estimated τ_2 and τ_1 are placed in Table 2, in order to compare them with those of Murthy *et al.*[26] of Eq. (15) and by the ratio of the individual slopes of the variations of χ_{ij}'' and χ_{ij}' with w_j in the limit w_j=0 of Eq.(16). The latter method seems to be better to calculate τ, since it eliminates polar-polar interaction almost completely. The linear plot of χ_{ij}'' against χ_{ij}' of Fig. 2 for different w_j of solute has intercepts, although it was expected from Eq. (15) that, they should pass through the origin. Nevertheless, values of τ are found to be in close agreement with those calculated from the ratio of the individual slopes of the variations of χ_{ij}'' and χ_{ij}' with w_j at $w_j \to 0$ of Eq. (16), as shown in Figs 3 and 4. The experimental points as shown in Figs 3 and 4 with the fit are presented (Table 2) to back up the results of Eq. (16) due to Debye model. Values of χ_{ij}'' increase monotonically with w_j and have a tendency to meet the origin for all the curves. This type of behaviour indicates that, under an electric field of 9.945 GHz, χ_{ij}'' tends to pass through the origin at $w_j \to 0$.

It is evident from Table 2 that, all the di-substituted benzenes exhibit the whole molecular rotation, while the di-substituted anilines show the rotation of the flexible parts under 10 GHz electric field when τ_1's and τ_2's are compared with the reported data. This indicates the flexible parts are more rigid in the di-substituted benzenes rather than the di-substituted anilines. The assumptions of symmetric and asymmetric relaxation behaviour from Eqs (8) and (9) for such non-rigid polar molecules yield τ_s and τ_{cs} from Eqs (11) and (13) to place them in the last two columns of Table 2. It reveals that the symmetric and asymmetric relaxation processes are more probable since, τ_s and τ_{cs} are almost in agreement with the reported τ values in a solution. The characteristic relaxation times τ_{cs} are sometimes very high through asymmetric distribution parameter δ and often could not be determined for most of the molecules.

The di-substituted benzenes showed τ_2's in agreement with the reported τ's and τ_{cs} except o-nitrobenzotrifluoride in C_6H_6, which agrees with τ_s only. But, 4-chloro 3-nitrobenzotrifluoride in CCl_4 and m-nitro-benzotrifluoride in C_6H_6 yield τ_2 in close agreement with reported τ's although, they showed $\tau_s \cong \tau_1$. Only 2-chloro-6-methyl aniline and 3-chloro 2-methyl aniline in C_6H_6 showed values of τ_1 in excellent agreement with the calculated values of τ_s. For the rest di-substituted anilines values of τ_1 agree well with the calculated values of τ_s, but the agreement is not better with the measured values of τ from Eqs (15) and (16). It thus reveals that, a part of the di-substituted anilines is rotating, obeying symmetric relaxation behaviour, while most of the di-substituted benzenes showed asymmetric relaxation process for their whole molecular rotations.

The relative weighted contributions c_1 and c_2 towards dielectric dispersions due to τ_1 and τ_2 are estimated and placed in Table 3, by using Fröhlich's Eqs (6) and (7). They are compared with the experimental c_1 and c_2 from the fitted curves of

$\chi_{ij}'/\chi_{\omega ij}$ and $\chi_{ij}''/\chi_{\omega ij}$ against w_j in the limit $w_j \to 0$ of Figs 5 and 6. The non-linear fit with only five points for III (–□–) and IV (–◎–) of Fig.5 appeared to be not convincing and in fact misguiding, but three accurate experimental points are enough for such a fit. However, the fit is done with a PC and appropriate software. All the curves of Figs 5 and 6 vary usually[12] except the convex curve V for o-nitrobenzotrifluoride in C_6H_6. The variations of $\chi_{ij}'/\chi_{\omega ij}$ with w_j are, however, concave and convex in nature for all systems as observed elsewhere[12]. The left hand sides of Eqs (1) and (2) vary with values of w_j in concave and convex manner according to Figs 5 and 6 are now fixed for τ_1 and τ_2 once estimated from intercept and slope of Eq. (3) to yield experimental c_1 and c_2 values from Eqs (4) and (5) at $w_j \to 0$.

This study is supposed to yield the accurate values of c_1 and c_2 unlike the earlier one[12], based on the graphical extrapolated values of $(\varepsilon_{ij}' - \varepsilon_{\infty ij})/(\varepsilon_{\omega ij} - \varepsilon_{\infty ij})$ and $\varepsilon_{ij}''/(\varepsilon_{\omega ij} - \varepsilon_{\infty ij})$ at $w_j \to 0$, drawn on the basis of scientific judgement. Although, the nature of variations remains unaltered, it is evident from Table 3 that, c_2 values are often negative for 4-chloro 3-nitrobenzotrifluoride in CCl_4, m-nitrobenzotrifluoride in C_6H_6 and for all the di-substituted anilines unlike other systems. This perhaps signifies that the rotation of the flexible parts of the polar molecules are not in accord with the whole molecular rotation due to inherent inertia of the substituted parts of the molecules under hf electric field. The theoretical values of c_1+c_2 are found to be greater than the sum of the experimental ones as listed in Table 3.

The experimental values of $c_1+c_2 \equiv 1$ for almost all the non-spherical polar liquid molecules. But (II) 4-chloro 3-nitrobenzotrifluoride in CCl_4 (–△–), (X) 4-chloro 2-methyl aniline (–▽–) and (XI) 5-chloro 2-methyl aniline (–⊠–) in C_6H_6 show considerably lower values of c_1+c_2. This may indicate the reliability of Eq. (3) so far derived for such molecules, although they show high correlation coefficients (r) and the corresponding very low % of errors to get the intercept and slope of Eq. (3). The largest theoretical c_1+c_2 value for (IV) 4-chloro 3-nitro toluene in CCl_4 (–●–) is 1.34, showing a deviation of nearly 34 %, unlike the other systems. The possible existence of more than two broad Debye-type dispersions may be taken into account for such molecules of varying complexities as reported in tables and figures.

Dipole moments μ_2 and μ_1 due to rotation of the whole molecule as well as the flexible parts were, however, measured from Eq. (19) using dimensionless parameters (b) involved with τ's by both the methods and slope β_1's of χ_{ij}' versus w_j curves of Fig. 4. The measured values of μ_2 and μ_1 are presented in Table 4. The variations of all the χ_{ij}' values of polar-nonpolar liquid mixtures are found to be parabolic with values of w_j of polar compounds as evident from Fig.4. They are found to cut the ordinate axis at $w_j = 0$ within $0.0238 \leq \chi_{ij}' \leq 0.0645$ except 4-chloro 3-nitrobenzotrifluoride in CCl_4 (–Δ–), 4-chloro 3-nitrotoluene in CCl_4 (–●–). This behaviour probably reflects the solvent effects on the polar compounds under investigation. The interaction of solute on solvent CCl_4 may occur due to slightly positive charge δ^+ on C atom of CCl_4 and negative charge δ^- on Cl atom of the substituted group in the benzene ring, as seen in Fig. 8. All the systems are of similar nature having monotonic increase of χ_{ij}' with w_j.

The dipole moments μ_2 and μ_1 are also derived from the conductivity measurement technique of Eq. (26) using the slope β_2's of σ_{ij} versus w_j curves of Fig.7 and are placed in Table 4 for comparison. The total hf conductivity σ_{ij} of all the polar-nonpolar liquid mixtures increase monotonically with w_j and cut the ordinate axis within the range $1.2233 \leq \sigma_{ij} \leq 1.2646$ at $w_j=0$ as seen in Fig.7. The slight disagreement of μ_1 and μ_2 derived from both the methods is due to the fact that the hf conductivity includes the fast polarization probably for the bound molecular charge associated with the molecule. All values of μ_2 for di-substituted benzenes and values of μ_1 for di-substituted anilines are found to agree with the reported values of μ presented in Table 4. This indicates that, the flexible parts of the di-substituted benzenes are more rigid in comparison to di-substituted anilines.

The hf dipole moment μ_j's are calculated by using τ from both the methods of direct slope of Eq. (15) and the ratio of the individual slopes of Eq. (16) in order to place them in.

Values of μ_j by using τ from the ratio of the individual slopes are in close agreement with the reported values, suggesting that, the latter method to

obtain τ is more realistic. In such a case, one polar molecule is surrounded by a large number of non-polar solvent molecules and remains in a quasi-isolated state.

A special attention is, therefore, paid to obtain the conformational structures of some of the complex molecules as shown schematically in Fig. 8. The inductive, electromeric and resonance effects combined with mesomeric effect of the substituted polar groups play the key role to yield the theoretical dipole moment μ_{theo} depending on the electron affinity of C–atom of the benzene ring. The molecules have C→CF_3, C←NH_2 ($\angle$142°), C→NO_2, C→Cl C←CH_3 polar groups of bond moments 9.53 × 10^{-30}, 4.93 × 10^{-30}, 14.10 × 10^{-30}, 5.63 × 10^{-30}, 1.23 × 10^{-30} C-m (Coulomb-metre) respectively[12,19] aligned in different angles in a plane to yield μ_{theo}. Out of these, only –NO_2 and –NH_2 groups are in the habit to show resonance effect (–R or +R) in the molecules either by pulling or pushing electrons towards C–atom of the benzene ring. This resonance effect is stronger than inductive effects (+I or –I) to exhibit the peculiar behaviours as seen in the $\chi_{ij}'/\chi_{o ij}$ versus w_j and $\chi_{ij}''/\chi_{o ij}$ versus w_j curves for the di-substituted benzenes II, IV, V, VI including all the di-substituted anilines.

The structure of these polar molecules is of special interest as sketched in Fig. 8 in view of rearrangement of charge-density in them. All the di-substituted anilines include –Cl, –NH_2 and –CH_3 polar groups, of which –Cl and –CH_3 have very weak inductive effects (+I or –I). They are easily influenced by the GHz electric field to show the rotation of their flexible parts. Further, the observed difference in μ values for a polar molecule in two aprotic nonpolar solvents may arise due to weak polarity of CCl_4 as shown in Fig. 8. The difference between μ_{theo} and experimental values of μ_j establishes the non-consideration of inductive and mesomeric effects. All these effects may be taken into account by the factor μ_{expt}/μ_{theo} to yield the exact μ_1 and μ_2 values of the molecules. All the polar molecules have sp^2 hybridized carbon atoms of benzene ring and the substituted parts are associated with sp^3 orbital. The interaction of orbitals may lead to gain knowledge on accumulation of charge on the substituted groups in addition to various effects present in them. The conformational structures of other molecules except six of Fig. 8 were already shown elsewhere[12,19].

Conclusions

The study of relaxation phenomena of di-substituted benzenes and anilines in C_6H_6 and CCl_4 by the modern established symbols of dielectric orientational susceptibilities χ_{ij} measured under a single frequency electric field is very encouraging. It seems to be more topical, significant and useful contribution to predict the conformational structures and various molecular associations of the molecules at any given temperature. The intercept and slope of the derived linear Eq. (3) by the regression analysis on the measured data of χ_{ij} of different values of w_j are used to get τ_2 and τ_1. The methodology so far developed in SI units is superior because of the unified, coherent and rationalized nature of the established symbols of dielectric terminologies and parameters, which are directly linked with orientational polarization of the molecules. The significant Eqs (15) and (16) to obtain values of τ_j and hence values of μ_j from Eq. (19) help the future workers to shed more light on the relaxation phenomena of the complicated non-spherical polar liquids and liquid crystals. The prescribed method to obtain values of τ_j from Eq. (16) with the use of the ratio of the individual slopes of χ_{ij}'' versus w_j and χ_{ij}' versus w_j curves at $w_j \to 0$ is a significant improvement over the existing ones, as it eliminates polar-polar interaction almost completely in τ_j's and μ_j's respectively.

Values of τ_j and μ_j are usually claimed to be accurate within 10 % and 5 %, respectively. But, the correlation coefficient r and % errors of Eq. (3) demand that, values of τ and μ are more than accurate. The non-spherical di-substituted benzene and aniline molecules absorb electric energy much more strongly, nearly 10 GHz electric field, at which the value of ε'' for absorption against frequency ω showed a peak. This invited the attention to get the double relaxation times τ_2 and τ_1 from Eq. (3). The corresponding sum of the experimental and theoretical values of weighted contributions c_1 and c_2 towards dielectric dispersions due to estimated τ_2 and τ_1 differ significantly to indicate more than two Debye type relaxations in such molecules because of their complexity. The values of τ for di-substituted benzenes as seen in

Table 2 show the whole molecular rotation, while the flexible parts of the di-substituted anilines rotates under 10 GHz electric field.

Di-substituted anilines exhibit the symmetric relaxation behaviour, while the asymmetric relaxation behaviour occurs in di-substituted benzenes in C_6H_6 except 4-chloro 3-nitrobenzotrifluoride in CCl_4 and m-nitro benzotrifluoride in C_6H_6, respectively. Values of μ_2 and μ_1 due to τ_2 and τ_1 are expected to be smaller when they are measured from the susceptibility measurement technique rather than the hf conductivity method, where the approximation of $\sigma_{ij} \cong \sigma_{ij}''$ is usually made. The difference of μ_2 for the first six systems and of μ_1 for the rest five systems of Table 4, between conductivity and susceptibility measurement may arise, either by elongation or reduction of the bond moments of the substituted polar groups by the factor μ_{expt} / μ_{theo} in agreement with the measured values of μ to take into account of the inductive, mesomeric and electromeric effects of the polar groups in the molecules. Thus, the correlation between the conformational structures with the observed results enhances the scientific content to add a new horizon of understanding to the existing knowledge of dielectric relaxation phenomena.

References

1 Dhull J S & Sharma D R, *J Phys D: Appl Phys*, 15 (1982) 2307.

2 Sharma A K & Sharma D R, *J Phys Soc Jpn*, 53 (1984) 4771.

3 Kumbharkhane A C, Puranic S M, Akode C G & Mehrotra S C, *Indian J Phys*, 74A (2000) 471.

4 Dutta K, Basak R C, Sit S K & Acharyya S, *J Molec Liq*, 88 (2000) 229.

5 Sit S K, Dutta K, Acharyya S, Palmajumder T & Roy S, *J Molec Liq*, 89 (2001) 111.

6 Khameshara S M & Sisodia M L, *Indian J Pure & Appl Phys*, 18 (1980) 110.

7 Gupta P C, Arrawatia M L & Sisodia M L, *Indian J Pure & Appl Phys*, 16 (1978) 451.

8 Arrawatia M L, Gupta P C & Sisodia M L, *Indian J Pure & Appl Phys*, 15 (1977) 770.

9 Gopalakrishna K V, *Trans Faraday Soc*, 53 (1957) 767.

10 Higasi K, *Bull Chem Soc Jpn*, 39 (1966) 2157.

11 Heston W M, Franklin A D, Henneley E J & Smyth C P, *J Am Chem Soc*, 72 (1950) 3443.

12 Saha U, Sit S K, Basak R C & Acharyya S, *J Phys D: Appl Phys*, 27 (1994) 596.

13 Jonscher A K, *Physics of dielectric solids*, invited papers (Ed) C H L Goodman, 1980.

14 Jonscher A K, *Universal Relaxation Law* (Chelsea Dielectric Press, London), 1996.

15 Ghosh N, Basak R C, Sit S K & Acharyya S, *J Molec Liq*, 85 (2000) 375.

16 Bergmann K, Roberti D M & Smyth C P, *J Phys Chem*, 64 (1960) 665.

17 Bhattacharyya J, Hasan A, Roy S B & Kastha G S, *J Phys Soc Jpn*, 28 (1970) 204.

18 Higasi K, Koga Y & Nakamura M, *Bull Chem Soc Jpn*, 44 (1971) 988.

19 Sit S K, Basak R C, Saha U & Acharyya S, *J Phys D: Appl Phys*, 27 (1994) 2194.

20 Fröhlich H, *Theory of dielectrics Oxford* (Oxford University Press, Oxford, UK).

21 Powles J G, *J Molec Liq*, 56 (1993) 35.

22 Hill N E, Vaughan W E, Price A H & Davies M, *Dielectric properties and molecular behaviour* (Van Nostrand Reinhold, London), 1969.

23 Smyth C P, *Dielectric behaviour and structure* (McGraw-Hill, UK), 1955.

24 Dutta K, Sit S K & Acharyya S, *Pramana: J Phys*, 57 (2001) 775.

25 Murphy F J & Morgan S O, *Bell Syst Tech J*, 18 (1939) 502.

26 Murthy M B R, Patil R L & Deshpande D K, *Indian J Phys*, 63B (1989) 491.

27 Cole K S & Cole R H, *J Chem Phys*, 9 (1941) 341.

28 Cole R H & Davidson D W, *J Chem Phys*, 19 (1951) 1484.